AD-770 300

AIRCRAFT ANTISKID ANALYSIS VERIFICATION AND REFINEMENT

Byron H. Anderson

General Dynamics

Prepared for:

Air Force Flight Dynamics Laboratory

September 1973

UNCLASSIFIED
Security Classification

DOCUMENT CONTROL DATA - R & D

(Security classification of title, body of abstract and indexing annotation must be entered when the overall report is classified)

1. ORIGINATING ACTIVITY (Corporate author)
General Dynamics Corporation
Convair Aerospace Division, Ft. Worth Operation
P.O. Box 748, Fort Worth, Texas 76101

2a. REPORT SECURITY CLASSIFICATION
UNCLASSIFIED

2b. GROUP

3. REPORT TITLE
AIRCRAFT ANTISKID ANALYSIS VERIFICATION AND REFINEMENT

4. DESCRIPTIVE NOTES (Type of report and inclusive dates)
Final Report (December 1970 thru April 1973)

5. AUTHOR(S) (First name, middle initial, last name)
Byron H. Anderson

6. REPORT DATE
September 1973

7a. TOTAL NO. OF PAGES
~~351~~ 365

7b. NO. OF REFS
17

8a. CONTRACT OR GRANT NO.
F33615-71-C-1109

b. PROJECT NO.
1369

c. Task Area No. 01

d. Work Unit No. 21

9a. ORIGINATOR'S REPORT NUMBER(S)

9b. OTHER REPORT NO(S) (Any other numbers that may be assigned this report)
AFFDL-TR-73-70

10. DISTRIBUTION STATEMENT
Approved for Public Release - Distribution Unlimited

11. SUPPLEMENTARY NOTES

12. SPONSORING MILITARY ACTIVITY
Air Force Flight Dynamics Laboratory
Wright-Patterson AFB, Ohio 45433

13. ABSTRACT

A program for verifying and refining a previously developed aircraft antiskid performance and system compatibility analysis procedure is described. Analysis verification was performed by comparing antiskid system operation as predicted by the analytical procedures with that recorded during laboratory testing. The laboratory tests were conducted at the Air Force Flight Dynamics Laboratory Landing Gear Test Facility at Wright-Patterson Air Force Base, Ohio using a set-up consisting of F-111 aircraft main landing gear, tire, wheel, brake, hydraulic brake actuation system and several antiskid control circuit variations. The aircraft landing gear equipment was mounted in a support fixture with movable load carriage installed over the 192 inch diameter brake test dynamometer. Analytical refinement consisted of modifying the mathematical equations describing antiskid operations to enhance computation economy and more accurately agree with test results. A discussion of parameters influencing antiskid operation is presented. Preliminary design of components for a fluidic controlled pneumatic brake actuation system is described.

DD FORM 1 NOV 65 1473

UNCLASSIFIED
Security Classification

UNCLASSIFIED
Security Classification

14. KEY WORDS	LINK A		LINK B		LINK C	
	ROLE	WT	ROLE	WT	ROLE	WT
Airplane Stopping Performance Antiskid Analysis Antiskid Dynamometer Testing Landing Gear Brake System Performance						

ib

UNCLASSIFIED
Security Classification

☆U.S.Government Printing Office: 1973 — 758-428/233

NOTICE

When Government drawings, specifications, or other data are used for any purpose other than in connection with a definitely related Government procurement operation, the United States Government thereby incurs no responsibility nor any obligation whatsoever; and the fact that the government may have formulated, furnished, or in any way supplied the said drawings, specifications, or other data, is not to be regarded by implication or otherwise as in any manner licensing the holder or any other person or corporation, or conveying any rights or permission to manufacture, use, or sell any patented invention that may in any way be related thereto.

NTIS		
BY		
Dist.	AVAIL. and or SPECIAL	
A		

Copies of this report should not be returned unless return is required by security considerations, contractual obligations, or notice on a specific document.

AIR FORCE/56780/19 November 1973 — 150

AIRCRAFT ANTISKID ANALYSIS
VERIFICATION AND REFINEMENT

BYRON H. ANDERSON

FOREWORD

The Analytical and Experimental Aircraft Antiskid Analysis Verification and Refinement work reported herein was performed by the Fort Worth Operation of General Dynamics Convair Aerospace Division under U. S. Air Force Contract F33615-71-C-1109. The contract was initiated under Project No. 1369, "Mechanical Systems for Advanced Flight Vehicles," and Task No. 136901, "High Performance Landing Gear." This program was administered under the direction of the Air Force Flight Dynamics Laboratory. Mr. Paul M. Wagner (AFFDL/FEM) was the Air Force Project Engineer.

This report describes work conducted during the period from December 1970 thru April 1973. The Convair Project Leader was R. C. Churchill and B. H. Anderson was the principal investigator. The design and installation of the verification test set-up and overhead load carriage fixture on the AFFDL Landing Gear Test Facility at Wright-Patterson AFB, Ohio was accomplished by Mr. J. F. Maverick and Mr. W. I. Streiff. Mr. W. C. Kreger formulated some of the mathematical models. Digital computer programing was performed by Mr. C. W. Austin, Mrs. L. J. Schnacke and Mr. J. D. Price.

The author wishes to thank Mr. Wagner for his guidance and assistance throughout the program. The generous assistance and cooperation of AFFDL Landing Gear Test Facility personnel and members of the Systems Research Laboratories, Inc., during the Verification Test Phase of the program is appreciated. This report was submitted by the author in June 1973.

K. H. Digges
KENNERLY H. DIGGES
Chief, Mechanical Branch
Vehicle Equipment Division
Air Force Flight Dynamics Laboratory

ABSTRACT

A program for verifying and refining a previously developed aircraft antiskid performance and system compatibility analysis procedure is described. Analysis verification was performed by comparing antiskid system operation as predicted by the analytical procedures with that recorded during laboratory testing. The laboratory tests were conducted at the Air Force Flight Dynamics Laboratory Landing Gear Test Facility at Wright-Patterson Air Force Base, Ohio using a set-up consisting of F-111 aircraft main landing gear, tire, wheel, brake, hydraulic brake actuation system and several antiskid control circuit variations. The aircraft landing gear equipment was mounted in a support fixture with movable load carriage installed over the 192 inch diameter brake test dynamometer. Analytical refinement consisted of modifying the mathematical equations describing antiskid operations to enhance computation economy and more accurately agree with test results. A discussion of parameters influencing antiskid operation is presented. Preliminary design of components for a fluidic controlled pneumatic brake actuation system is described.

CONTENTS

ILLUSTRATIONS

ILLUSTRATIONS

Appendix A

ILLUSTRATIONS

ILLUSTRATIONS

TABLES

APPENDIX A

SECTION I

INTRODUCTION

A. OBJECTIVE

The objectives of this program as stated in the contract statement of work are: (1) to verify, correlate and refine the Aircraft Antiskid Performance - Total System Compatibility Analysis Procedures previously developed under U.S. Air Force Contract F33615-70-C-1004 and as described in AFFDL-TR-70-128, and (2) to establish the feasibility of a fluidic-controlled pneumatic braking system.

B. SCOPE

This program for Aircraft Antiskid Performance - Total System Compatibility Analysis Verification, Correlation and Refinement consisted of the following:

(1) A total system verification test set-up was designed, fabricated and installed in the AFFDL Landing Gear Test Facility, Building 31, Area B, Wright-Patterson Air Force Base, Ohio. The test set-up is comprised of: (a) a structural steel framework attached to the 192 inch diameter inertia dynamometer, (b) a movable load carriage supported by the framework and providing simulated aircraft landing gear fuselage attachment provisions, (c) a carriage loading and positioning system, (d) one F-111 main landing gear tire-wheel-brake assembly assembled with the required aircraft landing gear structural components to complete an installation the same as that for the aircraft left wheel installation, (e) a mockup of the aircraft hydraulic brake actuation and control system including pilot's metering valve, accumulator, lines and fittings, (f) antiskid control circuits, an F-111 antiskid valve and wheel speed sensing unit and (g) instrumentation and recording equipment needed to measure and record parameter variations significant to antiskid operation.

(2) Verification testing consisting of a number of braked stops was performed utilizing the total system verification test set-up for thirty-six test conditions having various combinations of landing gear loading, antiskid control circuit type, two different tire sizes, various tire inflation pressures and various amounts of hydraulic brake actuation system flow restriction. During these stops the following parameters

were measured and recorded with respect to time: dynamometer flywheel speed and distance, braked wheel speed, hydraulic pressure at the brake and at the antiskid valve inlet, brake torque, radial and tangential forces between the tire and dynamometer flywheel and antiskid valve electrical signal.

(3) The results from some of the total system verification test runs were compared with analytically predicted parameter variations obtained from the antiskid performance and total system compatibility analysis procedures.

(4) The Antiskid Performance and Total System Compatibility Analysis procedures have been refined to enhance computation economy and to achieve agreement with verification test results.

(5) Components for a fluidic-controlled pneumatic braking system for operation with and skid control of an F-111 wheel/brake assembly have been designed. A comparison of fluidic to conventional brake control systems has been formulated.

C. BACKGROUND

The characteristics of modern high performance airplanes are such that there are many occasions where the pilot is very disadvantageously situated for perceiving the amount of wheel brake force which can be applied without causing tire skidding. Because of high airplane ground speeds required for takeoff or landing, relatively high wheel braking forces are frequently necessary for controlling the vehicle's velocity within the available runway distance. Since a relatively short duration tire skid at high speed may result in a blowout with consequent severe damage to other aircraft components or may cause loss of directional control, experience has established that a wheel brake antiskid feature is required for safe and predictable aircraft operation.

Figure 1 is a block diagram showing the typical arrangement of an aircraft landing gear wheel brake system and the relationship between the various elements within the total vehicle system. The brake system functions to inhibit wheel rotation in response to pilot command so that a force opposing aircraft motion is produced between the tires and runway surface. Most modern military aircraft are equipped with hydraulically actuated disc type brakes controlled by a full power brake control system which also incorporates an automatic antiskid feature as shown.

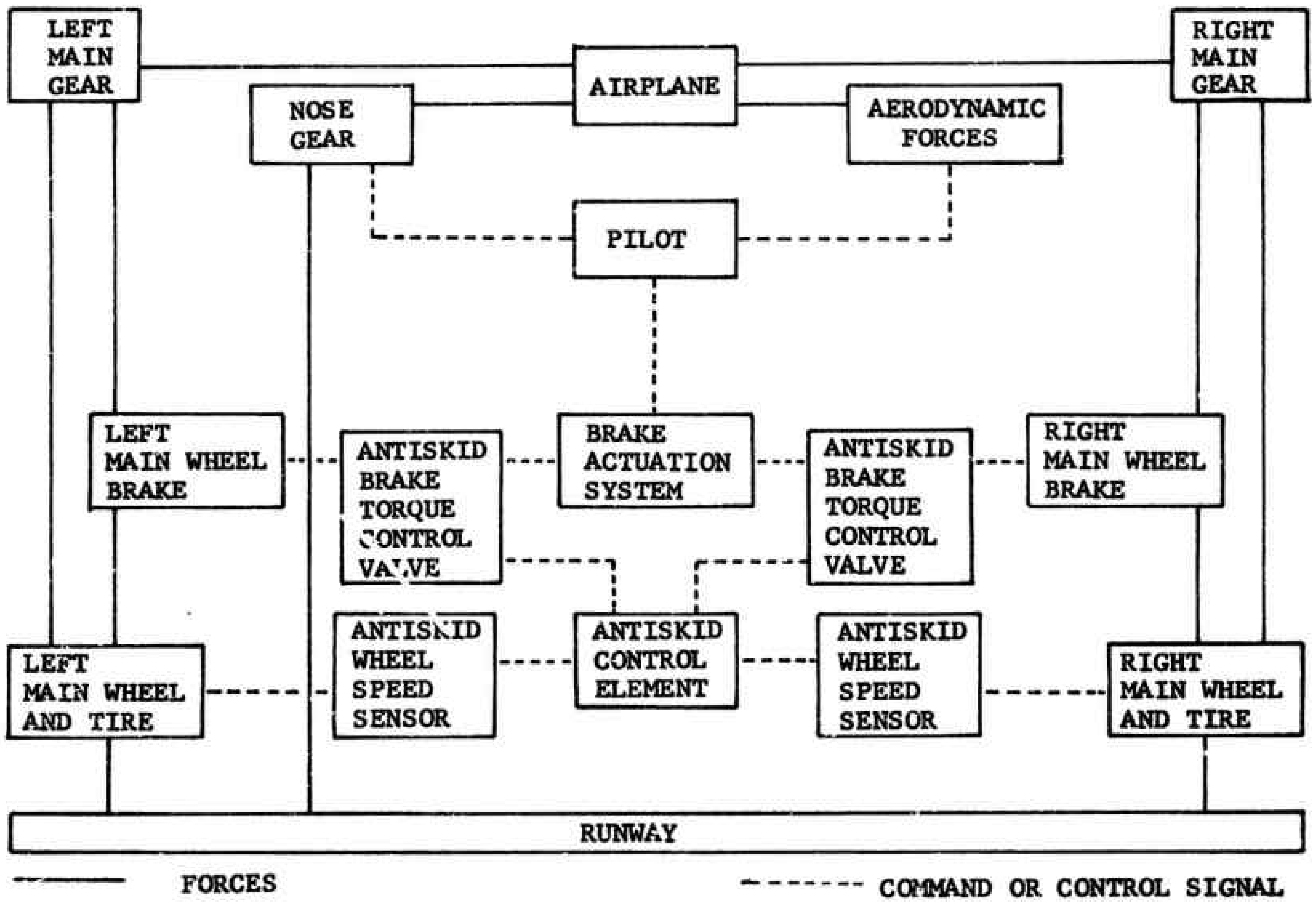

Figure 1 Aircraft Antiskid Arrangement Block Diagram

The antiskid function is accomplished by a group of components which automatically detect and alleviate incipient tire skidding by controlling brake torque. An incipient skid is alleviated by temporarily reducing brake torque to a value less than the torque being produced by the friction force at the tire-runway interface. Brake torque reduction is sustained for a time interval sufficiently long to allow the wheel to regain speed. After the wheel has regained speed, brake torque increase is initiated. Since brake torque is produced by applying fluid pressure to the brake actuating cylinders, torque is controlled indirectly by controlling actuation pressure.

Antiskid system components usually consist of wheel speed sensing units, antiskid control elements and antiskid brake torque control valves. For clarity, Figure 1 shows the arrangement of an aircraft having a tricycle landing gear arrangement with single wheel main gear configuration. For airplanes having multiple wheeled landing gears and/or multiple landing gears, the same basic arrangement prevails with the addition of additional similar type components as appropriate.

The reduction and subsequent reapplication of brake torque results in an oscillatory braking force being applied to the airplane. This oscillatory force has the potential for causing adverse dynamic loading of the airplane structure, for causing directional control difficulty and for degrading the aircraft's stopping performance. The need for evaluating antiskid operation to predict the effects of the potentially deleterious oscillatory braking force is now recognized because there have been a number of instances where failure to do so has resulted in severe operational difficulty and in some cases catastrophic landing gear failure.

The overall resultant effects of antiskid operation are dependent upon the characteristics of the antiskid equipment components along with the characteristics of the airplane and many of its other systems as well as the operating environment into which the vehicle is placed. If during the airplane's usage, within its intended operating envelope instances of unsafe conditions resulting from antiskid operation frequently occur, the braking system is deficient with respect to the attempted operational circumstances and is relatively unacceptable. Braking system deficiencies are caused by incompatibilities within the overall vehicle system which result in antiskid operation being different than was intended or which result in the practically

achievable braking effectiveness being incorrectly predicted. These incompatibilities result from inadequate consideration of significant design parameters or of the aircraft's required operating environment.

It is intended that the analytical techniques described herein be used for establishing the influence of the individual total vehicle system elements upon antiskid operation. The behavior of each equipment item can thereby be established or its performance requirements defined so that the relative compatibility between individual elements and between equipment items and basic aircraft characteristics can be determined. Whenever the practically achievable performance for each equipment item is established considering the applicable prevailing cost, weight, volume or other inherent physical property restraints, the overall system can then be evaluated with respect to the braking system equipment's acceptability and proper utilization.

As with any system or device the degree to which a braking system or one of its components may be adjudged acceptable is established by how well it operates to provide the performance expected without causing any trouble. Therefore, it is evident that the braking system equipment's acceptability for a particular usage is influenced by how well expectation is tempered with reason and judgement. For instance, it is possible that some aerodynamic or other vehicle characteristic prevents achievement of the desired or expected wet runway stopping performance with any conceivable antiskid equipment configuration. If experiencing this type of disappointing circumstance is to be avoid the expected braking system effectiveness must be established from basic material properties and proven fundamental principles which have been verified by substantial experimental evidence rather than from optimistic estimates or unsupported claims. The antiskid analysis techniques utilized during this program may be employed for such realistic establishment of braking system effectiveness. The following discussion of some fundamental aspects of antiskid operation and antiskid evaluation is presented to help establish a rational basis for applying the analysis procedure.

The dominant factor influencing the operation of an antiskid brake control system is the well known characteristic behavior of a rolling tire while being subjected to braking forces. This characteristic behavior, as shown on Figure 2 , is that as a small braking force is applied an apparent slippage develops between the tire and contacing surface. This apparent slippage is evidenced by the wheel angular velocity being less than the synchronous angular velocity by an amount proportional to the

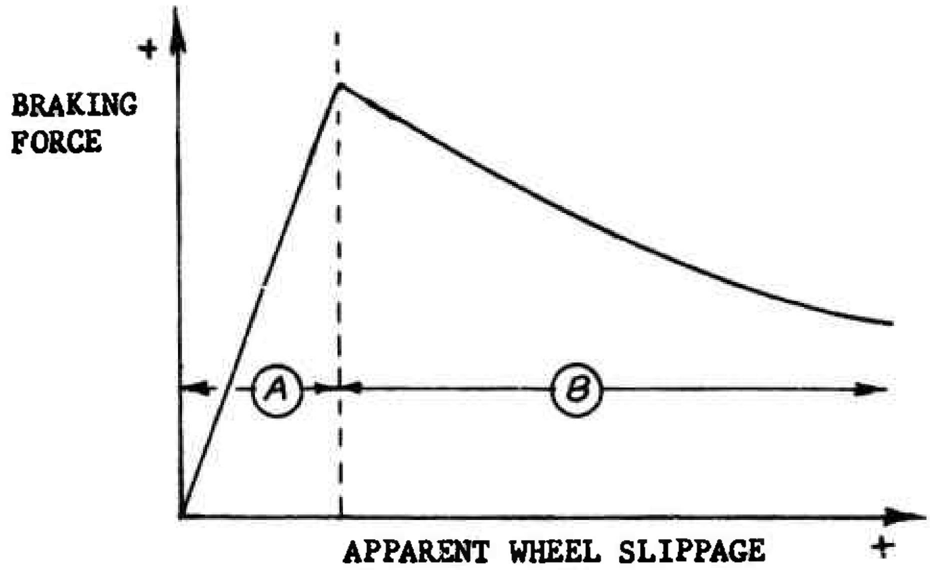

(A) ZONE OF NO TIRE FOOTPRINT SLIPPAGE

(B) ZONE OF INCREASING TIRE FOOTPRINT SLIPPAGE

APPARENT WHEEL SLIPPAGE = $\dot{X}_A - \dot{\Theta}_W R_e$

WHERE:

$\dot{X}_A$ = AXLE TRANSLATIONAL VELOCITY

$\dot{\Theta}_W$ = WHEEL ANGULAR VELOCITY

R_e = TIRE UNBRAKED APPARENT ROLLING RADIUS

Figure 2 Pneumatic Tire Slippage Versus Braking Force Characteristic

the braking force. The tire synchronous angular velocity is the value which results from unbraked rolling. The initial apparent slippage proportional to the braking force occurs without appreciable relative motion between the tire footprint and contacting surface because of elastic deformations within the tire. If an increase in the braking force to a value exceeding the maximum achievable for prevailing friction conditions is attempted, an actual slippage between the tire footprint and contacting surface results. When the tire footprint is actually sliding relative to the contacting surface the friction coefficient decreases as sliding velocity increases which is the usual case with any two sliding objects.

When the characteristics of the braking force - slippage relationship are considered while examining the equation of the tire's angular motion with applied brake torque as shown by Figure 3, it can be seen that when the applied brake torque is less than the available friction torque, a friction torque equal and opposite to the brake torque will develop by the tire increasing its slippage along the positive-slope portion of the characteristic relationship. If the applied brake torque is increased or if the tire-to-ground friction force potential decreases so that a condition occurs where the brake torque exceeds the available friction torque, tire slippage will increase into the negative-slope region of the brake force - slippage characteristic variation resulting in an unstable ever increasing negative wheel angular acceleration. A full skid will result if the brake torque is not quickly reduced to some value less than the instantaneous friction torque so that a positive wheel angular acceleration is produced causing the wheel to regain speed. To satisfactorily control brake torque an antiskid system must be capable of distinguishing between a tire's slippage in the stable or unstable condition.

Several control concepts and a number of different type devices for implementing some of these concepts have been used for antiskid brake control. Because of very competitive market conditions and the achievement of relatively acceptable performance, practically all of the antiskid systems in current general usage are of the class previously described in Figure 1. These systems measure a braked wheel's speed, compare the measured speed magnitude and/or rate of change to an "index-of-acceptability", and control brake torque according to the results of the comparison. The primary differences between systems supplied by different airframe or antiskid equipment manufacturers is the "index-of-acceptability" utilized and the methods by which it is established. The usual "index-of-acceptability" is the amount of wheel slippage or the rate of increase in wheel slippage.

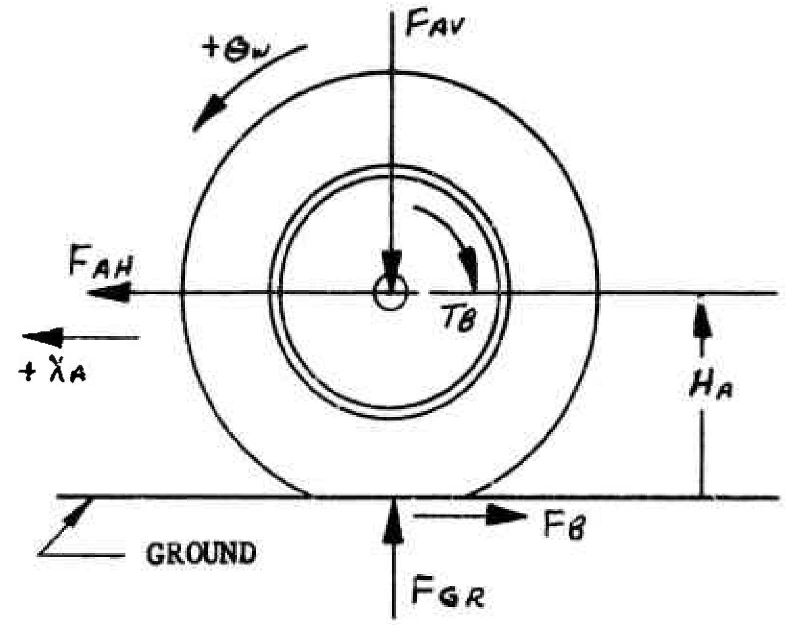

T_B = Brake torque
F_{GR} = Radial force on tire from ground
F_B = Braking force = μF_{GR}
F_{AV} = Vertical force on wheel from axle
F_{AH} = Horizontal force on wheel from axle
H_A = Height of axle above ground
μ = Friction coefficient between the footprints and ground
I_W = Tire-wheel assembly mass moment of inertia
X_A = Horizontal axle displacement
$\dot{X}_A$ = Horizontal axle velocity
θ_W = Wheel angular displacement
$\dot{\theta}_W$ = Wheel angular velocity
$\ddot{\theta}_W$ = Wheel angular acceleration

Equation of wheel angular motion: $I_W \ddot{\theta}_W = F_B H_A - T_B$

Figure 3 Braked Wheel Forces

Evaluating antiskid braking system performance and compatibility is aided by examining the physical operating characteristics of the applicable braking system equipment in the typical arrangement as shown schematically in Figure 4. The elements shown are: the pilot's metering valve, antiskid control valve, brake actuation cylinder, interconnecting fluid transmission lines with their flow resistances, brake discs, wheel and tire assembly, antiskid wheel speed sensor device and antiskid control circuit elements. The typical antiskid valve is a two element device having a control pressure producing first stage and a second stage power spool which controls the direction which fluid may flow thru the valve. Several different type first stage devices may be used and the range over which control pressure varies depends upon the type. Figure 4 shows the type where control pressure varies over the entire range between inlet port pressure and return port pressure. For other type first stage devices having different ranges of control pressure variation, the second stage spool areas upon which the control and brake port pressures act are sized so that a proper force balance is achieved. The antiskid valve operating principles are similar whichever type first stage type is used.

Figure 4 shows the antiskid valve second stage in the position for no antiskid control signal such that the fluid pressure as commanded by the pilot's pedal position is transmitted to the brake. The antiskid valve first stage produces a control pressure as a function of the antiskid valve control signal and inlet pressure. The control pressure is equal to antiskid valve inlet pressure with zero antiskid valve input signal and the control pressure is decreased as the valve signal increases. If the antiskid control valve input signal is increased the reduction in first stage control pressure imposes a pressure unbalance upon the second stage spool thereby causing spool movement to a position which allows fluid flow out of the brake cylinder to return. As the antiskid valve brake port presure becomes equal to the first stage control pressure, the pressure balance on the second stage spool causes it to be repositioned to shut off fluid flow. Whenever the antiskid valve input signal is reduced, first stage control pressure increases to cause an opposite pressure unbalance in the second stage which results in the spool being positioned to allow fluid flow from the pilot's metering valve to the brake cylinder until a new pressure balance is achieved.

A typical aircraft brake has a characteristic cylinder pressure versus fluid volume relationship and a characteristic cylinder pressure versus torque relationship as shown on Figure 5.

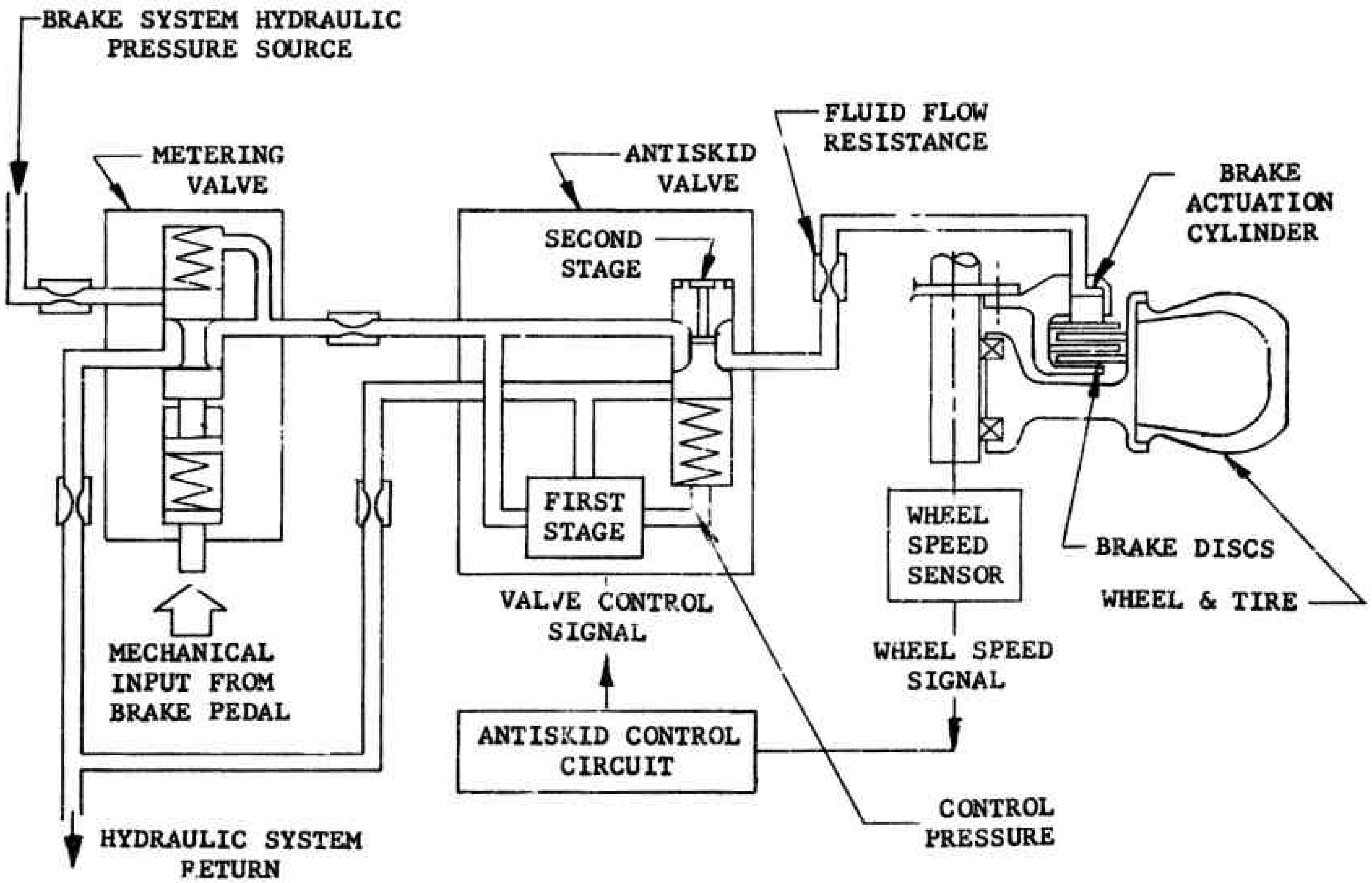

Figure 4 TYPICAL BRAKE CONTROL/ANTISKID FLUID POWER SYSTEM

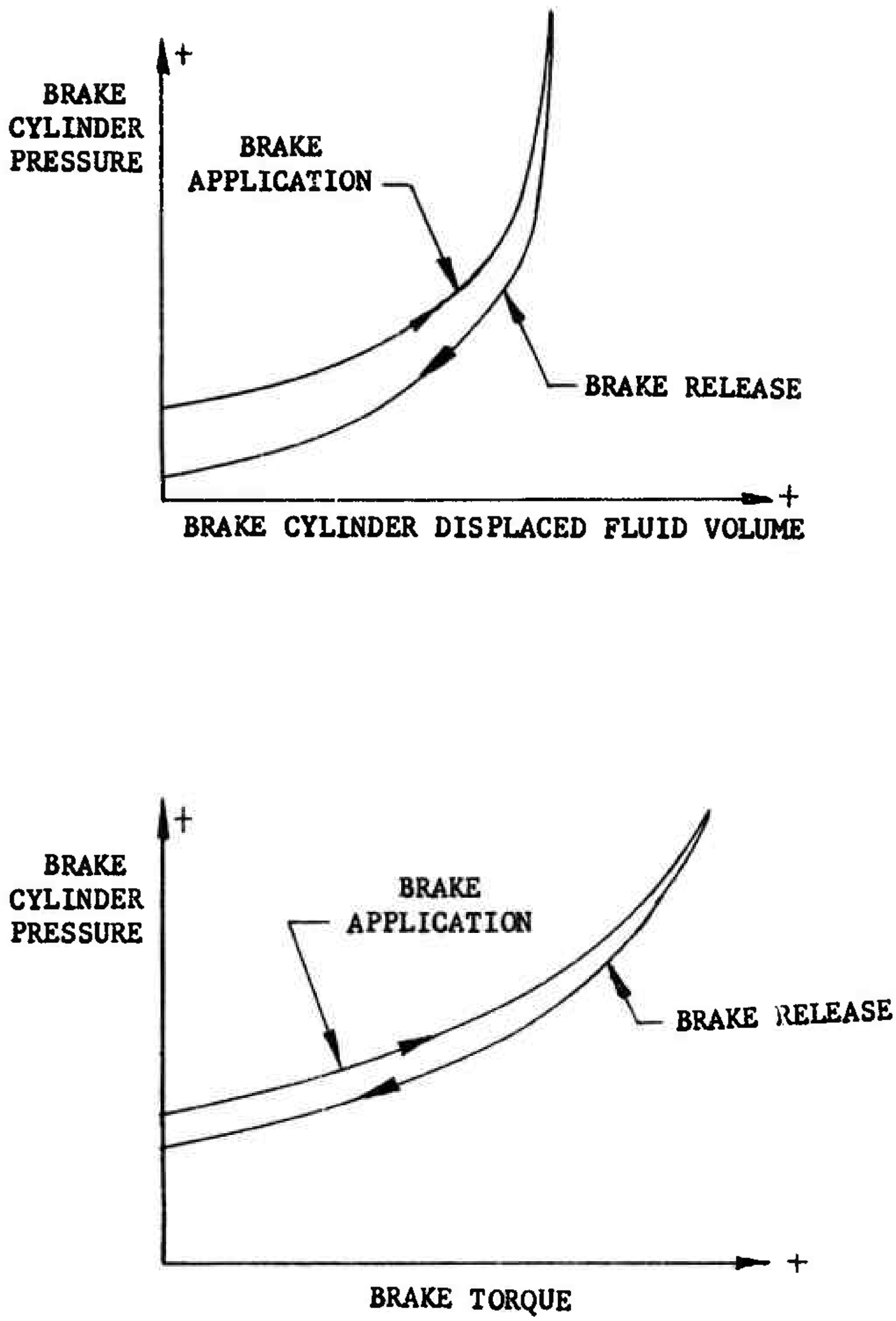

Figure 5 Typical Brake Characteristics

For occasions where the antiskid control circuit commands brake torque to be increased or decreased by changing the antiskid valve control signal, some amount of time must elapse during which sufficient fluid flow occurs to produce the change in brake cylinder volume corresponding with the required change in cylinder pressure. When changing brake cylinder pressure, the fluid flow rate at each instant is established by the difference between brake cylinder pressure and the system source pressure for brake application or by the difference between brake cylinder pressure and system return pressure for brake release and the combined resistance of the applicable fluid flow path. Since the antiskid valve is a mechanical device which must be positioned to permit fluid flow in the proper direction, some finite (usually small) time interval is required. Consequently, it must be recognized that the brake actuation system flow resistances, the antiskid valve dynamic response characteristics and the brake's characteristics have a very significant influence upon brake torque dynamic response to antiskid valve input control signals. In addition, the antiskid wheel speed sensing element and the control circuit elements usually have characteristics which result in the instantaneous values of the various signals lagging actual occurrences by some small amount. The relative compatibility of the brake actuation and control loop is established by how well the antiskid control element's characteristics are matched to the prevailing conditions of actuation fluid flow resistance, brake pressure-volume and pressure torque characteristics, and the dynamic response characteristics of the tire and wheel brake supporting structure.

Antiskid control has a cyclic nature because it involves detecting that braked wheel slippage has progressed from a stable condition to an unstable condition with subsequent brake torque adjustment in a manner such that wheel slippage returns to the stable condition. Figure 5 describes the sequential events which occur and the relative variation of wheel speed, brake torque and friction torque during a typical antiskid cycle. To emphasize the various events and fundamental characteristic variations, the magnitude and rate of the parameter changes shown have been arbitrarily assigned and are not intended to represent any specific case. The occurrences during the time intervals between events shown on Figure 5 are as follows:

TIME INTERVAL	OCCURRENCES
t_0-t_1	Brake torque increases and wheel angular velocity decreases in the stable region of the brake force - tire slippage characteristic producing an equal and opposite

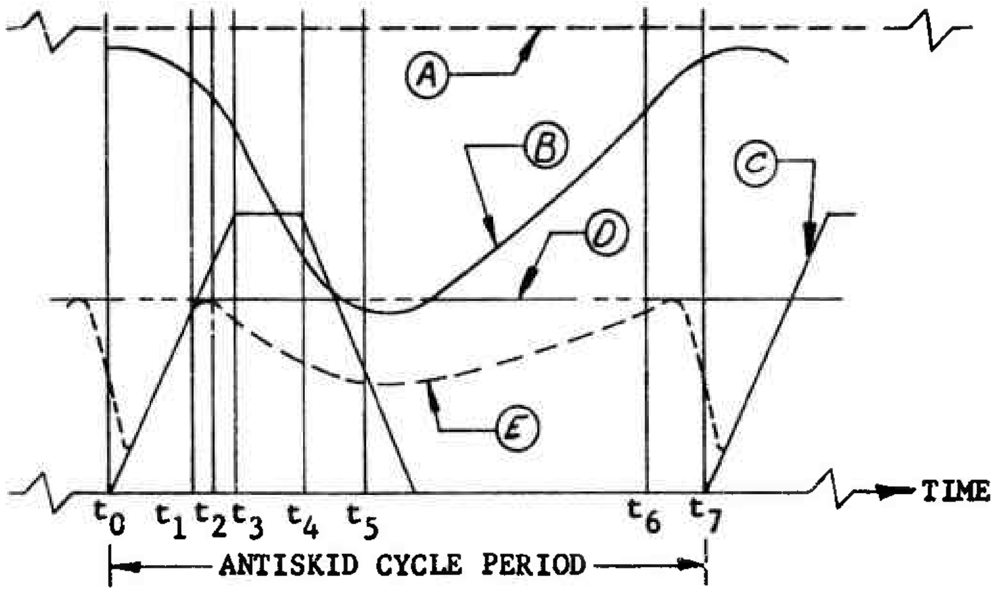

PARAMETERS

- Ⓐ Wheel synchronous angular velocity $\dot{X}_A/Re$
- Ⓑ Wheel angular velocity $\dot{\theta}_W$
- Ⓒ Applied brake torque T_B
- Ⓓ Maximum available friction torque μ max
- Ⓔ Achieved friction torque = μF_{GR}

EVENTS

t_0 - Instant brake application is initiated

t_1 - Instant when applied brake torque equals maximum available friction torque

t_2 - Instant of incipient skid detection, i.e., wheel slippage or slippage rate becomes equal to skid detection threshold

t_3 - Instant brake torque increase ceases (either because of brake torque reaching its applied value or because of skid control action preceding torque reduction)

t_4 - Instant brake torque reduction is initiated

t_5 - Instant brake torque equals friction torque and wheel negative acceleration ceases

t_6 - Instant wheel angular velocity has regained the required portion of its initial value (value at t_2) to cause initiation of brake reapplication, i.e., skid recovery signal threshold

t_7 - Instant brake application is initiated for next antiskid cycle

Figure 6 Antiskid Cycle Events

friction torque until the maximum available friction torque is achieved at t_1. Brake torque increase rate is controlled by the brake, brake actuation control system (hydraulic flow restriction) and skid control system characteristics.

t_1-t_2 Brake torque continues to increase producing increasing negative wheel acceleration into the unstable region of the brake force - tire slippage characteristic until wheel slippage or slippage increase rate reaches the skid-detection threshold.

t_2-t_3-t_4 Brake torque increase continues until it is terminated by either (a) the torque reaching the value commanded or (b) skid control system terminates the torque increase in preparation for torque reduction. Friction torque and wheel speed continue to decrease (total interval may be called skid control reaction time).

t_4-t_5 Brake torque decreases at a rate controlled by the brake, brake actuation system and antiskid control characteristics. Friction torque continues to decrease as wheel slippage increases. Wheel speed decreases to its minimum value.

t_5-t_6 Brake torque decreases until it becomes zero or until antiskid control system initiates brake torque increase. Wheel speed increases from its minimum value to an amount required to initiate brake torque increase (skid recovery signal).

t_6-t_7 Reaction time of the brake, brake actuation system and antiskid system between skid recovery signal and initiation of brake torque increase.

Figure 6 provides a graphic means for examining and evaluating the two most significant effects of antiskid cycling - the average braking force achieved (wheel braking system effectiveness) and the characteristics of dynamic forces being applied to the wheel supporting structure. From Figure 6 it can be seen that: the fundamental frequency of applied dynamic loading is established by the antiskid cyclic period (i.e., time interval t_0 -t_7), and assuming constant aircraft velocity during the cycle, the average braking force achieved is proportional to the area under the curve of friction torque versus time divided by the cyclic period.

The dynamic loading and average achieved brake force are not independent of each other but rather have a very complex interrelationship influenced by antiskid component and other brake system equipment characteristics.

An examination of Figure 6 considering the parameters shown and the effects of their variation with respect to evaluating braking system performance reveals that braking effectiveness is increased by: (a) moderate rates of brake torque increase, (b) high rates of brake torque decrease, (c) lower values of wheel slippage or rate of wheel slippage increase for skid detection threshold, (d) short antiskid system reaction time, (e) smaller amounts of excess applied brake torque and (f) least possible fraction of initial cycle velocity for skid recovery signal. Since most of the above tend to diminish the cyclic period, increased antiskid performance usually results in higher cyclic frequency potential.

Some particularly important aspects of antiskid operation are exemplified by Figure 7 which shows a comparison of the characteristic variation in braked wheel speed and braking force (friction torque) throughout an antiskid cycle for two extreme circumstances:

(a) An instance where the applied brake torque is a very large percentage greater than the available friction torque and the available friction torque is low, and

(b) An instance where the applied brake torque is a small percentage greater than the available friction torque and the available friction torque is high.

For both cases the interval between points ② and ③ is the time consumed by the required antiskid control circuit and antiskid valve actions, the interval between points ③ and ④ is the time required for sufficient fluid flow from the brake cylinders to cause brake torque reduction by an amount such that equality between brake torque and friction torque is achieved, the interval between points ④ and ⑤ is the time required for wheel spinup sufficiently to produce a skid recovery signal, the interval between points ⑤ and ⑥ is the time required for the antiskid control circuit and antiskid valve actions plus an interval required for sufficient fluid to flow such that the brake discs make contact if the brake was previously released to a degree for disc clearance to exist, and the interval between

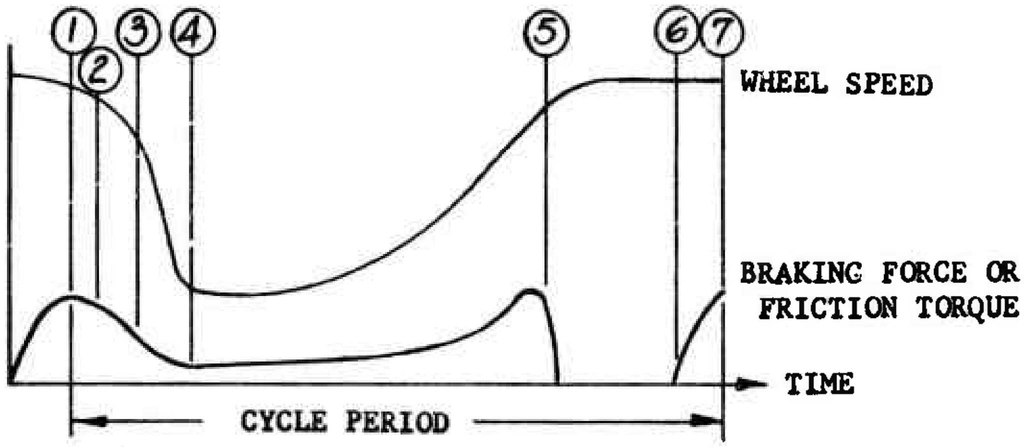

CASE (A): HIGH BRAKE TORQUE - LOW AVAILABLE FRICTION TORQUE

(1) Brake torque application to an amount equal to instantaneous available friction torque
(2) Skid detection
(3) Brake torque reduction initiated
(4) Brake torque reduced sufficiently to allow wheel decel to cease and wheel accel to begin
(5) Skid recovery signal - brake reapplication initiated
(6) Brake torque increase starts
(7) Brake reapplication to an amount equal to instantaneous available friction torque

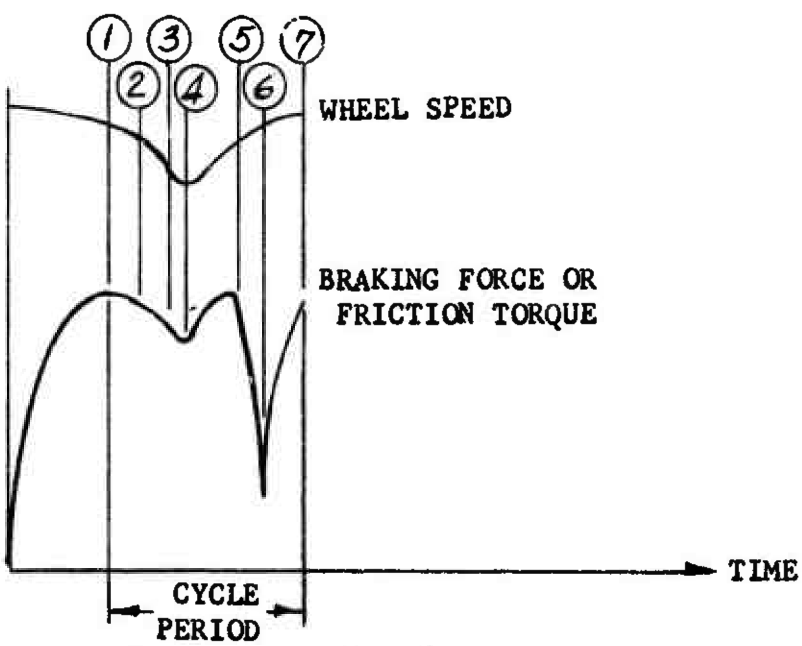

CASE (B): HIGH BRAKE TORQUE - HIGH AVAILABLE FRICTION TORQUE

Figure 7 Comparison of Antiskid Cycle Conditions

points (6) and (7) is the time for sufficient fluid flow to the brake for causing brake torque increase by an amount such that equality between brake torque and friction torque is again achieved.

It should be noted that the time interval between points (2) and (3) is approximately the same for both cases because the control circuit and antiskid valve consume about the same amount of operating time for any circumstance requiring brake pressure reduction. Since for case (a) the wheel has a much higher deceleration rate and a greater pressure reduction must be accomplished to prevent skidding with resultant greater time being consumed for removing fluid from the brake, the amount of wheel speed departure into the unstable slippage region is much greater. These factors along with the slower wheel spinup rate resulting from low available friction torque causes brake pressure reduction to be sustained for a longer time interval during which brake fluid volume usually decreases to an extent where clearance is produced between the friction surfaces. Upon brake reapplication a greater time interval is then required for replenishing the brake fluid volume to produce brake torque. The overall resultant effect is that the cyclic period for case (a) is greater than for case (b) and the average braking force achieved for case (a) is a smaller fraction of the maximum braking force produced than for case (b). Therefore, a major consequence of antiskid cycling is the trend toward reducing the achievable fraction of the instantaneous peak available braking force for conditions of low braking force potential (i.e., intensify the degradation of braking system effectiveness for conditions of reduced brake force potential). This inherent characteristic is unavoidable whenever any relatively "fixed time" elements are part of the control loop. The degree of degradation in braking system effectiveness is increased for larger amounts of excessive brake torque. This effect can be minimized if upon brake application the brake torque is reduced to more closely match the available friction torque. Modern "modulated" antiskid systems accomplish reduction of subsequent brake torque reapplication by using a servo type pressure regulating valve and providing a relatively slowly varying bias signal to the valve drive amplifier.

From the preceding discussion it can be established that the primary objectives of any brake control/antiskid system capable of achieving improved performance are: (1) to minimize the occurrence of antiskid cycles and (2) to minimize the amount of wheel speed departure into the unstable slippage region for cases where

cycling does occur. The degree to which these objectives are accomplished while permitting wheel brake application so as to achieve a large fraction of the potentially available friction force is a measure of the system's relative acceptability.

To accomplish its purpose an antiskid brake control system must function to cause a braked wheel's motion to be such that the relative velocity between the tire footprint and the ground is minimized for as much of the time as possible. An examination of the factors influencing tire footprint relative velocity reveals that the relative velocity between the tire footprint and the ground is equal to the horizontal velocity of the axle plus the horizontal velocity of the footprint relative to the axle, and that the horizontal velocity of the tire footprint relative to the axle is established by the rate of tire tread circumferential and radial displacement relative to the wheel and the wheel's angular velocity relative to the axle. At any instant all these velocity components are established by the relative distribution of elastic, thermal and kinetic energy resulting from the cumulative effects of the externally applied forces which have acted upon the tire-wheel assembly since spin-up and brake application.

As shown on Figure 3 the externally applied forces acting upon the tire-wheel assembly are the horizontal and vertical force components between the wheel and the axle, the brake torque, the radial force between the tire footprint and the ground and the horizontal friction force between the footprint and the ground. The runway profile along with the individual and collective elastic and inertia properties of the tire, wheel, supporting structure and vehicle influence the amount and nature of variations in radial ground force acting upon the tire-wheel assembly. The horizontal friction force acting upon the tire-wheel assembly is the product of the tire-to-ground radial force and the friction coefficient which in turn is affected by tire tread material elastic and strength properties as influenced by temperature and prior exposure to thermal and other environmental conditions, the nature and quantity of any contaminating substances, tire inflation pressure and footprint shape, and runway surface texture in addition to tire footprint relative velocity.

When braking system operation is examined within the context of the total vehicle system it is evident that the antiskid control elements must continually adjust brake torque in an attempt to achieve consonance with the other forces acting upon the tire wheel assembly. Since the forces acting upon the tire-wheel assembly are usually quite large compared to tire and wheel inertia, the antiskid system must accomplish brake torque

adjustment very rapidly. Figure 8 shows an oscillograph trace of axle vertical force component and brake torque recorded during landing of an F-111A aircraft on the main runway at Edwards AFB, California under dry conditions. This information was recorded for reasons other than antiskid system evaluation; however, it shows how axle vertical load variations resulting from airplane bouncing triggers antiskid operation as evidenced by brake torque varying in an attempt to follow the braking force potential. The higher frequency component of brake torque oscillation, at approximately 8 HZ, is caused by antiskid operation. It can be observed that each instance of large brake torque reduction corresponds with an instance of reduced axle vertical force. For this stop the pilot applied constant maximum braking during the interval shown. For any type airplane with any type antiskid system, antiskid cycling triggered by a sudden reduction in braking force potential incurred by either changes in tire-to-runway friction coefficient or by changes in radial wheel load can be expected to occur whenever the brake is applied with sufficient intensity.

As previously stated, the frequency and magnitude of the oscillatory braking force produced by antiskid cycling is not independent of braking system effectiveness. To achieve reasonably good braking performance under most conditions an antiskid brake control system should have approximately 10 HZ or greater cyclic frequency potential. Unfortunately, for many (perhaps most) airplanes 10 HZ is very near or above the landing gear fore and aft first mode natural frequency. Provisions must therefore be included within the brake control system to restrict the brake force oscillatory magnitude and/or cyclic frequency in a manner so that structurally damaging load magnification is prevented.

Figure 7 showed that the natural tendency is for the larger magnitude brake force oscillations to have a higher frequency than that for smaller magnitude oscillations. Since most of the antiskid system characteristics which promote achievement of improved braking performance for low braking force potential conditions such as wet runways, also produce higher antiskid cyclic rate potential, any steps taken to enhance braking performance for slippery conditions must be very carefully evaluated with respect to their effects upon dynamic loading whenever circumstances of high brake force potential are encountered. Therefore, the dominant consideration when evaluating total braking system compatibility is assuring that the antiskid induced oscillatory braking force does not have a combination of amplitude and frequency which is structurally detrimental under any condition of airplane usage. It is most often necessary to sacrifice braking system performance under some circumstances to achieve such compatibility.

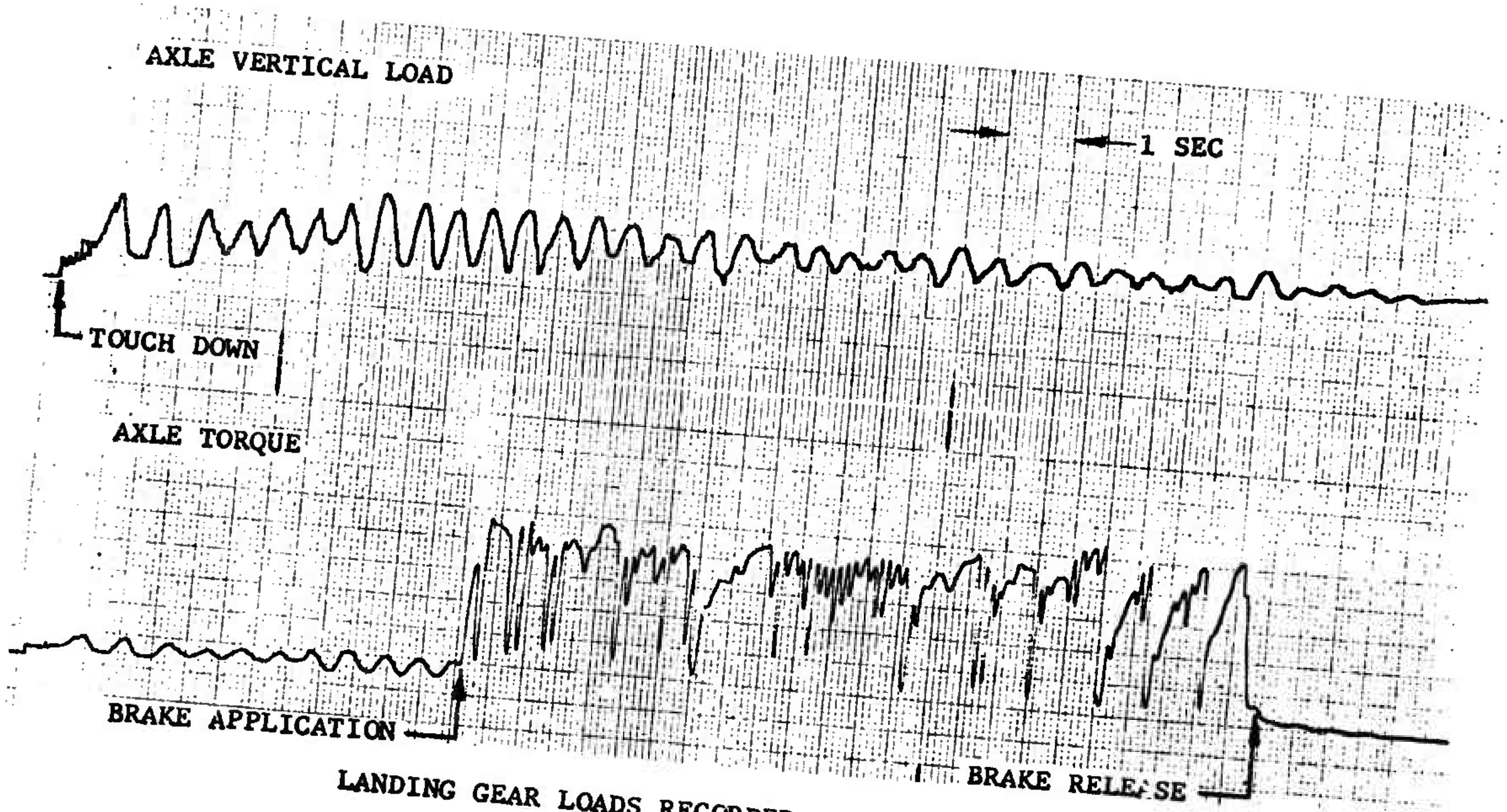

LANDING GEAR LOADS RECORDED ON F-111A NO. 12
FLT NO. 62 LANDING

Figure 8 Aircraft Landing Gear Vertical and Horizontal Loads

Antiskid system evaluation is usually performed during the initial design or system development phase for most new aircraft to assure stopping performance objectives can be achieved and to verify no adverse dynamic loading will be produced. These evaluations may be analytical, experimental or a combination of both and most often are performed as laboratory dynamometer tests, hybrid hardware-analog computer analyses and aircraft taxi tests. The analytical evaluation is usually accomplished by utilizing a setup composed of hardware representative of the aircraft components interfaced with an electronic analog computer. The computer is used to solve mathematical equations describing such parameters as aircraft motion, landing gear motion, tire and wheel motion, tire-to-runway friction, aerodynamic forces and brake torque. The actual behavior of a laboratory setup including such components as antiskid electronic circuitry, the brake, hydraulic control valves and interconnecting lines or other devices is measured by suitable instrumentation and fed into the computer to obtain a composite solution. This analysis procedure is used because a complete mathematical computer setup may be considered too expensive or because accurate mathematical descriptions for some components such as the electronic antiskid control circuit are not available. If any actual hardware is used in the computer setup, the analysis must be performed "real time".

While these hybrid hardware-computer analyses serve many useful purposes, several analytical limitations are incurred with a "real time" solution. Some of these analytical limitations are: (a) some significant parameters such as brake torsional displacement, tire circumferential displacement with respect to the wheel and unsprung mass position (position of the wheel, brake and axle suspended between springs representing the tire and shock absorber strut) have very high rates of vibration making their observation and interpretation very difficult. This same problem is encountered when attempting to interpret antiskid operation as recorded during vehicle testing, (b) if actual hardware is used as a part of the computer solution the effects of component characteristic variations cannot be evaluated unless such variations are physically produced. The large expenditure of time and money required to accomplish such evaluation is usually prohibitive, (c) the instrumentation used to interface the hardware with the computer introduces additional variables to an otherwise very complex system.

The above analytical difficulties can be overcome or significantly reduced by employing an all-mathematical approach and operating the analog computer at a reduced time scale or by

using a digital computer. As can be determined from the work accomplished under Contract F33615-70-C-1004 and described in AFFDL-TR-70-128, a major difficulty encountered with the all mathematical analysis approach is the large number and complexity of the mathematical operations result in relatively large computation expense. A part of the analytical refinement accomplished during this program has been directed toward reducing computation expense; however, with respect to total system analysis there are some relatively complex mathematical operations remaining. Depending upon particular circumstances and the type of problem to be solved, useful analytical results can be achieved either with an all-mathematical approach having various degrees of complexity or with the hybrid hardware-analog computer approach.

Laboratory dynamometer test evaluation of antiskid braking system operation provides a relatively low cost and very low risk means for examining many factors relative to system performance and compatibility. The dynamometer test results can be used to establish parameter values for analytical uses or to confirm analytical predictions. Even though dynamometer testing cannot be representative of aircraft operation in some respects, if properly conducted they will establish the limits of a particular equipment's capabilities and provide insight into how the equipment might be changed to achieve a more compatible system. A very advantageous aspect of dynamometer testing is that almost any conceivable parameter can be controlled or at least monitored with relative ease and a particular test can be duplicated if desired. Aircraft taxi or flight tests are needed to confirm that predicted brake system performance and compatibility are actually achieved. However, because of the great difficulties involved in controlling and/or measuring many parameters on an airplane and because of unacceptably high costs and/or high risks involved in producing a controlled demonstration under limiting conditions, it is not generally practical to consider aircraft testing as the only braking system evaluation technique.

Considering the previously described factors which influence antiskid operation whenever contemplating analysis of braking system effectiveness for use in establishing airplane stopping performance, it becomes evident that the random variation of such parameters as runway profile and tire-to-ground friction coefficient makes precise prediction of exact occurrences virtually impossible and impractical. However, since the random variations of many other factors such as brake application speed, wind direction and velocity, pilot brake system operating technique, and runway distance remaining from point of brake

application also significantly influence the relative success which will be achieved during an individual instance of brake system usage, it must be acknowledged that the relatively minor variations in antiskid operation from one instance to the next are not greatly significant. The primary benefits to be derived from analyzing antiskid effects upon airplane stopping performance are: to establish the relative capability of one aircraft type as compared to another for some defined runway condition, to evaluate the relative capabilities of one antiskid system type as compared to another on the same airplane, to evaluate the effects of possible variations in basic airplane configuration and landing gear characteristics upon braking system operation, and to establish braking system component performance requirements which are necessary for achieving some specified stopping performance for a particular aircraft type. By applying the antiskid evaluation techniques utilized during this program, answers may be provided for such questions as: Is it reasonable to expect that an airplane achieve the same stopping performance on any runway as might have been achieved during official performance demonstrations on the very smooth runway at Edwards AFB, California?, or Is it reasonable to expect the same level of braking system effectiveness from two different type airplanes equipped with the same type antiskid system if the airplanes differ with respect to tire size and landing gear elastic characteristics so as to affect the amount and frequency of load oscillation between the tire footprint and the ground? The answers to such questions can then provide the basis for judging braking system acceptability under particular circumstances and for establishing whether or not some change to the braking system equipment and/or some change in airplane operating procedures ought to be implemented.

Much of the preceeding discussion is recognized to be relatively common knowledge among those who routinely participate in the design, analysis and testing of aircraft braking systems. This discussion has been presented to establish the basis for parameters chosen for consideration and the rationale for the various analytical assumptions employed during this program. It is also hoped that by reviewing some of the fundamental aspects of antiskid operation, those who have not been previously exposed to the subject may be provided some insight into the problem and may thereby be able to achieve greater benefits from applying the antiskid analysis techniques.

D. PROBLEM DISCUSSION

A prior program, conducted under U.S. Air Force Contract F33615-70-C-1004 and administered by the Air Force Flight Dynamics Laboratory, resulted in development of an analysis procedure for predicting aircraft antiskid performance and total system compatibility. The results of this prior program are described in Report Number AFFDL-TR-70-128.

The analytical procedures consist of a complete mathematical description of the antiskid system components along with the airplane, other aircraft components and systems related to or influenced by antiskid operation, and the characteristics of the surface upon which the airplane is operating. The mathematical description includes such considerations as landing gear dynamic motion, tire elasticity, brake torque response, antiskid electronic circuitry, brake hydraulic control system dynamics, runway surface profile, and tire-to-runway friction characteristics. Both "On-Off" and "Modulated" antiskid systems are considered. Procedures for quantitative evaluation of the influencing parameters and examples of their usage are also presented. The mathematical description consists of analytical components as follows:

(1) Brake - Brake torque, hydraulic displacement and inlet flow rate are computed as functions of time considering applied brake pressure, relative velocity between the braking friction surfaces, axial elasticity, heat stack inertia, piston position and velocity, and the various friction coefficients (lining, torque tube and wheel splines, piston seals) as functions of velocity.

(2) Hydraulic System - Hydraulic pressure at the brake, at the antiskid valve inlet and outlet, and at the pilots metering valve is computed as a function of time considering pilot command, system supply pressure, compressibility and inertia of the actuation media, line flow resistance and elasticity, variable flow areas within the pilots metering valve and antiskid valve as functions of spool position, and volume of the various containment vessels (lines, valve bodies, brake housing).

(3) Airplane and Landing Gear - The position and velocity of the airplane and the landing gear elements with respect to the airplane are computed with respect to time considering forces from the wheel and brake, aerodynamic forces, runway profile, shock strut elasticity and damping, shock strut position, aircraft inertia, and control surface position.

(4) Wheel and Tire - The forces between the wheel-tire assembly and the airplane and between the wheel-tire assembly and the runway are computed with respect to time considering tire-to-runway friction coefficient as a function of relative velocity and runway surface condition including hydroplaning effects, tire radial and circumferential deformation and its rate, applied brake torque and axle velocity.

(5) Wheel Speed Sensor - Antiskid control circuit input signal is computed as a function of time considering wheel angular velocity and characteristics of the antiskid wheel speed sensor device.

(6) Antiskid Control Circuit - Antiskid valve voltage is computed as a function of time considering the input signal from the wheel speed sensor and the control circuit characteristics (the dynamic behavior of the various circuit elements is described).

(7) Antiskid Control Valve - Antiskid control valve spool position is computed as a function of time considering the applied valve voltage from the control circuit, first stage pressure response characteristics, and inlet, outlet and return port pressure.

(8) Control Surface Position - Horizontal tail position is computed as a function of time considering pilot command, stability augmentation system characteristics, and airplane pitch rate.

(9) Runway Surface Profile - Runway surface profile is defined as a function of the airplane's longitudinal displacement.

The analytical prediction procedure is implemented by combining the individual analytical components to obtain a total system composite solution. An electronic computer is used to produce a simultaneous solution of all mathematical equations. The mathematical descriptions previously developed with corrections and refinements resulting from work accomplished during this program are contained in Appendix A herein. To permit confident and useful employment of the analytical procedure a controlled physical demonstration to show its validity and to assure all significant parameters are included and properly accounted for should be performed, and simplification and refinement should be accomplished wherever possible to reduce complexity and consequent

computation expense. During the course of this program the second factor above became the major consideration in that only a very small fraction of the analytical effort planned could be accomplished.

As with the analysis of any physical phenomena the degree of complexity incurred with an analysis of antiskid operation is related to the degree of solution precision which is being attempted. At the onset of the analytical effort it was recognized that if any significant improvement in the analysis of antiskid compatibility was to be accomplished, some greater than usual analytical complexity would be required because the influence of such high frequency oscillations as brake squeal and tire tread circumferential displacement was to be accounted for. It was hoped that some way could be found to combine these complex analytical elements needed for compatibility evaluation with simpler analytical elements as are more appropriate for evaluating airplane stopping performance. Unfortunately, efforts expended toward accomplishing this goal have not produced very successful results. The following discussion describing various possible mathematical treatments of tire-to-ground friction illustrates the analytical dissonance between a procedure best suited for evaluating antiskid compatibility and a much less complex treatment suitable for airplane stopping performance evaluation.

A very important aspect of antiskid brake control system analysis is the mathematical treatment of the relationship between tire-to-runway friction force and the amount of tire-to-runway slippage. This mathematical treatment is influenced by budgetary considerations, computer setup and computer capabilities. For a real time analog computer setup the usual procedure is to define the friction coefficient between the tire and runway surface as a function of wheel slip ratio as shown in Figure 9(a). In this case, the amount of tire slippage is expressed as a fraction of the axles horizontal velocity. Figure 9(b) shows an alternate procedure where friction coefficient is expressed as a function of slip velocity. Figure 10 shows how these functions are used to compute the brake force and the brake force is then used in the computation of wheel slippage. Both of the above can give fairly good analytical results when evaluating braking system performance but do not produce computer operation which correlates very well with the effects of antiskid operation as recorded during vehicle tests.

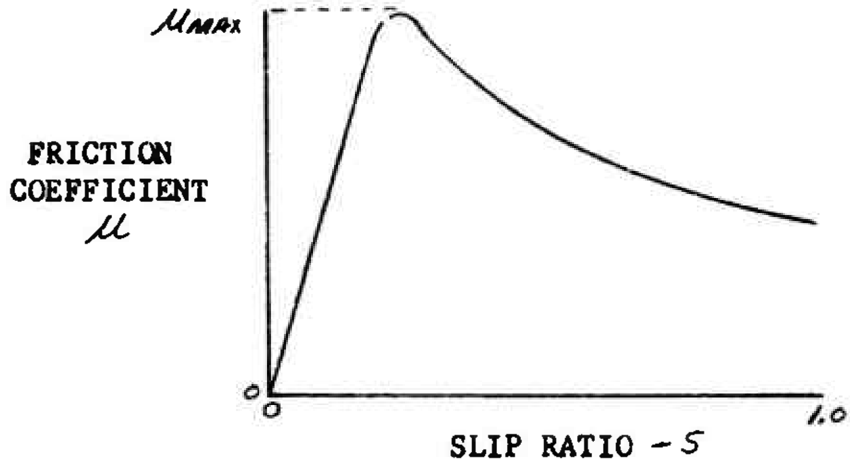

$S = 1 - \frac{\dot{\Theta}_W R_e}{\dot{X}_A}$

$\dot{\Theta}_W$ = TIRE ANGULAR VELOCITY

$\dot{X}_A$ = TRANSLATIONAL VELOCITY OF TIRE ROTATIONAL AXIS (AXLE) RELATIVE TO THE GROUND

R_e = TIRE UNBRAKED ROLLING RADIUS

(a) FRICTION COEFFICIENT - SLIP RATIO FUNCTION

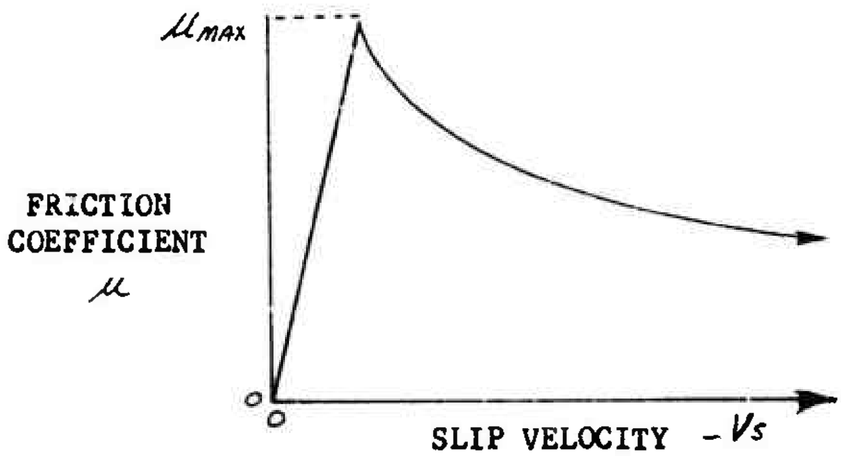

$V_S = \dot{X}_A - \dot{\Theta}_W R_e$

(b) FRICTION COEFFICIENT - SLIP VELOCITY FUNCTION

Figure 9 Tire Friction Coefficient Functions

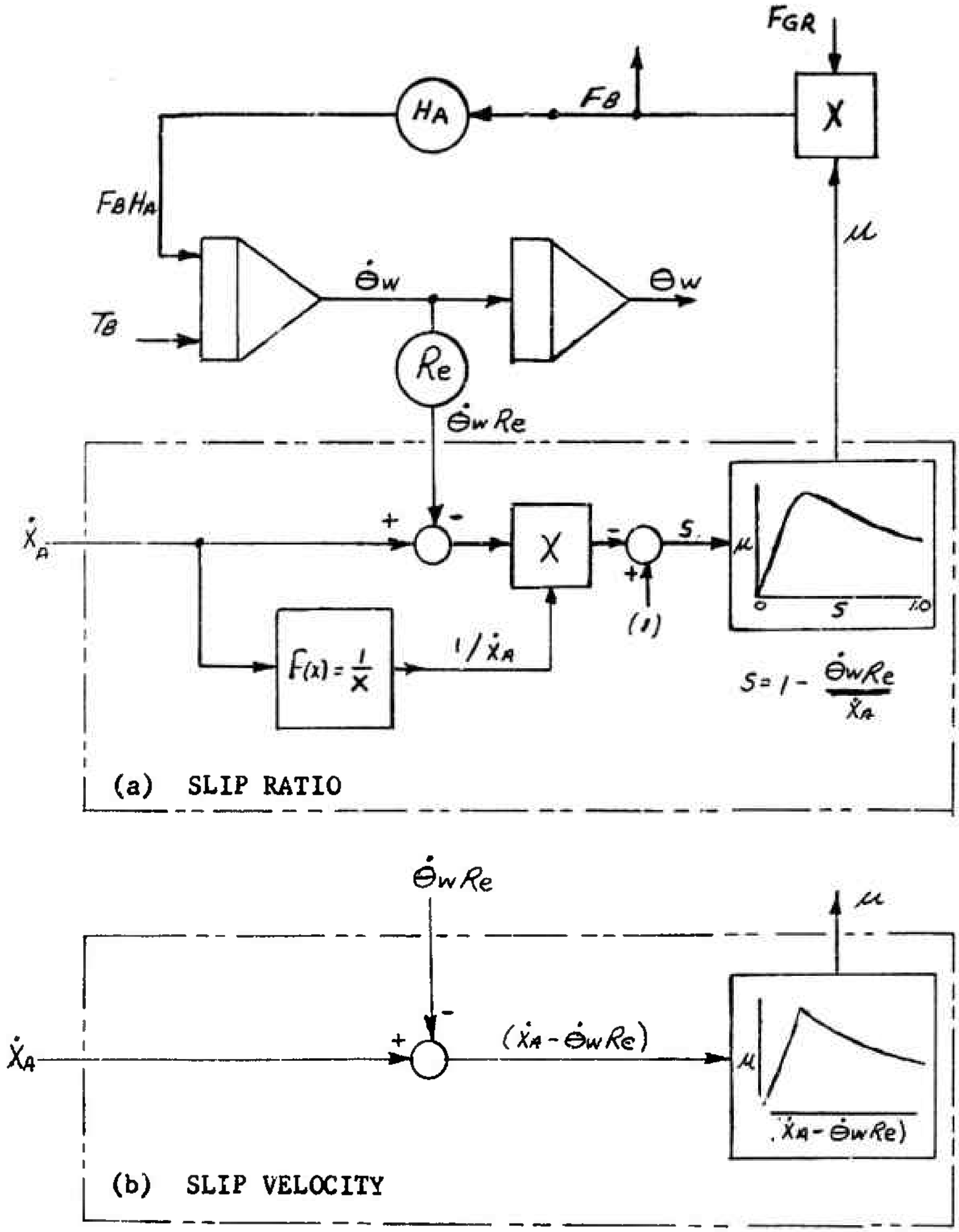

Figure 10 Tire Friction Computation

As described in Reference 17, a critical examination of the above mathematical treatment of the relationship between tire-to-runway friction force and tire-to-runway slippage will reveal that in the stable positive slope region of the friction force-slippage relationship the amount of apparent slippage is the result of the braking force and tire elastic deformation, not the cause of some value of friction coefficient being in existence, and that in the unstable negative slope region of the friction force-slippage relationship the amount of friction force decay is a function of the tire footprint actual slippage not some percentage of the axle velocity. Consequently, the characteristics of the friction coefficient-slip ratio function, if used, must be established relatively arbitrarily because of the very large variations which must be approximated over a wide range of conditions. It is not uncommon to set the initial slope of the friction coefficient-slip ratio function to be compatible with computer capabilities rather than attempt to simulate the tire elastic properties as would be more realistic.

Considering the above, using the analytical convenient slip ratio-friction coefficient technique cannot produce truly credible analytical results. Using the friction coefficient-slip velocity approach is capable of more believable analytical results if the function can be adequately defined. The mathematical treatment of the brake force-tire slippage phenomenon described in Appendix A herein better represents actual physical occurrences. This procedure is to account for the tire tread torsional and translational deformation relative to the wheel when computing footprint velocity relative to the runway. However, because of the tire treads' very high acceleration, a real time analog computer or relatively long integration time step digital computer solution is not practically achievable. Using the tire mathematical model described in Appendix A along with the definition of tire properties from Reference 1 allows the examination of such effects as tire size and inflation pressure upon braking system compatibility. These effects can be of considerable significance for the case of small high pressure tires.

There are other analytical elements such as brake torque computation and hydraulic valve operation where there are similar differences between the type of mathematical treatment which is best suited for compatibility analysis as compared with performance evaluation. It has been concluded that a single analysis procedure is not likely to ever be formulated which will be capable of general usage for all antiskid analysis tasks in an

economically feasible fashion. Accordingly, an alternate more simplified analysis procedure has been formulated. The analytical techniques of the simplified procedure are intended to be primarily used for performance evaluation. However, some compatibility aspects of antiskid operation can be analyzed.

SECTION II

VERIFICATION TESTING

The initial step toward verifying, correlating and refining the previously developed aircraft antiskid performance and total system compatibility analysis procedures was to conduct a controlled physical demonstration of total braking system operation. This demonstration consisted of a number of braked stops performed on a laboratory brake test dynamometer using a test set-up including an aircraft landing gear assembly to support the tire, wheel and brake, the brake actuation hydraulic system, and an antiskid system. During these braked stops various forces, hydraulic pressure and displacements describing the landing gear dynamic behavior, antiskid and hydraulic brake control systems' operation and braking performance were recorded so that this information could be compared with the corresponding information predicted by the analytical procedures for the same circumstances. The controlled demonstration was intended to show the effects upon braking performance and total system compatibility which result from varying such total system characteristics as:

(1) Hydraulic flow restriction at various points in the brake actuation system

(2) Tire radial and torsional stiffness

(3) Antiskid control characteristic

(4) Landing gear fore and aft natural frequency

(5) Tire-to-runway braking force potential.

A. TOTAL SYSTEM TEST INSTALLATION

The total system test installation consisted of:

(1) A support fixture equipped with a movable carriage simulating the aircraft landing gear attachment points. A carriage loading and control system was provided so that the landing gear could be landed on the 192 inch diameter flywheel of the inertia brake test dynamometer located in the AFFDL Landing Gear Test Facility, Building 31, Area B, Wright Patterson Air Force Base, Ohio.

(2) One F-111 main landing gear tire-wheel-brake assembly installed on the necessary F-111 landing gear structural components so as to complete an installation the same as that for the aircraft left main wheel.

(3) A mockup of the F-111 hydraulic brake actuation and control system including pilot's metering valve, accumulator, lines and fittings.

(4) An antiskid control system including wheel speed sensor, control circuit and antiskid valve.

(5) Instrumentation equipment as required to measure and record dynamometer flywheel speed and distance, braked wheel speed, hydraulic pressure at the brake and at the antiskid valve inlet, brake torque, radial and tangential forces between the tire and dynamometer flywheel, and electrical signal at the antiskid control valve. The instrumentation consisted of:

(a) Electrical resistance strain gage pressure transducers with appropriate excitation power supply and resistance measuring electronic circuitry (CEC System D) to measure hydraulic pressure at the brake and at the antiskid valve inlet. The accuracy of the pressure measurements was within $\pm$ 25 psig.

(b) The output from the antiskid wheel speed sensor (a D.C. tachometer) was used to measure braked wheel speed. The speed was determined within 2 percent by using the tachometer calibration curve and an electronic D.C. voltmeter (same as described in (e) for antiskid valve electrical signal).

(c) A light beam type electronic pulse generator and 200 hole perforated disc with appropriate electronic circuitry was used to measure dynamometer flywheel speed and distance. Distance measurement within $\pm$ .25 ft. and velocity measurement within $\pm$ 1.5 miles per hour was accomplished with an electronic counter and by the oscillograph.

(d) Electrical resistance strain gages installed on the axle were used to measure the radial and tangential forces between the tire and dynamometer flywheel and brake torque. CEC System D excitation power supply

and resistance measuring electronic circuitry were used for strain gage output recording. The axle was calibrated using a calibration fixture previously used for flight test load calibration.

(e) An electronic D.C. voltmeter was used to measure the electrical signal at the antiskid control valve. This voltmeter is the oscillograph galvanometer with appropriate shunt. Voltage measurement was within $\pm$ .5 volts.

Outputs from these measuring devices were recorded with respect to time on a CEC direct writing oscillograph and on magnetic tape.

Instrumentation calibration was accomplished by accepted laboratory practice with respect to standards traceable to the National Bureau of Standards.

During the course of the testing alternate equipment items such as different size tires, different antiskid control circuits and different hydraulic flow restrictors were assembled into the total system installation as appropriate to produce the desired overall system configuration for individual test conditions. The total system test installation is shown on Figures 11, 12, 13, 14, 15 and 16. Figure 17 shows two views of the 192 inch diameter inertia brake test dynamometer located in the AFFDL Landing Gear Test Facility prior to installation of the total system test support fixture. These two views correspond to those shown on Figure 11 and Figure 12 after the total system test support fixture was installed.

The total system test support fixture was designed and fabricated at the Fort Worth Operation of General Dynamics Convair Aerospace Division in Fort Worth, Texas. After assembly the support fixture was structurally proof tested at Fort Worth, Texas and then disassembled, shipped to Wright-Patterson Air Force Base, Ohio and installed in the AFFDL Landing Gear Test Facility. The support fixture has 28.0 inches carriage stroke and will accommodate a landing gear having up to 50.0 inches tire diameter. The movable carriage weighs approximately 15000 pounds and with the initially installed size actuator powered by the existing 1500 psi hydraulic system test loadings over the range of 0 - 30,000 pounds applied radially on the dynamometer flywheel can be accomplished. The support fixture structural capacity is 50,000 pounds and by increasing the size or number of load actuators or by increasing the capacity of the

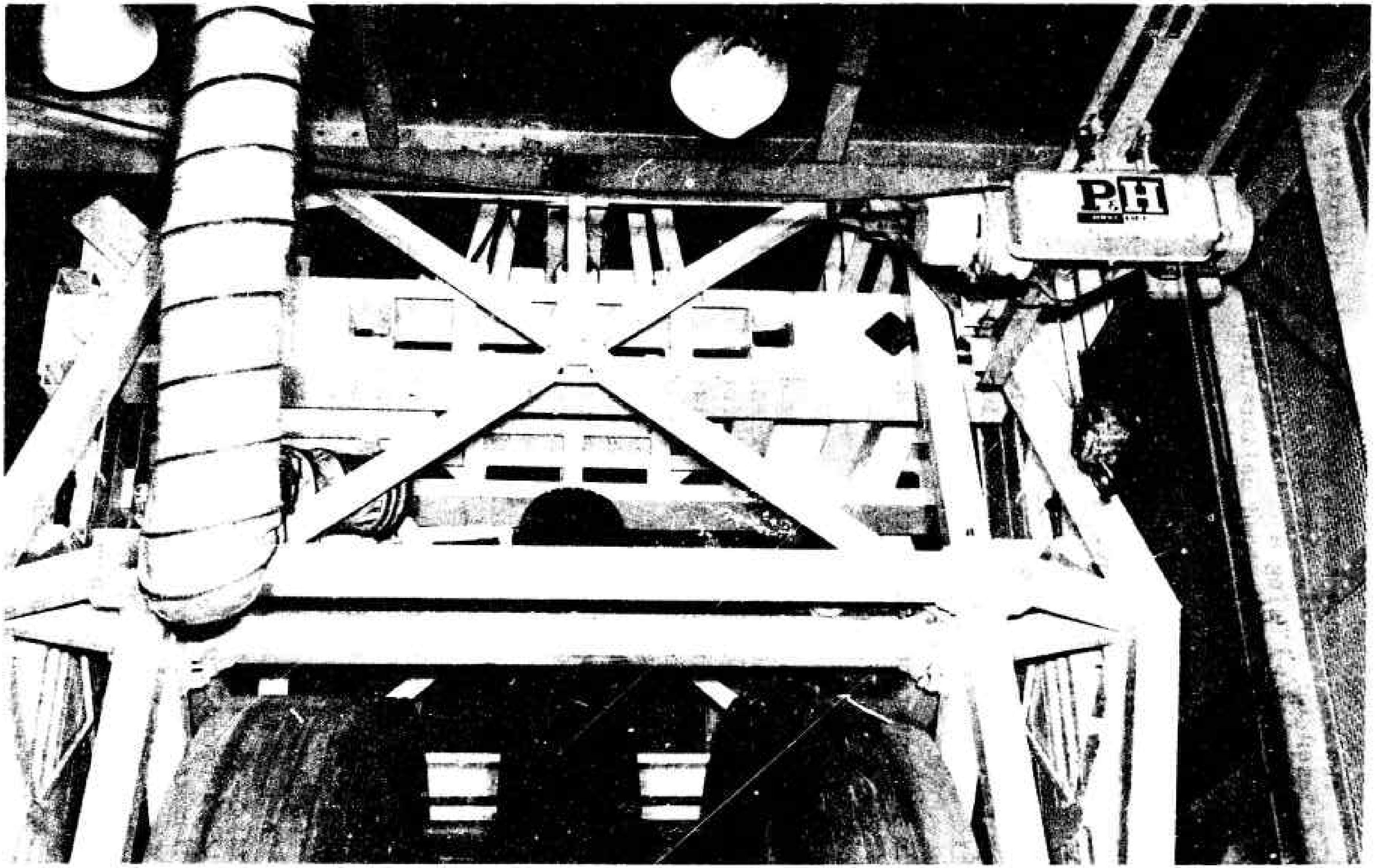

Figure 11 Total System Test Installation - Landing Gear and Support Fixture Viewed Looking North Inside Dynamometer Cage

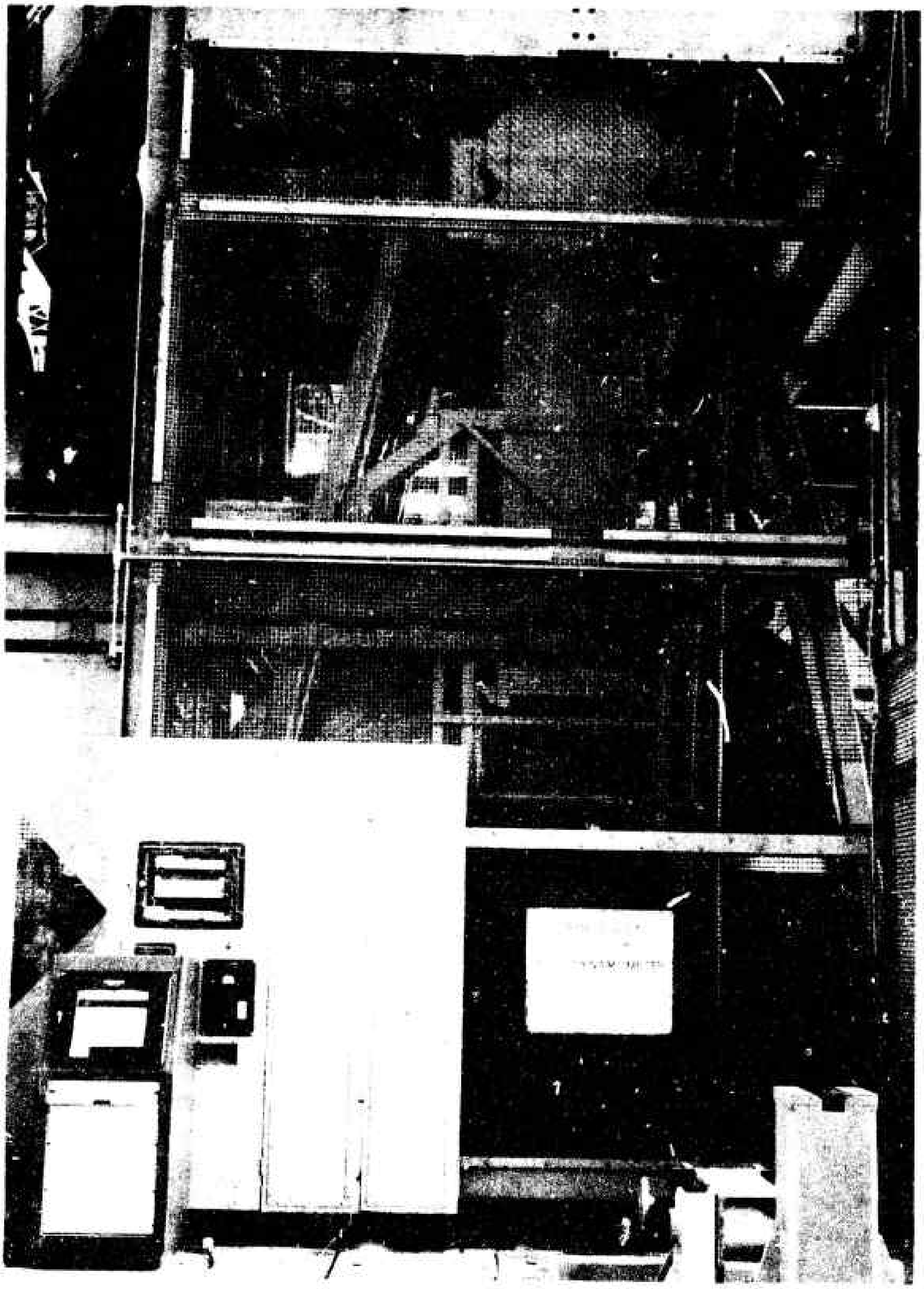

Figure 12   Total System Test Installation Support Fixture Viewed Looking East from Outside Dynamometer Cage

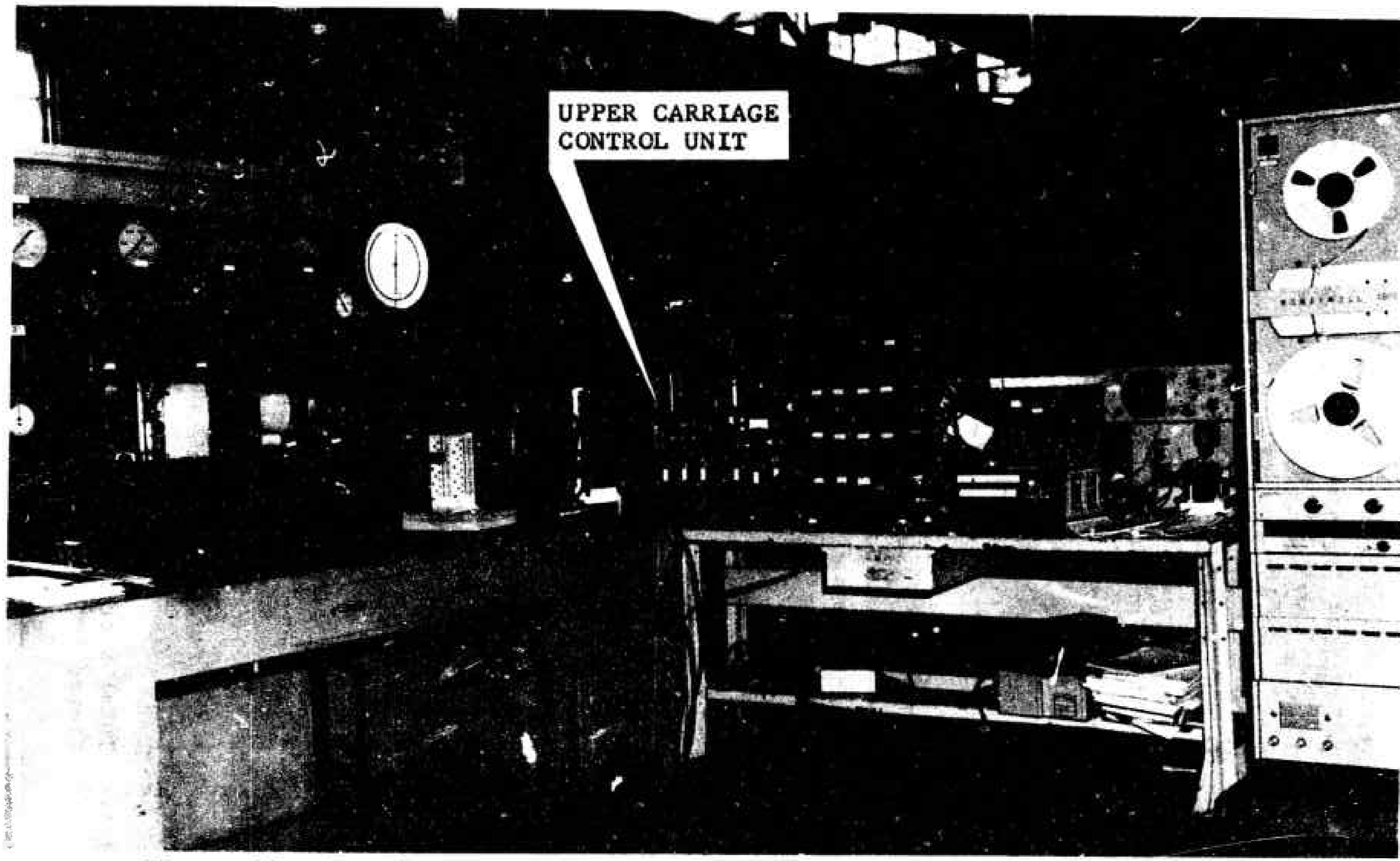

Figure 13 Total System Test Installation - Dynamometer Control Console, Upper Carriage Control Unit and Data Recording Equipment

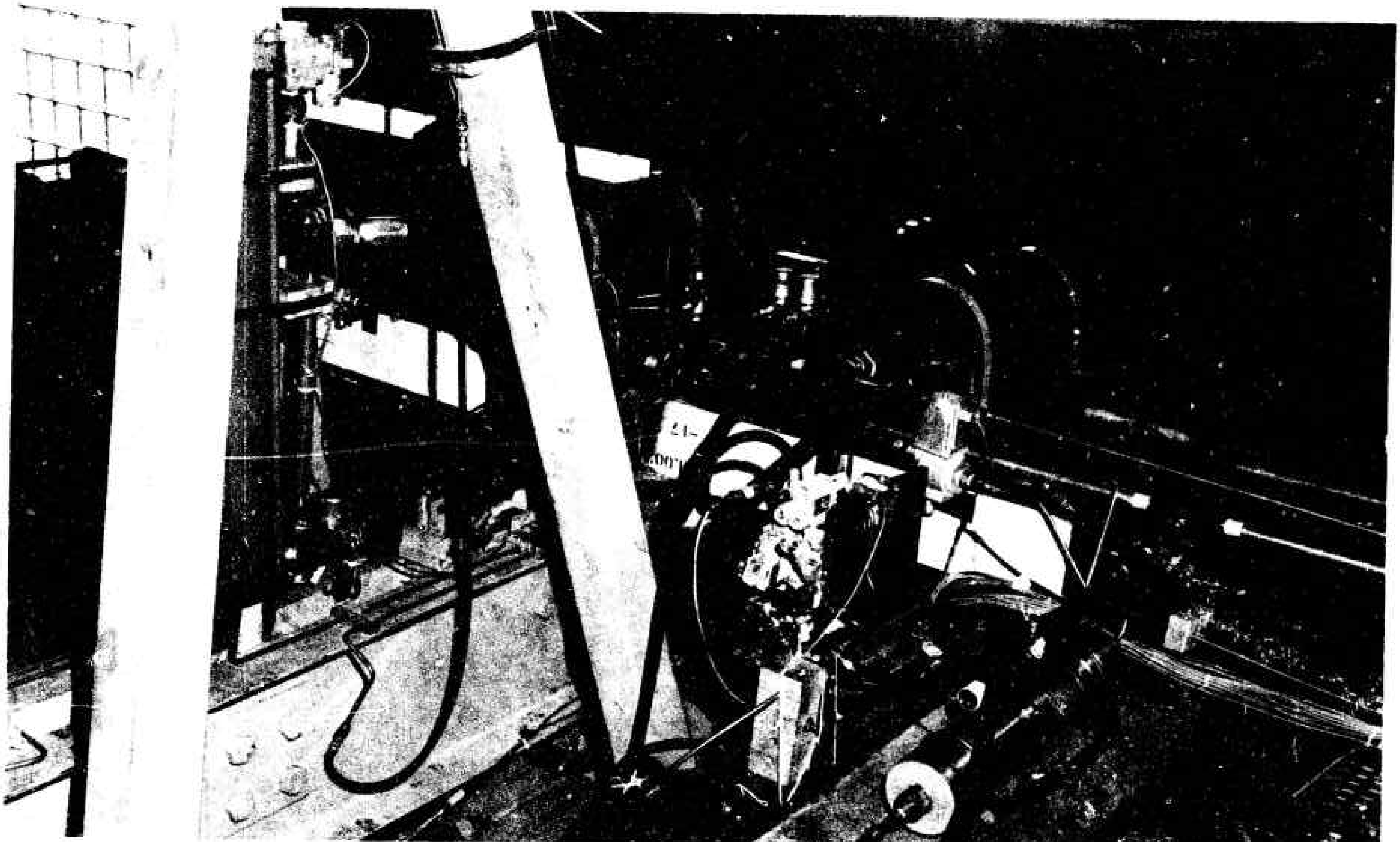

Figure 14 Total System Test Installation - Aircraft Brake Metering Valve and Accumulator with Upper Carriage Loading System Components Viewed from Top of Dynamometer Cage

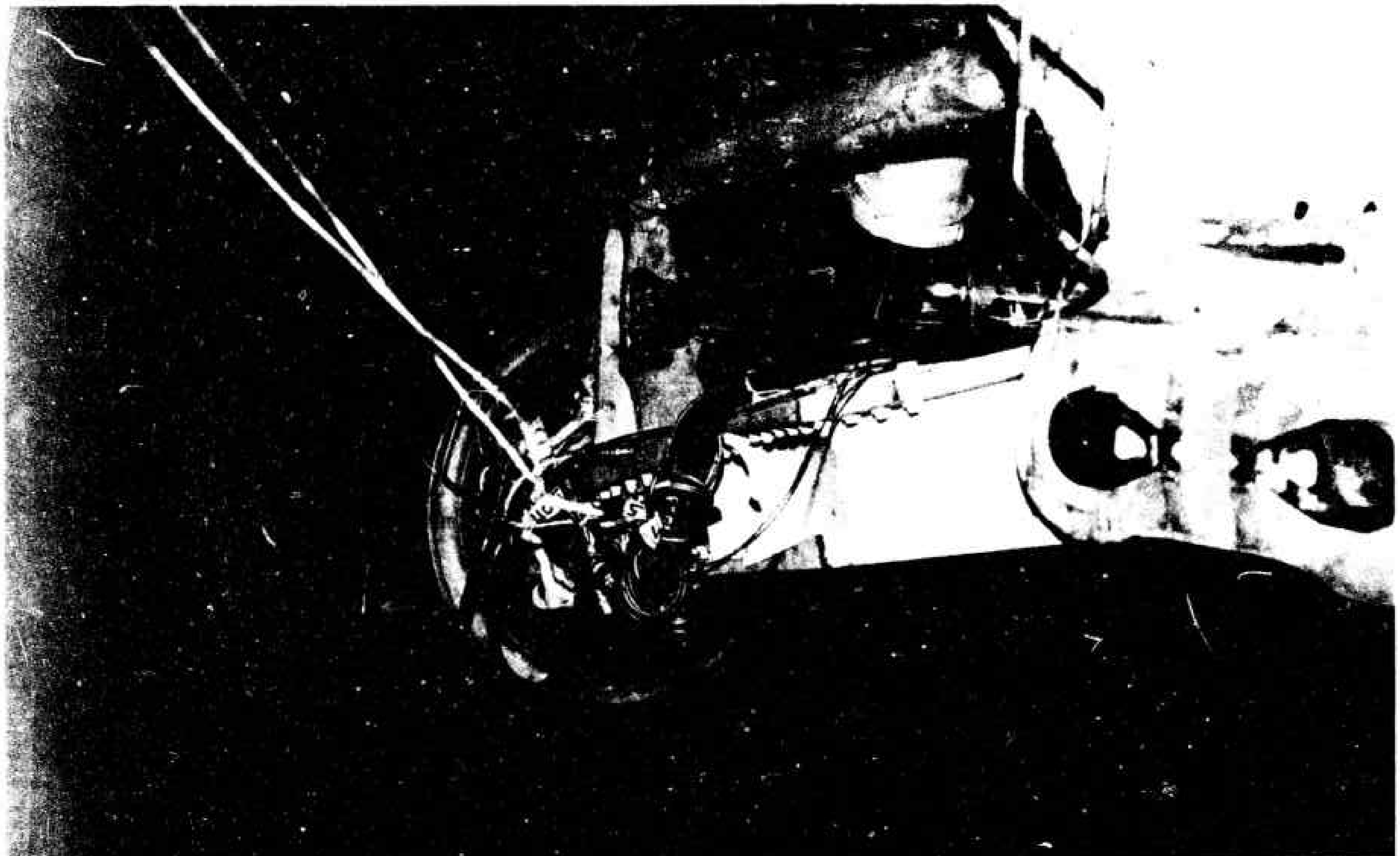

Figure 15 Total System Test Installation - F-111 Main Landing Gear Left Wheel Installed Over Dynamometer Flywheel - Viewed Looking Outboard and Forward

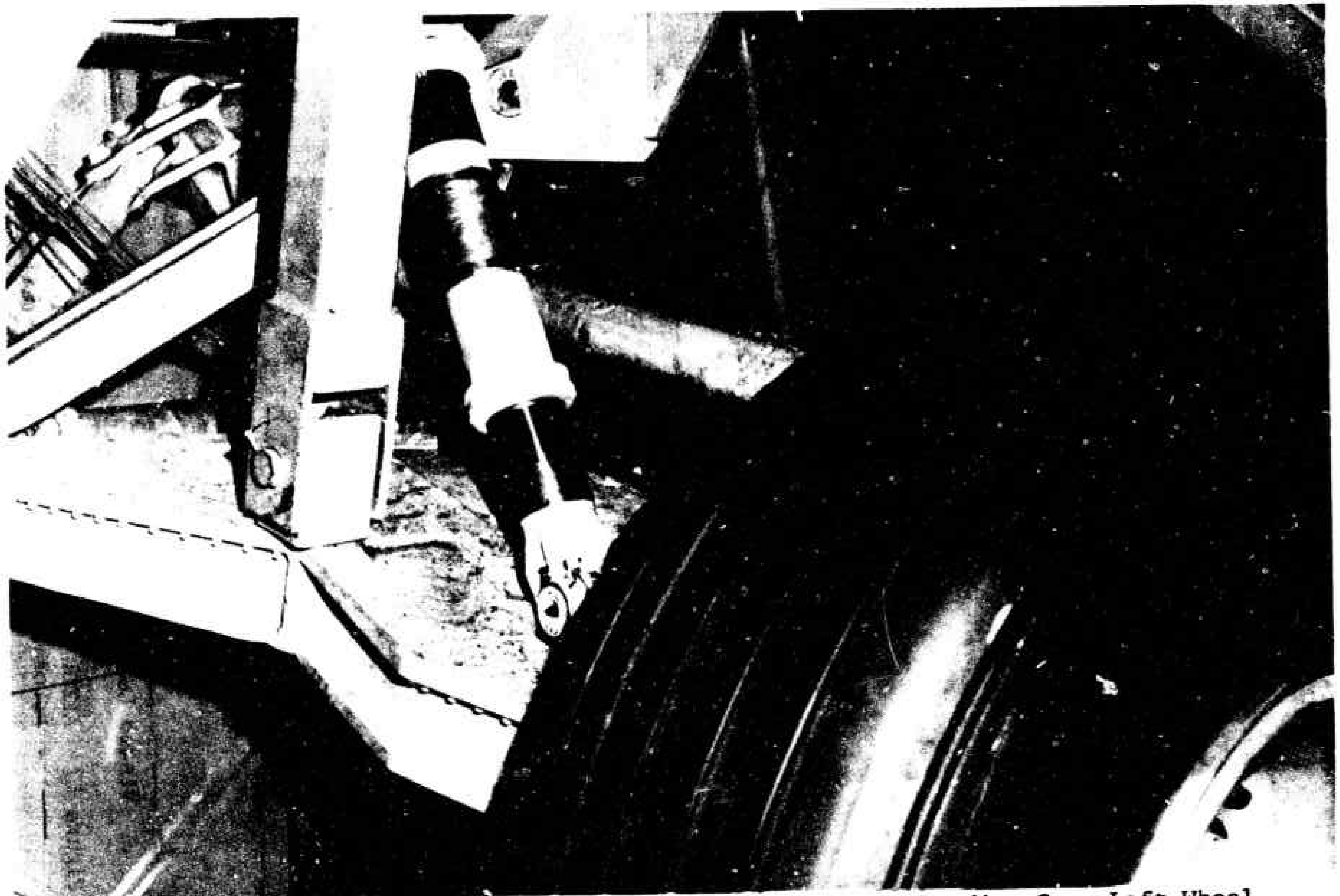

Figure 16 Total System Test Installation - F-111 Main Landing Gear Left Wheel Installed Over Dynamometer Flywheel - Viewed Looking Inboard and Aft

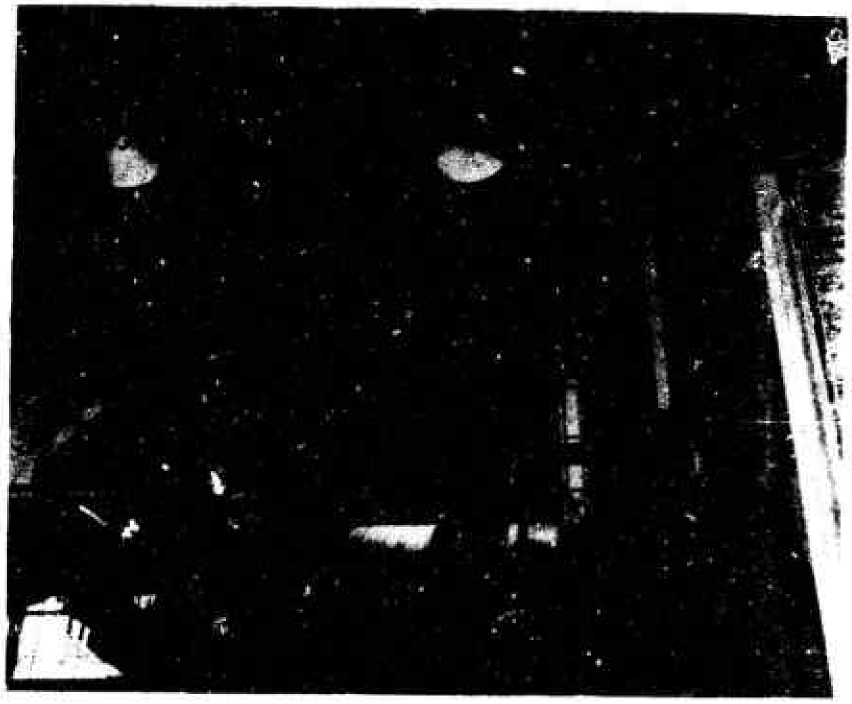

Viewed Looking North From Inside of Cage

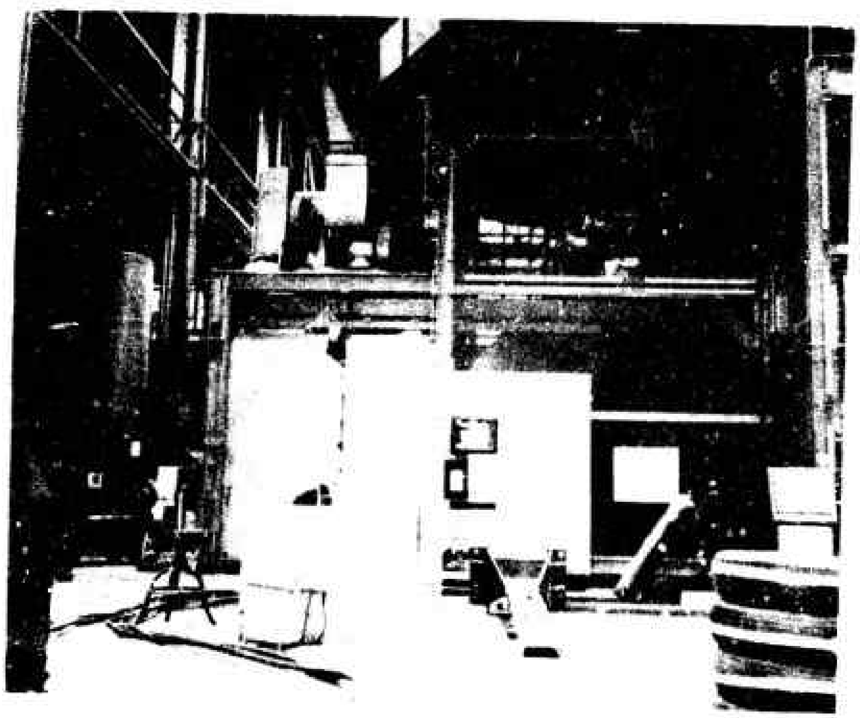

Viewed Looking East From Outside of Cage

Figure 17 AFFDL 192 Inch Diameter Brake Test Dynamometer Prior to Total System Test Installation

existing hydraulic system test loadings up to 50,000 pounds can be accomplished. Figure 18 shows the support fixture while being subjected to proof loading for the side load design condition and Figure 19 shows the fixture set up to apply proof loading for the landing design condition. Because the support fixture is not structurally symmetrical for loading applied in the plane of the flywheel, both landing and braking design proof loads were applied in each direction (i.e., as installed, horizontal loads acting both North and South). Because of support fixture symmetry in the plane of the flywheel shaft, proof loading for the side load condition was applied in the direction of horizontal load acting West only. The proof loadings applied are: for the landing design condition, 142,000 pounds (1.5 times the resultant of 75,000 pounds vertical combined with 57,750 pounds horizontal in a plane 19.0 inches above the flywheel), for the braking design condition 117,000 pounds (1.5 times the resultant of 50,000 pounds vertical combined with 60,000 pound horizontal in a plane tangent to the flywheel), and for the side load design condition (drift landing) 144,000 pounds which is 1.5 times the resultant of 75,000 pounds vertical combined with 60,000 pounds horizontal and in a plane tangent to the flywheel.

The support fixture carriage loading and control system consists of an electrohydraulic servo actuator in combination with a solid state electronic amplifier/comparator unit. The test fixture control unit as shown in Figure 13 allows the operator to lock or unlock the overhead carriage, command landing or unlanding, control the amount of landing load applied, apply or release the brake, bleed the carriage load hydraulic equipment and implement emergency unlanding.

B. TEST CONDITIONS AND PROCEDURES

The testing was accomplished by performing braked stops with a combination of different equipment configurations and different applied loading as listed in Table 1. The various equipment configurations listed are:

(1) Antiskid System - The antiskid systems used during the tests consisted of a production F-111 wheel speed sensor (Goodyear Part Number 9542613) and antiskid control valve (Goodyear Part Number 9550255) connected with one of the following antiskid control circuits:

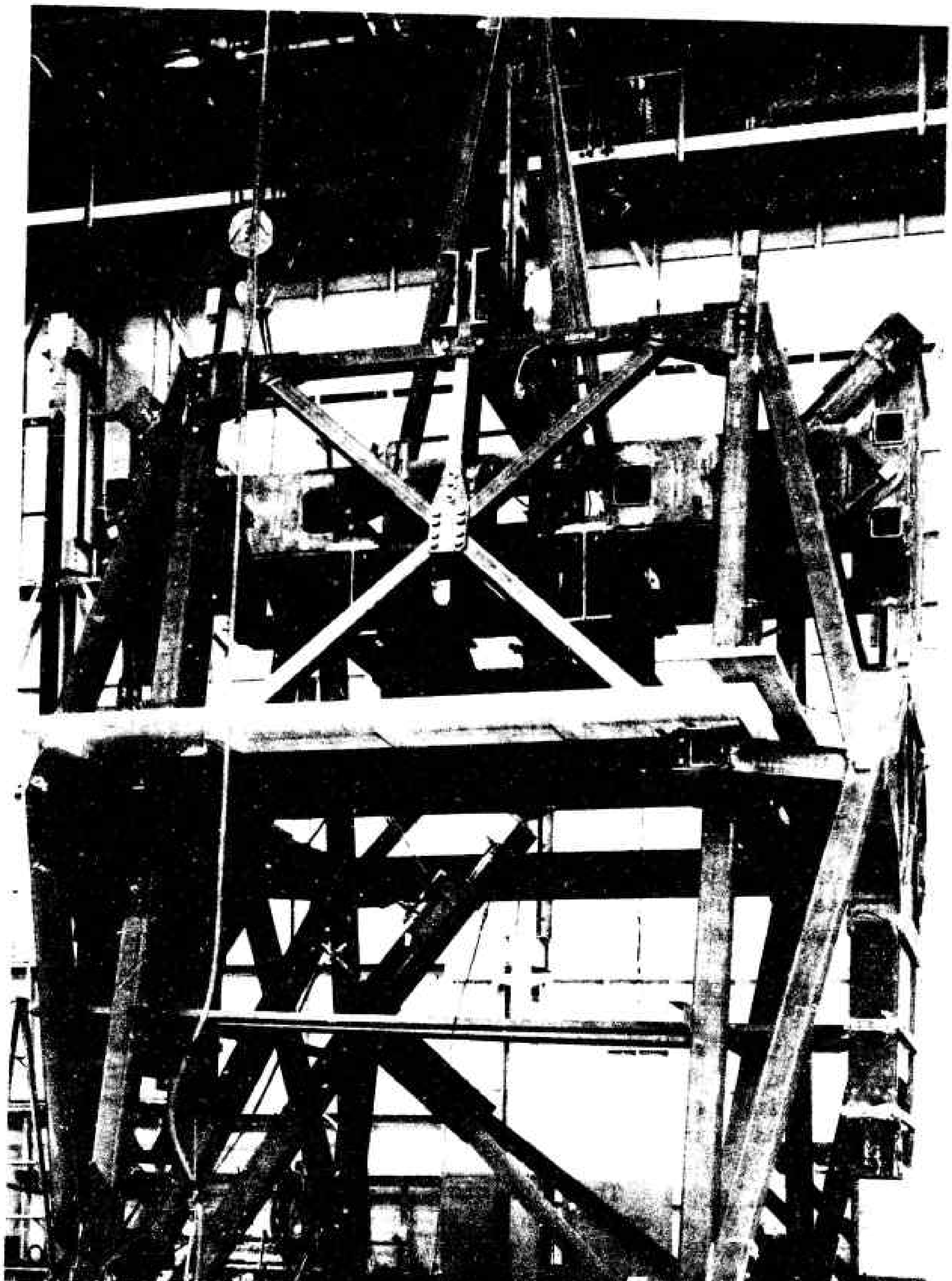

Figure 18 Landing Gear Support Fixture Structural Proof Test for Side Load Condition

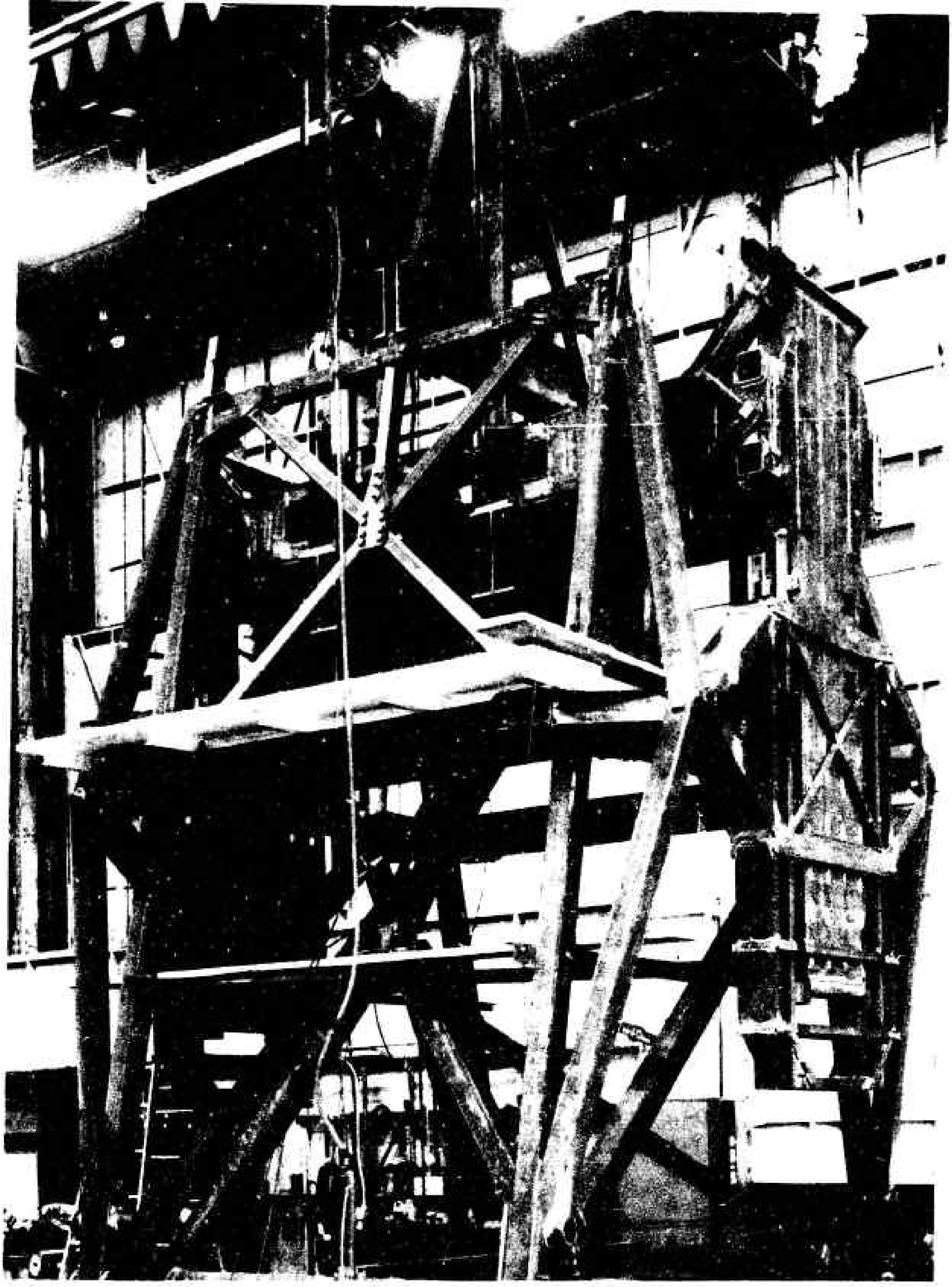

Figure 19 Landing Gear Support Fixture Structural Proof Test For Landing Load Condition

Table 1 Test Condition Summary

COND. NO.	ANTISKID SYSTEM	TIRE SIZE	TIRE AND SHOCK STRUT INFLATION	HYD. CONFIG.	APPLIED VERTICAL LOAD
1	ON-OFF-A	47 X 18	150-A	A	17,000
2	ON-OFF-A	47 X 18	150-A	A	13,000
3	ON-OFF-A	47 X 18	150-A	A	9,000
4	ON-OFF-A	47 X 18	150-A	A	5,000
5	ON-OFF-A	47 X 18	50-A	A	5,000
6	ON-OFF-A	47 X 18	50-A	A	13,000
7	ON-OFF-A	42 X 13	200-A	A	17,000
8	ON-OFF-A	42 X 13	200-A	A	13,000
9	ON-OFF-A	42 X 13	200-A	A	9,000
10	ON-OFF-A	42 X 13	200-A	A	5,000
11	ON-OFF-A	42 X 13	200-A	B	5,000
12	ON-OFF-A	42 X 13	200-A	B	13,000
13	ON-OFF-A	42 X 13	200-A	C	5,000
14	ON-OFF-A	42 X 13	200-A	C	13,000
15	ON-OFF-A	42 X 13	200-A	D	5,000
16	ON-OFF-A	42 X 13	200-A	D	13,000
17	ON-OFF-A	42 X 13	200-B	C	17,000
18	ON-OFF-A	42 X 13	200-B	C	13,000
19	ON-OFF-A	42 X 13	200-B	C	9,000
20	ON-OFF-A	42 X 13	200-B	C	5,000
21	ON-OFF-B	42 X 13	200-A	C	13,000
22	ON-OFF-B	42 X 13	200-A	C	5,000
23	ON-OFF-B	47 X 18	150-A	C	13,000
24	ON-OFF-B	47 X 18	150-A	C	5,000
25	MOD-A	47 X 18	150-A	C	13,000
26	MOD-A	47 X 18	150-A	C	5,000
27	MOD-A	47 X 18	150-B	A	13,000
28	MOD-A	47 X 18	50-A	A	5,000
29	MOD-A	47 X 18	150-A	A	17,000
30	MOD-A	47 X 18	150-A	A	13,000
31	MOD-A	47 X 18	150-A	A	9,000
32	MOD-A	47 X 18	150-A	A	5,000
33	MOD-A	42 X 13	200-A	A	17,000
34	MOD-A	42 X 13	200-A	A	13,000
35	MOD-A	42 X 13	200-A	A	9,000
36	MOD-A	42 X 13	200-A	A	5,000

(a) ON-OFF-A antiskid control circuit was a bread board version of the production F-104 and B-58 circuit except that an amplifier was added to the input in an attempt to achieve compatibility with the F-111 wheel speed sensor and to account for the difference in tire size.

(b) ON-OFF-B antiskid control circuit was the same as ON-OFF-A except the skid detection threshold and skid recovery signal settings were adjusted to achieve better stopping performance for the condition where high braking force potential exists.

(c) MOD-A antiskid control circuit was the production F-111 circuit with a modification of a resistance value in the modulating section. This modification was to facilitate the computation of analytically predicted performance and should have had negligible effect upon antiskid operation.

(2) Tire Size - The following two different size tire and wheel assemblies are physically interchangeable on the F-111 axle and fit with the F-111A brake assembly. The difference in weight of these two tire and wheel assemblies was expected to produce a preceivable change in landing gear fore and aft natural frequency.

(a) 47 X 18-18 size 26 ply rating tire mounted on a F-111A wheel assembly (B.F. Goodrich Part No. 3-1156-7) - This is the production F-111A equipment.

(b) 42 X 13-18 size 28 ply rating tire mounted on a F-111B wheel (B.F. Goodrich Part No. 3-1155-5).

(3) Hydraulic Configuration - The hydraulic brake actuation and control system used for these tests was a mockup of the production F-111 system with the following alterations:

(a) Hydraulic Configuration A was the production configuration with no alteration except that a single long hose was used in place of a combination of hard line and two short hoses between the metering valve and the landing gear.

(b) Hydraulic Configuration B was the production system modified by installing a moderate hydraulic flow restriction (.060 inch diameter orifices) between the antiskid valve and the brake.

(c) Hydraulic Configuration C was the production system modified by installing a moderate hydraulic flow restriction (.070 inch diameter orifices) between the pilot's metering valve and the antiskid valve.

(d) Hydraulic Configuration D was the production system modified by installing a very high hydraulic flow restriction (.035 inch diameter orifices) between the pilot's metering valve and the antiskid valve.

(4) Tire and Shock Strut Inflation Conditions - The test run conditions listed in Table I include variations in the total system configuration with respect to the shock strut and tire inflation pressures. The shock strut inflation pressure condition A is equivalent to that used on the F-111 and is sufficiently high to keep the shock struts upper stage fully extended. In the upper stage fully extended position and with the vertical loads associated with landing gross weights, shock strut stroking does not occur because there is insufficient compressive force to overcome the extending load. In this case the tire absorbs all of the airplane's vertical motion with respect to the ground and fairly large tire load variations result. Shock strut inflation pressure condition B is a lower pressure as is required to allow the upper stage to be compressed enough to produce two inches axle travel from the upper stage fully extended position when the test load is applied statically. This shock strut inflation condition would allow some of the vertical position variation in the aircraft's landing gear attachment to be absorbed by shock strut stroking as would occur with a conventional single stage strut arrangement. In this case the variation in tire loads should have been reduced. Even though these tests were performed with a laboratory set up where large vertical load variations should not occur the elastic deflection of the load carriage was expected to produce some variation of vertical load.

Different tire inflation pressure conditions were imposed to achieve changes in tire radial and torsional stiffness. The higher pressures were those which are usually used on the airplane (no flywheel correction applied) and the lower pressures were those which will produce approximately the same deflection for the test load imposed as is experienced on the airplane.

On Table 1 the tire and shock strut inflation condition is indicated by the tire inflation pressure in psig and the shock strut inflation condition letter as described above.

Since these tests were performed to produce information to be used for verification of the analytical prediction procedure, the test conditions were formulated to be compatible with the analytical procedure. The achievement of good (or even acceptable) braking performance was not expected for some test conditions. The reason for using the On-Off type antiskid control circuit for the majority of the test conditions was that the analytical prediction for On-Off operation was believed to be more economical than for the modulated control circuit operation. The objectives for the individual test conditions were:

- Test conditions number 1, 2, 3 and 4 were to examine the variation in braking system performance which results from variations in tire-to-runway braking force potential.

- Test conditions number 5 and 6 were to examine the effects of tire stiffness. The results of these test runs will be compared to conditions 2 and 4.

- Test conditions number 7, 8, 9 and 10 were to examine the effects of changing the landing gear fore and aft natural frequency.

- Test conditions number 11, 12, 13, 14, 15 and 16 were to examine the effects of variations in hydraulic system flow restrictions.

- Test conditions number 17, 18, 19 and 20 were to examine the effects of the landing gear's vertical compliance as influenced by shock strut characteristic.

- Test conditions number 21, 22, 23 and 24 were to examine the effects of changing the control circuit's operating characteristic.

- Test conditions number 25 and 26 were to determine the effects of varying the hydraulic system restriction in conjunction with modulat antiskid circuit operation.

- Run condition 27 was to de ne the effects of the landing gear's vertical compliance onjunction with modulated antiskid circuit operation.

- Test run condition 28 was to determine the effects of tire stiffness in conjunction with modulated antiskid circuit operation.

- Test conditions number 29, 30, 31 and 32 were to determine the variation in braking system performance with modulated antiskid circuitry resulting from variations in tire-to-runway braking force potential.

- Test conditions number 33, 34, 35 and 36 were to determine the effects of increased landing gear fore and aft natural frequency along with variations in tire-to-runway braking force potential with modulated antiskid system operation.

For all test conditions the dynamometer flywheel inertial equivalent was 10,147 pounds, the brake application speed was 135 mph and brake release speed was 10 mph. The resultant kinetic energy absorption was 6.15 million foot pounds as compared with 18 million foot pounds F-111A brake 45 stop energy capacity. This low energy condition was used for economy in that brake wear was minimized, test runs could be conducted more frequently because long brake cooling periods were avoided, and the computation expense required to analyze a complete test run was reduced. Each test run was performed as follows:

- The applicable total system installation test configuration was installed in the test set-up and the antiskid control circuit was functionally checked. The applicable landing load was set on the carriage load control system.

- The flywheel was accelerated to approximately 140 mph peripheral speed and the wheel was landed with the applicable applied load. When 135 mph flywheel speed was reached the brake was applied by positioning the aircraft pilot's metering valve for 1600 psi steady state output pressure. Prior to landing the instrumentation and recording equipment was started to record the applicable parameters during the test.

- When the flywheel speed had been reduced to 10 mph, the brake was released so that the aircraft wheel was allowed to coast. At approximately 2 mph flywheel speed the aircraft wheel was unlanded. The dynamometer flywheel was not brought to a complete stop because significant antiskid operation does not occur below 10 mph locked wheel detection speed and because repeated high torque low speed usage causes excessive brake wear and lining damage.

C. TEST RESULTS

Since this testing was performed for verification of the analytical prediction procedure, the criteria for evaluating the relative success or failure of an individual test run is established by the degree of agreement between actual occurrences and the analytically predicted occurrences. The nature of the testing was such that the test results could be evaluated by direct observation of the oscillograph traces showing the recorded data. Items which were evaluated are:

- Landing gear fore and aft load magnitude and oscillation frequency.
- The character and magnitude of braked wheel speed variation throughout individual antiskid cycles.
- Relative braking effectiveness as indicated by stopping distance and dynamometer flywheel deceleration rate.
- The ability of the antiskid system to prevent skids when conditions of low tire-to-runway friction potential are encountered.
- The overall compatibility between the various elements within the total system. For instance, was the hydraulic brake line flow restriction excessive such that satisfactory tire skid prevention or the achievement of satisfactory stopping performance was inhibited.

Test runs were performed for all of the 36 test conditions listed in Table 1 and the test data was recorded as intended. Figure 20 shows an oscillograph record for test condition No. 29 with a reduced time scale. This oscillograph is typical of the other test conditions except for length. As can be observed the antiskid system operated reasonably well.

In most respects practically all of the test results except for those from test condition No. 29 were unsatisfactory in that the circumstances of the test runs were beyond the bounds of the circumstances for which the analysis procedures were intended to represent. The primary difficulty was that the On-Off antiskid circuit operation was totally unsatisfactory and not representative of any type antiskid system which might ever be attempted to be used on an airplane. Unsatisfactory On-Off antiskid operation was caused by the wheel speed signal being severely

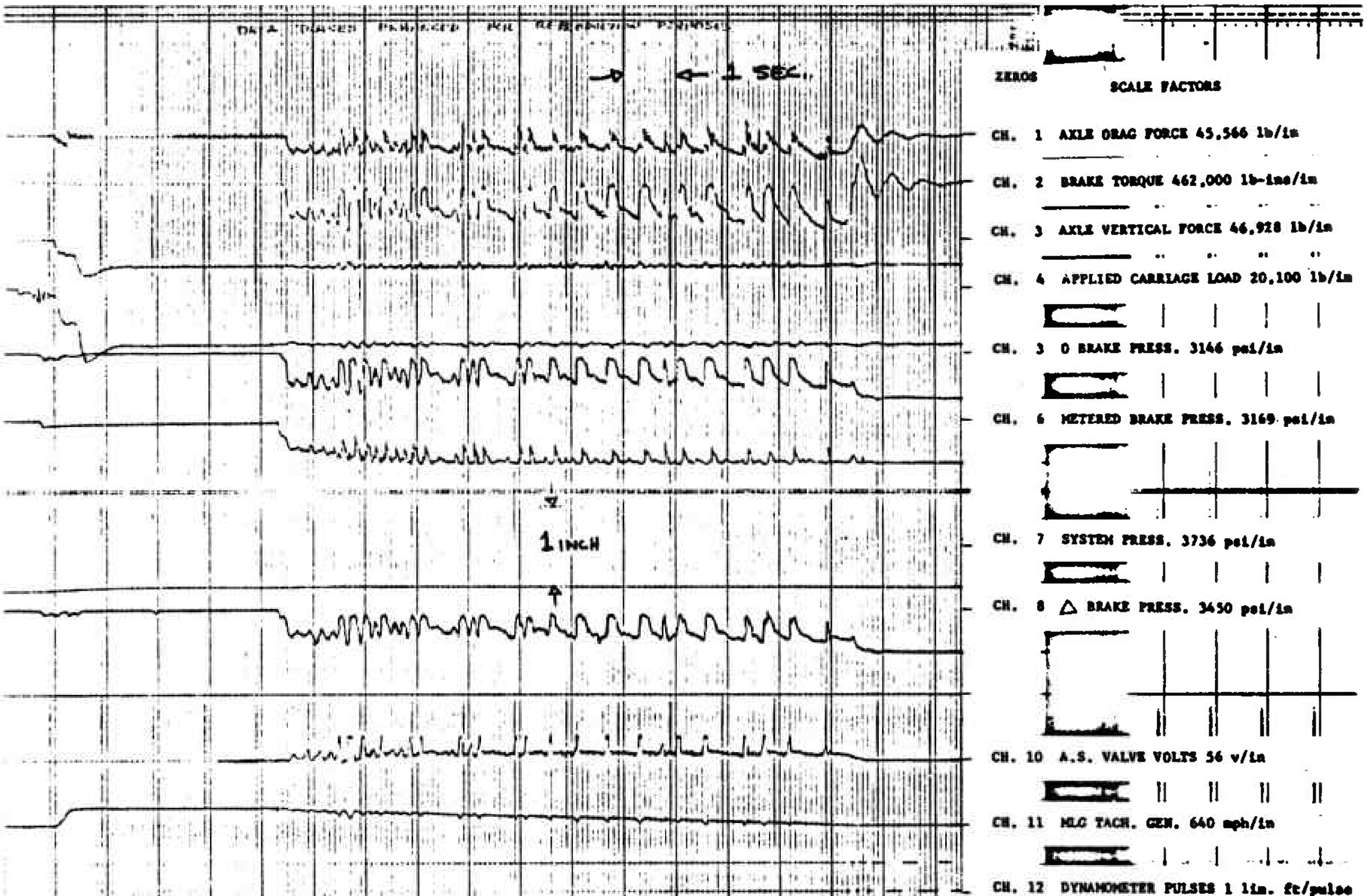

Figure 20 Test Condition No. 29 Oscillograph Recording

distorted by the amplifier which was intended for adapting the F-111 wheel speed sensor to provide the proper input to the F-104 type electronic circuit. The existance of the problem was recognized at the time the tests were being conducted; however, the means for prompt resolution was not available. Testing was continued because the degree of wheel speed signal distortion was not believed to be as great as it was later determined to be. When the magnitude of the problem was identified there was insufficient remaining time with which to implement suitable corrective action and repeat the test runs.

As a result of the unsatisfactory On-Off antiskid operation, a large number of severe tire skids occurred. These tire skids caused the tread compound to become reverted. Even though the flywheel surface was cleaned between test runs, the reverted tire tread compound contaminated the flywheel surface during the first few wheel revolutions such that tire-to-flywheel friction coefficient was much less than that which is usually available and which was planned for. Since the test runs for conditions using the modulated antiskid control circuit were performed such that they were interspersed with the tests using On-Off antiskid circuit, the results of these tests were adversely affected by the abnormal tire tread condition. This problem could have been avoided if additional tires had been available for replacement or if the tests had been performed so that those using modulated antiskid circuit had been performed first.

Observation of the oscillograph records during the course of the test revealed brake pressure increase and decrease was occurring at a rate less than that which had been expected. The test setup was inspected for possible unplanned excessive restriction in the hydraulic lines from the brake to the antiskid and brake metering valves and the antiskid valve was changed on one occasion; however, no cause for apparent high restriction could be found. This effect did not cause any significant difficulty with antiskid operation during testing but does cause an analytical problem as discussed in Section IV.

SECTION III

ANALYSIS REFINEMENT

Early in this program it was realized that if any appreciable amount of test data correlation was to be accomplished it would be necessary to devise some way to reduce analytical complexity because of the prohibitive computation expense which would otherwise be incurred. This problem was previously discussed in Section I herein. To permit evaluation of such effects as brake chatter and squeal, the tread circumferential and radial displacement with respect to the wheel, and hydraulic system resonant pressure surges, the analysis procedures as previously formulated contain a number of second order differential equations describing phenomena having very high oscillatory frequencies, some well above 100 HZ. Provisions for these effects were included because there have been instances where they have been the cause of braking system incompatibility problems. In addition, the examination of tire tread displacement with respect to the wheel provides the only known means of adequately explaining a tire's braking force versus apparent slippage relationship.

As a first step toward analytical refinement the antiskid valve mathematical model was revised as described in Section 7 of Appendix A. Additional damping was added between the tire tread and the wheel and the tire-to-ground friction coefficient versus slip velocity function was modified as described in Section 4 of Appendix A. These simplifications were helpful but did not significantly reduce computation expense. It is evident that there are infinitely many minor variations of the mathematical models formulated and that the useful analytical tool whereby "high gain" second order differential equations are replaced with first order equations could be employed in many more instances than it has. However, by these means establishing the simplest possible composite solution which could be useful requires a great deal of time consuming experimentation. To overcome this problem it was decided to revert to the more usual antiskid analytical techniques and formulate a simplified analysis procedure. For the following simplified mathematical description all of the elements previously described separately, except for the wheel speed sensor and antiskid control circuit, are combined into a single simplified model representing a brake test dynamometer type setup. This simplified model is essentially the same as that which would be (and has been) used on an analog computer operating at "real time" with actual aircraft antiskid control circuit hardware. For this case such high frequency

second order equations as those for axle torsional displacement, tire tread displacement relative to the wheel, brake disc axial displacement and hydraulic valve spool displacement are not included. There is also a significant difference in the treatment of the tire-to-ground friction force for this model in that the friction coefficient versus footprint relative slip velocity function has been modified to have a relatively moderate slope through zero as shown in Figure 24. This modification is required to represent the elastic displacement of the tire tread relative to the wheel which is not being computed. The same format as used in Appendix A is used.

A. MATHEMATICAL DESCRIPTION

Each major element of the system is described separately as in Appendix A even though all elements are combined into a single system.

Hydraulic System

The hydraulic system supplies brake actuation pressure, P_B, and consists of a pressure source, the antiskid valve flow control spool, the brake actuation cylinder and interconnecting piping as shown in Figure 21. As described in Appendix A hydraulic flow is established by the product of a pressure function ϕ and a flow coefficient function A_{CV} as follows.

(1) $$\phi\langle X, Y\rangle = \text{SIGN}(X-Y)\sqrt{|X-Y|}$$

(2) $$A_{CV}\langle X\rangle = A_{CVO} \qquad \text{IF } X \geq S_{CVO}$$
$$= \text{MAX}\{A_{CVL},\ X(A_{CVO}/S_{CVO})\} \qquad \text{IF } X < S_{CVO}$$

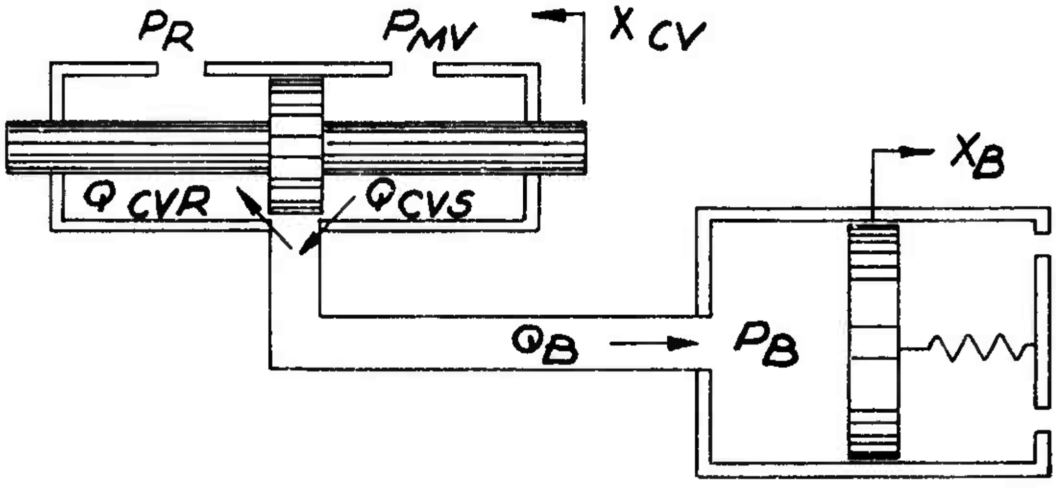

Figure 21 Simplified Brake Hydraulic System Schematic

The pressure source is the pilot's metering valve output having pressure P_{MV}. As the pilot applies the brakes, the metering valve output pressure increases from reservoir pressure, P_R, to the command pressure value, P_{CP}, as a function of time in accordance with equation (3).

$$(3) \quad P_{MV} = T(P_{CP} - P_R)/T_{CP} + P_R \qquad \text{IF } 0 \leq T \leq T_{CP}$$
$$= P_{CP} \qquad \text{IF } T > T_{CP}$$

The antiskid valve flow control spool position, X_{CV}, establishes the brake application or brake release flow coefficients, A_{CVS} and A_{CVR} respectively, according to equations (4) and (5).

$$(4) \quad A_{CVS} = A_{CVSO} \qquad \text{IF } (X_{CV} - S_{CL}) \geq S_{CVO}$$
$$= MAX\{A_{CVL}, (X_{CV} - S_{CL})(A_{CVSO}/S_{CVO})\} \qquad \text{IF } (X_{CV} - S_{CL}) < S_{CVO}$$

$$(5) \quad A_{CVR} = A_{CVRO} \qquad \text{IF } (-S_{CL} - X_{CV}) \geq S_{CVO}$$
$$= MAX\{A_{CVL}, (-S_{CL} - X_{CV})(A_{CVRO}/S_{CVO})\} \qquad \text{IF } (-S_{CL} - X_{CV}) < S_{CVO}$$

The flow thru the antiskid valve flow control spool is then given by equations (6), (7) and (8).

$$(6) \quad Q_{CVS} = A_{CVS}\,\phi\langle P_{MV}, P_B\rangle$$

$$(7) \quad Q_{CVR} = A_{CVR}\,\phi\langle P_B, P_R\rangle$$

$$(8) \quad Q_B = Q_{CVS} - Q_{CVR}$$

If the brake actuation piston area per line is A_{BPS}, then the piston velocity, $\dot{X}_B$, is given by equation (9).

$$(9) \quad \dot{X}_B = Q_B/A_{BPS}$$

The brake actuation pressure is established from the brake pressure volume characteristic as described by equation (10).

$$(10) \quad P_B = \begin{cases} C_{BPL} X_B + P_{BO} & \text{IF } X_B \leq 0 \\ C_{BPU} X_B + P_{BO} & \text{IF } X_B > 0 \end{cases}$$

The value for piston displacement X_B is established by integrating $\dot{X}_B$ from equation (9).

Antiskid Control Valve

The antiskid control valve mathematical description consists of the equations establishing the flow control spool position, X_{CV}, as a function of the valve's characteristics and the input control signal, E_V, as follows:

$$(11) \quad X_{SC} = C_{SCVR} E_V$$

$$(12) \quad \begin{aligned} R_{SC} &= 1.0 && \text{IF } X_{SC} \leq X_{SCM} \\ &= (X_{SCR} - X_{SC})/(X_{SCR} - X_{SCM}) && \text{IF } X_{SCM} < X_{SC} < X_{SCR} \\ &= 0.0 && \text{IF } X_{SC} \geq X_{SCR} \end{aligned}$$

$$(13) \quad P_{SC} = R_{SC}(P_{MV} - P_R) + P_R + P_{CVB}$$

$$(14) \quad V_{CV} = G_{CV}(P_{SC} - P_B)$$

$$(15) \quad \begin{aligned} \dot{X}_{CV} &= \mathrm{MIN}\{0, V_{CV}\} && \text{IF } S_{CVA} \leq X_{CV} \\ &= V_{CV} && \text{IF } S_{CVR} < X_{CV} < S_{CVA} \\ &= \mathrm{MAX}\{0, V_{CV}\} && \text{IF } X_{CV} \leq S_{CVR} \end{aligned}$$

Brake Torque System

Brake torque is the product of the number of friction surfaces, the normal force between friction surfaces, the friction coefficient between friction surfaces and the normal force radius. The normal force is the product of the effective actuation pressure, P_E, and the brake piston area, A_{BP}. The effective pressure is determined from equation (16) as follows:

(16) $P_E = \max\{0,\ P_B - P_{BDC} - P_{BF}\ \mathrm{SIGN}(\dot{X}_B)\}$

The brake torque, T_{BT}, is determined by equations (17), (18) and (19) where the friction coefficient is defined as a function of the relative velocity between the friction surfaces, V_B. W_T is the wheel angular velocity.

(17) $V_B = R_{BT} W_T$

(18)
$$\mu_B = \mu_{B1} + \mu_{B2}\ \mathrm{EXP}\langle -\alpha_B V_B \rangle \qquad \text{IF } V_B > 0$$
$$= 0 \qquad \text{IF } V_B = 0$$
$$= -\mu_{B1} - \mu_{B2}\ \mathrm{EXP}\langle \alpha_B V_B \rangle \qquad \text{IF } V_B < 0$$

(19) $T_{BT} = A_{BP}\, R_{BT}\, 2\, N_R\, (P_E)(\mu_B)$

In the above NR is the number of rotors. Since each rotor has a friction surface on each side, the number of friction surfaces is 2 NR.

Wheel and Tire System

Figure 22 shows the wheel and tire system representing a brake test dynamometer setup. The horizontal force, F_G, on the wheel (from the axle) is given by equation (20).

(20) $F_G = -C_G X_G - D_G \dot{X}_G$

If T_{BT} is the brake torque and F_{BT} is the friction force at the tire-flywheel interface, the tire and wheel equations of motion for horizontal translation and rotation are:

(21) $W_G \ddot{X}_G = F_G - F_{BT}$

(22) $W_{IT} \dot{W}_T = F_{BT} R_{TD} - T_{BT}$

The relative velocity between tire tread and the flywheel, V_R, is given by equation (23).

(23) $V_R = V_F + \dot{X}_G - R_R W_T$

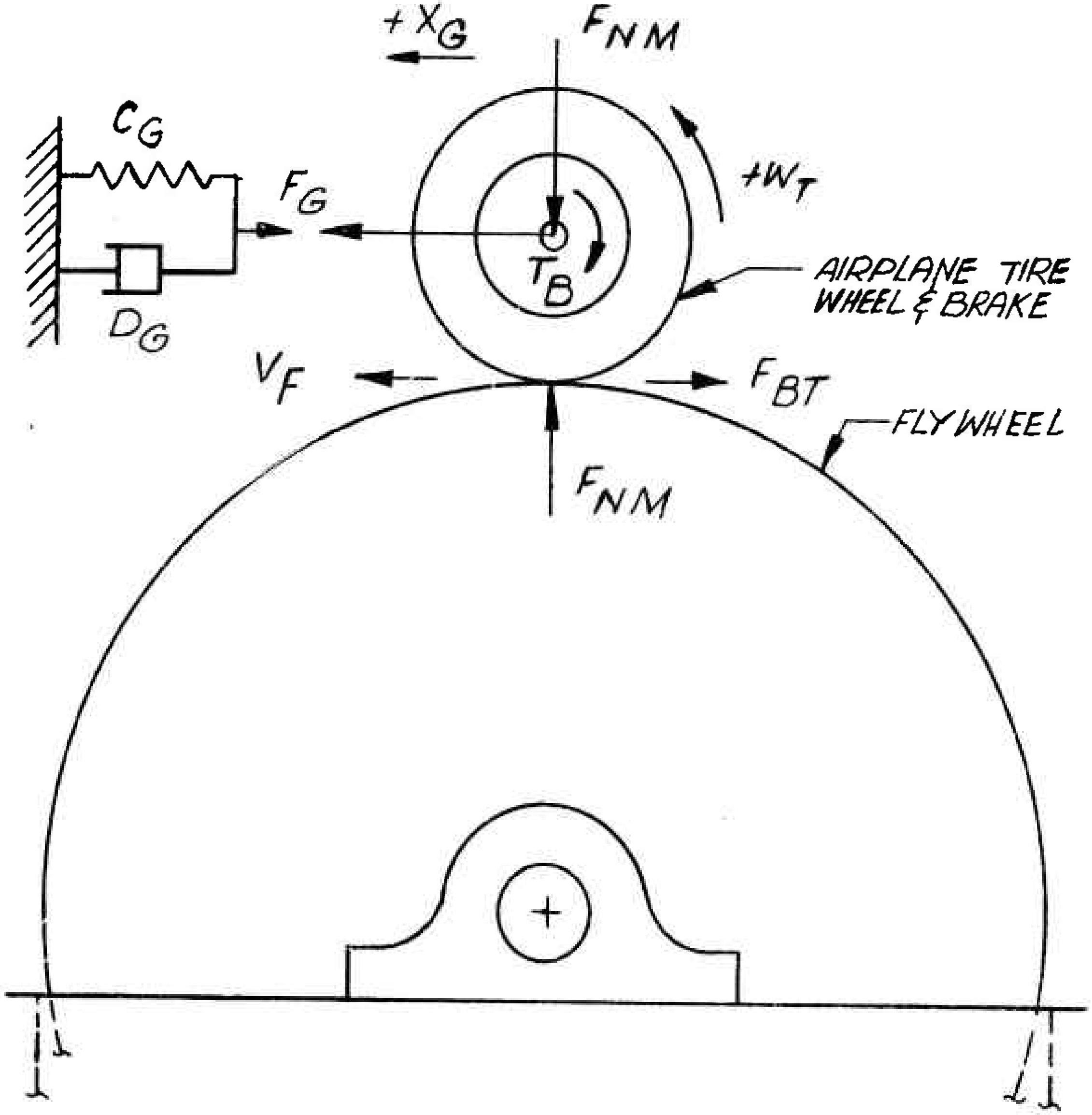

Figure 22 Dynamometer Flywheel Setup

The braking force, F_{BT}, is established by the tire vertical force, F_{Nm}, and the tire-to-ground friction coefficient, μ_T, by equations (24) and (25).

(24) $$F_{BT} = F_{Nm} \mu_T$$

(25) $$\begin{aligned} \mu_T &= \mu_{T1} + (\mu_{T2} - E_T V_F) EXP\langle -\alpha (V_R - V_{RO})\rangle \quad IF\ V_R > V_{RO} \\ &= (V_R/V_{RO})(\mu_{T1} + \mu_{T2} - E_T V_F) \quad IF\ -V_{RO} \leq V_R \leq V_{RO} \\ &= -\mu_{T1} - (\mu_{T2} - E_T V_F) EXP\langle \alpha (V_R + V_{RO})\rangle \quad IF\ V_R < -V_{RO} \end{aligned}$$

The flywheel velocity, V_F, and flywheel peripheral distance, X_F, are computed by integrating equations (26) and (27).

(26) $$\dot{V}_F = -F_{BT} / W_F$$

(27) $$\dot{X}_F = V_F / 12$$

Figure 23 shows the Simplified Antiskid Analysis System Equation Flow Diagram.

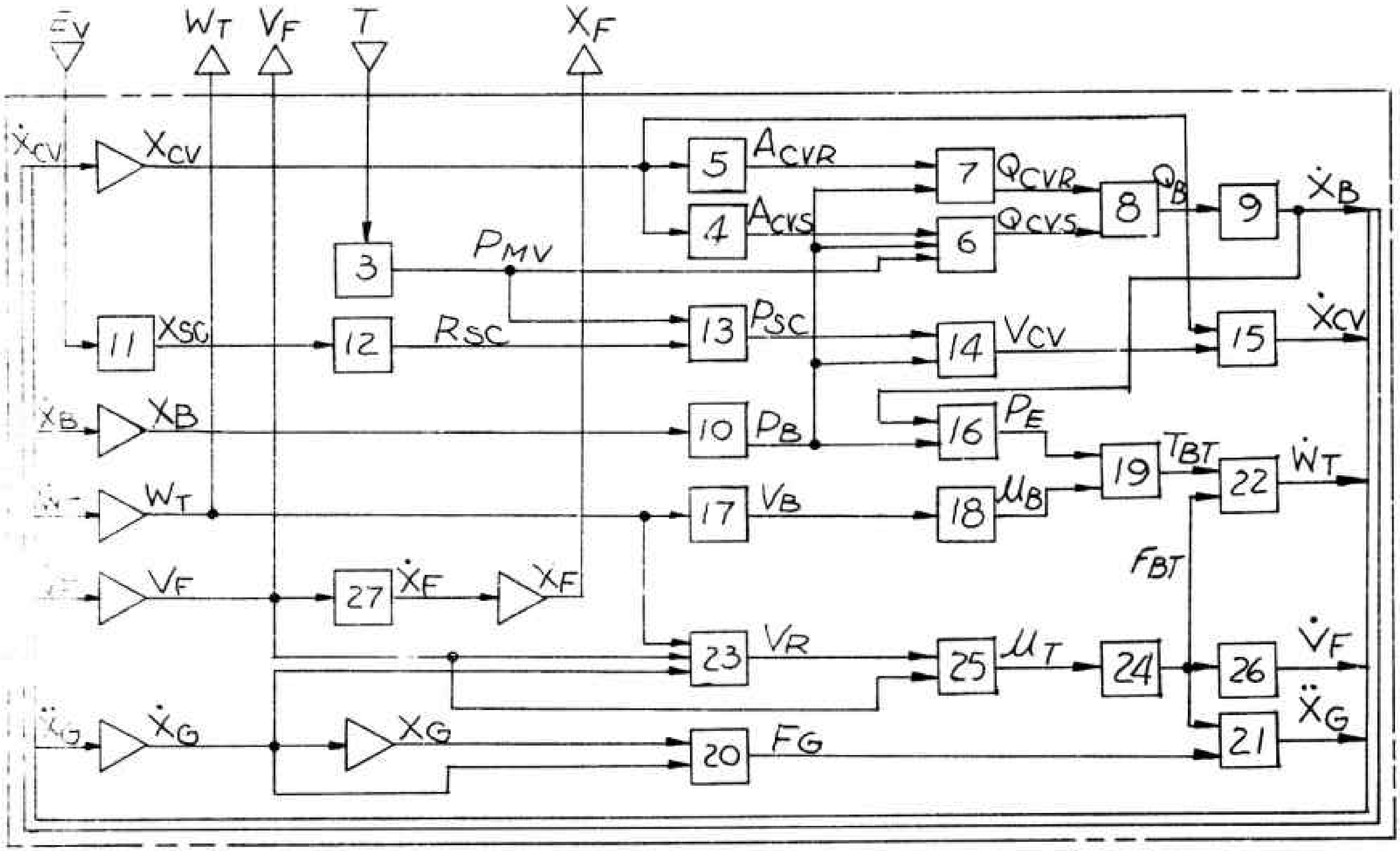

Figure 23 Simplified Antiskid Analysis System Equation Flow Diagram

B. PARAMETER EVALUATION

The parameters applicable to the simplified antiskid analysis procedure are listed in Table 2. The values for each parameter are that for test condition No. 29 as established by the procedures described in Appendix A for the applicable case except as follows:

The antiskid control valve gain, G_{CV}, is set at a value such that if the valve spool had constant velocity it would move through its entire travel in 0.010 seconds which is the step input response time of the valve with 1500 psi differential pressure. Therefore,

For .070 inches spool travel in .01 seconds,

$$\dot{X}_{CV} = .07/.01 = 7 \text{ inches per second.}$$

$$G_{CV} = \dot{X}_{CV}/\Delta P = 7/1500 = 0.0047 \text{ in}^3/\text{sec lbf}$$

The positive slope portion of the tire-to-ground friction coefficient function was established from information presented in Reference 1, for a 17.00-20 tire which is about the same size as the 47 X 18 tire used during testing:

From Figure 54 (page 38) of Reference 1:

$F_X = r K_X S_I$ for an axle velocity of approximately 100 ft/sec.

Where F_X = Braking force
r = Tire free radius
K_X = Tire fore and aft spring rate
S_I = slip ratio

By definition $S_I = \dfrac{\text{slip velocity}}{\text{axle velocity}}$

For a 47 X 18 tire with 13,000 pounds radial load and 150 psi inflation pressure, K_X = 6830 pounds/inch (see Reference 1, page 22, equation 47).

For a 47 X 18 tire r = 23.35 inches

Since $F_X = \mu F_Z = r K_X S_1$,

$$\mu = \frac{r K_X S_1}{F_Z} = \frac{(23.35)(6830)\ S_1}{13000}$$

$$\text{OR } \mu = 12.22 S_1 = 12.22 \frac{\text{SLIP VELOCITY}}{\text{AXLE VELOCITY}}$$

From Figure A40 in Appendix A μ_{MAX} = .496 for 2400 in/sec aircraft velocity. Use this value even though axle velocity for data from Reference 1 is only 1200 inches/sec.
Let V_{RO} = slip velocity for μ_{MAX} : Therefore,

$$V_{RO} = \text{Axle Velocity} \left(\frac{\mu_{MAX}}{12.22}\right)$$

$$V_{RO} = 1200 \left(\frac{.496}{12.22}\right)$$

$$V_{RO} = 48.7 \text{ inches/sec}$$

Figure 24 shows the resultant tire friction coefficient versus slip velocity function.

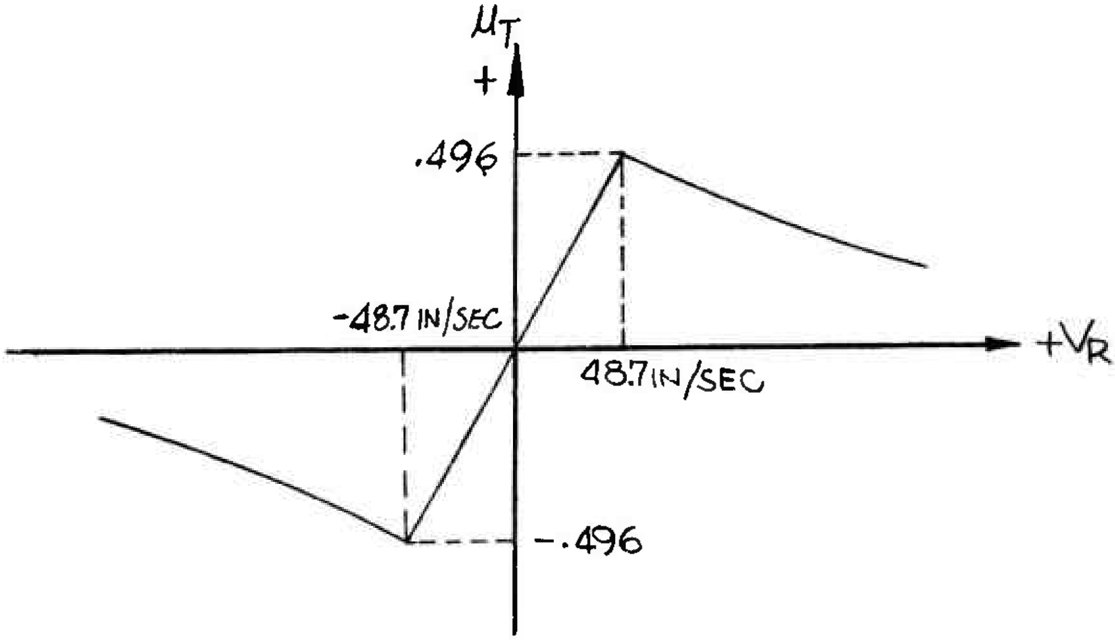

Figure 24 Tire-To-Ground Friction Coefficient Versus Relative Velocity

Table 2 Simplified Antiskid Analysis System Parameters (Sheet 1 of 4)

SYMBOL	TYPE	VALUE	UNITS	DESCRIPTION
α	c	0.25×10^{-2}	SEC/INCH	Tire Friction Parameter
α_B	c	0.30×10^{-1}	SEC/INCH	Brake Lining Friction Parameter
A_{BP}	c	0.133×10^{2}	$INCHES^2$	Piston Area per Brake
A_{BPS}	c	0.665×10	$INCHES^2$	Piston Area per Control Valve
$A_{CV}\langle X \rangle$	f			Control Valve Flow Coefficient Function
A_{CVL}	c	0.0	$IN^4/SEC\ LBF^{1/2}$	Control Valve Leakage Flow Coefficient
A_{CVR}	v		$IN^4/SEC\ LBF^{1/2}$	Control Valve Return Flow Coefficient
A_{CVS}	v		$IN^4/SEC\ LBF^{1/2}$	Control Valve Supply Flow Coefficient
A_{CVRO}	c	0.72×10	$IN^4/SEC\ LBF^{1/2}$	Control Valve Return Full Flow Coefficient
A_{CVSO}	c	0.34	$IN^4/SEC\ LBF^{1/2}$	Control Valve Supply Full Flow Coefficient
C_{BPL}	c	0.665×10^{3}	PSI/INCH	Brake P-V Slope (Discs not in contact)
C_{BPU}	c	0.4725×10^{5}	PSI/INCH	Brake P-V Slope (Discs in contact)
C_G	c	0.353×10^{5}	LBF/INCH	Fore and Aft Spring Rate at Axle
C_{SCVR}	c	0.12×10	INCHES/VOLT	Control Valve Input Coefficient
D_G	c	0.234×10^{2}	LBF SEC/INCH	Fore and Aft Damping Coefficient at Axle
E_V	v(I)		VOLTS	Antiskid Valve Volts
E_T	c	0.65×10^{-4}	DIMENSIONLESS	Tire Friction Velocity Correction Coefficient
F_G	v		POUNDS	Fore and Aft Force at Axle
F_{BT}	v		POUNDS	Friction Force Between Tire and Ground
F_{NM}	c	$.130 \times 10^{5}$	POUNDS	Vertical Force on Tire from Ground
G_{CV}	c	$.47 \times 10^{-2}$	$IN^3/SEC\ LBF$	Control Valve Gain
$\phi\langle X,Y \rangle$	f			Hydraulic Pressure Function
P_B	v		PSI	Brake Cylinder Pressure
P_{BO}	c	$.180 \times 10^{3}$	PSI	Brake Cylinder Pressure at Time Zero
P_{BR}	c	$.130 \times 10^{3}$	PSI	Brake Return Spring Preload Pressure
P_{BDC}	c	$.200 \times 10^{3}$	PSI	Brake Disc Contact Pressure
P_E	v		PSI	Effective Pressure for Brake Torque
P_{MV}	v		PSI	Metering Valve Output Pressure
P_{CP}	c	0.160×10^{4}	PSI	Pilots Command Brake Pressure

Table 2 Simplified Antiskid Analysis System Parameters (Sheet 2 of 4)

SYMBOL	TYPE	VALUE	UNITS	DESCRIPTION
P_{CVB}	c	0.25×10^{2}	PSI	Control Valve Bias Pressure
P_{FB}	c	0.219×10^{2}	PSI	Brake Piston Friction Hysteresis
P_{SC}	v		PSI	Antiskid Control Pressure
P_R	c	0.0	PSI	Hydraulic System Reservoir Pressure
Q_B	v		IN^3/SEC	Hydraulic Flow into the Brake
Q_{CVR}	v		IN^3/SEC	Hydraulic Flow thru Antiskid Valve to Return
Q_{CVS}	v		IN^3/SEC	Hydraulic Flow thru Antiskid Valve from Supply
R_{BT}	c	0.625×10	INCHES	Brake Piston Torque Producing Radius
R_R	c	0.228×10^{2}	INCHES	Tire Effective Rolling Radius
R_{SC}	v		DIMENSIONLESS	Control Valve Regulating Function
R_{TO}	c	0.2173×10^{2}	INCHES	Height of Axle Above Ground
S_{CL}	c	0.50×10^{-2}	INCHES	Control Valve Overlap
S_{CVO}	c	0.30×10^{-1}	INCHES	Control Valve Full Open Spool Travel
S_{CVA}	c	0.35×10^{-1}	INCHES	Control Valve Max Application Travel
S_{CVR}	c	-0.35×10^{-1}	INCHES	Control Valve Max Release Travel
T_{BT}	v		INCH LBF	Brake Torque
T	v(I)		SECONDS	Time
T_{CP}	c	0.10	SECONDS	Time to Reach Max Command Pressure
μ_B	v		DIMENSIONLESS	Brake Lining Friction Coefficient
μ_{B1}	c	0.15	DIMENSIONLESS	Brake Lining Friction Parameter
μ_{B2}	c	0.10	DIMENSIONLESS	Brake Lining Friction Parameter
μ_T	v		DIMENSIONLESS	Tire-to-Ground Friction Coefficient
μ_{T1}	c	0.20	DIMENSIONLESS	Tire Friction Parameter
μ_{T2}	c	0.45	DIMENSIONLESS	Tire Friction Parameter
V_B	v		INCHES/SEC	Brake Lining Velocity
V_{CV}	v		INCHES/SEC	Control Valve Spool Velocity
V_F	v		INCHES/SEC	Flywheel Peripheral Velocity
V_{FO}	c	$.240 \times 10^{4}$	INCHES/SEC	Flywheel Peripheral Velocity at Time Zero
$\dot{V}_F$	v		$INCHES/SEC^2$	Flywheel Peripheral Acceleration

Table 2 Simplified Antiskid Analysis System Parameters (Sheet 3 of 4

SYMBOL	TYPE	VALUE	UNITS	DESCRIPTION
$\dot{V}_{FO}$	c	0.0	INCHES/SEC^2	Flywheel Peripheral Acceleration at Time Zero
V_R	v		INCHES/SEC	Relative Velocity Between Tire Footprint & Groun
V_{RO}	c	0.487×10^2	INCHES/SEC	Tire Friction vs Velocity Parameter
W_G	c	0.155×10	LBF SEC^2/IN	Wheel, Tire, Brake & Supporting Structure Mass
W_{IT}	c	0.163×10^3	LBF IN SEC^2	Tire, Wheel & Brake Rotor Moment of Inertia
W_T	v(o)		RAD/SEC	Tire & Wheel Angular Velocity
W_{TO}	c	0.1053×10^3	RAD/SEC	Tire & Wheel Angular Velocity at Time Zero
$\dot{W}_T$	v		RAD/SEC^2	Tire & Wheel Angular Acceleration
$\dot{W}_{TO}$	c	0.0	RAD/SEC^2	Tire & Wheel Angular Acceleration at Time Zero
X_B	v		INCHES	Brake Piston Position
X_{BO}	c	0.0	INCHES	Brake Piston Position at Time Zero
$\dot{X}_B$	v		INCHES/SEC	Brake Piston Velocity
$\dot{X}_{BO}$	c	0.0	INCHES/SEC	Brake Piston Velocity at Time Zero
X_{BR}	c	0.275×10^{-2}	INCHES	Brake Piston Position for Full Release
X_{BDC}	c	0.1078	INCHES	Brake Piston Position at Disc Contact
X_{CV}	v		INCHES	Control Valve Spool Position
X_{CVO}	c	$+.35 \times 10^{-1}$	INCHES	Control Valve Spool Position at Time Zero
$\dot{X}_{CV}$	v		INCHES/SEC	Control Valve Spool Velocity
$\dot{X}_{CVO}$	c	0.0	INCHES/SEC	Control Valve Spool Velocity at Time Zero
X_F	v(o)		FEET	Flywheel Peripheral Distance
X_{SC}	v		INCHES	Control Valve Pressure Regulation Parameter
X_{SCM}	c		INCHES	Value of X_{SC} for Maximum Regulation
X_{SCR}	c		INCHES	Value of X_{SC} for Zero Regulation
X_G	v		INCHES	Axle Horizontal Position
X_{GO}	c	0.0	INCHES	Axle Horizontal Position at Time Zero
$\dot{X}_G$	v		IN/SEC	Axle Horizontal Velocity
$\dot{X}_{GO}$	c	0.0	IN/SEC	Axle Horizontal Velocity at Time Zero
$\ddot{X}_G$	v		IN/SEC^2	Axle Horizontal Acceleration
$\ddot{X}_{GO}$	c	0.0	IN/SEC^2	Axle Horizontal Acceleration at Time Zero

Table 2 Simplified Antiskid Analysis System Parameters (Sheet 4 of 4)

SYMBOL	TYPE	VALUE	UNITS	DESCRIPTION
WF	c	26.29	LBF-SEC^2/IN	Flywheel Mass
NR	c	7.0	DIMENSIONLESS	Number of Brake Rotors
V_{MIN}	c	160.0	INCHES/SEC	Flywheel Peripheral Velocity for Terminating Problem
$\dot{X}_{FO}$	c	200.0	FEET/SEC	Flywheel Peripheral Velocity at Time Zero
$\dot{X}_F$	v		FEET/SEC	Flywheel Peripheral Velocity
X_{FO}	c	0.0	FEET	Flywheel Peripheral Distance at Time Zero

In addition to formulating the simplified analysis procedure, some minor corrections have been made to the On-Off and modulated antiskid control circuit mathematical models as shown in Section 6 of Appendix A. For the On-Off circuit equation (N2) was not previously separately identified. Since Diode D2 is in the current path it is necessary to consider current AD2 separately so that its value can be limited to positive values only.

For the modulated antiskid circuit a minor modification of the computation sequence was required to place the proper limits on current AEQ2. For circuit conditions 3, 4, 7, 8, 11 and 12 where the valve drive amplifier is operating in the amplification mode, an upper current limit is necessary to represent the saturated condition. With the revised computation sequence, the value of AEQ2, once established and properly limited, is used for computing VB and AC4. Previously, the equation for AEQ2 was substituted into the equations for VB and AC4 so that all three parameters were computed from the instantaneous capacitor voltages.

SECTION IV

TEST DATA CORRELATION

Test data correlation was accomplished by comparing the analytical predictions for test condition number 29 with the test results. Figure 25 shows an expanded time scale oscillograph record of the first two seconds of the test for condition number 29. The variations of brake cylinder pressure, horizontal and vertical force on the axle, brake torque, braked wheel speed, and antiskid valve voltage are shown with respect to time. Two brake cylinder pressures, identified by "△" and "○", are shown because the F-111 brake has two independent sets of actuation cylinders and each set is controlled by separate metering valve and antiskid valve elements. Figure 26 shows the variation of the same or comparable quantities as predicted from the simplified analysis procedure for the first second of the stop. For the analytically generated information only one cylinder pressure is shown and the axle drag is shown in deflection units instead of force units. The information shown on Figure 26 was obtained from an electronic digital computer solution of simplified analysis procedure mathematical equations described in Section III combined with the Option 2 wheel speed sensor and modulated antiskid control circuit mathematical models from Sections 5 and 6 of Appendix A. The digital computer input data is shown on Table 3 and the computer program listing is in Appendix B.

A comparison between the test results shown on Figure 25 and the analytical predictions shown on Figure 26 reveals the following:

- The antiskid cyclic frequency is much higher for the Analytical prediction than was obtained in the test
- The brake pressure change rate in the test was much lower than analytically predicted
- The modulating antiskid circuit elements are not operating for the analytical prediction and were operating during the test.

It is believed that these differences are caused by both analytical and test difficulties. As was previously mentioned in Section II the brake pressure change rates were observed to be much lower than expected. Figure 27 shows part of an oscillograph record from an aircraft test performed by the Air

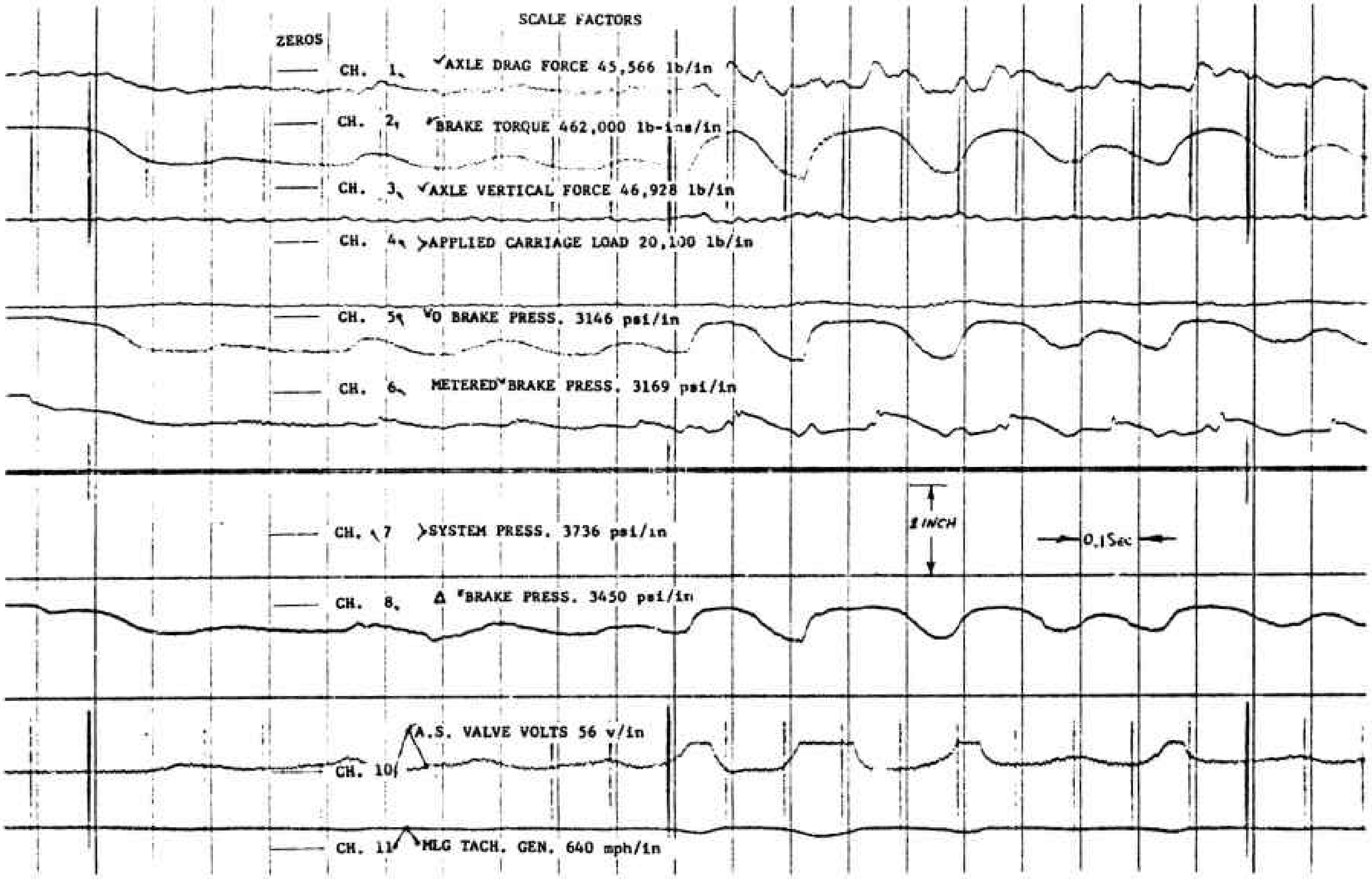

Figure 25 Expanded Time Scale Oscillograph Record of Test Condition No. 29

Figure 26 Analytically Predicted Antiskid Operation

Table 3 Computer Input Data for Test - Analysis Correlation

CENERAL DYNAMICS CONVAIR AEROSPACE DIVISION FORT WORTH OPERATION
6600 PROCEDURE A1C PROBLEM 463434-22 06/08/73 PAGE 0001

INPUT DATA

TIME BETWEEN STEPS= .2000E-03 SYSTEM RUN TIME = .1000E+01 SYSTEM PRINT INTERVAL = .1000E-02 CHECKOUT A6A MICROFILM OPT= 1

INTERNAL PRINT INTERVAL = .1000E-02

ACVRO = .7200E+00 ACVSO = .3400E+00 PCVB = .2500E+02 VMIN = .1600E+03 NR = 7

SIMPLIFIED BRAKE CONTROL

ALPHA=	.2500E-02	ALPHB=	.3900E-01	ABP=	.1330E+02	ABPS=	.6650E+01	ACR=	0.	ACVO=	0.
ACVL=	0.	CBPL=	.6650E+03	CBPU=	.4725E+05	CC=	.3530E+05	CSCVR=	.1200E+01	DC=	.2340E+02
ET=	.6500E-04	FNM=	.1300E+05	GCV=	.4700E-02	PBO=	.1800E+03	PCP=	.1600E+04	PFB=	.2190E+02
FR=	0.	RBT=	.6250E+01	RR=	.2280E+02	RTD=	.2173E+02	SCL=	.5000E-02	SCVO=	.3000E-01
SCVA=	.3500E-01	SCVR=	-.3500E-01	TCP=	.1000E+00	UB1=	.1500E+00	UB2=	.1000E+00	UT1=	.2000E+00
UT2=	.4500E+00	VF=	.2400E+04	VRO=	.4870E+02	WG=	.1550E+01	WTO=	.1053E+03	WIT=	.1630E+03
XCVO=	.3500E-01	XSCM=	.3600E+01	XSCR=	.1440E+02	XBO=	0.	XCO=	0.	XDGO=	0.
XFD=	0.	XFOO=	.2030E+03								

OPTION 2 WHEEL SPEED SENSOR

CWCC= .1147E+00 ESN= 0. EG= .1210E+02

CONTROLLER

CM=	.2300E+00	C404=	.2476E+04	C405=	.1060E+00	C406=	.6600E+02				
C407=	.1510E+01	C446=	.1825E-05	C447=	.1000E-08	C448=	.4650E-06	C449=	.1860E-05	C450=	.4740E-06
C451=	.1000E-08	C452=	-.1570E-05	C456=	.3400E-04	C457=	.2700E-07	C458=	-.1710E-04	C459=	.5200E-04
C460=	.2700E-07	C461=	.1325E-04	C462=	-.8340E-04	C526=	.1825E-05	C527=	.4650E-06	C528=	.4740E-06
C529=	.1860E-05	C530=	.1567E-05	C531=	.3400E-04	C532=	-.1710E-04	C533=	.1325E-04	C534=	.5720E-04
C535=	.8340E-04										
C565=	.3400E-04	C566=	.1400E-07	C567=	-.1710E-04	C568=	.1325E-04	C569=	.5200E-04	C570=	.1400E-07
C571=	.8340E-04	C575=	.1325E-05	C576=	.1000E-08	C577=	.4650E-06	C578=	.4740E-06	C579=	.1860E-05
C580=	.1000E-08	C581=	-.1570E-05								
C604=	.1610E-04	C605=	.7250E-05	C606=	.2920E+02	C607=	.1460E-05	C608=	.3700E+05	C609=	.3030E+07
C610=	.8333E+05	C611=	.2220E+06	C612=	.9010E+00	C613=	.5190E-05	C614=	.3600E+02	C615=	.3520E+03
C616=	.9200E+00	C617=	.3760E-05	C618=	.1000E-04	C619=	.7700E-05	C620=	.1000E-02	C621=	.6000E-03
C622=	.5460E-03	C623=	.5930E-03	C800=	.9940E+00	C801=	.9167E+04	C802=	.4290E-05	C803=	.5362E+03
C804=	.1091E-03	C805=	.5520E-03	C806=	.2166E+00	C807=	-.2304E-03	C808=	.2228E+03	C809=	.4530E-04
C810=	.1758E-03	C811=	.9300E-01	C812=	-.1501E-03	VC1=	.1208E+02	VC2=	0.	VC3=	0.
VC4=	0.	VC1D=	0.	VC2D=	0.	VC3D=	0.	VC4D=	0.	EV=	.1510E+01

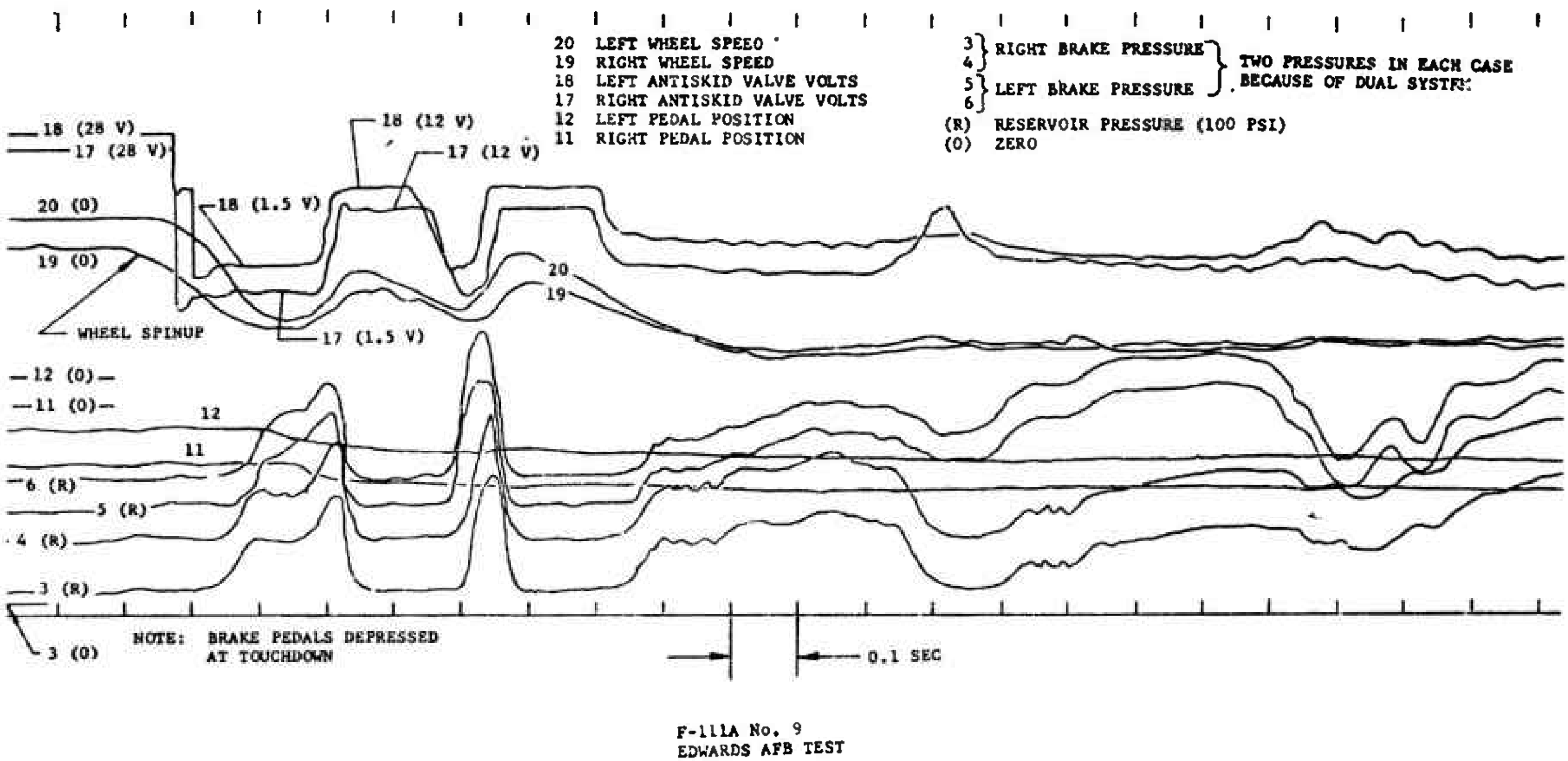

Figure 27 Antiskid Operation Recorded During Aircraft Landing

Force at Edwards Air Force Base, California. Many pertinent occurrences are shown on this record one of which is the brake pressure change rates. Records such as this were the basis for the pressure change rates expected during the testing phase of this program. It can be seen that for high rate valve voltage changes, the brake pressure changes on the airplane at about the same rate as was analytically predicted rather than as experienced during laboratory testing. To achieve agreement between analytical prediction and laboratory test result, the analytical parameters describing hydraulic flow restriction need to be modified to describe the laboratory test set-up. This could be done either by measuring the flow restriction in the laboratory (which should have been accomplished) or by trial and error experimentation with the analytical procedure. Neither has been accomplished. The differences in hydraulic flow restriction between the analytical prediction and the laboratory test set-up are primarily responsible for the different antiskid cyclic rates.

The failure of the analytical procedures to predict the operational characteristics of the antiskid control circuit modulating elements seems to be caused by two problems. The first is that for some undetermined reason, the computer program is not computing the same influence of capacitor C2 voltage upon antiskid valve voltage as a static check of the equations would indicate. The voltage of capacitor C2 controls the valve amplifier bias. Efforts toward finding the cause of this problem have not been successful. The second and most significant problem from a analytical viewpoint is that the "gain" for equations defining the current, AC2, which is charging capacitor C2, is so high that even with the .0002 second integration time step used, very large overshoots in capacitor C2 voltage occur. For this circumstance the valve amplifier bias is much too large which in turn causes the valve voltage to be too high. It is believed that the second difficulty is obscuring the cause of the first.

A related similar problem involving excessively high negative values of current AC4 was recognized prior to testing. Based on some experimental work accomplished by the Antiskid Engineering Department of the Goodyear Aerospace Corp., the value of R12, as shown on Figure A51 in Appendix A, was increased to limit the value of AC4 to an amount which could be analytically accommodated with a reasonable integration time step. This change in resistance value was previously mentioned in Section II. It is evident that a similar change could be implemented with regard to the excessively high positive values of current AC2.

The analytical difficulty experienced with the computation of antiskid control circuit parameter AC2, or any other parameter within the total system, should be recognized as typical of problems frequently encountered while attempting to mathematically analyze antiskid operation. For each instance a decision must be made to determine how the goals, toward which the analytical effort is directed, can be best accomplished either by implementing an appropriate simplifying mathematical technique so that a "brute force" solution is obtained, or by requiring some change be made to the equipment being evaluated. This decision is usually influenced by such factors as the analyst's experience, degree of prior equipment usage, cost of implementing the hardware change, consequence of enduring the problem, and the relative timing within the aircraft program when the problem is identified.

The specific analytical problem encountered during this program, wherein the equations for computing control circuit parameter AC2 have coefficients which necessitate an extremely small integration time step for obtaining a digital computer solution, could be resolved by any one of several ways. The practical significance of this analytical difficulty is that it indicates that the modulating circuit elements are susceptible to high frequency disturbances. If the problem is associated with circumstances where the absence of high frequency disturbance, such as brake squeal, can be assured, the best solution to the problem is to add a small resistance to current AC2 flow path so that its computation does not upset the whole analysis. For a case where the absence of high frequency disturbance cannot be assured it would be prudent to actually modify the antiskid circuit to reduce the "gain" on current AC2. For this second instance, the analytical difficulty is the definition of a real problem. It can be expected that similar situations regarding brake torque or hydraulic pressure computations may occur.

For the F-111 type Goodyear modulated antiskid circuit, the modulating elements susceptibility to high frequency disturbance is a very marginal situation in that actual occurrence of any indication of this effect during aircraft operation is extremely rare; however, such indication has occasionally occurred. When the digital computer solution was attempted with a 0.001 second integration time step, antiskid circuit operation was totally inhibited by capacitor C2 voltage overshoots. With the .0002 second time step computer solution, as shown on Figure 26, the valve signal "noise" during the last few cycles indicates that

the same inhibition is about to occur. If such analytical result had been available at the time this circuit was being formulated, it is very probable that some suitable corrective action would have been incorporated.

A significant aspect of the analytical procedures used for the test data correlation is type of computation equipment which was utilized. The digital computer solution using discrete time step integration will help identify some real incompatibilities within the brake system. However, the appearances of these incompatibilities may be exaggerated if the integration time step is not fairly small. The experience of this program is that, in general, the necessity for using an integration time step shorter than .0002 seconds to avoid computation difficulties indicates a situation where real incompatibility exists.

SECTION V

FLUIDIC CONTROLLED PNEUMATIC BRAKE ACTUATION SYSTEM DESIGN STUDY

Research studies have been conducted at Convair Aerospace and elsewhere to evaluate the application of fluidic control elements to aircraft wheel brake antiskid control systems. The results of the studies indicate that there is good potential for achieving more dependable braking system operation if a fluidic controlled brake actuation system is used instead of the more conventional hydraulic actuation system. The areas of primary improvement are reduced fire hazard and more constant antiskid control operation over a wide temperature range. For the case of modern carbon disc brakes which are operated at extremely high temperature, the fire hazard associated with hydraulic actuation is particularly significant. As an initial step in the evaluation of a fluidic controlled pneumatic braking system, antiskid brake control system components which are physically and functionally suitable for airplane usage have been designed. By having performed such detail design it is possible to establish the effects, if any, upon the other aircraft systems and components which might be required if the fluidic controlled pneumatic brake actuation system were installed. Such consideration is also necessary during the design of the components.

Figure 28 shows a block diagram of a fluidic controlled pneumatic braking system incorporating a modulated antiskid feature. For laboratory test evaluation the 3000 psi stored nitrogen pressure supply would be used. An aircraft installation might use either a stored nitrogen supply or a high pressure compressor combined with a smaller storage capacity.

Figure 29 shows a modulator type fluidic wheel speed sensor unit which is physically interchangeable with the F-111 D.C. electrical tachometer. The sensor consists of two-proximity sensors excited by a wheel driven slotted cup. The output of the sensors, a frequency signal, is the input to a frequency-to-analog converter module. The converter wheel speed signal is filtered and amplified to produce a linear analog output signal that is linearly proportional to wheel speed. The circuit diagram of the fluidic wheel speed sensor is shown on Figure 30.

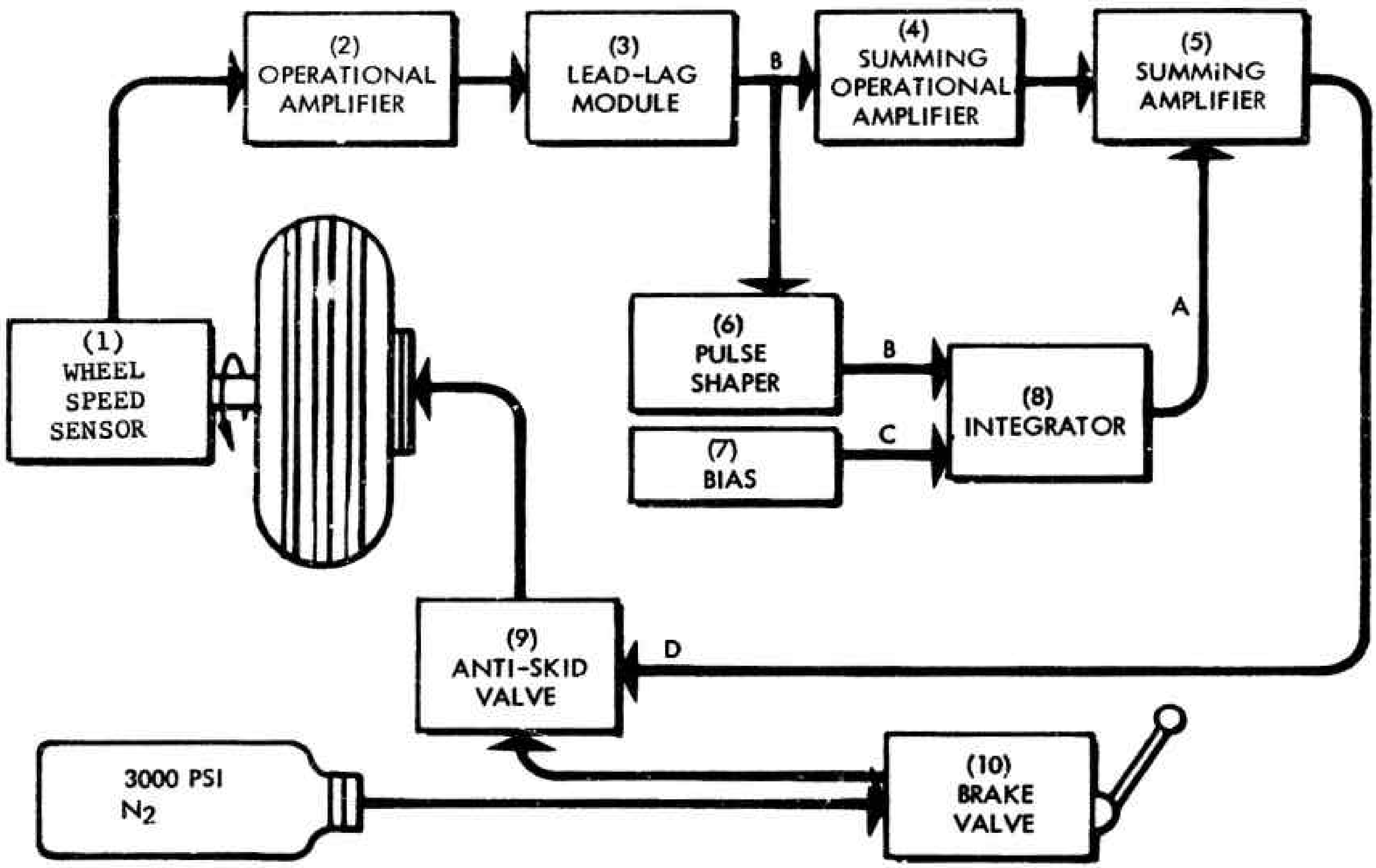

Figure 28 Fluidic Controlled Pneumatic Braking System

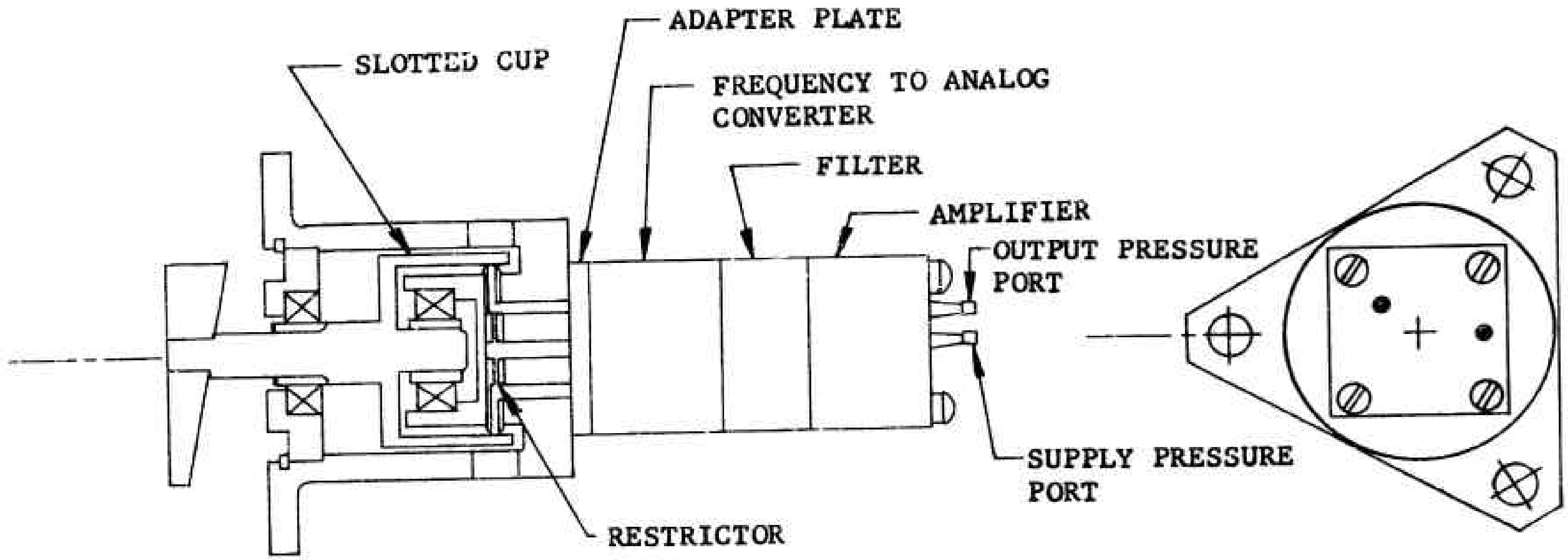

Figure 29 Fluidic Wheel Speed Sensor

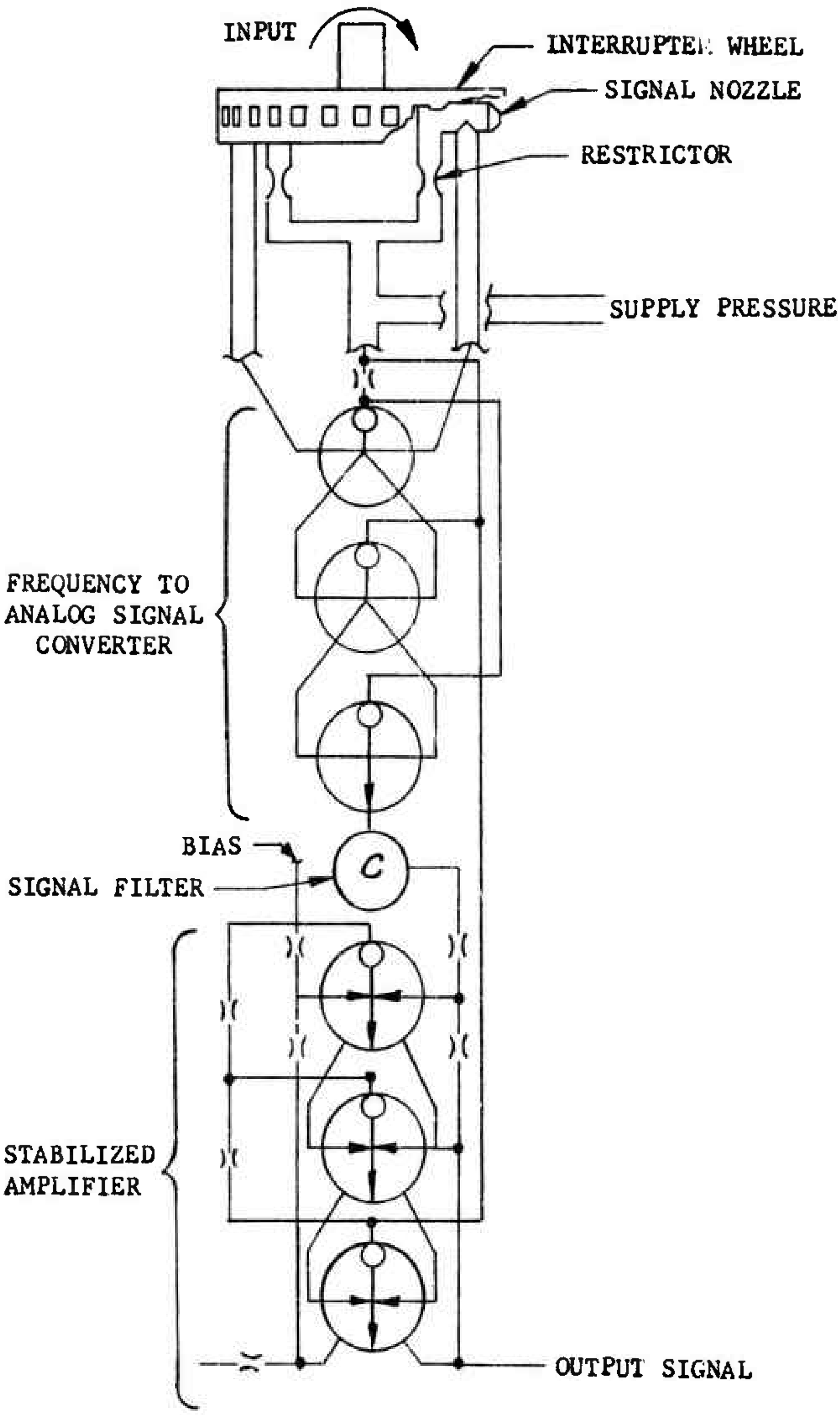

Figure 30 Fluidic Wheel Speed Sensor Schematic/Circuit Diagram

Figure 31 is a schematic showing how a F-111 hydraulic antiskid valve would be modified for pneumatic actuation by a pressure signal from a fluidic control circuit. To permit pneumatic actuation the electric linear force motor is replaced by a pressure bellows type linear force motor. For a limited evaluation test the hydraulic valve could be used for pneumatic pressure control if proper lubrication provisions are employed. For sustained pneumatic application the valve spool materials and perhaps a noninterflow poppet type second stage would be required; however, such a valve would have the same basic size, weight and cost as the hydraulic valve.

Since the fluidic control system will operate by relatively low level pneumatic pressure signals, it is necessary that all the control elements be physically located in close proximity to each other and the valve be located as close to the brake as is practical. The exact physical arrangement of the control circuit elements needs to be tailored to each application. The control circuit consists of items 2 thru 8 as shown on Figure 28. Item 2 is an operational amplifier providing gain and signal stability for the wheel speed sensor input to the lead-lag module. The lead-lag module, Item 3, is used for differentiating the wheel speed signal to produce a wheel acceleration signal. Item 4 is a variable gain operational amplifier for gain and impedance matching. A multi-input amplifier, identified as Item 5, is used for summing acceleration and bias circuit signals. The bias control circuit consists of Items 6, 7 and 8. The pulse shaper accepts and acceleration input signal and generates an output pulse of constant amplitude and adjustable time duration whenever the acceleration reaches a threshold value. The bias input consists of a linear restrictor. Integration is performed by a delayed (R-C) positive feedback circuit. These fluidic control circuit elements for one wheel can be packaged in a volume about two times as great as that for the equivalent electronic circuit elements - a space 3 x 3 x 4 inches. However, for many aircraft such as the F-111, these fluid elements could be installed inside the axle in a space not suitable for the electronic circuit elements or much of anything else.

The cost of a single set of fluidic components for laboratory evaluation is about four times as great as the production electric system; however, in comparable quantities the fluidic units would be approximately the same price and the electric units based on current catalog prices for fluidic elements. A major advantage of the fluidic system components is their ability to withstand intense vibration and high temperature. From this brief design study it has been concluded that fluidic control of a pneumatic brake actuation system can be practically accomplished.

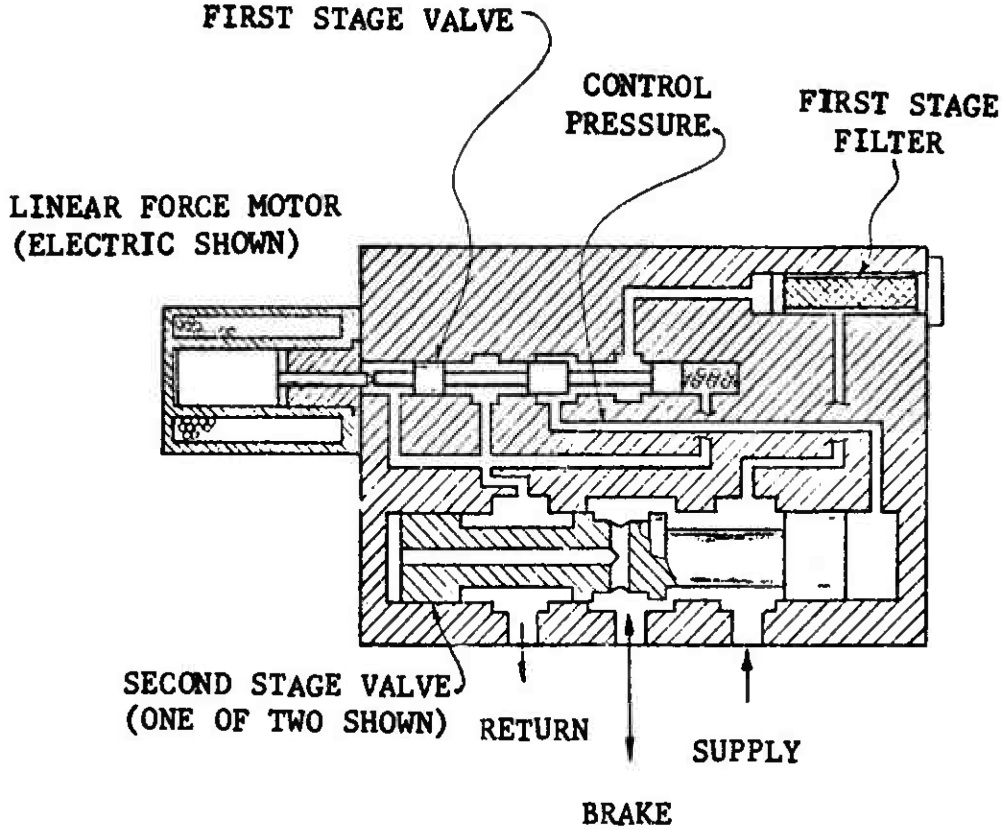

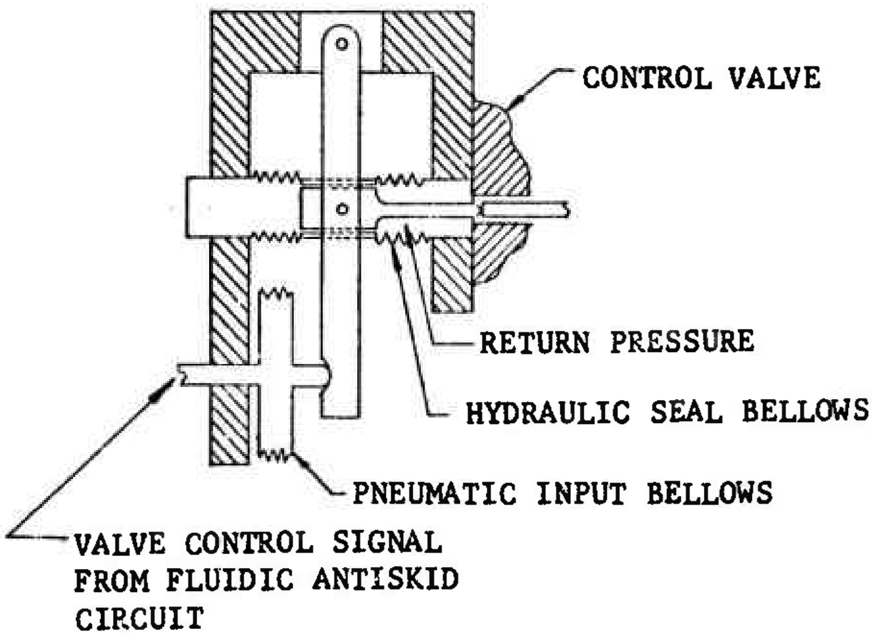

PNEUMATIC LINEAR FORCE MOTOR

Figure 31 Adaption of an Electrical Antiskid Valve for Pneumatic Actuation

REFERENCES

1. Smiley, Robert F. and Horne, Walter B. Mechanical Properties of Pneumatic Tires with Special Reference to Modern Aircraft Tires. NASA TR R-64.

2. Leland, T. J. W. and Taylor, G. R. Effects of Tread Wear on the Wet Runway Braking Effectiveness of Aircraft Tires. J. Aircraft Vol. 2 No. 2, March - April 1965.

3. Horne, W. B. and Leland, T. J. W. Influence of Tire Tread Pattern and Runway Surface Condition of Braking Friction and Rolling Resistance of a Modern Aircraft Tire. NASA TN D-1376.

4. Parker O-Ring Handbook, Parker Seal Company, Culver City, California, Cleveland, Ohio. Catalog 5700, June 1957

5. Daugherty, R. L. and Ingersoll, A. C. Fluid Mechanics McGraw-Hill 1954.

6. Blackburn, J. F., Reethof, G., and Shearer, J. L. Fluid Power Control. The M. I. T. Press 1960.

7. Lee, L. T. A Graphical Compilation of Damping Properties of Both Metallic and New Metallic Materials. AFML-TR-66-169. May 1966.

8. Ungar, E. E. and Hatch, D. K. High Damping Materials Prod. Eng. Vol. 32, No. 16, pp. 44-56, April 17, 1961.

9. Campbell, James E. Investigation of the Fundamental Characteristics of High Performance Hydraulic Systems, USAF Technical Report No. 5997, June 1950 ATI No. 91966.

10. Tanner, J. A. and Batterson, S. A. An Experimental Study of the Elastic Properties of Several Aircraft Tires During the Application of Braking Loads. Langley Working Paper 592. May 6, 1968.

11. Morris, J. G. Three Track Elevation Profiles Measured at Two United States Government Installations. NASA TN D-5545.

REFERENCES

(Continued)

12. Thomson, W. T. Mechanical Vibraticns. Prentice-Hall, Inc. 1953.

13. Technical Manual No. T. O. 4BA8-22-3, Overhaul Instructions with Illustrated Parts Breakdown, Skid Control Box Part No. 9543941 (Goodyear)

14. Transistor Circuit Design, Engineering Staff of Texas Instruments, Inc., Edited by Joseph A. Walston and John R. Miller, McGraw-Hill Book Co. 1963

15. Riddle, Robert L. and Ristenbatt, Marlin P. Transistor Physics and Circuits. Prentice Hall 1958.

16. Nanavati, Rajendra P. An Introduction to Semiconductor Electronics, McGraw-Hill Book Company 1963.

17. Batterson, Sidney A. A Study of the Dynamics of Airplane Braking Systems as Affected by Tire Elasticity and Brake Response. NASA TN D-3081

APPENDIX A

MATHEMATICAL MODELS

The analysis of antiskid operation is conducted using a modular approach whereby the problem is divided into several component parts, each having inputs and outputs defined so that the outputs from one or more components are provided as inputs to other components. By combining all the analytical components, a composite simultaneous solution is obtained. This Appendix lists analytical models formulated to mathematically describe the following aircraft components or systems (the computer program subroutine identification is given within parentheses after each item):

1. Brake Assembly
   (Brake System)
2. Brake Actuation Hydraulic System
   (Hydraulic System)
3. Vehicle and Wheel Structural Support
   (Airplane System)
4. Wheel and Tire
   (Wheel and Tire System)
5. Antiskid Wheel Speed Sensor
   (Wheel Speed Sensor)
6. Antiskid Control Circuit
   (Antiskid Control Circuit)
7. Antiskid Control Valve
   (Antiskid Control Valve)
8. Aerodynamic Control Surface Positioning System
   (Horizontal Tail Control)
9. Runway Profile
   (Runway System)

These component mathematical models are the same as those initially developed under Air Force Contract F33615-70-C-1004 as described in Report No. AFFDL-TR-70-128 except for corrections or modifications which have been incorporated as a result of analytical refinement conducted during this program. The analytical components are combined into composite solutions for three cases: 1. A laboratory inertia dynamometer set-up, 2. An airplane having three degrees of freedom (i.e., longitudinal and vertical translation and pitch rotation), 3. An airplane having six degrees of freedom (i.e., longitudinal, vertical and lateral translation and pitch, roll and yaw rotation). For the case of the

laboratory dynamometer set-up, two versions of the composite solution are provided. The first is the same as that previously described in Report No. AFFDL-TR-70-128 which utilizes the same analytical components as the airplane solutions and the second is a simplified solution combining all the analytical components with minimal mathematical complexity and is described in report Section III.

Alternate mathematical models have been formulated for some of the analytical components. These alternate mathematical models are listed in the applicable sections alphabetically and are provided for instances where they are needed to describe more than one type of equipment which might be used such as antiskid control circuits, where there are analytical benefits to be gained by utilizing a less complex mathematical model for circumstances where a more complex model is not required, or where modifications are needed for their proper application within the various composite solutions.

Format and Convention Usage

The presentation of the analytical component mathematical models follows a common format insofar as practical. The section describing each analytical component begins with an introductory explanation of its function or its characteristics relevant to antiskid operation. Following this introduction is the main body of the discussion under the heading, "A. Mathematical Description," containing the derivation of the equations that describe the system dynamically. This section is concluded with an equation flow diagram showing the relationship among the various system equations. A final discussion follows under the heading, "B. Parameter Evaluation," which sets forth methods of determining the values of the constants appearing in the system equations. The system presentation closes with a "Table of Parameters" which lists all of the system variables and constants.

The flow diagram which appears at the end of Section A is provided principally as an aid in the preparation of the digital computer program which solves the system equations. This flow diagram could also be used for an analog solution. The following conventions apply as to the usage of the flow diagrams: The triangles outside the enclosing phantom line denote variables which are used as inputs and outputs to other systems. The numbered rectangles refer to equations within the system. As an example, in Figure A3 the rectangle

numbered 9 indicates that T_{BT} is a function of μ_B and F_B and that the equation that gives the exact relationship is equation 1.9. No constants are shown in these diagrams. The triangles denoting integrators do not always contain an equation number. If the input to an integrator is $\dot{X}_P$ and its output is X_P, then the equation is implied. Thus, as in Figure A64, if the input to an integrator is $R4$ and the output is μ_{R4}, then the equation $\mu_{R4} = \int R4\,dt$, or equivantly, $\dot{\mu}_{R4} = R4$, is implied. Because of the size of the six degree airplane system, the flow diagram in Figure A32 is slightly different. Its use is strictly limited to the digital program generation. It says that all equations within one block must be written before proceeding to the next block. Thus, the first variables to be solved for are $\dot{Z}_{SN}$, Z_{SN}, Y_{DLN}, •••, S_{ML}. After this F_{VN}, F_{LN}, •••, Z_{GLR} are solved for.
After this X_{AXL}, $\dot{X}_{AXL}$, •••, F_{NN} etc.

The "Table of Parameters" is a listing of all variables and constants found in the equations of that system. Each variable is identified by its symbol, description, units, and "Type." The "Type" is listed a v, v(i), and v(o) depending on whether the variable is only used within the system, is received as an input from another system, or is an output to another system. Each constant is identified by its symbol, units, description, "type," and value. The "type" for each constant is always "c" and its value is that used with the F-111 antiskid system.

Table A1 lists the mathematical conventions utilized throughout this study.

Table A1 Explanation of Mathematical Convention

Convention	Description
$\dot{X}$	A dot over a variable denotes differentiation with respect to time
Computer Notation	All variables are expressed in a form to harmonize with Fortran character utilization. Thus a variable W_{TE} would appear as WTE Also, in general, the following practice is adhered to. If X_{TT} is a variable, then XTT is its Fortran form. The symbol for $\dot{X}_{TT}$ is XTTD. The symbol for $\ddot{X}_{TT}$ is XTTDD. The initial condition is denoted by adding 0 (zero). Thus $\dot{X}_{TT}$ at time = 0 is denoted by XTTDO.
$Z_{GD}\langle x \rangle$	The brackets "$\langle\ \rangle$" are used exclusively to denote the position of a function argument. The script x is used to denote an arbitrary variable. The parentheses "( )" are normally used to denote multiplication.
$\lvert T_{BT} \rvert$	Placing a parameter symbol between two vertical bars denotes the absolute value of the parameter. The absolute value of a signed number N is defined as N when N is positive and as -N when N is negative. For example: $\lvert 3 \rvert = 3$ and $\lvert -3 \rvert = 3$.
$MIN\{X_1, X_2, \cdots X_N, C_1\}$ OR $MAX\{X_1, X_2, \cdots X_N, C_1\}$	The braces preceded by "MIN" or "MAX" denote the value of the least (or largest) of the constant or the parameters enclosed within the braces.

Three different total system mathematical models have been formulated to perform antiskid analysis. The first model which is referred to as the flywheel system represents an antiskid system installed on a wheel and brake which are mounted on a dynamometer. The second system, referred to as the three degree system, represents an antiskid system installed on a wheel and brake mounted on a rigid airplane which is allowed three degrees of freedom (longitudinal translation down the runway, translation vertically, and pitch rotation). The third system, referred to as the six degree system, represents a rigid airplane having all six degrees of freedom and equipped with a conventional single wheeled main landing gear incorporating independent antiskid control of each brake. All of these systems are created utilizing the models described in Section III. The basic reason for utilizing three models is economics. The six degree system takes at least twice as long to run as the flywheel system and not all antiskid system parameters require the sophistication of the six degree system. However, it might be necessary to check certain effects under the most comprehensive circumstances.

The "Basic Control System" is made of the following elements:

1. Brake System
2. Hydraulic System
3. Wheel Speed Sensor
4. Control System
5. Antiskid Control Valve

To form the flywheel system, the "Basic Control System" is combined with the 3a. Airplane System (Flywheel), 4a. Wheel and Tire System (Flywheel), and the 9a. Runway System. To form the three degree system, the "Basic Control System" is combined with the 3b. Airplane System (3 Degree), 4b. Wheel and Tire System (3 Degree), 8. Horizontal Tail Control System, and 9a. Runway System. The six degree system incorporates two separate "Basic Control Systems" and two separate 4c. Wheel and Tire Systems. These are combined with a 3c. Airplane System (6 Degree) which utilizes the

8. Horizontal Tail Control and 9c. Runway System (6 Degree). When utilizing the "Basic Control Systems" with the six degree system, the variables communicating with the airplane model are reidentified to correspond to the right or left side of the airplane. Thus, X_{AXR} is X_{AX} in the right side and X_{AXL} is X_{AX} in the left side.

The high degree of modularity used in this analysis is desirable for three reasons. The first reason is that it is easy to combine the component models together to form different types of overall systems. This is true not only from modeling considerations but especially from programming aspects. As an example, the only basic change required to accommodate a twin or tandem gear would be to remodel the strut in the airplane system. The second reason for modularity is the difficulty in being completely general. Should a component arise which is not described by the existing models, it is easy to create a new program for the new model without having to modify the operation of other systems. Thus, from the programming point of view, to incorporate a new wheel speed sensor for example, the new model program can fall back on the existing read, write, and logic statements of the existing wheel speed model. The input and output variables of the new component model are automatically incorporated properly into the overall computational procedure, unless some new variables are defined. The following flow diagrams show the relationships between the various elements in the composite solutions.

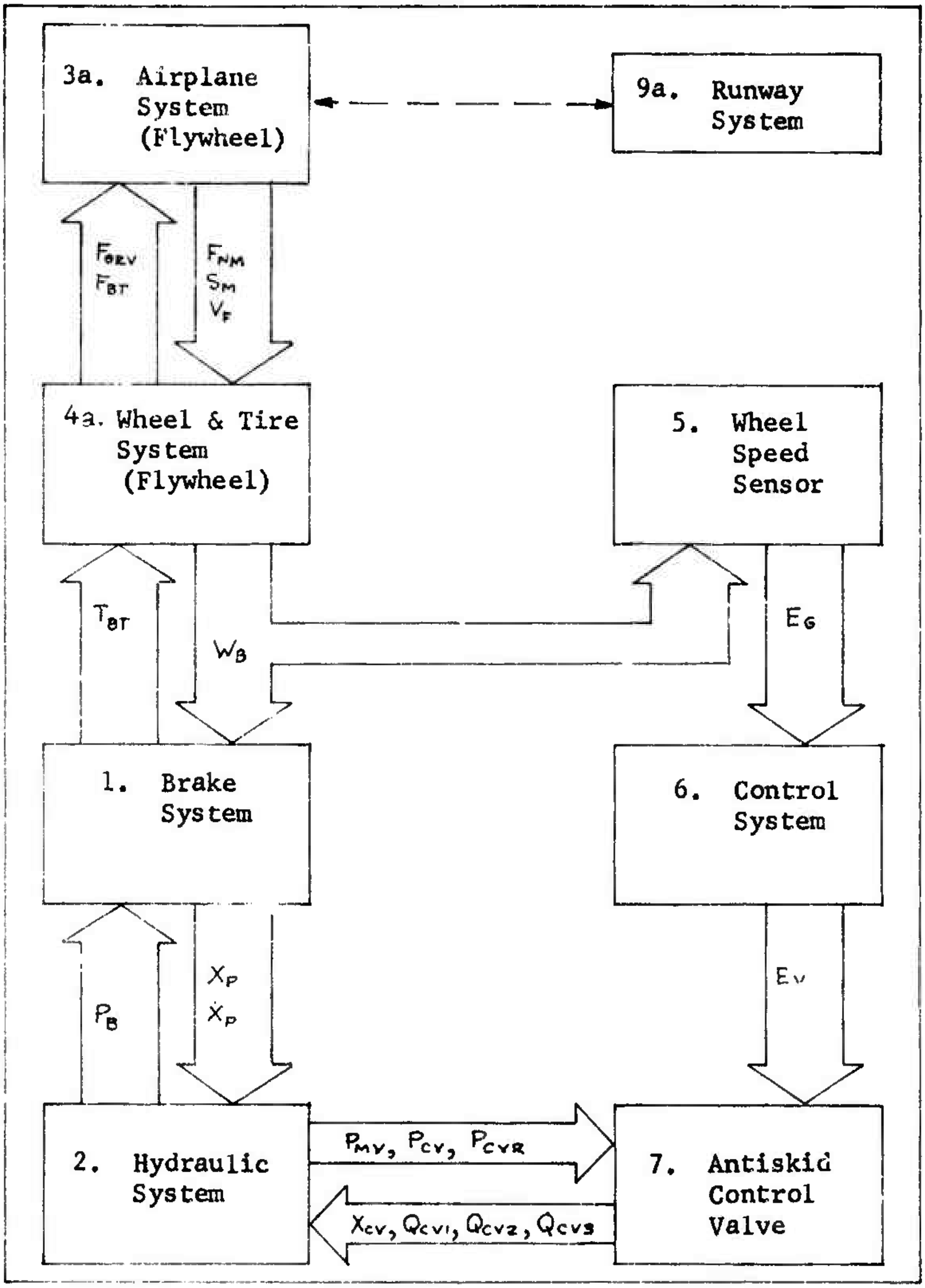

Flywheel System Composite Solution Flow Diagram

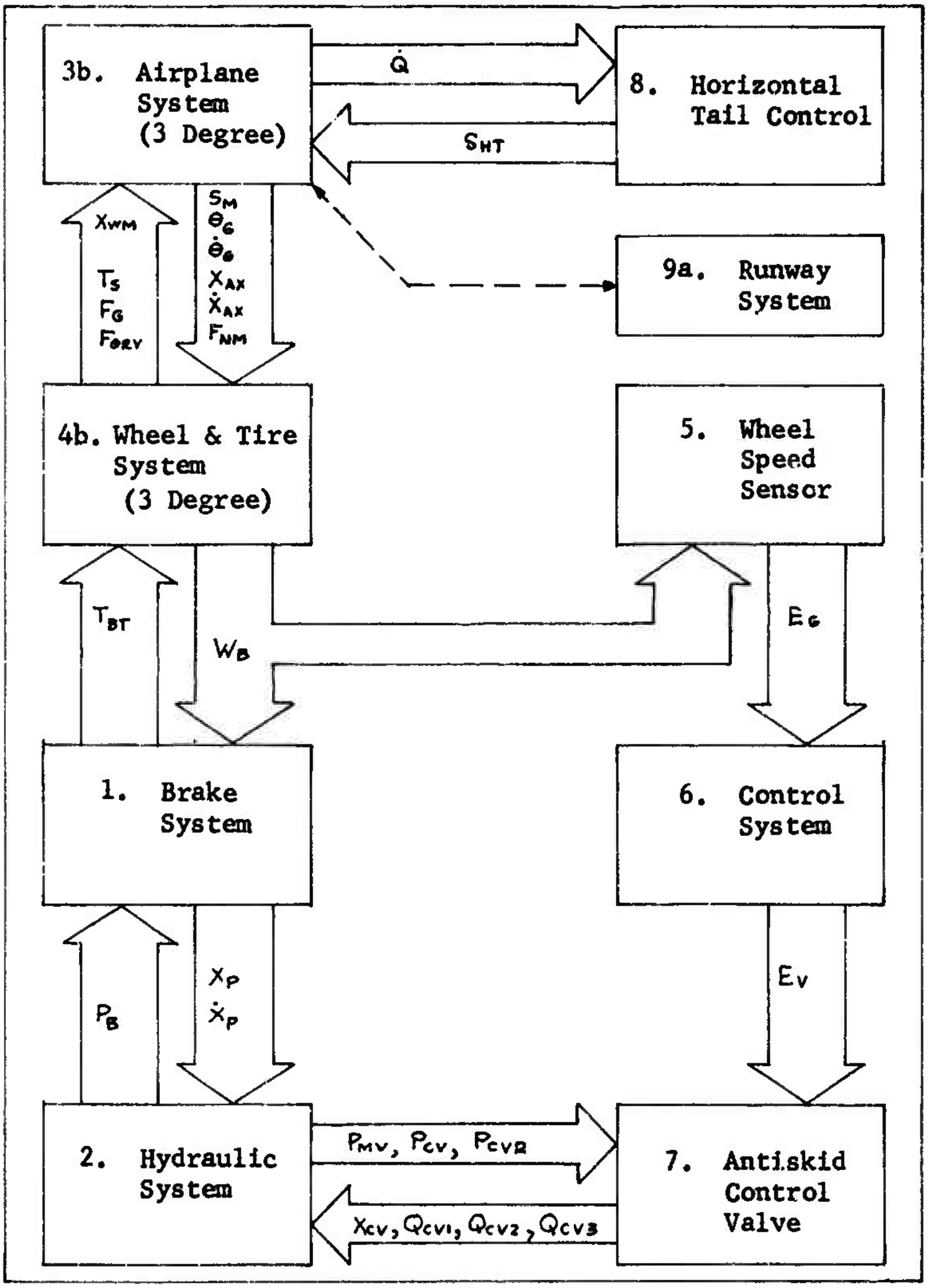

Three Degree System Composite Solution Flow Diagram

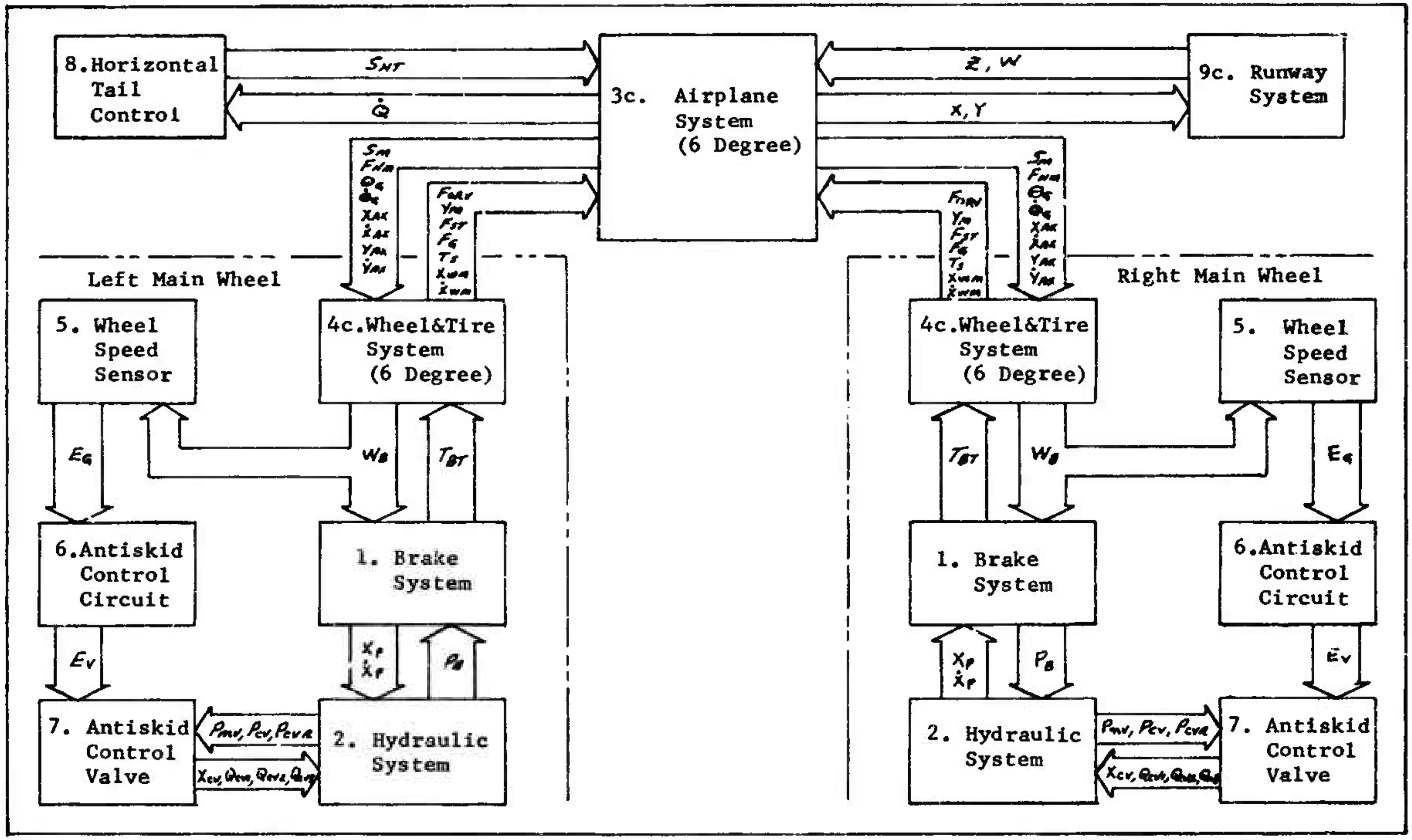

Six Degree System Composite Solution Flow Diagram

1. BRAKE ASSEMBLY

The conventional airplane brake consists of a series of discs which are alternately stators and rotors. The stators are restrained from rotating about the axle by splines or keyways. The rotors are similarly connected to the wheel and hence rotate with the wheel and tire. The brake torque is produced by axially compressing the disc stack; usually by hydraulically actuated pistons. Many brakes use return springs to release the brake stack against the return pressure of the hydraulic system. The amount of dynamic torque which is produced by the brake at any instant is the product of the friction force between the rubbing surfaces and the radial distance between the friction force and the axis of wheel rotation. The friction force ia the product of the normal force between the rubbing surfaces and the friction coefficient. A more simple mathematical treatment of the brake is a part of the simplified Antiskid Analysis Procedure.

A. Mathematical Description

In this analysis X_P will denote the brake piston linear displacement. The pistons, rotors, and ststors sre treated as a single mass system in the axial mode (X_P direction). The forces acting on the brake mass in the axial mode are:

a. Brake actuation force: equals(brake pressure) x (piston ares)
b. Force due to axial restraint
c. Keyway friction force
d. Brake piston seal friction force
e. Brake return spring force
f. Brake piston bottoming force

Figure A1 shows the brake system and the forces acting in the axial mode. Each of the axial forces is established as follows:

a. Brake Actuation Force

The brake actuation pressure P_B is received as an input from the hydraulic system. The brake actuation force is given by $P_B A_{BP}$, where A_{BP} is the total brake piston area.

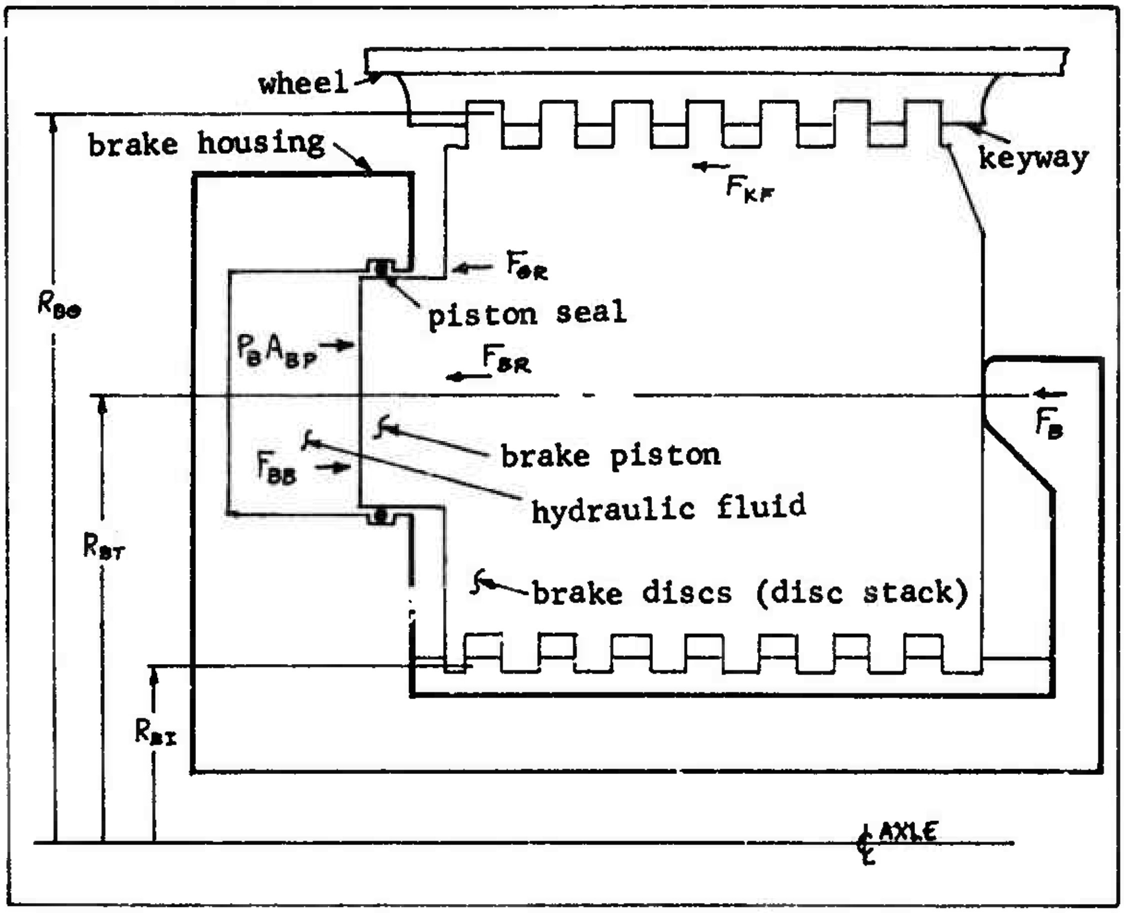

Figure A1 Forces Acting on the Brake Discs

b. Force due to Axial Restraint

The axial restraining force reflects the elasticity in the brake discs, the back plate, and the piston housing and is a function of their cumulative displacements. A way to derive this characteristic is from a curve of brake volumetric displacement vs. brake pressure. This characteristic does not include friction or return spring effects.

Let F_B denote the force due to axial restraint. And be defined by

(1.1) $$F_B = F_{B1} + F_{B2}$$

(1.2) $$F_{B1} = \begin{cases} C_{B1}\,(X_P - S_{B1}) + D_{B1}\,\dot{X}_P & \text{IF } X_P \geq S_{B1} \\ 0 & \text{IF } X_P < S_{B1} \end{cases}$$

(1.3) $$F_{B2} = \begin{cases} C_{B2}\,(X_P - S_{B2}) + D_{B2}\,\dot{X}_P & \text{IF } X_P \geq S_{B2} \\ 0 & X_P < S_{B2} \end{cases}$$

c. Keyway Friction Force

Let the keyway friction characteristic be defined by a function, G_F, as shown in Figure A2 and expressed mathematically as:

(1.4) $$G_F = \begin{cases} 1.0 & \text{IF } \dot{X}_P \geq V_{FS} \\ G_{FM} + (1 - G_{FM})\,\dot{X}_P / V_{FS} & \text{IF } V_{FS} > \dot{X}_P > 0 \\ 0.0 & \text{IF } \dot{X}_P = 0 \\ -G_{FM} + (1 - G_{FM})\,\dot{X}_P / V_{FS} & \text{IF } 0 > \dot{X}_P \geq -V_{FS} \\ -1.0 & \text{IF } -V_{FS} \geq \dot{X}_P \end{cases}$$

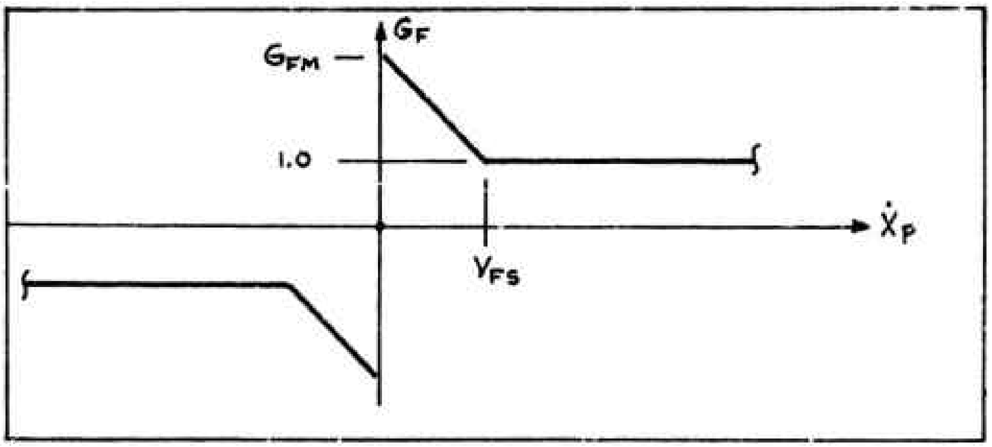

Figure A2 Keyway Friction Characteristic

The brake torque, T_{BT}, is tranferred to the wheel and tire through the rotor keyways. Torque, T_{BT}, is also transmitted to the axle. The major portion is transmitted through the stator keyways. The remaining portion of the torque is transmitted as piston side loading which results from friction between the pistons and the pressure plate. Let 100 H_{B1} denote the percentage of brake torque transferred through the stator keyways and let 100 H_{B2} denote the percentage of torque transferred through the pistons. Naturally, $H_{B1} + H_{B2} = 1$. The normal force on the stator keys is thus $H_{B1}|T_{BT}|/R_{BI}$, while the normal force on the rotor keys is $|T_{BT}|/R_{BO}$. The total keyway friction force is then given by

$$(1.5) \quad F_{KF} = |T_{BT}|\, G_F\, \mu_K \left(H_{B1}/R_{BI} + 1/R_{BO}\right)$$

d. <u>Brake Piston Seal Force</u>

Let F_{OR} denote the seal friction force. Then

$$(1.6) \quad F_{OR} = G_F \left(H_{OFC} + H_{OFP} P_B + |T_{BT}|\mu_{rp} H_{B2}/R_{BT}\right)$$

e. Brake Return Spring Force

The piston return force F_{BR} is given by

$$(1.7) \quad F_{BR} = F_{BRO} + C_{BR} X_P$$

f. Brake Piston Bottoming Force

In the brake released condition, an axial force is developed between the pistons and housing to balance return spring preload. This piston bottoming force is defined as:

$$(1.8) \quad F_{BB} = \begin{cases} -C_{BB}(X_P - S_{BB}) - D_{BB}\dot{X}_P & \text{FOR } X_P \le S_{BB} \\ 0 & \text{FOR } X_P > S_{BB} \end{cases}$$

This concludes the discussion of the axial brake forces.

Let R_{NR} be the number of rotors. Let W_B be the relative angular velocity between the rotors and stators as received from the wheel and tire system. The brake torque T_{BT} is then given by

$$(1.9) \quad T_{BT} = 2 R_{NR} F_B R_{BT} \mu_B$$

Where μ_B is:

$$(1.10) \quad \mu_B = \begin{cases} \mu_{B1} + \mu_{B2} e^{-\alpha_B V_B} & \text{IF } V_B > 0 \\ 0 & \text{IF } V_B = 0 \\ -\mu_{B1} - \mu_{B2} e^{+\alpha_B V_B} & \text{IF } V_B < 0 \end{cases}$$

Where V_B is:

$$(1.11) \quad V_B = R_{BT} W_B$$

Summing the forces in the axial direction yields:

$$(1.12) \quad W_{BE} \ddot{X}_P = P_B A_{BP} - F_B - F_{KF} - F_{BR} - F_{BR} + F_{BB}$$

In Equation (1.12) W_{BE} is the brake mass which experiences axial motion. Generally, W_{BE} is the brake heat sink mass. Figure A3 shows the relationship of the brake system equations. Table A2 lists the system parameters.

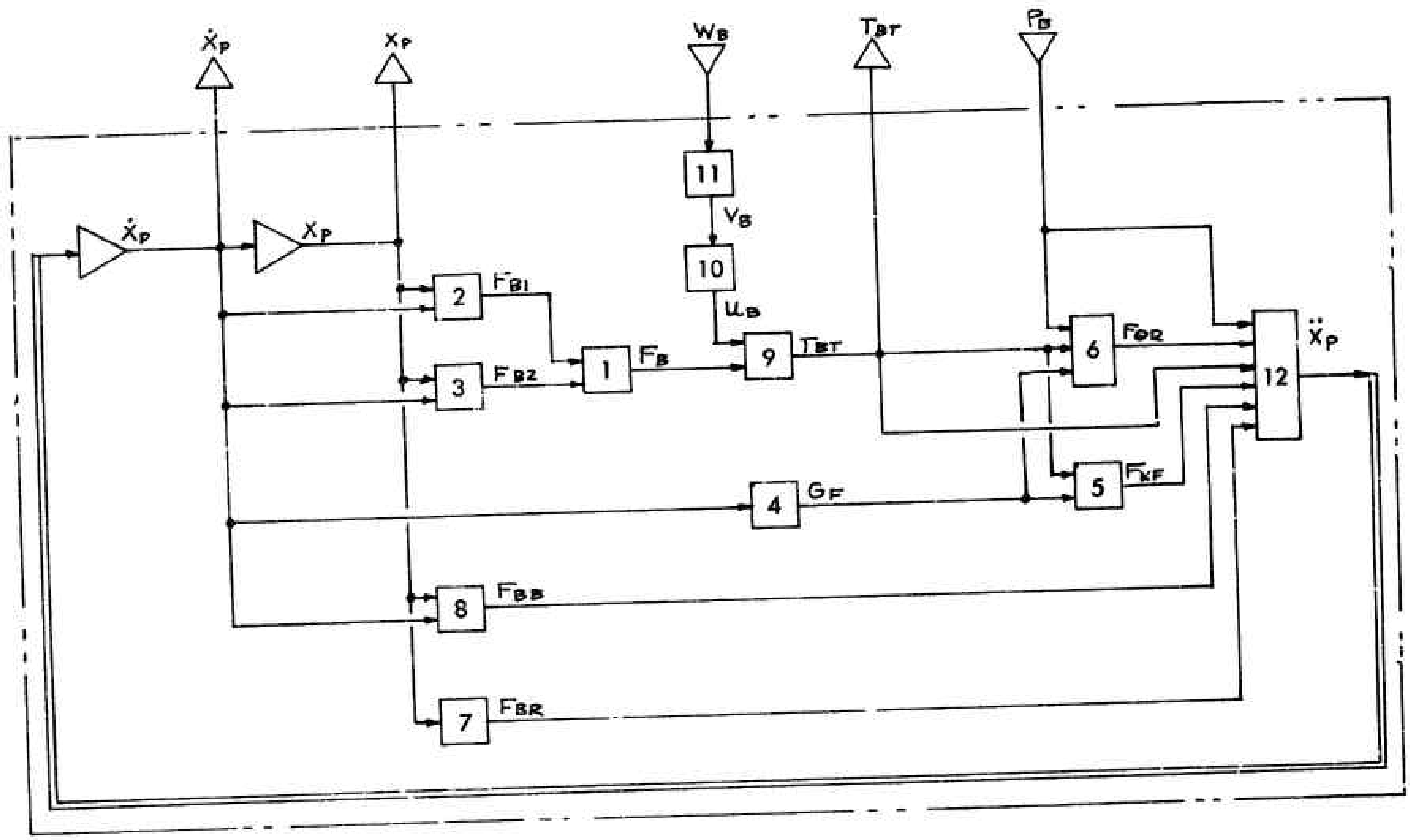

Figure A3 Brake Assembly Equation Flow Diagram

B. Parameter Evaluation

Figure A4 shows a plot of brake piston displacement as a function of brake application pressure for a new brake.

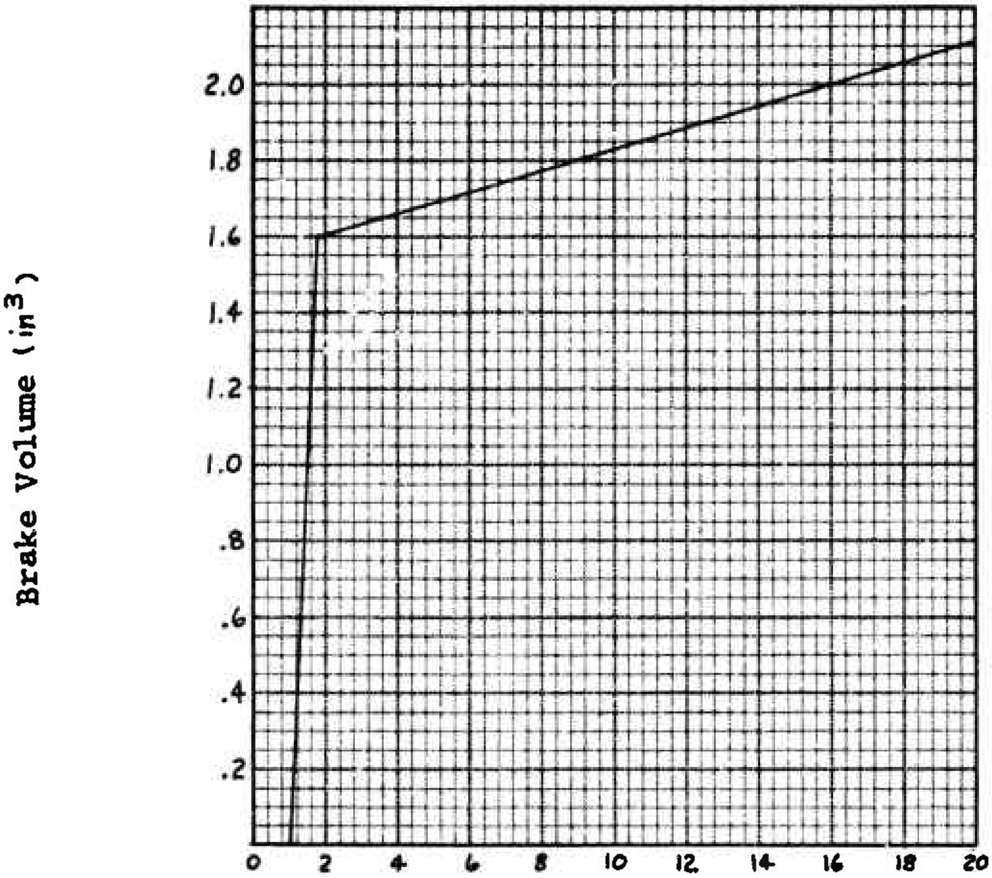

Figure A4 Brake Pressure Volume Characteristic

Assuming that no frictional effects are present, C_{BR} and C_{B1} can be derived as follows: Since the initial slope is due to spring return force only, then

$$(1.13)\quad C_{BR} = \left(\frac{\Delta P}{\Delta V}\right) A_{BP}^2 = \left(\frac{80}{1.6}\right)(13.3)^2 = 8850 \text{ lb/in}$$

From the other slope on the curve,

$$(1.14)\quad C_{B1} = \left(\frac{\Delta P}{\Delta V}\right) A_{BP}^2 = \left(\frac{1420}{.4}\right)(13.3)^2 - 8850 = 6.20\times 10^5 \text{ lb/in}$$

For a new brake $C_{B2} = 0$.

Assuming that the discs all move together, since the heat sink weight is 138 LBM, then W_{BE} = 138/386 = .358 LBF SEC^2/IN. The natural frequency is then $\omega_n = \sqrt{K/m}$ OR $\omega_n = \sqrt{(6.2\times10^5)/(.358)}$ = 1315 RAD/SEC

Assuming that η = .01 (see page 117),

$$(1.15) \quad D_{B1} = \frac{\eta C_{B1}}{\omega_n} = \frac{(.01)(6.2\times10^5)}{(1315)} = 4.71 \text{ lbf sec/in}$$

It is assumed that X_p = 0 when the brake pressure is 100 psi. Thus

$$(1.16) \quad F_{BPO} = A_{BP} P_B = (13.3)(100) = 1330 \text{ lbf}$$

Since the brake piston displacement is 1.55 IN^3 before the brake discs come into contact, then S_{B1} = 1.55/13.3 = .1165 in.

Since the F-111 brake has 8 stators with 14 rubbing surfaces, H_{B1} cannot be greater than 1/14. A conservatively high value of H_{B1} = .05 has been assumed and it follows that H_{B2} = .95.

The brake piston seals are equivalent to MS28775-219. The seal friction force is established using the procedures described in Reference 4. The seal sliding friction force is a function of rubber compound hardness, amount of installed compression, length of rubbing surface, seal groove projected area and applied hydraulic pressure. For the MS28775-219 size seal having 10 percent installed compression and 70 degree Shore A hardness the sliding friction force is 2.88 lbf plus 0.02 lbf per psi applied pressure per seal. There are 10 pistons in the brake housing; therefore,

$$(1.17) \quad H_{OFC} = (10)(2.88) = 28.8 \text{ lbf}$$

$$(1.18) \quad H_{OFP} = (10)(0.02) = 0.20 \text{ lbf/psi}$$

Conservatively high values for the friction coefficients μ_K and μ_{KP} are estimated as μ_K = .15 and μ_{KP} = .10. G_{FM} is estimated to be 1.50.

Values for the following brake dimensional characteristics are then from the appropriate brake component drawings: R_{BI} = 4.40 IN, R_{BT} = 6.25 IN, and R_{BD} = 8.25 IN.

Observations of braking stops indicate that for an average F-111 brake lining,

$$U_{B1} = .15$$

$$U_{B2} = .10$$

$$\alpha_B = .03 \text{ SEC/IN}$$

Table A2 Brake Assembly Parameters (Sheet 1 of 2)

SYMBOL	TYPE	VALUE	UNITS	DESCRIPTION
A_{BP}	c	13.3	IN	Piston area per brake
α_B	c	0.03	SEC/IN	Brake lining friction parameter
C_{B1}	c	6.2×10^5	LB/IN	Brake Disc spring rate characteristic
C_{B2}	c	0.0	LB/IN	
C_{BB}	c	1.0×10^5	LB/IN	Bottoming spring rate
C_{BR}	c	8850.	LB/IN	Return spring rate
D_{B1}	c	4.71	LB SEC/IN	Brake Disc damping coeff.
D_{B2}	c	0.0	LB SEC/IN	
D_{BB}	c	400.	LB SEC/IN	Bottoming damping coeff.
F_B	v		LB	Force between brake plates
F_{B1}	v		LB	$F_B = F_{B1} + F_{B2}$
F_{B2}	v		LB	
F_{BB}	v		LB	Bottoming Force
F_{BR}	v		LB	Return Force
F_{BRO}	c	1330.	LB	Return force when Xp = 0
F_{KF}	v		LB	Keyway friction force
$F_{\theta R}$	v		lb	"O-ring" friction force
G_F	v			Friction breakout function
G_{FM}	c	1.50	Dimensionless	Ratio of breakout friction to running friction
H_{B1}	c	0.05	Dimensionless	Fraction of brake torque removed by stator keys
H_{B2}	c	0.95	Dimensionless	Fraction of brake torque removed thru pistons
$H_{\theta FC}$	c	28.8	LBF	O-ring friction
$H_{\theta FP}$	c	0.20	LBF/PSI	

Table A2 Brake Assembly Parameters (Sheet 2 of 2)

SYMBOL	TYPE	VALUE	UNITS	DESCRIPTION
P_B	v (i)		LB/IN	Brake pressure
R_{BI}	c	4.40	IN	Radius to center of press on stator key
R_{BO}	c	8.25	IN	Radius to center of press on rotor key
R_{BT}	c	6.25	IN	Radius to piston centers
R_{NR}	c	7	Dimensionless	Number of rotors
S_{B1}	c	.1165	IN	Displacement of piston to engage C_{B1} Spring Rate
S_{B2}	c	0.0	IN	Displacement of piston to engage C_{B2} Spring Rate
S_{BB}	c	0.0	IN	Value of Xp when bottoming occurs
T_{BT}	v(o)		IN LB	Brake torque
u_B	v		Dimensionless	Brake lining friction coeff.
u_{B1}	c	0.15	Dimensionless	Brake lining friction characteristic
u_{B2}	c	0.10	Dimensionless	
u_K	c	0.15	Dimensionless	Friction coeff. of keyways (running)
u_{KP}	c	0.10	Dimensionless	Friction coeff. between pistons and walls (running)
V_B	v		IN/SEC	Velocity of brake lining
V_{FS}	c	0.10	IN/SEC	Friction breakout parameter
W_B	v(i)		RAD/SEC	Rotational speed between stators and rotors
W_{BE}	c	0.358	LB SEC /IN	Brake mass
X_P	v (o)		IN	Brake piston displacement
X_{PO}	c	0.0	IN	Brake piston displacement when t = o
$\dot{X}_P$	v (o)		IN/SEC	Brake Piston Velocity
$\dot{X}_{PO}$	c	0.0	IN/SEC	Brake piston velocity when t = o
$\ddot{X}_P$	v		IN/SEC	Brake piston accel.

2. BRAKE ACTUATION HYDRAULIC SYSTEM

The hydraulic system is the brake actuation power source and is made up of the four components as shown in Figure A5 : the pilot's metering valve, the antiskid control valve, the control line, and the brake piston housing. The pilot's metering valve is a pressure regulator, usually having a mechanical input, which has a steady state output pressure (Pmv) at a level commanded by the pilot (Pcom). The antiskid valve is a pressure regulator which has a steady state output as dictated by the antiskid control device. For a modulated antiskid system, the control valve is a variable pressure servo type regulator and for an ON-OFF antiskid system the control valve is an ON-OFF valve. The control line is simply the fluid transmission line or containment vessel connecting the control valve to the brake housing. The brake housing is a collection of cylinders and pistons which act to compress the brake discs. From a hydraulic system aspect, the control valve is a variable area orifice, where the orifice area is a function of spool position. The control valve spool position is received as an input from computations described in a section devoted to the operation of the control valve.

In the description of the brake actuation system, there are two principal effects which should be accounted for. The first is the time lag which exists between the control valve output pressure (Pcv) and the actual brake pressure (Pb). This lag is caused by the fluid's resistance to flow due to inertia and friction and by the brake pressure's dependence upon fluid volume within the pressure cavity. The second effect is the instantaneous brake pressure intensity as influenced by fluid inertia and the combined elasticity of the fluid and the pressure cavity. Rapid valve operation can cause pressure overshoot and oscillation due to "water hammer" effects. This overshoot can cause excessive brake torque and may interfere with proper control valve operation. The pilot's metering valve pressure drop and response characteristics are included in the actuating system description so that these effects upon antiskid operation can be examined. To allow for a variety of brake actuation systems which might be encountered, provision is made to accommodate both hydraulic and pneumatic actuation media. The line connecting the control valve and the brake can be treated as a separate fluid cavity or the effects of its volume may be lumped with the brake as would be appropriate for a short line.

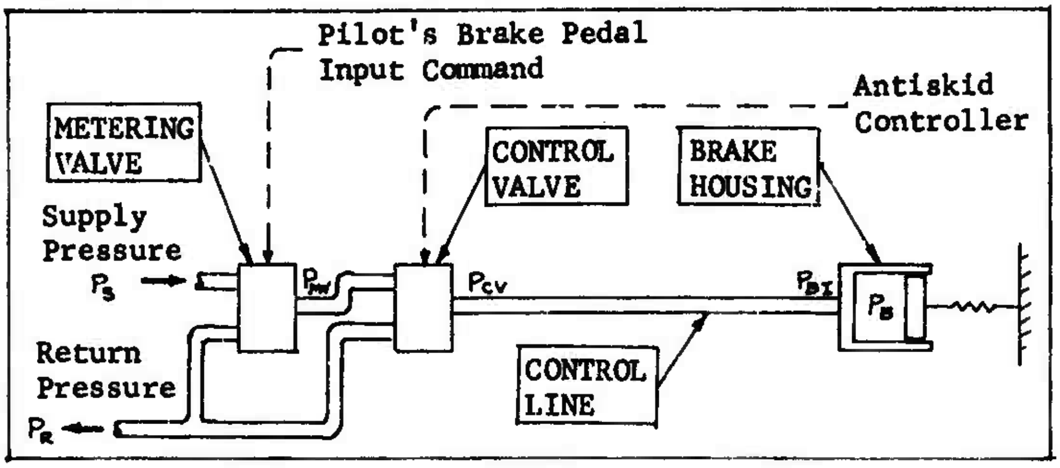

Figure A5 Hydraulic System Components

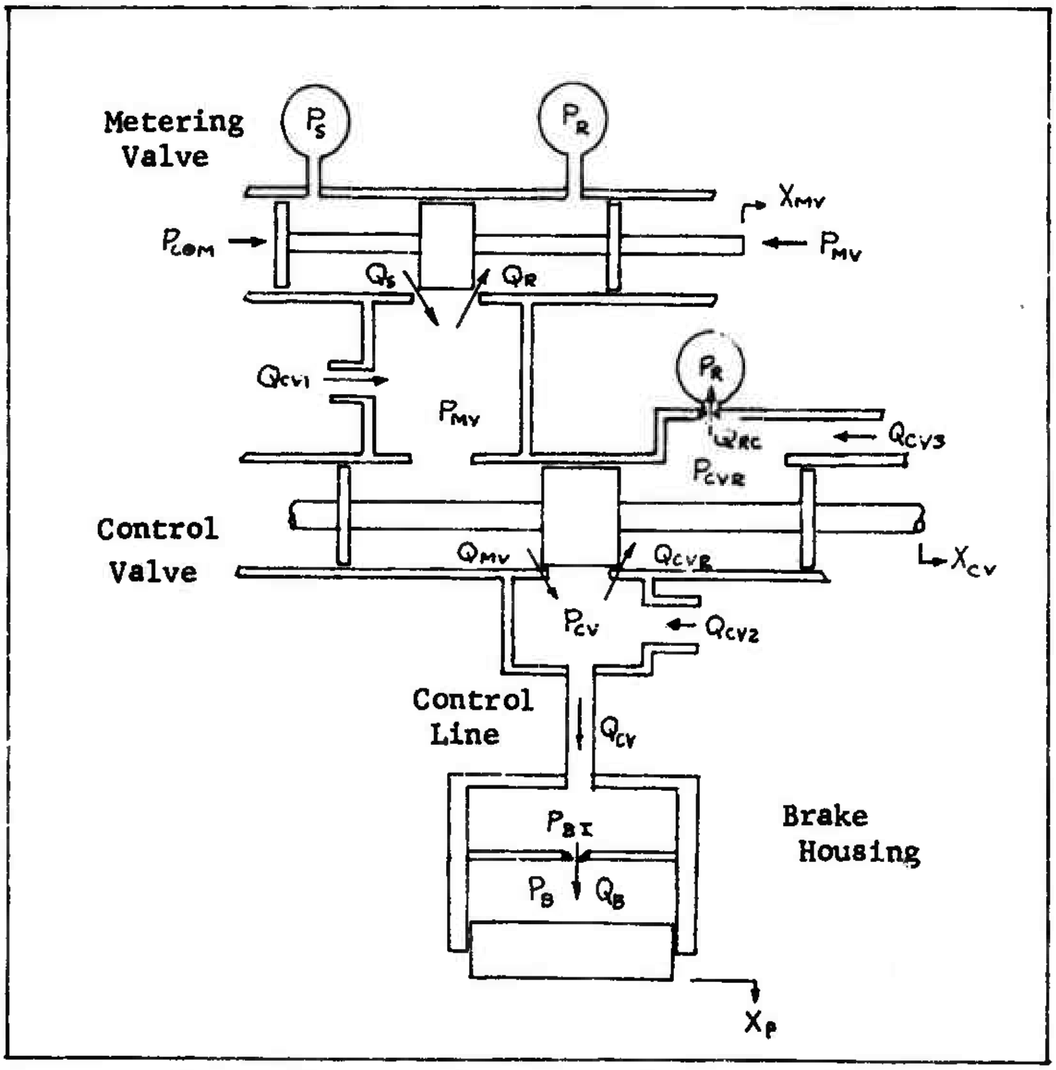

Figure A6 Hydraulic System Schematic for Options 1, 2 and 3

A. Mathematical Description (Options 1, 2 and 3)

Figure A6 is a schematic of the brake hydraulic system. The analytical procedures of References 5 and 6 are utilized to mathematically describe the system.

Let P_{COM} denote the brake pressure which is commanded by the pilot and define P_{COM} such that it increases from a minimum value, P_R, (reservoir pressure) to the desired steady state value P_{CP}, as a linear function of time over an interval, T_{CP}, as follows:

$$(2.1) \qquad P_{com} = \begin{cases} T\,(P_{CP} - P_R)/T_{CP} + P_R & \text{IF } 0 \le T \le T_{CP} \\ P_{CP} & \text{IF } T_{CP} < T \end{cases}$$

The metering valve attempts to maintain P_{MV} at the level of P_{COM}. The metering valve spool displacement X_{MV} is defined by equations (2.2) and (2.3).

$$(2.2) \qquad V_{MV} = G_{mv}\,(P_{com} - P_{mv})$$

$$(2.3) \qquad \dot{X}_{MV} = \begin{cases} \min\{0, V_{MV}\} & \text{if } S_{MVU} \le X_{MV} \\ V_{MV} & \text{if } S_{MVL} < X_{MV} < S_{MVU} \\ \max\{0, V_{MV}\} & \text{if } X_{MV} \le S_{MVL} \end{cases}$$

Let $\phi\langle X,Y\rangle$ be a function defined as follows:

(a) For hydraulic fluid

$$(2.4) \qquad \phi\langle X,Y\rangle = \mathrm{SIGN}\,(X-Y)\sqrt{|X-Y|}$$

(b) For compressible pneumatic fluids

(2.5) IF $X > Y$ and $X \ge Y/R_{CRIT}$ WHERE $R_{CRIT} = \left[2/(\gamma_a + 1)\right]^{\frac{\gamma_a}{(\gamma_a - 1)}}$

$$\phi\langle X,Y\rangle = X\left[1 - (R_{CRIT})^{\frac{\gamma_a - 1}{\gamma_a}}\right]^{1/2} \Big/ \left[(R_{CRIT})^{\gamma_a}\right]$$

IF $X \ge Y$ and $X \le Y/R_{CRIT}$

$$\phi\langle X,Y\rangle = X\left[1 - \left(\;/X\right)^{\frac{\gamma_a - 1}{\gamma_a}}\right]^{1/2} \Big/ \left(Y/X\right)^{\gamma_a}$$

IF $Y \ge X$ and $Y \le X/R_{CRIT}$

$$\phi\langle X,Y\rangle = -\phi\langle Y,X\rangle$$

IF $Y > X$ and $Y \ge X/R_{CRIT}$

$$\phi\langle X,Y\rangle = -\phi\langle Y,X\rangle$$

Let $A_{MV}\langle x\rangle$ be defined by:

$$(2.6)\quad A_{MV}\langle x\rangle = \begin{cases} A_{MVO} & \text{if } x \geq S_{MVO} \\ \max\{A_{MVL},\ x A_{MVO}/S_{MVO}\} & \text{if } x < S_{MVO} \end{cases}$$

Let A_{MVS} and A_{MVR} be defined by:

$$(2.7)\quad A_{MVS} = A_{MV}\langle X_{MV}\rangle$$

$$(2.8)\quad A_{MVR} = A_{MV}\langle -X_{MV}\rangle$$

Then

$$(2.9)\quad Q_S = A_{MVS}\,\phi\langle P_S, P_{MV}\rangle$$

$$(2.10)\quad Q_R = A_{MVR}\,\phi\langle P_{MV}, P_R\rangle$$

Let V_{MVV} be the fluid volume from the output of the metering valve up to the input of the control valve.
Then

$$(2.11)\quad \dot{P}_{MV} = (B_{MV}/V_{MVV})(Q_S - Q_R - Q_{MV} + Q_{CV1})$$

Let $A_{CV}\langle x\rangle$ be defined by:

$$(2.12)\quad A_{CV}\langle x\rangle = \begin{cases} A_{CVO} & \text{if } x \geq S_{CVO} \\ \max\{A_{CVL},\ x A_{CVO}/S_{CVO}\} & \text{if } x < S_{MVO} \end{cases}$$

Let A_{CVS} and A_{CVR} be defined by

$$(2.13)\quad A_{CVS} = A_{CV}\langle X_{CV} - S_{CL}\rangle$$

$$(2.14)\quad A_{CVR} = A_{CV}\langle -S_{CL} - X_{CV}\rangle$$

Then

$$(2.15)\quad Q_{MV} = A_{CVS}\,\phi\langle P_{MV}, P_{CV}\rangle$$

$$(2.16)\quad Q_{CVR} = A_{CVR}\,\phi\langle P_{CV}, P_{CVR}\rangle$$

$$(2.17)\quad \dot{P}_{CVR} = (B_{CVR}/V_{CVR})(Q_{CVR} - Q_{RC} + Q_{CV3})$$

$$(2.18)\quad Q_{RC} = A_{RC}\,\phi\langle P_{CVR}, P_R\rangle$$

The volume of the cavity occupied by the brake actuation media is established by equation (2.19) as follows:

$$(2.19) \quad V_B = V_{BO} + A_{BPS} X_P$$

Three options for the control line mathematical description are provided to cover a variety of circumstances which may be encountered. The third option is representative of a typical aircraft installation and is used in analyzing the F-111 system.

The first option is for a control line with hydraulic fluid considering volume effects only. This option will not predict "water hammer" but is satisfactory for many cases, particularly for the case of a short control line 50 inches or less in length. The following equations describe the first option:

$$(2.20a) \quad Q_{CV} = Q_{MV} - Q_{CVR} + Q_{CVZ}$$

$$(2.21a) \quad \dot{P}_{CV} = (B_B/V_B)(Q_{CV} - A_{BPS} \dot{X}_P)$$

$$(2.22a) \quad P_{BI} = P_{CV}$$

$$(2.23a) \quad P_B = P_{BI}$$

$$(2.24a) \quad Q_B = Q_{CV}$$

The following equations are applicable to the second option for the control line using compressible pneumatic fluid.

$$(2.20b) \quad Q_{CV} = Q_{MV} - Q_{CVR} + Q_{CVZ}$$

$$(2.21b) \quad \dot{P}_{CV} = (B_B/V_B)(Q_{CV} - P_{CV} A_{BPS} \dot{X}_P/B_B)$$

$$(2.22b) \quad P_{BI} = P_{CV}$$

$$(2.23b) \quad P_B = P_{BI}$$

$$(2.24b) \quad Q_B = Q_{CV}$$

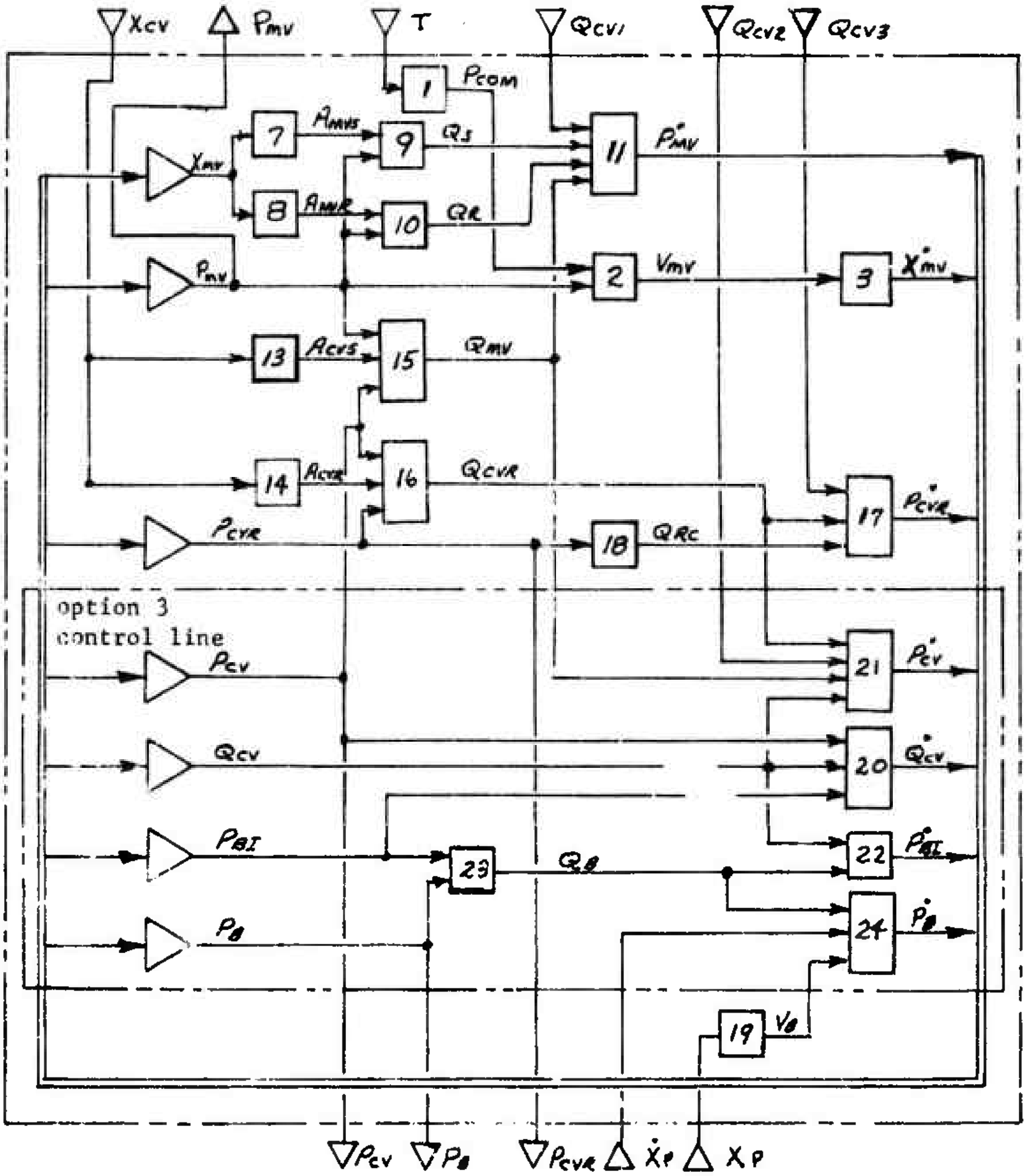

Note: Substitute partial equation flow diagram below for control line options 1 and 2.

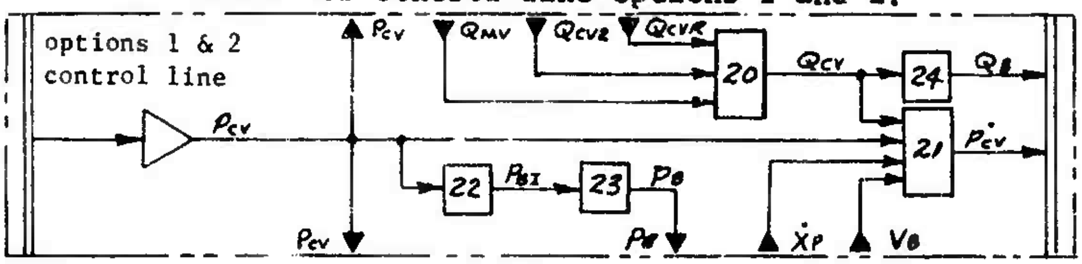

Figure A7 Hydraulic System Equation Flow Diagram for Options 1, 2 and 3

The third option is for a control line with hydraulic fluid where both volume and inertial effects are considered and is described by the following equations:

(2.20c) $\dot{Q}_{CV} = (A_{BL}/R_{HO}S_{BL})(P_{CV} - P_{BI} - D_{RBL}Q_{CV} - D_{TBL}Q_{CV}|Q_{CV}|)$

(2.21c) $\dot{P}_{CV} = (B_{BL}/V_{BL})(Q_{MV} - Q_{CVR} - Q_{CV} + Q_{CV2})$

(2.22c) $\dot{P}_{BI} = (B_{BL}/V_{BL})(Q_{CV} - Q_{B})$

(2.23c) $Q_{B} = A_{BO}\,\phi\langle P_{BI}, P_{B}\rangle$

(2.24c) $\dot{P}_{B} = (B_{B}/V_{B})(Q_{B} - A_{BPS}\dot{X}_{P})$

An Option 4 Hydraulic System is described to provide a simplified mathematical description of the hydraulic system which does not account for metering valve transient spool movement. For this model the metering valve is assumed to be full open for hydraulic flow the the brake and fully closed for hydraulic flow from the brake. Hydraulic flow direction and amount is established by control valve spool position as shown schematically in Figure A8. In addition the brake piston velocity is defined as the brake hydraulic flow rate divided by the piston area so that the hydraulic volume is the integral of the flow. Option 4 hydraulic system mathematical description is developed as follows:

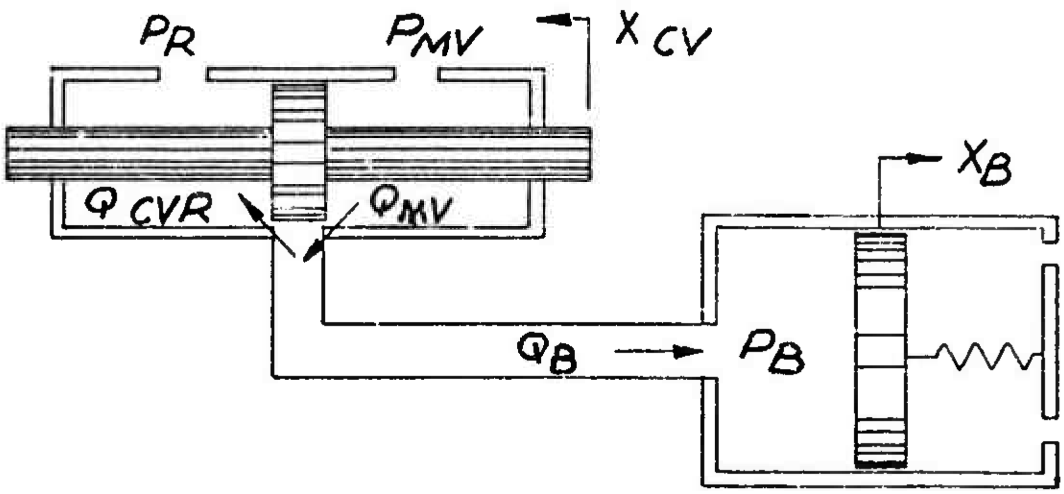

Figure A8 Option 4 Hydraulic System Schematic

Let P_{CP} denote the brake pressure which is commanded by the pilot. Let P_{MV}, metering valve output pressure increase from a minimum value, P_R, (reservoir pressure) to the desired steady state pressure, P_{COM}, as a linear function of time over an interval, T_{CP}, as follows:

$$(2.1d) \quad \begin{aligned} P_{MV} &= T(P_{CP}-P_R)/T_{CP} + P_R && \text{IF } 0 \leq T \leq T_{CP} \\ &= P_{CP} && \text{IF } T > T_{CP} \end{aligned}$$

Let the brake pressure, P_B, be a function of brake fluid volume as follows:

$$(2.2d) \quad P_B = P_{B1} + P_{B2}$$

$$(2.3d) \quad \begin{aligned} P_{B1} &= P_{BR1} + C_{BV1} V_B && \text{IF } 0 \leq V_B \leq V_{BC} \\ &= 0 && \text{IF } V_B > V_{BC} \end{aligned}$$

$$(2.4d) \quad \begin{aligned} P_{B2} &= P_{BR2} + C_{BV2} V_B && \text{IF } V_{BC} < V_B \\ &= 0 && \text{IF } 0 \leq V_B \leq V_{BC} \end{aligned}$$

Let the control valve flow area for brake application, A_{CVS}, be defined as a function of spool relative position:

$$(2.5d) \quad \begin{aligned} A_{CVS} &= A_{CVSO} && \text{IF } X_{CV} \geq S_{CVO} \\ & \text{MAX}\{A_{CVL}, X_{CV}(A_{CVSO})/S_{CVO}\} && \text{IF } X_{CV} \leq S_{CVO} \end{aligned}$$

In a similar way, let the control valve flow area for brake release, A_{CVR}, be defined as follows:

$$(2.6d) \quad \begin{aligned} A_{CVR} &= A_{CVRO} && \text{IF } X_{CV} \leq -S_{CVO} \\ & \text{MIN}\{A_{CVL}, X_{CV}(A_{CVRO})/S_{CVO}\} && \text{IF } X_{CV} > -S_{CVO} \end{aligned}$$

Then:

(2.7d) $$Q_{MV} = A_{CVS}\,\phi \langle P_{MV}, P_B \rangle$$

(2.8d) $$Q_{CVR} = A_{CVR}\,\phi \langle P_B, P_R \rangle$$

Where the function ϕ is as previously defined by equation (2.4)

(2.9d) $$Q_B = Q_{MV} - Q_{CVR}$$

(2.10d) $$V_B = \int Q_B$$

For compatibility with the other hydraulic system options as they interface with other systems:

(2.11d) $$P_{CV} = P_B$$

(2.12d) $$P_{CVR} = P_R$$

Figure A9 shows the Option 4 Hydraulic System Equation Flow diagram.

In this study the brake system hydraulic supply pressure, P_S, is treated as a constant. If P_S varies significantly due to operation of other aircraft hydraulic system equipment, this variable pressure defined as a function of time may be used.

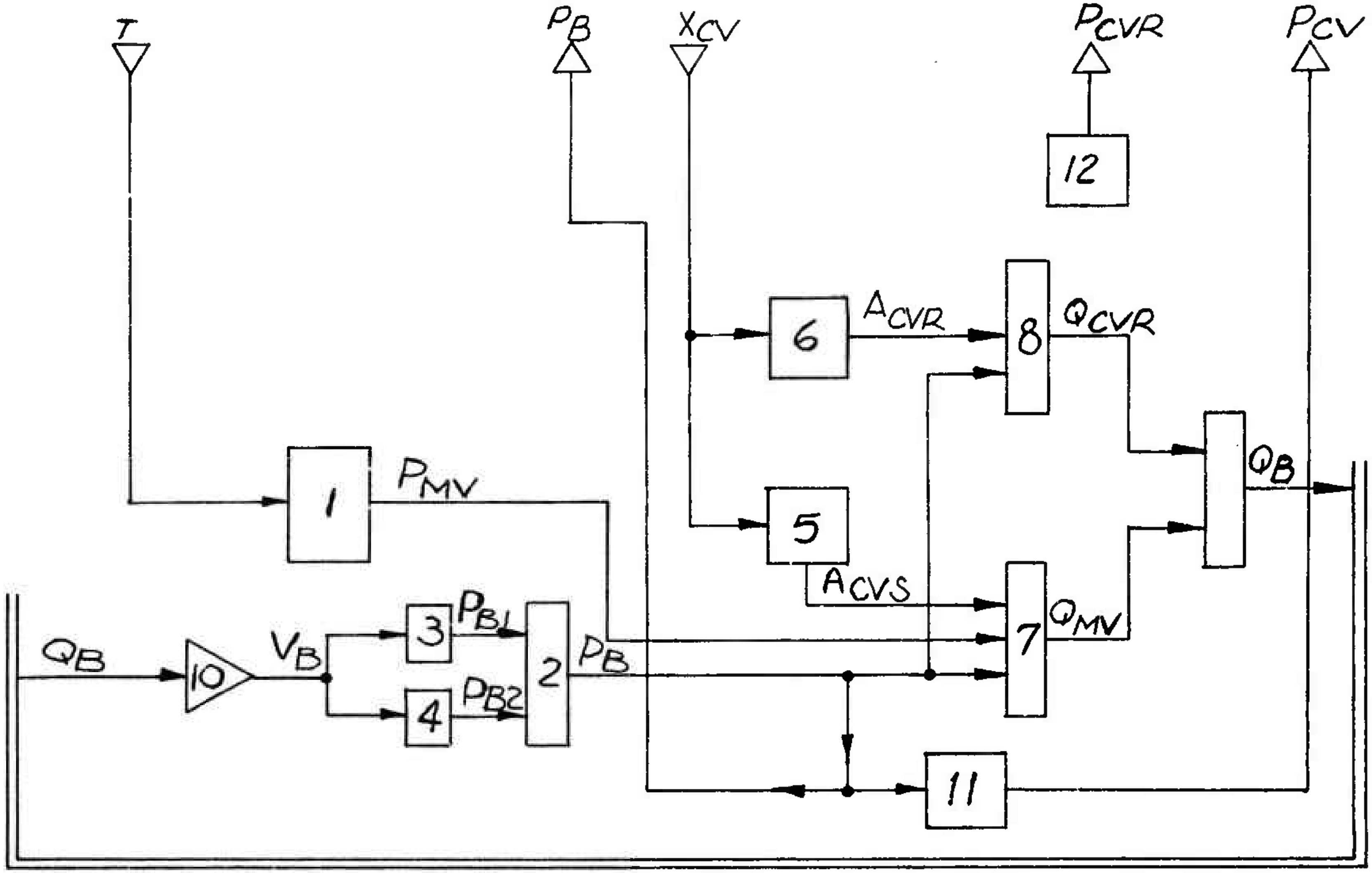

Figure A9 Option 4 Hydraulic System Equation Flow Diagram

B. Parameter Evaluation

For this study the third optional control line description as applied to the F-111 is of primary interest. For this case MIL-H-5606 hydraulic fluid is used. The hydraulic fluid properties for a mean temperature of 100°F and 1500 psi are:

(1) Adiabatic bulk modulus: $\beta = 248{,}000$ psi

(2) Density: $R_{HO} = .781 \times 10^{-4}$ LBF SEC^2/IN^4

(3) Kinematic viscosity: $\nu = .0267$ IN^2/SEC

The system supply pressure is 3000 psi and the return pressure is 100 psi. Initially, all flows are zero and all pressures except the supply pressure are at 100 psi. The pilot's input command pressure P_{COM} is also 100 psi. The pilot's input P_{COM} will go from 100 to 1500 psi in 0.2 seconds. Thus $T_{CP} = 0.2$ sec and $P_{CP} = 1500$ psi.

Metering Valve

When the metering valve spool is centered, the flow area is essentially zero for both the return and supply lines. In this spool position $X_{MV} = 0.0$. From equation (2.3) the spool is constrained to stay between S_{MVL} and S_{MVU}.

For the metering valve, $S_{MVL} = -.06$ in and $S_{MVU} = .06$ in. However, when X_{MV} is at + .05, the valve area has reached its maximum for the flow Q_S. When $X_{MV} = -.05$, the area is maximum for the return flow Q_R. Thus $S_{MVO} = .05$. By actual measurement, with the valve full open (area = A_{MVO}) at 100° F, the flow is 9.23 in^3/sec. at 200 psiΔP. Thus from (2.9) or (2.10),

$$(2.25) \quad A_{MVO} = Q/\sqrt{\Delta P} = 9.23/\sqrt{200} = .653 \ IN^4/(sec)(lbf)^{1/2}$$

In the F-111 system, the metering valve is situated next to the control valve so that the volume V_{MV} is quite small. V_{MV} was calculated from the valve drawing as being about 1.0 in^3. Also, the valve body is considered to be much stiffer than the hydraulic fluid so that the effective bulk modulus is the fluid modulus. Thus, B_M = 248,000 psi. G_{MV} was estimated from analog studies to be about .05.

<u>Control Valve</u>

For the control valve, X_{CV} = 0.0 when the spool is centered. At this point the flow area is zero so that A_{CVL} = 0.0. The flow area remains zero for $-.005 \le X_{CV} \le .005$. Thus the valve has an overlap of .005 in. and S_{CL} = .005. An additional movement of .030 in. produces full area so S_{CVO} = .030. By actual measurement at this position at 100°F, the flow is 7.7 in^3/sec. at 50 psi Δ P. Thus

$$(2.26) \quad A_{CVO} = Q/\sqrt{\Delta P} = 7.7/\sqrt{50} = 1.090 \ IN^4/(sec)(lbf)^{1/2}$$

The following values are estimates of the return characteristics of the control valve: V_{CVR} = 2.0 in^3, B_{CVR} = 248,000 psi, A_{RC} = 1.0 in^4/(sec)(lbf)1/2.

<u>Control Line</u>

The control line is 1/4 inch outside diameter steel tubing having 0.14 inch wall thickness and internal cross sectional area, A_{BL}, equal to .0386 in^2. Because of the thin wall, the tube elasticity greatly reduces the bulk modulus. The equivalent bulk modulus, B_e, may be calculated from

$$(2.27) \quad B_e = B\left(\frac{1}{\left(\frac{B}{E}\right)\left(\frac{D}{t}\right)+1}\right)$$

Where B = Fluid bulk modulus

E = Young's modulus of tube material

D = Mean tube diameter

t = Tube wall thickness

Thus

$$(2.28)\quad B_{BL} = \frac{248000}{\frac{(.248 \times 10^6)(.236)}{(30 \times 10^6)(.014)} + 1} = 217,700 \text{ PSI}$$

The control/line length, S_{BL}, is 191 inches with various types of flow restrictors according to the following table.

Table A3 Control Line Restrictions

Description	"K" Value*	Number n	nk
An815-4J Union	.54	1	.54
AN832-4J Union	.54	1	.54
AN821-4J Elbow (90°)	1.23	4	4.92
AN837-4J Elbow (45°)	.89	1	.89
90° Tube Bend	.01	12	.12
90° Hose Fitting	1.25	1	1.25
Total			8.26

*$\Delta h = KV^2/2g$ Where V is the velocity in the line.

The "K" values in Table A3 were derived from information contained in Reference 5.

Equation (2.20c) is the result of summing forces on the mass of fluid in the control line. The friction losses are depicted by a turbulent flow loss $D_{TBL}\,Q_{CV}^2$ and a laminar flow loss $D_{RBL}\,Q_{CV}$ It is assumed that all the turbulent flow losses come from elbows, etc., which are listed in Table 3. The loss due to the line itself is considered to be always laminar. This assumption of laminar flow for

the line is justified for two reasons: (1) the loss in the line is small compared to other losses in the system; (2) the flow is normally laminar anyway (Reynolds Number is less than 6000 for the F-111 system).

For the turbulent losses

$$(2.29)\quad \Delta P = \rho g \Delta h = K\rho V^2/2 = \left(K\rho/2A^2\right) Q^2$$

Thus

$$(2.30)\quad D_{TBL} = \frac{K\rho}{2\,(A_{BL})^2} = \frac{(8.26)(.781\times10^{-4})}{2\;(.0386)^2} = .216\ \text{lbf sec}^2/\text{IN}^8$$

For laminar losses, at temperatures normally encountered, the "oscillatory" friction is higher than the steady state friction. See Reference 9. The pressure loss can be written as

$$(2.31)\quad \Delta P = R_L\left(L/A^2\right) Q$$

For the steady state case as shown in Reference 6,

$$(2.32)\quad R_L = 8\pi\rho\nu$$

In Figure 10 values for this theoretical steady state R_L are compared over a range of temperatures to values from Reference 9 which were experimentally established for oscillatory flow. Since the hydraulic flow in the brake control line associated with antiskid operation is transitory, the laminar flow resistance base on experimental measurements for oscillatory flow is used.

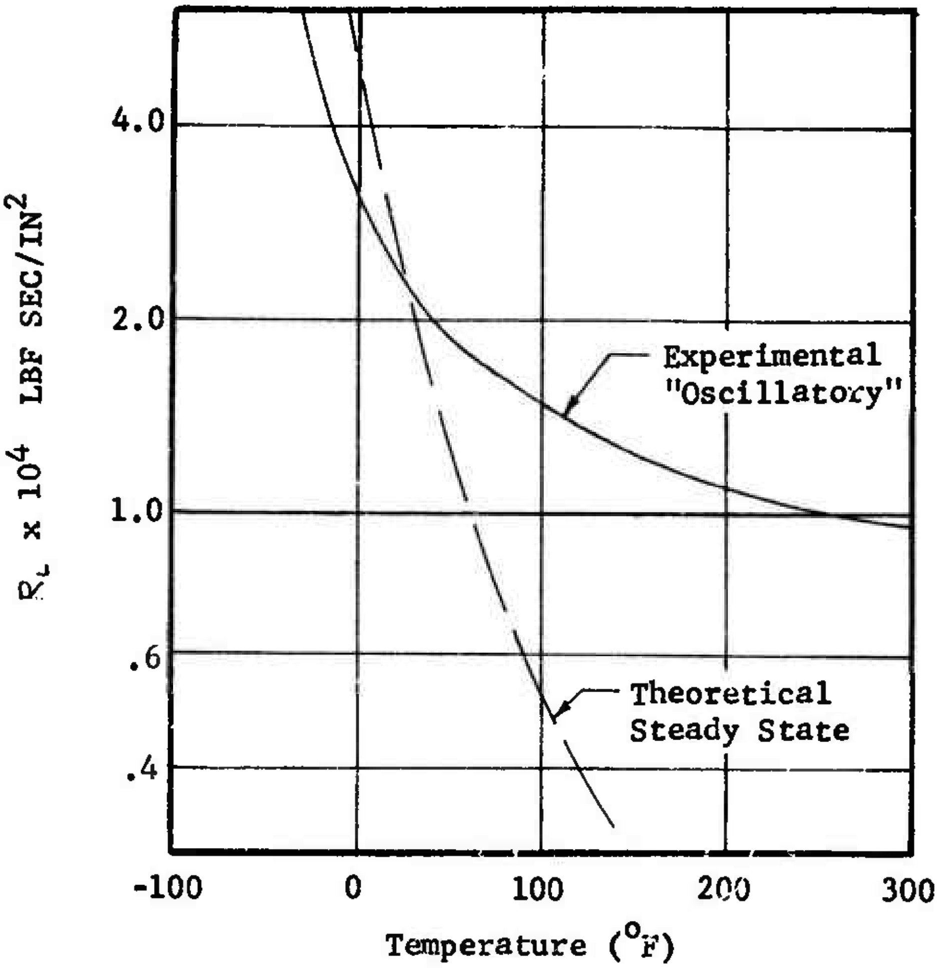

Figure A10 Hydraulic Fluid Damping Characteristic

From Figure A10 at 100^{o}F R_L for the experimental oscillatory case is 1.5 X 10^{-4}. LBF SEC/IN^2

Therefore:

$$(2.33) \qquad D_{RBL} = \frac{(R_L)(S_{BL})}{(A_{BL})^2} = \frac{(1.5 \times 10^{-4})(191)}{(.0386)^2}$$

$$= 19.22 \ \text{lbf sec/in}^5$$

When a "lumped parameter" type analysis as described by equations (2.20c), (2.21c) and (2.22c) is used for the control line the resulting natural frequency is somewhat lower than the actual line, if the actual line volume, V_{BL}, is used. The value of V_{BL} is adjusted as follows to achieve the correct natural frequency for the "lumped parameter" description.

Consider hydraulic fluid flowing through a line with cross sectional area, A, and divided into segments having equal length, S, as shown below.

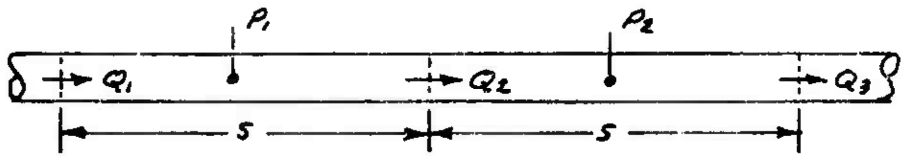

If each segment is treated as a separate pressure vessel having volume, V, with a flow in and a flow out, and if equations of the form of (2.20c) (2.21c) and (2.22c) are written for these pressure vessels, neglecting friction, the following expressions are obtained:

$$(2.34) \qquad \dot{Q}_2 = (A/\rho S)(P_1 - P_2)$$

$$(2.35) \qquad \dot{P}_1 = (B/V)(Q_1 - Q_2)$$

$$(2.36) \qquad \dot{P}_2 = (B/V)(Q_2 - Q_3)$$

By substituting equations (2.35) and (2.36) into equation (2.34) differentiated once with respect to time the following differential equation is formed:

$$(2.37) \qquad \ddot{Q}_2 = (A/\rho S)(B/V)\left[(Q_1 - Q_2) - (Q_2 - Q_3)\right]$$

or

$$(2.38) \qquad \ddot{Q}_2 + 2(AB/\rho SV)\,Q_2 = (AB/\rho SV)(Q_1 + Q_3)$$

Equation (2.38) establishes that the natural frequency of each line segment is:

$$(2.39) \qquad F_n = \frac{1}{2\pi}\sqrt{\frac{2AB}{\rho SV}} \quad \text{cps}$$

However, vibration theory considering distributed mass and elasticity establishes the speed of sound, C, in the line as:

$$(2.40) \qquad C = \sqrt{B/\rho} \quad \text{in/sec}$$

For fundamental mode oscillation in a closed end tube having length, S, the natural period, T_c, is:

(2.41) $$T_c = 2S/c \quad \text{SEC}$$

Therefore, the natural frequency, g_n, of an actual tube segment is:

(2.42) $$g_n = 1/T_c = (1/2S)\sqrt{B/\rho} \quad \text{CPS}$$

By equating the two expressions for natural frequency, equations (2.39) and (2.42), the volume of the line segment which will have the same natural frequency as the actual is established as:

(2.43) $$V = 2AS/\pi^2$$

Thus,

(2.44) $$V_{BL} = \frac{2}{\pi^2} A_{BL} S_{BL} = \frac{(2)(.0386)(191)}{\pi^2} = 1.495 \text{ IN}^3$$

Brake Housing

The brake housing has ten pistons of 1.33 in^2 area each. Since the number of pistons serviced by one control line is five, then $A_{BPS} = 5(1.33) = 6.65$ in^2. The fluid volume in the brake housing with the pistons bottomed $(X_P = 0)$ is 8.00 in^3. Thus $V_{BO} = 4.00$ in^3 or one-half the total volume. The orifice coefficient A_{BO} was estimated to be about 2.0 $IN^4/SEC\ LBF^{1/2}$.

Optional Systems

The option 1 system neglects the line inertial effects. The parameters have the same value as the corresponding parameters for the option 3 system, except that V_{BO} should include any line volume. Thus, for the F-111 system, with the option 1 system, $V_{BO} = 4.00 + .0386(191) = 11.36 \text{ IN}^3$.

The option 2 description is used for systems with compressible pneumatic fluid. The appropriate parameters will be evaluated for nitrogen at 100°F as the fluid media and isothermal processes are assumed except for orifice flow calculations. While the heat transfer characteristics of the brake system components have not been rigorously evaluated, the usual component installation is such that assuming isothermal processes is valid. The mathematical description of the brake actuation control system using compressible pneumatic fluid is written using equations of the same general form as for those describing the hydraulic system, thereby minimizing the

the number of equations and enhancing computation flexibility. Utilizing the hydraulic equations when pneumatic fluid is used requires that the appropriate parameters be expressed in suitable mathematically equivalent terms. Consider the characteristic equation of state for a perfect gas:

$$(2.45) \qquad P = \frac{MRT}{V}$$

And the definition:

$$(2.46) \qquad \frac{dP}{dt} = \frac{\partial P}{\partial m}\frac{dm}{dt} + \frac{\partial P}{\partial V}\frac{dV}{dt} + \frac{\partial P}{\partial T}\frac{dT}{dt}$$

For the assumed isothermal process, substitution of equation (2.45) into equation (2.46) gives:

$$(2.47) \qquad \dot{P} = \left(\frac{RT}{V}\right)\dot{m} - \left(\frac{RT}{V}\right)\frac{m}{V}\dot{V}$$

For those cases, such as for the metering valve and control valve pressure cavities, where the volume is not changing, $\dot{V}$ is zero and equation (2.47) reduces to:

$$(2.48) \qquad \dot{P} = \left(\frac{RT}{V}\right)\dot{m}$$

For hydraulic fluid, $\dot{P}$ is described by equations having the form of equation (2.49) below. (See equation (2.11) for instance.)

$$(2.49) \qquad \dot{P} = \left(\frac{B}{V}\right)Q$$

Noting the similarity between equation (2.48) and equation (2.49) it is obvious that if RT is used in place of B and if $\dot{m}$ is used in place of Q, the "Hydraulic" equations can be used for computing performance of a system using pneumatic fluid. Thus, $B_B = B_{CVR} = B_{MV} = RT$.
For nitrogen R = 662.4 $in\ lbf/lbm\,^\circ F$ and at 100°F
RT = (662.4) (460 + 100) = 371 x 10^6 $in\ lbf/lbm$.

Since P/RT = M/V, equation (2.47) can be written as

$$(2.50) \qquad \dot{P} = \left(\frac{RT}{V}\right)\left[\dot{m} - \left(\frac{P}{RT}\right)\dot{V}\right]$$

Equation (2.21b) is obtained by substituting B_B for RT, $A_{BPS}\dot{X}_P$ for $\dot{V}$, and Q for $\dot{m}$ in equation (2.50), thereby accounting for the change in brake volume caused by piston movement.

Equation (2.51) below, from Reference 6, describes the mass flow rate of a gas from a container having high pressure, P_H, through an orifice of area, A_o, to a container having

low pressure, P_L .

$$(2.51)\quad \dot{m} = \left(\frac{C_O A_O}{R}\sqrt{\frac{2GC_P}{T}}\right) P_H \left(\frac{P_H}{P_L}\right)^{1/\gamma} \sqrt{1-\left(\frac{P_H}{P_L}\right)^{\frac{\gamma-1}{\gamma}}}$$

Equation (2.52) below, from Reference 6, describes the volumetric flow rate of hydraulic fluid through an orifice under similar circumstances.

$$(2.52)\quad Q = C_O A_O \left(\sqrt{2/\rho}\right)\sqrt{P_H - P_L}$$

Both equations (2.51) and (2.52) can be written in the form $Q = A_F \phi\langle P_H, P_L\rangle$ where $\phi\langle P_H, P_L\rangle$ is a flow function as defined by equations (2.4) and (2.5) for the appropriate circumstances and where A_F is a flow coefficient accounting for orifice and fluid properties. For the case of hydraulic fluids a value of $C_O\sqrt{2/\rho} = 103.5\ in^2/lbf^{1/2} sec$ has been established by experience as being representative of an average orifice (i.e., $C_O \approx 0.65$). The metering valve flow coefficient, A_{MVO} , previously computed is 0.653 $in^4/sec\ lbf^{1/2}$; therefore, the apparent actual orifice area, A_O , for the metering valve is $A_O = 0.653/103.5 = .631 \times 10^{-2}\ in^2$.

For the case of the pneumatic system with nitrogen at 100°F as the working fluid and using $C_P =$ 2300 in lbf/lbm$^\circ$ F, and R = 662.4 in lbf/lbm $^\circ$F:

$$\begin{aligned}(2.53)\quad A_{MVO} &= \frac{C_O A_O}{R}\sqrt{\frac{2GC_P}{T}} \\ &= \frac{(.8)(.631\times10^{-2})}{662.4}\sqrt{\frac{(2)(386)(2300)}{560}} \\ &= 0.43\times10^{-3}\ lb_m\ in^2/lbf\ sec\end{aligned}$$

Using the same procedure establishes that:

$$A_{CVO} = 0.716\times10^{-3}\ lbm\ in^2/lbf\ sec$$

$$A_{RC} = 0.658\times10^{-3}\ lbm\ in^2/lbf\ sec$$

Table A4 lists the parameters for Hydraulic System Options 1, 2 and 3. The parameters which apply for the Option 4 Hydraulic System are listed in Table A5.

Table A4 Option 1, 2 and 3 Hydraulic System Parameters (Sheet 1 of 5)

SYMBOL	TYPE	VALUE	UNITS	OP* 1	OP* 2	OP* 3	DESCRIPTION
A_{BL}	c	.0386	IN^2			X	Cross sectional area of brake control line
$A_{B\theta}$	c	2.00	$IN^4/SEC\ LBF^{1/2}$			X	Brake housing orifice coefficient
A_{BPS}	c	6.65	IN^2	X	X	X	Brake piston area (per brake line)
$A_{CV}\langle x\rangle$	f			X	X	X	Control valve flow area function
A_{CVL}	c	0.00	$IN^4/SEC\ LBF^{1/2}$	X		X	Control valve leakage flow coeff.
		0.00	$LBM\ IN^2/LBF^{1/2}\ SEC$		X		
A_{CVO}	c	1.09	$IN^4/SEC\ LBF^{1/2}$	X		X	Control valve full open flow coeff.
		$.716X10^{-3}$	$LBM\ IN^2/LBF^{1/2}\ SEC$		X		
A_{CVR}	v		$IN^4/SEC\ LBF^{1/2}$	X		X	Control valve return flow coeff.
			$LBM\ IN^2/LBF^{1/2}\ SEC$		X		
A_{CVS}	v		$IN^4/SEC\ LBF^{1/2}$	X		X	Control valve supply coeff.
			$LBM\ IN^2/LBF\ SEC$		X		
$A_{MV}\langle x\rangle$	f			X	X	X	Metering valve flow area function.
A_{MVL}	c	0.00	$IN^4/SEC\ LBF^{1/2}$	X		X	Metering valve leakage coeff.
		0.00	$LBM\ IN^2/SEC\ LBF^{1/2}$		X		
A_{MVO}	c	.653	$IN^4/SEC\ LBF^{1/2}$	X		X	Metering valve full open flow coeff.
		$.429X10^{-3}$	$LBM\ IN^2/SEC\ LBF^{1/2}$		X		
A_{MVR}	v		$IN^4/SEC\ LBF^{1/2}$	X		X	Metering valve return flow coeff.
			$LBM\ IN^2/SEC\ LBF^{1/2}$		X		
A_{MVS}	v		$IN^4/SEC\ LBF^{1/2}$	X		X	Metering valve supply flow coeff.
			$LBM\ IN^2/SEC\ LBF^{1/2}$		X		
A_{RC}	c	1.00	$IN^4/SEC\ LBF^{1/2}$	X		X	Control valve return line restriction.
		$.658X10^{-3}$	$LBM\ IN^2/LBF\ SEC$		X		
B_B	c	$.248X10^6$	LBF/IN^2	X		X	Bulk modulus within the brake housing.
	c	$.371X10^6$	IN LBF/LBM		X		Temp X gas constant.

*See notes on Sheet 5

Table A4 Option 1, 2 and 3 Hydraulic System Parameters (Sheet 2 of 5)

SYMBOL	TYPE	VALUE	UNITS	OP* 1	OP* 2	OP* 3	DESCRIPTION
B_{SL}	c	.218 X 10^6	LBF/IN^2			X	Fluid bulk modulus in control line.
B_{CVR}	c	.248 X 10^6	LBF/IN^2	X			Fluid bulk modulus in return of control V.
	c	.371 X 10^6	IN LBF/LBM		X		Temp. X gas constant, Cont Valve Return Cavity
B_{MV}	c	.248 X 10^6	LBF/IN^2	X		X	Bulk modulus at MV outlet
	c	.371 X 10^6	IN LBF/LBM		X		Temp X gas constant, metering valve outlet
D_{RBL}	c	19.22	LBF SEC/IN^5			X	Laminar line loss coeff.
D_{TBL}	c	.216	LBF SEC^2/IN^8			X	Turbulent line loss coeff.
G_{MV}	c	.05	IN^3/SEC LBF	X		X	Metering valve gain
	c	.05	IN^3/SEC LBF		X		
γ_a	c	1.40	Dimensionless		X		Ratio of specific heats $\gamma_a = (c_p/c_y)$
P_B	v(o)		LBF/IN^2	X	X	X	Brake Pressure
P_{BO}	c	100	LBF/IN^2			X	Brake pressure at time = 0.
	v		LBF/IN^2	X	X		
$\dot{P}_B$	v		LBF/IN^2 SEC			X	Time derivative of brake press.
P_{BI}	v		LBF/IN^2	X	X	X	Press. at brake inlet.
P_{BIO}	c	100	LBF/IN^2			X	Brake inlet press at time = 0.
	v		LBF/IN^2	X	X		
$\dot{P}_{BI}$	v		LBF/IN^2 SEC			X	Brake inlet press time derivative
P_{COM}	v		LBF/IN^2	X	X	X	Pilot's command press.
P_{CP}	c	1500	LBF/IN^2	X	X	X	Steady state command press.
P_{CV}	v(o)		LBF/IN^2	X	X	X	Control valve output press.
P_{CVO}	c	100	LBF/IN^2	X		X	Control valve press at time = 0.
	c	14.7	LBF/IN^2		X		
$\dot{P}_{CV}$	v		LBF/IN^2 SEC	X	X	X	Derivative of control valve press.

Table A4 Option 1, 2 and 3 Hydraulic System Parameters (Sheet 3 of 5)

SYMBOL	TYPE	VALUE	UNITS	OP 1	OP 2	OP 3	DESCRIPTION
P_{CVR}	v(o)		LBF/IN^2	X	X	X	Return press in cont. valve.
P_{CVRO}	c	100	LBF/IN^2	X		X	Cont valve ret press time 0
	c	14.7	LBF/IN^2		X		
$\dot{P}_{CVR}$	v		LBF/IN^2 SEC	X	X	X	Derivative of cont VA press ret
$\phi(x,y)$	f			X	X	X	Flow function
P_{MV}	v(o)		LBF/IN^2	X	X	X	Metering valve output press.
P_{MVO}	c	100	LBF/IN^2	X		X	Metering valve press at time = 0.
	c	14.7	LBF/IN^2		X		
$\dot{P}_{MV}$	v		LBF/IN^2 SEC	X	X	X	Time derivative of MV press
P_R	c	100	LBF/IN^2	X		X	Return pressure
	c	14.7	LBF/IN^2		X		
P_S	c	3000	LBF/IN^2	X	X	X	System supply pressure.
Q_B	v		IN^3/SEC	X		X	Flow into brake (per line)
			LBM/SEC		X		
Q_{CV}	v		IN^3/SEC	X		X	Flow out of control valve
	v		LBM/SEC		X		
Q_{CVO}	c	0.0	IN^3/SEC			X	Control valve flow at time = 0
	v		IN^3/SEC	X			
	v		LBM/SEC		X		
$\dot{Q}_{CV}$	v		IN^3/SEC			X	Time derivative cont VA flow
Q_{CV1}	v(i)		IN^3/SEC	X		X	
			LBM/SEC		X		
Q_{CV2}	v(i)		IN^3/SEC	X		X	Feedback flows from
			LBM/SEC		X		control valve.
Q_{CV3}	v(i)		IN^3/SEC	X		X	
			LBM/SEC		X		

Table A4 Option 1, 2 and 3 Hydraulic System Parameters (Sheet 4 of 5)

SYMBOL	TYPE	VALUE	UNITS	OP 1	OP 2	OP 3	DESCRIPTION
Q_{CVR}	v		IN^3/SEC	X		X	Return flow in control valve
			LBM/SEC		X		
Q_{MV}	v		IN^3/SEC	X		X	Metering valve flow
			LBM/SEC		X		
Q_R	v		IN^3/SEC	X		X	Return flow from metering valve
			LBM/SEC		X		
Q_{RC}	v		IN^3/SEC	X		X	Return flow from control valve
			LBM/SEC		X		
Q_S	v		IN^3/SEC	X		X	Flow into system
			LBM/SEC		X		
R_{CRIT}	c	‡	Dimensionless		X		Critical pressure ratio
R_{HO}	c	$.781 \times 10^{-4}$	$LBF\ SEC^2/IN^4$	X		X	Fluid density
S_{BL}	c	191.0	IN			X	Control line length
S_{CL}	c	.005	IN	X	X	X	Control valve overlap
S_{CVO}	c	.030	IN	X	X	X	Spool distance from full closed to full open (C.V)
S_{MVL}	c	-.060	IN	X	X	X	Min. Neg. spool travel (met. valve)
S_{MVO}	c	.050	IN	X	X	X	Spool travel from full closed to full open (met. valve)
S_{MVU}	c	.060	IN	X	X	X	Max. Pos. Spool travel (met. valve)
T	v(i)		SEC	X	X	X	Time
T_{CP}	c	.200	SEC	X	X	X	Time for $P_{com} = P_{cp}$
V_B	v		IN^3	X	X	X	Brake fluid volume (per line)
V_{BO}	c	4.00	IN^3	X	X	X	Brake fluid volume when Xp = 0
V_{BL}	c	1.495	IN^3			X	Corrected line volume

‡ Calculate from γ_α, see Equation (2.5)

Table A4 Option 1, 2 and 3 Hydraulic System Parameters (Sheet 5 of 5)

SYMBOL	TYPE	VALUE	UNITS	OP* 1	OP* 2	OP* 3	DESCRIPTION
V_{CVR}	c	2.00	IN^3	X	X	X	Control valve return volume.
V_{MV}	v		IN/SEC	X	X	X	Metering valve control variable.
V_{MVV}	c	1.00	IN^3	X	X	X	Volume between metering & control valve.
X_{CV}	v(i)		IN	X	X	X	Control valve spool position.
X_{MV}	v		IN	X	X	X	Metering valve spool position.
X_{MVO}	c	0.0	IN	X	X	X	Metering valve spool position at time=0
$\dot{X}_{MV}$	v		IN/SEC	X	X	X	Metering valve spool velocity.
X_P	v(i)		IN	X	X	X	Brake piston displacement
$\dot{X}_P$	v(i)		IN/SEC	X	X	X	Brake piston velocity

*An x denotes application in option 1, 2, or 3 as explained on page 35-37.

Option 1 Brake actuation system using hydraulic fluid where the control line description considers volume effects only.

Option 2 Brake actuation system using compressible pneumatic fluid.

Option 3 Brake actuation system using hydraulic fluid where the control line description considers both volume and inertia effects.

Table A5 Option 4 Hydraulic System Parameters (Sheet 1 of 2)

SYMBOL	TYPE	VALUE	UNITS	DESCRIPTION
ACVR	v		$IN^4/SEC\ LBF^{1/2}$	Hydraulic flow coefficient, control valve return
ACVRO	c	1.09	$IN^4/SEC\ LBF^{1/2}$	Hydraulic flow coeff, control valve return, full open to return
ACVS	v		$IN^4/SEC\ LBF^{1/2}$	Hydraulic flow coeff, control valve supply
ACVSO	c	1.09	$IN^4/SEC\ LBF^{1/2}$	Hydraulic flow coeff, control valve supply, full open to supply
ACVL	c	0	$IN^4/SEC\ LBF^{1/2}$	Hydraulic flow coeff, Control valve null position
CBV1	c	50	LBF/IN^5	Brake pressure - Volume coefficient - Before disc contact
CBV2	c	3550	LBF/IN^5	Brake pressure - Volume coefficient - After disc contact
PCP	-	1500	LBF/IN^2	Pilot command brake pressure
PCV	v(o)		LBF/IN^2	Control valve output pressure
PCVR	v(o)		LBF/IN^2	Return pressure in control valve
PR	c	100	LBF/IN^2	Reservoir pressure
PB	v(o)		LBF/IN^2	Brake pressure
PBR1	c	100	LBF/IN^2	Brake bias pressure before disc contact
PBR2	c	-5480	LBF/IN^2	Brake bias pressure after disc contact
PB1	v		LBF/IN^2	Brake pressure before disc contact
PB2	v		LBF/IN^2	Brake pressure after disc contact
QMV	v		IN^3/SEC	Hydraulic flow rate out of metering valve
QCVR	v		IN^3/SEC	Hydraulic flow rate from control valve to return
QB	v		IN^3/SEC	Hydraulic flow rate into brake
SCVO	c	0.030	IN	Position of control valve spool for max flow

Table A5 Option 4 Hydraulic System Parameters (Sheet 2 of 2)

SYMBOL	TYPE	VALUE	UNITS	DESCRIPTION
T	v(1)		SEC	Time
TCP	c	0.1	SEC	Time for $PMV = PCP$
XCV	v(1)		IN	Control Valve Spool position
VB	v		IN^3	Brake hydraulic volume
VBO	c	0	IN^3	Brake hydraulic volume at time zero
PMV	v		LBF/IN^3	Metering valve output pressure
VBC	c	1.6	IN^3	Brake volume at disc contact

3a VEHICLE AND WHEEL STRUCTURAL SUPPORT (FLYWHEEL)

Figure A11 shows the model for the airplane system as it might be simulated with a dynamometer flywheel set-up. The mass W_A is supported by the tire and is determined by the percentage of the airplane weight carried on one main gear. The mass W_{AR} represents some part of the airplane structure which could vibrate in sympathy with certain ground discontinuities such as wing mounted fuel tanks or armament. The forces F_{LO} and F_{AL} act on W_A because of gravity and aerodynamic lift, respectively.

A. Mathematical Description

The shock strut stroke is denoted by Z_{SM}.
This stroke is determined by Z and Z_{WM}.

(3a.1) $$Z_{SM} = Z_{WM} - Z + S_{MGL}$$

(3a.2) $$\dot{Z}_{SM} = \dot{Z}_{WM} - \dot{Z}$$

The shock strut force F_{VM} is given by equation (3a.3)

(3a.3) $$F_{VM} = F_{VMS}\langle Z_{SM}\rangle + D_{VM}\dot{Z}_{SM} + A_{VM}\langle Z_{SM}\rangle \dot{Z}_{SM}|\dot{Z}_{SM}| + D_{VMC}\, G_M\langle \dot{Z}_{SM}\rangle$$

Where
$$G_M\langle X\rangle = \begin{cases} +1.0 & \text{FOR } X > 0 \\ 0 & \text{FOR } X = 0 \\ -1.0 & \text{FOR } X < 0 \end{cases}$$

Let Z_{GO} and Z_{GOP} denote the height and slope of the ground (or flywheel surface). Let S_M denote the tire deflection. Then S_M and $\dot{S}_M$ are determined by

(3a.4) $$S_M = \max\{0.0,\ Z_{GO}\langle X_F\rangle - Z_{WM} + R_{OT}\}$$

(3a.5) $$\dot{S}_M = Z_{GOP}\langle X_F\rangle V_F - \dot{Z}_{WM}$$

The force F_{NM} acting vertically upward on the tire is then given by

(3a.6) $$F_{NM} = S_M\left(C_{MT} + D_{MT}\dot{S}_M\right)$$

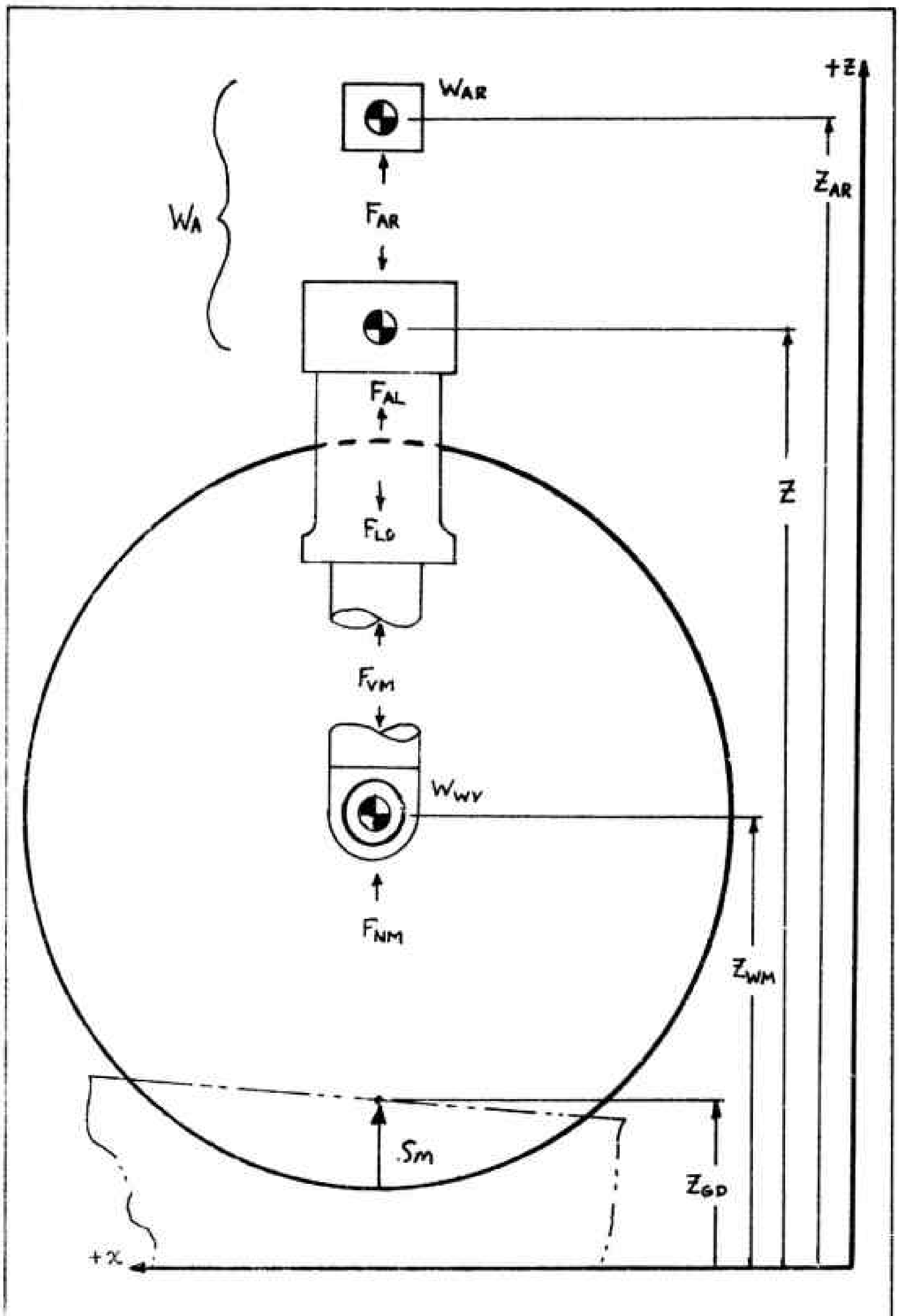

Figure A1 Flywheel System Model

Summing forces in the vertical direction on the unsprung mass W_{WV}, there follows:

$$(3a.7)\quad W_{WV}\ddot{Z}_{WM} = F_{NM} - F_{VM} + F_{\theta RV}$$

Where $F_{\theta RV}$ is the tire unbalance force.
For the mass W_{AR}, summing forces vertically gives:

$$(3a.8)\quad W_{AR}\ddot{Z}_{AR} = F_{AR}$$

$$(3a.9)\quad F_{AR} = C_{AR}(Z - Z_{AR}) + D_{AR}(\dot{Z} - \dot{Z}_{AR})$$

The aerodynamic lift and drag forces F_{AL} and F_{AD} are defined as follows:

$$(3a.10)\quad F_{AL} = C_{AL}V_F^2$$

$$(3a.11)\quad F_{AD} = C_{AD}V_F^2$$

The equation which determines Z is given as

$$(3a.12)\quad (W_A - W_{AR})\ddot{Z} = F_{VM} + F_{AL} - F_{LD} - F_{AR}$$

The equation for the flywheel velocity is given by

$$(3a.13)\quad W_{AT}\dot{V}_F = F_{TH} - F_{AD} - 2F_{BT}$$

Where F_{TH} is a force equivalent to engine thrust and W_{AT} is the airplane mass. The aircraft's longitudinal displacement is established by

$$(3a.14)\quad X_F = \int V_F\,dt + X_{FO}$$

The equation flow diagram for the airplane system (flywheel) is shown on Figure A12.

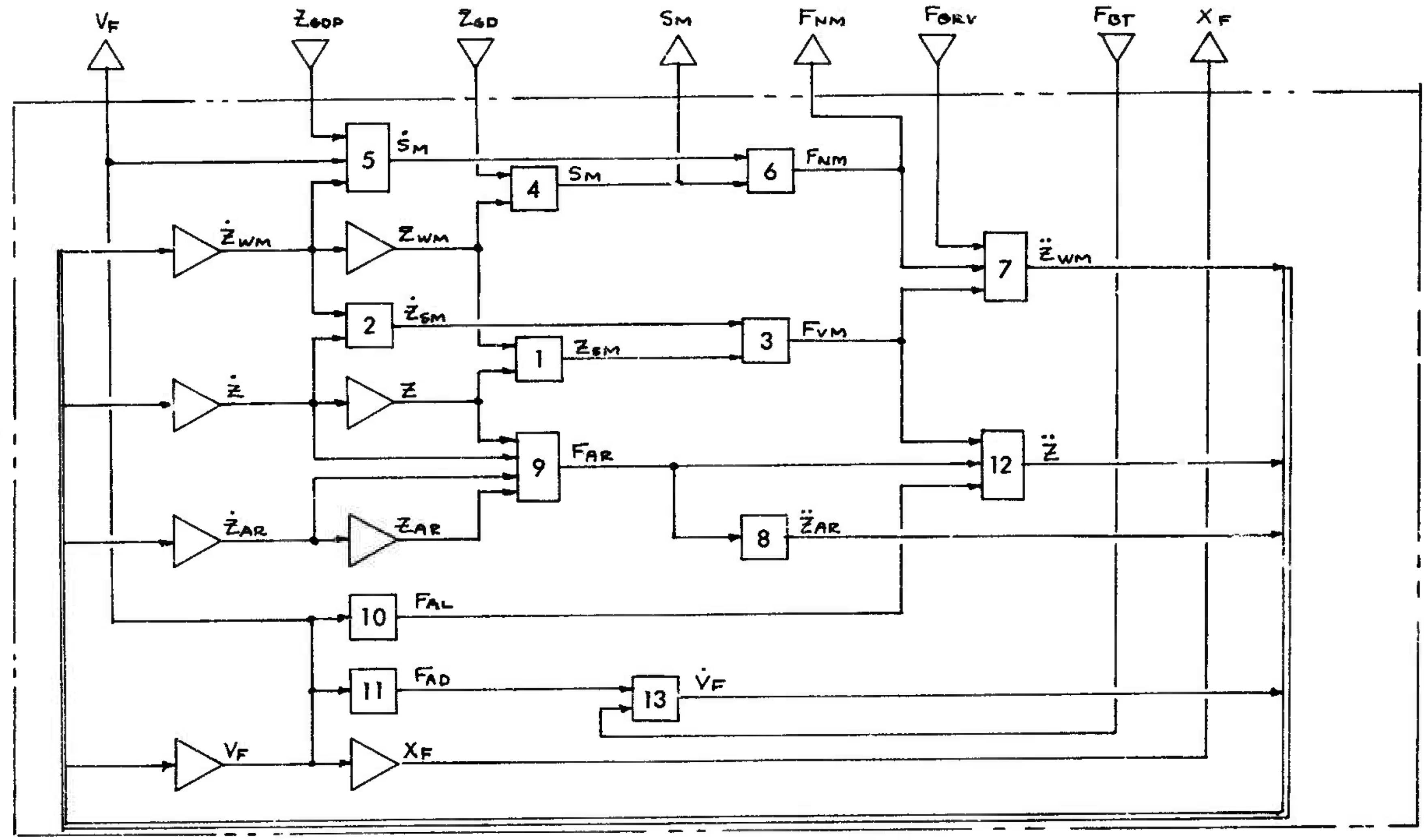

Figure A12 Airplane System (Flywheel) Equation Flow Diagram

B. Parameter Evaluation

Shock Strut Characteristics

Figures A13 and A14 show the main gear load and damping characteristics for one gear.

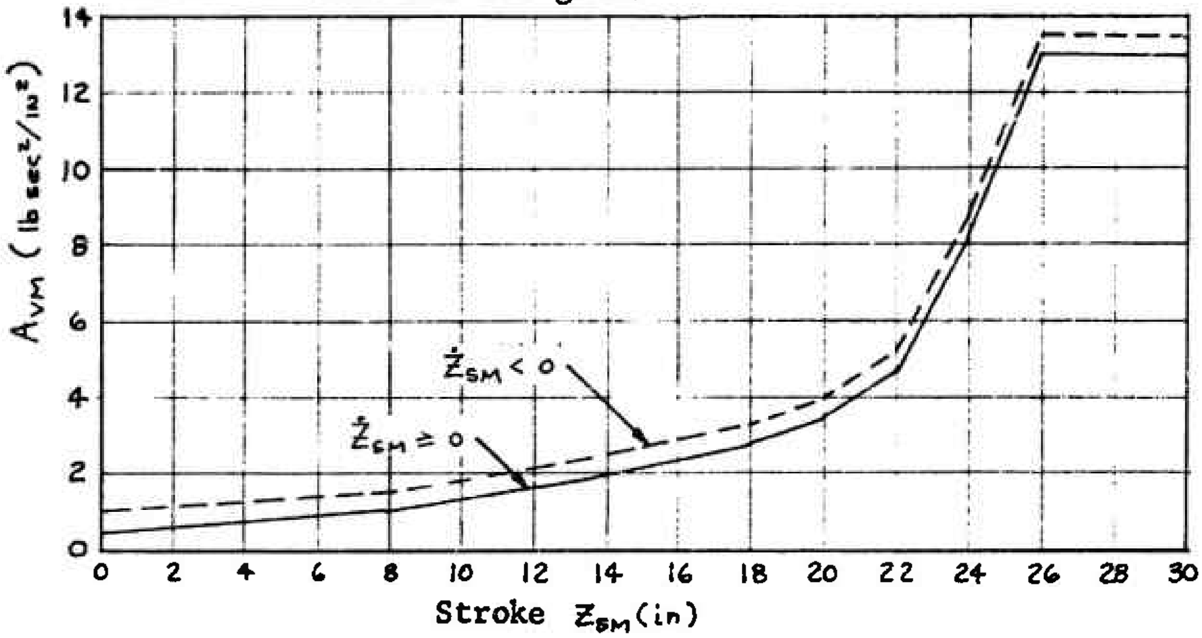

Figure A13 Main Gear Damping Curve

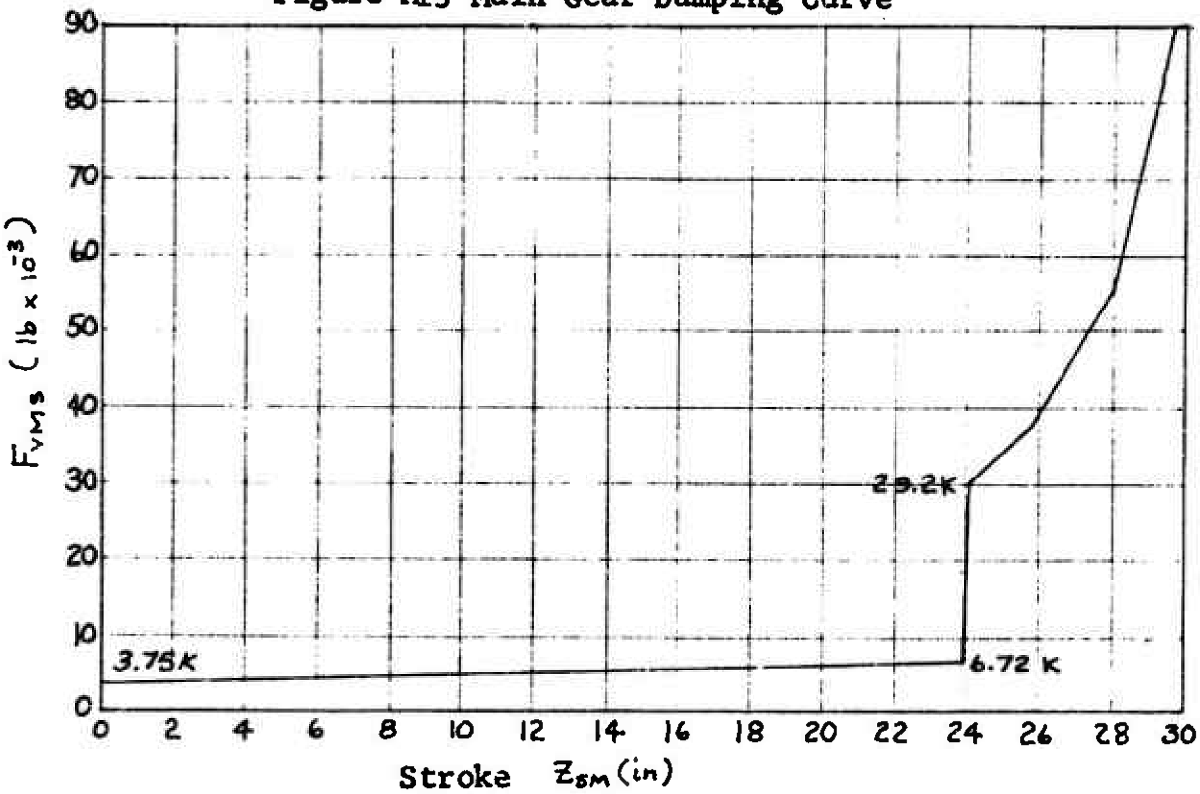

Figure A14 Main Gear Air Load Curve

Vertical Tire Characteristics

In equation (3a.6) it has been assumed that the tire loading characteristic is given by an equation of the form

(3a.15) $$F = S(C + D\dot{S})$$

Let the following terms be defined for a tire:

F_R = Rated load

P_R = Rated pressure

S_R = Rated deflection

If P is the actual pressure, then obviously the tire spring rate, C , is

(3a.16) $$C = \left(\frac{P}{P_R}\right)\left(\frac{F_R}{S_R}\right)$$

From reference 1 (Equation 132) the damping force, F_D , is established as:

(3a.17) $$F_D = \left(\frac{\eta C}{\omega}\right)\dot{S}$$

It is assumed that the damping force is related to the undamped natural frequency at rated conditions. The undamped natural frequency, ω , is established as:

(3a.18) $$\omega = \sqrt{\frac{K}{m}} = \sqrt{\frac{F_R}{S_R}\frac{G}{F_R}} = \sqrt{\frac{G}{S_R}}$$

Where G = 386 IN/SEC^2. Also from Equations 137 and 138 of Reference 1:

(3a.19) $$\eta = 2\,\eta_R \Big/ \left[1 + (P/P_R)\right]$$

Where $\eta_R = 0.1.$

The main landing gear shock strut linear damping coefficient, D_{VM}, is set equal to zero for the example problem.

The unsprung mass, W_{WV}, experiencing vertical motion is 6.44 lbm. Thus, W_{WV} = (644)/386 = 1.667 lbf sec^2/in.

As previously assumed in Equation (3a.15), $F_0 = S_0 \dot{S}$
Equating the two expressions for F_0 at rated deflection

(3a.20) $$\frac{\eta C}{\omega} = S_R D$$

Or

(3a.21) $$D = \frac{\eta C}{\omega S_R} = \frac{\eta F_R}{(S_R)^2}\left(\frac{P}{P_R}\right)\sqrt{\frac{S_R}{G}}$$

For the 47 x 18 - 18 26 ply rating F-111 main tire,
$P = P_R =$ 150 psi

F_R = 38,100 lb. and S_R = 4.00 IN.

Thus

(3a.22) $$C_{MT} = \left(\frac{P}{P_R}\right)\left(\frac{F_R}{S_R}\right) = \frac{(150)(38100)}{(150)(4.00)} = 9530 \text{ lbf/IN}$$

(3a.23) $$D_{MT} = \left(\frac{P}{P_R}\right)\left(\frac{\eta F_R}{S_R^2}\right)\sqrt{\frac{S_R}{G}}$$

$$= \frac{(150)}{(150)}\frac{(.1)(38100)}{(4.00)^2}\sqrt{\frac{4.0}{386}} = 24.24 \text{ lbf sec/IN}^2$$

<u>Aircraft Characteristics</u>

For the example problem, an airplane weight of 57,000 lb. is used. The static vertical load on one main gear is 25,200 lbs. so that

(3a.24) $$W_A = 25{,}200/G = 65.0 \text{ lbf sec}^2\text{/IN.}$$

For a velocity of V_F = 2400 IN/SEC and a representative tire-to-runway braking coefficient of .45 at the main wheel, the tire load is 21,400 lbs. Thus F_{LO} = 21,400 lb.

The total aircraft mass is $W_{AT} = 57000/G = 147.8$ lbf sec^2/IN.

The mass W_{AR} is used to simulate some airplane resonant effect. For illustrative purposes, it is assumed that $W_{AR} = 1000$ LBM = 2.59 LBF SEC^2/IN and has a natural frequency of 12 cps. Therefore, since $\omega = 2\pi(12) = 75.4$ rad/sec and $k = m\omega^2$,

$$(3a.25)\quad C_{AR} = \omega^2 W_{AR} = (75.4)^2(2.59) = 14{,}720 \text{ lb/in}$$

Using 3 percent critical damping gives

$$(3a.26)\quad D_{AR} = (.03)\,2\sqrt{C_{AR} W_{AR}} =$$
$$= (.03)\,2\sqrt{(14{,}720)(2.59)} = 11.72 \text{ lb sec/in}$$

The initial conditions are calculated for equilibrium. At time = 0, let $X_F = 0$ so that $Z_{GD}\langle X_F\rangle = 0$ since $Z_{GD}\langle 0\rangle$ is always 0. Let V_{FO} = 1200 IN/SEC and assume that $C_{AL} = C_{AD} = 0$

From equation (3a.6),

$$(3a.27)\quad S_m = F_{NM}/C_{MT} = 26000/9530 = 2.73 \text{ in}$$

From equation (3a.4),

$$(3a.28)\quad Z_{WMO} = (0 - 2.73 + 23.32) = 20.59 \text{ IN}$$

From figure A14 when $F_{VMS} = 26000$ lb.,

Z_{SM} = 23.98 in and from equation (3a.1),

$$(3a.29)\quad Z_0 = Z_{WMO} - Z_{SM} + S_{MEL} = 20.59 - 23.98 + 83.41 = 80.0 \text{ IN.}$$

Also $Z_{ARO} = Z_O = 80.0$ in.

For the example problem the effects of aerodynamic forces are not included in the flywheel simulation; therefore, C_{AD} = 0.0 and C_{AL} = 0.0.

The unsprung mass moving vertically, W_{WV}, is the same as W_{GW} described in the Section 4a Wheel and Tire System (Flywheel) for horizontal motion. Therefore, W_{WV} = 1.60 lbf sec^2/in.

The average engine idle thrust is 1000 lbf. Therefore, F_{TH} = 1000 lbf.

Table A6 Vehicle and Wheel Structural Support (Flywheel) Parameters (Sheet 1 of 3)

SYMBOL	TYPE	VALUE	UNITS	DESCRIPTION
A_{VM}	v*		lb sec²/in²	Shock strut damping characteristic.
C_{AD}	c	0.0	lb sec²/in²	Aerodynamic drag coefficient.
C_{AL}	c	0.0	lb sec²/in²	Aerodynamic lift coefficient.
C_{AR}	c	14,720	lb/in	Spring rate associated with mass W_{AR}
C_{MT}	c	9530	lb/in	Tire vertical spring rate
D_{AR}	c	11.72	lb sec/in	Damping coeff. associated with mass W_{AR}
D_{MT}	c	38.8	lb sec/in²	Tire damping coefficient
D_{VM}	c	0.0	lb sec/in	Shock strut linear damping coeff.
F_{AD}	v		lb	Aerodynamic drag force on airplane.
F_{AL}	v		lb	Aerodynamic lift force on airplane
F_{AR}	v		lb	Force associated with mass W_{AR}
F_{BT}	v(i)		lb	Braking force
F_{LD}	c	21,400	lb	Static force on tire
$F_{\theta RV}$	v(i)		lb	Tire unbalance force (vertical)
F_{NM}	v(o)		lb	Tire normal force
F_{TH}	c	1000	lb	Engine thrust
F_{VM}	v		lb	Shock strut force
F_{VMS}	v**		lb	Shock strut force with $\dot{Z}_{SM} = 0$
S_M	v(o)		in	Tire deflection
$\dot{S}_M$	v		in/sec	Rate of tire deflection
V_F	v		in/sec	Flywheel velocity
Y_{FO}	c	2400	in/sec	Flywheel velocity at time = 0

*Point plot input see Figure 13
**Point plot input see Figure 14

Table A6 Vehicle and Wheel Structural Support (Flywheel) Parameters (Sheet 2 of 3)

SYMBOL	TYPE	VALUE	UNITS	DESCRIPTION
W_A	c	65.0	lb sec²/in	Airplane mass carried on main gear.
W_{AR}	c	2.59	lb sec²/in	Mass of airplane substructure.
W_{AT}	c	147.8	lb sec²/in	Total airplane mass
W_{WV}	c	1.667	lb sec²/in	Unsprung mass
X_F	v(o)		in	Flywheel surface distance traveled.
X_{FO}	c	0.0	in	Flywheel distance at time = 0.
Z	v		in	Vertical location of equivalent apl. mass C.G.
Z_o	c	80.0	in	Vertical location of equivalent mass at time = 0
$\dot{Z}$	v		in/sec	Velocity of apl. mass
$\dot{Z}_o$	c	0.0	in/sec	Velocity of apl mass at time = 0
$\ddot{Z}$	v		in/sec²	Acceleration of apl mass
Z_{AR}	v		in	Auxiliary mass location
Z_{ARO}	c	80.0	in	Auxiliary mass location at time = 0
$\dot{Z}_{AR}$	v		in/sec	Auxiliary mass velocity
$\dot{Z}_{ARO}$	c	0.0	in/sec	Auxiliary mass velocity at time = 0
$\ddot{Z}_{AR}$	v		in/sec²	Auxiliary mass acceleration
Z_{GD}	v(i)		in.	Ground height
Z_{GDP}	v(i)		in/in	Ground slope
Z_{SM}	v		in	Shock Strut Stroke
$\dot{Z}_{SM}$	v		in/sec	Shock strut stroke velocity

Table A6 Vehicle and Wheel Structural Support (Flywheel) Parameters (Sheet 3 of 3)

SYMBOL	TYPE	VALUE	UNITS	DESCRIPTION
Z_{WM}	v		in	Axle location (vertical)
Z_{WMO}	c	20.59	in	Axle location at time = 0
$\dot{Z}_{WM}$	v		in/sec	Axle velocity (vertical)
$\dot{Z}_{WMO}$	c	0.0	in/sec	Axle location at time = 0
$\ddot{Z}_{NM}$	v		IN/SEC²	Axle acceleration
D_{VMC}	c	200	LB	Coulomb friction coeff
$G_m\langle K\rangle$	f			Coulomb friction function
R_{OT}	c	23.32	IN	Undeflected tire radius*
S_{MCL}	c	83.41	IN	Fully extended shock strut length
$\dot{V}_F$	v		IN/SEC²	Flywheel acceleration
$\dot{V}_{FO}$	c	7.0	IN/SEC²	Flywheel acceleration at time zero

*Same as for tire and wheel system

3b. VEHICLE AND WHEEL STRUCTURAL SUPPORT (3 DEGREE AIRPLANE SYSTEM)

The three degree airplane system is built around a rigid body airplane which is allowed to move vertically, horizontally (parallel to the runway centerline), and rotationally in the pitch mode. This model provides for the interaction of the anti-skid system with those effects which are related to airplane pitch. This includes such pitch effects as change in the aerodynamic lift, drag, and moment due to change in wing angle of attack, change in the aerodynamic lift, drag, and moment due to changes in elevator deflection as dictated by the stability augmentation system (pitch mode), change in tire loading due to braking pitch moment, and the effect of ground slope and roughness as reacted through both the main and nose gears.

A. Mathematical Description

Figure A15 shows the three coordinates which describe the airplane position relative to reference points on the earth's surface.

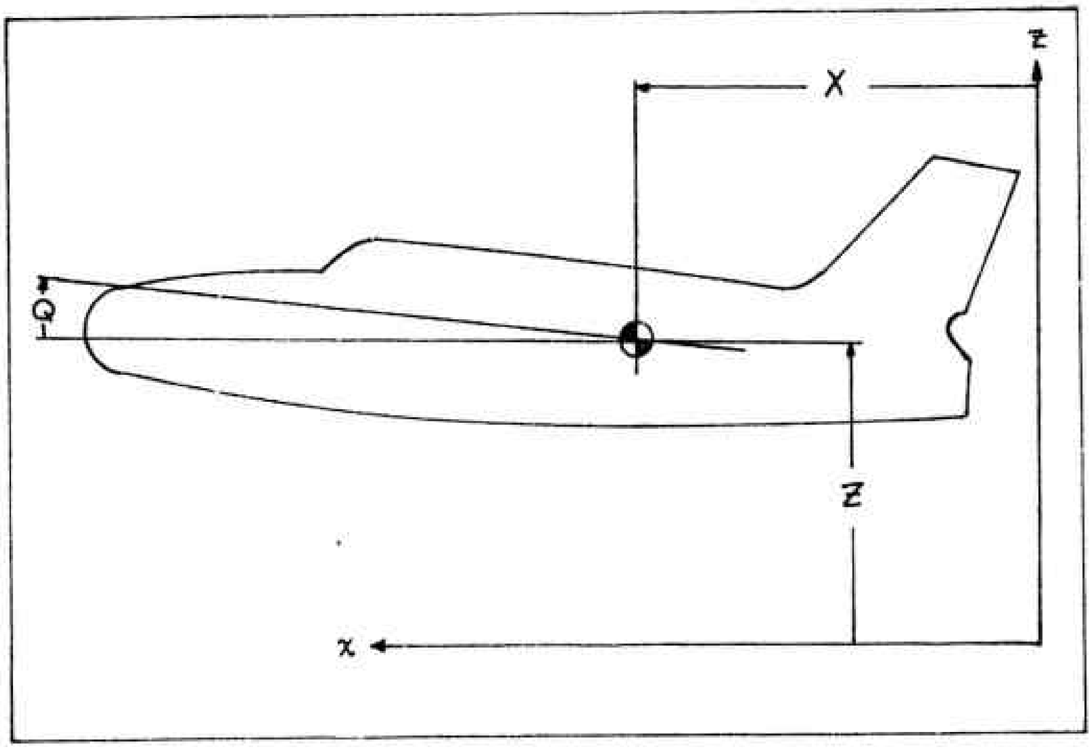

Figure A15 Airplane Coordinates

Figure A16 shows the gear extended dimensions as measured in the airplane's water line-fuselage station reference system.

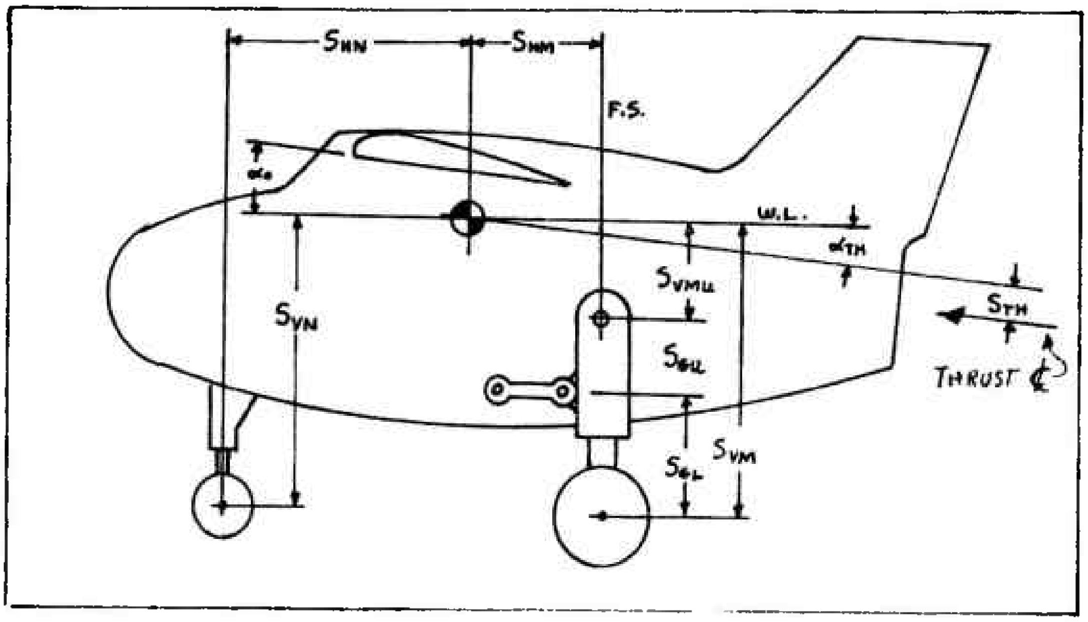

Figure A16 Airplane Geometry

Let $Z_{GD}\langle x \rangle$ denote the runway profile height and let $Z_{GDP}\langle x \rangle$ denote the runway profile slope.

Nose Gear

Let Z_{SN} and $\dot{Z}_{SN}$ denote the nose strut stroke and stroke velocity. From Figure A17 , Z_{SN} and $\dot{Z}_{SN}$ are given by

$$(3b.1)\quad Z_{SN} = Z_{WN} + S_{VN} - Z - S_{HN} Q$$

$$(3b.2)\quad \dot{Z}_{SN} = \dot{Z}_{WN} - \dot{Z} - S_{HN} \dot{Q}$$

The nose gear shock strut force is then given by

$$(3b.3)\quad F_{VN} = F_{VNS}\langle Z_{SN} \rangle + D_{NN} \dot{Z}_{SN} + A_{VN}\langle Z_{SN} \rangle \dot{Z}_{SN} \left| \dot{Z}_{SN} \right|$$

F_{NN}, the normal ground force at the nose gear is given by

$$(3b.4)\quad F_{NN} = S_N \left(C_{NT} + D_{NT} \dot{S}_N \right)$$

where S_N is the nose tire deflection. S_N and $\dot{S}_N$ are given by:

$$(3b.5)\quad S_N = max\{0.0, Z_{GD}\langle X_{WN}\rangle + R_{OTN} - Z_{WN}\}$$

$$(3b.6)\quad \dot{S}_N = Z_{GDP}\langle X_{WN}\rangle \dot{X}_{WN} - \dot{Z}_{WN}$$

Summing vertical forces on the nose wheel,

$$(3b.7)\quad W_{WN}\ddot{Z}_{WN} = F_{NN} - F_{VN}$$

$$(3b.8)\quad F_{DN} = U_{RRN} F_{NN}$$

Main Gear

Let Z_{SM} and $\dot{Z}_{SM}$ denote the main gear stroke and stroke velocity:

$$(3b.9)\quad Z_{SM} = Z_{WM} - Z + S_{VM} + S_{HM}Q$$

$$(3b.10)\quad \dot{Z}_{SM} = \dot{Z}_{WM} - \dot{Z} + S_{HM}\dot{Q}$$

The main gear shock strut force is given by:

$$(3b.11)\quad F_{VM} = F_{VMS}\langle Z_{SM}\rangle + D_{VM}\dot{Z}_{SM} + A_{VM}\langle Z_{SM}\rangle \dot{Z}_{SM}|\dot{Z}_{SM}| + OVMC\ GM\langle \dot{Z}_{SM}\rangle$$

Let S_M denote the main gear tire deflection. Then the tire normal force is given by:

$$(3b.12)\quad F_{NM} = S_M(C_{MT} + D_{MT}\dot{S}_M)$$

$$(3b.13)\quad S_M = max\{0.0, Z_{GD}\langle X_{AX}\rangle + R_{OTM} - Z_{WM}\}$$

$$(3b.14)\quad \dot{S}_M = Z_{GDP}\langle X_{AX}\rangle \dot{X}_{AX} - \dot{Z}_{WM}$$

Summing vertical forces on the main wheel, where $FORV$ is the vertical component of the tire unbalance force,

$$(3b.15)\quad W_{WM} Z_{WM} = F_{NM} - F_{VM} + F_{ORV}$$

Figure A18 shows the model of the main gear. With the assumption that the gear weight is much less than the airplane weight (that is, $W_u \ll W_A$), it follows that:

$$(3b.16)\quad W_u S_{Gu}^2 \ddot{\theta}_G = F_u S_{Gu} - F_G(S_{Gu} + Z_{GL}) - T_S$$

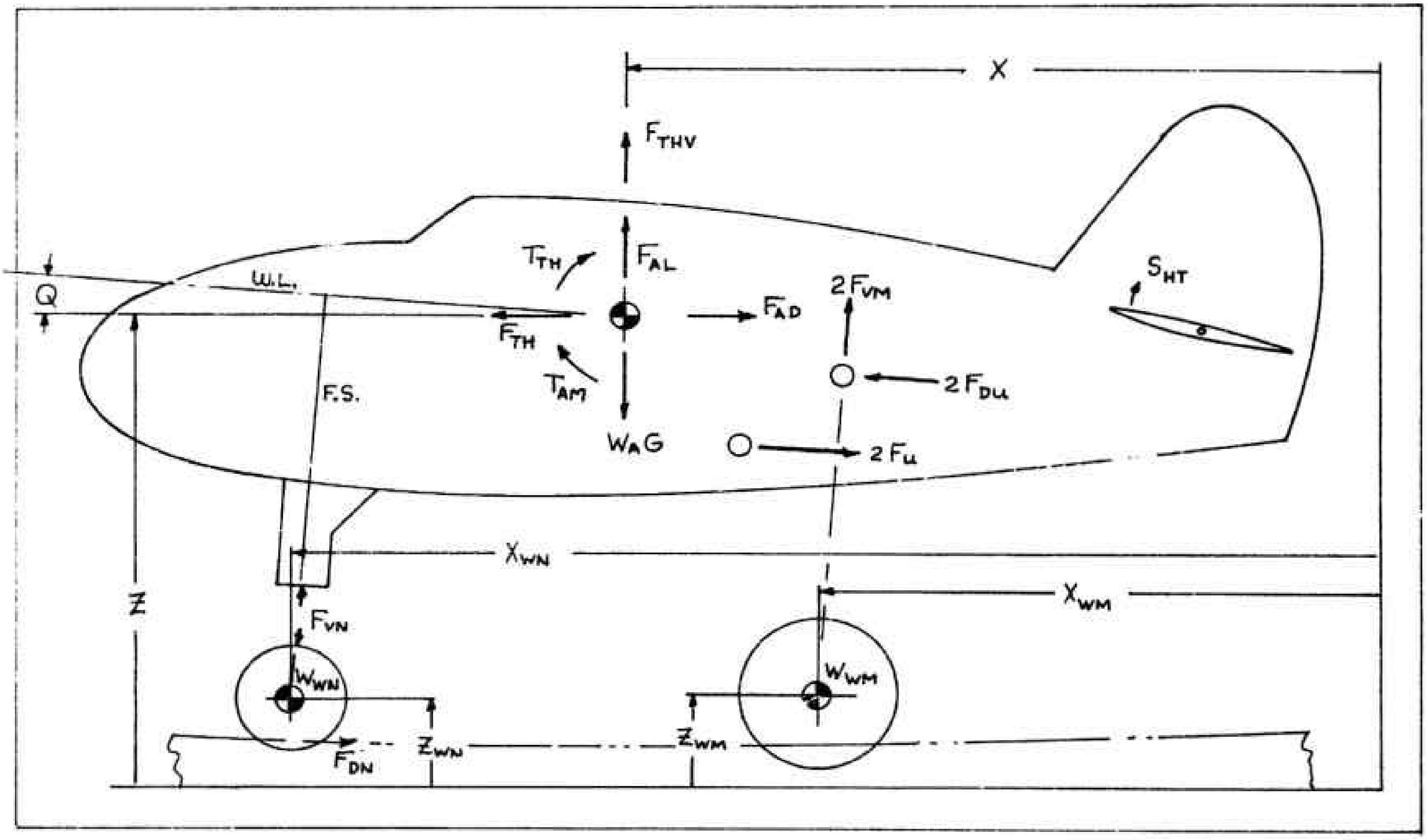

Figure A17 Airplane Dynamics

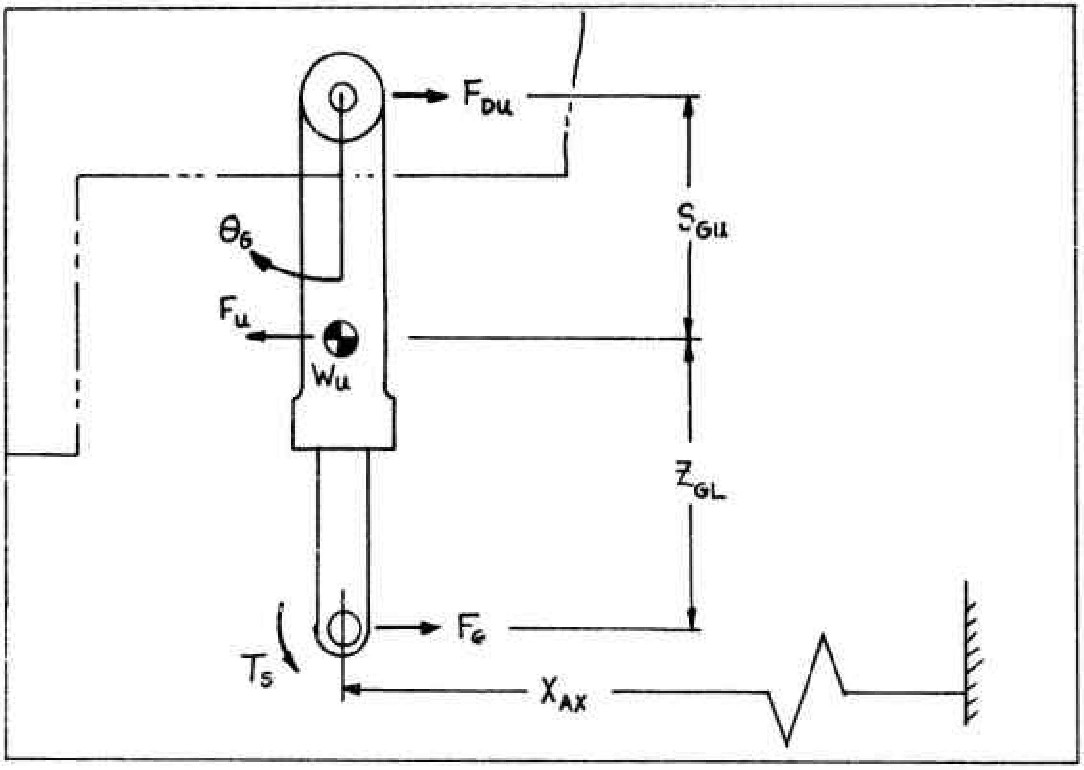

Figure A18 Main Strut Model

where Z_{GL} is determined by:

(3b.17) $Z_{GL} = S_{GL} - Z_{SM}$

F_{DU} can then be computed by summing moments about the CG,

(3b.18) $F_{DU} = (F_G Z_{GL} + T_S)/S_{GU}$

where

(3b.19) $F_U = S_{GU}(C_U(Q - \theta_G) + D_U(\dot{Q} - \dot{\theta}_G))$

T_S and F_G are outputs from the tire and wheel system. The horizontal axle reference location is denoted by X_{AX}. X_{AX} is given by:

(3b.20) $X_{AX} = X - S_{HM} + (S_{GU} + Z_{GL})\theta_G$

(3b.21) $\dot{X}_{AX} = \dot{X} + (S_{GU} + Z_{GL})\dot{\theta}_G$

Thrust

Referring to Figures A16 and A17 , if F_{TH} is the thrust, then

$$(3b.22)\quad F_{THV} = F_{TH}\,(\alpha_{TH} + Q)$$

$$(3b.23)\quad T_{TH} = S_{TH}\,F_{TH}$$

Aerodynamics

The dynamic Air Force Q_A is given by:

$$(3b.24)\quad Q_A = \dot{X}^2 A_{REF} R_{HA} / 288.0$$

The aerodynamic lift, drag, and moment are then given by:

$$(3b.25)\quad F_{AL} = C_{AL} Q_A$$

$$(3b.26)\quad F_{AD} = C_{AD} Q_A$$

$$(3b.27)\quad T_{AM} = C_{AM} Q_A$$

If α_W denotes the wing angle of attack relative to the air, then:

$$(3b.28)\quad \alpha_W = \alpha_0 + (180/\pi)(Q - \dot{Z}/\dot{X})$$

Let S_{HT} denote the horizontal tail deflection. Then the aerodynamic coefficients are given by:

$$(3b.29)\quad C_{AL} = G_{AL} + B_{AL}\alpha_W + E_{AL} S_{HT}$$

$$(3b.30)\quad C_{AD} = G_{AD} + B_{AD}\alpha_W + E_{AD} S_{HT}$$

$$(3b.31)\quad C_{AM} = G_{AM} + B_{AM}\alpha_W + E_{AM} S_{HT}$$

Dynamics

Referring to Figure A17,

$$(3b.32)\quad W_A \ddot{Z} = F_{AL} + F_{THV} - W_A G + 2F_{VM} + F_{VN}$$

$$(3b.33)\quad W_A \ddot{X} = F_{TH} - F_{AD} + 2F_{DU} - 2F_{U} - F_{DN}$$

$$(3b.34)\quad W_{IQ}\ddot{Q} = F_{VN}S_{HN} - 2F_{VM}S_{HM} + 2F_{DU}S_{VMU} + T_{TH} + T_{AM} - 2F_{U}(S_{GU} + S_{VMU}) - F_{DN}(Z - Z_{GD}\langle X_{WN}\rangle$$

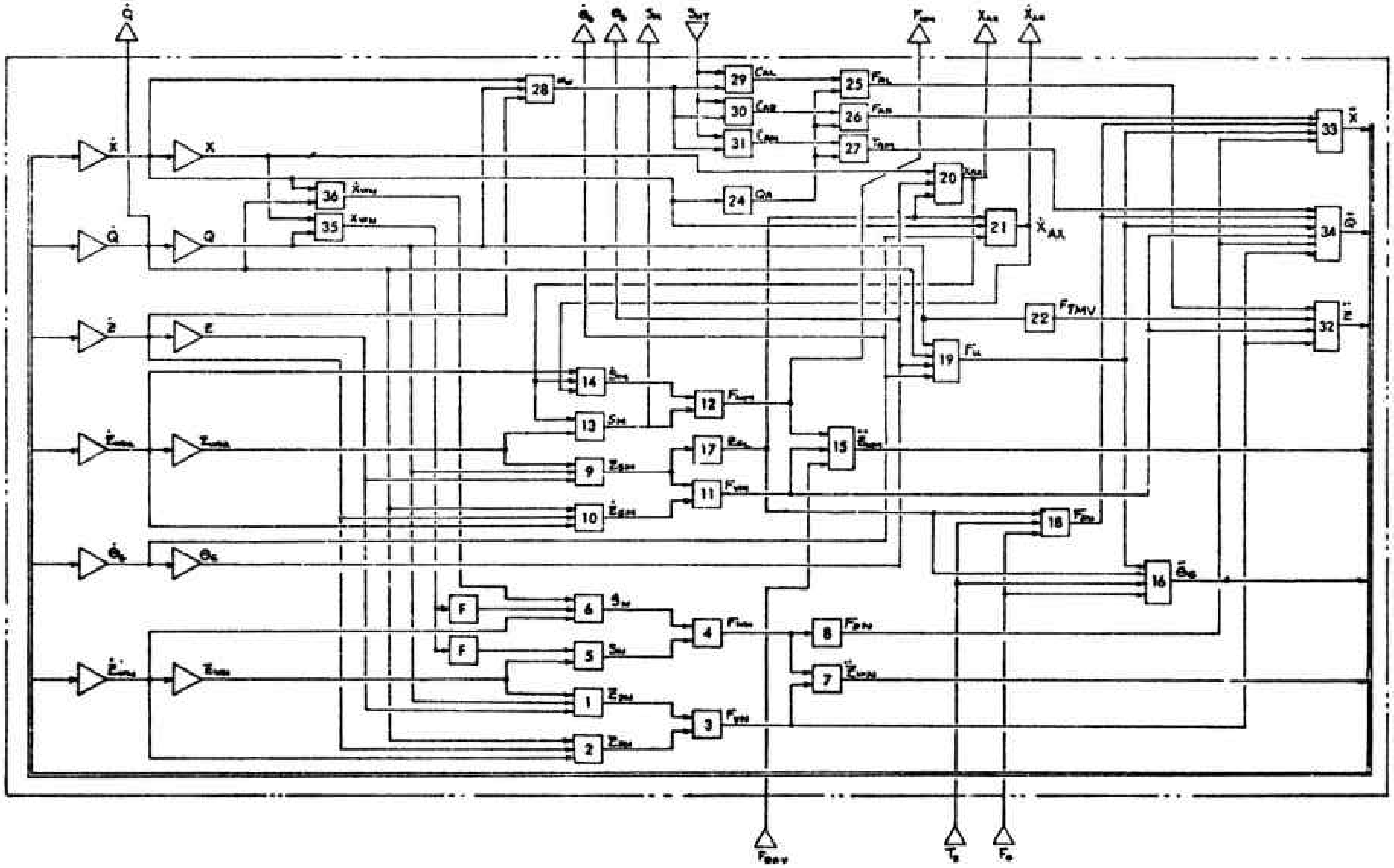

Figure A19 Airplane System (3 Degree) Equation Flow Diagram

where

$$(3b.35)\quad X_{WN} = X + S_{HN} + S_{VN} Q$$

$$(3b.36)\quad \dot{X}_{WN} = \dot{X} + S_{VN} \dot{Q}$$

Figure A19 shows the system flow diagram.

B. PARAMETER EVALUATION

Shock Strut Characteristics

Figures A20 and A21 show the nose gear load and damping characteristics.

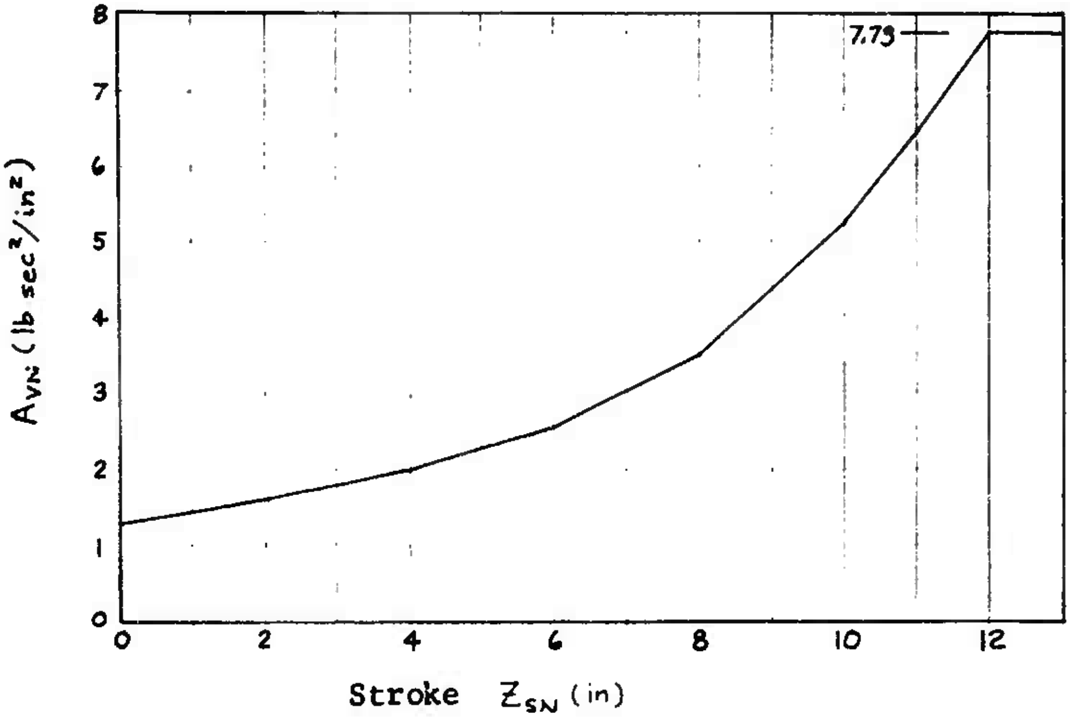

Figure A20 Nose Gear Damping Curve

Nose Tire Characteristics

See also page 135 of the flywheel system. The 22 x 6.6-10 16-ply rating nose tire has a rating of 9150 lbs. at 190 psi. The a flection is 1.50 inches. The operating pressure is 190 psi. Since these are two nose tires,

$$(3b.37)\quad C_{NT} = \left(\frac{P}{P_R}\right)\frac{F_R}{\delta_R} = \left(\frac{190}{190}\right)\frac{(2)(9150)}{(1.50)} = 12{,}200 \text{ lb/in}$$

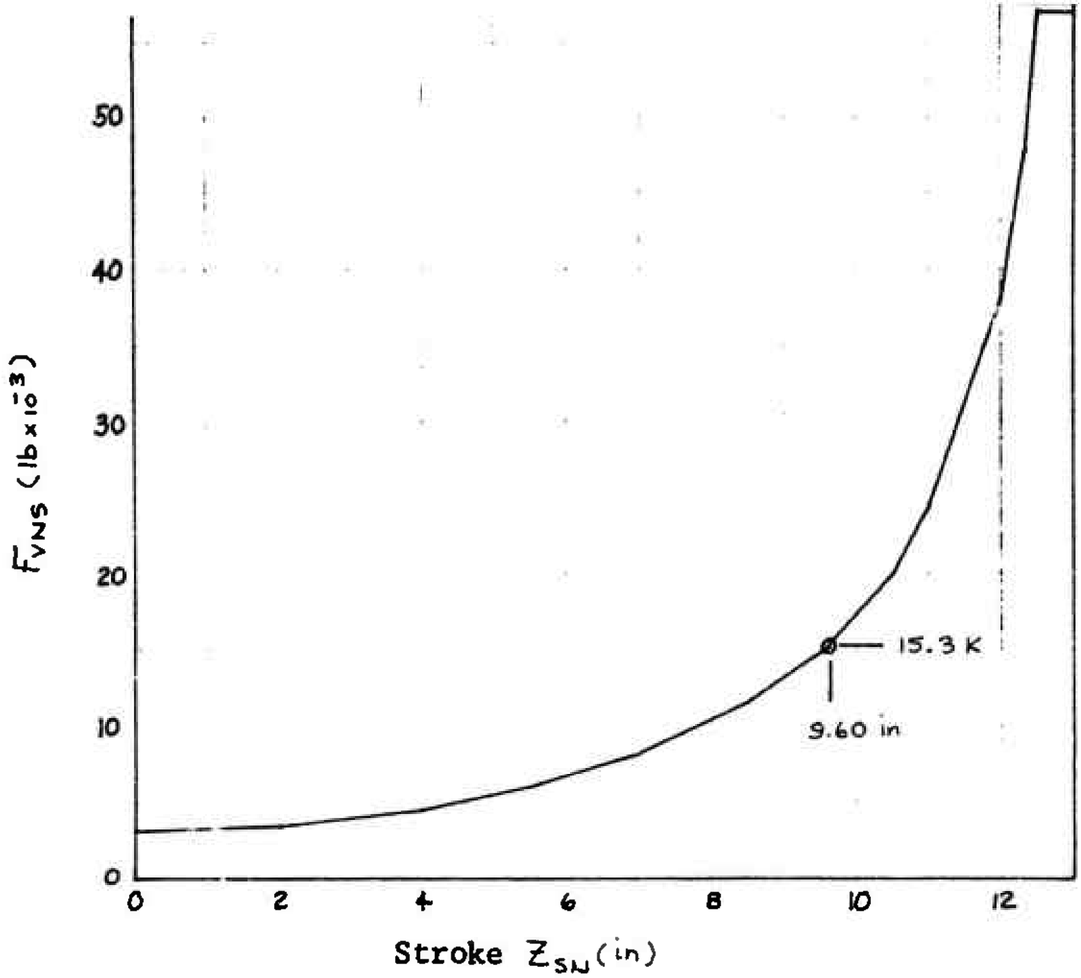

Figure A21 Nose Gear Air Load Curve

Since $\eta = 0.1$,

$$(3b.38)\ C_{NT} = \frac{\eta F_R}{\delta_R^2}\left(\frac{P}{P_R}\right)\sqrt{\frac{S_R}{G}}$$

$$= \frac{(.1)(2)(9150)}{(1.50)^2}\left(\frac{190}{190}\right)\sqrt{\frac{1.50}{386}} = 50.6\ \frac{\text{lb sec}}{\text{in}^2}$$

The nose tire rolling resistance coefficient is U_{RRN} = .020 and the unsprung nose tire mass (mass of tires, wheels, axle, and lower shock strut) is W_{WN} = 175/386 = .453 LBF SEC^2/IN. The nose tire undeflected radius, R_{OTN}, is 10.8 in.

Main Tire Characteristics

The main tire undeflected radius, R_{OTM}, is 23.32 inches. The other main tire characteristics are computed as shown on page 134.

Main Gear Characteristics

The F-111 main gear spring rate parameters were computed from load-deflection data recorded during structural testing and correlated with data from jig drop tests and from flight tests.

Figure A22 shows the model which has the same form as that described in equations (3b.16) through (3b.21) and in the wheel and tire system. The rotational spring rate of one main gear about its pivot is 26×10^6 in lb/rad.
The remaining values are calculated (at static position) as:

$$
(3b.39) \quad \begin{cases} S_{GU} = 21.0 \text{ in} \\ W_u = 279 \text{ lbm} = .723 \text{ lb sec}^2/\text{in} \\ W_{GW} = W_{WM} = 644 \text{ lbm} = 1.667 \text{ lbf sec}^2/\text{in} \\ C_G = 200{,}000 \text{ lb/in} \end{cases}
$$

Thus from figure 22, C_u is given by

$$
(3b.40) \quad C_u = C_{u(ROT)} / S_{GU}^2 = 26 \times 10^6 / 21^2 = 59{,}000 \text{ lb/in}
$$

The first mode natural frequency of the model is 21.84 cps. Assuming that η is .054 (about 3% critical), then evaluating the damping at $\omega = (2\pi)(21.84) = 137.5$ rad/sec there follows:

$$
(3b.41) \quad D_G = \frac{\eta C_G}{\omega} = \frac{(.054)(200{,}000)}{(137.5)} = 78.6 \ \frac{\text{lb sec}}{\text{in}}
$$

$$
(3b.42) \quad D_U = \frac{\eta C_U}{\omega} = \frac{(.054)(59{,}000)}{(137.5)} = 23.2 \ \frac{\text{lb sec}}{\text{in}}
$$

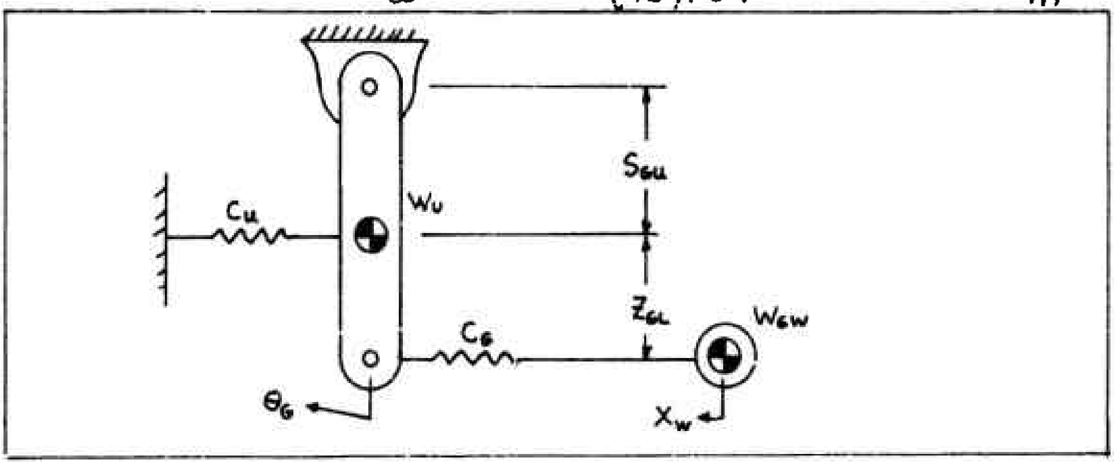

Figure A22 Main Gear Strut and Wheel Model

Aerodynamic Data

For finding the aerodynamic data, the F-111A is landing with flaps at 34°, wings swept to 26°, and spoilers applied. An equilibrium airplane condition of $\alpha_W = 2^\circ$ and $\delta_{HT} = -5^\circ$ is assumed. For these conditions,

$$(3b.43)\quad C_L = 0.13 \qquad \frac{\partial C_L}{\partial \alpha_W} = .128\ deg^{-1} \qquad \frac{\partial C_L}{\partial \delta_{HT}} = .022\ deg^{-1}$$

$$(3b.44)\quad C_D = .258 \qquad \frac{\partial C_D}{\partial \alpha_W} = .000\ deg^{-1} \qquad \frac{\partial C_D}{\partial \delta_{HT}} = -.0036\ deg^{-1}$$

$$(3b.45)\quad C_{M_A} = 0.00 \qquad \frac{\partial C_{MA}}{\partial \alpha_W} = -.025\ deg^{-1} \qquad \frac{\partial C_{MA}}{\partial \delta_{HT}} = -.0352\ deg^{-1}$$

The aerodynamic reference point is F.S. 526.8, WL 197.2. Assuming the airplane C.G. at F.S. 519.0, WL 180.0, if ΔX and ΔY are given by:

$$(3b.46)\quad \Delta X = FSA - FSCG = 526.8 - 519.0 = 7.8 \text{ inches}$$

$$(3b.47)\quad \Delta Y = WLA - WLCG = 197.2 - 180.0 = 17.2 \text{ inches}$$

Then if $\bar{C} = 108.5$ inches is the length of the M.A.C., then $C_m\bar{C}$ at the airplane C.G. is given by:

$$(3b.48)\quad C_M\bar{C} = C_{MA}\bar{C} - C_L\Delta X + C_D\Delta Y$$

$$= (0.0)(108.5) - (0.13)(7.8) + (.258)(17.2) = 3.424 \text{ inches}$$

Also,

$$(3b.49)\quad \frac{\partial C_M\bar{C}}{\partial \alpha_W} = \frac{\partial C_{MA}\bar{C}}{\partial \alpha_W} - \frac{\partial C_L}{\partial \alpha_W}\Delta X + \frac{\partial C_D}{\partial \alpha_W}\Delta Y$$

$$= (-.025)(108.5) - (.128)(7.8) + (0.0)(17.2) = -.371$$

$$(3b.50)\quad \frac{\partial C_M\bar{C}}{\partial \delta_{HT}} = \frac{\partial C_{MA}\bar{C}}{\partial \delta_{HT}} - \frac{\partial C_L}{\partial \delta_{HT}}\Delta X + \frac{\partial C_D}{\partial \delta_{HT}}\Delta Y$$

$$= (-.0352)(108.5) - (.022)(7.8) - (.0036)(17.2) = -3.759$$

Thus from equations (3b.29), (3b.30), and (3b.31),

(3b.51) $\begin{cases} C_{AL} = C_L = 0.13 \\ B_{AL} = (\partial C_L/\partial \alpha_W) = .128 \text{ deg}^{-1} \\ E_{AL} = (\partial C_L/\partial S_{HT}) = .022 \text{ deg}^{-1} \end{cases}$

(3b.52) $\begin{cases} C_{AD} = C_D = .258 \\ B_{AD} = (\partial C_D/\partial \alpha_W) = 0.0 \text{ deg}^{-1} \\ E_{AD} = (\partial C_D/\partial S_{HT}) = -.0036 \text{ deg}^{-1} \end{cases}$

(3b.53) $\begin{cases} C_{AM} = C_M\bar{C} = 3.424 \text{ in} \\ B_{AM} = (\partial C_M\bar{C}/\partial \alpha_W) = -.371 \text{ in/deg} \\ E_{AM} = (\partial C_M\bar{C}/\partial S_{HT}) = -3.759 \text{ in/deg} \end{cases}$

(3b.54)

$$G_{AL} = C_{AL} - B_{AL}\alpha_W - E_{AL} S_{HT}$$
$$= .013 - (.128)(2) - (.022)(-5.0) = -.016$$

(3b.55)

$$G_{AD} = C_{AD} - B_{AD}\alpha_W - E_{AD} S_{HT}$$
$$= .258 - (0.0)(2) - (-.0036)(-5) = .240$$

(3b.56)

$$G_{AM} = C_{AM} - B_{AM}\alpha_W - E_{AM} S_{HT}$$
$$= 3.424 - (-.371)(2) - (-.3759)(-5) = 2.286 \text{ IN}$$

<u>Initial Conditions</u>

Assume that at time = 0.0 seconds the airplane velocity is 2400 in/sec = $\dot{X}o$. The airplane is shown in Figure 23 with brakes off.

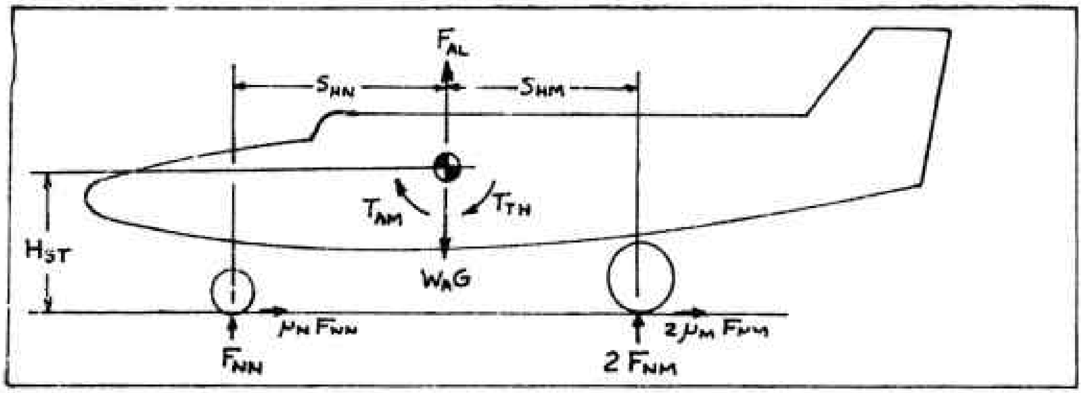

Figure A23 Airplane Initial Equilibrium Forces

Assume that $\alpha_W = 3^\circ$ and $S_{HT} = -5^\circ$, then from equations (3b.29) (3b.30) and (3b.31), there follows:

$$(3b.57)\quad C_{AL} = (-.016) + (.128)(3) + (.022)(-5) = 0.222$$

$$(3b.58)\quad C_{AM} = (2.286) + (-.371)(3) + (-3.759)(-5) = 19.973$$

Since $S_{HN} = 258.9$, $S_{HM} = 32.6$ inches, $T_{TH} = 20{,}000$ in/lb., and if the estimated value for H_{ST} is 97.2 inches, then

$$(3b.59)\quad F_{NM} = \left(\frac{(T_{TH} + T_{AM}) + (S_{HN} - H_{ST}\mu_N)(W_AG - F_{AL})}{(S_{HN} + S_{HM}) + H_{ST}(\mu_M - \mu_N)}\right)\frac{1}{2}$$

Now from equations (3b.24), (3b.25), and (3b.26),

$$(3b.60)\quad Q_A = (2400)^2(525)(.00238)/288 = 25000 \text{ lb}$$

$$(3b.61)\quad F_{AL} = (.222)(25000) = 5500 \text{ lb}$$

$$(3b.62)\quad T_{AM} = (19.973)(25000) = 499{,}300 \text{ in lb}$$

Thus,

$$(3b.63)\quad F_{NM} = \frac{1}{2}\left(\frac{(519300) + (257)(57000 - 5500)}{(295.1) + (97.2)(0)}\right)$$

So

$$(3b.64)\quad F_{NM} = 22988 \text{ lb}$$

and

$$(3b.65)\quad F_{NN} = W_AG - F_{AL} - 2F_{NM}$$
$$= 57000 - 5500 - 2(22988) = 5524 \text{ lb}$$

Assume that when time = 0 that $X_{WM} = 0.0$ inches, then $Z_{GD}\langle X_{WM}\rangle = 0.0$. Then $X_{WN} = 295.1$ inches so that $Z_{GD}\langle X_{WN}\rangle = (9.676-9.703)12 = -.32$ inches. Refer to the runway system for values of Z_{GD}. From equation (3b.12):

$$(3b.66)\quad S_M = (22988)/(9530) = 2.41 \text{ in}$$

Thus from equation (3b.13)

(3b.67) $Z_{WMO} = 23.32 - 2.41 = 20.91$ in

From Figure A14 in the flywheel system, if F_{VMS} = 22,950 lbs, then Z_{SM} = 24.00 inches. Now, from equation (3b.4)

(3b.68) $S_N = (5524)/(12{,}200) = .46$ in

From equation (3b.5), there follows:

(3b.69) $Z_{WNO} = (-.32) + (10.80) - (.46) = 10.02$ in

Also, from Figure 21, if F_{VNS} = 5,600 lbs. then: $Z_{SN} = 5$ in

Rearranging equations (3b.1) and (3b.9)

(3b.70) $Z_o + S_{HN} Q_o = S_{VN} + Z_{WNO} - Z_{SN}$

(3b.71) $Z_o - S_{HM} Q_o = S_{VM} + Z_{WMO} - Z_{SM}$

Solving these two equations,

(3b.72) $Q_o = .0329$ RADIANS

(3b.73) $Z_o = 82.36$ in

Finally,

(3b.74) $X_o = X_{WMO} + S_{HM} = 36.20$ in

(3b.75) $\Theta_{GO} = Q_o = .0329$ RADIANS

The values of the following parameters as listed in Table A7 are established by the airplane's dimensional and mass characteristics: ALO, ALTH, AREF, SGL, SHM, SHN, SVM, SVN, SGU, STH, WA, WIQ, and SVMU.

For the example problem the density of air at standard conditions, sea level and 59.6°F, is assumed. Thus, RHA = .00238 Slugs/Ft³

The shock strut linear damping coefficients, DVN for the nose gear and DVM for the main gear, are set equal to zero for the example problem.

Table A7 3 Degree Airplane System Parameters (Sheet 1 of 5)

SYMBOL	TYPE	VALUE	UNITS	DESCRIPTION
α_o	c	1.00	deg	Wing Angle of Incidence
α_{TH}	c	-.052	rad	Angle between Thrust ℄ and W.L.
α_W	v		deg	Wing Angle of Attack
A_{REF}	c	525	ft^2	Wing Ref. Area
A_{VM}	v*		$lb\ sec^2/in^2$	M.G. Shock Strut Damping Characteristic
A_{VN}	v*		$lb\ sec^2/in^2$	N.G. Shock Strut Damping Characteristic
B_{AD}	c	0.0	deg^{-1}	Aero Drag Parameter
B_{AL}	c	.128	deg^{-1}	Aero Lift Parameter
B_{AM}	c	-.371	in/deg	Aero Moment Parameter
C_{AD}	v		-	Aero Drag Coefficient
C_{AL}	v		-	Aero Lift Coefficient
C_{AM}	v		in	Aero Moment Coefficient
C_{MT}	c	9530	lb/in	M.G. Tire Vertical Spring Rate
C_{NT}	c	12,200	lb/in	N.G. Tire(s) Vertical Spring Rate
C_{u}	c	59,000	lb/in	Drag Brace - Strut Spring Rate
D_{MT}	c	38.8	$lb\ sec/in^2$	M.G. Tire Vertical Damping Coeff.
D_{NT}	c	50.6	$lb\ sec/in^2$	N.G. Tire Vertical Damping Coeff.
D_{u}	c	23.2	lb sec/in	Drag Brace - Strut Damping Coeff.
D_{VM}	c	0.0	lb sec/in	M.G. Strut Damping Coefficient
D_{VN}	c	0.0	lb sec/in	N.G. Strut Damping Coefficient
E_{AD}	c	-.0036	deg^{-1}	Aero Drag Coefficient
E_{AL}	c	.022	deg^{-1}	Aero Lift Coefficient
E_{AM}	c	-3.755	in/deg	Aero Moment Coefficient
F_{AD}	v		lb	Aero Drag
F_{AL}	v		lb	Aero Lift
F_{DN}	v		lb	Nose Tire Drag
F_{Du}	v		lb	Horizontal Load at M.G. Pivot

* Point Plot Input

Table A7 3 Degree Airplane System Parameters (Sheet 2 of 5)

SYMBOL	TYPE	VALUE	UNITS	DESCRIPTION
F_G	v(I)		lb	Horizontal Load on M.G. Axle
F_{NM}	v(o)		lb	M.G. Tire Normal Load
F_{NN}	v		lb	N.G. Tire Normal Load
F_{TH}	c	1000	lb	Engine Thrust
F_{THV}	v		lb	Vertical Component of Engine Thrust
F_u	v		lb	Load in Fictitious Drag Brace
F_{VM}	v		lb	Shock Strut Loag (M.G.)
F_{VMS} *	v		lb	Shock Strut Air Load (M.G.)
F_{VN}	v		lb	Shock Strut Load (N.G.)
F_{VNS} *	v		lb	Shock Strut Air Load (N.G.)
G	c	386	in/sec^2	Gravitational Constant
G_{AD}	c	.240	—	Aero Drag Parameter
G_{AL}	c	-.016	—	Aero Lift Parameter
G_{AM}	c	2.286	in	Aero Moment Parameter
Θ_G	v(o)		rad	M.G. Rotation from Vertical
Θ_{GO}	c	.0329	rad	Θ_G at Time = 0 Sec.
$\dot{\Theta}_G$	v(o)		rad/sec	Angular Velocity of Main Gear Strut
$\dot{\Theta}_{GO}$	c	0.0	rad/sec	$\dot{\Theta}_G$ at Time = 0 Sec.
$\ddot{\Theta}_G$	v		rad/sec^2	Angular Acceleration of Main Gear Strut
$F_{\Theta RV}$	v(I)		lb	Tire Vertical Unbalance
Q	v		rad	Angle of APL W.L. to Horizontal (Pitch)
Q_o	c	.0329	rad	Q at Time = 0.0 Sec.
$\dot{Q}$	v(o)		rad/sec	APL Pitch Rate
$\dot{Q}_o$	c	0.0	rad/sec	APL Pitch Rate at Time = 0.0 Sec.

* Point Plot Input

Table A7 3 Degree Airplane System Parameters (Sheet 3 of 5)

SYMBOL	TYPE	VALUE	UNITS	DESCRIPTION
$\ddot{Q}$	v		rad/sec^2	APL Pitch Acceleration
Q_A	v		lb	Aerodynamic Pressure x AREF
R_{HA}	c	.00238	slug/ft^3	Air Density
$R_{\theta TM}$	c	23.32	in	M.G. Tire Undeflected Radius
$R_{\theta TN}$	c	10.80	in	N.G. Tire Undeflected Radius
S_{GL}	c	93.61	in	*
S_{GU}	c	20.0	in	*
S_{HM}	c	49.0	in	*
S_{HN}	c	222.4	in	*
S_{HT}	v(I)		deg	Horizontal Tail Deflection
S_M	v(o)		in	M.G. Tire Deflection
$\dot{S}_M$	v		in/sec	M.G. Tire Deflection Rate
S_{VMU}	c	34.875	in	*
S_N	v		in	N.G. Tire Deflection
$\dot{S}_N$	v		in/sec	N.G. Tire Deflection Rate
S_{VM}	c	84.24	in	*
S_{VN}	c	85.4	in	*
S_{TH}	v	20.00	in	*
T_{AM}	v		in lb	Aero Moment
T_S	v(I)		in lb	Moment on M.G. Axle
T_{TH}	c	20,000	in lb	Moment at C.C. due to Thrust
U_{RRN}	c	.020	—	N.G. Tire Rolling Resistance Coefficient
W_A	c	147.6	lb sec^2/in	APL Mass
W_{IQ}	c	3.66×10^6	lb sec^2 in	APL Pitch Moment of Inertia About C.G.
W_U	c	.723	lb sec^2/in	M.G. Upper Strut Mass
W_{WM}	c	1.667	lb sec^2/in	M.G. Unsprung Mass

* See Figure A16

Table A7 3 Degree Airplane System Parameters (Sheet 4 of 5)

SYMBOL	TYPE	VALUE	UNITS	DESCRIPTION
W_{WN}	c	.453	lb sec^2/in	N.G. Unsprung Mass
X	v		in	Horizontal C.G. Location of APL
X_o	c	36.20	in	C.G. Location at Time = 0
$\dot{X}$	v		in/sec	APL Velocity
$\dot{X}_o$	c	2400	in/sec	APL Velocity at Time = 0
$\ddot{X}$	v		in/sec^2	APL Acceleration
X_{AX}	v(o)		in	M.G. Axle (Undeflected) Location
$\dot{X}_{AX}$	v(o)		in/sec	M.G. Axle Velocity (Undeflected)
X_{WM}	v(I)		in	M.G. Axle Location (Horizontal)
$\dot{X}_{WM}$	v(I)		in/sec	M.G. Axle Velocity
X_{WN}	v		in	N.G. Axle Location (Horizontal)
$\dot{X}_{WN}$	v		in/sec	N.G. Axle Velocity
Z	v		in	Vertical Location of APL C.G.
Z_o	c	82.36	in	Vertical Location of APL C.G. at Time = 0
$\dot{Z}$	v		in/sec	APL Vertical Velocity
$\dot{Z}_o$	c	0.0	in/sec	APL Vertical Velocity at Time = 0
$\ddot{Z}$	v		in/sec^2	APL Vertical Acceleration
Z_{GD}	v(I)		in	Runway Contour Height
Z_{GDP}	v(I)		in/in	Runway Contour Slope
Z_{GL}	v		in	Distance from Mass W_u to Strut Axle
Z_{SM}	v		in	M.G. Stroke
$\dot{Z}_{SM}$	v		in/sec	M.G. Stroke Velocity
Z_{SN}	v		in	N.G. Stroke
$\dot{Z}_{SN}$	v		in/sec	N.G. Stroke Velocity

Table A7 3 Degree Airplane System Parameters (Sheet 5 of 5)

SYMBOL	TYPE	VALUE	UNITS	DESCRIPTION
$\ddot{Z}_{WM}$	v		IN/SEC^2	M.G. Axle Vertical Acceleration
Z_{WN}	v		IN	N.G. Axle Height
Z_{WNO}	c	10.02	IN	N.G. Axle Height at Time = 0
$\dot{Z}_{WN}$	v		IN/SEC	N.G. Axle Vertical Velocity
$\dot{Z}_{WNO}$	c	0.0	IN/SEC	N.G. Axle Vertical Velocity at Time = 0
$\ddot{Z}_{WN}$	v		IN/SEC^2	N.G. Axle Vertical Acceleration
OVMC	c	200	LBS	Coulomb Friction Coefficient
GM	f			Coulomb Friction Function (See Flywheel System)

3c. AIRPLANE SYSTEM (6 DEGREE)

The six-degree airplane system is built around a rigid body airplane which is allowed to move vertically and horizontally (both parallel and perpendicular to the runway centerline). Also, the airplane's yaw, pitch, and roll effects are considered. This model considers all the effects found in the three-degree airplane system. The purpose of the six-degree airplane is primarily two-fold: the first is to evaluate the effects of the anti-skid system on the airplane's directional stability; the second is to evaluate any anti-skid system degradation caused by airplane yaw and side drift movement.

For the nose gear, the model considers the tire and strut characteristics in the vertical direction. Also, the nose tire's yawed rooling characteristics are included. The steering loop is closed by providing a "pilot" function which provides an input to the nose tire. The "pilot" function depends on the airplane's yaw angle. The two main gears are treated as two distinct systems except for any structural coupling which may exist between the two. Provisions are made for side wind perturbation and for aerodynamic effects caused by airplane yaw and roll.

A. Mathematical Description

Figure A24 shows the six coordinates which describe the airplane position relative to reference points on the earth's surface.

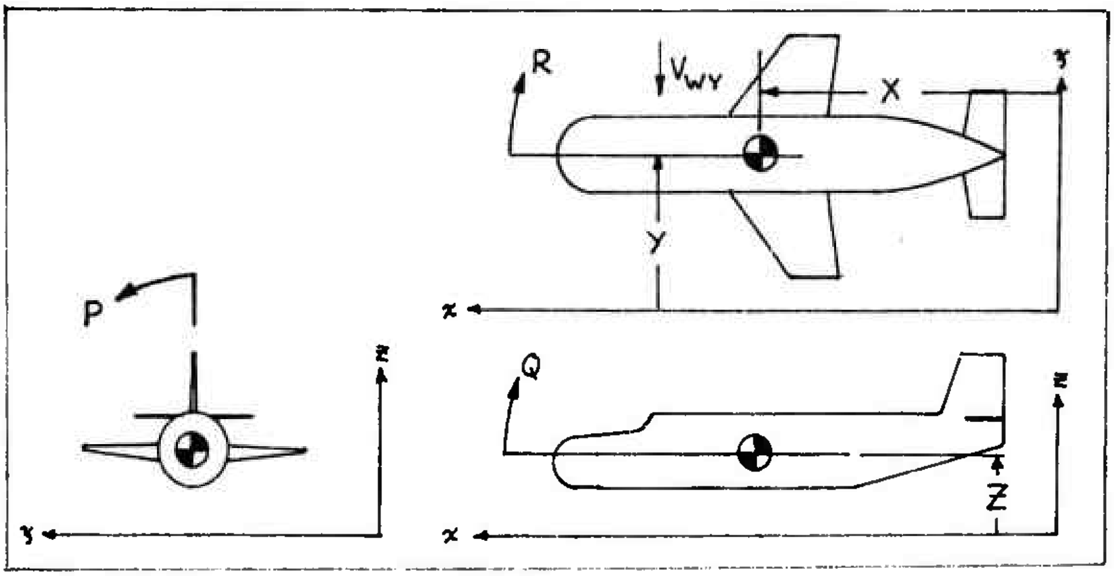

Figure A24 Airplane Coordinates

V_{WY} is a crosswind. The runway is oriented so that its centerline coincides with the x axis for 0 inch runway heights ($Z_{GD} = 0$). This analysis assumes that the pitch (Q) and roll (P) angles are small. Let $Z_{GD}\langle x,y\rangle$ denote the runway profile and let $Z_{GDP}\langle x,y\rangle$ denote the runway slope ($Z_{GDP}\langle x,y\rangle = \partial Z_{GD}\langle x,y\rangle/\partial x$). Figure A25 shows the airplane as measured in the fuselage station-water line reference system.

Nose Gear

Let Z_{SN} and $\dot{Z}_{SN}$ denote the nose gear stroke and stroke velocity. Then we have that:

$$\text{(3c.1)}\quad Z_{SN} = Z_{WN} + S_{VN} - Z - S_{HN}Q$$

$$\text{(3c.2)}\quad \dot{Z}_{SN} = \dot{Z}_{WN} - \dot{Z} - S_{HN}\dot{Q}$$

The nose gear shock strut force F_{VN} is then given by:

$$\text{(3c.3)}\quad F_{VN} = F_{VNS}\langle Z_{SN}\rangle + D_{VN}\dot{Z}_{SN} + A_{VN}\langle Z_{SN}\rangle \dot{Z}_{SN}|\dot{Z}_{SN}|$$

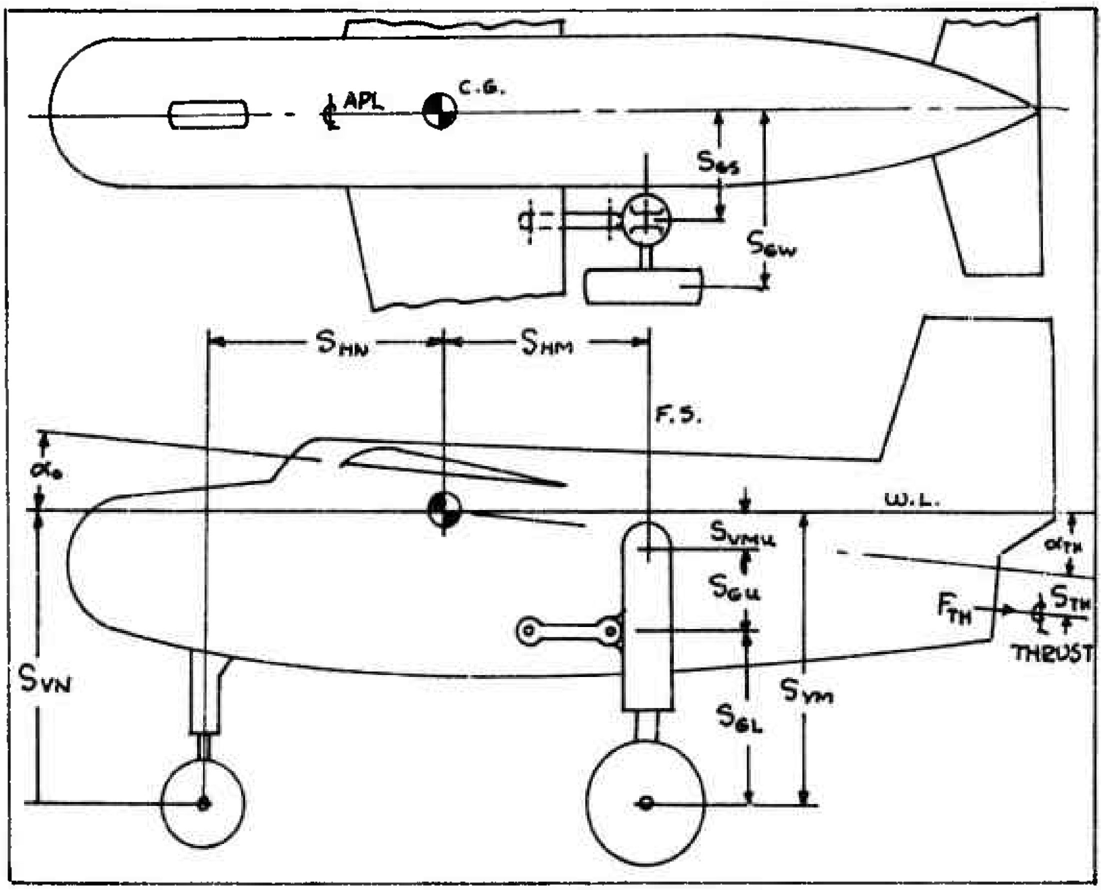

Figure A 25 Airplane Geometry

Figures A26, A27 and A28 show the forces acting on the airplane as seen in the different planes. Let F_{LN} denote the lateral force on the nose wheel at the axle. Then:

$$(3c.4)\quad W_{WN}\ddot{Y}_N = F_{SNS} - F_{LN}$$

Where F_{SNS} is the lateral component of the sliding or cornering force of the nose tire. The load F_{LN} is caused by the nose wheel trying to move laterally relative to the airplane. If this lateral displacement is denoted by Y_{DLN}, then:

$$(3c.5)\quad F_{LN} = C_{LN}Y_{DLN} + D_{LN}\dot{Y}_{DLN}$$

$$(3c.6)\quad Y_{DLN} = Y_N - Y + (Z + S_{HN}Q)P - S_{HN}R$$

$$(3c.7)\quad \dot{Y}_{DLN} = \dot{Y}_N - \dot{Y} + (Z + S_{HN}Q)\dot{P} + (\dot{Z} + S_{HN}\dot{Q})P - S_{HN}\dot{R}$$

Now F_{NN} is given by:

$$(3c.8)\quad F_{NN} = S_N(C_{NT} + D_{NT}\dot{S}_N)$$

where

$$(3c.9)\quad S_N = \max\{0.0,\ Z_{GD}\langle X_{WN}, Y_N\rangle + R_{OTN} - Z_{WN}\}$$

$$(3c.10)\quad \dot{S}_N = Z_{GDP}\langle X_{WN}, Y_N\rangle \dot{X}_{WN} - \dot{Z}_{WN}$$

Summing vertical forces on the nose gear unsprung weight:

$$(3c.11)\quad W_{WN}\ddot{Z}_{WN} = F_{NN} - F_{VN}$$

Assume that the pilot positions the nose wheel with a rate proportional to the airplane yaw angle. Thus:

$$(3c.12)\quad \dot{\Theta}_N = \begin{cases} \min\{0,\ -G_{PIL}R & \text{if } \Theta_N \geq \Theta_{NMAX} \\ -G_{PIL}R & \text{if } |\Theta_N| < |\Theta_{NMAX}| \\ \max\{0,\ -G_{PIL}R & \text{if } \Theta_N \leq -\Theta_{NMAX} \end{cases}$$

Θ_N gives the yaw angle of the nose wheel with respect to the airplane ℄. The yaw angle of the tire with respect to its direction of motion is given by Θ_{YAW}.

$$(3c.13)\quad \Theta_{YAW} = \Theta_N + R - (\dot{Y}_N / \dot{X}_{WN})$$

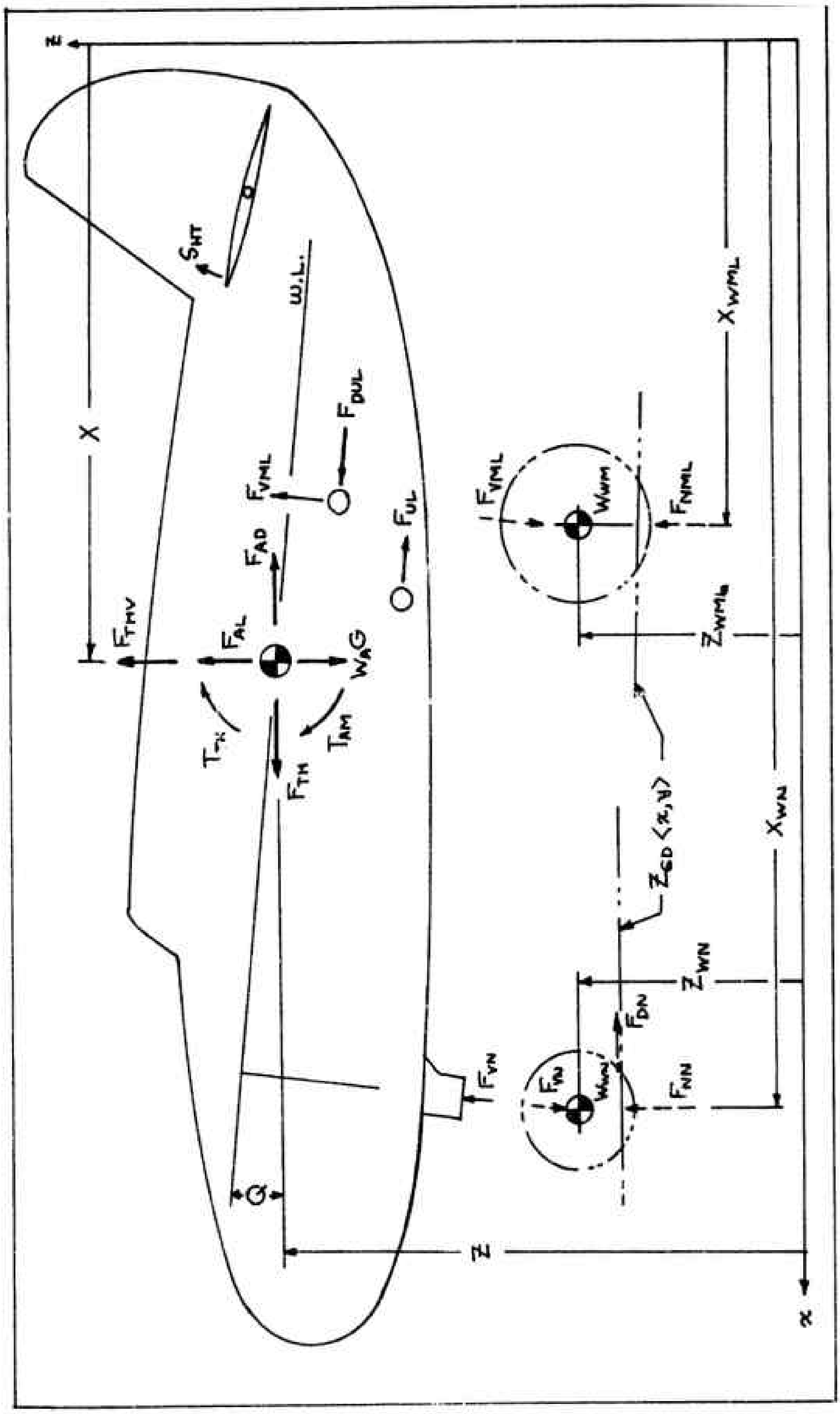

Figure A26 Airplane Dynamics (Pitch)

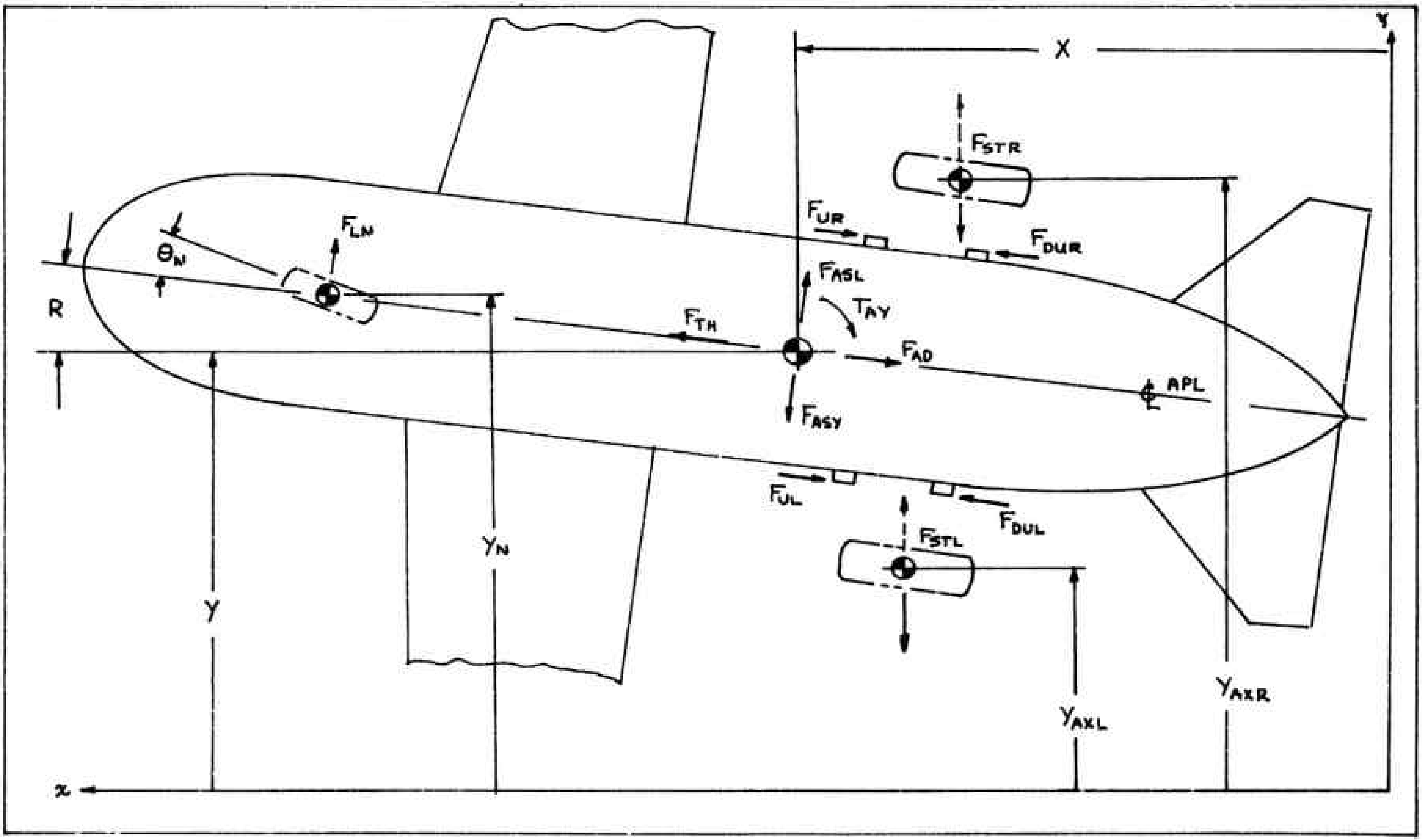

Figure A27 Airplane Dynamics (Yaw)

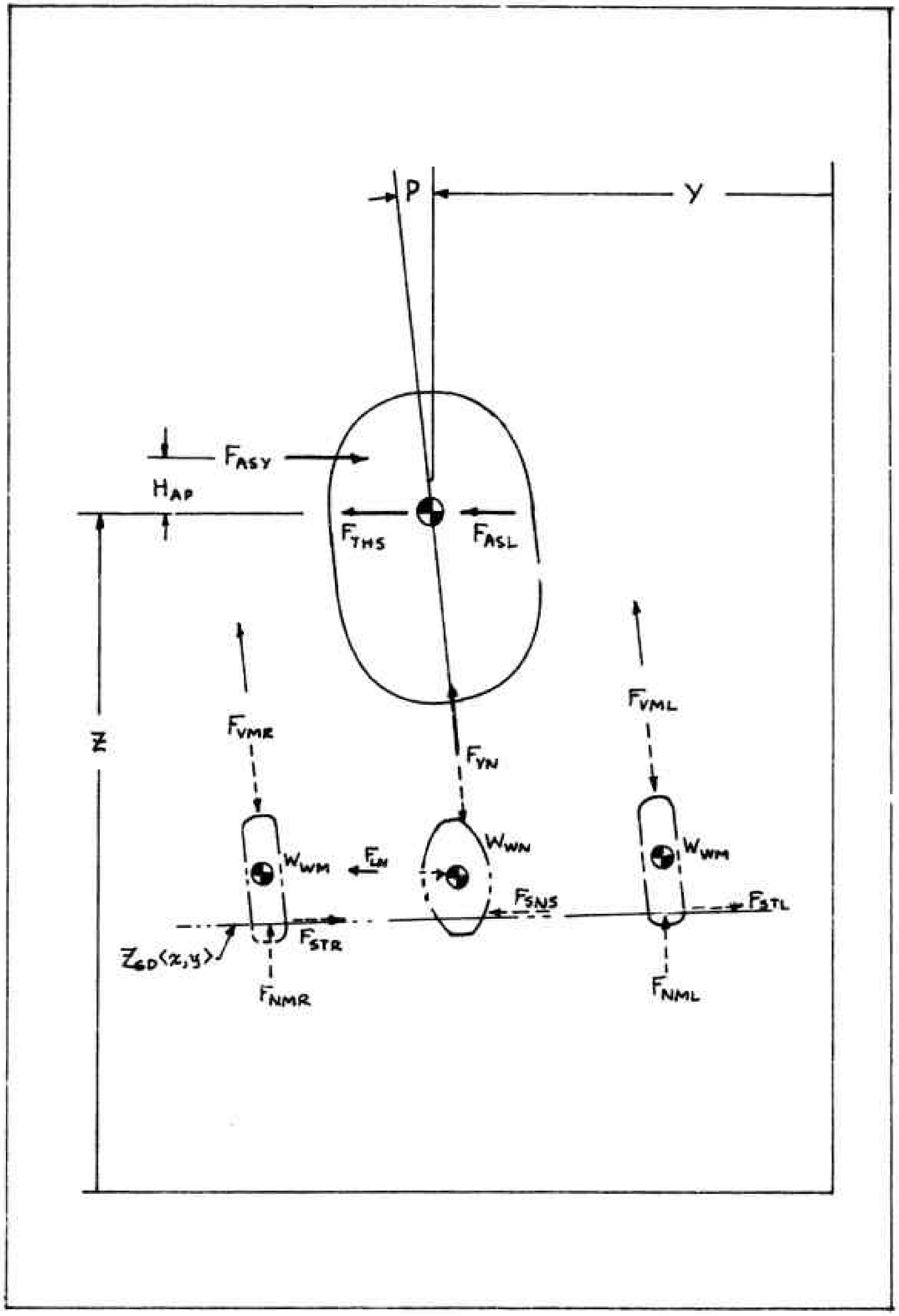

Figure A28 Airplane Dynamics (Roll)

The steering characteristic is developed from Reference 1 (p. 30). Let U_{NTF} be the coefficient of friction between the nose tire and the ground. Then the maximum force normal to the tire in the plane of the ground is F_{NTF} where:

$$\text{(3c.14)} \quad F_{NTF} = U_{NTF} F_{NN}$$

Using equation (79) and 80) from Reference 1 :

$$\text{(3c.15)} \quad U_{RT} = \begin{cases} P_{WC}\,\Theta_{YAW}/F_{NTF} & \text{if } F_{NTF} > 0 \\ 0 & \text{if } F_{NTF} \leq 0 \end{cases}$$

$$\text{(3c.16)} \quad F_{NCFS} = \begin{cases} F_{NTF} & \text{if } U_{RT} \geq 1.5 \\ F_{NTF}\left(U_{RT} - 4\,U_{RT}^{3}/27\right) & \text{if } |U_{RT}| < 1.5 \\ -F_{NTF} & \text{if } U_{RT} \leq -1.5 \end{cases}$$

Thus, F_{NCFS} corresponds to $F_{\psi,r,e}$ in Reference 1 and Pwc is the cornering power given by:

$$\text{(3c.17)} \quad P_{WC} = \begin{cases} C_{P1} S_N - C_{P2} S_N^{2} & \text{if } S_N \leq S_{P1} \\ C_{P3} - C_{P4} S_N & \text{if } S_N > S_{P1} \end{cases}$$

The actual normal cornering force F_{NCF} is not F_{NCFS} , but lags F_{NCFS} because of the tire relaxation length. The expression for F_{NCF} is given by:

$$\text{(3c.18)} \quad \dot{F}_{NCF} = \left(F_{NCFS} - F_{NCF}\right)\left(\dot{X}_{WN}/S_{YRL}\right)$$

Having obtained F_{NCF} , then from Figure A29,

$$\text{(3c.19)} \quad F_{SNS} = F_{NCF} \cos\langle \Theta_N + R\rangle - U_{RRN} F_{NN} \sin\langle \Theta_N + R\rangle$$

$$\text{(3c.20)} \quad F_{DN} = F_{NCF} \sin\langle \Theta_N + R\rangle + U_{RRN} F_{NN} \cos\langle \Theta_N + R\rangle$$

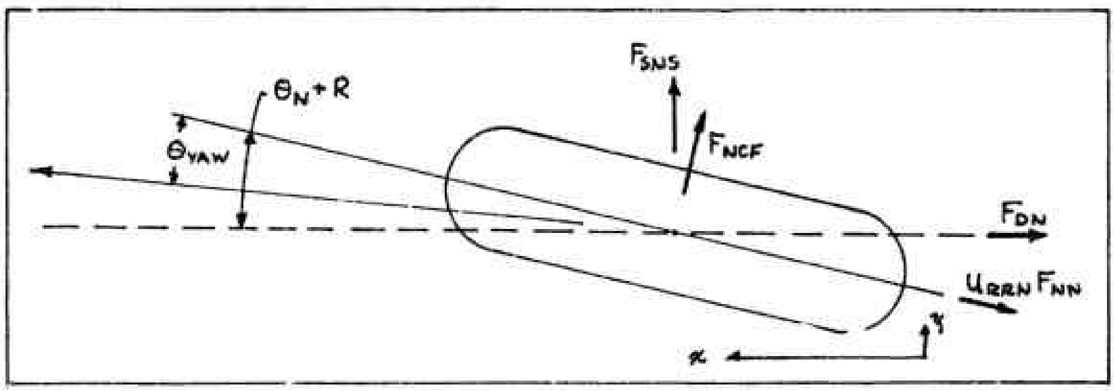

Figure A29 Nose Tire Cornering Force

Main Gear

Let Z_{SM} and $\dot{Z}_{SM}$ denote the stroke and stroke velocity. The additional subscripts L and R refer to the left and right side of the airplane (looking forward).

$$(3c.21)\quad Z_{SMR} = Z_{WMR} - Z + S_{VM} + S_{HM}Q + S_{GW}P$$

$$(3c.22)\quad \dot{Z}_{SMR} = \dot{Z}_{WMR} - \dot{Z} + S_{HM}\dot{Q} + S_{GW}\dot{P}$$

$$(3c.23)\quad Z_{SML} = Z_{WML} - Z + S_{VM} + S_{HM}Q - S_{GW}P$$

$$(3c.24)\quad \dot{Z}_{SML} = \dot{Z}_{WML} - \dot{Z} + S_{HM}\dot{Q} - S_{GW}\dot{P}$$

The main gear shock strut forces are then given by:

$$(3c.25)\quad F_{VMR} = F_{VMS}\langle Z_{SMR}\rangle + D_{VM}\dot{Z}_{SMR} + A_{VM}\langle Z_{SMR}\rangle \dot{Z}_{SMR}|\dot{Z}_{SMR}|$$

$$(3c.26)\quad F_{VML} = F_{VMS}\langle Z_{SML}\rangle + D_{VM}\dot{Z}_{SML} + A_{VM}\langle Z_{SML}\rangle \dot{Z}_{SML}|\dot{Z}_{SML}|$$

Let S_M denote the main gear tire deflection and let F_{NM} be the associated load. Thus, in the vertical direction, the relation between the load and tire deflection is given as follows:

$$(3c.27)\quad F_{NMR} = S_{MR}(C_{MT} + D_{MT}\dot{S}_{MR})$$

$$(3c.28)\quad F_{NML} = S_{ML}(C_{MT} + D_{MT}\dot{S}_{ML})$$

$$(3c.29)\quad S_{MR} = \max\{0, Z_{GD}\langle X_{WMR}, Y_{MR}\rangle + R_{\theta TM} - Z_{WMR}\}$$

$$(3c.30)\quad \dot{S}_{MR} = Z_{GDP}\langle X_{WMR}, Y_{MR}\rangle \dot{X}_{WMR} - \dot{Z}_{WMR}$$

$$(3c.31)\quad S_{ML} = \max\{0, Z_{GD}\langle X_{WML}, Y_{ML}\rangle + R_{\theta TM} - Z_{WML}\}$$

$$(3c.32)\quad \dot{S}_{ML} = Z_{GDP}\langle X_{WML}, Y_{ML}\rangle \dot{X}_{WML} - \dot{Z}_{WML}$$

Summing forces in the vertical direction on the main gear wheels,

$$(3c.33)\quad W_{WM}\ddot{Z}_{WMR} = F_{NMR} - F_{VMR} + F_{\theta RVR}$$

$$(3c.34)\quad W_{WM}\ddot{Z}_{WML} = F_{NML} - F_{VML} + F_{\theta RVL}$$

Figure A30 shows a side view of the left hand main gear. With the assumption that $W_u << W_A$, Θ_{GR} and Θ_{GL} are described by:

$$(3c.35)\ W_u S_{GU}^2 \ddot{\theta}_{GR} = S_{GU} F_{UR} + (S_{GU} + Z_{GLR})(F_{TL} - F_{TR} - F_{GR}) - T_{SR}$$

$$(3c.36)\ W_u S_{GU}^2 \ddot{\theta}_{GL} = S_{GU} F_{UL} + (S_{GU} + Z_{GLL})(F_{TR} - F_{TL} - F_{GL}) - T_{SL}$$

where

$$(3c.37)\ Z_{GLR} = S_{GL} - Z_{SMR}$$

$$(3c.38)\ Z_{GLL} = S_{GL} - Z_{SML}$$

The forces F_{TR} and F_{TL} are used to impart the correct moment into the gear.

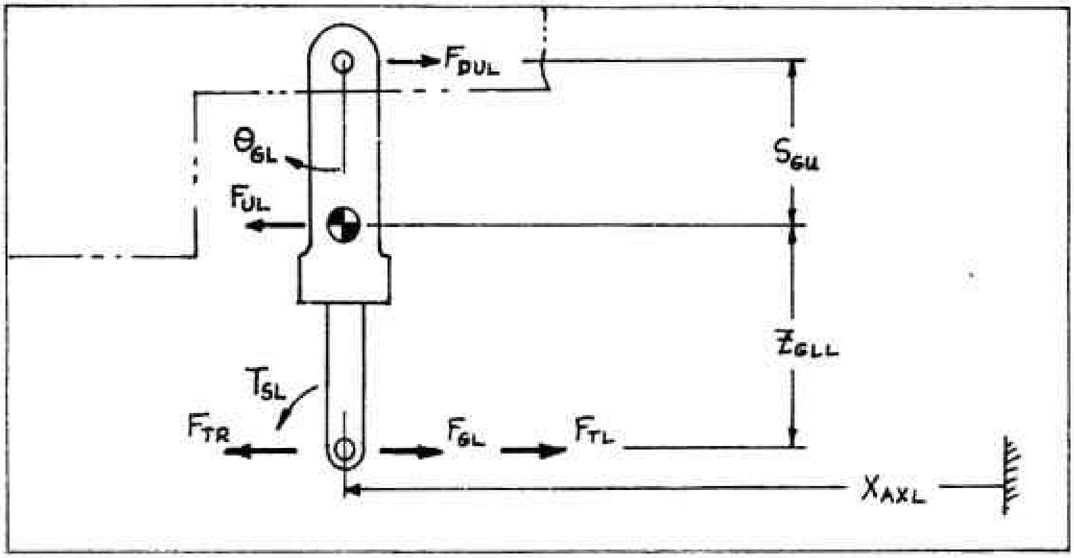

Figure A30 Side View of the Main Gear Strut

The overall gear system model is shown in Figure A31. In order to transmit torque properly, the forces $F_{TR\theta}$ and $F_{TL\theta}$ are applied equal and opposite on different sides of the gear. Thus,

$$(3c.39)\ F_{TR\theta} = F_{GR}(S_{GW} - S_{GS})/2S_{GS}$$

$$(3c.40)\ F_{TL\theta} = F_{GL}(S_{GW} - S_{GS})/2S_{GS}$$

If it is assumed that 100 H_A percent of this torque is taken directly into the airplane, then 100 H_G = 100-100 H_A percent is transmitted through the gear. Thus,

$$(3c.41)\ F_{TR} = H_G F_{TR\theta}$$

$$(3c.42)\ F_{TL} = H_G F_{TL\theta}$$

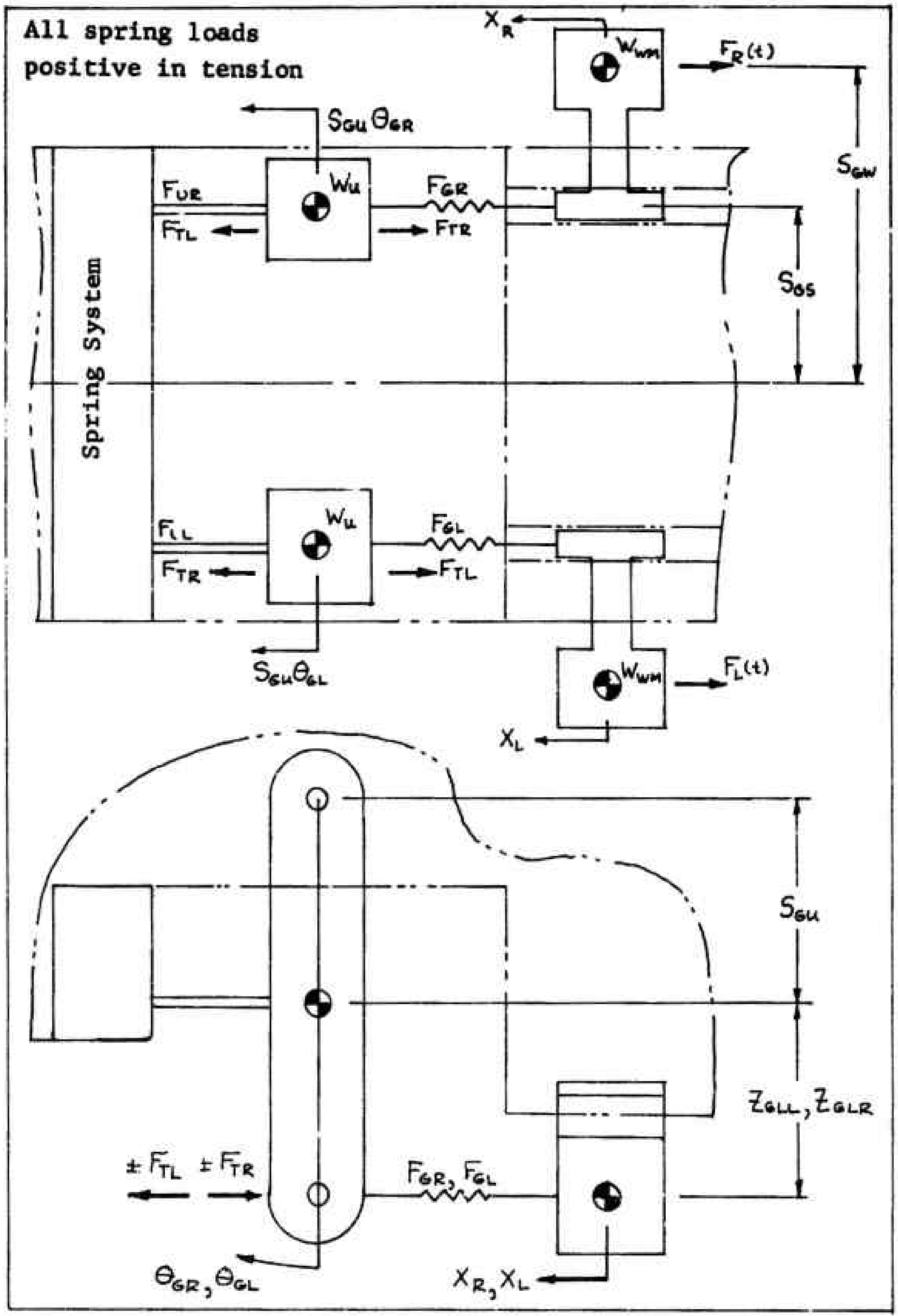

Figure A31 Main Gear Model

Let Q_R and Q_L be the difference between the gear rotation and the airplane rotation. That is,

$$(3c.43)\quad Q_R = Q - \theta_{GR}$$

$$(3c.44)\quad Q_L = Q - \theta_{GL}$$

$$(3c.45)\quad \dot{Q}_R = \dot{Q} - \dot{\theta}_{GR}$$

$$(3c.46)\quad \dot{Q}_L = \dot{Q} - \dot{\theta}_{GL}$$

Then we can find constants C_{u1}, C_{u2}, D_{u1}, and D_{u2} such that:

$$(3c.47)\quad F_{UR} = S_{GU}(C_{u1}Q_R - C_{u2}Q_L) + S_{GU}(D_{u1}\dot{Q}_R - D_{u2}\dot{Q}_L)$$

$$(3c.48)\quad F_{UL} = S_{GU}(C_{u1}Q_L - C_{u2}Q_R) + S_{GU}(D_{u1}\dot{Q}_L - D_{u2}\dot{Q}_R)$$

It then follows, assuming negligible strut moment of inertia that:

$$(3.49)\quad F_{DUR} = ((F_{GR} + F_{TR} - F_{TL})\bar{z}_{GLR} + T_{SR})/S_{GU}$$

$$(3c.50)\quad F_{DUL} = ((F_{GL} + F_{TL} - F_{TR})Z_{GLL} + T_{SL})/S_{GU}$$

As outputs to the tire and wheel systems we need to compute X_{AX} and Y_{AX}. X_{AX} is shown in Figure 30. Y_{AX} is assumed to be the undeflected tire footprint position in the y direction.

$$(3c.51)\quad X_{AXL} = X + S_{GW}R + S_{VMU}Q + (S_{GU} + Z_{GLL})\theta_{GL} - S_{HM}$$

$$(3c.52)\quad X_{AXR} = X - S_{GW}R + S_{VMU}Q + (S_{GU} + Z_{GLR})\theta_{GR} - S_{HM}$$

$$(3c.53)\quad \dot{X}_{AXL} = \dot{X} + S_{GW}\dot{R} + S_{VMU}\dot{Q} + (S_{GU} + Z_{GLL})\dot{\theta}_{GL}$$

$$(3c.54)\quad \dot{X}_{AXR} = \dot{X} - S_{GW}\dot{R} + S_{VMU}\dot{Q} + (S_{GU} + Z_{GLR})\dot{\theta}_{GR}$$

$$(3c.55)\quad Y_{AXL} = Y - S_{GW} - (S_{HM} - S_{VMU}Q - (S_{GU} + Z_{GLL})\theta_{GL})R \\ - (S_{VMU} + S_{GU} + Z_{GLL})P$$

$$(3c.56)\quad Y_{AXR} = Y + S_{GW} - (S_{HM} - S_{VMU}Q - (S_{GU} + Z_{GLR})\theta_{GR})R \\ - (S_{VMU} + S_{GU} + Z_{GLR})P$$

$$(3c.57)\quad \dot{Y}_{AXL} = \dot{Y} - (S_{HM} - S_{VMU}Q - (S_{GU} + Z_{GLL})\theta_{GL})\dot{R} \\ + (S_{VMU}\dot{Q} + (S_{GU} + Z_{GLL})\dot{\theta}_{GL})R \\ - (S_{VMU} + S_{GU} + Z_{GLL})\dot{P}$$

$$(3c.58)\ \dot{Y}_{AXR} = \dot{Y} - (S_{HM} - S_{VMU}Q - (S_{GU} + Z_{GLR})\Theta_{GR})\dot{R} + (S_{VMU}\dot{Q} + (S_{GU} + Z_{GLR})\dot{\Theta}_{GR})R - (S_{VMU} + S_{GU} + Z_{GLR})\dot{P}$$

Engine Thrust

Referring to Figures A26 and A27, if F_{TH} is the engine thrust, then

$$(3c.59)\ F_{THV} = F_{TH}(\alpha_{TH} + Q)$$

$$(3c.60)\ T_{TH} = S_{TH}F_{TH}$$

$$(3c.61)\ F_{THS} = F_{TH}R$$

Aerodynamics

The following eight equations apply as in the three-degree model.

$$(3c.62)\ Q_A = \dot{X}^2 A_{REF} R_{HA}/288$$

$$(3c.63)\ F_{AL} = C_{AL}Q_A$$

$$(3c.64)\ F_{AD} = C_{AD}Q_A$$

$$(3c.65)\ T_{AM} = C_{AM}Q_A$$

$$(3c.66)\ \alpha_W = \alpha_0 + (180/\pi)(Q - \dot{Z}/\dot{X})$$

$$(3c.67)\ C_{AL} = G_{AL} + B_{AL}\alpha_W + E_{AL}S_{HT}$$

$$(3c.68)\ C_{AD} = G_{AD} + B_{AD}\alpha_W + E_{AD}S_{HT}$$

$$(3c.69)\ C_{AM} = G_{AM} + B_{AM}\alpha_W + E_{AM}S_{HT}$$

Let V_{WY} denote the wind gust velocity as shown in Figure A24 If Ψ and β are defined by:

$$(3c.70)\ \Psi = (V_{WY} + \dot{Y})/\dot{X}$$

$$(3c.71)\ \beta = (180/\pi)(\Psi - R)$$

Then β is the angle of sideslip.

Let Q_{AT} denote the dynamic air pressure (including side wind) multiplied by the reference area. Then:

$$(3c.72)\quad Q_{AT} = ((V_{WY} + \dot{Y})^2 + \dot{X}^2) A_{REF} R_{HA}/288$$

Then the aerodynamic yaw moment is given by:

$$(3c.73)\quad T_{AY} = C_{AN}\beta Q_{AT}$$

and the aerodynamic side force is given by:

$$(3c.74)\quad F_{ASY} = C_{AY}\beta Q_{AT}$$

Finally, an aerodynamic force F_{ASL} due to a combination of lift and pitch is:

$$(3c.75)\quad F_{ASL} = F_{AL} P$$

Refer to Figure A27 as to the direction of these forces.

Dynamics

Referring to Figures A26 and A27, summing forces in the x, y, and z direction,

$$(3c.76)\quad W_A \ddot{Z} = F_{AL} + F_{THV} - W_A G + F_{VMR} + F_{VML} + F_{VN}$$

$$(3c.77)\quad W_A \ddot{X} = F_{TH} - F_{AD} + F_{DUR} + F_{DUL} - F_{UR} - F_{UL} - F_{DN}$$

$$(3c.78)\quad W_A \ddot{Y} = F_{THS} - F_{STR} - F_{STL} + F_{LN} + F_{ASL} - F_{ASY}$$

Summing moments about the C.G. we have:

$$\begin{aligned}(3c.79)\quad W_{IQ}\ddot{Q} = {} & F_{VN}S_{HN} - F_{VMR}S_{HM} - F_{VML}S_{HM} + F_{DUR}S_{VMU} \\ & + F_{DUL}S_{VMU} + T_{TH} + T_{AM} - F_{UR}(S_{GU} + S_{VMU}) \\ & - F_{UL}(S_{GU} + S_{VMU}) - F_{DN}(Z - Z_{GD}\langle X_{WN}\rangle)\end{aligned}$$

$$\begin{aligned}(3c.80)\quad W_{IR}\ddot{R} = {} & F_{LN}S_{HN} + S_{GS}(F_{UR} - F_{UL} + F_{DUL} - F_{DUR}) + T_{AY} \\ & + 2H_A(F_{TR\theta} - F_{TL\theta})S_{GS}\end{aligned}$$

$$\begin{aligned}(3c.81)\quad W_{IP}\ddot{P} = {} & (F_{VML} - F_{VMR})S_{GW} + F_{ASY}H_{AP} \\ & -(Z - Z_{GD}\langle X, Y\rangle)(F_{STR} + F_{STL} + F_{LN})\end{aligned}$$

$$(3c.82)\quad X_{WN} = X + S_{HN} + S_{VN}Q$$

$$(3c.83)\quad \dot{X}_{WN} = \dot{X} + S_{VN}\dot{Q}$$

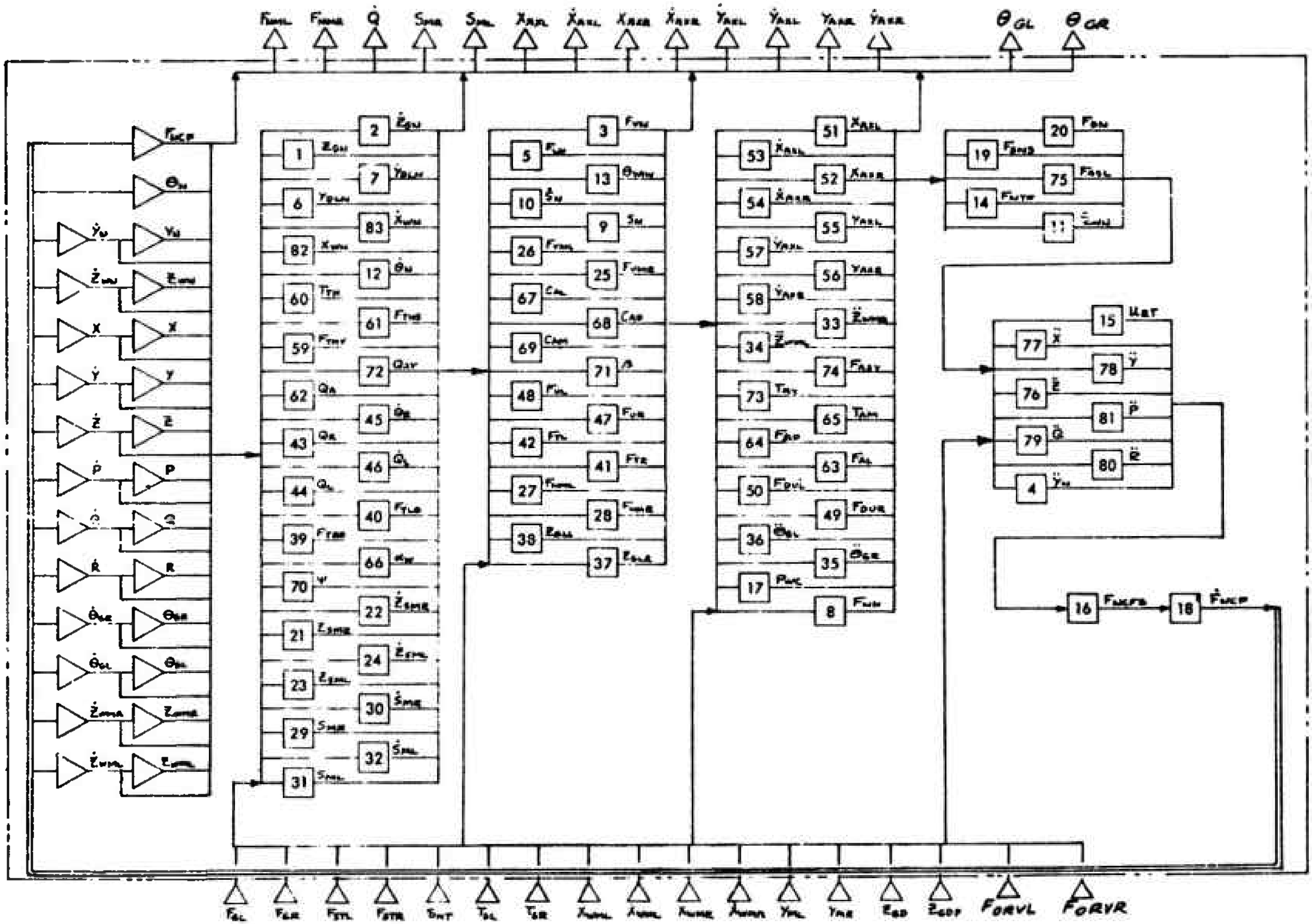

Figure A32 Airplane System (6 Degree) Equation Flow Diagram

B. Parameter Evaluation

Nose Gear Characteristics

Based on a nose gear lateral natural frequency of 12 cps, we have $\omega_n = 2\pi(12) = 75.5$ RAD/SEC. Since $W_{WN} = .435$, then:

$$(3c.84)\ C_{LN} = W_{WN}\,\omega_n^2 = .435\,(75.5)^2 = 2480 \text{ lb/in}$$

Using $\eta = .054$ as in the calculation of D_θ in the three-degree model,

$$(3c.85)\ D_{LN} = \eta\, C_{LN}/\omega_n = (.054)(2480)/75.5 = 1.78 \text{ lb sec/in}$$

The steering or cornering characteristic parameters are obtained from Reference 1. Based on Figure44(a) in Reference 1, the value for U_{NTF} is:

$$(3c.86)\ U_{NTF} = F_{\psi,r,e(max)}/F_z = 25000/45200 = .553$$

Using equation 82 from Reference 1, if $K = (P + .44P_R)w^2 = (1.44)(190)(6.6)^2 = 11{,}920$ lb. then:

$$(3c.87)\ C_{P1} = 1.2\,C_c K/d = (1.2)(57)(11920)/22 = 37060 \text{ lb/Rad in}$$

$$(3c.88)\ C_{P2} = 8.8\,C_c K/d^2 = (8.8)(57)(11920)/(22)^2 = 12353 \text{ lb/Rad in}^2$$

$$(3c.89)\ C_{P3} = .0674\,C_c K = (.0674)(57)(11920) = 45794 \text{ lb/Rad}$$

$$(3c.90)\ C_{P4} = .34\,C_c K/d = (.34)(57)(11920)/22 = 10500 \text{ lb/Rad in}$$

$$(3c.91)\ S_{P1} = .0875\,d = (.0875)(22) = 1.925 \text{ in}$$

From Figure 43 in Reference 1 we see that the cornering force lags the yaw angle. Equation 63 in Reference 1 shows that the equation which describes the curves in Figure 43 is given by:

$$(3c.92)\ F_{y,r} = (1 - e^{-x/L_y})\, F_{y,r\,max}\langle\Theta_{YAW}\rangle$$

where Ly is the tire yawed rolling relaxation length. Differentiating this equation, there follows:

$$(3c.93)\ \frac{dF_{y,r}}{dx} = \frac{e^{-x/L_y}}{L_y}\, F_{y,r\,max}\langle\Theta_{YAW}\rangle$$

Eliminating e^{-x/L_Y} results in:

$$(3c.94)\quad F_{Y,r} + L_Y \frac{dF_{Y,r}}{dx} = F_{Y,r\,max}\langle\Theta_{YAW}\rangle$$

Equation (3c.18) is obtained by using:

$$(3c.95)\quad \frac{dF_{Y,r}}{dx} = \frac{dF_{Y,r}}{dt} \Big/ \frac{dx}{dt} \approx \frac{\dot{F}_{NCF}}{\dot{X}_{WN}}$$

where it is assumed for large airplane velocities that $\dot{X}_{WN} = dx/dt$. We see that the parameter S_{YRL} is the relaxation length. From Figure 39 of Reference 1, for most conditions, S_{YRL} is obtained from:

$$(3c.96)\quad S_{YRL} = .6\,w\,(2.8 - .8\,P/P_r)$$
$$= (.6)(6.6)(2.8 - .8) = 7.92 \text{ in}$$

Main Gear Characteristics

For many airplanes which have a conventional strut arrangement (similar to a B-58) most of the moment about the shock strut ℄ is taken out through the shock strut. In this case equations (3c.41) and (3c.42) would use $H_G = 0.0$. In the case of the F-111 gear the opposite result occurs so that $H_G = 1.0$ and $H_A = 0.0$. The following values apply to the F-111 gear:

$$(3c.97)\quad \begin{cases} W_u = .723 \text{ lb sec}^2/\text{in} \\ W_{WM} = W_{WV} = 1.667 \text{ lb sec}^2/\text{in} \\ S_{Gu} = 21.00 \text{ in} \\ S_{GW} = 60.00 \text{ in} \\ S_{GS} = 20.00 \text{ in} \\ H_G = 1.0 \\ H_A = 0.0 \end{cases}$$

If loads $F_R(t) = F_L(t) = F_o$ are applied as shown in figure 31 , then because of symmetry, the result will be that $Q_R = Q_L$. But then equation (3c.47) says that $C_{u1} - C_{u2} = F_{UR}/S_{Gu}Q_R$ but $C_u = F_{UR}/S_{Gu}Q_R$ as shown in the 3 degree model. Thus

$$(3c.98)\quad C_{u1} - C_{u2} = C_u = 59{,}000 \text{ lb/in}$$

With the main gear at static, if a drag load of 18,000 lb. is applied to the left gear at the ground and -18,000 lb. is applied to the right gear at the ground the observed deflections with $Q = 0$ are $Q_L = .0236$ rad and $Q_R = -.0236$ rad. (Assuming a lateral beam torsional spring rate of 43.0×10^6 in lb/rad).

In the equations which describe the gear loading T_{SR} and T_{SL} can be chosen as 0 if Z_{GLL} and Z_{GLR} are the dimensions to the ground instead of the axle. Thus $Z_{GL} = Z_{GLL} = Z_{GLR} = 2.2 + 12.9 = 21.4$ in. Equations (3c.35), (3c.36), (3c.39), (3c.40), (3c.41) and (3c.42) can then be combined to give

$$(3c.99)\quad F_{UR} - F_{UL} = \left(\frac{S_{GU} + Z_{GL}}{S_{GU}}\right)(F_{GR} - F_{GL})\left(1 + H_G\left(\frac{S_{GW} - S_{GS}}{S_{GS}}\right)\right)$$

$$= \left(\frac{21.0 + 21.4}{21.0}\right)(-36000)\left(1 + \left(\frac{60-20}{20}\right)\right) = -212{,}000 \text{ lb}$$

Subtracting equation (3c.48) from (3.47) results in

$$(3c.100)\quad F_{UR} - F_{UL} = (C_{U1} + C_{U2}) S_{GU} Q_R - (C_{U1} + C_{U2}) S_{GU} Q_L$$

So that

$$(3c.101)\quad C_{U1} + C_{U2} = \frac{-212000}{(2)(21.0)(-.0236)} = 214{,}000 \text{ lb/in}$$

Adding and subtracting equations (3c.98) and (3c.101) results in

$$(3c.102)\quad C_{U1} = \frac{59000 + 214000}{2} = 136{,}500 \text{ lb/in}$$

$$(3c.103)\quad C_{U2} = \frac{214{,}000 - 59000}{2} = 77{,}500 \text{ lb/in}$$

At a fore and aft natural frequency of 137.5 rad/sec, the damping coefficients D_{U1} and D_{U2} are given as

$$(3c.104)\quad D_{U1} = \eta C_{U1}/\omega = \frac{(.054)(1.36 \times 10^5)}{(137.5)} = 53.4 \text{ lb sec/in}$$

$$(3c.105)\quad D_{U2} = \eta C_{U2}/\omega = \frac{(.054)(.775 \times 10^5)}{(137.5)} = 30.5 \text{ lb sec/in}$$

Aerodynamic Characteristics

The coefficients for equations (3c.62) thru (3c.69) have been derived in the 3 degree model. For the F-111A in the landing configuration and wings swept to 26 degrees as described in the 3 degree system, $C_{N\beta} = .0014$ and $C_{Y\beta} = -.021$. Then the coefficient C_{AY} is calculated from

$$\text{(3c.106)} \quad C_{AY} = -C_{Y\beta} = .021 \ deg^{-1}$$

Let ΔX = FSA - FSCG as in the 3 degree system where FSA = 526.8 and FSCG = 519.0. Let b be the wing span. If b = 756 in., then

$$\text{(3c.107)} \quad C_{AN} = b\,C_{N\beta} - \Delta X\,C_{Y\beta}$$

$$\text{(3c.108)} \quad C_{AN} = (756)(.0014) - (7.80)(-.021) = 1.222 \ in/deg$$

Airplane Characteristics

The parameters listed in Table A8 describing the airplane's dimensional and mass characteristics are those previously derived in the 3 degree model or simply a listing of the appropriate values applicable to the F-111 for which no derivation or computation is required.

Table A8 Airplane System (6 Degree) Parameters (Sheet 1 of 9)

SYMBOL	TYPE	VALUE	UNITS	DESCRIPTION
α_O	c	1.00	deg	Wing Angle of Incidence
α_{TH}	c	-.052	rad	Angle between Thrust & W.L.
α_W	v		deg	Wing Angle of Attack
A_{REF}	c	525.0	ft^2	Wing Reference Area
A_{VM}	v*		$lb\ sec^2/in^2$	M.G. Shock Strut Damping Coeff.
A_{VN}	v*		$lb\ sec^2/in^2$	N.G. Shock Strut Damping Coeff.
B_{AD}	c	0.00	deg^{-1}	Aero Drag Parameter
B_{AL}	c	.128	deg^{-1}	Aero Lift Parameter
B_{AM}	c	-.371	in/deg	Aero Moment Parameter
β	v		deg	Angle of Sideslip
C_{AD}	v		-	Aero Drag Coefficient
C_{AL}	v		-	Aero Lift Coefficient
C_{AM}	v		in	Aero Moment Coeff. (Pitch)
C_{AN}	c	1.222	in/deg	Aero Moment Coeff. (Yaw)
C_{AY}	c	.021	deg^{-1}	Aero Side Force Coeff.
C_{LN}	c	2480	lb/in	Nose Gear Lateral Spring Rate
C_{MT}	c	9530	lb/in	M.G. Tire Vertical Spring Rate
C_{NT}	c	12,200	lb/in	N.G. Tire(s) Vertical Spring Rate
C_{P1}	c	37,060	lb/rad in	Parameters for P_{WC}
C_{P2}	c	12,353	$lb/rad\ in^2$	
C_{P3}	c	45,794	lb/rad	
C_{P4}	c	10,500	lb/rad in	
C_{U1}	c	1.365×10^5	lb/in	Drag Brace Characteristic Spring Rates
C_{U2}	c	$.775 \times 10^5$	lb/in	
D_{LN}	c	1.78	lb sec/in	Nose Gear Lateral Damping Coeff.
D_{MT}	c	38.8	$lb\ sec/in^2$	M.G. Tire Vertical Damping Coeff.
D_{NT}	c	50.6	$lb\ sec/in^2$	N.G. Tire(s) Vertical Damping Coefficient

Table A8 Airplane System (6 Degree) Parameters (Sheet 2 of 9)

SYMBOL	TYPE	VALUE	UNITS	DESCRIPTION
D_{U1}	c	53.4	lb sec/in	Drag Brace Characteristic Damping Coefficient
D_{U2}	c	30.5	lb sec/in	
D_{VM}	c	0.0	lb sec/in	M. G. Shock Strut Linear Damping Coefficient
D_{VN}	c	0.0	lb sec/in	N. G. Shock Strut Linear Damping Coefficient
E_{AD}	c	-.0036	deg^{-1}	Aero Drag Coefficient
E_{AL}	c	.022	deg^{-1}	Aero Lift Coefficient
E_{AM}	c	- 3.759	in/deg	Aero Moment Coefficient
F_{AD}	v		lb	Aero Drag
F_{AL}	v		lb	Aero Lift
F_{ASL}	v		lb	Side Force Due to Aero Lift
F_{ASY}	v		lb	Side Force Due to Yaw
F_{DN}	v		lb	N. G. Rolling Resistance
F_{DUL}	v		lb	Horizontal Load at M. G. Pivot
F_{DUR}	v		lb	
F_{GL}	v(I)		lb	Horizontal Load on M. G. Axle
F_{GR}	v(I)		lb	
F_{LN}	v		lb	Lateral Nose Gear Load
F_{NCF}	v		lb	Normal Cornering Force
F_{NCFO}	c	0.0	lb	Normal Cornering Force at Time = 0
$\dot{F}_{NCF}$	v		lb/sec	Time Derivative of Normal Cornering Force
F_{NCFS}	v		lb	Steady State Normal Cornering Force
F_{NML}	v(o)		lb	M. G. Tire Normal Load
F_{NMR}	v(o)		lb	

Table A8 Airplane System (6 Degree) Parameters (Sheet 3 of 9)

SYMBOL	TYPE	VALUE	UNITS	DESCRIPTION
F_{NN}	v		lb	N.G. Tire Normal Load
F_{NTF}	v		lb	Nose Tire Friction Force
F_{SNS}	v		lb	Nose Tire Lateral Force
F_{STL}	v(I)		lb	M. G. Lateral Tire Force
F_{STR}	v(I)		lb	
F_{TL}	v		lb	M. G. Loads for Torque Takeout Correction
$F_{TL\theta}$	v		lb	
F_{TR}	v		lb	
$F_{TR\theta}$	v		lb	
F_{TH}	c	1000.	lb	Engine Thrust
F_{THV}	v		lb	Vertical Component of Engine Thrust
F_{THS}	v		lb	Side Component of Engine Thrust
F_{UL}	v		lb	M. G. Loads in Ficticious Drag Brace
F_{UR}	v		lb	
F_{VML}	v		lb	M. G. Shock Strut Load
F_{VMR}	v		lb	
F_{VMS}	v*		lb	M. G. Shock Strut Air Load Curve
F_{VN}	v		lb	N. G. Shock Strut Load
F_{VNS}	v*		lb	N. G. Shock Strut Air Load Curve
G	c	386	in/sec^2	Gravitational Constant
G_{AD}	c	.240	-	Aero Drag Parameter
G_{AL}	c	-.016	-	Aero Lift Parameter
G_{AM}	c	2.286	in	Aero Moment (Pitch) Parameter
G_{PIL}	c	3.0	sec^{-1}	Pilot's Steering Gain
H_A	c	0.0	-	Torque Adjustment Parameter $H_A + H_6 = 1$
H_{AP}	c	0.0	in	Height of Center of Pressure above C. G.

*Point Plot Input

Table A8 Airplane System (6 Degree) Parameters (Sheet 4 of 9)

SYMBOL	TYPE	VALUE	UNITS	DESCRIPTION
H_G	c	1.0	-	Torque Adjustment Parameter
Θ_N	v		rad	Nose Wheel Turn Angle Relative to Apl ℄.
Θ_{NO}	c	0.0	rad	Θ_N at Time = 0
$\dot{\Theta}_N$	v		rad/sec	d Θ_N/dt
Θ_{GR}	v		rad	M. G. Strut Rotation from Horizontal
Θ_{GL}	v		rad	
Θ_{GLO}	c	.0329	rad	Θ_G at Time = 0
Θ_{GRO}	c	.0329	rad	
$\dot{\Theta}_{GL}$	v		rad/sec	Angular Velocity of M. G. Strut
$\dot{\Theta}_{GR}$	v		rad/sec	
$\dot{\Theta}_{GLO}$	c	0.0	rad/sec	$\dot{\Theta}_G$ at time = 0
$\dot{\Theta}_{GRO}$	c	0.0	rad/sec	
$\ddot{\Theta}_{GL}$	v		rad/sec^2	Angular Acceleration of M. G. Strut
$\ddot{\Theta}_{GR}$	v		rad/sec^2	
Θ_{NMAX}	c	0.7	rad	Maximum Nose Wheel Turning Angle
Θ_{YAW}	v		rad	Nose Wheel Turning Yaw Angle
Ψ	v		rad	Angle of Relative Wind
P	v		rad	Airplane Roll Angle
P_o	c	0.0	rad	P at Time = 0
$\dot{P}$	v		rad/sec	Airplane Roll Rate
$\dot{P}_o$	c	0.0	rad/sec	$\dot{P}$ at Time = 0
$\ddot{P}$	v		rad/sec^2	Roll Acceleration
P_{WC}	v		lb/rad	Nose Tire Cornering Power
Q	v		rad	Airplane Pitch Angle
Q_o	c	.0329	rad	Q at Time = 0
$\dot{Q}$	v(o)		rad/sec	Pitch Rate

Table A8 Airplane System (ζ Degree) Parameters (Sheet 5 of 9)

SYMBOL	TYPE	VALUE	UNITS	DESCRIPTION
$\dot{Q}_o$	c	0.0	rad/sec	Q at Time = 0
$\ddot{Q}$	v		rad/sec²	Pitch Acceleration
Q_A	v		lb	Aero Press X Aref
Q_{AT}	v		lb	Aero Press X Aref (Includes Vwy)
Q_L	v		rad	Angular Position and Velocity
$\dot{Q}_L$	v		rad/sec	of M. G. Relative to the Airplane
Q_R	v		rad	
$\dot{Q}_R$	v		rad/sec	
R	v		rad	Airplane Yaw Angle
R_o	c	0.0	rad	R at Time = 0
$\dot{R}$	v		rad/sec	Yaw Rate
$\dot{R}_o$	c	0.0	rad/sec	$\dot{R}$ at Time = 0
$\ddot{R}$	v		rad/sec²	Yaw Acceleration
$R_{\theta TM}$	c	23.32	in	M. G. Tire Undeflected Radius
$R_{\theta TN}$	c	10.80	in	N. G. Tire Undeflected Radius
R_{HA}	c	.00238	slug/ft³	Air Density
S_{GL}	c	26.50	in	≠
S_{GS}	c	20.00	in	≠
S_{GU}	c	21.00	in	≠
S_{GW}	c	60.00	in	≠
S_{HM}	c	36.20	in	≠
S_{HN}	c	258.90	in	≠
S_{HT}	v(I)		deg	Horizontal Tail Deflection
S_{MR}	v(o)		in	M. G. Tire Deflection
S_{ML}	v(o)		in	
$\dot{S}_{MR}$	v		in/sec	M. G. Tire Deflection Rate
$\dot{S}_{ML}$	v		in/sec	
S_N	v		in	N. G. Tire Deflection
$\dot{S}_N$	v		in/sec	N. G. Tire Deflection Rate

≠ See Figure 25

Table A8 Airplane System (6 Degree) Parameters (Sheet 6 of 9)

SYMBOL	TYPE	VALUE	UNITS	DESCRIPTION
S_{PI}	c	1.925	in	Parameter of Cornering Power Pwc
S_{TH}	c	20.00	in	#
S_{VM}	c	84.24	in	#
S_{VMU}	c	36.74	in	#
S_{VN}	c	85.86	in	#
S_{YRL}	c	7.92	in	Nose Tire Relaxation Length (Yaw)
T_{AM}	v		in lb	Aero Pitching Moment
T_{AY}	v		in lb	Aero Yawing Moment
T_{SL}	v(I)		in lb	Moment on M. G. Axle
T_{SR}	v(I)		in lb	
T_{TH}	c	20,000	in lb	Thrust Moment about C. G.
U_{NTF}	c	.553	—	Nose Tire Friction Coefficient
U_{RRN}	c	.02	—	Nose Tire Rolling Resistance Coefficient
U_{RT}	v		—	Nose Tire Cornering Parameter
V_{WY}	v*		in/sec	Crosswind
W_A	c	147.6	lb sec²/in	Airplane Mass
W_{IP}	c	1.465×10^6	lb sec² in	Roll Moment of Inertia
W_{IQ}	c	3.66×10^6	lb sec² in	Pitch Moment of Inertia
W_{IR}	c	4.93×10^6	lb sec² in	Yaw Moment of Inertia
W_{WM}	c	1.667	lb sec²/in	M. G. Unsprung Mass
W_{WN}	c	.453	lb sec²/in	N. G. Unsprung Mass
W_u	c	.723	lb sec²/in	M. G. Upper Strut Mass
X	v		in	Horizontal Position of A_{PL} C.G.
X_o	c	36.20	in	X at Time = 0
$\dot{X}$	v		in/sec	Airplane Velocity in the x Direction
$\dot{X}_o$	c	2400	in/sec	Velocity at Time = 0
$\ddot{X}$	v		in/sec²	Airplane Acceleration in the X Direction

*Point Plot Input

Table A8 Airplane System (6 Degree) Parameters (Sheet 7 of 9)

SYMBOL	TYPE	VALUE	UNITS	DESCRIPTION
X_{AXL}	v(o)		in	M.G. Axle Undeflected Location (x Direction)
$\dot{X}_{AXL}$	v(o)		in/sec	M.G. Axle Undeflected Velocity (x Direction)
X_{WML}	v(I)		in	M.G. Tire Footprint Location and Velocity in the x direction
$\dot{X}_{WML}$	v(I)		in/sec	
X_{WMR}	v(I)		in	
$\dot{X}_{WMR}$	v(I)		in/sec	
X_{WN}	v		in	N.G. Tire Location (X direction)
$\dot{X}_{WN}$	v		in/sec	N.G. Tire Velocity (X direction)
X_{AXR}	v(o)		in	M.G. Undeflected Axle Location (x Direction)
$\dot{X}_{AXR}$	v(o)		in/sec	M.G. Undeflected Axle Velocity (x Direction)
Y	v		in	Horizontal C. G. Location (Y Direction)
Y_o	c	0.0	in	Y at Time = 0
$\dot{Y}$	v		in/sec	Airplane C.G. Velocity in Y Direction
$\dot{Y}_o$	c	0.0	in/sec	$\dot{Y}$ at Time = 0
$\ddot{Y}$	v		in/sec^2	Airplane C.G. acceleration in Y Direction
Y_{AXL}	v(o)		in	M.G. Undeflected Axle Location and Velocity in the Y Direction
$\dot{Y}_{AXL}$	v(o)		in/sec	
Y_{AXR}	v(o)		in	
$\dot{Y}_{AXR}$	v(o)		in/sec	
Y_{DLN}	v		in	N.G. Lateral Deflection
$\dot{Y}_{DLN}$	v		in/sec	N.G. Lateral Delta Velocity
Y_{ML}	v(I)		in	M.G. Tire Footprint Location In the Y Direction
Y_{MR}	v(I)		in	

Table A8 Airplane System (6 Degree) Parameters (Sheet 8 of 9)

SYMBOL	TYPE	VALUE	UNITS	DESCRIPTION
Y_N	v		in	N.G. Lateral Location (Y Direction)
Y_{NO}	c	0.0	in	Y_N at Time = 0
$\dot{Y}_N$	v		in/sec	N.G. Lateral Velocity
$\dot{Y}_{NO}$	c	0.0	in/sec	$\dot{Y}_N$ at Time = 0
$\ddot{Y}_N$	v		in/sec^2	N.G. Lateral Acceleration
Z	v		in	Height of Apl C.G. above ground ref.
Z_o	c	82.36	in	Z at Time = 0
$\dot{Z}$	v		in/sec	Apl vertical velocity
$\dot{Z}_o$	c	0.0	in/sec	$\dot{Z}$ at Time = C
$\ddot{Z}$	v		in/sec^2	Apl Vertical acceleration
Z_{GO}	v(I)		in	Runway contour height
Z_{GOP}	v(I)		in/in	Runway contour slope (x Direction)
Z_{BLL}	v		in	Distance from Wu position to Axle
Z_{GLR}	v		in	
Z_{SML}	v		in	M.G. Strut Velocity and Stroke
$\dot{Z}_{SML}$	v		in/sec	
Z_{SMR}	v		in	
$\dot{Z}_{SMR}$	v		in/sec	
Z_{SN}	v		in	N. G. Stroke
$\dot{Z}_{SN}$	v		in/sec	N.G. Stroke Velocity
Z_{WML}	v		in	M. G. Axle Height
Z_{WMR}	v		in	
Z_{WMLO}	c	20.91	in	M.G. Axle Height at Time = 0
Z_{WMRO}	c	20.91	in	
$\dot{Z}_{WML}$	v		in/sec	M.G. Axle Velocity
$\dot{Z}_{WMR}$	v		in/sec	

Table A8 Airplane System (6 Degree) Parameters (Sheet 9 of 9)

SYMBOL	TYPE	VALUE	UNITS	DESCRIPTION
$\dot{Z}_{WMLO}$	c	0.0	in/sec	M.G. Axle Velocity at Time = 0
$\dot{Z}_{WMRO}$	c	0.0	in/sec	
$\ddot{Z}_{WML}$	v		in/sec^2	M.G. Axle Vertical Acceleration
$\ddot{Z}_{WMR}$	v		in/sec^2	
Z_{WN}	v		in	N. G. Axle Vertical Location
Z_{WNO}	c	10.02	in	Z_{WN} at Time = 0
$\dot{Z}_{WN}$	v		in/sec	N.G. Axle Vertical Velocity
$\dot{Z}_{WNO}$	c	0.0	in/sec	$\dot{Z}_{WN}$ at Time = 0
$\ddot{Z}_{WN}$	v		in/sec^2	N. G. Axle Vertical Acceleration
F_{ORVL}	v(I)		lb	M. G. Tire Unbalance
F_{ORVR}	v(I)		lb	

4a. WHEEL AND TIRE SYSTEM (FLYWHEEL)

Figure A33 shows the components of the wheel and tire system.

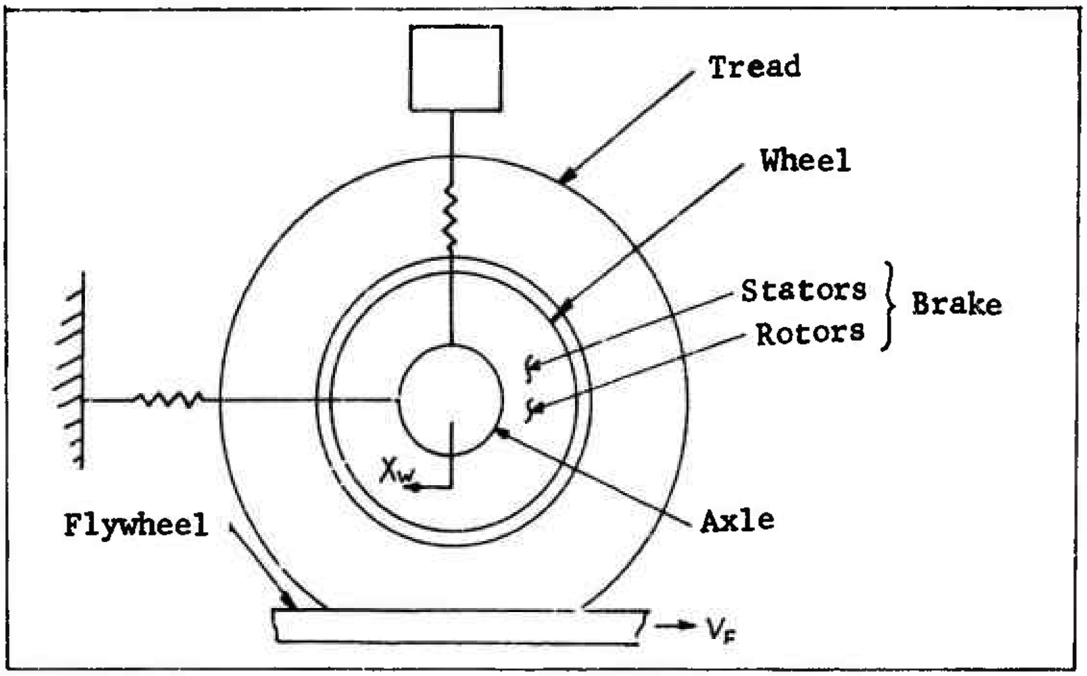

Figure A33 Components of the Wheel and Tire System

In the vertical, or Z direction, the axle, brake, wheel, tire, and lower shock strut are combined and operate as a single mass point. A description of this mode is found in the airplane system. The airplane system furnishes various inputs to the tire and wheel: V_F the airplane (flywheel surface) velocity; F_{NM} , the vertical load between the tire and pavement; S_M , the tire deflection. The brake torque T_{ST} is an input from the brake system.

The horizontal displacement of two mass points is considered. One mass point is made up of the axle, brake, wheel, and the inner part of the tire and its location is designated as X_W. The other mass point is the tire tread and its location is designated as X_{TT}.

In rotation, there are three mass points: the axle and stationary brake elements make up the first; the brake rotors, wheel, and inner tire make up the second; and the tire tread makes up the third. The angular positions of these three mass points are denoted respectively as θ_S, θ_W, and θ_T. Let F_G be the horizontal force acting on the

axle and let F_{TT} be the net horizontal force between the wheel and tire tread. Figure A34 shows the location of these forces. F_{BT} is the horizontal force between the tire and the flywheel surface.

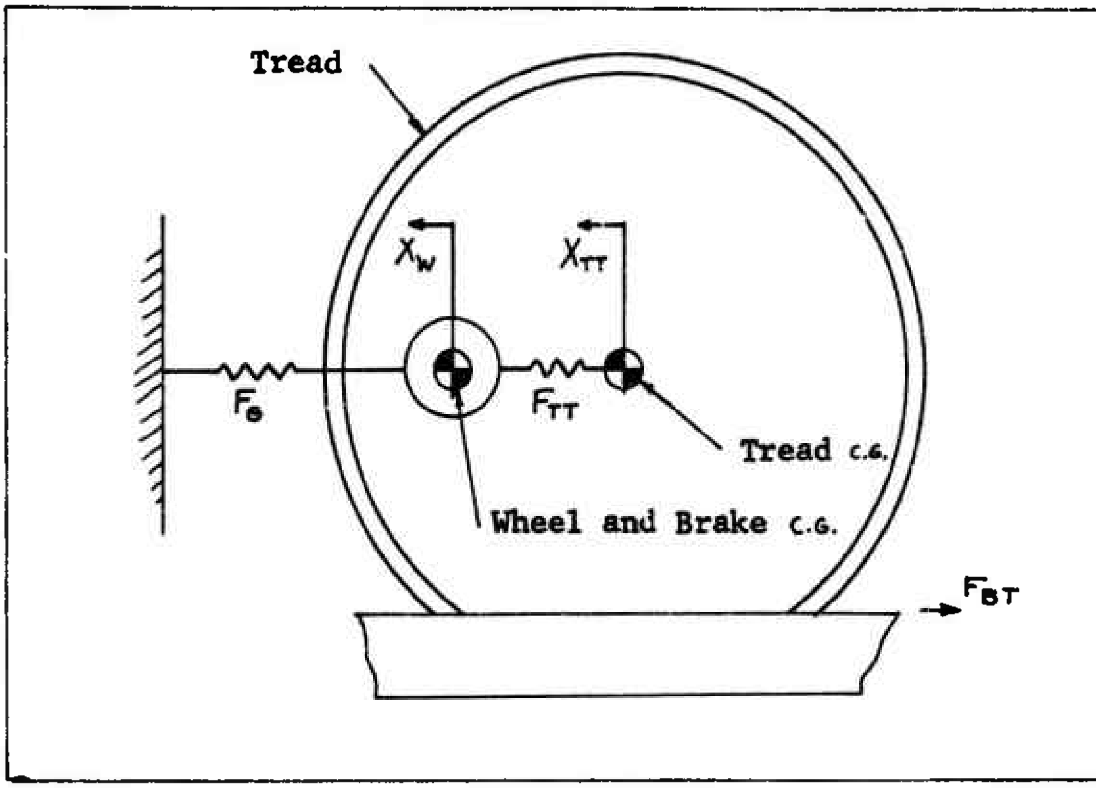

Figure A34 Tire Horizontal Model

A. Mathematical Description

Equations describing the tire and wheel behavior are developed by referring to Figure A34. Forces F_G and F_{TT} are defined by equations (4a.1), (4a.2), and (4a.3) as follows:

(4a.1) $F_G = -C_{GH} X_W - D_{GH} \dot{X}_W$

(4a.2) $F_{TT} = C_{TT}(X_{TT} - X_W) + E_{TT}(X_{TT} - X_Y) + D_{TLV}(\dot{X}_{TT} - \dot{X}_W)$

(4a.3) $D_{TT}(\dot{X}_Y - \dot{X}_W) = E_{TT}(X_{TT} - X_Y)$

Equations (4a.2) and (4a.3) describe a type 2 spring-damper system as defined by Figure A38 and discussed in the parameter evaluation.

Let W_{GW} denote the mass of the axle, wheel, brake and inner part of the tire. Let W_{TE} denote the appropriate tire tread mass. Summing forces in the horizontal direction gives:

$$(4a.4)\quad W_{GW}\ddot{X}_W = F_G + F_{TT}$$

$$(4a.5)\quad W_{TE}\ddot{X}_{TT} = -F_{TT} - F_{BT} + F_{\theta RH}$$

Where $F_{\theta RH}$ is a force produced by tire unbalance, the corresponding vertical part of this unbalance force is denoted by $F_{\theta RV}$. These two forces are given in equations (4a.6) and (4a.7).

$$(4a.6)\quad F_{\theta RH} = R_{K\theta} W_T^2 \sin\langle\theta_T\rangle$$

$$(4a.7)\quad F_{\theta RV} = R_{K\theta} W_T^2 \cos\langle\theta_T\rangle$$

W_T and θ_T are the rotational speed and position ot the tire tread.

The rotational schematic of the wheel and tire system is shown in Figure A35 .

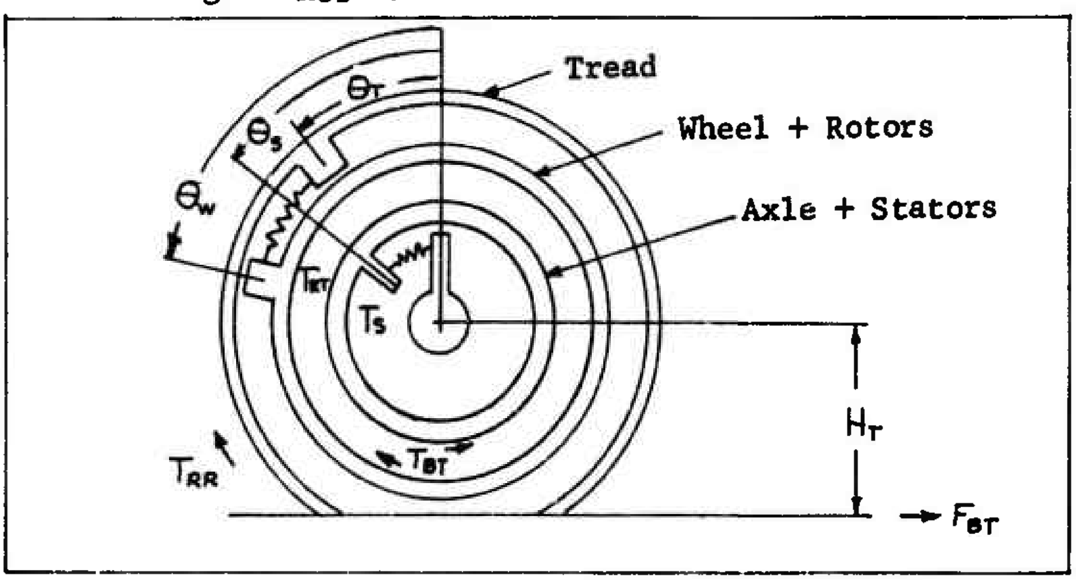

Figure A35 Tire Rotational Model

Let T_{RT} and T_S be defined by equations (4a.8), (4a.9), and (4a.10) as follows:

$$(4a.8)\quad T_{KT} = C_{RT}(\theta_W - \theta_T) + E_{RT}(\theta_W - \theta_Y) + D_{TRV}(\dot{\theta}_W - \dot{\theta}_T)$$

$$(4a.9)\quad D_{RT}(\dot{\theta}_Y - \dot{\theta}_T) = E_{RT}(\theta_W - \theta_Y)$$

$$(4a.10)\quad T_S = C_{RS}\theta_S + D_{RS}\dot{\theta}_S$$

Let H_T be the height of the axle above the ground. Let T_{RR} be the torque on the tire that produces rolling resistance. These two quantities are given by:

$$(4a.11)\quad H_T = R_{0T} - S_M$$

$$(4a.12)\quad T_{RR} = \begin{cases} S_M(D_{SR} + D_{VR}W_T) & \text{if } W_T > 0 \\ 0 & \text{if } W_T = 0 \\ S_M(-D_{SR} + D_{VR}W_T) & \text{if } W_T < 0 \end{cases}$$

If T_{BT} is the brake torque, then torques can be summed to obtain the following three equations:

$$(4a.13)\quad W_{IS}\ddot{\theta}_S = T_{BT} - T_S$$

$$(4a.14)\quad W_{IW}\ddot{\theta}_W = -T_{RT} - T_{BT}$$

$$(4a.15)\quad W_{IT}\ddot{\theta}_T = H_T F_{BT} + T_{RT} - T_{RR}$$

The rolling radius of the tire is obtained using the methods of Reference 1. Denoting the rolling radius as R_T, it is defined as:

$$(4a.16)\quad R_T = R_{0T} - \tfrac{1}{3}S_M - U_{RR}(X_{TT} - X_W)$$

Let V_{RS} denote the velocity of the tire footprint relative to the flywheel surface with $W_T = 0$, let V_R be the relative velocity including W_T.

$$(4a.17)\quad V_{RS} = V_F + \dot{X}_{TT}$$

$$(4a.18)\quad V_R = V_{RS} - R_T W_T$$

Here V_F is the velocity of the flywheel surface. Adopting the convention, $W_T = \dot{\theta}_T$; $W_S = \dot{\theta}_S$; and $W_W = \dot{\theta}_W$, the relative angular velocity between the stators and rotors is denoted by W_B and is established by:

$$(4a.19)\quad W_B = W_W - W_S$$

When a tire is moving over a runway with any appreciable amount of standing water or slush, a hydrodynamic "wedge"

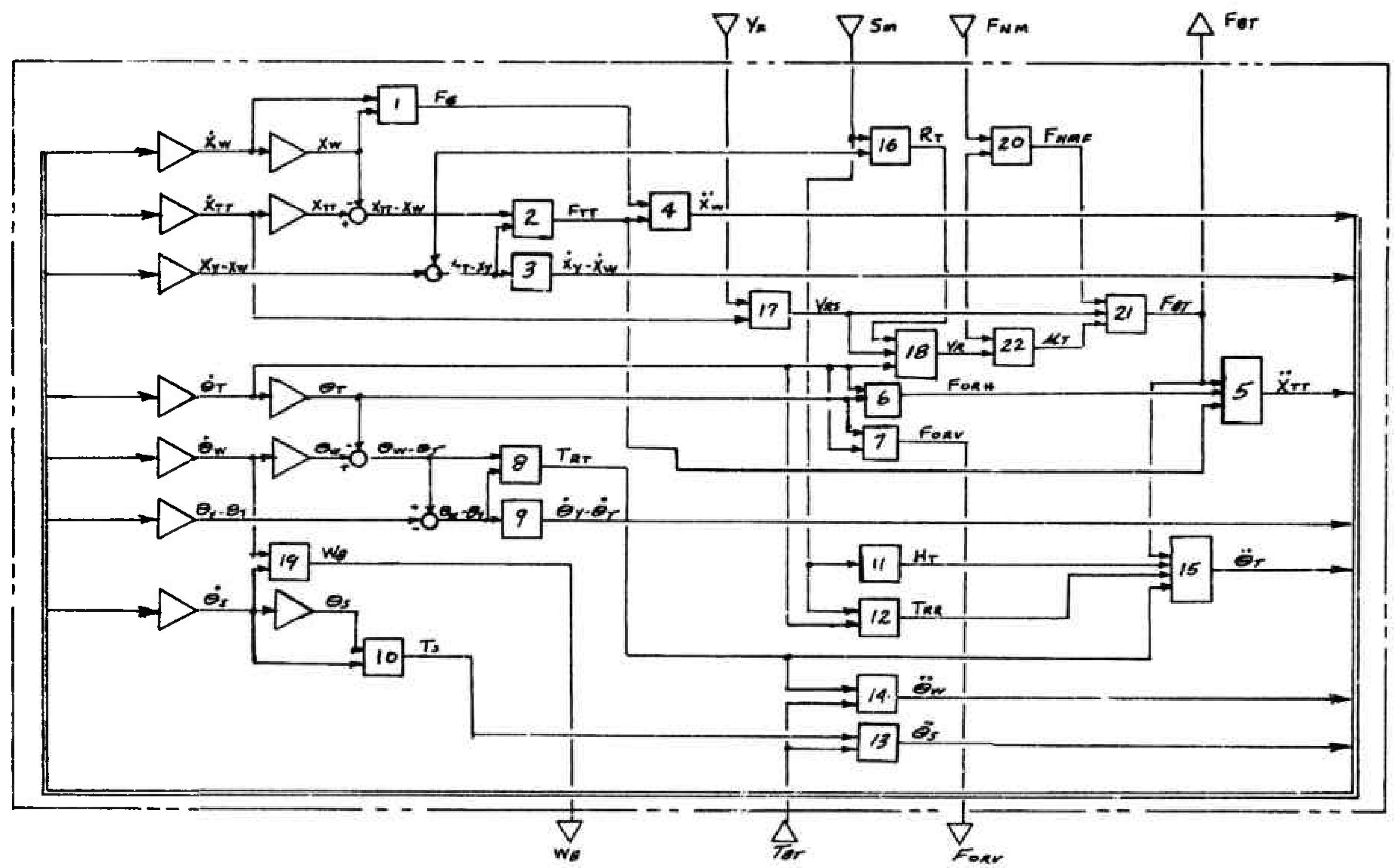

Figure A36 Wheel and Tire System (Flywheel) Equation Flow Diagram

of water starts separating the tread and runway surface. It is assumed that the length of this "wedge" is proportional to V_{RS}^2 and at hydroplaning speed, V_{HY}, the tread is completely separated from the runway. In equations (4a.20) and (4a.20) the coefficients C_{HY} and D_{HY} are used to define hydroplaning effects and water drag on the wheel. For dry runway conditions, C_{HY} and D_{HY} are zero. The horizontal force between the tire tread footprint and the runway surface is established by equations (4a.20), (4a.21), and (4a.22) as follows:

(4a.20) $F_{NMF} = F_{NM}(1 - C_{HY}(V_{RS}/V_{HY})^2)$

(4a.21) $F_{BT} = F_{NMF}U_T + D_H V_{RS}^2$

(4a.22) $U_T = \begin{cases} U_{T1} + (U_{T2} - E_T V_{RS})\, e^{-\alpha V_R} & \text{if } V_R > V_{RO} \\ \{[U_{T1} + (U_{T2} - E_T V_{RS})\, e^{-\alpha V_{RO}}]\, 1/V_{RO}\} V_R & \text{if } V_{RO} > V_R > -V_{RO} \\ -U_{T1} \quad (U_{T2} - E_T V_{RS})\, e^{\alpha V_R} & \text{if } V_R < V_{RO} \end{cases}$

Figure A36 is an equation flow diagram showing the relation between equations (4a.1) through (4a.22).

B. Parameter Evaluation

Gear Characteristics

The mass W_{GW} is made up of the mass of half the shock strut, half the lateral beam, the axle, the wheel, the brakes, and all but one-third of the tire tread. The sum of the masses of these components totals 616 LBM. Thus, $W_{GW} = 616/386 = 1.60$ lb sec²/in. The fore and aft natural frequency of the gear (as calculated from deflection data) is 21.84 cps = 137.5 rad/sec. Using the gear mass, with all of the tire included (644 LBM), the spring rate C_{GH} can be calculated as:

(4a.23) $C_{GH} = m\omega_n^2 = \left(\frac{644}{386}\right)(137.5)^2 = 31{,}500$ lb/in

A typical approach to estimate the damping coefficient is to use 3% critical. Thus,

(4a.24) $D_{GH} = (.03)\, 2\sqrt{mC_G} = (.06)\sqrt{\left(\frac{644}{386}\right)31500} = 13.8\ \frac{\text{lb sec}}{\text{in}}$

Tire Tread Characteristics

The principle underlying the calculation of the tire friction coefficient is that compared to the rest of the tire, the tire "footprint" is totally inelastic. (The tire "footprint" is that portion of the tire tread which is in contact with the ground). Thus, if the velocity of the footprint and the friction vs. velocity curve for the rubber-surface interface are defined, the tire friction coefficient is established. In order to predict the motion of the footprint, the tire tread is assumed to behave like an inelastic ring which is supported on the wheel as shown in Figure A37.

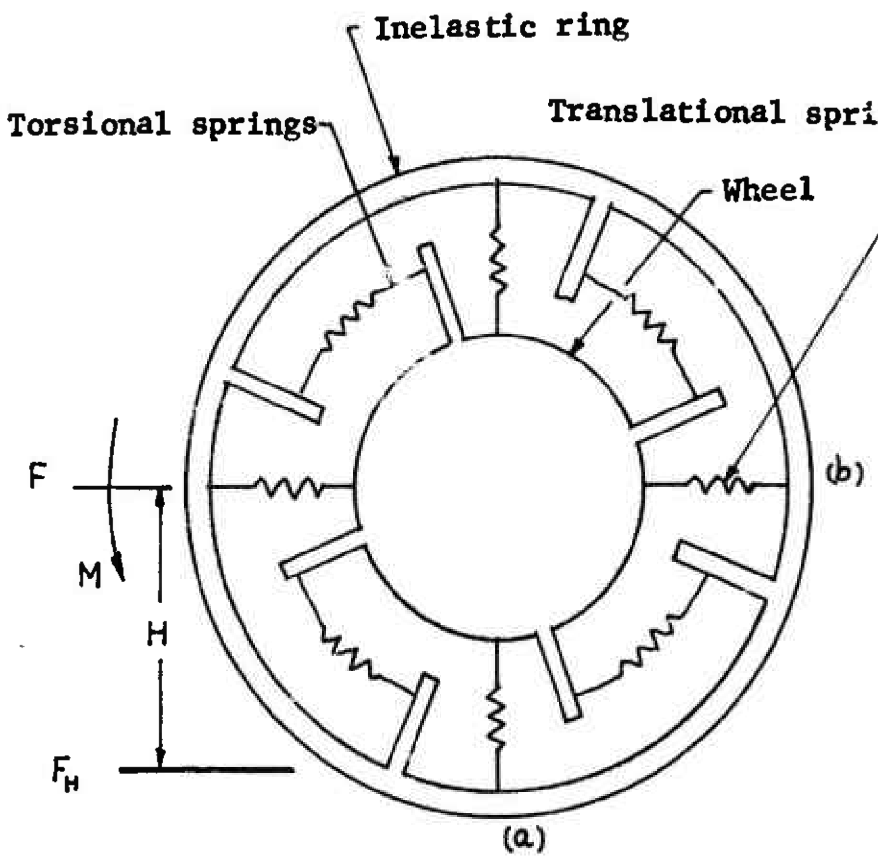

Figure A37 Tire Tread Model

The horizontal position of the footprint is assumed to be the same as the horizontal position of the ring center of gravity. A frictional force F_H applied at the ground can be resolved into a translational force $F = F_H$ acting at the ring C.G., plus a moment $M = F_H \cdot H$ acting about the ring C.G.

For an actual tire with distributed mass and elasticity approximately one-third of the tire would move with the footprint in response to force, F_H. Therefore, it is assumed for translation the mass of the ring, W_{TE}, is one-third of the tire tread mass, which is 84 LBM. Thus, $W_{TE} = (84)/(3 \times 386) = 0.0725$ LBF SEC^2/IN.

For rotation the total tire tread mass is assumed to move in response to moment, M. Thus, the moment of inertia about its center of gravity is $W_{IT} = MR^2 = (84/386)(23^2) = 115$ LBF SEC^2/IN.

References 1 (page 22) and 10 (Figure 8) are used to obtain values for the torsional and translational spring rates as shown in Figure A37. Under the application of the force F_H, the peripheral movement at point (b) is about 20% of the peripheral movement at point (a) in Figure A37. The expression for the footprint spring rate from Reference 1 is:

$$(4a.25)\quad K_x = .6\, d\,(P + 4P_r)\sqrt[3]{S_o/d}$$

Where for the F-111 with a vertical tire load of 25,000 lb,

d = 46.65 in.	=	Tire diameter
P = 150 psi	=	Tire operating pressure
Pr = 150 psi	=	Tire rated pressure
So = 2.75 in.	=	Operating (static) deflection

Thus,

$$(4a.26)\quad K_x = (.6)(46.65)(5)(150)\sqrt[3]{2.75/46.65} = 8150 \text{ lb/in}$$

The application of F_H = 8150 lb. causes the footprint to move one inch. At point b, the movement is .2 inches. Assuming that the movement at point b is all due to rotation, the apparent torsional spring rate is:

$$(4a.27)\quad C_{RT} = \left(\frac{d}{2}\right)\frac{H\,F_H}{(.2)} = \frac{(23.32)(20.57)(8150)}{(.2)} = 19.5\times10^6 \text{ IN LBF/RAD}$$

Since .8 inches of the 1.0 inch footprint motion is due to tread C.G. fore and aft translation, the apparent spring rate is:

$$(4a.28)\quad C_{TT} = \frac{F_H}{.8} = \frac{8150}{.8} = 10{,}200 \text{ lb/in}$$

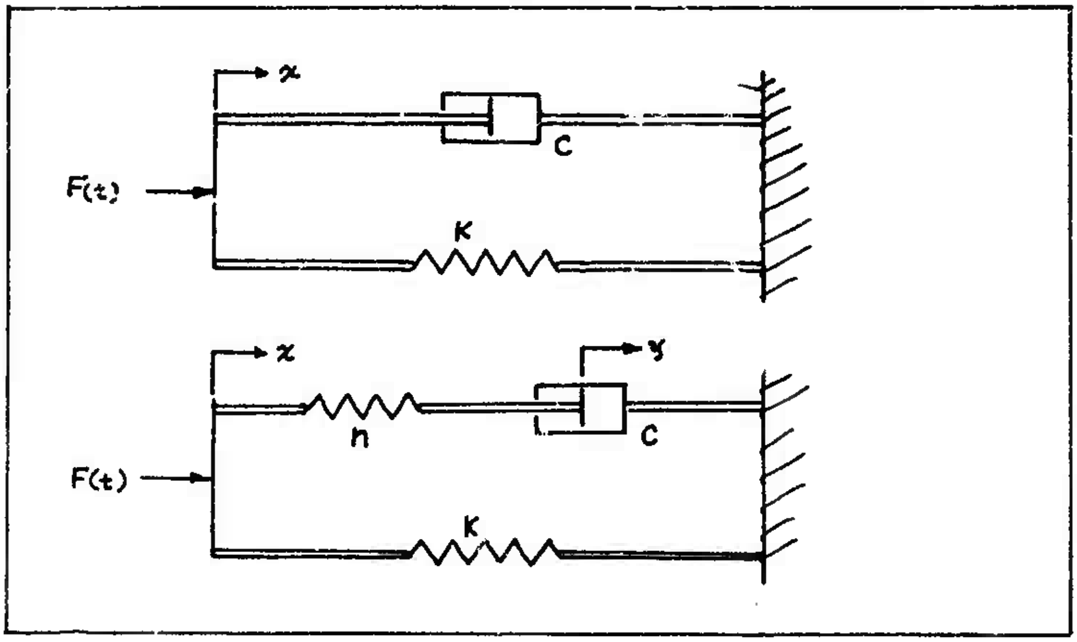

Figure A38 Tire Damping Models

It is well publicized and generally accepted that the elastic and damping characteristics of tires and other structural devices are not accurately described by the mathematically convenient linear spring-viscous damper representation over a wide frequency range. The behavior of rubber-like materials is particularly different than that described by the conventional model. To establish suitable mathematical descriptions of the various damping forces for tires and other elements of this study, several models were explored. Figure A38 depicts the two types of elastic systems which are used. The Type 1 model is a conventional system with viscous damping and Type 2 is a visco-elastic system, having elasticity and damping which varies with frequency. To compare the two, consider the effects of driving each with a variable force F(t) = Fo $\cos \omega t$. In each case, the resultant deflection is $x = x_0 \cos(\omega t - \varphi)$

The loss coefficient, β, is defined by $\beta = \tan\varphi$. For a conventional system (Type 1 with c and k constant), the loss coefficient which is a measure of the damping is

given by:

$$(4a.29)\quad \beta = c\omega/k$$

Reference 1 assumes that c is of the form $c = \eta\, k/\omega$ where η and k are constant. From this:

$$(4a.30)\quad \beta = \eta$$

Reference 8 seems to indicate (p. 55) that the loss coefficient for tire tread rubber is somewhere between the above two values.

For the Type 2 system, shown in Figure constant, the loss coefficient is given by:

$$(4a.31)\quad \beta = \left(\frac{c\omega}{k}\right) \Big/ \left(1 + \left(\frac{c\omega}{n}\right)^2 \left(1 + \frac{n}{k}\right)\right)$$

To represent a tire, the values $(c/k) = 1.56 \times 10^{-3}$ sec. and $(n/k) = 0.520$, were used to compute values of β for a range of frequencies. β versus ω is shown in Figure A39 for both Type 1 and Type 2 models, along with values of β taken from References 1 and 8. The value from Reference 1 is shown constant at all frequencies because the value is not identified with any frequency. The above values of (c/k) and (n/k) were chosen because they gave β values in best agreement with authoritative data.

Figure A39 shows both Type 1 and Type 2 models have relatively poor correlation with both data sources. Reference 8 indicates β is highly dependent upon temperature and tire rubber compound as might be expected. During damping model exploration, both Type 1 and Type 2 systems were examined dynamically on an analog computer. It was found that differences in their behavior were observable; however, since the damping forces are relatively small compared to the other forces, this difference was small. Either model is equally satisfactory for evaluating anti-skid operation. The Type 2 system is used for the tire because it is in closer agreement with recorded observations. The peak in the β versus frequency curve for the Type 2 system is in keeping with most of the contour plots for rubber-like materials as shown in Reference 7 and 8.

The tire elastic and damping coefficients are:

$$(4a.32)\quad \begin{cases} D_{TT} = (1.56\times10^{-3})\,C_{TT} = 15.9 \text{ lb sec/in} \\ E_{TT} = (.52)\,C_{TT} = 5300 \text{ lb/in} \\ D_{RT} = (1.56\times10^{-3})\,C_{RT} = 30{,}400 \text{ in lb sec/rad} \\ E_{RT} = (.52)\,C_{RT} = 10.15\times10^{6} \text{ in lb/rad} \end{cases}$$

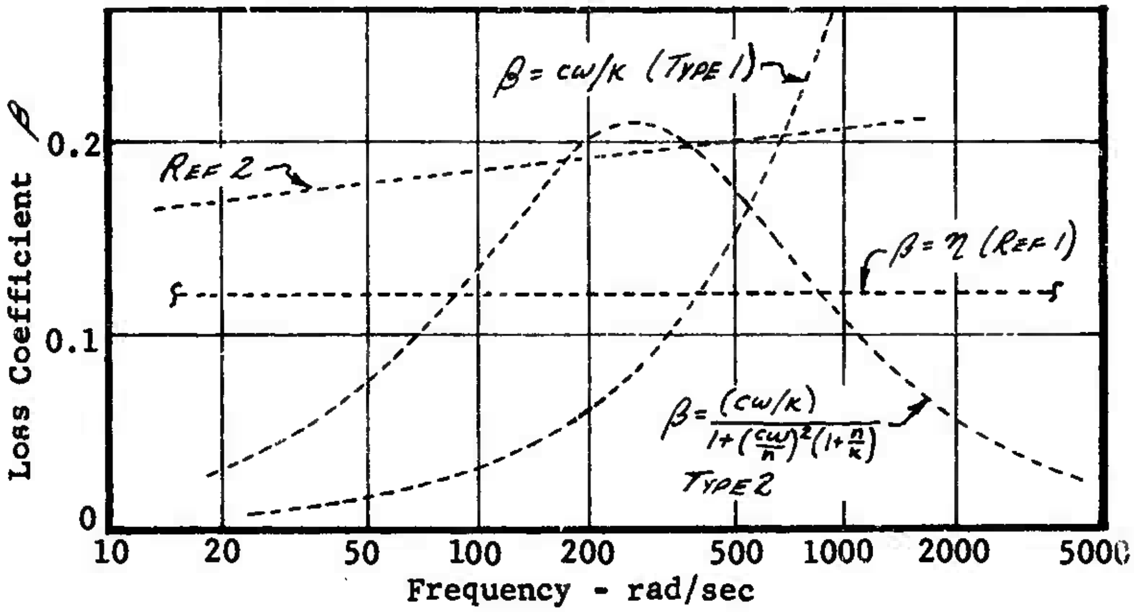

Figure A39 Model Loss Factors

The equation (4a.16) for the rolling radius R_T is a restatement of equation (76 b) of Reference 1. To allow for circumferential decay length other than those equal to the outside free tire radius, a coefficient U_{RR} is provided. For this study U_{RR} is set equal to 1.0.

Axle Parameters

The observed torsional natural frequency of the axle (with brake stators) is 125 cps. The calculated value for its moment of inertia is 16.8 LBF SEC^2/IN. Thus, the torsional spring rate, C_{RS}, is established as:

$$(4a.33)\quad C_{RS} = (2\pi\,125)^2(16.8) = 10.4\times10^{6} \text{ in lb/rad}$$

For the steel axle, a value for η (in the Type 1 system in Figure 38) is probably something less than .01 (Reference 7). Thus, at resonance, if $c\omega/k = \eta$, then the damping coefficient is established as:

$$(4a.34)\quad D_{RS} = k\eta/\omega = (10.4\times10^{6})(.01)/(2\pi125) = 132 \text{ in lb sec/rad}$$

Tire Rolling Resistance

From Figure 17a of Reference 2, the rolling resistance coefficient, μ_r is given by $\mu_r = .012 + 1 \times 10^{-5} v$ where v is the axle speed in INCHES/SEC. Thus,

$$(4a.35)\quad T_{RR} = \mu_r F_{RR} R_T = (.012 + 1 \times 10^{-5} V) F_{RR} R_T$$

Or alternately, $= (.012 + 1 \times 10^{-5} \dot{\theta}_T R_T)(F_{RR}/\delta)(\delta) R_T$

Since $F_{RR}/\delta = C_{MT}$, the rolling resistance coefficients are established as:

$$(4a.36)\quad D_{SR} = .012\, C_{MT} R_T = (.012)(9530)(20.57) = 2350 \text{ lb}$$

$$(4a.37)\quad D_{VR} = 1 \times 10^{-5} C_{MT} R_T^2 = (9530 \times 10^{-5})(20.57)^2 = 40.3 \text{ lb sec}$$

Figure A40 shows the friction coefficient for a tire sliding (i.e. full skid) on a dry concrete runway as a function of velocity. This data is taken from Reference 3 and is applicable to a typical runway contaminated with rubber deposits from previous airplane operations. Table A9 below lists the appropriate coefficients for equation (4a.22) which apply for dry and wet runway surface conditions.

Table A9 Runway Friction Characteristics

SYMBOL	UNITS	WET CONCRETE	DRY CONCRETE
u_{T1}	-----	.050	.200
u_{T2}	-----	.180	.450
E_T	SEC/IN	$.065 \times 10^{-3}$	$.065 \times 10^{-3}$
α	SEC/IN	1.0×10^{-3}	2.5×10^{-3}

Initial Conditions

All initial conditions, except wheel and tire rotational speed, will be set to zero. From the airplane system at time = 0, $V_F = 2400$ and $S_M = 2.245$. Using equation (4a.16) results in:

$$(4a.38)\quad R_T = R_{\theta T} - \tfrac{1}{3} S_M = 23.32 - \tfrac{1}{3}(2.245) = 22.67 \text{ in}$$

In order that V_R be zero, equations (4a.18) and (4a.19) show that:

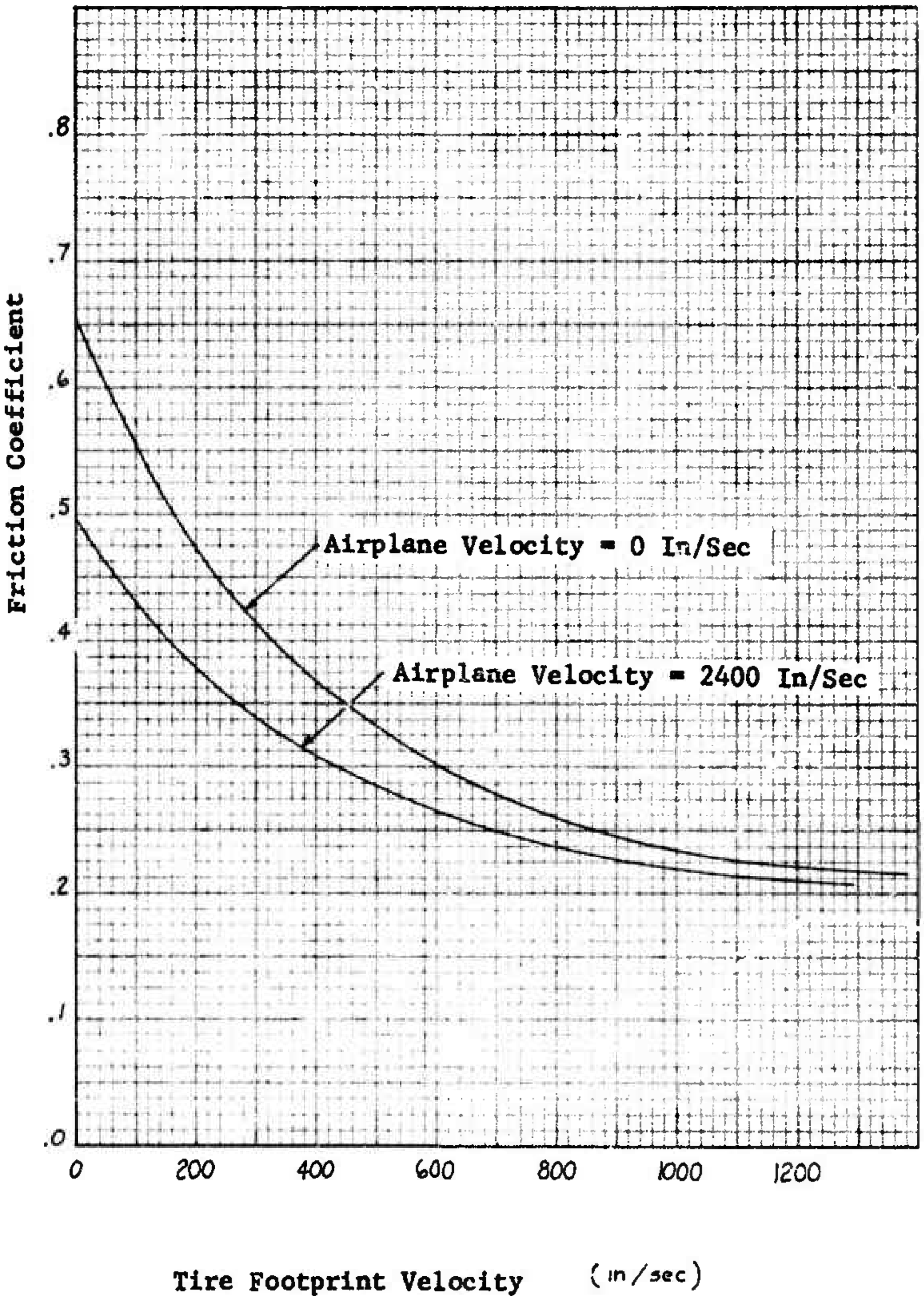

Figure A40 Tire Sliding Friction Coefficient

(4a.39) $\dot{\Theta}_{To} = \dot{\Theta}_{Wo} = V_F / R_T = 2400/22.67 = 105.9$ rad/sec

Table A10 Wheel and Tire System (Flywheel) Parameters (Sheet 1 of 4)

SYMBOL	TYPE	VALUE	UNITS	DESCRIPTION
α	c	2.5×10^{-3}	sec/in	Tire Friction Parameter
C_{GH}	c	3/500	lb/in	Fore and Aft Spring Rate at Axle
C_{RS}	c	10.4×10^{6}	in lb/rad	Axle Rotational Spring Rate
C_{RT}	c	19.5×10^{6}	in lb/rad	Tire to Wheel Rotational Spring Rate
C_{HY}	c	0.0	–	Controls Hydroplaning Influence
C_{TT}	c	10,200	lb/in	Tread to Wheel Spring Rate
D_{GH}	c	13.8	lb sec/in	Fore and Aft Damping Coefficient at Axle
D_{HY}	c	0.0	lb sec^2/in^2	Water Resistance Coefficient
D_{RS}	c	132.0	in lb sec/rad	Gear to Axle Rotational Damping Coefficient
D_{RT}	c	30,400	in lb sec/rad	Tire to Wheel Rotational Damping Coefficient
D_{SR}	c	2350	lb	Rolling Resistance Parameter
D_{TT}	c	15.9	lb sec/in	Tread to Wheel Damping Coefficient
D_{VR}	c	40.3	lb sec/rad	Rolling Resistance Parameter
E_{RT}	c	10.15×10^{6}	in lb/rad	Tire to Wheel Coupling Spring Rate
E_{T}	c	$.65 \times 10^{-4}$	sec/in	Tire Friction Correction Coeff.
E_{TT}	c	5300	lb/in	Tread to Wheel Coupling Spring Rate
F_{BT}	v(o)		lb	Horizontal Force on Tire Foot-print from Ground
F_{G}	v		lb	Horizontal Force at Axle
$F_{\theta RH}$	v		lb	Horizontal Wheel Unbalance Force
$F_{\theta RV}$	v(o)		lb	Vertical Wheel Unbalance Force
F_{NM}	v(I)		lb	Vertical Force between Time and Ground
F_{NMF}	v		lb	Vertical Force not Supported by Water Film

Table A10 Wheel and Tire System (Flywheel) Parameters (Sheet 2 of 4)

SYMBOL	TYPE	VALUE	UNITS	DESCRIPTION
F_{TT}	v		lb	Net Force Between Tread & Wheel
H_T	v		in	Axle Height Above Ground ($H_T \le R_{\theta T}$)
θ_S	v		rad	Axle Rotation
θ_{SO}	c	0.0	rad	Axle Rotation at Time = 0
$\dot{\theta}_S$	v		rad/sec	Axle Rotational Speed
$\dot{\theta}_{SO}$	c	0.0	rad/sec	Axle Rotational Speed at Time = 0
$\ddot{\theta}_S$	v		rad/sec^2	Axle Rotational Acceleration
θ_T	v		rad	Tire Tread Rotation
θ_{TO}	c	0.0	rad	Tire Tread Rotation at Time = 0
$\dot{\theta}_T$	v		rad/sec	Tire Tread Rotational Speed
$\dot{\theta}_{TO}$	c	105.9	rad/sec	Tire Tread Rotational Speed at Time = 0
$\ddot{\theta}_T$	v		rad/sec^2	Tire Tread Rotational Acceleration
θ_W	v		rad	Wheel Rotation
θ_{WO}	c	0.0	rad	Wheel Rotation at Time = 0
$\dot{\theta}_W$	v		rad/sec	Wheel Rotational Speed
$\dot{\theta}_{WO}$	c	105.9	rad/sec	Wheel Rotational Speed at Time = 0
$\ddot{\theta}_W$	v		rad/sec^2	Wheel Rotational Acceleration
θ_Y	v		rad	Dummy Variables used to
θ_{YO}	c	0.0	rad	Simulate Visco-elastic Tire
$\dot{\theta}_Y$	v		rad/sec	Characteristic
R_{KO}	c	0.0	lb sec^2/rad^2	Unbalance Coefficient
$R_{\theta T}$	c	23.32	in	Undeflected Tire Radius
R_T	v		in	Tire Rolling Radius
S_M	v(I)		in	Tire Deflection
T_{BT}	v(I)		in lb	Brake Torque

Table A10 Wheel and Tire System (Flywheel) Parameters (Sheet 3 of 4)

SYMBOL	TYPE	VALUE	UNITS	DESCRIPTION
T_{RR}	v		in lb	Torque Producing Rolling Resistance
T_{RT}	v		in lb	Torque between Tire (Tread) and Wheel
T_S	v		in lb	Axle Torque
U_{RR}	c	1.0	–	Rolling Radius Parameter
U_T	v		–	Tire Friction Coefficient
U_{T1}	c	.20	–	Tire Friction Parameters
U_{T2}	c	.45	–	
V_F	v(I)		in/sec	Flywheel Surface Velocity
V_{HY}	c	2400	in/sec	Tire Hydroplaning Speed
V_R	v		in/sec	Velocity of Tire Footprint Relative to Flywheel
V_{RS}	v		in/sec	Same as V_R except Rotational Effects Ignored
W_B	v(o)		rad/sec	Relative Rotational Speed Between Stators and Rotors
W_{EW}	c	1.60	lb sec²/in	Effective Tire, Wheel, and Brake Mass
W_{IS}	c	16.8	in lb sec²/rad	Axle Moment of Inertia (+ Stators)
W_{IT}	c	115.0	in lb sec²/rad	Tread Moment of Inertia
W_{IW}	c	66.0	in lb sec²/rad	Wheel & Rotors Moment of Inertia
W_S	v		rad/sec	$W_S = \dot{\theta}_S$
W_T	v		rad/sec	$W_T = \dot{\theta}_T$
W_{TE}	c	.0725	lb sec²/in	Equivalent Tire Tread Mass
W_W	v		rad/sec	$W_W = \dot{\theta}_W$
X_{TT}	v		in	Location of Tire Tread C.G.
X_{TTO}	c	0.0	in	Location of Tire Tread C.G. at Time = 0

Table A10 Wheel and Tire System (Flywheel) Parameters (Sheet 4 of 4)

SYMBOL	TYPE	VALUE	UNITS	DESCRIPTION
$\dot{X}_{TT}$	v		IN/SEC	Tread CG Velocity
$\dot{X}_{TTO}$	c	0.0	IN/SEC	Tread CG Velocity at Time = 0
$\ddot{X}_{TT}$	v		IN/SEC^2	Tread CG Acceleration
X_W	v		IN	Horizontal Axle Location
X_{WO}	c	0.0	IN	Horizontal Axle Location at Time = 0
$\dot{X}_W$	v		IN/SEC	Horizontal Axle Velocity
$\dot{X}_{WO}$	c	0.0	IN/SEC	Horizontal Axle Velocity at Time = 0
$\ddot{X}_W$	v		IN/SEC^2	Horizontal Axle Acceleration
X_Y	v		IN	Dummy Variables Used to
X_{YO}	c	0.0	IN	Simulate Visco-elastic Tire
$\dot{X}_Y$	v		IN/SEC	Characteristic
D_{TRV}	c	9500	IN LBF SEC/RAD	Tire Tread Radial Damping Coeff
D_{TRL}	c	5.45	LBF SEC/IN	Tire Tread Longitudinal Damping Coeff
V_{RO}	c	25.0	IN/SEC	Tire Friction Threshold Velocity

4b. WHEEL AND TIRE SYSTEM (3 DEGREE)

Figure A41 shows the components of the wheel and tire system. The wheel and tire system

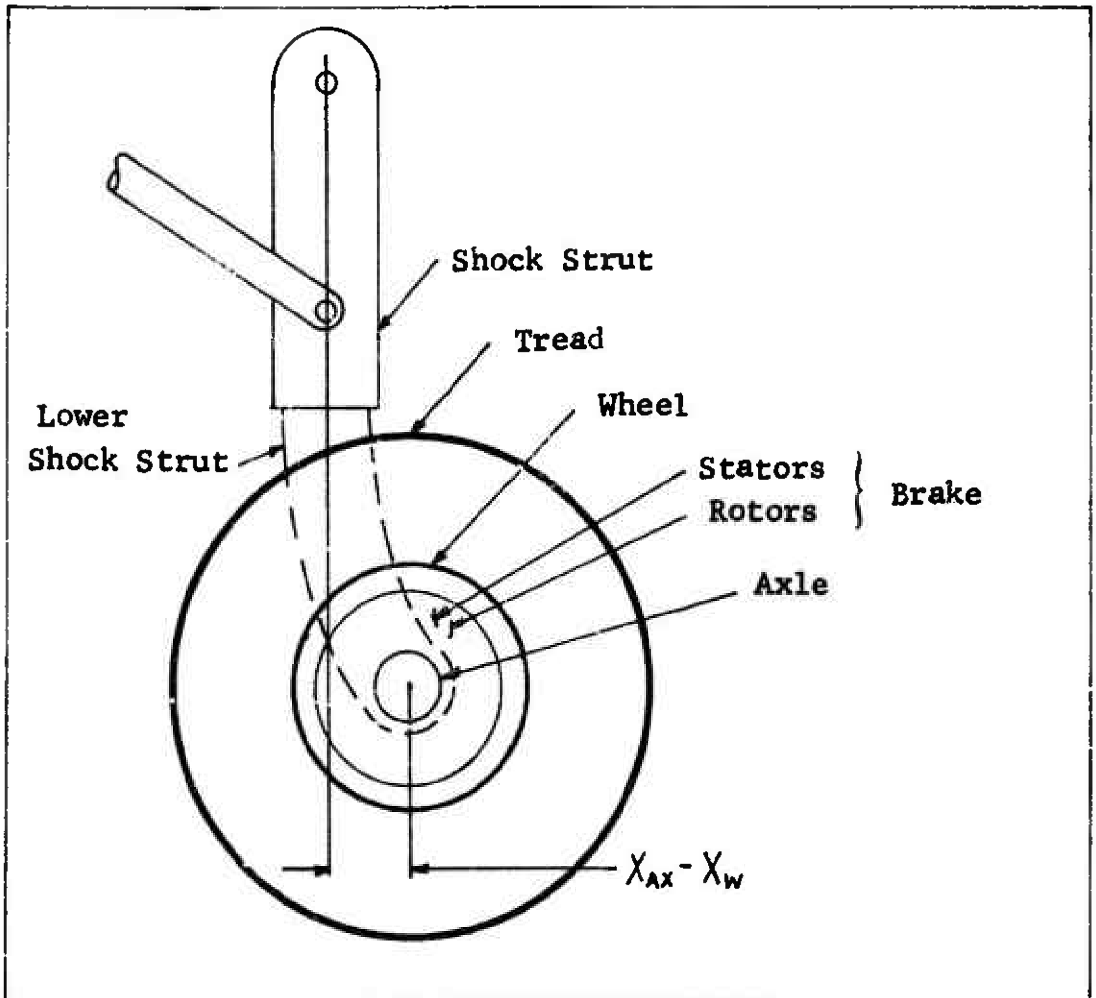

Figure A41 Components of the Wheel and Tire System

for the 3 degree airplane system is essentially the same as for the flywheel model. The Airplane System still furnishes the tire deflection S_M and the tire vertical load F_{NM} . The ground speed, however, is no longer furnished by the Airplane System, but is found by summing forces on the tire, wheel, brake, and axle mass. The horizontal force exerted on the axle by the airplane is calculated by obtaining the translational (X_{AX}) and rotational (θ_G) gear positions from the Airplane System.

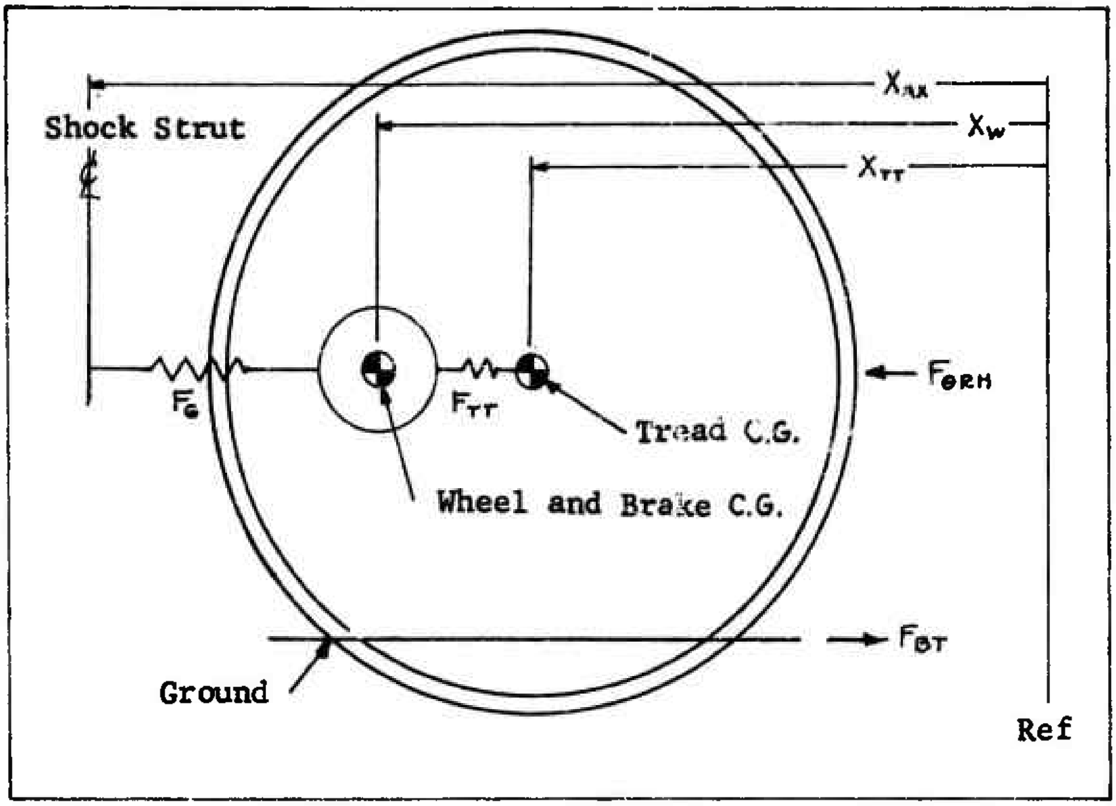

Figure A42 Tire Horizontal Model

Referring to Figure A42 equation (4a.1) in the flywheel system changes to

(4b.1) $F_G = C_G(X_{AX} - X_W) + D_G(\dot{X}_{AX} - \dot{X}_W)$

Equations (4b.2) through (4b.9) are listed for completeness, although they are the same as (4a.2) through (4a.9).

(4b.2) $F_{TT} = C_{TT}(X_{TT} - X_W) + E_{TT}(X_{TT} - X_Y) + D_{TLV}(\dot{X}_{TT} - \dot{X}_W)$

(4b.3) $D_{TT}(\dot{X}_Y - \dot{X}_W) = E_{TT}(X_{TT} - X_Y)$

(4b.4) $W_{GW}\ddot{X}_W = F_G + F_{TT}$

(4b.5) $W_{TE}\ddot{X}_{TT} = -F_{TT} - F_{BT} + F_{\theta RH}$

(4b.6) $F_{\theta RH} = R_{K\theta} W_T^2 \sin\langle\theta_T\rangle$

(4b.7) $F_{\theta RV} = R_{K\theta} W_T^2 \cos\langle\theta_T\rangle$

Figure A43 shows the rotational model of the wheel, tire, axle, and lower strut with the gear rotation Θ_G added. Including the effect of Θ_G there follows:

$$(4b.8)\quad T_{RT} = C_{RT}(\Theta_W - \Theta_T) + E_{RT}(\Theta_W - \Theta_Y) + D_{TRV}(\dot{\Theta}_W - \dot{\Theta}_T)$$

$$(4b.9)\quad D_{RT}(\dot{\Theta}_Y - \dot{\Theta}_T) = E_{RT}(\Theta_W - \Theta_Y)$$

$$(4b.10)\quad T_S = C_{RS}(\Theta_S + \Theta_G) + D_{RS}(\dot{\Theta}_S + \dot{\Theta}_G)$$

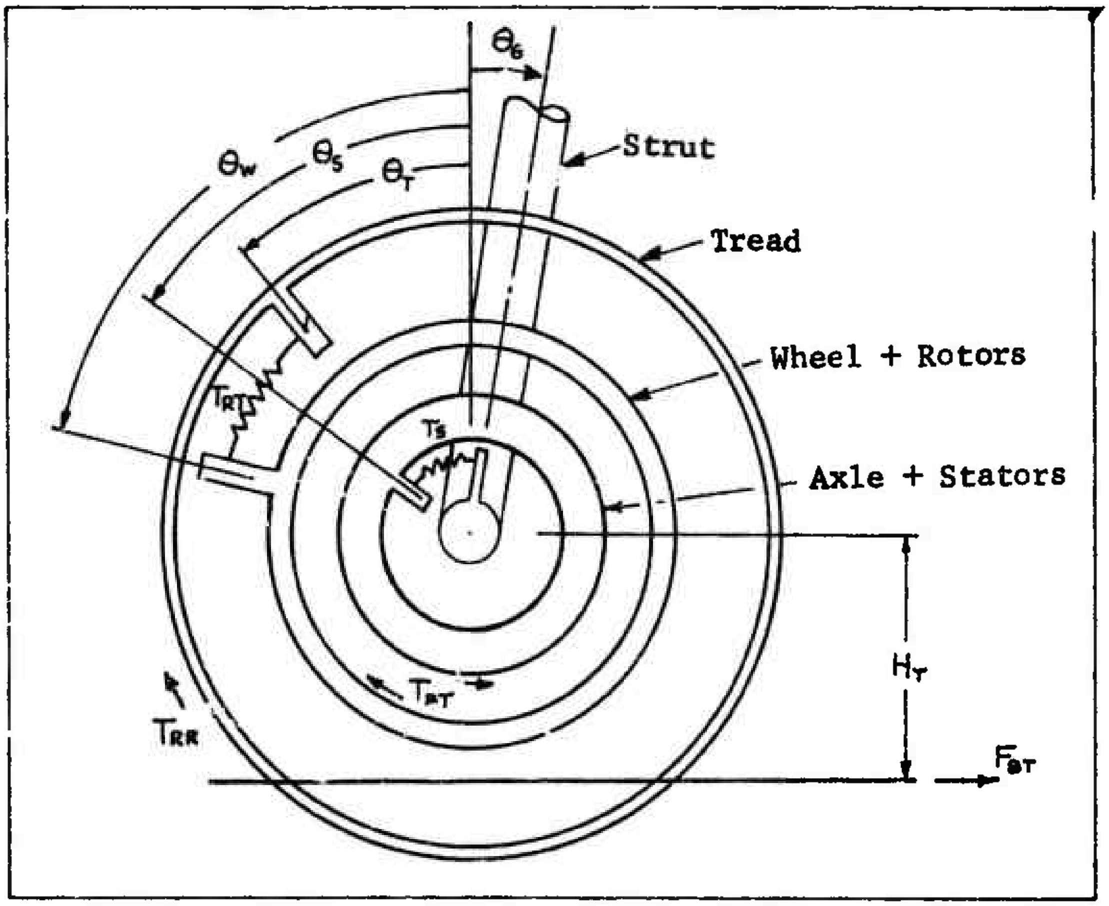

Figure A43 Tire Rotational Model

Equations (4b.11) through (4b.16) are the same as (4a.11) through (4a.16).

$$(4b.11)\quad H_T = R_{OT} - S_M$$

$$(4b.12)\quad T_{RR} = \begin{cases} S_M(D_{SR} + D_{VR}W_T) & \text{if } W_T > 0 \\ 0 & \text{if } W_T = 0 \\ S_M(-D_{SR} + D_{VR}W_T) & \text{if } W_T < 0 \end{cases}$$

$$(4b.13)\quad W_{IS}\ddot{\theta}_S = T_{BT} - T_S$$

$$(4b.14)\quad W_{IW}\ddot{\theta}_W = -T_{RT} - T_{BT}$$

$$(4b.15)\quad W_{IT}\ddot{\theta}_T = H_T F_{BT} + T_{RT} - T_{RR}$$

$$(4b.16)\quad R_T = R_{BT} - \tfrac{1}{3} S_M - U_{RR}(X_{TT} - X_W)$$

Because the ground is now stationary equation (4a.17) becomes

$$(4b.17)\quad V_{RS} = \dot{X}_{TT}$$

The remaining equations are unchanged except for noting that the outputs X_{WM} and $\dot{X}_{WM}$ required for the Airplane System are obtained by renaming X_{TT}. Thus $X_{WM} = X_{TT}$ and $\dot{X}_{WM} = \dot{X}_{TT}$. Continuing,

$$(4b.18)\quad V_R = V_{RS} - R_T W_T \qquad (\text{WHERE } W_T = \dot{\theta}_T)$$

$$(4b.19)\quad W_B = W_W - W_S$$

$$(4b.20)\quad F_{NMF} = F_{NM}\left(1 - C_{HY}(V_{RS}/V_{HY})^2\right)$$

$$(4b.21)\quad F_{BT} = F_{NMF} U_T + D_{HY} V_{RS}^2$$

$$(4b.22)\quad U_T = \begin{cases} \mu_{T1} + (\mu_{T2} - E_T V_{RS})e^{-\alpha V_R} & \text{if } V_R > V_{R0} \\ \left\{\left[\mu_{T1} + (\mu_{T2} - E_T V_{RS})e^{-\alpha V_{R0}}\right] 1/V_{R0}\right\} V_R & \text{if } V_{R0} > V_R > -V_{R0} \\ -\mu_{T1} - (\mu_{T2} - E_T V_{RS})e^{\alpha V_R} & \text{if } V_R < -V_{R0} \end{cases}$$

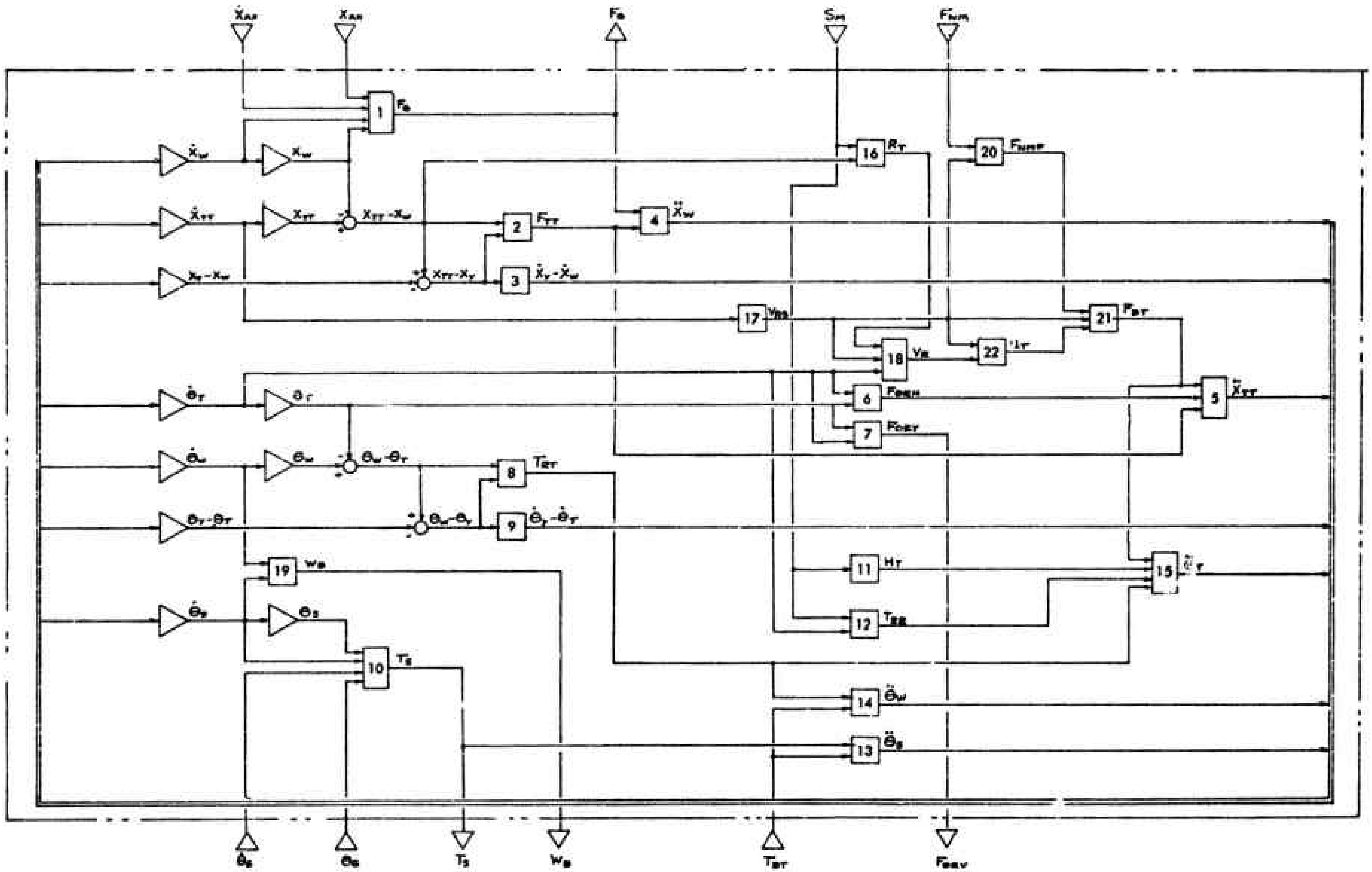

Figure A44 Wheel and Tire System (3 Degree) Equation Flow Diagram

B. Parameter Evaluation

The parameter values for this system are essentially the same as for the wheel and tire system that corresponds to the flywheel system. One difference is the values for C_G and D_G which are derived in the Airplane System (3 degree). These values are

$$(4b.23) \quad \begin{cases} C_G = 200{,}000 \text{ lb/in} \\ D_G = 78.6 \text{ lb sec/in} \end{cases}$$

Since this system moves with the airplane the initial conditions should match the Airplane model. Thus

$$(4b.24) \quad \begin{cases} X_{TTO} = 0.774 \text{ in} \\ \dot{X}_{TTO} = 2400 \text{ in/sec} \end{cases}$$

$$(4b.25) \quad \begin{cases} X_{WO} = 0.774 \text{ in} \\ \dot{X}_{WO} = 2400 \text{ in/sec} \end{cases}$$

From equation (4b.16)

$$(4b.26) \quad R_T = R_{eT} - \tfrac{1}{3} S_M = 23.32 - .80 = 22.52 \text{ IN}$$

Thus for a "spun up" tire, we have from equation (18)

$$(4b.27) \quad W_T = V_{RS}/R_T = 2400/22.52 = 106.7 \text{ rad/sec}$$

Then

$$(4b.28) \quad \dot{\theta}_{TO} = \dot{\theta}_{WO} = 106.7 \text{ rad/sec}$$

Also from equation (10), choose θ_{SO} so that zero torque is produced.

$$(4b.29) \quad \theta_{SO} = \theta_{GO} = .0329 \text{ rad/sec}$$

Table A11 Wheel and Tire System (3 Degree) Parameters (Sheet 1 of 4)

SYMBOL	TYPE	VALUE	UNITS	DESCRIPTION
α	c	2.5×10^{-3}	sec/in	Tire Friction Parameter
C_G	c	2.0×10^{5}	lb/in	Fore and Aft Spring Rate at Axle
C_{RS}	c	10.4×10^{6}	in lb/rad	Axle Rotational Spring Rate
C_{RT}	c	19.5×10^{6}	in lb/rad	Tire to Wheel Rotational Spring Rate
C_{HY}	c	0.0	—	Controls Hydroplanning Influence
C_{TT}	c	10,200	lb/in	Tread to Wheel Spring Rate
D_G	c	78.6	lb sec/in	Fore and Aft Damping Coeff. at Axle
D_{HY}	c	0.0	lb sec²/in²	Water Resistance Coeff.
D_{RS}	c	132	in lb sec/rad	Gear To Axle Rotational Damping Coeff.
D_{RT}	c	30,400	in lb sec/rad	Tire to Wheel Rotational Damping Coeff.
D_{SR}	c	2350	lb	Rolling Resistance Parameter
D_{TT}	c	15.9	lb sec/in	Tread to Wheel Damping Coeff.
D_{VR}	c	40.3	lb sec/rad	Rolling Resistance Parameter
E_{RT}	c	10.15×10^{6}	in lb/rad	Tire to Wheel Coupling Spring Rate
E_T	c	$.65\times10^{-4}$	sec/in	Tire Friction Correction Coeff.
E_{TT}	c	5300	lb/in	Tread to Wheel Coupling Spring Rate
F_{BT}	v		lb	Horizontal Force on Tire Footprint from Ground
F_G	v(o)		lb	Horizontal Force at Axle
$F_{\theta RH}$	v		lb	Horizontal Wheel Unbalance Force
$F_{\theta RV}$	v(o)		lb	Vertical Wheel Unbalance Force
F_{NM}	v(i)		lb	Vertical Force Between Tire and Ground
F_{NMF}	v		lb	Vertical Force Not Supported by Water Film
F_{TT}	v		lb	Net Force Between Tread and Wheel

Table A11 Wheel and Tire System (3 Degree) Parameters (Sheet 2 of 4)

SYMBOL	TYPE	VALUE	UNITS	DESCRIPTION
H_T	v		in	Axle Height Above Ground ($H_T \leq R_{\theta T}$)
θ_s	v		rad	Axle Rotation
θ_{so}	c	.0329	rad	Axle Rotation at Time = 0
$\dot{\theta}_s$	v		rad/sec	Axle Rotational Speed
$\dot{\theta}_{so}$	c	0.0	rad/sec	Axle Rotational Speed at Time = 0
$\ddot{\theta}_s$	v		rad/sec^2	Axle Rotational Acceleration
θ_T	v		rad	Tire Tread Rotation
θ_{TO}	c	0.0	rad	Tire Tread Rotation at Time = 0
$\dot{\theta}_T$	v		rad/sec	Tire Tread Rotational Speed
$\dot{\theta}_{TO}$	c	106.7	rad/sec	Tire Tread Rotational Speed at Time = 0
$\ddot{\theta}_T$	v		rad/sec^2	Tire Tread Rotational Acceleration
θ_W	v		rad	Wheel Rotation
θ_{WO}	c	0.0	rad	Wheel Rotation at Time = 0
$\dot{\theta}_W$	v		rad/sec	Wheel Rotational Speed
$\dot{\theta}_{WO}$	c	106.7	rad/sec	Wheel Rotational Speed at Time = 0
$\ddot{\theta}_W$	v		rad/sec^2	Wheel Rotational Acceleration
θ_Y	v		rad	Dummy Variables Used to
θ_{YO}	c	0.0	rad	Simulate Visco-Elastic Tire
$\dot{\theta}_Y$	v		rad/sec	Characteristic.
$R_{K\theta}$	c	0.0	lb sec^2/rad^2	Unbalance Coeff.
$R_{\theta T}$	c	23.32	in	Undeflected Tire Radius
R_T	v		in	Tire Rolling Radius
S_n	v(i)		in	Tire Deflection

Table All Wheel and Tire System (3 Degree) Parameters (Sheet 3 of 4)

SYMBOL	TYPE	VALUE	UNITS	DESCRIPTION
T_{BT}	v(i)		in lb	Brake Torque
T_{RE}	v		in lb	Torque Producing Rolling Resistance
T_{RT}	v		in lb	Torque Between Tire (Tread) and Wheel
T_S	v(o)		in lb	Axle Torque
U_{ER}	c	1.0	—	Rolling Radius Parameter
U_T	v		—	Tire Friction Coefficient
U_{T1}	c	.20	—	Tire Friction Parameters
U_{T2}	c	.45	—	
V_{HY}	c	2400	in/sec	Tire Hydroplanning Speed
V_R	v		in/sec	Velocity of Tire Footprint Relative to Flywheel
V_{ES}	v		in/sec	Same as V_R except Rotational Effects Ignored
W_B	v(o)		rad/sec	Relating Rotational Speed Between Stators & Rotors
W_{GW}	c	1.6	$lb\ sec^2/in$	Effective Tire, Wheel, & Brake Mass
W_{IS}	c	16.8	$in\ lb\ sec^2/rad$	Axle Moment of Inertia (+ Stators)
W_{IT}	c	115.0	$in\ lb\ sec^2/rad$	Tread Moment of Inertia
W_{IW}	c	66.0	$in\ lb\ sec^2/rad$	Wheel and Rotors Moment of Inertia
W_S	v		rad/sec	$W_S = \dot{\theta}_S$
W_T	v		rad/sec	$W_T = \dot{\theta}_T$
W_{TE}	c	.0725	$lb\ sec^2/in$	Equivalent Tire Tread Mass
W_W	v		rad/sec	$W_W = \dot{\theta}_W$
X_{TT}	v		in	Location of Tire Tread C.G.
X_{TTO}	c	0.774	in	Location of Tire Tread C.G. at Time = 0

Table A11 Wheel and Tire System (3 Degree) Parameters (Sheet 4 of 4)

SYMBOL	TYPE	VALUE	UNITS	DESCRIPTION
$\dot{X}_{TT}$	v		in/sec	Tread C.G. Velocity
$\dot{X}_{TTO}$	c	2400	in/sec	Tread C.G. Velocity at Time = 0
$\ddot{X}_{TT}$	v		in/sec^2	Tread C.G. Acceleration
X_W	v		in	Horizontal Axle Location
X_{WO}	c	0.774	in	Horizontal Axle Location at Time = 0
$\dot{X}_W$	v		in/sec	Horizontal Axle Velocity
$\dot{X}_{WO}$	c	2400	in/sec	Horizontal Axle Velocity at Time = 0
$\ddot{X}_W$	v		in/sec^2	Horizontal Axle Acceleration
X_Y	v		in	Dummy Variables Used to
X_{YO}	c	0.0	in	Simulate Visco-Elastic Tire
$\dot{X}_Y$	v		in/sec	Characteristic.
θ_G	v(i)		rad	Gear Rotation
$\dot{\theta}_G$	v(i)		rad/sec	Gear Rotational Velocity
X_{AX}	v(i)		in	Undeflected Axle Position
$\dot{X}_{AX}$	v(i)		in/sec	Undeflected Axle Velocity
X_{WM}	v(o)		in	Footprint Location (x Direction)
$\dot{X}_{WM}$	v(o)		in/sec	Footprint Velocity (x Direction)
D_{TRV}	c	9500	IN LBF SEC/RAD	Tire Tread Radial Damping Coeff.
D_{TLV}	c	5.45	LBF SEC/IN	Tire Tread Longitudinal Damping Coeff.
V_{RO}	c	25.0	IN/SEC	Tire Friction Threshold Velocity

4c. TIRE AND WHEEL SYSTEM (6 DEGREE)

The wheel and tire system for the six degree problem is the same as that described in the three degree system except for inclusion of the lateral mode. Equations (4c.1) through (4c.17) are the same as (4b.1) through (4b.17) in the three degree system.

A. Mathematical Description

(4c.1) $F_G = C_G(X_{AX} - X_W) + D_G(\dot{X}_{AX} - \dot{X}_W)$

(4c.2) $F_{TT} = C_{TT}(X_{TT} - X_W) + E_{TT}(X_{TT} - X_Y) + D_{TLV}(\dot{X}_{TT} - \dot{X}_W)$

(4c.3) $D_{TT}(\dot{X}_Y - \dot{X}_W) = E_{TT}(X_{TT} - X_Y)$

(4c.4) $W_{GW}\ddot{X}_W = F_G + F_{TT}$

(4c.5) $W_{TE}\ddot{X}_{TT} = -F_{TT} - F_{BT} + F_{ORH}$

(4c.6) $F_{ORH} = R_{KO} W_T^2 \sin\langle\theta_T\rangle$

(4c.7) $F_{ORV} = R_{KO} W_T^2 \cos\langle\theta_T\rangle$

(4c.8) $T_{RT} = C_{RT}(\theta_W - \theta_T) + E_{RT}(\theta_W - \theta_Y) + D_{TRV}(\dot{\theta}_W - \dot{\theta}_T)$

(4c.9) $D_{RT}(\dot{\theta}_Y - \dot{\theta}_T) = E_{RT}(\theta_W - \theta_Y)$

(4c.10) $T_S = C_{RS}(\theta_S - \theta_G) + D_{RS}(\dot{\theta}_S - \dot{\theta}_G)$

(4c.11) $H_T = R_{OT} - S_M$

(4c.12) $T_{RR} = \begin{cases} S_M(D_{SR} + D_{VR}W_T) & \text{if } W_T > 0 \\ 0 & \text{if } W_T = 0 \\ S_M(-D_{SR} + D_{VR}W_T) & \text{if } W_T < 0 \end{cases}$

(4c.13) $W_{IS}\ddot{\theta}_S = T_{BT} - T_S$

(4c.14) $W_{IW}\ddot{\theta}_W = -T_{RT} - T_{BT}$

(4c.15) $W_{IT}\ddot{\theta}_T = H_T F_{BT} + T_{RT} - T_{RR}$

(4c.16) $R_T = R_{OT} - \frac{1}{3}S_M - U_{RR}(X_{TT} - X_W)$

(4c.17) $V_{RS} = \dot{X}_{TT} = \dot{X}_{WM}$ also $X_{WM} = X_{TT}$

Equation (4b.18) which gives the relative velocity between the footprint and the ground is changed to account for the lateral footprint velocity $\dot{Y}_M$.

$$(4c.18) \quad V_R = \sqrt{V_{RX}^2 + \dot{Y}_M^2}$$

Equations (4b.19) and (4b.20) are unchanged.

$$(4c.19) \quad W_B = W_W - W_S$$

$$(4c.20) \quad F_{NMF} = F_{NM}(1 - C_{HY}(V_{RS}/V_{HY})^2)$$

Now V_{RX} is the relative velocity in the x direction so

$$(4c.21) \quad V_{RX} = V_{RS} - R_T W_T$$

Thus, the angle β_T which defines the friction force direction as shown in Figure A45 is given by

$$(4c.22) \quad \beta_T = \tan^{-1}\langle \dot{Y}_M / V_{RX} \rangle$$

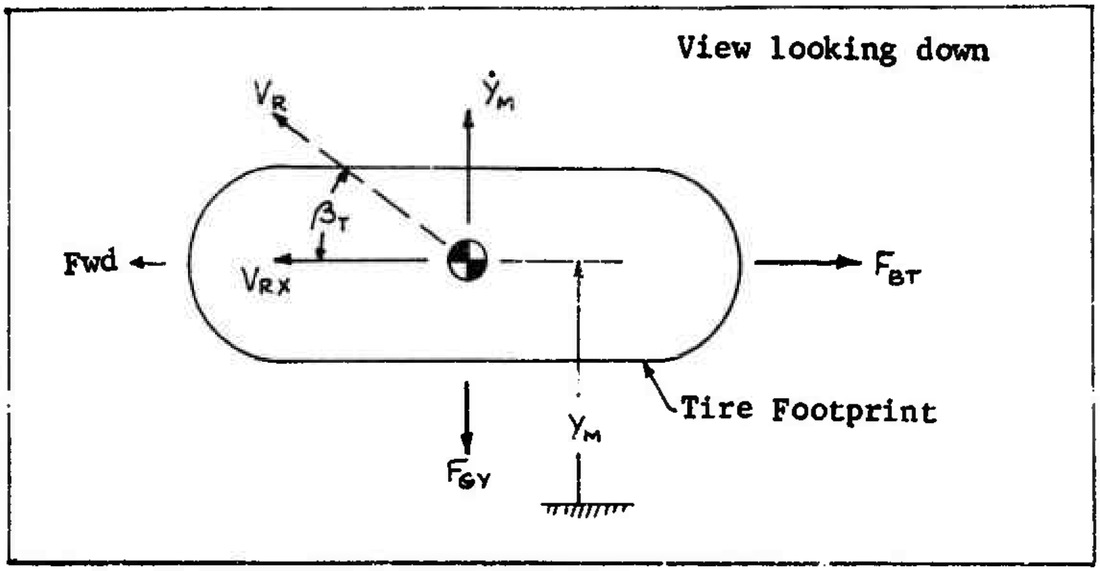

Figure A45 Footprint Friction Components

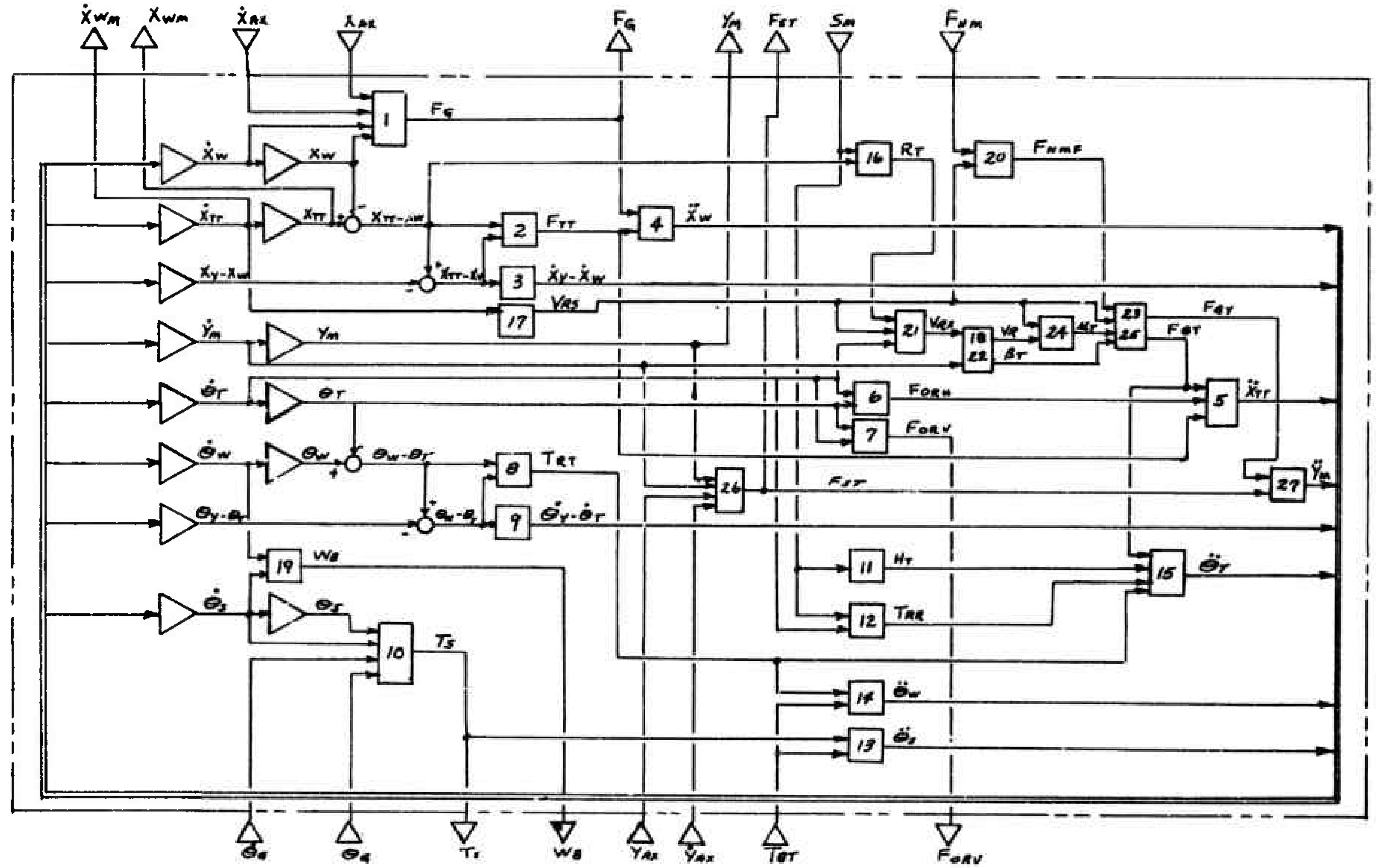

Figure A46 Wheel and Tire System (6 Degree) Equation Flow Diagram

Thus, F_{BT} is now given by

$$(4c.23)\quad F_{BT} = F_{NMF}\, U_T \cos\langle \beta_T \rangle + D_{KY} V_{RS}^2$$

and

$$(4c.24)\quad U_T = \begin{cases} \mu_{T1} + (\mu_{T2} - E_T V_{RS}) e^{-\alpha V_R} & \text{if } V_R > V_{R0} \\ \{[\mu_{T1} + (\mu_{T2} - E_T V_{RS}) e^{-\alpha V_{R0}}]\, 1/V_{R0}\} V_R & \text{if } V_{R0} > V_R \geq 0 \end{cases}$$

The lateral friction force F_{GY} is given by

$$(4c.25)\quad F_{GY} = F_{NMF}\, U_T \sin\langle \beta_T \rangle$$

The airplane produces a lateral position Y_{AX} of the axle. If Y_M is the lateral location of the footprint, then a lateral force F_{ST} is produced and

$$(4c.26)\quad F_{ST} = C_{ST}(Y_{AX} - Y_M) + D_{ST}(\dot{Y}_{AX} - \dot{Y}_M)$$

Finally, forces can be summed laterally on the footprint to obtain

$$(4c.27)\quad W_{TE}\, \ddot{Y}_M = F_{ST} - F_{GY}$$

B. Parameter Evaluation

<u>Wheel and Tire System Parameters</u>

Most of the parameter values were derived in the wheel and tire system that was used with the flywheel. The only addition is the evaluation of C_{ST} and D_{ST}.

From reference 1 (p.15)

$$(4c.28)\quad K_\lambda = \tau_\lambda w (P + .24 P_R)(1 - .7(\delta_0/w))$$

Assuming that δ_0 = 2.245 in., then

$$(4c.29)\quad C_{ST} = (2)(18)(1.24)(150)(1 - .7(2.245/18))$$

$$(4c.30)\quad C_{ST} = 6460 \text{ lb/in}$$

Using $\omega_n = \sqrt{K/m} = \sqrt{6460/.0725} = 298.4$

Using η = .1 (from page 50 of Ref. 1) results in

$$(4c.31)\quad D_{ST} = \eta C_{ST}/\omega_n = (.1)(6460)/298.4 = 2.165$$

Initial Conditions

The only difference between this and the three degree system is evaluating Y_{MO} and $\dot{Y}_{MO}$. It should be that $Y_{MO} = Y_{AX}(0)$ Since this system is used for both right and left sides, then Y_{MO} will differ. Assume that this system is used as the right wheel and tire. Then, $Y_{MO} = Y_{AXR}$ as in equation (4c.56). From this equation at Time = 0, (since R = P = 0), then

$$(4c.32)\quad Y_{MO} = Y_{AXR} = Y_0 + S_{GW} = 0 + 60 = 60 \text{ in}$$

Similarly

$$(4c.33\quad \dot{Y}_{MO} = \dot{Y}_{AXR} = \dot{Y}_0 = 0.0 \text{ in/sec}$$

Table A12 Wheel and Tire System (6 Degree) Parameters (Sheet 1 of 5)

SYMBOL	TYPE	VALUE	UNITS	DESCRIPTION
α	c	2.5×10^{-3}	sec/in	Tire Friction Parameter
β_T	v		rad	Tire Footprint Friction Angle
C_G	c	2.0×10^5	lb/in	Fore and Aft Spring Rate at Axle
C_{RS}	c	10.4×10^6	in lb/rad	Axle Rotational Spring Rate
C_{RT}	c	19.5×10^6	in lb/rad	Tire to Wheel Rotational Spring Rate
C_{HY}	c	0.0	–	Controls Hydroplaning influence
C_{ST}	c	6460	lb/in	Tire Lateral Spring Rate
C_{TT}	c	10,200	lb/in	Tread to Wheel Spring Rate
D_G	c	78.6	lb sec/in	Fore and Aft Damping Coefficient at Axle
D_{HY}	c	0.0	lb sec^2/in^2	Water Resistance Coefficient
D_{RS}	c	132	in lb sec/rad	Gear to Axle Rotational Damping Coeff.
D_{RT}	c	30,400	in lb sec/rad	Tire to Wheel Rotational Damping Coeff.
D_{SR}	c	2350	lb	Rolling Resistance Parameter
D_{ST}	c	2.165	lb sec/in	Tire Lateral Damping Coefficient
D_{TT}	c	15.9	lb sec/in	Tread to Wheel Damping Coefficient
D_{VR}	c	40.3	lb sec/rad	Rolling Resistance Parameter
E_{RT}	c	10.15×10^6	in lb/rad	Tire to Wheel Coupling Spring Rate
E_T	c	$.65 \times 10^{-4}$	sec/in	Tire Friction Correction Coefficient
E_{TT}	c	5300	lb/in	Tread to Wheel Coupling Spring Rate
F_{BT}	v		lb	Horizontal Force on Tire Footprint from Ground
F_G	v(o)		lb	Horizontal Force at Axle
F_{GY}	v		lb	Lateral Tire Load (On Ground)
F_{GRH}	v		lb	Horizontal Wheel Unbalance Force
F_{GRV}	v(o)		lb	Vertical Wheel Unbalance Force

Table A12 Wheel and Tire System (6 Degree) Parameters (Sheet 2 of 5)

SYMBOL	TYPE	VALUE	UNITS	DESCRIPTION
F_{NM}	v(I)		lb	Vertical Force between Tire and Ground
F_{NMF}	v		lb	Vertical Force not supported by Water Film
F_{ST}	v(o)		lb	Lateral Tire Load (On Apl)
F_{TT}	v		lb	Net Force between Tread and Wheel
H_T	v		in	Axle Height Above Ground
θ_G	v(I)		rad	Gear Rotation
$\dot{\theta}_G$	v(I)		rad/sec	Gear Rotational Velocity
θ_S	v		rad	Axle Rotation
θ_{SO}	c	-.0329	rad	Axle Rotation at Time = 0
$\dot{\theta}_S$	v		rad/sec	Axle Rotational Speed
$\dot{\theta}_{SO}$	c	0.0	rad/sec	Axle Rotational Speed at Time = 0
$\ddot{\theta}_S$	v		rad/sec^2	Axle Rotational Acceleration
θ_T	v		rad	Tire Tread Rotation
θ_{TO}	c	0.0	rad	Tire Tread Rotation at Time = 0
$\dot{\theta}_T$	v		rad/sec	Tire Tread Rotational Speed
$\dot{\theta}_{TO}$	c	106.7	rad/sec	Tire Tread Rotational Speed at Time = 0
$\ddot{\theta}_T$	v		rad/sec^2	Tire Tread Rotational Acceleration
θ_W	v		rad	Wheel Rotation
θ_{WO}	c	0.0		Wheel Rotation at Time = 0
$\dot{\theta}_W$	v		rad/sec	Wheel Rotational Speed
$\dot{\theta}_{WO}$	c	106.7	rad/sec	Wheel Rotational Speed at Time = 0
$\ddot{\theta}_W$	v		rad/sec^2	Wheel Rotational Acceleration
θ_Y	v		rad	Dummy Variables used to
θ_{YO}	c	0.0	rad	Simulate Visco-Elastic Tire
$\dot{\theta}_Y$	v		rad/sec	Characteristic

Table A12 Wheel and Tire System (6 Degree) Parameters (Sheet 3 of 5)

SYMBOL	TYPE	VALUE	UNITS	DESCRIPTION
$R_{K\theta}$	c	0.0	lb sec^2/rad^2	Unbalance Coefficient
$R_{\theta T}$	c	23.32	in	Undeflected Tire Radius
R_T	v		in	Tire Rolling Radius
S_M	v(I)		in	Tire Deflection
T_{BT}	v(I)		in lb	Brake Torque
T_{RR}	v		in lb	Torque Producing Rolling Resistance
T_{RT}	v		in lb	Torque Between Tire (Tread) and Wheel
T_S	v(o)		in lb	Axle Torque
U_{RR}	c	1.0	—	Rolling Radius Parameter
U_T	v		—	Tire Friction Coefficient
U_{T1}	c	.20	—	Tire Friction Parameters
U_{T2}	c	.45	—	
V_{HY}	c	2400	in/sec	Tire Hydroplanning Speed
V_R	v		in/sec	Velocity of Tire Footprint Relative to Flywheel
V_{RS}	v		in/sec	Same as Vrx except rotational effects ignored
V_{RX}	v		in/sec	Tire Footprint Relative Velocity in X Direction
W_B	v(o)		rad/sec	Relative Rotational Speed between Stators and Rotors
$W_{\theta W}$	c	1.6	lb sec^2/in	Effective Tire, Wheel, and Brake Mass
W_{IS}	c	16.8	in lb sec^2/rad	Axle Moment of Inertia (+ Stators)
W_{IT}	c	115	in lb sec^2/rad	Tread Moment of Inertia
W_{IW}	c	66.0	in lb sec^2/rad	Wheel and Rotors Moment of Inertia

Table A12 Wheel and Tire System (6 Degree) Parameters (Sheet 4 of 5)

SYMBOL	TYPE	VALUE	UNITS	DESCRIPTION
W_S	v		rad/sec	$W_S = \dot{\theta}_S$
W_T	v		rad/sec	$W_T = \dot{\theta}_T$
W_{TE}	c	0.0725	$lb\ sec^2/in$	Equivalent Tire Tread Mass
W_W	v		rad/sec	$W_W = \dot{\theta}_W$
X_{TT}	v		in	Location of Tire Tread C. G.
X_{TTO}	c	0.0	in	Location of Tire Tread C. G. at Time = 0
$\dot{X}_{TT}$	v		in/sec	Tread C. G. Velocity
$\dot{X}_{TTO}$	c	2400	in/sec	Tread C. G. Velocity at Time = 0
$\ddot{X}_{TT}$	v		in/sec^2	Tread C. G. Acceleration
X_W	v		in	Horizontal Axle Location
X_{WO}	c	0.0	in	Horizontal Axle Location at Time = 0
$\dot{X}_W$	v		in/sec	Horizontal Axle Velocity
$\dot{X}_{WO}$	c	2400	in/sec	Horizontal Axle Velocity at Time = 0
$\ddot{X}_W$	v		in/sec^2	Horizontal Axle Acceleration
X_Y	v		in	Dummy Variables used to
X_{YO}	c	0.0	in	Simulate Visco-Elastic Tire
$\dot{X}_Y$	v		in/sec	Characteristic
Y_{AX}	v(I)		in	Undeflected Axle Location (y Direction)
$\dot{Y}_{AX}$	v(I)		in/sec	Undeflected Axle Velocity (y Direction)
X_{AX}	v(I)		in	Undeflected Axle Location (x Direction)
$\dot{X}_{AX}$	v(I)		in/sec	Undeflected Axle Velocity (x Direction)
Y_M	v(o)		in	Footprint Location (y Direction)
Y_{MO}	c	±60.0	in	Ym at Time = 0 ($Y_{MRO} = +60$, $Y_{MLO} = -60$)
$\dot{Y}_M$	v		in/see	Footprint Velocity
$\dot{Y}_{MO}$	c	0.0	in/sec	$\dot{Y}m$ at Time = 0

Table A12 Wheel and Tire System (6 Degree) Parameters (Sheet 5 of 5)

SYMBOL	TYPE	VALUE	UNITS	DESCRIPTION
$\ddot{Y}_M$	v		in/sec^2	Footprint Acceleration
X_{WM}	v(o)		in	Footprint Position (x Direction)
$\dot{X}_{WM}$	v(o)		in/sec	Footprint Velocity
DTRV	c	9500	in LBF SEC/RAD	Tire Tread Radial Damping Coeff.
DTLV	c	5.45	LBF SEC/IN	Tire Tread Longitudinal Damping Coeff.
VRO	c	25.0	in/sec	Tire Friction Threshold Velocity

5. WHEEL SPEED SENSOR

The primary input parameter to an electronic antiskid control circuit is an airplane wheel speed signal. For conventional control circuitry the input must be a direct current voltage. The wheel speed sensor may have any of several forms such as a D.C. tachometer or an A.C. tachometer with variable voltage or frequency converted to a direct current voltage by suitable electronic circuitry. The control circuit input signal, E_G , is a function of the wheel's angular velocity relative to the axle (tachometer mount) and the characteristics of any associated electronic circuitry used for radio interference suppression and/or for conversion of A.C. frequency or voltage signals to D.C. voltage. To provide the means for mathematically describing the control circuit input signal for a variety of wheel speed sensors, two approaches are taken. The first, identified as Option 1, is applicable whenever there is a perceptible phase lag between actual wheel speed and the antiskid circuit input as is generally the case where A.C. voltage signals are converted to D.C. or where a D.C. tachometer is driven through an elastic coupling. A second simpler mathematical description, called Option 2, is provided to minimize computation difficulty and expense where no significant phase lag exists.

A. Mathematical Description

Option 1

Assume that a D.C. tachometer generator is mounted on the axle and is driven by the wheel. The output of the hypothetical generator is assumed to be applied to a linear force motor which acts upon a single degree of freedom damped spring mass system as shown on Figure A47. The control circuit input signal, E_G , is proportional to the mass displacement. By adjusting the relative characteristics of the linear force motor, hypothetical generator, spring, mass and damper a mathematical description of a wide variety of wheel speed sensors can be accommodated.

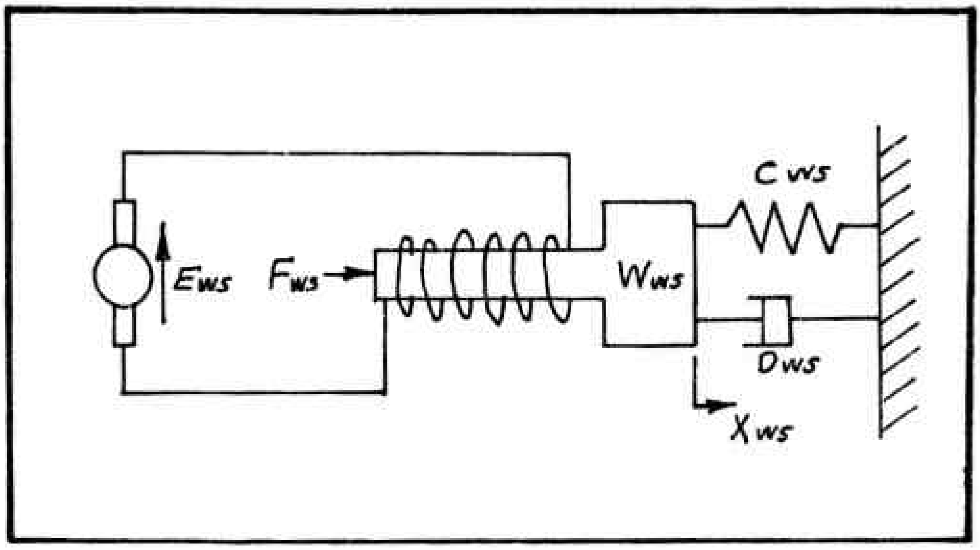

Figure A47 Wheel Speed Signal System

The output of the hypothetical generator, E_{WS}, is proportional to the wheel's angular velocity relative to the axle, W_B, as defined by equation (5.1). Angular velocity, W_B, is obtained as an output of the tire and wheel system.

$$E_{WS} = G_{WS} W_B \tag{5.1}$$

The force produced by the linear force motor, F_{WS}, is proportional to the generator output, E_{WS}, as defined by equation (5.2).

$$F_{WS} = C_{WG} E_{WS} \tag{5.2}$$

The hypothetical mass displacement, X_{WS}, is obtained from equation (5.3) which results from summing forces on the hypothetical mass, W_{WS}.

$$\ddot{X}_{WS} = \frac{F_{WS}}{W_{WS}} - \frac{C_{WS}}{W_{WS}}(X_{WS}) - \frac{D_{WS}}{W_{WS}}(\dot{X}_{WS}) \tag{5.3}$$

The antiskid circuit wheel speed input voltage signal, E_G, is proportional to the hypothetical mass displacement, X_{WS}, as defined by equation (5.4).

$$E_G = C_{CGV} X_{WS} + E_{SN} \tag{5.4}$$

In equation (5.4), E_{SN} is any extraneous "noise" which might be present due to the operation of other aircraft systems, etc.

The equation flow diagram is shown on Figure A48.

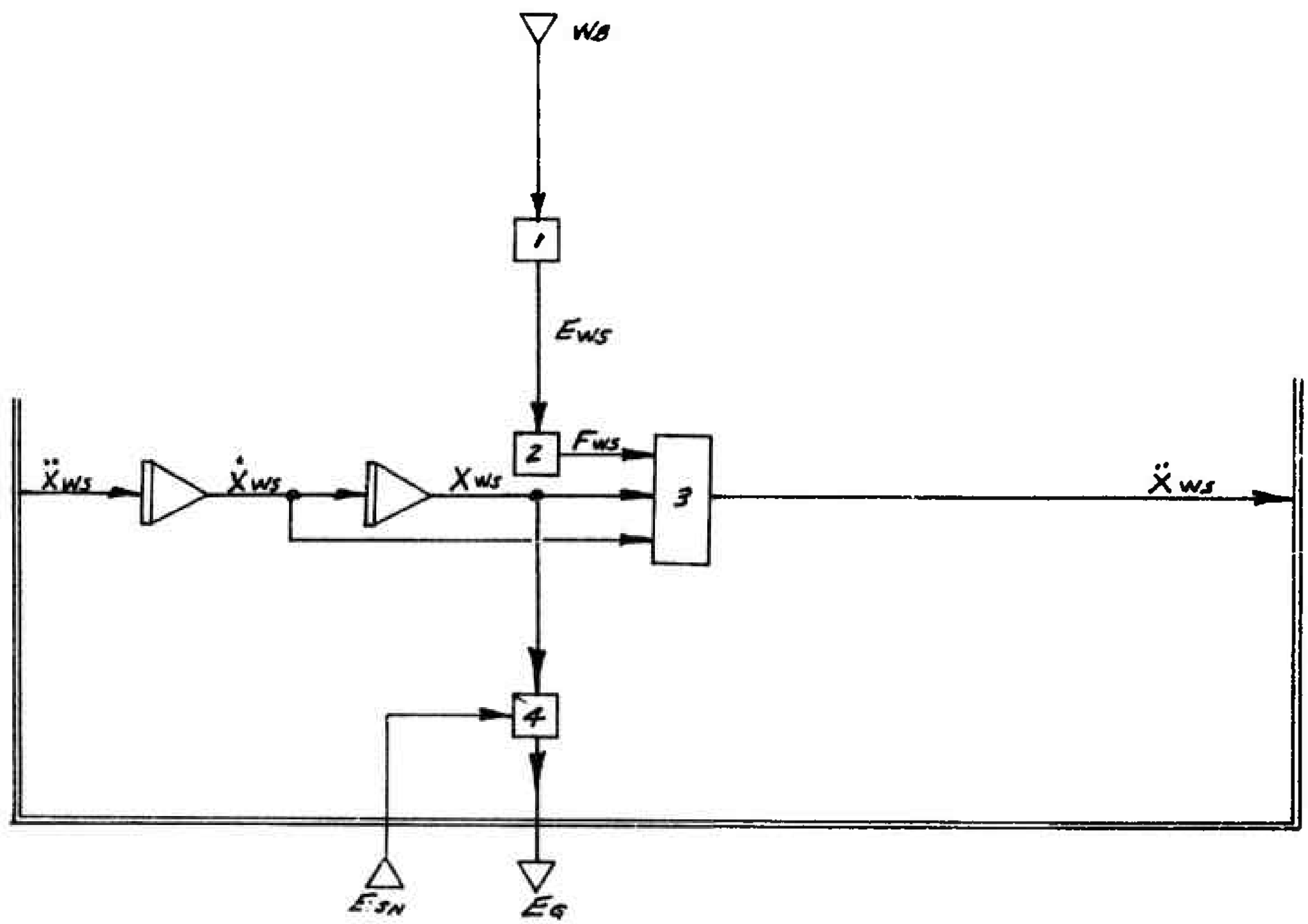

Figure A48 Wheel Speed Sensor Equation Flow Diagram (Option 1)

Option 2

For cases where the wheel speed transducer is a D.C. tachometer, or equivalent, driven through a rigid coupling (such as the F-104 and F-111) there is usually very small difference between the actual wheel speed and antiskid control circuit input (i.e., very low phase lag or attenuation) and the extra mathematical complication incurred by using a very high gain second order equation is not justified. For these cases the antiskid control circuit input voltage may be considered proportional to the wheel's angular velocity as defined by equation (5.5).

$$(5.5) \qquad E_G = G_{WOC} W_B + E_{SN}$$

No equation flow diagram is shown for Option 2.

B. Parameter Evaluation

Option 1

The objective of using a single degree of freedom damped spring mass system to describe the antiskid control circuit input is to provide a mathematical "tool" whereby phase lag within the wheel speed sensor device can be accounted for. Consequently, the values for mass, spring rate and damping coefficient are chosen to produce the desired effect rather than to describe physical devices. The other coefficients are chosen to achieve compatibility with the control circuit. For the F-111 modulated antiskid circuit let the hypothetical tachometer coefficient be the same as for the actual F-111 tachometer, 12 volts per thousand RPM. Therefore:

$$(5.6) \qquad G_{WS} = \frac{12 \times 60}{1000 \times 2\pi} = 0.1147 \text{ VOLT SEC/RAD}$$

Let the force motor coefficient, the elastic system spring rate and output voltage coefficient all be equal to unity so that for steady state conditions the control circuit input, E_G, is the tachometer output. Therefore:

$$(5.7) \qquad \begin{aligned} C_{WG} &= 1.0 \text{ lbf/VOLT} \\ C_{WS} &= 1.0 \text{ lbf/INCH} \\ C_{CGV} &= 1.0 \text{ VOLT/INCH} \end{aligned}$$

Based on information furnished by the Goodyear Aerospace Corp. the component characteristics and arrangement which is usually utilized for converting A.C. frequency to D.C. voltage produces about 30 degrees (or greater) phase lag at 5 cps. The following equations from reference 12 describe the single degree of freedom system's behavior when an oscillatory force $X_o K \sin \omega t$ is applied.

$$\frac{X}{X_o} = \frac{1}{\sqrt{\left[1-(\omega/\omega_n)^2\right]^2 + \left(2\zeta\,\omega/\omega_n\right)^2}} \tag{5.8}$$

$$\tan\phi = \frac{2\,(\omega/\omega_n)}{1-(\omega/\omega_n)^2}$$

In these equations ϕ is the phase angle, $\zeta = D_{WS}/2W_{WS}\,\omega_n$ is the damping factor, $\omega_n = \sqrt{C_{WS}/W_{WS}}$ is the undamped natural frequency, ω is the frequency of applied oscillatory loading, and X/X_o is the magnification factor. If the degree of attenuation and phase angle are known at a particular frequency, the undamped natural frequency and damping factor are established. Assuming two percent attenuation and 30 degree phase lag at 5 cps, the equations above give an undamped natural frequency of 14.6 cps (91.8 RAD/SEC) and a damping factor of 0.746.

For an undamped natural frequency of 91.8 RAD/SEC and a spring rate, C_{WS}, of 1.0 lbf/IN the mass, W_{WS}, is established as 0.1185×10^{-3} lbf-sec^2/IN. The damping coefficient, D_{WS}, is established from the mass and damping factor as

$$D_{WS} = 0.1623 \times 10^{-2} \text{ lbf sec/IN} \tag{5.9}$$

Option 2

For use with the F-111 modulated antiskid control circuit, use the actual F-111 tachometer output of 12 volts D.C. per 1000 RPM. Therefore:

$$G_{WDC} = \frac{12 \times 60}{1000 \times 2\pi} = 0.1147 \text{ VOLT SEC/RAD} \tag{5.10}$$

For use with the on-off antiskid circuit as installed on the F-104 (and B-58) the tachometer output is 20 volts per 1000 RPM. To make the on-off circuit compatible with the F-111 requires that the difference in tire size (46.5 inch dia. for F-111 versus 22 inch dia. for B-58) also be accounted for. Therefore, for the on-off antiskid circuit use:

$$G_{WOC} = (0.1147)\left(\frac{46.5}{22}\right)\left(\frac{20}{12}\right) = 0.4 \text{ VOLT SEC/RAD} \tag{5.11}$$

Table A13 Wheel Speed Sensor Parameters (Sheet 1 of 2)

SYMBOL	TYPE	VALUE	UNITS	DESCRIPTION
		OPTION 1 FOR USE WITH F-111 MODULATED CIRCUIT		
C_{CGV}	c	1.0	VOLT/IN	Output Voltage Coefficient
C_{WG}	c	1.0	lbf/VOLT	Hypothetical Liner Force Motor Coefficient
C_{WS}	c	1.0	lbf/IN	Spring Rate (Hypothetical Spring)
D_{WS}	c	0.1623×10^{-2}	lbf SEC/IN	Damping Coefficient (Hypothetical Damper)
E_G	v(o)		VOLTS	Antiskid Control Circuit Input Signal
E_{WS}	v		VOLTS	Hypothetical Tachometer Voltage
F_{WS}	v		lbf	Hypothetical Linear Force Motor Output Force
G_{WS}	c	0.1147	VOLT SEC/RAD	Hypothetical Tachometer Voltage-Speed Coefficient
E_{SN}	v(I)	0.0	VOLTS	Input Signal "Noise"
W_{WS}	c	0.1185×10^{-3}	lbf SEC^2/IN	Mass (Hypothetical Mass)
W_B	v(I)		RAD/SEC	Wheel Angular Velocity Relative to Angle
X_{WS}	v		INCH	Hypothetical Mass Displacement
X_{WSO}	c	0.0	INCH	Hypothetical Mass Displacement at Time Zero
$\dot{X}_{WS}$	v		IN/SEC	Hypothetical Mass Velocity
$\dot{X}_{WSO}$	c	0.0	IN/SEC	Hypothetical Mass Velocity at Time Zero
$\ddot{X}_{WS}$	v		IN/SEC^2	Hypothetical Mass Acceleration
		OPTION 2 FOR USE WITH F-111 MODULATED CIRCUIT		
G_{WOC}	c	0.1147	VOLT SEC/RAD	
E_{SN}	v(I)	0.0	VOLTS	

Table A13 Wheel Speed Sensor Parameters (Sheet 2 of 2)

SYMBOL	TYPE	VALUE	UNITS	DESCRIPTION
		OPTION 2 FOR USE WITH F104 ON-OFF CIRCUIT		
G_{WOC}	c	0.4	VOLT SEC/RAD	
E_{SN}	v(I)	0.0	VOLTS	

6a. MODULATED ANTISKID CONTROL CIRCUIT

After introduction of on-off type antiskid systems, it became apparent from various analyses and studies of test results and operational performance that braking effectiveness could be increased if the number of antiskid cycles and their intensity could be minimized. To minimize antiskid cycling occurrences and intensity, it is necessary to control the amount of brake torque being applied such that the available friction torque is not exceeded for as much of the time as is possible. A number of devices utilizing various principles of operation have been used for this purpose. These devices predominately utilize the principle of regulating or "modulating" brake pressure to keep its value as near as possible to that which will produce a skid. One of the first of these type devices is a hydraulic pressure modulator comprised of an orifice and accumulator installed upstream from the pilot's metering valve and configured such that repetitive antiskid cycling causes a temporary reduction in pilot's metered pressure. The Convair Model 880 airplane's Hytrol MKI antiskid system with hydraulic modulation is a typical example of this type installation.

A subsequent development was the Bendix system which is used on Grumman A6A and Lockheed C141 aircraft. This system combines hydraulic modulation accomplished within the off-on type control valve with two levels of skid detection, (i.e., brake pressure reduction in two steps controlled by skid intensity). Further improvements have been achieved by utilizing a servo type pressure regulating valve with electronic control to achieve a wide range of control characteristics and better accommodate widely varying runway friction conditions encountered during aircraft operation. The Goodyear Adaptive system used on General Dynamics F-111 aircraft and the Hytrol MK II system used on McDonnell-Douglas F4C and LTV A7A aircraft are examples of the servo valve type systems. Within each of the types or classes of systems there are a number of variations in circuitry and component arrangement depending upon the aircraft type, landing gear arrangement and configuration, and the airplane's mission requirements. For this program a mathematical model of the F-111 airplane's Goodyear Adaptive Antiskid Control Circuit is developed. Models for other type circuits can be developed using similar procedures.

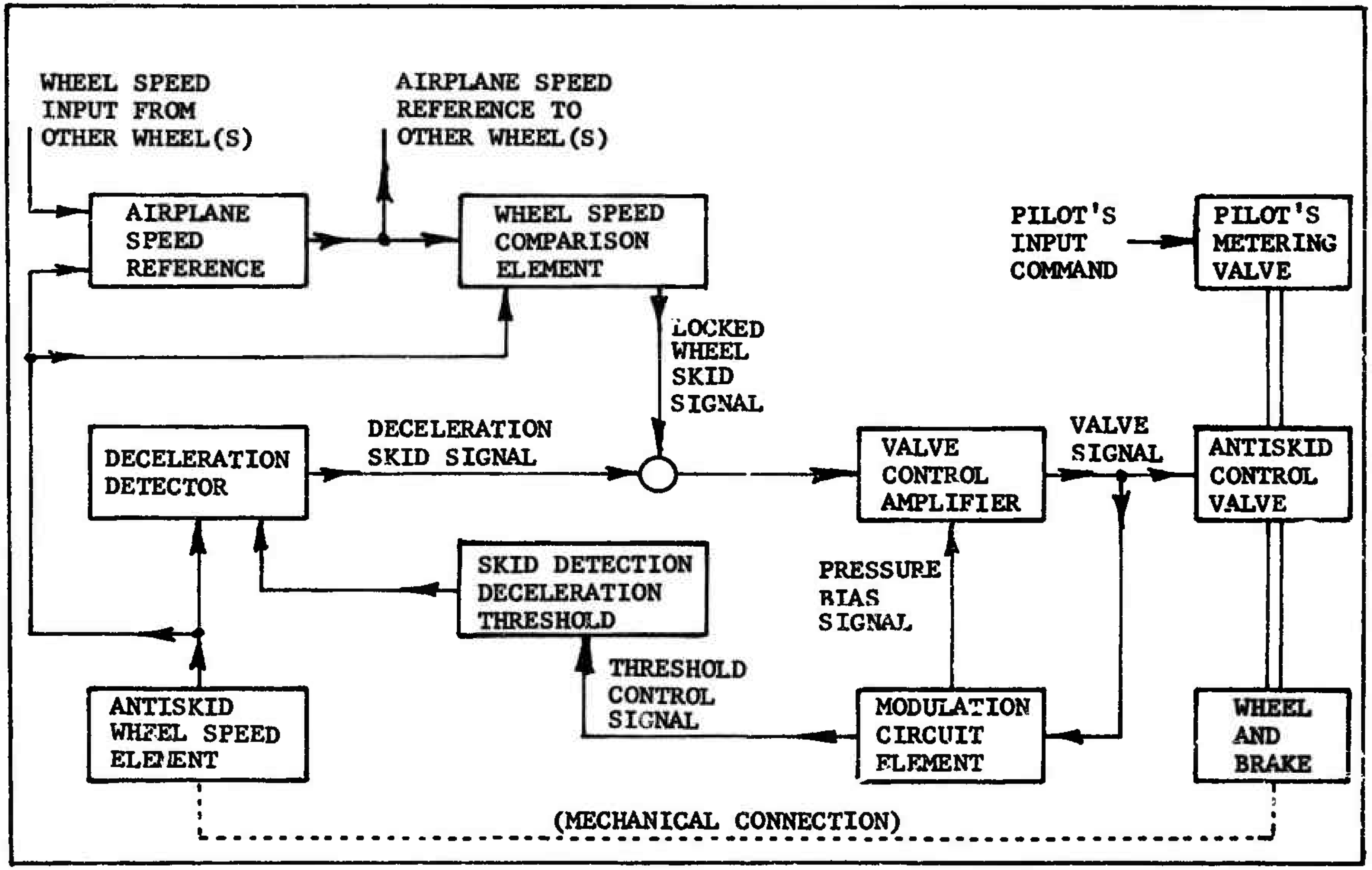

Figure A49 Modulated Antiskid Control Functional Block Diagram

Figure A49 is a block diagram showing the basic functional elements of the Goodyear adaptive antiskid control circuit as used on the F-111 airplane and showing the relationship of the control circuit to the other brake system components. During antiskid circuit operation, a wheel speed signal is provided as an input to a deceleration detector. Within the deceleration detector the wheel's deceleration rate is computed and compared to a threshold value provided by a skid detection threshold circuit element. The deceleration detector produces a skid signal proportional to the amount by which the wheel's deceleration rate exceeds the threshold value. The skid signal is applied to a valve control amplifier which in turn produces a valve control signal proportional to the input skid signal plus any pressure bias signal which might exist. The valve control signal is supplied to the antiskid control valve (a servo type pressure regulator) for brake pressure control and to a modulation circuit element. The modulation circuit element interprets the valve control signal and provides a pressure bias signal to the valve control amplifier and a threshold control signal to the skid detection threshold circuit element. The wheel speed signal is also supplied to the locked wheel prevention circuit elements consisting of an airplane speed reference and a wheel speed comparison element. When the airplane speed reference indicates that the airplane's speed exceeds "locked wheel arming speed" (usually 20 mph) and simultaneously the wheel speed is less than that which should exist for a slightly lower airplane speed (usually 10 mph), the wheel speed comparison circuit element produces a skid signal sufficient to fully release the brake. Locked wheel arming speed is chosen as some reasonably low speed below which a locked wheel is not particularly detrimental. The locked wheel feature is deactivated below locked wheel arming speed so that the airplane can be brought to a complete stop. The aircraft circuit also incorporates circuit elements for failure detection, automatic cutoff and prevention of brake application prior to touchdown. These logic type functions do not affect aircraft stopping performance and are not included in this analysis.

A. Modulated Antiskid Circuit Mathematical Description

A simplified schematic diagram of the Goodyear adaptive antiskid circuit for one wheel as used on F-111 type aircraft is shown on Figure A50. This circuit accom-

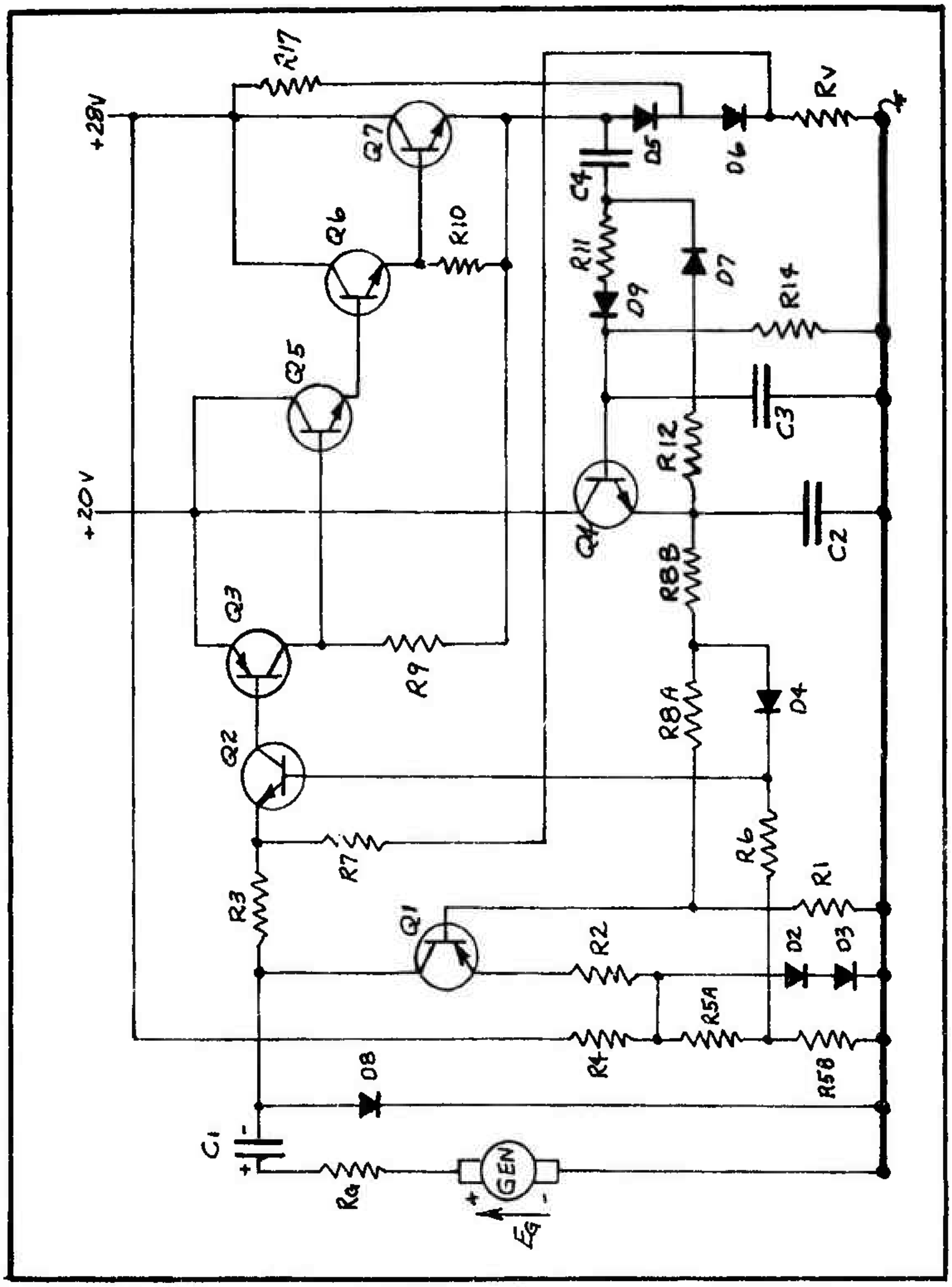

Figure A 50 Modulated Antiskid Control Circuit Schematic

plishes deceleration skid control as previously described in the control circuit functional description as follows. An input voltage, E_G, is provided by a wheel driven D. C. tachometer generator (GEN). E_G charges the deceleration detector, capacitor, C_1, through resistance R_G and diode D_8 during wheel spin-up. For normal wheel deceleration rates, with no incipient skidding, the generator voltage will decrease relatively slowly and a small current will flow from the positive side of C_1 through R_G, the generator, R_4, R_2, and transistor Q_1 to the negative side of C_1. This current discharges capacitor C_1 and causes its voltage to closely follow E_G. Transistor Q_1 is the skid detection threshold circuit element. Q_1 is a current-limiting device that offers very low impedance to current below its threshold value and extremely high impedance to any current above that threshold. The threshold is controlled by R_2. Diodes D_2 and D_3 provided bias voltage for the operation of Q_1. When an incipient skid occurs, the generator voltage decreases rapidly and since Q_1 limits the discharge current into C_1, the voltage at the negative side of C_1 decreases and causes current to flow through R_{5A}, R_6, Q_2, and R_3. The current into the base of Q_2 is amplified by Q_2, Q_3, Q_5, Q_6 and Q_7, (the valve control amplifier) to produce a voltage across R_V, the antiskid valve coil. Voltage applied to the antiskid valve causes brake pressure to be reduced proportionally and thereby alleviate the incipient skid. Antiskid valve voltage is feedback to the amplifier input through R_7 to stabilize amplifier gain against changes due to temperature and component characteristic variations.

Antiskid valve voltage pulses are transmitted to the modulation circuit elements through capacitor C_4. Within the modulation circuit element, consisting of C_4, R_{11}, R_{14}, R_{12}, D_7, C_3, C_2, D_9 and Q_4, each increase in voltage to the valve produces an increase in the charge on C_3. Voltage on C_3 causes Q_4 to charge C_2. Since C_2 discharges through R_{8B}, R_{8A}, and R_1, the voltage on C_2 provides a threshold control signal to Q_1. The charge on C_3, and in turn on C_2, is a function of the amp'itude and frequency of valve voltage pulses. Voltage on C_2 is also applied to Q_2 through R_{8B} and D_4 to provide a pressure bias signal to the valve control amplifier. The operation of the modulation circuit element results in an automatic threshold change to the skid sensing circuit and a bias to the valve control amplifier to match the braking conditions being encountered.

The mathematical description of the operation of the Goodyear adaptive electronic antiskid control circuit as shown on Figure A50 is developed with conventional circuit analysis techniques using Kirchhoff's Laws. Figure A51 is the schematic diagram from Figure A50 with the transistors and diodes shown in terms of their equivalent circuits and the various currents and voltages identified. The transistor and diode equivalent circuits are adaptations of equivalent circuits developed and described in references 13, 14 and 15. Some of the diode forward resistances are combined with other resistance in series with the diodes and are not shown separately. Also, since the current through R_G (the output resistance of the wheel speed signal source) has three non-mutually influencing components, R_G is included in R_3 , R_{08} and R_{15} to simplify equations. Other simplifications will be described and discussed during the development of equations.

Referring to Figure A51, the ci·cuit equations are developed as follows:

The voltage across capacitor C_1 is defined as:

(1) $$V_{C1} = \int \dot{V}_{C1}\, dt$$

(A1) $$\dot{V}_{C1} = A_{C1}/C_1 \quad \text{OR} \quad \dot{V}_{C1} = A_{C1}\, C_{608}$$

A_{C1} is the current through C_1 and C_1 is the capacitance. A_{C1} is established by summing currents at node N11 as:

(N11) $$A_{C1} = A_{08} - A_{12}$$

Using Ohm's law and summing voltages around the loop of which R_{08} is a part, A_{08} is established as:

(R10) $$A_{08} = (E_G - V_{C1} - E_{08})/R_{08} \quad \text{FOR } (E_G - V_{C1} - E_{08}) > 0$$
$$= 0 \quad \text{FOR } (E_G - V_{C1} - E_{08}) \leq 0$$

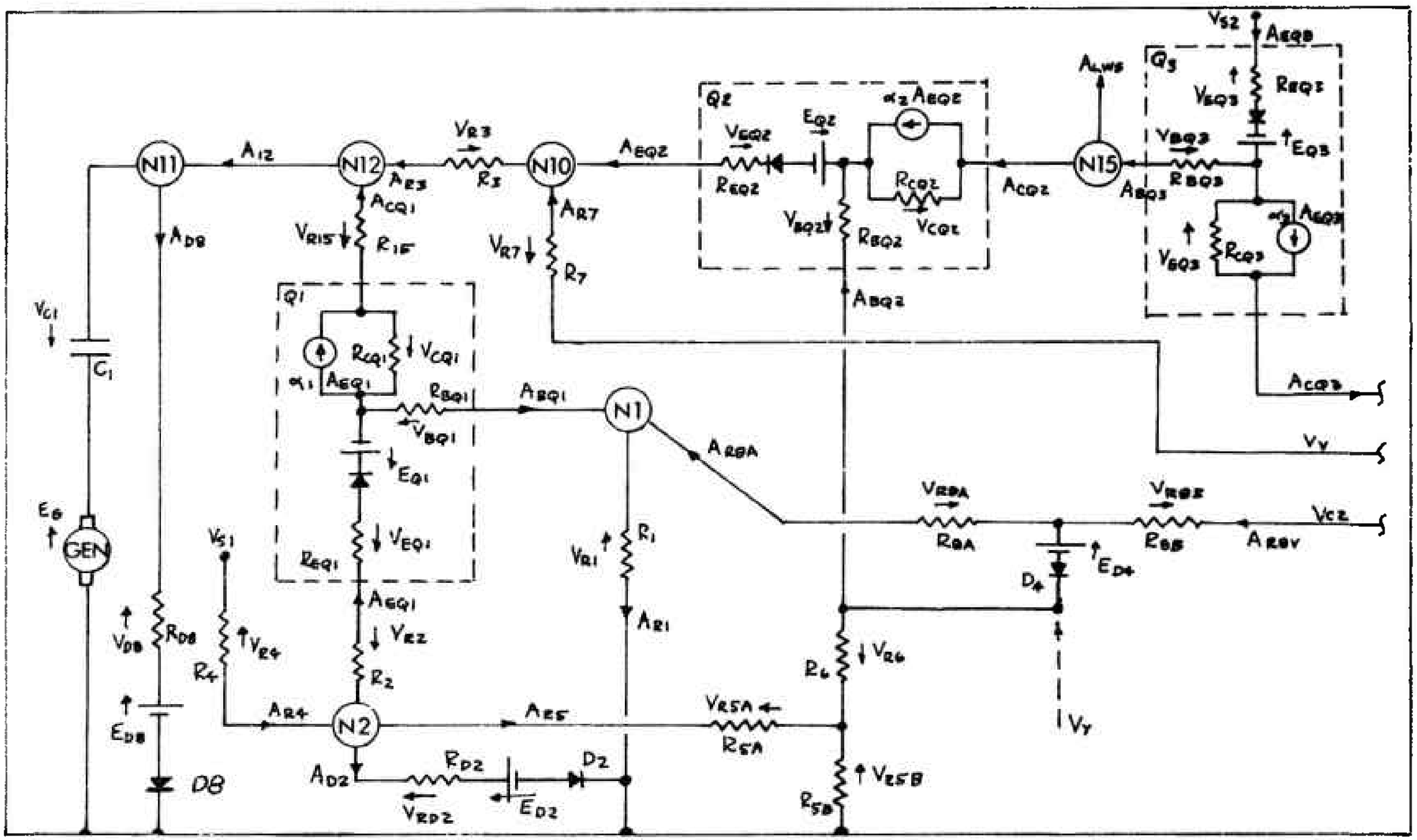

Figure A51 Modulated Antiskid Schematic with Mathematical Identification and Incorporating Equivalent Circuits for Transistors and Diodes (Sheet 1 of 2)

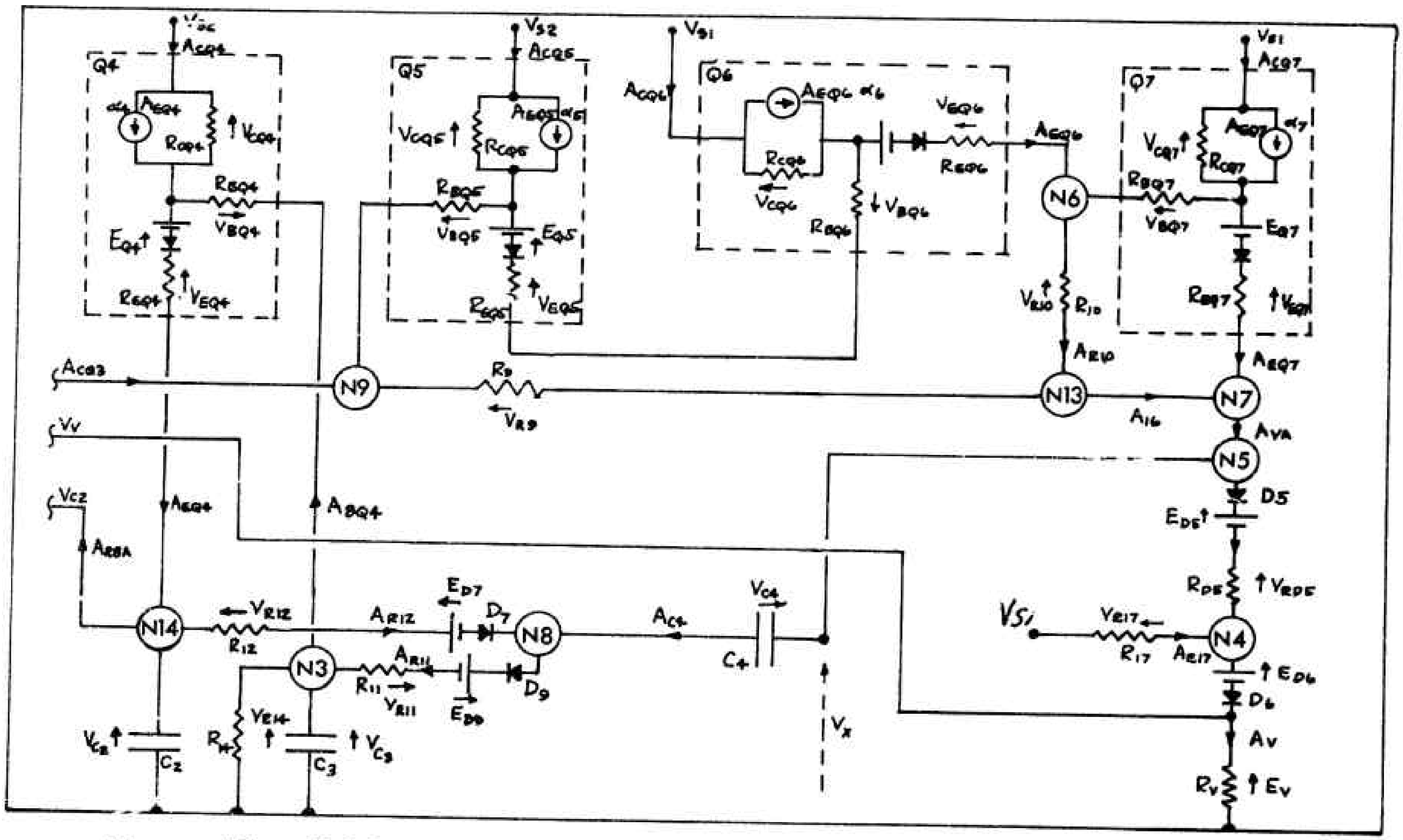

Figure A51 Modulated Antiskid Schematic with Mathematical Identification and Incorporating Equivalent Circuits for Transistors and Diodes (Sheet 2 of 2)

Noting that because of diode D_8, A_{D8} is restricted to positive values only.

To combine constants, write equation (R10) as:

$$\text{(R10)} \quad A_{D8} = (E_G - V_{C_1})C_{620} - C_{621} \qquad \text{FOR } (E_G - V_{C_1}) > C_{620}/C_{621}$$

$$= 0 \qquad \text{FOR } (E_G - V_{C_1}) \leq C_{620}/C_{621}$$

By summing currents at Node N12, current A_{12} is established as:

$$\text{(N12)} \quad A_{12} = A_{R3} + A_{CQ1}$$

Substituting equation (N12) into equation (N11) gives:

$$\text{(N11)}' \quad A_{C1} = A_{D8} - A_{R3} - A_{CQ1}$$

To compute A_{CQ1} it is desirable to first obtain equations for the voltages at the base and emitter of Q_1 in terms of the base and emitter currents and the appropriate voltage sources. The voltage at the base of Q_1 is V_{R1} . Summing currents at Node N1 establishes current A_{R1} as:

$$\text{(N1)} \quad A_{R1} = A_{BQ1} + A_{R8A}$$

Summing voltages around the loop R_1, R_{8A}, R_{8B} to V_{C2} gives: $V_{R8A} + V_{R8B} = V_{C2} - V_{R1}$. If the current through diode $D4$ is assumed negligible, then $A_{R8A} = A_{R8B}$. (Because of the relative resistances, the current through $D4$ is a very small fraction of the current through R_{8B}). By Ohm's law, $V_{R8A} + V_{R8B} = A_{R8A}(R_{8A} + R_{8B})$ and $V_{R1} = A_{R1} R_1$, Substitution into equation (N1) and solving for V_{R1} gives:

$$\text{(N1)}' \quad V_{R1} = R_1\left(A_{BQ1} + \frac{V_{C2}}{R_{8A}+R_{8B}}\right) \Big/ \left(1 + \frac{R_1}{R_{8A}+R_{8B}}\right)$$

The voltage at Node (N2) is $E_{D2}+V_{RD2}$. (Here two diodes D_2 and D_3 as shown on Figure 50 are combined in an equivalent single diode). Summing currents at Node (N2) establishes current A_{D2} as:

(N2): $$A_{D2} = A_{R4} - A_{R5} - A_{EQ1}$$

By Ohm's law, $V_{RD2} = A_{D2} R_{D2}$, $V_{R4} = A_{R4} R_4$, and $(V_{R5A} + V_{R5B}) = A_{R5}(R_{5A} + R_{5B})$ (Note: Because of the relative resistances, A_{R6} is a very small component of the current in R_{5A} and is assumed to be zero when computing V_{RD2}.) Summing voltages around the appropriate loops establishes that $V_{R4} = V_{S1} - V_{RD2} - E_{D2}$ and $V_{R5A} + V_{R5B} = V_{RD2} + E_{D2}$. By substitution into equation (N2) and solving for V_{RD2} gives:

(N2)' $$V_{RD2} = \frac{\left[\frac{V_{S1}}{R_4} - E_{D2}\left(\frac{1}{R_4} + \frac{1}{R_{5A}+R_{5B}}\right) - A_{EQ1} \right]}{\left(\frac{1}{R_{D2}} + \frac{1}{R_4} + \frac{1}{R_{5A}+R_{5B}}\right)}$$

Summing voltages around the loop through which A_{BQ1} (the base of current Q_1) flows results in:

(Q-1) $$E_{D2} + V_{RD2} - V_{R2} - V_{EQ1} - E_{Q1} - V_{BQ1} - V_{R1} = 0$$

By substituting $V_{R2} = A_{EQ1} R_2$, $V_{EQ1} = A_{EQ1} R_{EQ1}$ amd $V_{BQ1} = A_{BQ1} R_{BQ1}$ (From Ohm's Law) along with equations (N1)', (N2)', and the basic transistor relationship $A_{EQ1} = (h_{FE1}+1) A_{BQ1}$ into equation (Q-1) and solving for A_{EQ1}

(Q-1)' $$A_{EQ1} = C_{602} - C_{603} V_{C2} \quad \text{, WHERE}$$

$$C_{602} = \frac{\left\{ E_{D2}\left[1 - \left(\frac{1}{R_4}+\frac{1}{R_5}\right) \Big/ \left(\frac{1}{R_{D2}}+\frac{1}{R_4}+\frac{1}{R_5}\right)\right] + V_{S1}\left(\frac{1}{R_4}\right) \Big/ \left(\frac{1}{R_{D2}}+\frac{1}{R_4}+\frac{1}{R_5}\right) - E_{Q1} \right\}}{\left\{ R_2 + R_{EQ1} + \frac{R_{BQ1}}{(h_{FE1}+1)} + \frac{R_1}{(h_{FE1}+1)} \Big/ \left(1+\frac{R_1}{R_B}\right) + 1 \Big/ \left(\frac{1}{R_{D2}}+\frac{1}{R_4}+\frac{1}{R_5}\right) \right\}}$$

$$C_{603} = \frac{\frac{R_1}{R_1+R_B}}{\left\{ R_2 + R_{EQ1} + \frac{R_{BQ1}}{(h_{FE1}+1)} + \frac{R}{(h_{FE1}+1)} \Big/ \left(1+\frac{R_1}{R_B}\right) + 1 \Big/ \left(\frac{1}{R_{D2}}+\frac{1}{R_4}+\frac{1}{R_5}\right) \right\}}$$

And where in the above $R_S = R_{SA} + R_{SB}$ and $R_B = R_{BA} + R_{BB}$.

For Q_1 to operate as a transistor, V_{CQ1} must be positive. Using equation $(Q\text{-}1)'$, the basic transistor characteristic (Q2) $A_{CQ1} = h_{FE1} A_{EQ1}/(h_{FE1}+1)$ and by writing the voltage loop equation through $D2, Q1, R_{15}, C_1$ and (GEN) it can be shown that V_{CQ1} is positive for $(E_G - V_{C1})$ negative; therefore, equation (Q-1)' is applicable only for $(E_G - V_{C1}) < 0$. Substituting (Q-1) into (Q-2) gives the following equation:

$$\text{(Q-1C)} \quad A_{CQ1} = C_{604} - C_{605} V_{C2} \qquad \text{FOR } (E_G - V_{C1}) < 0$$
$$= 0 \qquad \text{FOR } (E_G - V_{C1}) \geq 0$$
$$= 0 \qquad \text{FOR } V_{C2} \geq C_{604}/C_{605}$$

$$C_{604} = C_{602} \left(\frac{h_{FE1}}{h_{FE1}+1} \right)$$

$$C_{605} = C_{603} \left(\frac{h_{FE1}}{h_{FE1}+1} \right)$$

By summing currents at node N10, current A_{R3} is established as:

$$\text{(N10)} \quad A_{R3} = A_{EQ2} + A_{R7}$$

To compute the components of A_{R3} (i.e., A_{EQ2} and A_{R7}) it is desirable to have equation (N10) in a form where A_{R7} is expressed in terms of the appropriate voltages and resistances. By summing voltages around the loop R_V, R_7, R_3, C_1 and GEN, V_{R7} is established as:

$$\text{(V7)} \quad V_{R7} = E_V - V_{R3} - (E_G - V_{C1})$$

Substituting equation (V7) along with $V_{R3} = A_{R3} R_3$ and $V_{R7} = A_{R7} R_7$ into (N10) gives:

$$\text{(N10)'} \quad A_{R3} = \frac{A_{EQ2}}{1 + R_3/R_7} + \frac{E_V}{(R_7 + R_3)} - \frac{(E_G - V_{C1})}{(R_7 + R_2)}$$

To combine constants write as:

$$\text{(N10)'} \quad A_{R3} = A_{EQ2} C_{612} + \left[E_V - (E_G - V_{C1}) \right] C_{613}$$

To compute current A_{EQ2} , sum voltages around the loop through which A_{BQ2} flows:

$$(Q\text{-}2) \quad V_Y - V_{BQ2} - E_{Q2} - V_{EQ2} - V_{R3} - (E_6 - V_{C1}) = 0$$

Here voltage V_Y is the base voltage on Q2 and is either $(V_{R5B} - V_{R6})$ or $(V_{C2} - V_{R8B} - E_{D4})$ whichever is the largest; therefore, there will be a version of equation (Q-2) for each of these conditions. To establish which condition exists, it is necessary to compute $(V_{R5B} - V_{R6})$ and $(V_{C2} - V_{R8B} - E_{D4})$

During derivation of Equation (N2)' it was observed that $V_{R5A} + V_{R5B} = V_{RD2} + E_{D2}$ and it was assumed that A_{R6} was small when compared to A_{R5} . Using the same assumption V_{R5B} is established as follows by Ohm's Law:

$$(R\text{-}5) \qquad V_{R5B} = A_{R5}\, R_{5B}$$

By substituting $A_{R5}\,(R_{5A} + R_{5B}) = V_{R5A} + V_{R5B}$ into equation (R-5) above gives:

$$(R\text{-}5)' \qquad V_{R5B} = R_{5B}\,(V_{RD2} + E_{D2}) / (R_{5A} + R_{5B})$$

By substituting equation (N2)' for V_{RD2} and investigating the influence of A_{EQ1} within its allowable range, it can be seen that for practical purposes V_{R5B} is a constant.

To compute V_{R6} , it can be seen that A_{R6} equals A_{BQ2} when V_Y is $V_{R5B} - V_{R6}$; therefore, $V_{R6} = A_{BQ2}\, R_6$ by Ohm's law.

By Ohm's Law $V_{R8B} = A_{R8B}\, R_{8B}$. Since the current through D4 is very small and may be assumed zero, and since A_{BQ1} is such a small component of the current through R1 that it can be assumed zero, by Ohm's Law:

$$(V8) \quad A_{R8B} = A_{R8A} = V_{C2} / (R_1 + R_{8A} + R_{8B})$$

Therefore:

$$\left(V_{C2} - V_{R8B} - E_{D4}\right) = \left[V_{C2}\left(\frac{R_1 + R_{8A}}{R_1 + R_{8A} + R_{8B}}\right) - E_{D4}\right]$$

To establish whether $V_Y = (V_{R5B} - V_{R6})$ OR

$$V_Y = \left[V_{C2}\left(\frac{R_1 + R_{8A}}{R_1 + R_{8A} + R_{8B}}\right) - E_{D4}\right]$$

A voltage VB will be defined as follows:

(VB) $$V_B = \left[V_{C2}\left(\frac{R_1 + R_{8A}}{R_1 + R_{8A} + R_{8B}}\right) - E_{D4}\right] - \left(V_{R5B} - R_6 A_{BQ2}\right)$$

if $V_B > 0$, (VY-1) $$V_Y = \left[V_{C2} C_m - E_{D4}\right]$$

if $V_B \leq 0$, (VY-2) $$V_Y = \left[V_{R5B} - R_6 A_{BQ2}\right]$$

where C_m above is defined as:

$$C_m = \left(\frac{R_1 + R_{8A}}{R_1 + R_{8A} + R_{8B}}\right)$$

To combine constants and expressing A_{BQ2} as $A_{EQ2}/h_{FE2}+1$ equation(V_B) may be written in the following form:

(VB) $$V_B = V_{C2} C_m + A_{EQ2} C_{801} - C_{800}$$

Before proceeding with the computation of A_{R3}, the valve control amplifier and modulation circuit elements will be examined to develop equations for E_V and V_{C2}.

By summing currents at Node N5 current A_{D5} is established as:

(N5) $$A_{D5} = A_{VA} - A_{C4}$$

The voltage at Node N5 is defined as V_X. Summing voltages around the loop R_V, D_6, D_5 and V_X gives:

(VX) $$V_X = E_V + E_{D6} + V_{RD5} + E_{D5}$$

By summing currents at Node N4, current A_{R17} is established as:

(N4) $$A_{R17} = A_V - A_{05}$$

By substituting equations (N4), (N5), and (EV) into equation (VX) and by using Ohm's Law to establish that $E_V = A_V R_V$, $V_{R17} = A_{R17} R_{17}$ and $V_{R05} = A_{05} R_{05}$, VX is established as:

(VX)' $$V_X = A_{05} C_{400} + C_{401}$$

By substituting equation (EV) into (N4) and using the relationships $E_V = A_V R_V$ and $V_{R17} = A_{R17} R_{17}$ EV is established as:

(N4)' $$E_V = A_{05} C_{406} + C_{407}$$

The operation of transistors Q2, Q3, Q5, Q6, and Q7 will now be considered to develop an equation for current A_{VA} (Valve Control Amplifier Output Current).

By summing currents at Node N7, current A_{VA} is established as:

(N7) $$A_{VA} = A_{EQ7} + A_{I6}$$

By summing currents at Node N13, current A_{I6} is established as:

(N13) $$A_{I6} = A_{R10} + A_{R9}$$

By summing currents at Node N6, current A_{R10} is established as:

(N6) $$A_{R10} = A_{EQ6} - A_{BQ7}$$

By summing currents at Node N9, current A_{R9} is established as:

(N9) $$A_{R9} = A_{CQ3} - A_{BQ5}$$

Summing voltages around the loop, R_{EQ7}, R_{BQ7} and R_{10} gives:

$$(V10) \qquad V_{R10} = V_{EQ7} + E_{Q7} + V_{BQ7}$$

By using the relationships $V_{R10} = A_{R10} R_{10}$, $V_{EQ7} = A_{EQ7} R_{EQ7}$ and $V_{BQ7} = A_{BQ7} R_{BQ7}$ as established by Ohm's law along with the transistor characteristic $A_{EQ7} = (h_{FE7}+1) A_{BQ7}$ and substitution equation (N6) into (V10) and solving for A_{BQ7}:

$$(V10)' \qquad A_{BQ7} = \frac{A_{EQ6} R_{10} - E_{Q7}}{\left[(h_{FE7}+1) R_{EQ7} + R_{BQ7} + R_{10}\right]}$$

By substituting (V10)' and (N6) into the relationship $V_{R10} = A_{R10} R_{10}$

$$(A10) \qquad V_{R10} = A_{EQ6} C_{402} + C_{403} E_{Q7}$$

Summing voltages around the loop R10, R_{EQ6}, R_{BQ6}, R_{EQ5}, R_{BQ5} and R_9 gives:

$$(V9) \qquad 0 = V_{R10} + V_{EQ6} + E_{Q6} + V_{BQ6} + V_{EQ5} + E_{Q5} + V_{BQ5} - V_{R9}$$

By substituting equations (A10) and (N9) into (V9) along with transistor characteristics $A_{EQ6} = (h_{FE6}+1) A_{BQ6}$ and $A_{EQ5} = (h_{FE5}+1) A_{BQ5}$ and the Ohm's Law relationships $V_{R9} = A_{R9} R_9$, $V_{EQ6} = A_{EQ6} R_{EQ6}$, $V_{BQ6} = A_{BQ6} R_{BQ6}$, $V_{EQ5} = A_{EQ5} R_{EQ5}$ and $V_{BQ5} = A_{BQ5} R_{BQ5}$ and solving for A_{EQ6}:

(V9)'

$$A_{EQ6} = \frac{A_{CQ3} R_9 - (E_{Q6} + E_{Q5} + C_{403} E_{Q7})}{\left[C_{402} + R_{EQ6} + \dfrac{R_{BQ6} + R_{EQ5}}{(h_{FE6}+1)} + \dfrac{R_{BQ5} + R_9}{(h_{FE5}+1)(h_{FE6}+1)}\right]}$$

Substituting equations (N13), (N6), (N9), and (V9)' into equation (N7) along with transistor characteristics $A_{EQ5} = (h_{FE5}+1)\, A_{BQ5}$ and $A_{EQ6} = (h_{FE6}+1)\, A_{BQ6}$ and solving for A_{VA} gives:

$$\text{(N7)'} \qquad A_{VA} = A_{CQ3}\, C_{404} - C_{405}$$

It should be noted that these operations involving Q5, Q6, and Q7 assume that A_{CQ3} is large enough such that A_{VA} is not negative and that the applicable supply voltages, VS1 and VS2, are large enough to keep V_{CQ7}, V_{CQ6} and V_{CQ5} positive at all times. The latter assumption can be proven to be true for the range of currents experienced during circuit operation. If A_{CQ3} is not greater than C405/C404, insufficient voltage is developed across R9 to cause Q5, Q6 and Q7 to operate. For A_{CQ3} less than C405/C404 all of A_{CQ3} goes through R9 and $A_{VA} = A_{CQ3}$; therefore, equation (N7)' has two forms depending on the value of A_{CQ3}. Write these two forms as follows:

$$\text{(N7)''} \qquad \begin{aligned} A_{VA} &= A_{CQ3}\, C_{404} - C_{405} && \text{FOR } A_{CQ3} > C_{405}/C_{404} \\ &= A_{CQ3} && \text{FOR } A_{CQ3} \le C_{405}/C_{404} \end{aligned}$$

Supply voltage VS2 is large enough so that voltages V_{CQ3} and V_{EQ3} are always positive and a small leakage current A_{CQ3O} flows. All the equations developed here are for the increment of A_{CQ3} above the leakage value.

By using the transistor characteristics $A_{CQ3} = h_{FE3}\, A_{BQ3}$
$A_{CQ2} = A_{EQ2}\, h_{FE2} / (h_{FE2}+1)$

And if at Node N15 $A_{LWS} = 0$, $A_{BQ3} = A_{CQ2}$
then:

$$\text{(Q3)} \qquad A_{CQ3} = A_{EQ2}\, C_{606}$$

$$\text{WHERE} \qquad C_{606} = \frac{(h_{FE2})(h_{FE2})}{(h_{FE2}+1)}$$

The operation of the modulating circuit element will now be examined. To compute valve voltage EV from equation (N4)' the value of current A_{D5} which is established by Equation (N5) is required. Equation (N5) shows that a

component of A_{D5} is A_{C4}. Before developing equations for computing A_{C4} some observations relative to the operation of C4 and Q4 are helpful.

By summing currents at Node (N8) current A_{C4} is established as:

$$\text{(N8)} \qquad A_{C4} = A_{R11} - A_{R12}$$

However, because of diodes D7 and D9 currents A_{R11} and A_{R12} have limitations depending upon the direction of voltage across the diodes. Summ'ng voltages around the loop C3, R11, D9, C4 to VX gives:

$$\text{(V11)} \qquad V_{C3} + V_{R11} + E_{D9} + V_{C4} - V_X = 0$$

Substituting equation (V11) into the expression $V_{R11} = A_{R11} R_{11}$ as established by Ohm's law gives:

$$\text{(V11)}' \qquad A_{R11} = \frac{V_X - V_{C4} - E_{D9} - V_{C3}}{R_{11}} \quad \text{FOR } (V_X - V_{C4} - E_{D9} - V_{C3}) > 0$$

Because of D9, $A_{R11} = 0$ $\qquad$ FOR $(V_X - V_{C4} - E_{D9} - V_{C3}) \leq 0$

Summing voltages around the loop C3, R12, D7, C4, to VX gives:

$$\text{(V12)} \qquad V_{C2} - V_{R12} - E_{D7} + V_{C4} - V_X = 0$$

Substituting equation (V12) into the expression $V_{R12} = A_{R12} R_{12}$ as established by Ohm's law gives:

$$\text{(V12)}' \qquad A_{R12} = \frac{V_{C2} - E_{D7} + V_{C4} - V_X}{R_{12}} \quad \text{FOR } (V_{C2} - E_{D7} + V_{C4} - V_X) > 0$$

Because of D7 $A_{R12} = 0$ $\qquad$ FOR $(V_{C2} - E_{D7} + V_{C4} - V_X) \leq 0$

Summing voltages around the loop C3 through Q4 to C2 gives:

$$\text{(V-Q4)} \qquad V_{C3} - V_{BQ4} - E_{Q4} - V_{EQ4} - V_{C2} = 0$$

Since the currents A_{BQ4} and A_{EQ4} in transistor Q4 are restricted to positive values only, voltages VBQ4 and VEQ4 are always positive; therefore, equation (V-Q4) shows that VC2 is always less than VC3 by an amount at least equal to EQ4. Also, because of diodes D7 and D9, no current can flow from C3 through R11, D9, D7 and R12 to C2. For these circumstances, it is observed (1) that for A_{C4} positive, all of A_{C4} passes through R11 and all of A_{R11} is A_{C4} and (2) that for A_{C4} negative, all of A_{C4} passes through R12 and all of A_{R12} is $-A_{C4}$.

Since there cannot be positive A_{R11} and positive A_{R12} simultaneously, equation (N8) evolves to:

$$\text{(N8)}' \quad \begin{aligned} A_{C4} &= A_{R11} && \text{FOR } A_{R11} > 0 \\ A_{C4} &= 0 && \text{FOR } A_{R11} = 0 \text{ AND } A_{R12} = 0 \\ A_{C4} &= -A_{R12} && \text{FOR } A_{R12} > 0 \end{aligned}$$

By substituting equations (N5), (VX)' and (N7)" into equations (V11)' and (V12)', equations for A_{C4} are developed for each case.

The remaining equations for the modulation circuit element will now be developed. Substituting the expressions $V_{BQ4} = A_{BQ4} R_{BQ4}$ and $V_{EQ4} = A_{EQ4} R_{EQ4}$ as established by Ohm's law along with the transistor characteristic $A_{EQ4} = (h_{FE4}+1) A_{BQ4}$ into equation (V-Q4) and solving for A_{BQ4} gives:

$$\text{(V-Q4)}' \quad A_{BQ4} = \frac{V_{C3} - E_{Q4} - V_{C2}}{\left[R_{BQ4} + (h_{FE4}+1) R_{EQ4}\right]} \qquad \text{FOR } (V_{C3} - E_{Q4} - V_{C2}) > 0$$

$$= 0 \qquad \text{FOR } (V_{C3} - E_{Q4} - V_{C2}) \leq 0$$

To combine constants, write equation (V-Q4) as:

$$(\text{V-Q4}) \quad A_{BQ4} = (V_{C3} - V_{C2})\, C_{622} - C_{623} \quad \text{FOR } (V_{C3} - V_{C2}) > C_{623}/C_{622}$$

$$= 0 \quad \text{FOR } (V_{C3} - V_{C2}) \leq C_{623}/C_{622}$$

Also, since current AEQ4 is needed, define the transistor characteristic as equation Q4:

$$(\text{Q-4}) \quad A_{EQ4} = A_{BQ4}\, C_{614}$$

where $C_{614} = (h_{FE4} + 1)$

By summing currents at Node (N14) current A_{C2} is established as:

$$(\text{N14}) \quad A_{C2} = A_{EQ4} - A_{R12} - A_{R8A}$$

Using the same assumption relative to A_{R8A} as was made for equations (N1)' and (V8) and by Ohm's Law A_{R8A} is established by equation (V8) as:

$$(\text{V8}) \quad A_{R8A} = \frac{V_{C2}}{R_1 + R_{8A} + R_{8B}} \qquad \text{(Repeated)}$$

By summing currents at Node (N3) current A_{C3} is established as:

$$(\text{N3}) \quad A_{C3} = A_{R11} - A_{R14} - A_{BQ4}$$

Current A_{R14} is computed from $V_{C3} = A_{R14} R_{14}$ established by Ohm's law and A_{BQ4} is computed from equation (V-Q4)' and Equation (Q-4).

Equation (N8)' establishes that:

$$A_{R12} = -A_{C4} \qquad \text{FOR } A_{C4} < 0$$
$$= 0 \qquad \text{FOR } A_{C4} \geq 0$$

$$A_{R11} = A_{C4} \qquad \text{FOR } A_{C4} > 0$$
$$= 0 \qquad \text{FOR } A_{C4} \leq 0$$

Substituting the above and equations (V8) and (Q-4) into equation (N14) gives:

(N14)' $$A_{C2} = A_{BQ4} C_{614} + A_{C4} - V_{C2} C_{618} \qquad \text{FOR } A_{C4} < 0$$
$$= A_{BQ4} C_{614} - V_{C2} C_{618} \qquad \text{FOR } A_{C4} \geq 0$$

Similarly, by substituting the above A_{R11} to A_{C4} relationship and $V_{C3} = A_{R14} R_{14}$ into equation (N3) A_{C3} is established as:

(N3)' $$A_{C3} = A_{C4} - V_{C3} C_{619} - A_{BQ4} \qquad \text{FOR } A_{C4} > 0$$
$$= -V_{C3} C_{619} - A_{BQ4} \qquad \text{FOR } A_{C4} \leq 0$$

The voltages across capacitors C2, C3 and C4 are established by:

(2) $$V_{C2} = \int \dot{V}_{C2}\, dt$$

(A2) $$\dot{V}_{C2} = C_{609} A_{C2}$$

(3) $$V_{C3} = \int \dot{V}_{C3}\, dt$$

(A3) $$\dot{V}_{C3} = C_{610} A_{C3}$$

(4) $$V_{C4} = \int \dot{V}_{C4}\, dt$$

(A4) $\dot{V}_{C4} = C_{611} A_{C4}$

All of the equations describing the antiskid circuit's operation have now been developed; however, to obtain a computer solution of these equations, they have to be converted to a suitable form so that there are no "closed loops." Also, since the equations for A_{EQ2}, A_{VA} and A_{C4} have different forms depending upon which circumstances exist, a procedure must be established to define which form of equations (Q2), (N7)" and (N8)' applies for each instance. There are twelve (12) possible combinations of circumstances as shown on Table A14. The procedure for defining which condition exists will be to assume a condition and develop a set of equations based on the assumption. Using these equations, the assumption will be tested. If the test is affirmative, the assumed condition exists. If the test is negative, the assumption is incorrect and other assumed conditions are tested until an affirmative test result is obtained. To illustrate this procedure, the equations for circuit condition 4 will be developed:

For circuit condition 4 A_{C4} is positive, A_{CQ3} greater than C_{405}/C_{404} and VB greater than zero. Substitute equation (N5) and the applicable version of equation (N7)" into equation (VX)'.

(VX)'-4 $V_X = \left(A_{CQ3}\, C_{404} - C_{405} - A_{C4}\right) C_{400} + C_{401}$

From equations (N8)' and (V11)' A_{C4} is established as:

(N8)' - P $$A_{C4} = \frac{V_X - V_{C4} - E_{09} - V_{C3}}{R_{11}}$$

Substitute (VX)'-4 into (N8)'-P and solve for A_{C4}

(N8)'-P4

$$A_{C4} = \frac{A_{CQ3}\, C_{404} C_{400}}{R_{11} + C_{400}} - \frac{(V_{C4} + V_{C3})}{R_{11} + C_{400}} - \frac{(E_{09} + C_{405} C_{400} \cdot C_{401})}{R_{11} + C_{400}}$$

Table A14 Modulated Antiskid Circuit Conditions

Circuit Condition	Capacitor C4 Current Mode (See Note 1)	Valve Amplifier Operating Mode (See Note 2)	Pressure Bias Signal Condition (See Note 3)
1	$A_{C4} > 0$	$A_{EQ2} \leq C_{607}$	$V_B \leq 0$
2	$A_{C4} > 0$	$A_{EQ2} \leq C_{607}$	$V_B > 0$
3	$A_{C4} > 0$	$A_{EQ2} > C_{607}$	$V_B \leq 0$
4	$A_{C4} > 0$	$A_{EQ2} > C_{607}$	$V_B > 0$
5	$A_{C4} = 0$	$A_{EQ2} \leq C_{607}$	$V_B \leq 0$
6	$A_{C4} = 0$	$A_{EQ2} \leq C_{607}$	$V_B > 0$
7	$A_{C4} = 0$	$A_{EQ2} > C_{607}$	$V_B \leq 0$
8	$A_{C4} = 0$	$A_{EQ2} > C_{607}$	$V_B > 0$
9	$A_{C4} < 0$	$A_{EQ2} \leq C_{607}$	$V_B \leq 0$
10	$A_{C4} < 0$	$A_{EQ2} \leq C_{607}$	$V_B > 0$
11	$A_{C4} < 0$	$A_{EQ2} > C_{607}$	$V_B \leq 0$
12	$A_{C4} < 0$	$A_{EQ2} > C_{607}$	$V_B > 0$

Notes:

1. Capacitor $C4$ is charging for $A_{C4} > 0$, static for $A_{C4} = 0$ and discharging for $A_{C4} < 0$.
2. The valve amplifier is amplifying for $A_{EQ2} > C_{607}$ and is cutoff for $A_{EQ2} \leq C_{607}$.
3. A pressure bias signal exists for $V_B > 0$ and does not exist for $V_B \leq 0$.

Now substitute equations (N5), (N7)" and (N8)'-P4 into equation (N4)' and solve for EV

(N4)'-4

$$E_V = \frac{R_V}{R_{11}+C_{400}}\Big[A_{CQ3}\,C_{404}\,R_{11}C_{406} + (V_{C4}+V_{C2})\,C_{406} - (C_{405}R_{11} - E_{D5} + C_{401})\,C_{406} + C_{407}(R_{11}+C_{406})\Big]$$

Substituting equations (N4)'-4, (N10)', (Vy-1), and (Q3) into equation (Q-2) and solving for A_{EQ2} gives:

(Q-2)-4 $$A_{EQ2} = -(E_6 - V_{C1})\,C_{449} + V_{C2}\,C_{450} - (V_{C3}+V_{C4})\,C_{451} + C_{452}$$

By substituting equation (Q3) into equation (N8)'-P4 an equation is obtained for computing AC4 using the value of A_{EQ2} obtained from equation (Q-2)-4 above and making this substitution and combining constants, equation (N8)'-P4 can be written as:

(N8)-4 $$A_{C4} = (A_{EQ2})\,C_{806} - (V_{C3}+V_{C4})\,C_{804} - C_{807}$$

if $$\left[(A_{EQ2})\,C_{806} - (V_{C3}+V_{C4})\,C_{804} - C_{807}\right] > 0$$

The value of A_{EQ2} from equation (Q-2)-4 may also be used for computing VB.

Using equations (Q-2)-3, (VB) and (N8)-4 the assumption that $A_{C4} > 0$, $A_{CQ3} > C_{405}/C_{404}$ and VB > 0 can be tested. If the test is affirmative, then values for A_{C4}, A_{R3} and EV can be computed. If the test is negative another conditions must be tested for.

Tables A15 and A16 are a summary of test equations developed in the same manner as above. Since equation (Q3) establishes a linear relationship between A_{EQ2} and A_{CQ3} and since A_{EQ2} needs to be computed as a step in the computation of A_{R3}, the test equations for A_{CQ3} will be performed implicitly by computing A_{EQ2} and comparing its computed value to C607 where C607 is defined as:

$$C607 = \frac{C_{405}}{(C_{404})(C_{606})}$$

Currents A_{C4} and A_{EQ2} are computed using the applicable test condition equations.

Table A15 Valve Amplifier Operating Mode Test Equations

Circuit Condition, n	Applicable Equation (6a-Q2-n) (See Note)
1	$A_{EQ2} = -(E_G - V_{C1})C456 - (V_{C3} + V_{C4})C457 + C458$
2	$A_{EQ2} = V_{C2}C461 - (E_G - V_{C1})C459 - (V_{C3} + V_{C4})C460 + C462$
3	$A_{EQ2} = -(E_G - V_{C1})C446 - (V_{C3} + V_{C4})C447 + C448$
4	$A_{EQ2} = V_{C2}C450 - (E_G - V_{C1})C449 - (V_{C3} + V_{C4})C451 + C452$
5	$A_{EQ2} = -(E_G - V_{C1})C531 + C532$
6	$A_{EQ2} = V_{C2}C533 - (E_G - V_{C1})C534 - C535$
7	$A_{EQ2} = -(E_G - V_{C1})C526 + C527$
8	$A_{EQ2} = V_{C2}C528 - (E_G - V_{C1})C529 - C530$
9	$A_{EQ2} = -(E_G - V_{C1})C565 - (V_{C2} + V_{C4})C566 + C567$
10	$A_{EQ2} = V_{C2}C568 - (E_G - V_{C1})C569 - (V_{C2} + V_{C4})C570 - C571$
11	$A_{EQ2} = -(E_G - V_{C1})C575 - (V_{C2} + V_{C4})C576 + C577$
12	$A_{EQ2} = V_{C2}C578 - (E_G - V_{C1})C579 - (V_{C2} + V_{C4})C580 - C581$

Notes:

1. For circuit conditions 1, 2, 5, 6, 9 and 10 - if $AEQ2 < 0$, set $AEQ2 = 0$
2. For circuit conditions 3, 4, 7, 8, 11 and 12 - if $AEQ2 > C802$, set $AEQ2 = C802$

Table A16   Capacitor C4 Current Mode Test Equations

Circuit Condition, n	Applicable Equation (6a-N8-n)
1 & 2	$A_{C4} = (A_{EQ2})C_{806} - (V_{C3}+V_{C4})C_{804} - C_{807}$ IF $[(A_{EQ2})C_{806} - (V_{C3}+V_{C4})C_{804} - C_{807}] > 0$
3 & 4	$A_{C4} = (A_{EQ2})C_{803} - (V_{C3}+V_{C4})C_{804} - C_{805}$ IF $[(A_{EQ2})C_{803} - (V_{C3}+V_{C4})C_{804} - C_{805}] > 0$
5 & 6	$A_{C4} = 0$ IF $[(A_{EQ2})C_{806} - (V_{C3}+V_{C4})C_{804} - C_{807}] \leq 0$ AND $[(A_{EQ2})C_{811} - (V_{C2}+V_{C4})C_{809} - C_{812}] \geq 0$
7 & 8	$A_{C4} = 0$ IF $[(A_{EQ2})C_{803} - (V_{C3}+V_{C4})C_{804} - C_{805}] \leq 0$ AND $[(A_{EQ2})C_{808} - (V_{C2}+V_{C4})C_{809} - C_{810}] \geq 0$
9 & 10	$A_{C4} = (A_{EQ2})C_{811} - (V_{C2}+V_{C4})C_{809} - C_{812}$ IF $[(A_{EQ2})C_{811} - (V_{C2}+V_{C4})C_{809} - C_{812}] < 0$
11 & 12	$A_{C4} = (A_{EQ2})C_{808} - (V_{C2}+V_{C4})C_{809} - C_{810}$ IF $[(A_{EQ2})C_{808} - (V_{C2}+V_{C4})C_{809} - C_{810}] < 0$

For the cases where $A_{EQ2} >$ C607 an upper limit must be established to represent saturation of the valve drive amplifier. This upper limit is called C802 and applies to the applicable circuit conditions noted on Table A15.

Table A17 Summary of Equations for Computing Current A_{05}

Circuit Condition, n	Applicable Equation 6a-N5-n (See Note)
1 & 2	$A_{05} = A_{VAI}\, C_{606} - A_{C4}$
3 & 4	$A_{05} = A_{VAI}\, C_{606}\, C_{404} - C_{405} - A_{C4}$
5 & 6	$A_{05} = A_{VAI}\, C_{606}$
7 & 8	$A_{05} = A_{VAI}\, C_{606}\, C_{404} - C_{405}$
9 & 10	$A_{05} = A_{VAI}\, C_{606} - A_{C4}$
11 & 12	$A_{05} = A_{VAI}\, C_{606}\, C_{404} - C_{405} - A_{C4}$
Note: For all circuit conditions if $A_{05} < 0$, set $A_{05} = 0$	

As shown on Figure A49 the locked wheel prevention circuit elements also have an input to the valve control amplifier. In the equations thus far it has been assumed that the locked wheel skid signal, A_{LWS} at node (N15), is zero. When computing the valve voltage, it is necessary that the non-zero value of A_{LWS} be accounted for. If A_{LWS} is not zero then equation (Q3) is:

$$\text{(Q3-1)} \qquad A_{CQ3} = C_{606}\, A_{EQ2} + h_{FE3}\, A_{LWS}$$

Since A_{LWS} is a two valued variable (i.e. either zero or the value required to drive the amplifier as necessary to achieve full brake release) insofar as valve voltage computation is concerned, it can be considered as a current which can be added to A_{EQ2} in Equation (Q3). If we define a current A_{VAI} , valve amplifier input current, as:

$$\text{(LW-1)} \qquad A_{VAI} = A_{EQ2} + A_{LWS}$$

and treat this current like A_{EQ2} in equation (Q3) and if we substitute equations (Q3) and (N7)" into equation (N5) an equation for computing A_{DS} is formulated for each circuit condition. Current A_{DS} is then used in equation (N4) to compute EV. Table A17 lists the version of equation (N5) which is to be used for computing current A_{DS} for each circuit condition.

Since the variables EG and VC1 are always used in the form of their difference, we will define the difference as equation (5)

$$\text{(5)} \qquad E_G - V_{C1} = (E_G - V_{C1})$$

For the cases where the antiskid control circuit mathematical model is used with the flywheel system or three dimensional airplane system, the flywheel velocity, VF, or the airplane velocity, X, as applicable, will be used as the airplane speed reference circuit element. The wheel speed comparison element will be described as follows:

$$\text{(6)} \qquad \begin{aligned} A_{LWS} &= C_{617} \quad \text{FOR } V_F > C_{615} \text{ AND } E_G < C_{616} \\ &= 0 \quad \text{FOR } V_F \leq C_{615} \text{ OR } E_G \geq C_{616} \end{aligned}$$

Table A18 Modulated Antiskid Circuit Equation Summary (Sheet 1 of 2)

Equation No.	Equation
(6a-1)	$V_{C1} = \int \dot{V}_{C1}\, dt$
(6a-A1)	$\dot{V}_{C1} = A_{C1}\, C_{608}$
(6a-2)	$V_{C2} = \int \dot{V}_{C2}\, dt$
(6a-A2)	$\dot{V}_{C2} = A_{C2}\, C_{609}$
(6a-3)	$V_{C3} = \int \dot{V}_{C3}\, dt$
(6a-A3)	$\dot{V}_{C3} = A_{C3}\, C_{610}$
(6a-4)	$V_{C4} = \int \dot{V}_{C4}\, dt$
(6a-4A)	$\dot{V}_{C4} = A_{C4}\, C_{611}$
(6a-5)	$(E_G - V_{C1}) = E_G - V_{C1}$
(6a-6)	$A_{LWS} = \begin{cases} C_{617} & \text{FOR } V_F > C_{615} \text{ AND } E_G < C_{616} \\ 0 & \text{FOR } V_F \leq C_{615} \text{ OR } E_G \geq C_{616} \end{cases}$
(6a-LW-1)	$A_{VAI} = A_{EQ2} + A_{LWS}$
(6a-N3)	$A_{C3} = \begin{cases} A_{C4} - V_{C3}\, C_{619} - A_{BQ4} & \text{FOR } A_{C4} > 0 \\ - V_{C3}\, C_{619} - A_{BQ4} & \text{FOR } A_{C4} \leq 0 \end{cases}$
(6a-N4)	$E_V = A_{D5}\, C_{406} + C_{407}$
(6a-N5-n)	See Table A17
(6a-N8-n)	See Table A16

Table A18 Modulated Antiskid Circuit Equation Summary (Sheet 2 of 2)

Equation No.	Equation
(6a-N10)	$A_{R3} = A_{EQ2} C_{612} + [E_V - (E_G - V_{C1})] C_{613}$
(6a-N11)	$A_{C1} = A_{D8} - A_{R3} - A_{CQ1}$
(6a-N14)	$A_{C2} = \begin{cases} A_{BQ4} C_{614} + A_{C4} - V_{C2} C_{618} & \text{FOR } A_{C4} < 0 \\ A_{BQ4} C_{614} - V_{C2} C_{618} & \text{FOR } A_{C4} \geq 0 \end{cases}$
(6a-Q2-n)	See Table A15
(6a-Q-1C)	$A_{CQ1} = \begin{cases} C_{604} - C_{605} V_{C2} & \text{FOR } (E_G - V_{C1}) < 0 \\ 0 & \text{FOR } (E_G - V_{C1}) \geq 0 \\ 0 & \text{FOR } V_{C2} \geq C_{604}/C_{605} \end{cases}$
(6a-R10)	$A_{D8} = \begin{cases} (E_G - V_{C1}) C_{620} - C_{621} & \text{FOR } (E_G - V_{C1}) > C_{621}/C_{620} \\ 0 & \text{FOR } (E_G - V_{C1}) \leq C_{621}/C_{620} \end{cases}$
(6a-VB)	$V_B = V_{C2} C_M + A_{EQ2} C_{801} - C_{800}$
(6a-VQ4)	$A_{BQ4} = \begin{cases} (V_{C3} - V_{C2}) C_{622} - C_{623} & \text{FOR } (V_{C3} - V_{C2}) > C_{623}/C_{622} \\ 0 & \text{FOR } (V_{C3} - V_{C2}) \leq C_{623}/C_{622} \end{cases}$

The conditions which define the circuit's mode of operation at a particular instant are: (1) the current, $AC4$, into capacitor $C4$ is either positive, negative or zero, (2) the valve control amplifier is operating either in the cutoff mode or in the amplification mode, and (3) the modulating circuit element is either providing a pressure bias signal or it is not. The valve amplifier condition is indicated by current $AEQ2$ being equal to or less than C607 in the cutoff mode and being greater than C607 in the amplification mode. The pressure bias signal is indicated as existing when voltage VB is greater than zero and as not existing when VB is equal to or less than zero.

Table A18 summarizes the modulated antiskid circuit equations and the equation flow diagram is shown on Figure A52.

B. Parameter Evaluation

Table A19 lists the parameters defining the modulated circuit's operation. The values for the constants are computed from various circuit element characteristics (resistance, capacitance, etc.) as described in reference 13 and in the semiconductor component manufacturers catalogs.

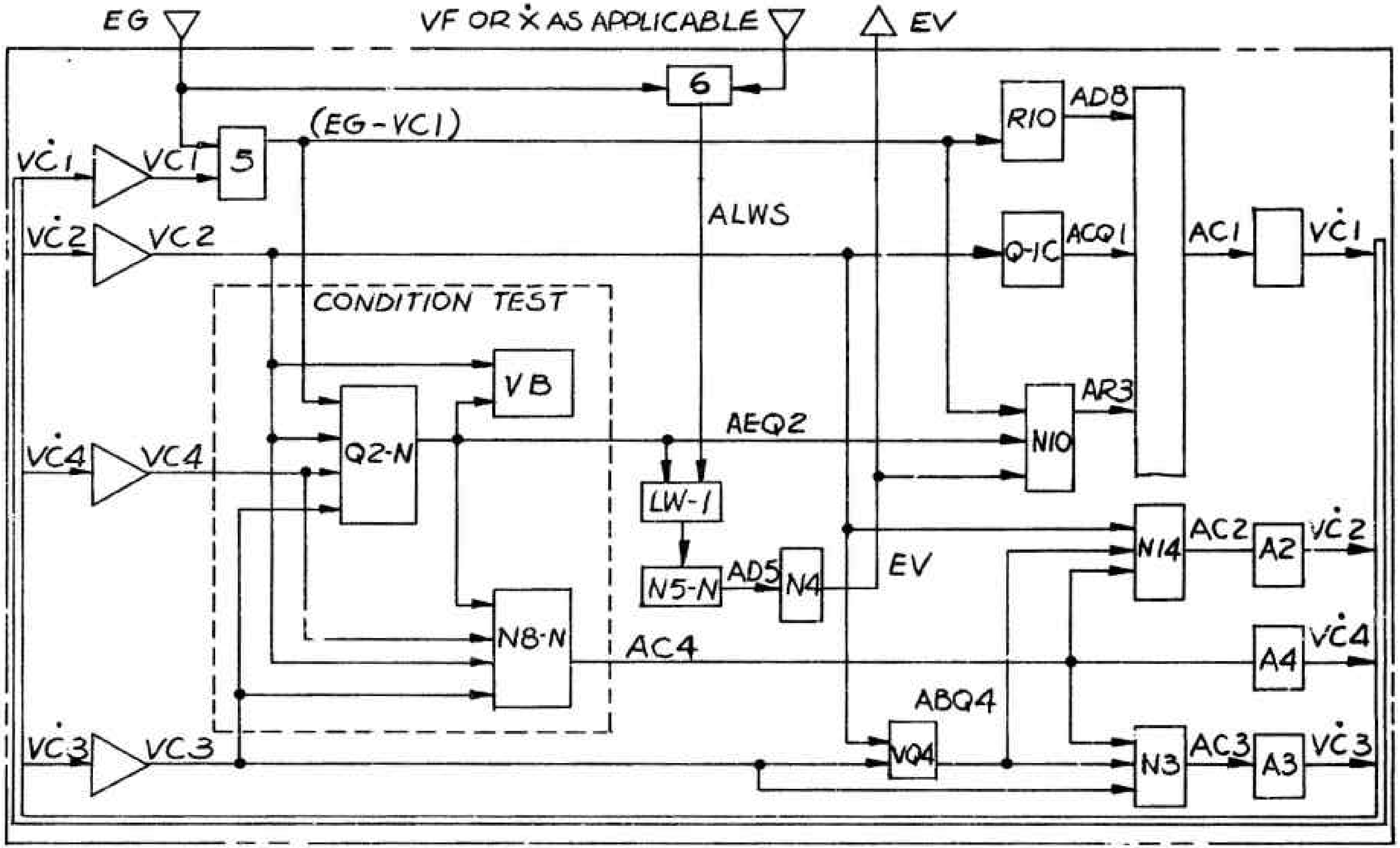

Figure A52 Modulated Antiskid Circuit Equation Flow Diagram

Table A19 Modulated Control System Parameters (Sheet 1 of 4)

Symbol	Type	Value	Units	Description (See Note)
A_{BQ4}	v		Amps	Transistor Q4 Base Current
A_{C1}	v		Amps	Current thru Capacitor C1
A_{C2}	v		Amps	Current thru Capacitor C2
A_{C3}	v		Amps	Current thru Capacitor C3
A_{C4}	v		Amps	Current thru Capacitor C4
A_{CQ1}	v		Amps	Transistor Q1 Collector Current
A_{D5}	v		Amps	Current thru Diode D5
A_{D8}	v		Amps	Current thru Diode D8
A_{EQ2}	v		Amps	Transistor Q2 Emitter Current
A_{EQ4}	v		Amps	Transistor Q4 Emitter Current
A_{R3}	v		Amps	Current thru Resistor R3
E_G	v(I)		Volts	Input Signal from Wheel Speed Sensor
V_B	v		Volts	Circuit Condition Determination Voltage
V_{C1}	v		Volts	Voltage Across Capacitor C1
V_{C10}	c	12.08	Volts	Voltage across Capacitor C1 at Time Zero
V_{C2}	v		Volts	Voltage across Capacitor C2
V_{C20}	c	0.0	Volts	Voltage across Capacitor C2 at Time Zero
V_{C3}	v		Volts	Voltage across Capacitor C3
V_{C30}	c	0.0	Volts	Voltage across Capacitor C3 at Time Zero
V_{C4}	v		Volts	Voltage across Capacitor C4
V_{C40}	c	0.0	Volts	Voltage across Capacitor C4 at Time Zero
E_V	v(o)		Volts	Antiskid Valve Voltage
A_{LWS}	v		Amps	Locked Wheel Skid Signal
V_F	v(I)		In/Sec	Flywheel Velocity
C_M	c	0.23	Dimls	VG2 Voltage Coefficient EQU VB-n
N	v		Dimls	Circuit Condition Number, Integer 1-12

Note: All equation numbers in Description are preceded by 6a. For example, EQU VB-n means equations number 6a-VB-n.

Table A19 Modulated Control System Parameters (Sheet 2 of 4)

Symbol	Type	Value	Units	Description (See Note page)
C404	c	2476.0	Dimls	ACQ3 Coeff. EQU N7, N5-3-4, N5-7-8, N5-11-12
C405	c	0.106	Amps	Const EQU N7, N5-3-4, N5-78, N5-11-12
C406	c	66.0	Ohms	AD5 Coefficient EQU N4
C407	c	1.51	Volts	Const. EQU N4
C446	c	1.825×10^{-6}	Mhos	(EG-VC1) Coefficient EQU Q2-3
C447	c	0.144×10^{-8}	Mhos	(VC3 + VC4) Coefficient EQU Q2-3
C448	c	0.465×10^{-6}	Amps	Const EQU Q2-3
C449	c	1.86×10^{-6}	Mhos	(EG-VC1) Coefficient EQU Q2-4
C450	c	0.474×10^{-6}	Mhos	VC2 Coefficient EQU Q2-4
C451	c	0.144×10^{-8}	Mhos	(VC3 + VC4) Coefficient EQU Q2-4
C452	c	-1.567×10^{-6}	Amps	Const EQU Q2-4
C456	c	34.0×10^{-6}	Mhos	(EG-VC1) Coefficient EQU Q2-1
C457	c	0.027×10^{-6}	Mhos	(VC3 + VC4) Coefficient EQU Q2-1
C458	c	-17.1×10^{-6}	Amps	Const EQU QL-1
C459	c	52.0×10^{-6}	Mhos	(EG-VC1) Coefficient EQU Q2-2
C460	c	0.027×10^{-6}	Mhos	(VC3 + VC4) Coefficient EQU Q2-2
C461	c	13.25×10^{-6}	Mhos	VC2 Coefficient EQU Q2-2
C462	c	-83.4×10^{-6}	Amps	Const EQU Q2-2
C526	c	1.825×10^{-6}	Mhos	(EG-VC1) Coefficient EQU Q2-7
C527	c	0.465×10^{-6}	Amps	Const EQU Q2-7
C528	c	0.474×10^{-6}	Mhos	VC2 Coefficient EQU Q2-8
C529	c	1.86×10^{-6}	Mhos	(EG-VC1) Coefficient EQU Q2-8
C530	c	1.567×10^{-6}	Amps	Const. EQU Q2-8
C531	c	34.0×10^{-6}	Mhos	(EG-VC1) Coefficient EQU Q2-5
C532	c	-17.1×10^{-6}	Amps	Const. EQU Q2-5
C533	c	13.25×10^{-6}	Mhos	VC2 Coefficient EQU Q2-6
C534	c	52.0×10^{-6}	Mhos	(EG-VC1) Coefficient EQU Q2-6
C535	c	83.4×10^{-6}	Amps	Const. EQU Q2-6
C56[illegible]	c	34.0×10^{-6}	Mhos	(EG-VC1) Coefficient EQU Q2-9

Table A19 Modulated Control System Parameters (Sheet 3 of 4)

Symbol	Type	Value	Units	Description (See Note page)
C566	c	0.014×10^{-6}	Mhos	(VC2 + VC4) Coefficient EQU Q2-9
C567	c	-17.1×10^{-6}	Amps	Const. EQU Q2-9
C568	c	13.25×10^{-6}	Mhos	VC2 Coefficient EQU Q2-10
C569	c	52.0×10^{-6}	Mhos	(EG-VC1) Coefficient EQU Q2-10
C570	c	0.014×10^{-6}	Mhos	(VC2 + VC4) Coefficient EQU Q2-10
C571	c	66.5×10^{-6}	Amps	Const. EQU Q2-10
C575	c	1.825×10^{-6}	Mhos	(EG-VC1) Coefficient EQU Q2-11
C576	c	0.001×10^{-6}	Mhos	(VC2 + VC4) Coefficient EQU Q2-11
C577	c	0.465×10^{-6}	Amps	Const. EQU Q2-11
C578	c	0.474×10^{-6}	Mhos	VC2 Coefficient EQU Q2-12
C579	c	1.86×10^{-6}	Mhos	(EG-VC1) Coefficient EQU Q2-12
C580	c	0.001×10^{-6}	Mhos	(VC2 + VC4) Coefficient EQU Q2-12
C581	c	-1.567×10^{-6}	Amps	Const. EQU Q2-12
C604	c	16.1×10^{-6}	Amps	Const. EQU Q-1C
C605	c	7.25×10^{-6}	Mhos	VC2 Coefficient EQU Q-1C
C606	c	29.2	Dimensionless	Q3 Collector - Q2 Emitter Current Ratio
C607	c	1.46×10^{-6}	Amps	AEQ2 Comparison Constant
C608	c	$0.037 \times 10^{+6}$	Volts/Amp Sec	Reciprocal of Capacitance C1
C609	c	$3.03 \times 10^{+6}$	Volt/Amp Sec	Reciprocal of Capacitance C2
C610	c	$0.833 \times 10^{+5}$	Volt/Amp Sec	Reciprocal of Capacitance C3
C611	c	$0.222 \times 10^{+6}$	Volt/Amp Sec	Reciprocal of Capacitance C4
C612	c	0.901	Dimensionless	AEQ2 Coefficient EQU N10
C613	c	5.19×10^{-6}	Mhos	EV-(EG-VC1) Coefficient EQU N10
C614	c	36.0	Dimensionless	ABQ4 Coefficient EQU N14 - Q4
C615	c	352.0	In/Sec	Locked Wheel Arming Speed
C616	c	0.92	Volts	Locked Wheel Signal Detection Speed
C617	c	3.76×10^{-6}	Amps	Locked Wheel Signal Current
C618	c	7.7×10^{-6}	Mhos	VC2 Coefficient EQU N14
C619	c	7.7×10^{-6}	Mhos	VC3 Coefficient EQU N3

Table A19 Modulated Control System Parameters (Sheet 4 of 4)

Symbol	Type	Value	Units	Description (See Note page)
C620	c	0.001	Mhos	(EG-VC1) Coefficient EQU R10
C621	c	600.0×10^{-6}	Amps	Const. EQU R10
C622	c	846.0×10^{-6}	Mhos	(VC3-VC2) Coefficient EQU VQ4
C623	c	593.0×10^{-6}	Amps	Const. EQU VQ4
C800	c	0.994	Volts	Constant EQU VB
C801	c	9167	Ohms	AEQ2 Coefficient EQU VB
C802	c	4.29×10^{-6}	Amps	Maximum Value for AEQ2 in EQU-Q2-N
C803	c	536.2	Dimls	AEQ2 Coefficient EQU N8-3, 4, 7 & 8
C804	c	109.1×10^{-6}	Mhos	(VC3 + VC4) Coefficient EQU N8-1,2,3,4,5,6,7,8
C805	c	552.0×10^{-6}	Amps	Constant EQU N8-3, 4, 7 & 8
C806	c	0.2166	Dimls	AEQ2 Coefficient EQU N8-1, 2, 5 & 6
C807	c	-230.4×10^{-6}	Amps	Constant EQU N8-1, 2, 5 & 6
C808	c	222.8	Dimls	AEQ2 Coefficient EQU N8-7, 8, 11 & 12
C809	c	45.3×10^{-6}	Mhos	(VC2 + VC4) Coefficient EQU N8-5, 6, 7, 8, 9, 10, 11 & 12
C810	c	175.8×10^{-6}	Amps	Constant EQU N8-7, 8, 11 & 12
C811	c	0.090	Dimls	AEQ2 Coefficient EQU N8-5, 6, 9 & 10
C812	c	-150.1×10^{-6}	Amps	Constant EQU N8-5, 6, 9 & 10
No	c	1	Dimls	Circuit Condition at Time Zero
$\dot{V}C1$	v		Volts/Sec	Capacitor C1 Voltage Change Rate
$\dot{V}C10$	c	0.0	Volts/Sec	Capacitor C1 Voltage Change Rate at Time Zero
$\dot{V}C2$	v		Volts/Sec	Capacitor C2 Voltage Change Rate
$\dot{V}C20$	c	0.0	Volts/Sec	Capacitor C2 Voltage Change Rate at Time Zero
$\dot{V}C3$	v		Volts/Sec	Capacitor C3 Voltage Change Rate
$\dot{V}C30$	c	0.0	Volts/Sec	Capacitor C3 Voltage Change Rate at Time Zero
$\dot{V}C4$	v		Volts/Sec	Capacitor C4 Voltage Change Rate
$\dot{V}C40$	c	0.0	Volts/Sec	Capacitor C4 Voltage Change Rate at Time Zero

6b. ON-OFF ANTISKID CONTROL CIRCUIT

Most aircraft on-off type antiskid systems operate according to the functional block diagram shown on Figure A53 The various functional elements may be electrical, mechanical or a combination of electrical and mechanical devices. If during braking the brake torque applied to the wheel exceeds the amount which can be reacted by friction at the tire-ground interface, the antiskid system operates to prevent tire skids as follows. A wheel speed signal is provided to a deceleration detection element where the wheel's deceleration rate is computed and compared to a threshold value which is provided by a skid detection threshold element. The deceleration detector produces a skid signal whenever the wheel's deceleration rate exceeds the threshold value. The wheel speed signal is also supplied to a wheel speed reference element and a wheel speed comparison element. The wheel speed reference element is a "memory" device which produces a "comparison index." The "comparison index" is the wheel's initial unbraked speed minus an adjustment to account for the aircraft's deceleration. The wheel speed comparison element compares wheel speed to the "comparison index" and produces a skid signal whenever the wheel speed is less than the "comparison index." The deceleration detection element initiates a skid signal and the wheel speed comparison element maintains the skid signal until the wheel has regained most of its initial speed. The skid signals from both the deceleration detection element and the wheel speed comparison element are transmitted to a valve control element which acts to control the antiskid valve such that the brake is released when a skid signal exists and the brake is applied when a skid signal does not exist.

An electrical system of the form shown on Figure A54 or a mechanical device as shown on Figure A56 are the most common means used for implementing the on-off antiskid system function.

Electrical On-Off Antiskid System

Figure A54 is a schematic diagram of the Goodyear electrical on-off antiskid control circuit as used on the Lockheed F104 and General Dynamics B-58 aircraft. This circuit accomplishes on-off antiskid control according to the preceding functional description as follows: The wheel speed

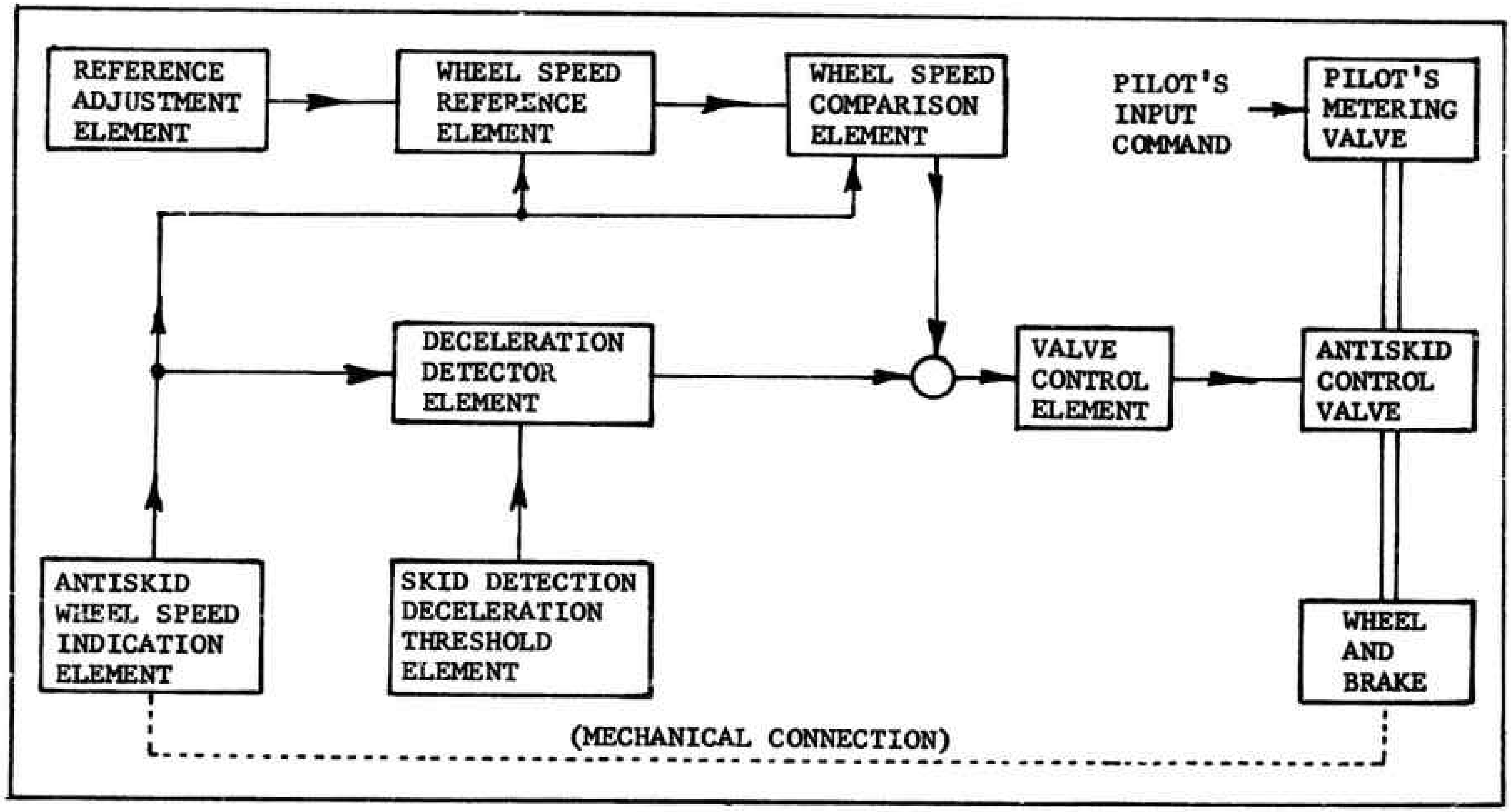

Figure A53 On-Off Antiskid Control Functional Block Diagram

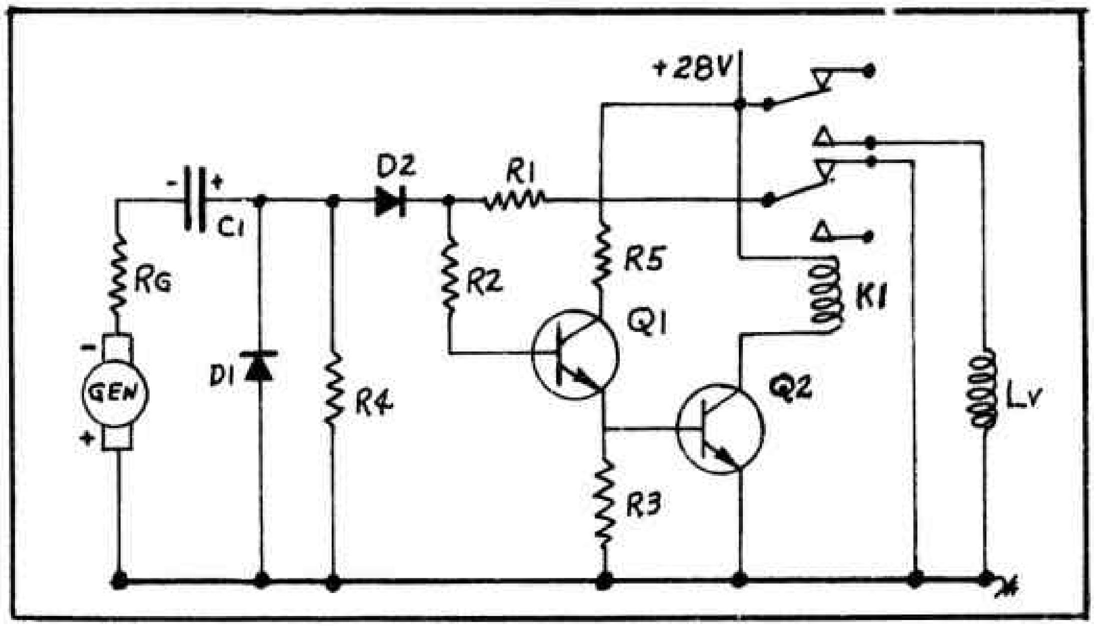

(A) Schematic Diagram

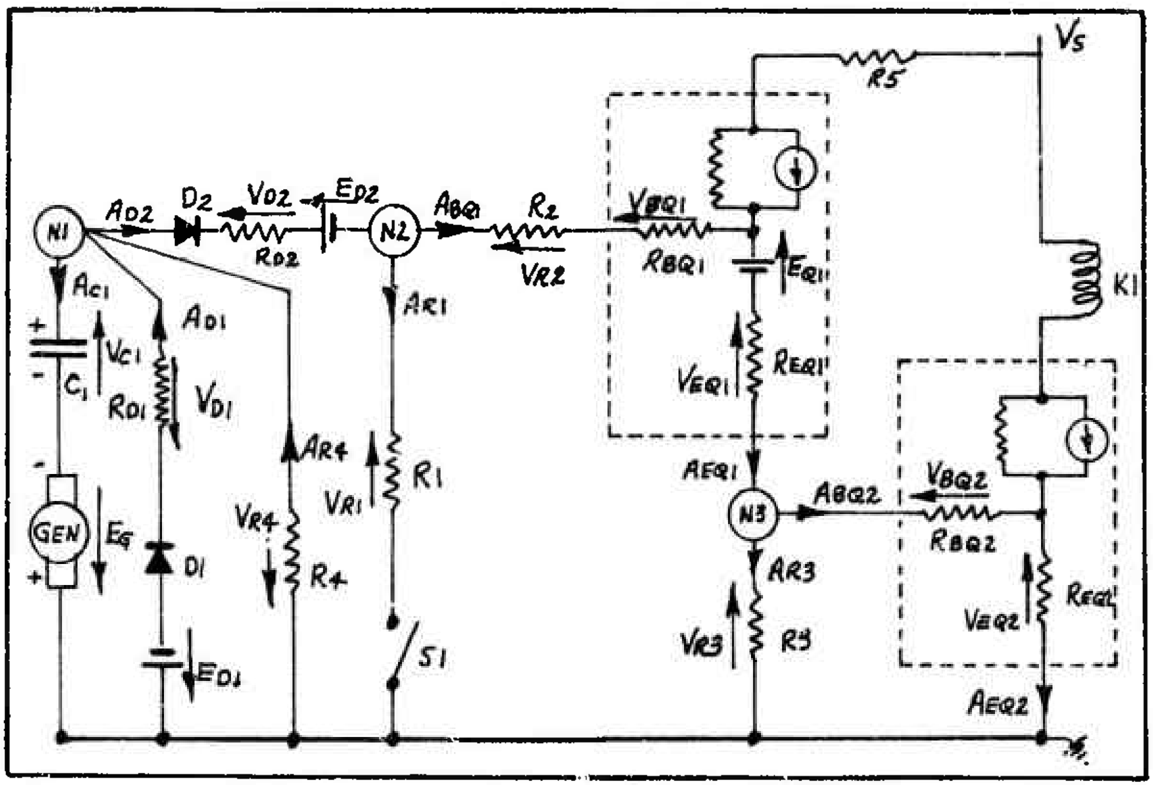

(B) Mathematical Identification Showing Transistors and Diodes in Terms of their Equivalent Circuits

Figure A54 Electrical On-Off Antiskid Control Circuit

indication element, a wheel driven D. C. tachometer generator (GEN), supplies an input voltage EG which is proportional to wheel speed. EG charges capacitor C1 through R5, Diode D1 and Resistance RG during wheel spin-up. Capacitor C1 is both the deceleration detector and the wheel speed reference element. For normal wheel deceleration rates, with no incipient skidding, the generator voltage decreases relatively slowly and a small current will flow from the positive side of C1 through R5 and through D2 and R1, (GEN) and RG to the negative side of C1. This current discharges C1 and causes its voltage to closely follow EG. The amplifier comprised of R2, Q1, R3, R4 and Q2 acts as the skid detection deceleration threshold element, the wheel speed comparison element, and, in conjunction with relay K1, the valve control element. When an incipient skid occurs, the generator voltage decreases rapidly. R5 and R1 limit the discharge current flow into C1 so that the voltage at the positive side of C1 increases. The value of the voltage at the positive side of C1 is proportional to wheel deceleration rate. The amplifier characteristics are set so that when the voltage at the positive side of C1 is a value V_{SDT} or greater, enough current flows into the base of Q1 to cause Q2 to conduct sufficiently for relay K1 to actuate. When relay K1 actuates the supply voltage is applied to the antiskid valve coil LV. The voltage across the antiskid valve coil, EV, is equal to the supply voltage. Actuation of relay K1 also causes R1 to be disconnected from ground so that the resistance in the discharge path of C1 is increased to aid its action as a wheel speed reference. Voltage V_{SDT} is the skid detection threshold. More modern versions of this circuit utilize transistors to perform the function of relay K1; however, their operation is the same. Resistor R5 is the speed reference adjustment element.

A-1 Electrical On-Off Mathematical Description

The mathematical description of the electrical circuit's operation is developed from Figure A54(b) which is the schematic from Figure A54(a) with the transistors and diodes shown in terms of their equivalent circuits and the appropriate currents and voltages identified.

The voltage across capacitor C1 is defined by:

(6b-1-1) $$V_{C1} = \int \dot{V}_{C1}\, dt$$

where (6b-1-A1) $\dot{V}_{C1} = A_{C1} C_{705} \qquad (C_{705} = 1/C_1)$

Current AC1 is established by summing currents at node N1 as:

(6b-1-N1) $$A_{C1} = A_{D1} + A_{R4} - A_{D2}$$

Using Ohm's law and summing voltages around the loop of which RD1 is a part, current AD1 is established as:

(6b-1-R1) $$A_{D1} = E_G - V_{C1} - E_{D1} / R_{D1} \qquad \text{FOR } (E_G - V_{C1} - E_{D1}) > 0$$
$$= 0 \qquad \text{FOR } (E_G - V_{C1} - E_{D1}) \leq 0$$

To combine constants, write equation (6b-1-R1) as:

$$A_{D1} = (E_G - V_{C1}) C_{706} - C_{707} \qquad \text{FOR } (E_G - V_{C1}) > \frac{C_{707}}{C_{706}}$$
$$= 0 \qquad \text{FOR } (E_G - V_{C1}) \leq \frac{C_{707}}{C_{706}}$$

Noting that because of diode D1, A_{D1} is restricted to positive values only.

In a similar manner, using Ohm's law and summing voltages around the loop containing R4, current A_{R4} is established as:

(6b-1-V2) $$A_{R4} = (E_G - V_{C1}) / R_4 \quad \text{OR} \quad A_{R4} = (E_G - V_{C1}) C_{708}$$

Summing currents at node N2 and noting that because of diode D2, current AD2 cannot be negative gives:

(6b-1-N2) $$A_{D2} = A_{BQ1} + A_{R1} \quad \text{FOR } (A_{BQ1} + A_{R1}) \geq 0$$
$$= 0 \quad \text{FOR } (A_{BQ1} + A_{R1}) < 0$$

By Ohm's law the voltage across RD2 is

(6b-1-V3) $$V_{D2} = A_{D2} R_{D2}$$

For the case where no skid signal exists and relay K1 is not actuated, R1 is connected to ground and a current AR1 may flow. Using Ohm's law and by summing voltages around the loop R1, D2, C1 and (GEN), A_{R1} is established as :

(6b-1-V4) $$A_{R1} = V_{C1} - E_G - E_{D2} - V_{D2} / R_1$$

Since the variables EG and VC1 are always used in the form of their difference, define the difference as:

(6b-1-3) $$(E_G - V_{C1}) = E_G - V_{C1}$$

By substituting (6b-1-V3) and (6b-1-N2) into (6b-1-V4),

(6v-1-V4)' $$A_{R1} = \frac{(V_{C1} - E_G - E_{D2})}{R_{D2} + R_1} - \frac{A_{BQ1} R_{D2}}{R_{D2} - R_1}$$

By summing currents at node N3, current AEQ1 is

(6b-1-N3) $$A_{EQ1} = A_{BQ2} + A_{R3}$$

By summing voltages around the loop containing R3 and the base and emitter of Q2,

(6b-1-V5) $$0 = V_{R3} - V_{BQ2} - V_{EQ2}$$

Note: For Q2 the base-emitted junction potential has been omitted to reduce mathematical complexity. This is justified because whether or not Q2 is conducting has negligible effect on current A_{C1}.

By substituting (6b-1-N3) along with the Ohm's law expressions $A_{BQ2} = V_{BQ2}/R_{BQ2}$ AND $A_{EQ2} = V_{EQ2}/R_{EQ2}$ and the transistor characteristic $A_{EQ2} = (h_{FE2}+1)A_{BQ2}$ into (6b-1-V5) and solving for A_{BQ2},

(6b-1-V5)' $$A_{BQ2} = \frac{A_{EQ1}\, R_3}{R_{BQ2} + R_3 + R_{EQ2}\,(h_{FE2}+1)}$$

By substituting (6b-1-V5)' and (6b-1-N3) into the Ohm's law expression $V_{R3} = A_{R3}\, R_3$

(6b-1-2) $$V_{R3} = R_3\, A_{EQ1}\left[1 - \frac{R_3}{R_{BQ2} + R_3 + R_{EQ2}(h_{FE2}+1)}\right]$$

By summing voltages around the loop R3, REQ1, EQ1, RBQ1, R2, RD2, C1 and (GEN)

(6b-1-V6) $0 = V_{R3} + V_{EQ1} + E_{Q1} + V_{BQ1} + V_{R2} + E_{D2} + V_{D2} - V_{C1} + E_G$

By substituting (6b-1-2) and (6b-1-V4) along with the Ohm's law expressions $V_{EQ1} = A_{EQ1}\, R_{EQ1}$, $V_{BQ1} = A_{BQ1}\, R_{BQ1}$ and $V_{R2} = A_{BQ1}\, R_2$ and the transistor characteristic $A_{EQ1} = (h_{FE1}+1)\, A_{BQ1}$ into (6b-1-V6) and solving for A_{BQ1}:

(6b-1-V6)' $$A_{BQ1} = (V_{C1} - E_G)\, C_{701} - C_{702} \quad \text{FOR } (V_{C1}-E_G) > \frac{C_{702}}{C_{701}}$$
$$= 0 \quad \text{FOR } (V_{C1}-E_G) \le \frac{C_{702}}{C_{701}}$$

For the case where relay K1 is actuated and R1 is disconnected from ground the same substitution is made except that $V_{D2} = A_{BQ1}\, R_{D2}$ is used in place of equation (6b-1-V4)'. For the actual circuit components used on the aircraft, the resulting equation has coefficients that are negligibly different from (6b-1-V6)'; therefore, equation

(6b-1-V6)' will be used for both cases.

The value of A_{BQ1} which causes relay K1 to be actuated is defined as, C700, the skid detection threshold current. From this definition and equation (6b-1-V4)'

(6b-1-V4-1) $$A_{R1} = (V_{C1} - E_G)C_{709} - C_{710} - A_{BQ1}C_{711} \quad \text{FOR } A_{BQ1} < C_{700}$$
$$= 0 \quad \text{FOR } A_{BQ1} \geq C_{700}$$

When relay K1 is not actuated EV = 0, when relay K1 is actuated EV = VS; therefore,

(6b-1-EV) $$E_V = 0 \quad \text{FOR } A_{BQ1} < C_{700}$$
$$= V_S \quad \text{FOR } A_{BQ1} \geq C_{700}$$

The equation flow diagram for the electrical on-off control circuit is shown on Figure A55.

B-1 Electrical On-Off Parameter Evaluation

Table A20 lists the parameters and their values as applicable for the General Dynamics B-58 control circuit. (The same circuit is used on the Lockheed F-104.)

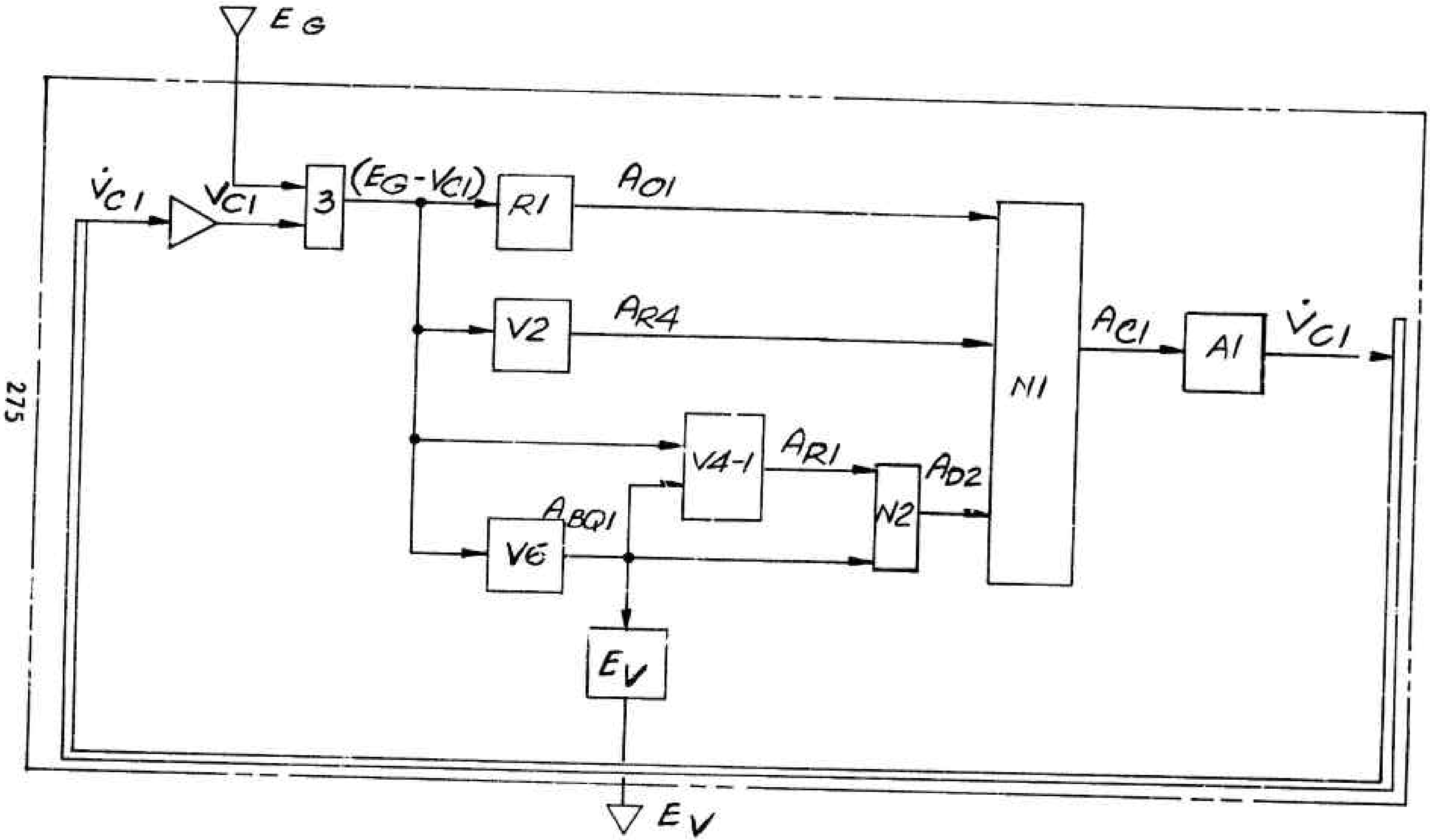

Figure A55 Electrical On-Off Circuit Equation Flow Diagram

Table A20 On-Off Control System Parameters

Symbol	Type	Value	Units	Description
A_{BQ1}	v		Amps	Transistor Q1 Base Current
A_{C1}	v		Amps	Current thru Capacitor C1
A_{D1}	v		Amps	Current thru Diode D1
A_{R1}	v		Amps	Current thru Resistor R1
A_{R4}	v		Amps	Current thru Resistor R4
E_G	v(I)		Volts	Input Signal from Wheel Speed Sensor
E_V	v(c)		Volts	Antiskid Valve Voltage
V_{C1}	v		Volts	Voltage across Capacitor C1
V_{C10}	c	0.0	Volts	Voltage across Capacitor C1 at Time Zero
V_{C1}	v		Volts/Sec	Capacitor C1 Voltage Change Rate
V_S	c	28.0	Volts	Supply Voltage
$C700$	c	17.5×10^{-6}	Amps	Skid Detection Threshold Current
$C701$	c	6.6×10^{-6}	Mhos	(EG - VC1) Coefficient EQU V6
$C702$	c	0.86×10^{-6}	Amps	Constant EQU V6
$C705$	c	$0.04 \times 10^{+6}$	Volt/Amp Sec	Reciprocal of Capacitance C1
$C706$	c	1667.0×10^{-6}	Mhos	(EG - VC1) Coefficient EQU R1
$C707$	c	1000.0×10^{-6}	Amps	Constant EQU R1
$C708$	c	19.35×10^{-6}	Mhos	(EG-VC1) Coefficient EQU V2
$C709$	c	161×10^{-6}	Mhos	(EG-VC1) Coefficient EQU V4-1
$C710$	c	96.8×10^{-6}	Amps	Constant EQU V4-1
$C711$	c	0.0968	Dimls	ABQ1 Coefficient EQU V4-1

Mechanical On-Off Antiskid Device

Figure A56 is a schematic drawing showing the operating principles of a commonly used mechanical on-off antiskid device of which the Hydroaire Hytrol Mk I and Dunlop Maxaret units are typical examples. The device operates as follows. The rotor (the wheel speed indication element) is connected to the aircraft wheel by some positive means such as a direct connection or gear train, etc., so that the rotor's angular velocity is a constant ratio of aircraft wheel speed. During spinup the motion of the rotor is transmitted through the clutch to the drum. The clutch is configured such that it is self-energizing for rotation in the direction of wheel rotation associated with forward airplane motion, shown here as counterclockwise. Stop (DS1) on the drum engages stop (FS1) on the flywheel, thereby transmitting torque to cause the velocity of the flywheel to be the same as the drum. The flywheel and the drum are connected by spring (CA)and damper (DA). As the aircraft wheel and rotor decelerate, a clockwise torque is transmitted through the clutch to the drum and from the drum through spring (CA) and damper (DA) to the flywheel. The amount of this torque is proportional to the product of the rotor's deceleration rate and the flywheel's inertia. The torque compresses spring (CA) so that the flywheel moves counterclockwise with respect to the drum. For steady airplane wheel deceleration the amount of relative motion between the flywheel and drum is proportional to the deceleration rate. A suitable mechanism (usually a set of electrical contact points or a cam device) connected between the flywheel and drum causes a valve to be actuated so that brake pressure is relieved whenever a pre-established amount of relative motion occurs. The clutch is also configured so that when the torque from the rotor to the drum is clockwise, the torque capacity is limited to some slightly greater amount than that required to initiate brake release. If the rotor experiences greater deceleration than that required to initiate brake release, the clutch slips and allows the drum and flywheel to overrun the rotor. The flywheel's inertia reacted by the drag of the clutch maintains a torque on spring (CA) so that the relative motion between the drum and flywheel (skid signal) is sustained until the flywheel's kinetic energy is dissipated or until the rotor has regained sufficient speed to eliminate clutch slippage. For this device the flywheel's inertia causing displacement of spring (CA) and damper (DA) is the

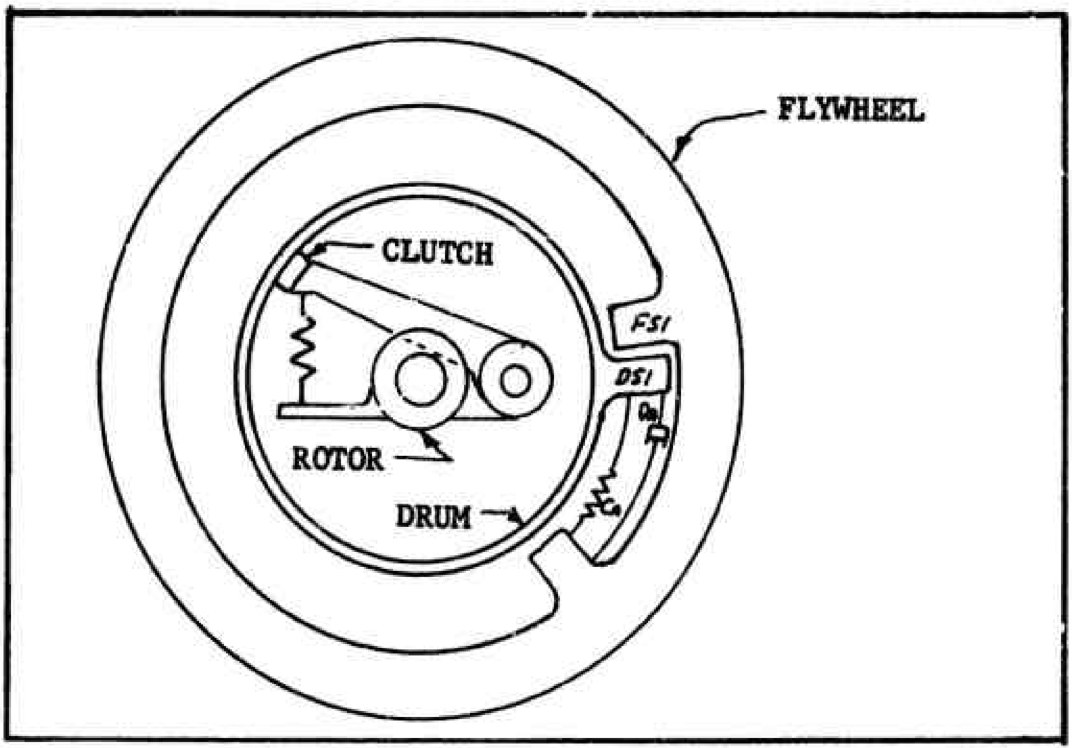

A. Functional Schematic

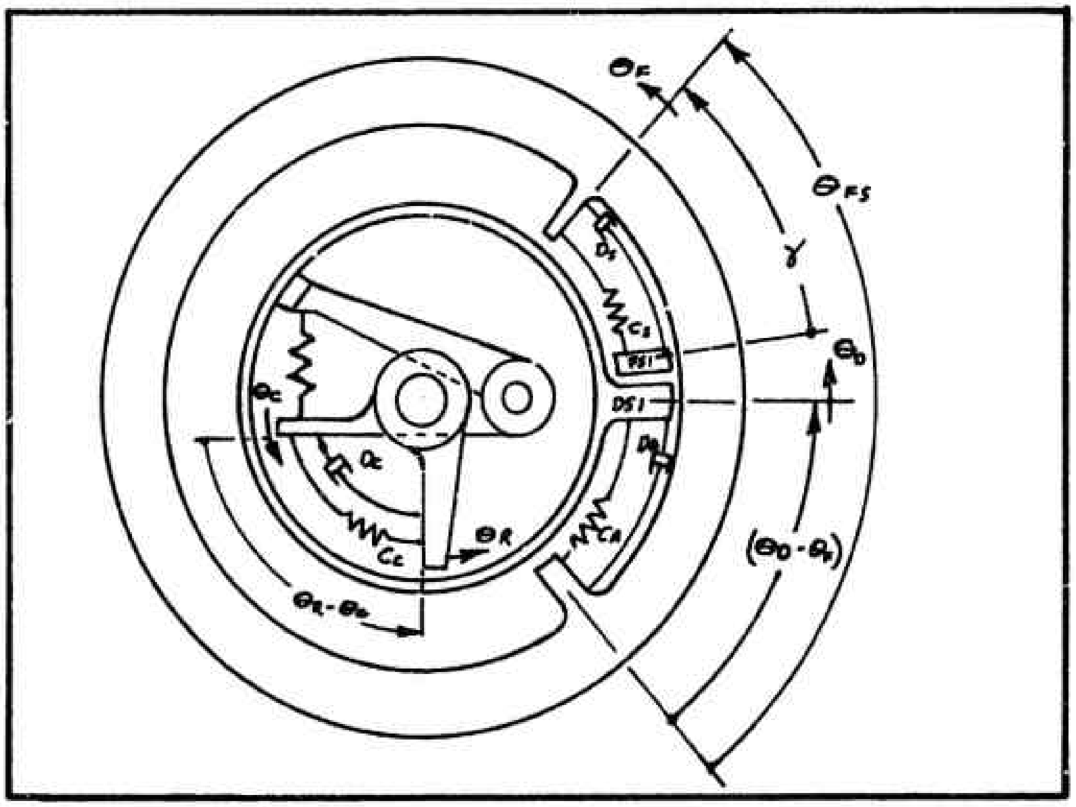

B. Mathematical Representation

Figure A56 Mechanical On-Off Antiskid Device

deceleration detector element, the clutch's overrunning drag torque on the drum is the reference adjustment element, the clutch is the wheel speed comparison element and the rotational kinetic energy of the flywheel is the wheel speed reference element.

A-2 Mechanical On-Off Mathematical Description

The mathematical description of the mechanical on-off anti-skid device is developed by referring to figure A56(B) which defines the applicable parameters and shows flywheel stop (FS1) represented by a spring-damper system. Also, a spring-damper system is added between the rotor and clutch carrier to represent the small motion which actually occurs during clutch operation.

At flywheel stop (FS1) there is a torque, TS, which is exerted on the flywheel by the drum, if drum stop (DS1) is in contact with FS1. If the mass of FS1 is considered small in comparison to the stop spring (CS) and stop damper (DS) then, setting the sum of torques on FS1 at zero:

(6b-2-1) $$T_S = C_S\,(\gamma_0 - \gamma) - D_S\,\dot{\gamma}$$

Where $C_S(\gamma_0 - \gamma)$ is the stop spring torque, $(-D_S\dot{\gamma})$ is the stop damper torque and γ_0 is the free length of spring CS.

Since TS results from a contact force, it cannot be less than zero; therefore, if $\gamma + (\theta_0 - \theta_F)$ is less than θ_{FS} then TS = 0. Rewriting equation (1) solving for $\dot{\gamma}$ gives:

(6b-2-2) $$\dot{\gamma} = C_S\,(\gamma_0 - \gamma) - T_S / D_S$$

γ is then established by:

(6b-2-3) $$\gamma = \int \dot{\gamma}\, dt$$

γ as computed from (6b-2-2) and (6b-2-3) is compared to $\theta_{FS} - (\theta_0 - \theta_F)$ to establish TS. If TS is other than zero, it is computed from (6b-2-1) using $\gamma = \theta_{FS} - (\theta_0 - \theta_F)$ AND $\dot{\gamma} = -(\dot{\theta}_0 - \dot{\theta}_F)$.

Substituting the above expressions for γ and $\dot{\gamma}$ into (6b-2-1) gives:

(6b-2-1-1) $TS = CS\left[\gamma_0 - \theta_{FS} + (\theta_D - \theta_F)\right] + D_S\,(\dot{\theta}_D - \dot{\theta}_F)$

$\qquad$ FOR $[\gamma + (\theta_D - \theta_F) - \theta_{FS}] \geq 0$

$= 0 \qquad$ FOR $[\gamma + (\theta_D - \theta_F) - \theta_{FS}] < 0$

Summing torques on the flywheel gives:

(6b-2-4) $$\ddot{\theta}_F = \left[T_S + C_A(\theta_D - \theta_F) + D_A(\dot{\theta}_D - \dot{\theta}_F)\right] / W_{FW}$$

Summing torques on the drum gives:

(6b-2-5) $$\ddot{\theta}_D = \left[-T_S - C_A(\theta_D - \theta_F) - D_A(\dot{\theta}_D - \dot{\theta}_F) + T_C\right] / W_D$$

Where T_C is the clutch torque.

Subtracting (6b-2-4) from (6b-2-5) results in:

(6b-2-6) $$(\ddot{\theta}_D - \ddot{\theta}_F) = \left(\frac{1}{W_D} + \frac{1}{W_{FW}}\right)\left[-T_S - C_A(\theta_D - \theta_F) - D_A(\dot{\theta}_D - \dot{\theta}_F)\right] + T_C / W_D$$

By integrating (6b-2-6) twice, $(\dot{\theta}_D - \dot{\theta}_F)$ and $(\theta_D - \theta_F)$ are established as

(6b-2-7) $$(\dot{\theta}_D - \dot{\theta}_F) = \int (\ddot{\theta}_D - \ddot{\theta}_F)\,dt$$

(6b-2-8) $$(\theta_D - \theta_F) = \int (\dot{\theta}_D - \dot{\theta}_F)\,dt$$

Substituting values for $(\theta_D - \theta_F)$ and $(\dot{\theta}_D - \dot{\theta}_F)$ computed from (6b-2-7) and (6b-2-8) into equation (6b-2-4) and integrating once establishes $\dot{\theta}_F$ as follows:

(6b-2-9) $$\dot{\theta}_F = \int \ddot{\theta}_F\,dt$$

Combining the results from (6b-2-7) and (6b-2-9) establishes $\dot{\theta}_D$ as:

(6b-2-10) $$\dot{\theta}_D = (\dot{\theta}_D - \dot{\theta}_F) + \dot{\theta}_F$$

The clutch will now be examined.

The torque exerted on the clutch carrier by the rotor, T_C, is defined by:

(6b-2-11) $$T_C = C_C\,(\theta_R - \theta_C) + D_C\,(\dot{\theta}_R - \dot{\theta}_C)$$

If, as for the flywheel stop, it is assumed that the clutch carrier inertia is negligibly small, the torque between the clutch and the drum equals the torque between the rotor and the clutch carrier. In this case equation (6b-2-11) may be solved for $(\dot{\theta}_R - \dot{\theta}_C)$ and by integrating once $(\theta_R - \theta_C)$ is obtained:

(6b-2-12) $$(\theta_R - \theta_C) = \int (\dot{\theta}_R - \dot{\theta}_C)\,dt$$

Where $(\dot{\theta}_R - \dot{\theta}_C)$ is obtained from the following version of (6b-2-11)

(6b-2-11-1) $$(\dot{\theta}_R - \dot{\theta}_C) = \left[T_C - C_C\,(\theta_R - \theta_C)\right] \Big/ D_C$$

It follows that:

(6b-2-13) $$\dot{\theta}_C = \dot{\theta}_R - (\dot{\theta}_R - \dot{\theta}_C)$$

If the clutch is configured so that there is no slipping for counterclockwise torque on the drum, $\dot{\theta}_C$ must equal $\dot{\theta}_D$ and any difference between $\dot{\theta}_R$ and $\dot{\theta}_D$ must be relative velocity between the clutch carrier and the rotor (i.e. $\dot{\theta}_R - \dot{\theta}_C$). If $\dot{\theta}_D$ is substituted for $\dot{\theta}_C$ in equation (6b-2-11) then the resulting equation can be used to compute the torque required to force $\dot{\theta}_C$ to be equal to $\dot{\theta}_D$. Therefore, making this substitution,

(6b-2-11-2) $$T_C = C_C\,(\theta_R - \theta_C) + D_C\,(\dot{\theta}_R - \dot{\theta}_D)$$

Equation (6b-2-11-2) adequately describes the component of clutch torque due to relative velocity; however, the component due to relative displacement is not satisfactorily described because the torque direction is independent of relative position. To compute the clutch torque for all conditions, equation (6b-2-11-2) will be modified and

a procedure for establishing the clutch condition will be defined. The clutch condition is established by the torque direction. The torque direction is determined by examining the direction the drum is attempting to move relative to the clutch. The direction of the drum's attempted movement relative to the clutch is established by comparing the drum velocity, $\dot{\theta}_D$, to the velocity, $\dot{\theta}_{CH}$, of a hypothetical or "index" clutch. The "index" clutch will be permitted to have slight slippage on the drum for counterclockwise torque so that there is a preceivable circumstance to indicate torque direction. To describe the "index" clutch motion relative to the rotor, equation (6b-2-11-1) is modified by substituting θ_{CH} and $\dot{\theta}_{CH}$ for θ_C and $\dot{\theta}_C$ as follows:

(6b-2-11-1M) $$(\dot{\theta}_R - \dot{\theta}_{CH}) = \left[T_C - C_C(\theta_R - \theta_{CH})\right] / D_C$$

The clutch torque, T_C , is defined by equation (6b-2-11-3). $(\theta_R - \theta_{CH})$ is obtained from equation (6b-2-12) and $\dot{\theta}_{CH}$ is then established from equation (6b-2-13), noting that in each case θ_{CH} and $\dot{\theta}_{CH}$ are used in place of θ_C and $\dot{\theta}_C$. The clutch condition is established by the difference between $\dot{\theta}_{CH}$ and $\dot{\theta}_D$ as follows:

For $(\dot{\theta}_{CH} - \dot{\theta}_D) > 0$	Clutch torque is positive on the drum (clutch attempting to have positive velocity with respect to drum)
For $(\dot{\theta}_{CH} - \dot{\theta}_D) = 0$	Clutch is not attempting to move relative to drum
For $(\dot{\theta}_{CH} - \dot{\theta}_D) < 0$	Clutch torque is negative on the drum. (Drum is attempting to have positive velocity with respect to clutch).

Now that the clutch condition is defined, equation (6b-2-11-2) is modified so that the torque direction is established by the direction of relative velocity between the drum and the clutch as follows:

(6b-2-11-3) $T_C = G_C\langle\dot\theta_{CH}-\dot\theta_D\rangle\left|C_C(\theta_R-\theta_{CH})\right| + D_C(\dot\theta_R-\dot\theta_D)$

$$\text{FOR}\left\{G_C\langle\dot\theta_{CH}-\dot\theta_D\rangle\left|C_C(\theta_R-\theta_{CH})\right|+D_C(\dot\theta_R-\dot\theta_D)\right\} > C750$$

$$= C750$$

$$\text{FOR}\left\{G_C\langle\dot\theta_{CH}-\dot\theta_D\rangle\left|C_C(\theta_R-\theta_{CH})\right|+D_C(\dot\theta_R-\dot\theta_D)\right\} \le C750$$

The function $G_C\langle\dot\theta_{CH}-\dot\theta_D\rangle$ is defined as follows:

(6b-2-14)
$$G_C\langle\dot\theta_{CH}-\dot\theta_D\rangle = +1.0 \quad \text{FOR } (\dot\theta_{CH}-\dot\theta_D) > 0$$
$$= 0 \quad \text{FOR } (\dot\theta_{CH}-\dot\theta_D) = 0$$
$$= -1.0 \quad \text{FOR } (\dot\theta_{CH}-\dot\theta_D) < 0$$

The constant C750 is the value of clutch drag torque when the drum is overrunning the clutch.

The amount of relative motion between the flywheel and drum $(\theta_D-\theta_F)$ is the skid signal. To be compatible with the electrical antiskid control circuits, assume the skid signal is produced by a set of electrical contact points; therefore,

(6b-2-15)
$$E_V = V_S \quad \text{FOR } (\theta_D-\theta_F) \ge C751$$
$$= 0 \quad \text{FOR } (\theta_D-\theta_F) < C751$$

C751 is the skid detection threshold value of $(\theta_D-\theta_F)$ Also, for compatibility with the other parts of the analysis, let the input be derived from the wheel speed sensor output, EG, as follows:

(6b-2-16)
$$\dot\theta_R = C752\ E_G$$

C752 is the conversion coefficient. The equation flow diagram for the mechanical on-off antiskid device is shown on Figure A56a.

B-2 Mechanical On-Off Parameter Evaluation

No parameter evaluation has been accomplished for the mechanical on-off device because it is not applicable to the aircraft being considered.

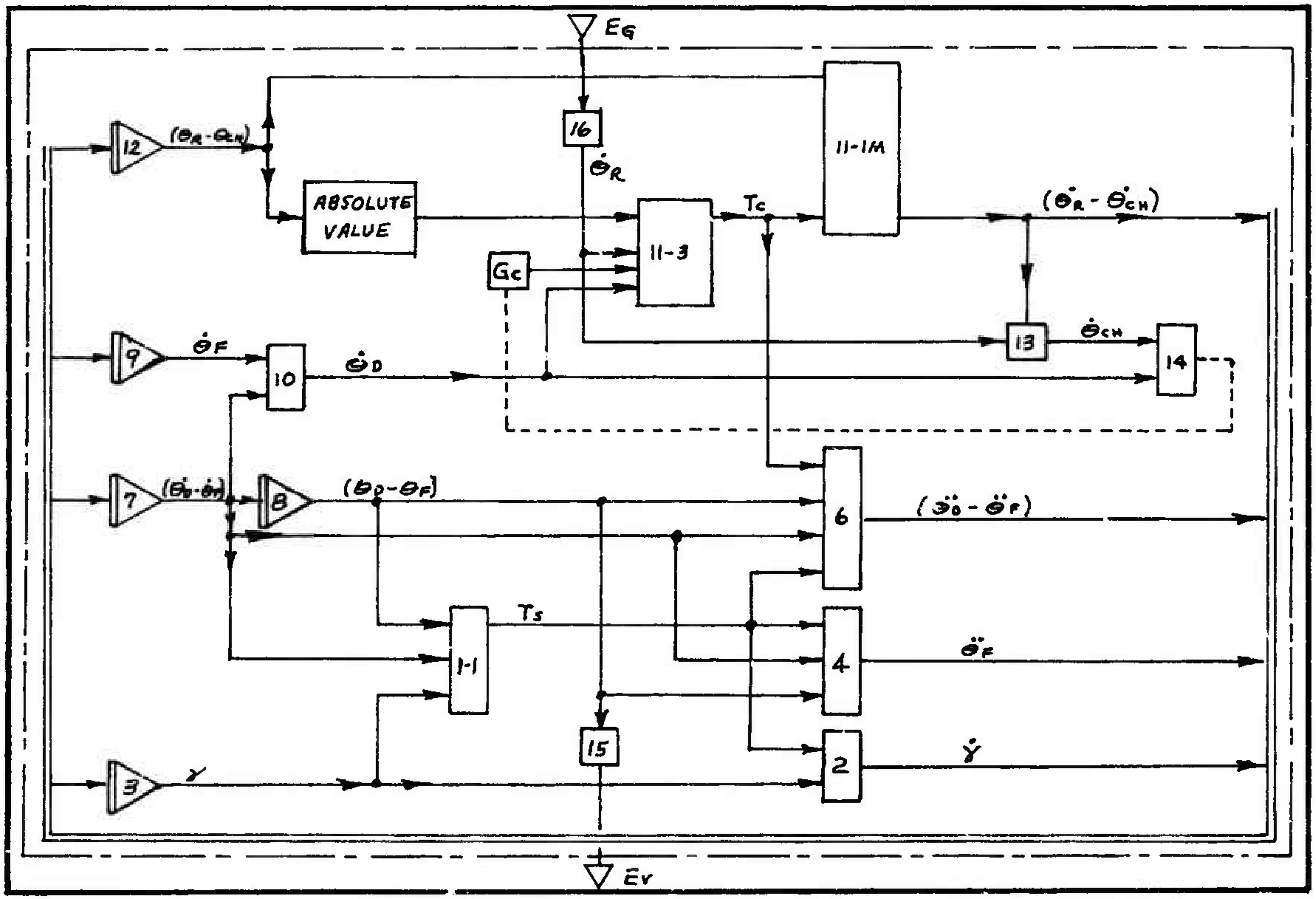

Figure A56a Mechanical On-Off Device Equation Flow Diagram

7. ANTISKID CONTROL VALVE

Aircraft antiskid control systems typically utilize a two-stage electrically operated pressure control valve. The first stage contains an electro-mechanical device such as a torque motor, solenoid or linear force motor which positions a hydraulic flow regulating element (flapper, nozzle or spool) such that a control pressure is produced. The control pressure is a function of the valve input pressure and the electrical input signal. The first stage control pressure is applied to the second stage hydraulic flow controlling power spool. The second stage spool is positioned by forces produced by the control pressure and valve output pressure in a manner such that output pressure is controlled in proportion to the first stage control pressure.

A. Mathematical Description

First Stage

The function of the first stage can be described mathematically by considering the control pressure producing element to be a single degree of freedom damped spring mass system as shown in Figure A57 acted upon by a force, F_{cv} , proportional to the electrical input signal.

$$F_{cv} = C_{scv} E_v \tag{7.1}$$

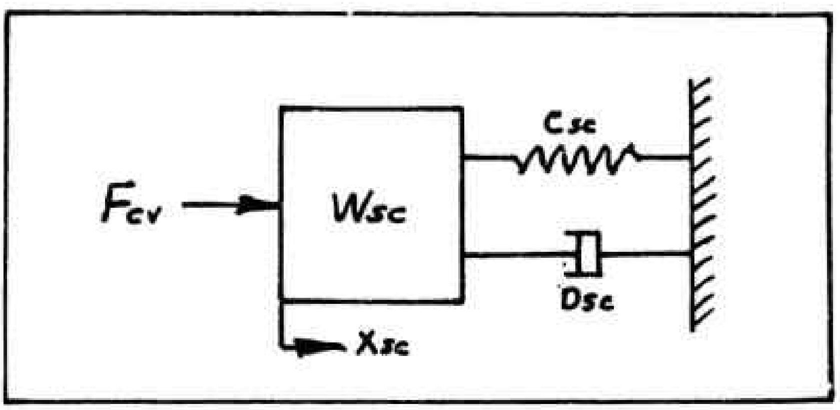

Figure A57 First Stage Spring Mass System

The first stage control pressure, P_{sc}, is defined as a function of the mass position, X_{sc}, according to Figure A58. X_{sc} is established by equation (7.2) which results from summing forces on the first stage mass, W_{sc}.

$$\text{(7.2)} \qquad \ddot{X}_{sc} = \frac{F_{cv}}{W_{sc}} - \frac{C_{sc}}{W_{sc}} X_{sc} - \frac{D_{sc}}{W_{sc}} \dot{X}_{sc}$$

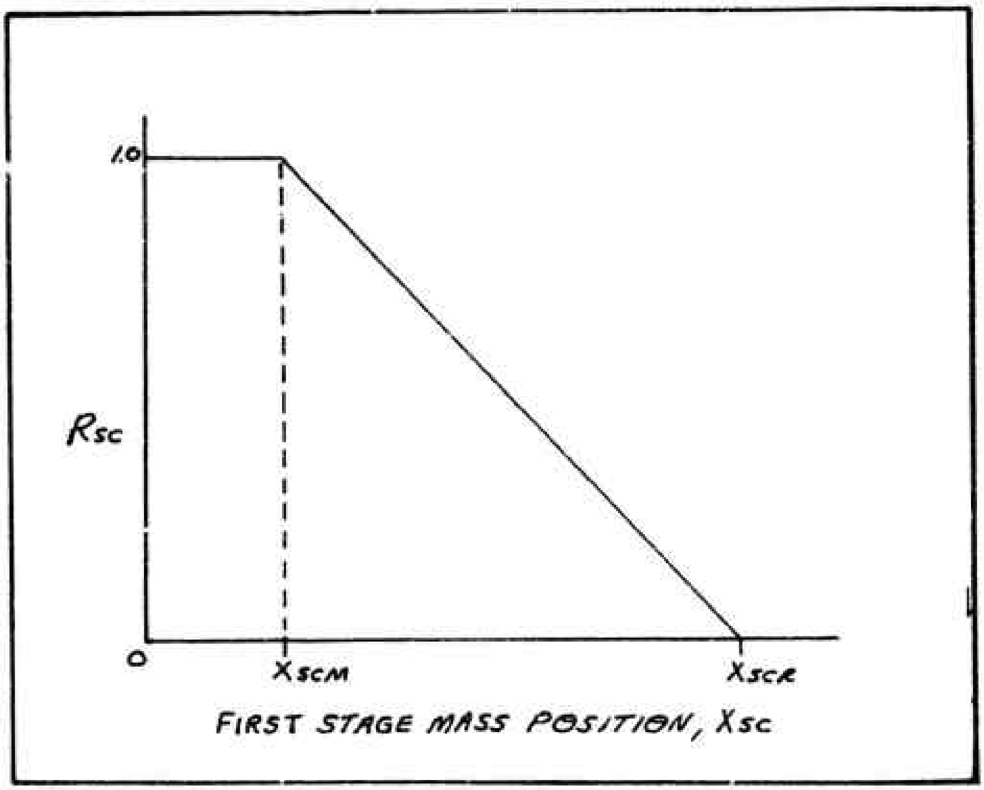

Figure A 58 First Stage Control Pressure - Mass Position Relationship

$$\text{(7.3)} \qquad P_{sc} = R_{sc}\,(P_{MV} - P_{CVR}) + P_{CVR}$$

$$\text{(7.4)} \qquad R_{sc} = \begin{cases} 1.0 & \text{IF } X_{sc} \leq X_{scm} \\ \dfrac{X_{scR} - X_{sc}}{X_{scR} - X_{scm}} & \text{IF } X_{scm} < X_{sc} < X_{scR} \\ 0 & \text{IF } X_{sc} \geq X_{scR} \end{cases}$$

Second Stage

The physical arrangement of the F-111 antiskid valve second stage is shown schematically in Figure A59. Most other antiskid valves have the same operating principles.

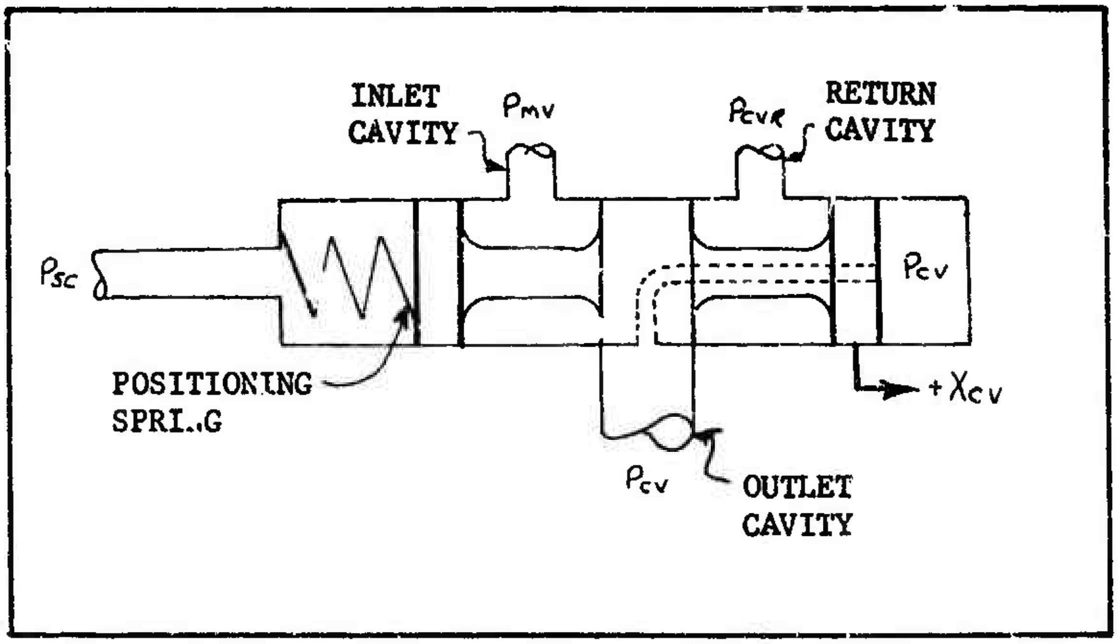

Figure A 59 Antiskid Valve Second Stage

As described in the hydraulic system, the metering valve output pressure, P_{MV}, is supplied to the antiskid control valve second stage inlet. When the second stage spool is displaced in a positive direction a fluid passage opens permitting hydraulic flow from the metering valve to the antiskid valve outlet cavity. When the second stage spool is displaced in a negative direction a fluid passage opens permitting hydraulic flow from the outlet cavity to return. Therefore, the second stage spool position defines the hydraulic flow areas. To permit computation flexibility and economy, two options for establishing the second stage spool position are provided.

Option No. 1

For Option No. 1 the second stage spool position, X_{CV}, is established by equation (7.5) which results from summing forces on the spool mass, W_{CV}. Figure A60 shows a schematic of a single degree of freedom damped spring mass system representing the antiskid valve second stage spool. Springs, C_{CVS}, and dampers, D_{CVS}, are stops representing the spool's longitudinal restraing caused by its contact with the valve body. The forces acting on the second stage spool are the positioning spring force, damping force, stop forces and forces due to outlet cavity pressure, P_{CV}, and first stage control pressure, P_{SC}.

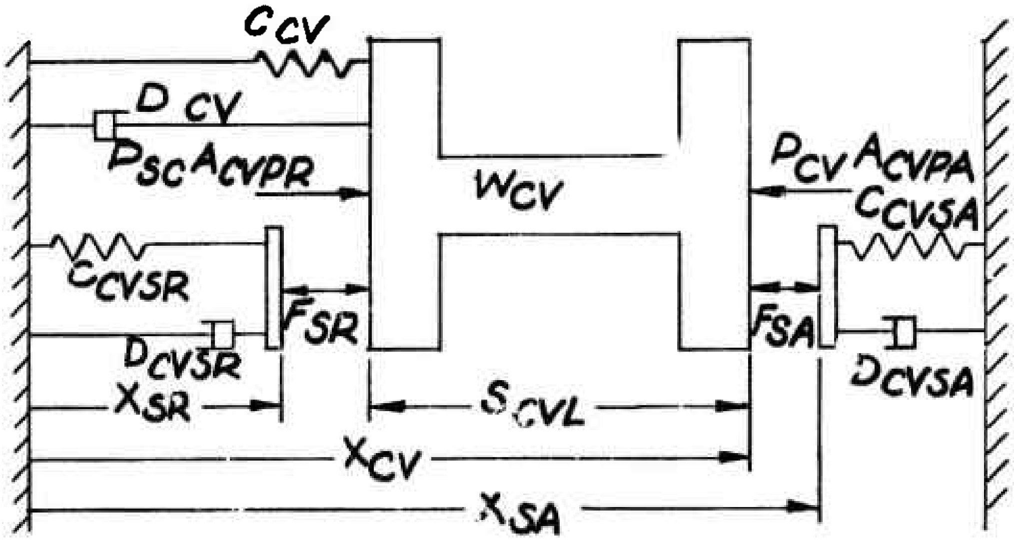

Figure A60 Second Stage Spool Forces

Summing forces on the second stage spool gives:

$$(7.5)\quad \ddot{X}_{CV} = \left[(P_{SC})(A_{CVPR}) - (P_{CV})(A_{CVPA})\right] / W_{CV} + (X_{CVP} - X_{CV})\, C_{CV}/W_{CV} - \dot{X}_{CV}(D_{CV})/W_{CV} + F_{SR}/W_{CV} - F_{SA}/W_{CV}$$

Integrating twice gives:

$$(7.6)\quad \dot{X}_{CV} = \int \ddot{X}_{CV}\, dt$$

(7.7) $$X_{CV} = \int \dot{X}_{CV}\, dt$$

In equation (7.5) the forces F_{SA} and F_{SR} are the forces between the spool and the stops. Since the stop forces are contact forces, they cannot be less than zero. Forces F_{SA} and F_{SR} are defined as follows:

(7.8) $$F_{SA} = 0 \qquad , \text{FOR } X_{CV} \leq X_{SA}$$

$$F_{SA} = C_{CVS}(X_{SA} - S_{SA}) + \dot{X}_{CV} D_{CVS} \qquad , \text{FOR } X_{CV} > X_{SA}$$

(7.9) $$F_{SR} = 0 \qquad , \text{FOR } (X_{CV} - S_{CVL}) \geq X_{SR}$$

$$F_{SR} = C_{CVS}(S_{SR} - X_{SR}) - \dot{X}_{CV} D_{CVS} \qquad , \text{FOR } (X_{CV} - S_{CVL}) < X_{SR}$$

In equation (7.9), S_{CVL} , is the spool length and S_{SR} is the undflected position of stop, S_R . The positions of the spool stops, X_{SA} and X_{SR} , are established as follows: Let the mass of the stop in the brake application direction of spool movement, S_A , be zero. Therefore, summing forces on S_A and solving for $\dot{X}_{SA}$ gives:

(7.10) $$\dot{X}_{SA} = \left[F_{SA} - (X_{SA} - S_{SA}) C_{CVS} \right] / D_{CVS}$$

In equations (7.8) and (7.10), S_{SA} is the undeflected position of stop, S_A. It follows that:

(7.11) $$X_{SA} = \int \dot{X}_{SA}\, dt$$

Using the same procedure as above for the stop in the brake release direction of spool movement, S_R ;

(7.12) $$\dot{X}_{SR} = \left[C_{CVS}(S_{SR} - X_{SR}) - F_{SR} \right] / D_{CVS}$$

And it follows that:

(7.13) $$X_{SR} = \int \dot{X}_{SR}\, dt$$

The hydraulic system contains provision for leakage flow associated with first stage pressure regulation and spool fit. Since these small flows have no effect on the valve's performance in the case under consideration, they have not been computed. Therefore, the following equations apply:

$$Q_{CV1} = 0 \tag{7.14}$$

$$Q_{CV2} = 0 \tag{7.15}$$

$$Q_{CV3} = 0 \tag{7.16}$$

Figure A61 shows the Option No. 1 Control Valve Equation Flow Diagram.

<u>Option No. 2</u>

Since the time interval which elapses during second stage spool movement from one extreme position to the other is very short in comparison with overall control valve response time and since all of the control valve lag can be accounted for in the first stage, the second stage spool position, X_{CV}, can be established as a function of the direction of pressure differential thusly:

$$\begin{aligned} X_{CV} &= 0 && \text{FOR } (P_{CV} - P_{CVB}) = P_{SC} \\ X_{CV} &= +S_{CVO} && \text{FOR } (P_{CV} - P_{CVB}) < P_{SC} \\ X_{CV} &= -S_{CVO} && \text{FOR } (P_{CV} - P_{CVB}) > P_{SC} \end{aligned} \tag{7.17}$$

In equation (7.17) S_{CVO} is the second stage spool position for full flow area as described in the hydraulic system and P_{CVB} is the second stage apparent bias pressure equivalent to the positioning spring force.

Figure A62 is the Equation Flow Diagram for Option No. 2.

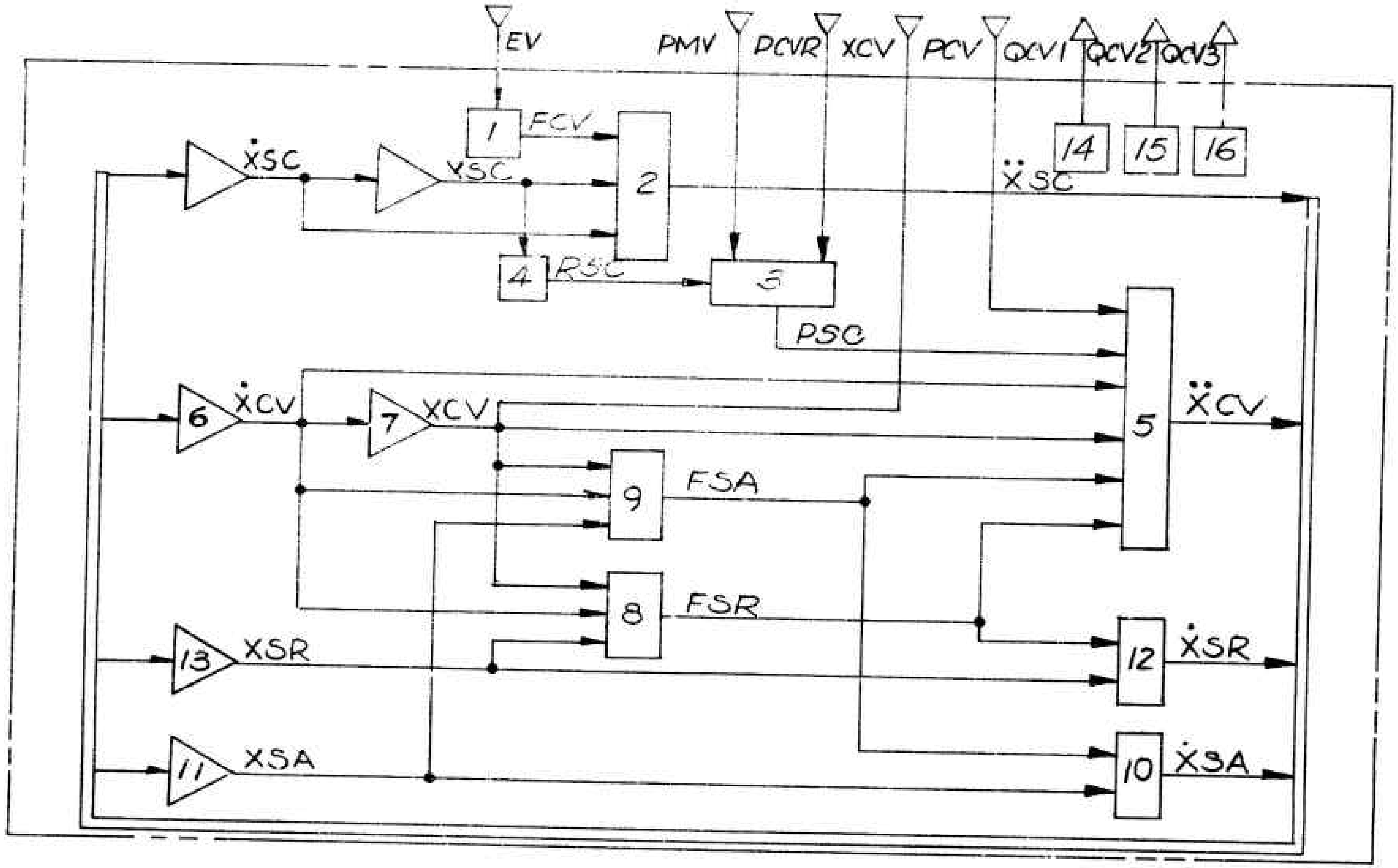

Figure A61 Antiskid Control Valve Equation Flow Diagram (Option No. 1)

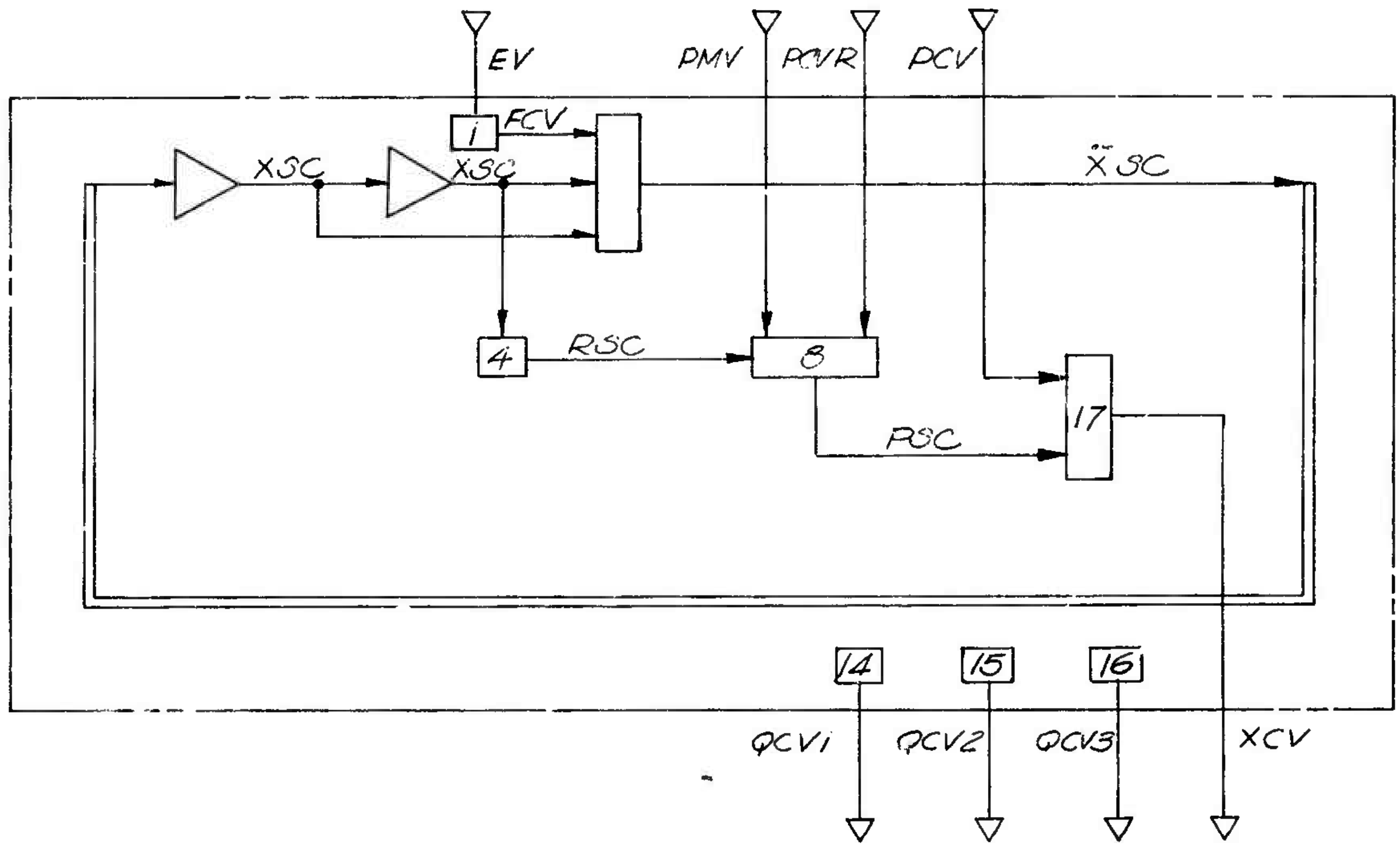

Figure A62 Antiskid Control Valve Equation Flow Diagram (Option No. 2)

B. Parameter Evaluation

The parameters used for describing the antiskid valve's first stage behavior are established from measured frequency response performance characteristics along with some features of its physical construction. Frequency response test results from the F-111 antiskid valve show 25 degrees phase lag at 5 cps. From various experiments it is known that the first stage accounts for most of the phase lag. The F-111 valve's approximate 700 cps undamped natural frequency is quite high compared to a more usual 100 cps value. Since antiskid operation is generally 10 cps or less and since the low frequency phase lag can be accurately described with a lower natural frequency system, an undamped natural frequency of 100 cps will be used to minimize computation difficulty.

Coefficients C_{scv} and C_{sc} are set arbitrarily so that static values of X_{sc} will be compatible with values of X_{scm} and X_{scR} (which are also arbitrarily chosen) and the proper valve voltage - output pressure relationship is achieved. In this example the following values are assigned:

$$\begin{aligned} C_{scv} &= 1.2 \text{ lbf/volt} \\ C_{sc} &= 1.0 \text{ lbf/inch} \\ X_{scm} &= 3.6 \text{ inches} \\ X_{scR} &= 14.4 \text{ inches} \end{aligned} \tag{7.14}$$

For 100 cps (628 rad/sec) undamped natural frequency and $C_{sc} = 1.0$ lbf/in, the mass W_{sc} is computed from $(\omega_n)^2 = C_{sc}/W_{sc}$

$$W_{sc} = 2.54 \times 10^{-6} \text{ lbf sec}^2\text{/in} \tag{7.15}$$

Using the equations relating natural frequency and phase angle listed in the wheel speed sensor parameter evaluation and assuming the first stage has 20 degrees phase lag at 5 cps, the damping factor is established as 3.63. For the values of W_{sc} and C_{sc} above this damping factor results in:

$$D_{sc} = 11.6 \times 10^{-3} \text{ lbf sec/inch} \tag{7.16}$$

The area, A_{CVP}, the stop clearances, S_{CVA} and S_{CVR}, and the mass of the second stage spool, W_{CV}, are computed from the spool's physical dimensions as shown on the valve drawing.

$$
\begin{aligned}
A_{CVP} &= 0.05 \text{ IN}^2 \\
W_{CV} &= 41.5 \times 10^{-6} \text{ lbf sec}^2/\text{IN} \\
S_{CVA} &= 0.03 \text{ INCH} \\
S_{CVR} &= 0.03 \text{ INCH}
\end{aligned}
\tag{7.17}
$$

The positioning spring rate, C_{CV}, and spool damping coefficient were established based on the valve's transient response characteristic where it was observed that a 50 cps about .5 critically damped transient pressure oscillation appeared. From this observation

$$
\begin{aligned}
C_{CV} &= 4.0 \text{ lbf/IN} \\
D_{CV} &= 13.0 \times 10^{-3} \text{ lbf sec/IN}
\end{aligned}
\tag{7.18}
$$

The stop spring, C_{CVS}, and damper, D_{CVS}, characteristics are arbitrarily chosen to be as high as possible within computation capability.

$$
\begin{aligned}
C_{CVS} &= 5000 \text{ lbf/IN} \\
D_{CVS} &= 50 \text{ lbf sec/IN}
\end{aligned}
\tag{7.19}
$$

The undeflected positioning spring length was computed assuming it produced approximately the same force on the valve spool as 25 PSI pressure differential.

$$X_{CVP} = 0.2 \text{ INCH} \tag{7.20}$$

Table A21 lists the parameters and their values which are applicable to the F-111 antiskid control valve. For Option 1 mathematical description and Table A22 lists the parameters which are applicable to Option 2.

Table A21 Antiskid Control Valve Parameters (Option No. 1) (Sheet 1 of 2)

SYMBOL	TYPE	VALUE	UNITS	DESCRIPTION
ACVPA	c	0.05	IN^2	Second Stage Spool Area, Output Pressure End
ACVPR	c	0.05	IN^2	Second Stage Spool Area, Control Pressure End
CSCV	c	1.2	LBF/VOLT	First Stage Volts - Force Coefficient
CSC	c	1.0	LBF/IN	First Stage Spring Rate
CCV	c	4.0	LBF/IN	Second Stage Positioning Spring Rate
CCVS	c	5000	LBF/IN	Second Stage Stop Spring Rate
DSC	c	11.6×10^{-3}	LBF-SEC/IN	First Stage Damping Coefficient
DCV	c	13.0×10^{-3}	LBF SEC/IN	Second Stage Damping Coefficient
DCVS	c	50	LBF SEC/IN	Second Stage Stop Damping Coefficient
EV	v(I)		VOLTS	Antiskid Valve Volts
FCV	v		LBF	First Stage Driving Force
FSA	v		LBF	Second Stage Stop Force - Positive Spool Displacement
FSR	v		LBF	Second Stage Stop Force - Netative Spool Displacement
PCV	v(I)		LBF/IN^2	Antiskid Valve Outlet Cavity Pressure
PMV	v(I)		LBF/IN^2	Metering Valve Output Pressure
PSC	v		LBF/IN^2	First Stage Output Control Pressure
PCVR	v(I)		LBF/IN^2	Antiskid Valve Return Cavity Pressure
QCV1	v(o)		IN^3/SEC	Leakage Flow into Control Valve Inlet Cavity
QCV2	v(o)		IN^3/SEC	Leakage Flow into Control Valve Outlet Cavity
QCV3	v(o)		IN^3/SEC	Leakage Flow into Control Valve Return Cavity
RSC	v		DIMENSIONLESS	First Stage Pressure Regulation Coefficient
SSA	c	0.03	IN	Undeflected Stop Position - Second Stage Spool Positive Displacement
SSR	c	-0.03	IN	Undeflected Stop Position - Second Stage Spool Negative Displacement
SCVL	c	1.0	IN	Second Stage Spool Length

Table A21 Antiskid Control Valve Parameters (Option No. 1) (Sheet 2 of 2)

SYMBOL	TYPE	VALUE	UNITS	DESCRIPTION
W_{SC}	c	2.54×10^{-6}	LBF SEC²/IN	First Stage Mass
W_{CV}	c	41.5×10^{-6}	LBF SEC²/IN	Second Stage Spool Mass
X_{SC}	v		IN	First Stage Mass Displacement
X_{SCO}	c	0.0	IN	First Stage Mass Displacement at Time Zero
$\dot{X}_{SC}$	v		IN/SEC	First Stage Mass Velocity
$\dot{X}_{SCO}$	c	0.0	IN/SEC	First Stage Mass Velocity at Time Zero
$\ddot{X}_{SC}$	v		IN/SEC²	First Stage Mass Acceleration
X_{SCM}	c	3.6	IN	First Stage Mass Position for Zero Regulation
X_{SCR}	c	14.4	IN	First Stage Mass Position for Max Regulation
X_{CV}	v		IN	Second Stage Spool Displacement
X_{CVO}	c	0.03	IN	Second Stage Spool Displacement at Time Zero
$\dot{X}_{CV}$	v		IN/SEC	Second Stage Spool Velocity
$\dot{X}_{CVO}$	c	0.0	IN/SEC	Second Stage Spool Velocity at Time Zero
$\ddot{X}_{CV}$	v		IN/SEC²	Second Stage Spool Acceleration
X_{SA}	v		IN	Positive Motion Stop Displacement
X_{SAO}	c	0.03	IN	Positive Motion Stop Displacement at Time Zero
$\dot{X}_{SA}$	v		IN/SEC	Positive Motion Stop Velocity
X_{SR}	v		IN	Negative Motion Stop Displacement
X_{SRO}	c	-1.03	IN	Negative Motion Stop Displacement at Time Zero
$\dot{X}_{SR}$	v		IN/SEC	Negative Motion Stop Velocity
X_{CVP}	c	0.2	IN	Second Stage Positioning Spring Undeflected Spool Position

Table A22 Antiskid Control Valve Parameters (Option No. 2)

SYMBOL	TYPE	VALUE	UNITS	DESCRIPTION
C_{SCV}	c	1.2	LBF/VOLT	First Stage Volts - Force Coefficient
C_{SC}	c	1.0	LBF/IN	First Stage Spring Rate
D_{SC}	c	11.6×10^{-3}	LBF SEC/IN	First Stage Damping Coefficient
E_{V}	v(I)		VOLTS	Antiskid Valve Volts
F_{CV}	v		LBF	First Stage Driving Force
P_{CV}	v(I)		LBF/IN^2	Antiskid Valve Outlet Cavity Pressure
P_{CVB}	c	15	LBF/IN^2	Second Stage Bias Pressure
P_{CVR}	v(I)		LBF/IN^2	Antiskid Valve Return Cavity Pressure
P_{MV}	v(I)		LBF/IN^2	Metering Valve Output Pressure
P_{SC}	v		LBF/IN^2	First Stage Output Control Pressure
R_{SC}	v		DIMENSIONLESS	First Stage Regulation Coefficient
* S_{CVO}	c	0.03	IN	Second Stage Spool Displacement for Max Flow Area
W_{SC}	c	2.54×10^{-6}	$LBF\,SEC^2/IN$	First Stage Mass
X_{CV}	v(c)		IN	Second Stage Spool Displacement
X_{SC}	v		IN	First Stage Mass Displacement
X_{SCO}	c	0.0	IN	First Stage Mass Displacement at Time Zero
$\dot{X}_{SC}$	v		IN/SEC	First Stage Mass Velocity
$\dot{X}_{SCO}$	c	0.0	IN/SEC	First Stage Mass Velocity at Time Zero
$\ddot{X}_{SC}$	v		IN/SEC^2	First Stage Mass Acceleration
X_{SCM}	c	3.6	IN	First Stage Position for Zero Regulation
X_{SCR}	c	14.4	IN	First Stage Position for Maximum Regulation
Q_{CV1}	v(o)	0.0	IN^3/SEC	Leakage Flow into Control Valve Inlet Cavity
Q_{CV2}	v(o)	0.0	IN^3/SEC	Leakage Flow into Control Valve Outlet Cavity
Q_{CV3}	v(o)	0.0	IN^3/SEC	Leakage Flow into Control Valve Return Cavity

*See Hydraulic System

8. HORIZONTAL TAIL CONTROL

In the 3 degree and 6 degree airplane models, the tail position can be controlled by two different means. The first is simply to require that the horizontal tail rotation be fixed at some value S_{HT}. The second is to fix the input commands S_{EST} and F_{PX} and then let the stability augmentation system adjust the tail setting S_{HT}.

A. Mathematical Description

Figure A63 shows a control system representation of the stability augmentation system.

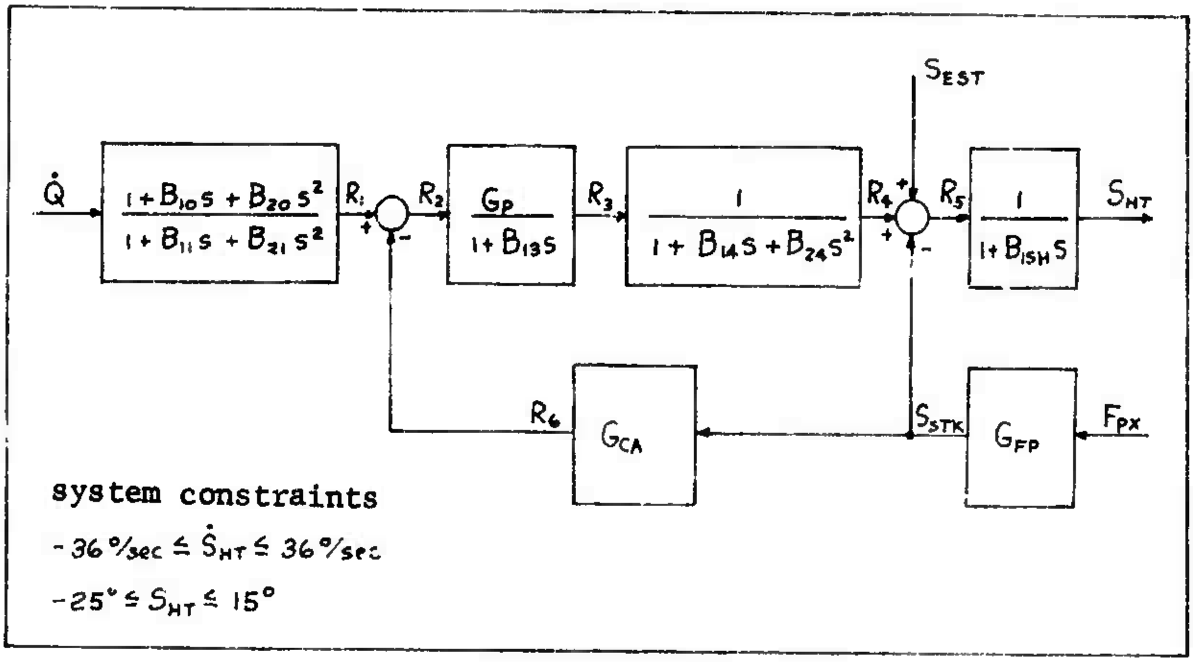

Figure A63 Stability Augmentation System

Using figure A63 as a guide, the following equations describe the stability augmentation system.

(8.1) $S_{STK} = G_{FP} F_{PX}$

Where F_{PX} is the force exerted by the pilot on the stick.

(8.2) $R_6 = G_{CA} S_{STK}$

Let U_Q and U_{QQ} be defined by

$$(8.3)\quad U_Q = \left(\frac{180}{\pi}\right)\int \dot{Q}\, dt$$

$$(8.4)\quad U_{QQ} = \int U_Q\, dt$$

Also, let U_{R1} and U_{RR1} be defined by

$$(8.5)\quad U_{R1} = \int R_1\, dt$$

$$(8.6)\quad U_{RR1} = \int U_{R1}\, dt$$

Then

$$(8.7)\quad R_1 = (U_{QQ} + B_{10} U_Q + B_{20}\dot{Q} - U_{RR1} - B_{11} U_{R1})/B_{21}$$

$$(8.8)\quad R_2 = R_1 - R_6$$

Let U_{R2}, U_{R3}, U_{RR3}, U_{R4}, and U_{RR4} be defined by

$$(8.9)\quad U_{R2} = \int R_2\, dt$$

$$(8.10)\quad U_{R3} = \int R_3\, dt$$

$$(8.11)\quad U_{RR3} = \int U_{R3}\, dt$$

$$(8.12)\quad U_{R4} = \int R_4\, dt$$

$$(8.13)\quad U_{RR4} = \int U_{R4}\, dt$$

Then

$$(8.14)\quad R_3 = (G_P U_{R2} - U_{R3})/B_{13}$$

$$(8.15)\quad R_4 = (U_{RR3} - U_{RR4} - B_{14} U_{R4})/B_{24}$$

$$(8.16)\quad R_5 = R_4 + S_{EST} - S_{STK}$$

Because of rate and position limits, the equations that describe S_{HT} in terms of R_5 must be modified to reflect these limits. Let S_{HTP} be defined by

$$(8.17)\quad S_{HTP} = (R_5 - S_{HT})/B_{15H}$$

Then

$$(8.18)\quad S_{HTI} = \begin{cases} S_{HTDMX} & \text{if } S_{HTP} > S_{HTDMX} \\ S_{HTP} & \text{if } -S_{HTDMX} \le S_{HTP} \le S_{HTDMX} \\ -S_{HTDMX} & \text{if } S_{HTP} < -S_{HTDMX} \end{cases}$$

$$(8.19)\quad \dot{S}_{HT} = \begin{cases} \min\{0.0, S_{HTI}\} & \text{if } S_{HT} \ge S_{HTMAX} \\ S_{HTI} & \text{if } S_{HTMIN} < S_{HT} < S_{HTMAX} \\ \max\{0.0, S_{HTI}\} & \text{if } S_{HT} \le S_{HTMIN} \end{cases}$$

Finally the stick position F_{PX} may be positioned as a function of time by specifying two times and two loads.

$$(8.20)\quad F_{PX} = \begin{cases} 0 & \text{if } T_{PX2} \le T_{PX1} \\ F_{PX1} & \text{if } T \le T_{PX1} < T_{PX2} \\ F_{PX2} & \text{if } T_{PX1} < T_{PX2} \le T \\ F_{PX1} + (F_{PX2} - F_{PX1})(T - T_{PX1})/(T_{PX2} - T_{PX1}) & \\ & \text{if } T_{PX1} < T < T_{PX2} \end{cases}$$

B. Parameter Evaluation

The values for the F-111A system parameters are listed in Table A23. In using this system for a braking problem the usual procedure is to first choose a steadystate value for $S_{HT}(S_{HTSS})$. Set $S_{HTO} = S_{HSS} = S_{EST}$ and set $F_{PX} = 0$ $(T_{PX1} = T_{PX2} = 0)$.
Set all other initial conditions to zero.

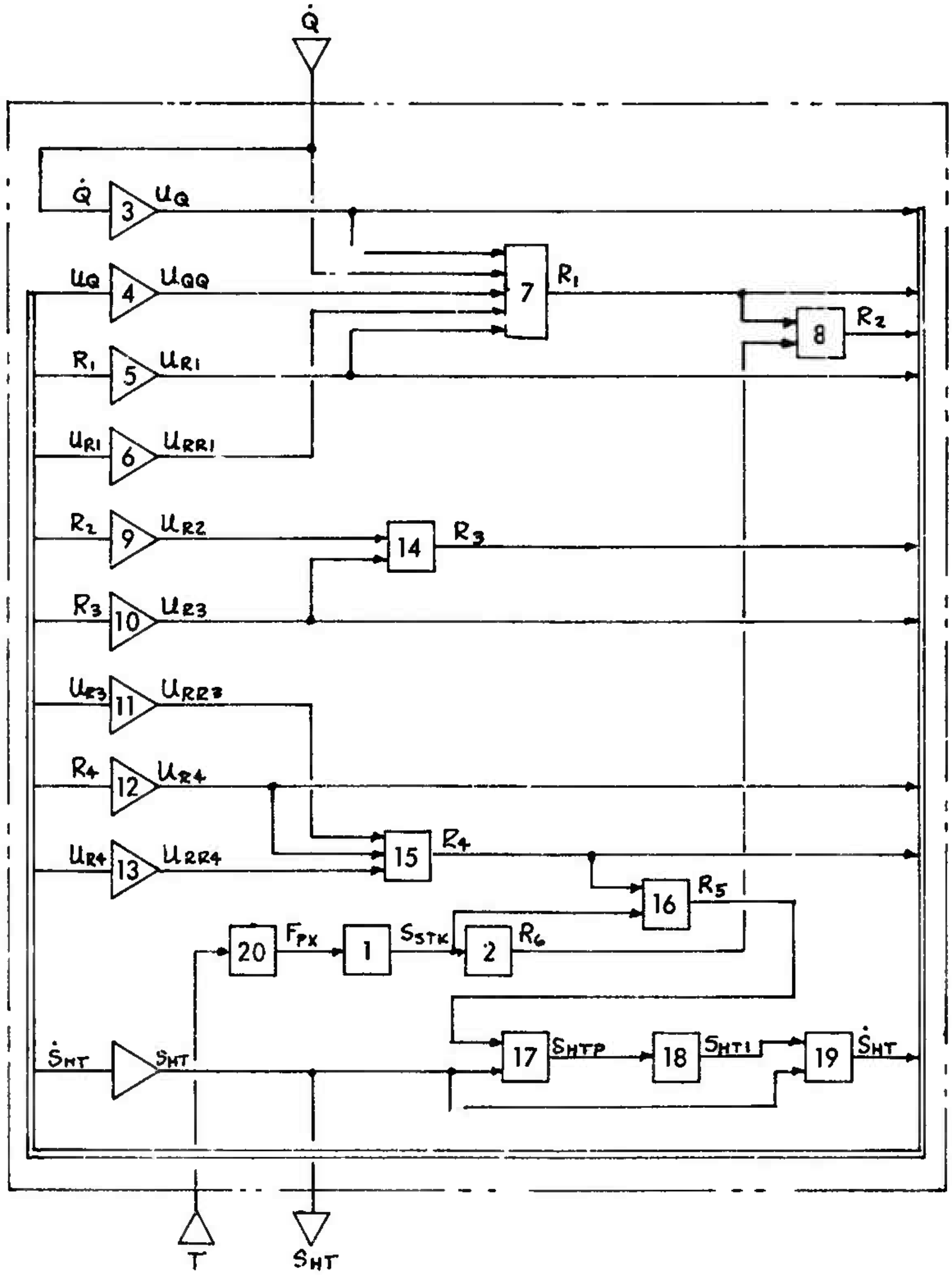

Figure A 64 Horizontal Tail Control Equation Flow Diagram

Table A23 Horizontal Tail Control Parameters (Sheet 1 of 3)

SYMBOL	TYPE	VALUE	UNITS	DESCRIPTION
B_{10}	c	0.4	sec	SAS Constants
B_{11}	c	0.05	sec	
B_{13}	c	0.50	sec	
B_{14}	c	0.00269	sec	
B_{15H}	c	0.05	sec	
B_{20}	c	3.58	sec^2 deg/RAD	
B_{21}	c	0.000555	sec^2	
B_{24}	c	0.00037	sec^2	
F_{PX}	v		lb	Stick Force
F_{PX1}	c	0.0	lb	Determine Stick Force
F_{PX2}	c	0.0	lb	
G_{CA}	c	3.6	sec^{-1}	Command Augmentation Gain
G_{FP}	c	0.51	deg/lb	Stick Force Gain
G_P	c	0.375	sec^{-1}	Augmentation Gain
$\dot{Q}$	v(i)		RAD/sec	Airplane Pitch Rate
R_1	v		deg/sec	Intermediate SAS Variables
R_2	v		deg/sec	
R_3	v		deg/sec	
R_4	v		deg	
R_5	v		deg	
R_6	v		deg/sec	
S_{EST}	c	-5.0	deg	Series Trim Input

Table A23 Horizontal Tail Control Parameters (Sheet 2 of 3)

SYMBOL	TYPE	VALUE	UNITS	DESCRIPTION
δ_{HT}	v(o)		deg	Horizontal Tail Deflection when Time = 0
δ_{HTO}	c	-5.0	deg	
$\dot{\delta}_{HT}$	v		deg/sec	Horizontal Tail Deflection Rate
δ_{HT1}	v		deg/sec	Used to Calculate $\dot{\delta}_{HT}$
δ_{HTP}	v		deg/sec	
δ_{HTDMX}	c	36.0	deg/sec	Maximum Tail Deflection Rate
δ_{HTMAX}	c	15.0	deg	Maximum Tail Deflection
δ_{HTMIN}	c	-25.0	deg	Minimum Tail Deflection
δ_{STK}	v		deg	Stick Position
T	v(i)		sec	Time
T_{PX1}	c	0.0	sec	Used to Determine $\bar{F}_{PX}$
T_{PX2}	c	0.0	sec	
U_Q	v		deg	SAS Variables and Initial Conditions
U_{QO}	c	0.0	deg	
U_{QQ}	v		deg sec	
U_{QQO}	c	0.0	deg sec	
U_{R1}	v		deg	
U_{R1O}	c	0.0	deg	
U_{RR1}	v		deg sec	
U_{RR1O}	c	0.0	deg sec	
U_{R2}	v		deg	
U_{R2O}	c	0.0	deg	

Table A23 Horizontal Tail Control Parameters (Sheet 3 of 3)

SYMBOL	TYPE	VALUE	UNITS	DESCRIPTION
u_{R3}	v		deg	SAS Variables and Initial Conditions
u_{R30}	c	0.0	deg	
u_{RR3}	v		deg sec	
u_{RR30}	c	0.0	deg sec	
u_{R4}	v		deg sec	
u_{R40}	c	0.0	deg sec	
u_{RR4}	v		deg sec^2	
u_{RR40}	c	0.0	deg sec^2	

9a. RUNWAY SYSTEM (FLYWHEEL AND 3 DEGREE)

This runway system is essentially the same as the runway system for the 6 degree. In fact, the relation between the two is given by $Z_{GD}\langle x\rangle = Z_{GD}\langle x,0\rangle$ and $Z_{GDP}\langle x\rangle = Z_{GPP}\langle x,0\rangle$. Even though this system is like the 6 degree system, the equations are listed below which take advantage of the fact that it takes less computer time to calculate $Z_{GD}\langle x\rangle$ than $Z_{GD}\langle x,0\rangle$.
The data describing the runway is in tabular form and consists of runway elevation values as shown in table A25 as described in discussion of the 6 degree runway system. The data is from the center strip from station 4574 to station 6574.

A. Mathematical Description

Let $H_{RC}(i)$, $i = 1, 2, \cdots, 1001$ denote the elevations at two foot intervals. As an example, $H_{RC}(5) = 9.686$
If x is a distance measured down the runway where x is in inches, then $z = Z_{GD}\langle x\rangle$ and $w = Z_{GDP}\langle x\rangle$ correspond to the elevation in inches and the slope in inches per inch. The values for z and w are determined as outlined below. The function Z_{GD} will have the property that $Z_{GD}\langle 0\rangle = 0$.

Let X_{LRO} be a constant such that $0 \le X_{LRO} < 2000$.
The input X_{LRF} in feet is derived from x such that $0 \le X_{LRF} < 2000$ and for some integer k

$$(9a.1)\quad X_{LRF} = X_{LRO} + x/12 - 2000k$$

Let n be an integer such that $2(n-1) \le X_{LRO} < 2n$ and define Z_{GCO} by

$$(9a.2)\quad Z_{GCO} = H_{RC}(n) + (H_{RC}(n+1) - H_{RC}(n))(X_{LRO} - 2n + 2)/2$$

If m is an integer such that $2(m-1) \le X_{LRF} < 2m$ then z and w are given by

$$(9a.3)\quad z = 12\left(H_{RC}(m) + (H_{RC}(m+1) - H_{RC}(m))(X_{LRF} - 2m + 2)/2 - Z_{CGO}\right)$$

$$(9a.4)\quad w = (H_{RC}(m+1) - H_{RC}(m))/2$$

Table A24 Runway System Parameters (Flywheel and 3 Degree)

SYMBOL	TYPE	VALUE	UNITS	DESCRIPTION
$H_{RC}(i)$	c	*	Ft.	Center Runway Elevation Profile
ω	v(o)		In/In	Runway Slope at x ($\omega = Z_{GOP}\langle x \rangle$)
x	v(i)		In.	Distance Down Runway
X_{LRO}	c	0.0	Ft.	Determines starting point (at time = 0) on Runway Profile
X_{LRF}	v		Ft.	Determines position on runway profile
z	v(o)		In.	Runway elevation at x
Z_{GCO}	c ‡		Ft.	Correction height

‡ Determined from the constant X_{LRO}

* See Table A24 of the 6 degree runway system (use center, sta. 4574 to 6574)

9b. RUNWAY SYSTEM (6 DEGREE)

The runway system is not actually a "system" in the same sense as the brake system, for example. The runway system is simply a function called by the airplane system to supply values for ground slope and elevation. The data describing the runway is in tabular form and consists of runway elevation values as shown in Table A25. Except for a slight modification, the data in Table A25 is taken from station 4574 to station 6574 of runway 25 from reference 11. The left elevations and right elevations are 10 ft. to the left and 10 ft. to the right of center respectively. The elevations have been modified slightly so that the elevations at station 4574 match those as station 6574. This is done to provide an essentially "endless" runway by repeated use of a basic 2000 ft. strip.

A. Mathematical Description

Let $H_{RR}(i)$, $H_{RC}(i)$, $H_{RL}(i)$, $i = 1, 2, \cdots, 1001$ denote the elevations at two foot increments of the right, center, and left runway strips respectively. As an example, $H_{RL}(11) = 9.550$ and $H_{RC}(5) = 9.686$. If x is a distance measured down the runway, and y is a distance measured out from the center of the runway where x and y are in inches, then $z = Z_{GD}\langle x, y\rangle$ and $\omega = Z_{GDP}\langle x, y\rangle$ correspond to the elevation in inches and the slope in inches per inch. The values for z and ω are determined as outlined below. The function Z_{GD} will be chosen in such a way that $Z_{GD}\langle 0, y\rangle = 0.0$ inches.

Let X_{LRF} and Y_{LRF} be the inputs in feet. Thus,

(9c.1) $Y_{LRF} = y/12$

Let X_{LRO} be a constant such that $0 \leq X_{LRO} < 2000$. X_{LRF} is a number such that $0 \leq X_{LRF} < 2000$ and which also satisfies the following equation for some integer K.

(9c.2) $X_{LRF} = X_{LRO} + x/12 - 2000\,K$

Now let n be an integer such that $2(n-1) \leq X_{LRO} < 2n$. Define Z_{GRO}, Z_{GCO}, Z_{GLO} as follows:

$$(9c.3)\quad Z_{GRO} = H_{RR}(n) + \tfrac{1}{2}(H_{RR}(n+1) - H_{RR}(n))(X_{LRO} - 2n + 2)$$

$$(9c.4)\quad Z_{GCO} = H_{RC}(n) + \tfrac{1}{2}(H_{RC}(n+1) - H_{RC}(n))(X_{LRO} - 2n + 2)$$

$$(9c.5)\quad Z_{GLO} = H_{RL}(n) + \tfrac{1}{2}(H_{RL}(n+1) - H_{RL}(n))(X_{LRO} - 2n + 2)$$

Now let m be an integer such that $2(m-1) \leq X_{LRF} < 2m$ Define Z_{GRX}, Z_{GCX}, and Z_{GLX} as follows:

$$(9c.6)\quad Z_{GRX} = H_{RR}(m) + \tfrac{1}{2}(H_{RR}(m+1) - H_{RR}(m))(X_{LRF} - 2m + 2) - Z_{GRO}$$

$$(9c.7)\quad Z_{GCX} = H_{RC}(m) + \tfrac{1}{2}(H_{RC}(m+1) - H_{RC}(m))(X_{LRF} - 2m + 2) - Z_{GCO}$$

$$(9c.8)\quad Z_{GLX} = H_{RL}(m) + \tfrac{1}{2}(H_{RL}(m+1) - H_{RL}(m))(X_{LRF} - 2m + 2) - Z_{GLO}$$

If $Y_{LRF} \geq 0$, then

$$(9c.10)\quad z = 12\,(Z_{GCX} + (Z_{GRX} - Z_{GCX})(Y_{LRF}/10))$$

$$(9c.11)\quad w = (Y_{LRF}/20)(H_{RR}(m+1) - H_{RR}(m) - H_{RC}(m+1) + H_{RC}(m)) + \tfrac{1}{2}(H_{RC}(m+1) - H_{RC}(m))$$

If $Y_{LRF} < 0$, then

$$(9c.12)\quad z = 12\,(Z_{GCX} + (Z_{GCX} - Z_{GLX})(Y_{LRF}/10))$$

$$(9c.13)\quad w = (Y_{LRF}/20)(H_{RC}(m+1) - H_{RC}(m) - H_{RL}(m+1) + H_{RL}(m)) + \tfrac{1}{2}(H_{RC}(m+1) - H_{RC}(m))$$

Table A.25 Three Track Elevation Profiles

(Stations and elevations are in feet)

(Sheet 1 of 6)

STATION	ELEVATION		
	LEFT	CENTER	RIGHT
4574	9.597	9.703	9.593
4576	9.596	9.699	9.586
4578	9.593	9.696	9.581
4580	9.590	9.696	9.580
4582	9.590	9.686	9.580
4584	9.589	9.696	9.622
4586	9.580	9.688	9.629
4588	9.574	9.685	9.625
4590	9.570	9.686	9.616
4592	9.563	9.693	9.622
4594	9.564	9.704	9.634
4596	9.563	9.692	9.616
4598	9.556	9.676	9.611
4600	9.558	9.676	9.613
4602	9.592	9.694	9.612
4604	9.594	9.699	9.627
4606	9.595	9.711	9.641
4608	9.600	9.704	9.601
4610	9.604	9.703	9.605
4612	9.594	9.696	9.602
4614	9.585	9.697	9.606
4616	9.572	9.699	9.608
4618	9.569	9.702	9.607

Table A25 Three Track Elevation Profiles

(Stations and elevations are in feet)
(Sheet 2 of 6)

Station	Elevation Left	Elevation Center	Elevation Right
4620	9.565	9.697	9.591
4622	9.572	9.698	9.601
4624	9.578	9.677	9.594
4626	9.583	9.687	9.589
4628	9.583	9.690	9.593
4630	9.583	9.681	9.593
4632	9.584	9.694	9.597
4634	9.591	9.699	9.604
4636	9.593	9.658	9.601
4638	9.594	9.693	9.597
4640	9.590	9.691	9.570
4642	9.588	9.691	9.578
4644	9.586	9.687	9.559
4646	9.594	9.667	9.590
4648	9.583	9.668	9.569
4650	9.568	9.673	9.557
4652	9.573	9.669	9.569
4654	9.574	9.674	9.559
4656	9.572	9.681	9.554
4658	9.565	9.665	9.567
4660	9.570	9.654	9.564
4662	9.573	9.659	9.561
4664	9.575	9.674	9.554
4666	9.574	9.669	9.569
4668	9.572	9.677	9.555
4670	9.577	9.677	9.554
4672	9.570	9.694	9.974
4674	9.568	9.491	9.551
4676	9.571	9.685	9.587
4678	9.577	9.690	9.591
4680	9.576	9.687	9.595
4682	9.554	9.631	9.599
4684	9.564	9.690	9.587
4686	9.555	9.692	9.586
4688	9.569	9.687	9.590
4690	9.571	9.656	9.594
4692	9.578	9.685	9.597
4694	9.578	9.692	9.597
4696	9.577	9.693	9.602
4698	9.555	9.703	9.606
4700	9.570	9.694	9.591
4702	9.567	9.696	9.600
4704	9.557	9.705	9.599
4706	9.571	9.702	9.996
4708	9.570	9.704	9.600
4710	9.568	9.696	9.598
4712	9.556	9.694	9.595
4714	9.562	9.695	9.593
4716	9.558	9.691	9.596
4718	9.560	9.698	9.591
4720	9.562	9.691	9.593
4722	9.554	9.699	9.593
4724	9.565	9.658	9.592
4726	9.555	9.687	9.592
4728	9.576	9.690	9.596
4730	9.590	9.693	9.602
4732	9.582	9.690	9.604
4734	9.579	9.699	9.533
4736	9.579	9.693	9.599
4738	9.578	9.691	9.594
4740	9.578	9.696	9.587
4742	9.575	9.674	9.587
4744	9.570	9.676	9.575
4746	9.577	9.695	9.572
4748	9.583	9.685	9.573
4750	9.587	9.670	9.571
4752	9.582	9.664	9.570
4754	9.581	9.680	9.572
4756	9.583	9.675	9.574
4758	9.572	9.674	9.571

Station	Elevation Left	Elevation Center	Elevation Right
4760	.557	9.667	9.567
4762	9.560	9.668	9.564
4764	9.560	9.668	9.561
4766	9.565	9.676	9.568
4768	9.567	9.676	9.567
4770	9.563	9.564	9.564
4772	9.551	9.660	9.557
4774	9.563	9.570	9.561
4776	9.565	9.676	9.561
4778	9.554	9.677	9.567
4780	9.560	9.678	9.574
4782	9.557	9.678	9.575
4784	9.552	9.683	9.574
4786	9.554	9.686	9.580
4788	9.571	9.582	9.586
4790	9.572	9.703	9.587
4792	9.573	9.702	9.591
4794	9.580	9.704	9.594
4796	9.582	9.703	9.597
4798	9.576	9.702	9.588
4800	9.567	9.697	9.590
4802	9.580	9.696	9.586
4804	9.553	9.699	9.593
4806	9.590	9.700	9.588
4808	9.590	9.698	9.585
4810	9.588	9.594	9.579
4812	9.555	9.697	9.581
4814	9.581	9.698	9.593
4816	9.578	9.700	9.583
4818	9.579	9.693	9.579
4820	9.572	9.686	9.578
4822	9.534	9.679	9.574
4824	9.589	9.676	9.574
4826	9.589	9.680	9.568
4828	9.590	9.586	9.571
4830	9.593	9.689	9.574
4832	9.595	9.584	9.581
4834	9.596	9.693	9.585
4836	9.595	9.595	9.594
4838	9.590	9.698	9.599
4840	9.590	9.701	9.603
4842	9.598	9.710	9.598
4844	9.586	9.704	9.596
4846	9.590	9.691	9.597
4848	9.591	9.689	9.596
4850	9.586	9.595	9.595
4852	9.579	9.694	9.598
4854	9.577	9.583	9.595
4856	9.582	9.693	9.595
4858	9.586	9.696	9.593
4860	9.588	9.694	9.587
4862	9.591	9.690	9.585
4864	9.595	9.686	9.595
4866	9.595	9.683	9.602
4868	9.594	9.680	9.601
4870	9.589	9.692	9.603
4872	9.590	9.685	9.600
4874	9.587	9.685	9.598
4876	9.591	9.578	9.596
4878	9.584	9.677	9.595
4880	9.593	9.673	9.594
4882	9.595	9.685	9.594
4884	9.599	9.688	9.595
4886	9.600	9.693	9.594
4888	9.602	9.699	9.596
4890	9.602	9.704	9.599
4892	9.596	9.703	9.598
4894	9.590	9.719	9.597
4896	9.595	9.715	9.596
4898	9.596	9.715	9.593

Station	Elevation Left	Elevation Center	Elevation Right
4900	9.590	9.716	9.603
4902	9.593	9.714	9.582
4904	9.593	9.717	9.585
4906	9.598	9.714	9.580
4908	9.591	9.711	9.584
4910	9.589	9.716	9.578
4912	9.589	9.713	9.585
4914	9.592	9.712	9.581
4916	9.588	9.711	9.585
4918	9.587	9.710	9.592
4920	9.589	9.705	9.585
4922	9.586	9.696	9.578
4924	9.588	9.685	9.576
4926	9.589	9.695	9.572
4928	9.585	9.701	9.571
4930	9.586	9.702	9.570
4932	9.590	9.711	9.571
4934	9.594	9.707	9.568
4936	9.590	9.699	9.569
4938	9.590	9.692	9.567
4940	9.588	9.684	9.566
4942	9.583	9.687	9.570
4944	9.581	9.688	9.566
4946	9.582	9.682	9.562
4948	9.580	9.692	9.567
4950	9.576	9.679	9.569
4952	9.576	9.678	9.578
4954	9.571	9.687	9.578
4956	9.575	9.682	9.579
4958	9.581	9.689	9.585
4960	9.581	9.686	9.581
4962	9.582	9.678	9.585
4964	9.583	9.695	9.589
4966	9.580	9.699	9.588
4968	9.576	9.709	9.587
4970	9.574	9.696	9.585
4972	9.576	9.685	9.585
4974	9.571	9.682	9.584
4976	9.576	9.690	9.579
4978	9.576	9.685	9.580
4980	9.573	9.679	9.583
4982	9.580	9.678	9.588
4984	9.579	9.691	9.592
4986	9.585	9.698	9.591
4988	9.593	9.695	9.595
4990	9.590	9.699	9.589
4992	9.589	9.689	9.591
4994	9.593	9.695	9.592
4996	9.597	9.704	9.597
4998	9.598	9.709	9.590
5000	9.603	9.702	9.594
5002	9.602	9.715	9.602
5004	9.608	9.703	9.610
5006	9.607	9.724	9.609
5008	9.605	9.728	9.610
5010	9.608	9.730	9.613
5012	9.609	9.721	9.614
5014	9.607	9.710	9.611
5016	9.597	9.703	9.604
5018	9.587	9.711	9.599
5020	9.586	9.701	9.592
5022	9.587	9.691	9.583
5024	9.588	9.682	9.580
5026	9.581	9.666	9.577
5028	9.582	9.671	9.575
5030	9.581	9.672	9.574
5032	9.582	9.679	9.578
5034	9.590	9.684	9.583
5036	9.589	9.692	9.585
5038	9.588	9.691	9.587

Table A25 Three Track Elevation Profiles

(Stations and elevations are in feet)
(Sheet 3 of 6)

Station	Elevation			Station	Elevation			Station	Elevation		
	Left	Center	Right		Left	Center	Right		Left	Center	Right
5040	9.581	9.689	9.587	5180	9.586	9.735	9.630	5320	9.657	9.805	9.695
5042	9.589	9.686	9.582	5182	9.577	9.743	9.633	5322	9.658	9.810	9.692
5044	5.57[illegible]	9.682	9.578	5184	9.597	9.745	9.638	5324	9.667	9.803	9.693
5046	9.585	9.683	9.570	5186	9.602	9.755	9.643	5326	9.668	9.799	9.692
5048	9.572	9.680	9.570	5188	9.599	9.756	9.640	5328	9.576	9.797	9.689
5050	9.571	9.683	9.567	5190	9.591	9.750	9.637	5330	9.675	9.803	9.690
5052	9.575	9.684	9.568	5192	9.595	5.757	9.641	5332	9.677	9.806	9.695
5054	9.579	9.686	9.575	5194	9.601	9.756	9.650	5334	9.680	9.812	9.697
5056	9.580	9.655	9.588	5196	9.597	9.750	9.552	5336	9.686	9.811	9.702
5058	9.589	9.699	9.531	5198	9.595	9.745	9.639	5338	9.689	9.823	9.702
5060	9.568	9.702	9.593	5200	9.595	9.741	9.533	5340	9.683	9.812	9.704
5062	9.582	9.696	9.591	5202	9.591	9.747	9.635	5342	9.680	9.811	9.703
5064	9.577	9.686	9.593	5204	9.601	9.758	9.648	5344	9.675	9.807	9.705
5066	9.558	9.679	9.579	5206	9.610	9.759	9.655	5346	9.572	9.813	9.699
5068	9.569	9.663	9.555	5208	9.623	9.767	9.559	5348	9.680	9.816	9.701
5070	9.575	9.662	9.557	5210	9.630	9.779	9.662	5350	9.694	9.818	9.704
5072	9.574	9.665	9.550	5212	9.623	9.772	9.661	5352	9.699	9.810	9.704
5074	9.568	9.666	9.562	5214	9.624	9.755	9.559	5354	9.705	9.813	9.706
5076	9.571	9.670	9.557	5216	9.623	9.768	9.660	5356	9.710	9.811	9.708
5878	9.569	9.675	9.555	5218	9.619	9.773	9.557	5358	9.714	9.817	9.707
5380	9.558	9.679	9.566	5220	9.620	9.772	5.650	5360	9.707	9.809	9.699
5082	9.565	9.690	9.563	5222	9.622	5.765	9.659	5362	9.699	9.813	9.700
5084	9.559	9.697	9.570	5224	9.627	9.761	9.648	5364	9.697	9.804	9.700
5086	9.566	9.685	9.555	5226	9.628	9.766	9.652	5366	9.697	9.808	9.701
5088	9.555	9.664	9.557	5228	9.624	9.757	9.658	5368	9.702	9.802	9.708
5090	9.553	9.664	9.556	5230	9.630	9.756	9.657	5370	9.708	9.797	9.706
5092	9.565	9.663	9.557	5232	9.634	9.772	9.661	5372	9.713	9.799	9.706
5094	9.565	9.674	9.553	5234	9.643	9.777	9.661	5374	9.719	9.811	9.705
5096	9.564	5.672	9.566	5236	9.637	9.765	9.662	5376	9.731	9.822	9.711
5099	9.552	9.675	9.559	5238	9.625	9.777	9.659	5378	9.737	9.835	9.715
5100	9.565	9.694	9.574	5240	9.627	9.778	9.550	5380	9.744	9.832	9.721
5102	9.555	9.702	9.576	5242	9.622	9.775	9.668	5382	9.746	9.833	9.722
5104	9.565	9.706	9.577	5244	9.638	9.779	9.675	5384	9.751	9.835	9.732
5106	9.570	9.704	9.581	5246	9.643	9.780	9.684	5386	9.760	9.837	9.733
5108	9.569	9.702	9.575	5248	9.641	9.779	9.689	5388	9.764	9.852	9.729
5110	9.564	5.699	9.582	5250	9.645	9.780	9.695	5390	9.768	9.850	9.733
5112	9.571	9.697	9.577	5252	9.653	9.771	9.697	5392	9.769	9.854	9.735
5114	9.568	9.694	9.583	5254	9.655	9.783	9.702	5394	9.770	9.865	9.736
5116	9.554	9.698	9.577	5256	9.656	9.783	9.703	5396	9.780	9.862	9.731
5118	9.561	9.659	9.575	5258	9.657	9.790	9.725	5398	9.781	9.865	9.735
5120	9.552	9.676	9.557	5260	5.662	9.793	9.714	5400	9.777	9.871	9.737
5122	9.542	9.675	9.555	5262	9.653	9.787	9.709	5402	9.777	9.860	9.737
5124	9.544	9.676	9.570	5264	9.663	9.782	9.708	5404	9.777	9.870	9.743
5126	9.539	9.677	9.571	5266	9.664	9.784	9.705	5406	9.783	9.862	9.742
5128	9.537	9.672	9.567	5268	9.664	9.786	9.592	5408	9.783	9.858	9.745
5130	9.536	9.657	9.555	5270	9.650	9.787	9.675	5410	9.782	9.868	9.757
5132	9.547	9.667	9.567	5272	5.657	9.785	5.683	5412	9.785	9.865	9.760
5134	9.549	9.657	9.555	5274	9.655	9.782	9.681	5414	9.786	9.864	9.763
5136	9.539	9.661	9.561	5276	9.650	9.789	5.575	5416	9.783	9.871	9.763
5138	9.535	9.652	9.553	5278	9.641	9.780	9.667	5418	9.777	9.873	9.762
5140	9.542	9.653	5.549	5280	9.633	9.776	5.562	5420	9.775	9.877	9.760
5142	9.545	9.651	9.557	5282	9.629	9.766	9.662	5422	9.780	9.883	9.766
5144	9.548	9.664	9.555	5284	9.626	9.757	9.557	5424	9.787	9.880	9.770
5146	9.552	9.678	9.573	5286	9.621	9.775	9.665	5426	9.783	9.872	9.775
5148	9.555	9.672	9.574	5288	9.635	9.775	9.557	5428	9.785	9.869	9.777
5150	9.552	9.675	9.573	5290	9.639	9.773	9.667	5430	9.787	9.862	9.784
5152	9.565	5.664	9.570	5292	9.643	9.775	9.666	5432	9.790	9.857	9.786
5154	9.565	9.674	9.573	5294	9.655	9.780	9.666	5434	9.797	9.875	9.793
5156	9.578	9.698	5.595	5296	9.664	9.793	9.659	5436	9.796	9.887	9.793
5158	9.590	9.705	9.590	5298	9.652	9.801	9.567	5438	9.795	9.883	9.792
5160	9.599	9.715	9.601	5300	9.657	9.801	9.674	5440	9.787	9.882	9.787
5162	9.589	9.718	9.604	5302	5.653	9.805	9.557	5442	9.786	9.887	9.785
5164	9.599	9.723	9.607	5304	9.661	9.808	9.689	5444	9.781	9.877	5.783
5166	9.598	9.719	9.513	5306	9.557	9.806	9.685	5446	9.777	9.870	9.774
5168	9.632	9.723	9.617	5308	9.657	9.803	7.691	5448	9.785	9.866	9.773
5170	9.631	9.735	9.515	5310	9.659	9.801	9.664	5450	9.791	9.865	9.767
5172	9.599	5.730	9.623	5312	9.652	9.809	5.699	5452	9.754	9.857	9.764
5174	9.592	9.738	9.527	5314	9.650	9.808	9.701	5454	9.770	9.855	9.763
5176	9.592	9.732	9.633	5316	9.655	9.807	9.700	5456	[illegible]	9.866	9.747
5179	9.597	9.734	9.534	5318	9.660	9.805	9.702	5458	9.772	9.850	9.767

Table A25 Three Track Elevation Profiles

(Stations and elevations are in feet)
(Sheet 4 of 6)

Station	Elevation		
	Left	Center	Right
5460	9.770	9.860	9.753
5462	9.769	9.861	9.789
5464	9.769	9.859	9.787
5466	9.767	9.868	9.791
5468	9.769	9.852	9.788
5470	9.785	9.886	9.792
5472	9.797	9.893	9.795
5474	9.801	9.897	9.900
5476	9.803	9.900	9.797
5478	9.804	9.896	9.735
5480	9.810	9.915	9.799
5482	9.811	9.920	9.803
5484	9.812	9.927	9.806
5486	9.819	9.929	9.810
5488	9.818	9.922	9.807
5490	9.815	9.927	9.807
5492	9.807	9.901	9.801
5494	9.807	9.920	9.793
5496	9.793	9.919	9.783
5498	9.792	9.908	9.776
5500	9.795	9.905	9.774
5502	9.797	9.903	9.771
5504	9.800	9.905	9.775
5506	9.797	9.906	9.779
5508	9.799	9.905	9.754
5510	9.799	9.906	9.788
5512	9.802	9.902	9.735
5514	9.801	9.904	9.784
5516	9.801	9.903	9.795
5518	9.803	9.902	9.790
5520	9.800	9.904	9.795
5522	9.802	9.892	9.800
5524	9.801	9.900	9.803
5526	9.806	9.904	9.514
5528	9.800	9.889	9.837
5530	9.797	9.387	9.515
5532	9.797	9.904	9.824
5534	9.799	9.913	9.827
5536	9.814	9.909	9.826
5538	9.818	9.929	9.827
5540	9.817	9.933	9.827
5542	9.825	9.937	9.525
5544	9.820	9.903	9.835
5546	9.820	9.927	9.535
5548	9.828	9.938	9.839
5550	9.826	9.927	9.543
5552	9.820	9.930	9.843
5554	9.822	9.903	9.547
5556	9.821	9.922	9.850
5558	9.822	9.930	9.554
5560	9.829	9.95[illegible]	9.863
5562	9.830	9.947	9.855
5564	9.847	9.956	9.858
5566	9.890	9.947	9.862
5568	9.849	9.947	9.861
5570	9.849	9.961	9.860
5572	9.806	9.948	9.854
5574	9.841	9.963	9.871
5576	9.841	9.962	9.578
5578	9.840	9.960	9.877
5580	9.845	9.963	9.575
5582	9.840	9.970	9.875
5584	9.839	9.953	9.374
5586	9.841	9.954	9.862
5588	9.840	9.954	9.861
5590	9.835	9.940	9.541
5592	9.836	9.934	9.862
5594	9.834	9.939	9.862
5596	9.800	9.911	9.865
5598	9.830	9.916	9.850

Station	Elevation		
	Left	Center	Right
5600	9.838	9.917	9.862
5602	9.837	9.926	9.861
5604	9.831	9.921	9.862
5606	9.801	9.901	9.866
5608	9.836	9.937	9.876
5610	9.828	9.936	9.875
5612	9.827	9.926	9.874
5614	9.824	9.939	9.876
5616	9.8[illegible]8	9.946	9.879
5618	9.829	9.953	9.876
5620	9.837	9.952	9.887
5622	9.841	9.956	9.884
5624	9.846	9.953	9.881
5626	9.846	9.961	9.879
5628	9.846	9.973	9.885
5630	9.843	9.972	9.887
5632	9.849	9.978	9.890
5634	9.850	9.977	9.896
5636	9.859	9.979	9.906
5638	9.860	9.986	9.909
5640	9.864	9.993	9.916
5642	9.867	9.999	9.925
5644	9.862	10.006	9.927
5646	9.857	10.008	9.929
5648	9.862	10.011	9.936
5650	9.870	10.017	9.945
5652	9.880	10.021	9.951
5654	9.897	10.023	9.952
5656	9.897	10.041	9.955
5658	9.903	10.040	9.956
5660	9.907	10.039	9.956
5662	9.910	10.039	9.954
5664	9.91[illegible]	[illegible]	9.949
5666	9.914	10.039	9.945
5668	9.911	10.030	9.942
5670	9.910	10.033	9.939
5672	9.916	10.020	9.932
5674	9.914	10.028	9.926
5676	9.926	10.037	9.929
5678	9.929	10.044	9.937
5680	9.926	10.049	9.944
5682	9.925	10.057	9.950
5684	9.934	10.042	9.949
5686	9.933	10.052	9.949
5688	9.930	10.052	9.951
5690	9.929	10.054	9.954
5692	9.936	10.055	9.952
5694	9.947	10.053	9.949
5696	9.944	10.045	9.942
5698	9.939	10.028	9.937
5700	9.939	10.032	9.929
5702	9.914	10.029	9.929
5704	9.917	10.024	9.925
5706	9.913	10.030	9.932
5708	9.921	10.036	9.936
5710	9.929	10.040	9.943
5712	9.931	10.044	9.957
5714	9.929	10.044	9.949
5716	9.935	10.052	9.952
5718	9.930	10.055	9.954
5720	9.934	10.056	9.950
5722	9.939	10.048	9.942
5724	9.938	10.050	9.949
5726	9.940	10.054	9.957
5728	9.945	10.049	9.956
5730	9.945	10.054	9.955
5732	9.950	10.053	9.956
5734	9.953	10.040	9.949
5736	9.958	10.041	9.949
5738	9.956	10.049	9.939

Station	Elevation		
	Left	Center	Right
5740	9.964	10.058	9.944
5742	9.967	10.052	9.940
5744	9.964	10.056	9.945
5746	9.962	10.049	9.946
5748	9.970	10.056	9.959
5750	9.972	10.064	9.966
5752	9.972	10.089	9.974
5754	9.967	10.088	9.977
5756	9.966	10.092	9.981
5758	9.974	10.091	9.980
5760	9.982	10.098	9.985
5762	9.980	10.101	9.982
5764	9.976	10.097	9.985
5766	9.975	10.098	9.980
5768	9.979	10.100	9.976
5770	9.978	10.087	9.975
5772	9.967	10.094	9.976
5774	9.970	10.087	9.975
5776	9.970	10.092	9.974
5778	9.967	10.097	9.975
5780	9.960	10.095	9.976
5782	9.960	10.089	9.979
5784	9.957	10.084	9.976
5786	9.940	10.077	9.977
5788	9.934	10.067	9.979
5790	9.930	10.067	9.980
5792	9.927	10.064	9.982
5794	9.914	10.062	9.980
5796	9.915	10.066	9.978
5798	9.912	10.074	9.975
5800	9.910	10.071	9.975
5802	9.920	10.073	9.984
5804	9.925	10.091	9.987
5806	9.927	10.088	9.994
5808	9.933	10.105	10.001
5810	9.942	10.101	10.002
5812	9.947	10.125	9.994
5814	9.963	10.120	9.991
5816	9.965	10.108	9.984
5818	9.973	10.110	9.987
5820	9.970	10.104	9.985
5822	9.975	10.101	9.985
5824	9.970	10.095	9.986
5826	9.967	10.091	9.987
5828	9.960	10.095	9.998
5830	9.961	10.105	10.004
5832	9.963	10.107	10.011
5834	9.960	10.118	10.015
5836	9.959	10.121	10.014
5838	9.963	10.115	10.013
5840	9.960	10.111	10.017
5842	9.967	10.105	10.015
5844	9.963	10.108	10.009
5846	9.957	10.115	10.004
5848	9.964	10.112	10.000
5850	9.977	10.100	9.996
5852	9.985	10.115	9.995
5854	9.990	10.111	9.993
5856	9.991	10.105	9.990
5858	9.988	10.105	9.994
5860	9.987	10.100	10.003
5862	9.988	10.095	10.003
5864	9.983	10.091	9.999
5866	9.971	10.088	9.992
5868	9.962	10.082	9.988
5870	9.957	10.081	9.985
5872	9.952	10.088	9.979
5874	9.950	10.073	9.976
5876	9.940	10.064	9.974
5878	9.947	10.061	9.965

Table A25 Three Track Elevation Profiles

(Stations and elevations are in feet)
(Sheet 5 of 6)

Station	Elevation			Station	Elevation			Station	Elevation		
	Left	Center	Right		Left	Center	Right		Left	Center	Right
5880	9.945	10.055	9.957	6020	9.962	10.082	9.979	6160	9.937	10.079	10.011
5882	9.943	10.041	9.954	6022	9.954	10.083	9.975	6162	9.957	10.086	10.012
5884	9.947	10.025	9.947	6024	9.955	10.086	9.972	6164	9.938	10.078	10.015
5886	9.943	10.026	9.946	6026	9.953	10.080	9.975	6166	9.940	10.096	10.016
5888	9.945	10.028	9.952	6028	9.957	10.076	9.971	6168	9.940	10.095	10.014
5890	9.952	10.021	9.957	6030	9.960	10.085	9.975	6170	9.958	10.096	10.009
5892	9.957	10.038	9.957	6032	9.963	10.096	9.972	6172	9.940	10.076	9.999
5894	9.961	10.053	9.980	6034	9.969	10.092	9.959	6174	9.945	10.085	10.006
5896	9.953	10.065	9.994	6036	9.973	10.096	9.964	6176	9.942	10.080	10.005
5898	9.971	10.071	10.005	6038	9.970	10.093	9.960	6178	9.939	10.079	10.002
5900	9.973	10.075	10.006	6040	9.973	10.089	9.959	6180	9.942	10.070	10.002
5902	9.989	10.072	10.008	6042	9.978	10.089	9.958	6182	9.938	10.062	9.999
5904	10.002	10.081	10.009	6044	9.976	10.087	9.955	6184	9.942	10.059	9.995
5906	10.008	10.089	10.007	6046	9.975	10.088	9.955	6186	9.955	10.063	9.995
5908	10.017	10.102	10.003	6048	9.970	10.054	9.951	6188	9.946	10.057	9.986
5910	10.032	10.112	9.997	6050	9.972	10.084	9.946	6190	9.943	10.065	9.985
5912	10.027	10.114	10.002	6052	9.950	10.073	9.946	6192	9.934	10.062	9.973
5914	10.039	10.117	10.004	6054	9.931	10.082	9.946	6194	9.936	10.049	9.962
5916	10.038	10.116	10.008	6056	9.952	10.089	9.951	6196	9.930	10.048	9.955
5918	10.040	10.115	10.010	6058	9.958	10.093	9.945	6198	9.929	10.059	9.954
5920	10.041	10.115	10.005	6060	9.990	10.092	9.954	6200	9.927	10.049	9.954
5922	10.038	10.109	10.001	6062	9.956	10.090	9.952	6202	9.929	10.081	9.955
5924	10.050	10.123	10.002	6064	9.979	10.091	9.942	6204	9.922	10.075	9.949
5926	10.013	10.113	9.998	6066	9.970	10.093	9.943	6206	9.914	10.071	9.945
5928	9.994	10.105	10.002	6068	9.970	10.082	9.942	6208	9.912	10.061	9.945
5930	9.983	10.111	10.004	6070	9.975	10.076	9.955	6210	9.900	10.071	9.949
5932	9.990	10.110	10.004	6072	9.976	10.085	9.963	6212	9.897	10.060	9.953
5934	9.957	10.098	10.000	6074	9.977	10.086	9.968	6214	9.894	10.058	9.949
5936	9.987	10.104	9.997	6076	9.953	10.085	9.973	6216	9.887	10.062	9.949
5938	9.953	10.098	9.990	6078	9.955	10.088	9.981	6218	9.889	10.061	9.944
5940	9.982	10.093	9.991	6080	9.980	10.103	9.980	6220	9.887	10.063	9.941
5942	9.983	10.091	9.956	6082	9.993	10.108	9.986	6222	9.886	10.068	9.935
5944	9.980	10.099	9.980	6084	9.987	10.095	9.985	6224	9.880	10.061	9.929
5946	9.976	10.098	9.975	6086	9.990	10.089	9.996	6226	9.877	10.055	9.925
5948	9.982	10.092	9.980	6088	9.990	10.092	9.998	6228	9.873	10.065	9.916
5950	9.993	10.091	9.984	6090	9.993	10.085	9.996	6230	9.867	10.061	9.914
5952	10.003	10.095	9.987	6092	9.977	10.096	9.996	6232	9.860	10.055	9.912
5954	10.008	10.101	9.992	6094	9.976	10.089	9.991	6234	9.853	10.043	9.915
5956	10.009	10.125	9.997	6096	9.964	10.092	9.982	6236	9.850	10.044	9.922
5958	10.010	10.123	10.010	6098	9.965	10.083	9.983	6238	9.846	10.041	9.921
5960	10.003	10.135	10.007	6100	9.950	10.085	9.986	6240	9.841	10.031	9.919
5962	10.000	10.138	10.002	6102	9.956	10.076	9.988	6242	9.844	10.021	9.918
5964	9.995	10.128	9.997	6104	9.941	10.081	9.988	6244	9.854	10.015	9.909
5966	9.994	10.115	9.988	6106	9.957	10.079	9.986	6246	9.848	10.008	9.903
5968	9.958	10.103	9.954	6108	9.955	10.076	9.987	6248	9.840	9.997	9.899
5970	9.987	10.100	9.977	6110	9.952	10.074	9.958	6250	9.844	10.009	9.898
5972	9.957	10.094	9.974	6112	9.946	10.072	9.985	6252	9.840	10.018	9.896
5974	9.984	10.097	9.955	6114	9.944	10.077	9.952	6254	9.836	10.015	9.899
5976	9.957	10.099	9.959	6116	9.943	10.075	9.975	6256	9.853	10.022	9.903
5978	9.991	10.095	9.954	6118	9.941	10.071	9.977	6258	9.827	10.013	9.899
5980	9.993	10.098	9.955	6120	9.941	10.079	9.975	6260	9.820	10.001	9.891
5982	9.992	10.095	9.950	6122	9.938	10.063	9.960	6262	9.821	10.004	9.886
5984	9.997	10.090	9.947	6124	9.938	10.070	9.969	6264	9.821	9.982	9.883
5986	9.995	10.092	9.955	6126	9.935	10.074	9.968	6266	9.826	9.956	9.879
5988	9.987	10.094	9.957	6128	9.940	10.073	9.972	6268	9.828	9.958	9.881
5990	9.954	10.093	9.963	6130	9.936	10.077	9.977	6270	9.830	9.963	9.882
5992	9.983	10.083	9.957	6132	9.935	10.076	9.974	6272	9.830	9.964	9.881
5994	9.975	10.038	9.966	6134	9.937	10.059	9.970	6274	9.831	9.972	9.879
5996	9.976	10.098	9.954	6136	9.943	10.077	9.969	6276	9.832	9.978	9.884
5998	9.975	10.086	9.965	6138	9.940	10.070	9.967	6278	9.830	9.984	9.886
6000	9.977	10.075	9.954	6140	9.934	10.061	9.970	6280	9.827	9.984	9.885
6002	9.960	10.071	9.959	6142	9.935	10.070	9.971	6282	9.823	9.974	9.890
6004	9.953	10.070	9.955	6144	9.937	10.066	9.972	6284	9.824	9.973	9.891
6006	9.945	10.073	9.965	6146	9.933	10.067	9.977	6286	9.824	9.967	9.890
6008	9.950	10.071	9.968	6148	9.936	10.066	9.981	6288	9.823	9.958	9.882
6010	9.956	10.068	9.977	6150	9.932	10.074	9.987	6290	9.820	9.949	9.879
6012	[illegible]	10.077	9.981	6152	9.930	10.069	9.996	6292	9.815	9.957	9.870
6014	9.955	10.079	9.934	6154	9.930	10.066	10.004	6294	9.806	9.952	9.863
6016	9.967	10.083	9.987	6156	9.932	10.082	10.005	6296	9.807	9.948	9.855
6018	9.955	10.079	9.955	6158	9.936	10.071	10.006	6298	9.819	9.941	9.853

Table A25 Three Track Elevation Profiles

(Stations and elevations are in feet)
(Sheet 6 of 6)

Station	Elevation		
	Left	Center	Right
6300	9.818	9.937	9.852
6302	9.817	9.935	9.853
6304	9.822	9.937	9.849
6306	9.815	9.934	9.955
6308	9.811	9.928	9.852
6310	9.809	9.931	9.951
6312	9.807	9.936	9.847
6314	9.806	9.937	9.855
6316	9.803	9.939	9.843
6318	9.796	9.943	9.841
6320	9.794	9.944	9.835
6322	9.789	9.949	9.822
6324	9.784	9.947	9.829
6326	9.781	9.948	9.830
6328	9.783	9.949	9.832
6330	9.782	9.941	9.833
6332	9.783	9.944	9.832
6334	9.786	9.938	9.83[illegible]
6336	9.787	9.956	9.842
6338	9.794	9.956	9.841
6340	9.796	9.950	9.839
6342	9.790	9.954	9.835
6344	9.792	9.934	9.834
6346	9.794	9.938	9.820
6348	9.790	9.923	9.826
6350	9.784	9.931	9.823
6352	9.783	9.921	9.825
6354	9.780	9.929	9.820
6356	9.779	9.924	9.812
6358	9.782	9.914	9.814
6360	9.786	9.927	9.804
6362	9.790	9.910	9.798
6364	9.794	9.905	9.793
6366	9.797	9.914	9.786
6368	9.795	9.912	9.786
6370	9.794	9.914	9.785
6372	9.794	9.906	9.794
6374	9.790	9.905	9.786
6376	9.787	9.904	9.789
6378	9.782	9.898	9.791
6380	9.790	9.908	9.788
6382	9.778	9.903	9.784
6384	9.776	9.901	9.789
6386	9.774	9.888	9.784
6388	9.773	9.884	9.779
6390	9.762	9.879	9.776
6392	9.754	9.864	9.779
6394	9.740	9.856	9.775
6396	9.727	9.853	9.772
6398	9.720	9.846	9.765
6400	9.719	9.854	9.781
6402	9.716	9.849	9.780
6404	9.721	9.855	9.779
6406	9.727	9.854	9.780
6408	9.734	9.846	9.784
6410	9.744	9.849	9.787
6412	9.750	9.850	9.786
6414	9.753	9.855	9.776
6416	9.757	9.856	9.774
6418	9.759	9.858	9.773
6420	9.758	9.862	9.770
6422	9.755	9.859	9.770
6424	9.752	9.861	9.765
6426	9.754	9.862	9.753
6428	9.751	9.856	9.760
6430	9.744	9.859	9.755
6432	9.739	9.852	9.751
6434	9.732	9.847	9.743
6436	9.729	9.834	9.733
6438	9.724	9.830	9.724
6440	9.721	9.831	9.720
6442	9.717	9.827	9.720
6444	9.716	9.826	9.714
6446	9.716	9.822	9.713
6448	9.717	9.822	9.707
6450	9.720	9.821	9.711
6452	9.721	9.827	9.713
6454	9.718	9.834	9.714
6456	9.721	9.832	9.719
6458	9.721	9.830	9.720
6460	9.720	9.824	9.720
6462	9.724	9.829	9.711
6464	9.718	9.827	9.711
6466	9.707	9.817	9.710
6468	9.698	9.812	9.704
6470	9.693	9.808	9.696
6472	9.693	9.811	9.683
6474	9.682	9.799	9.692
6476	9.680	9.786	9.681
6478	9.673	9.777	9.680
6480	9.660	9.766	9.673
6482	9.653	9.758	9.663
6484	9.651	9.752	9.657
6486	9.651	9.755	9.657
6488	9.648	9.751	9.649
6490	9.643	9.737	9.645
6492	9.641	9.734	9.639
6494	9.636	9.730	9.637
6496	9.636	9.732	9.640
6498	9.635	9.730	9.643
6500	9.637	9.734	9.637
6502	9.641	9.736	9.635
6504	9.642	9.738	9.641
6506	9.640	9.736	9.642
6508	9.641	9.739	9.641
6510	9.640	9.737	9.639
6512	9.638	9.739	9.637
6514	9.639	9.736	9.639
6516	9.637	9.735	9.637
6518	9.634	9.733	9.635
6520	9.633	9.736	9.638
6522	9.627	9.742	9.637
6524	9.626	9.733	9.634
6526	9.623	9.731	9.630
6528	9.620	9.727	9.625
6530	9.612	9.721	9.620
6532	9.608	9.713	9.616
6534	9.610	9.704	9.609
6536	9.607	9.702	9.574
6538	9.602	9.713	9.597
6540	9.597	9.695	9.594
6542	9.599	9.701	9.595
6544	9.597	9.698	9.592
6546	9.674	9.696	9.591
6548	9.622	9.699	9.593
6550	9.593	9.702	9.620
6552	9.588	9.706	9.604
6554	9.588	9.692	9.625
6556	9.590	9.704	9.605
6558	9.591	9.707	9.633
6560	9.588	9.708	9.621
6562	9.589	9.704	9.594
6564	9.591	9.692	9.567
6566	9.590	9.695	9.585
6568	9.590	9.696	9.589
6570	9.591	9.702	9.594
6572	9.597	9.701	9.573
6574	9.597	9.703	9.583

Table A26 Runway System Parameters (6 Degree)

SYMBOL	TYPE	VALUE	UNITS	DESCRIPTION
$H_{RC}(i)$	C	*	Ft	Center runway elevation profile
$H_{RL}(i)$	C	*	Ft	Left runway elevation profile
$H_{RR}(i)$	C	*	Ft	Right runway elevation profile
ω	V (o)		In/In	Runway slope at coordinate (X,Y)
x	V (I)		In	Distance down the runway
X_{LRO} ★	C	0.0	Ft	Determines starting point (at time = 0) on runway profile
X_{LRF}	V		Ft	Determines position on runway profile
y	V (I)		In	Distance from runway ℄., Inches
Y_{LRF}	V		Ft	Distance from runway ℄., Feet
z	V (o)		In	Runway elevation at coordinate (X,Y)
Z_{GCO}	C	‡	Ft	Center profile height at time = 0
Z_{GCX}	V		Ft	Center profile height
Z_{GLO}	C	‡	Ft	Left profile height at time = 0
Z_{GLX}	V		Ft	Left profile height
Z_{GRO}	C	‡	Ft	Right profile height at time = 0
Z_{GRX}	V		Ft	Right profile height

* See Table A25 for values of H_{RC}, H_{RL} and H_{RR} . Use station 4574 to 6574.

‡ Determined from the constant X_{LRO}

★ This input allows starting the airplane on a different part of the runway profile even though its distance down the runway is the same.

APPENDIX B

DIGITAL COMPUTER PROGRAM FOR SIMPLIFIED ANTISKID ANALYSIS PROCEDURE

The user's instructions for CDC 6600 procedure A6A which is a program for solving the equations for the simplified antiskid analysis procedure as described in Section III are as follows:

INPUT DATA

Input card data shall be tabulated on Data Sheets according to the following format for all cards:

1-66	67-72	73	74-75	76-79
Problem Data	Job	"P"	PN	CS

PN-- problem number, CS--card sequence number (numbered sequentially from 0001).

The problem data is defined by the following formats. Unless otherwise indicated, data should be entered as floating point.

Card 1

Card Columns

1-30		37-45		47
ID		JOB		M

Columns	Variable Description
1-30	ID -- Alphanumeric Identification
37-45	JOB -- Problem Name (alphanumeric)
47	M = 1 printed output only = 2 microfilm output only = 3 printed and microfilm output

Card 2

Card Columns

1-10	11-20	21-30	31-40
TSTEP	TINTP	TEND	TRITE

Variable	Description
TSTEP	Time between steps
TINTP	Internal print interval
TEND	System run time
TRITE	System print interval

Card 3

Card Columns

1-10	11-20	21-30	31-40	41-45
ACVRO	ACVSO	PCVB	VMIN	NR

Variable	Description
ACVRO	Control valve return full flow coefficient
ACVSO	Control valve supply full flow coefficient
PCVB	Control valve bias pressure
VMIN	Flywheel velocity for terminating problem
NR	Number of Brake rotors

Simplified Brake Control System (Cards 4-11)

1-10	11-20	21-30	31-40	41-50	51-60	Cards.
ALPHA	ALPHB	ABP	ABPS	XGDD	VFD	4
ACVL	CBPL	CBPU	CG	CSCVR	DG	5
ET	FNM	GCV	PBO	PCP	PFB	6
PR	RBT	RR	RTD	SCL	SCVO	7
SCVA	SCVR	TCP	UB1	UB2	UT1	8
UT2	VF	VRO	WG	WTO	WIT	9
XCVO	XSCM	XSCR	XBO	XGO	XDGO	10
XFO	XFDO					11

Variable	Description
ALPHA	Tire Friction Parameter (α)
ALPHB	Brake Lining Friction Parameter (α_B)
ABP	Piston area/brake
ABPS	Piston area/control valve
XGDD	Axle horizontal acceleration ($\ddot{x}_g$)
VFD	Flywheel peripheral acceleration ($\dot{V}_f$)
ACVL	Control valve leakage flow coefficient
CBPL	Brake P-V slope (disk not in contact)
CBPU	Brake P-V slope (disc in contact)
CG	Fore and aft spring rate at axle
CSCVR	Control valve input coefficient
DG	Fore and aft damping coefficient at axle.
ET	Tire friction velocity correction coefficient
FNM	Vertical force on tire from ground
GCV	Control valve gain
PBO	Brake pressure (at time zero)
PCP	Pilots command brake pressure
PFB	Brake piston friction hysterisis pressure
PR	Hydraulic system reservoir pressure
RBT	Brake piston torque producing radius
RR	Tire effective rolling radius
RTD	Axle height (above ground)
SCL	Control valve overlap

Variable	Description
SCVO	Control valve full open spool travel
SCVA	Control valve maximum application travel
SCVR	Control valve maximum release travel
TCP	Time to reach maximum command pressure
UB1	Brake lining friction parameter
UB2	Brake lining friction parameter
UT1	Tire friction parameter
UT2	Tire friction parameter
VF	Flywheel peripheral velocity
VRO	Tire - friction vs. velocity - parameter
WG	Mass of: Wheel, Tire, Brake, & supporting structure
WTO	Angular velocity of Tire & Wheel (at time zero)
WIT	Moment of Inertia: Tire, Wheel, & Brake rotor
XCVO	Control valve spool position (at time zero)
XSCM	Value of X_{SC} for maximum regulation '
XSCR	Value of X_{SC} for zero regulation'
XBO	Brake piston position (at time zero)
XGO	Axle horizontal position (at time zero) (X_{GO})
XDGO	Axle horizontal velocity (at time zero) (X_{GO})
XFO	Flywheel peripheral distance (at time zero) (X_{FO})
XFDO	Flywheel peripheral velocity (at time zero)(X_{FO})

1) X_{SC} is the control valve pressure regulation parameter.

Wheel Speed Sensor System

Card 12 (follows the Simplified Brake Control Systems cards)

2	Card
IOPT	12

Variable	Description
IOPT=1	the control circuit input signal is proportional to the mass displacement
IOPT=2	the control circuit input voltage is considered proportional to the wheel's angular velocity.

The wheel speed sensor system has two approaches as mentioned above. The problem data varies for each approach taken.

IOPT=1

Card Columns

1-10	11-20	21-30	31-40	41-50	51-60	Card
CCGV	CWG	CWS	DWS	GWS	WWS	13
ESN	XWS	XWS	EG			14

Variable	Description
CCGV	Output voltage coefficient (volt/in)
CWG	Hypothetical linear force motor coefficient (lbf/volt)
CWS	Spring rate (hypothethical spring) (lbf/in)
DWS	Damping coefficient (hypothetical damper) (lbf/in)
GWS	Hypothetical tachometer voltage-speed coefficient (volt sec/rad)
WWS	Mass (hypothetical mass) (lbf sec^2/in)
ESN	Input signal "noise" (volts)
XWS	Hypothetical mass displacement at time=0 (in)
$\dot{X}$WS	Hypothetical mass velocity at time=0 (in/sec)
EG	Anti-skid control circuit input signal (volts)

IOPT=2

Card Columns

1-10	11-20	21-30	Card
GWOC	ESN	EG	13

Variable	Description
GWOC	D.C. tachometer voltage-speed coefficient (volt sec/rad)
ESN	Input signal "noise" (volts)
EG	Anti-skid control circuit input signal (volts)

Card Group A (follows wheel)

2	Card
I	A1

Variable	Description
I=1	a modulated (brake pressure) circuit will be used to simulate the control system.
I=2	an electrical on-off circuit will be used to simulate the control system.

Modulated Circuit

Card Columns

1-10	11-20	21-30	31-40	41-50	51-60	Card
CM	C404	C405	C406	C407	C446	A2
C447	C448	C449	C450	C451	C452	A3
C456	C457	C458	C459	C460	C461	A4
C462	C526	C527	C528	C529	C530	A5
C531	C532	C533	C534	C535	C565	A6
C566	C567	C568	C569	C570	C571	A7
C575	C576	C577	C578	C579	C580	A8
C581	C604	C605	C606	C607	C608	A9
C609	C610	C611	C612	C613	C614	A10
C615	C616	C617	C618	C619	C620	A11
C621	C622	C623	C800	C801	C802	A12
C803	C804	C805	C806	C807	C808	A13
C809	C810	C811	C812	VC1	VC2	A14
VC3	VC4	VĊ1	VĊ2	VĊ3	VĊ4	A15
EV						A16

Variable	Description
CM	VC2 voltage coefficient equ VB
C404	ACQ3 coeff equ N7, N5-3-4, N5-7-8, N5-11-12 (DIMLS)
C405	Const equ N7, N5-3-4, N5-78, N5-11-12 (AMPS)
C406	AD5 coeff equ N4 (OHMS)
C407	Const equ N4 (VOLTS)
C446	(EG-VC1) coeff equ Q2-3 (MHOS)
C447	(VC3+VC4) coeff equ Q2-3 (MHOS)
C448	Const equ Q2-3 (AMPS)
C449	(EG-VC1) coeff equ Q2-4 (MHOS)
C450	VC2 coeff equ Q2-4 (MHOS)
C451	(VC3+VC4) coeff equ Q2-4 (MHOS)
C452	Const equ Q2-4 (AMPS)
C456	(EG-VC1) coeff equ Q2-1 (MHOS)
C457	(VC3+VC4) coeff equ Q2-1 (MHOS)
C458	Const equ Q2-1 (AMPS)
C459	(EG-VC1) coeff equ Q2-2 (MHOS)
C460	(VC3+VC4) coeff equ Q2-2 (MHOS)
C461	VC2 coeff equ Q2-2 (MHOS)
C462	Const equ Q202 (AMPS)

Variable	Description
C526	(EG-VC1) coeff equ Q2-7 (MHOS)
C527	Const equ Q2-7 (AMPS)
C528	VC2 coeff equ Q2-8 (MHOS)
C529	(EG-VC1) coeff equ Q2-8 (MHOS)
C530	Const equ Q2-8 (AMPS)
C531	(EG-VC1) Coeff equ Q2-5 (MHOS)
C532	Const Equ Q2-5 (AMPS)
C533	VC2 coeff equ Q2-6 (MHOS)
C534	(EG-VC1) coeff equ Q2-6 (MHOS)
C535	Const equ Q2-6 (AMPS)
C565	(EG-VC1) coeff equ Q2-9 (MHOS)
C566	(VC2+VC4) coeff equ Q2-9 (MHOS)
C567	Const equ Q2-9 (AMPS)
C568	VC2 coeff equ Q2-10 (MHOS)
C569	(EG-VC1) coeff equ Q2-10 (MHOS)
C570	(VC2+VC4) coeff equ Q2-10 (MHOS)
C571	Const equ Q2-10 (AMPS)
C575	(EG-VC1) coeff equ Q2-11 (MHOS)
C576	(VC2+VC4) coeff equ Q2-11 (MHOS)
C577	Const equ Q2-11 (AMPS)
C578	VC2 coeff equ Q2-12 (MHOS)
C579	(EG-VC1) coeff equ Q2-12 (MHOS)
C580	(VC2+VC4) coeff equ Q2-12 (MHOS)
C581	Const equ Q2-12 (AMPS)
C604	Const equ Q1C (AMPS)
C605	VC2 coeff equ Q-1C (MHOS)
C606	Q3 collector - Q2 emitter current ratio
C607	AEQ2 comparison constant (AMPS)
C608	Reciprocal of capacitance C1 (VOLT/AMP SEC)
C609	Reciprocal of capacitance C2 (VOLT/AMP SEC)
C610	Reciprocal of capacitance C3 (VOLT/AMP SEC)
C611	Reciprocal of capacitance C4 (VOLT/AMP SEC)
C612	AEQ2 coeff equ N10
C613	VV-EG+VC1 coeff equ N10 (MHOS)
C614	Emitter-base current ratio - Q4
C615	Locked wheel arming speed (IN/SEC)
C616	Locked wheel signal detection speed (VOLTS)
C617	Locked wheel signal current (AMPS)
C618	VC2 coeff equ 14 (MHOS)
C619	VC3 coeff equ N3 (MHOS)
C620	(EG-VC1) coeff equ R10 (MHOS)
C621	Const equ R10 (AMPS)
C622	(VC3-VC2) coeff equ VC4 (MHOS)
C623	Const equ VQ4 (AMPS)
C800	Constant equ VB (VOLTS)

Variable	Description
C801	AEQ2 coeff equ VB (OHMS)
C802	Max. valve for AEQ2 equ Q2-N (AMPS)
C803	AEQ2 coeff equ N8-3, 4, 7 & 8 (DIMLS)
C804	(VC3+VC4) coeff equ N8-1 to N8-8 (MHOS)
C805	Constant equ N8-3, 4, 7 & 8 (AMPS)
C806	AEQ2 coeff equ N8-1, 2, 5 & 6 (DIMLS)
C807	Constant equ N8-1, 2, 5 & 6 (AMPS)
C808	AEQ2 coeff equ N8-7, 8, 11 & 12 (DIMLS)
C809	(VC2+VC4) coeff equ N8-5 to N8-12 (MHOS)
C810	Constant equ N8-7, 8, 11 & 12 (AMPS)
C811	AEQ2 coeff equ N8-5, 6, 9 & 10 (DIMLS)
C812	Constant equ N8-5, 6, 9 & 10 (AMPS)
VC1	Voltage across capacitor C1 at time=0 (VOLTS)
VC2	Voltage across capacitor C2 at time=0 (VOLTS)
VC3	Voltage across capacitor C3 at time=0 (VOLTS)
VC4	Voltage across capacitor C4 at time=0 (VOLTS)
$V\dot{C}1$	Capacitor C1 voltage change rate (volts/sec)
$V\dot{C}2$	Capacitor C2 voltage change rate (volts/sec)
$V\dot{C}3$	Capacitor C3 voltage change rate (volts/sec)
$V\dot{C}4$	Capacitor C4 voltage change rate (volts/sec)
EV	Anti-skid valve voltage (VOLTS)

Electrical On-Off Circuit

Card Columns

1-10	11-20	21-30	31-40	41-50	51-60	Card
VS	C700	C701	C702	C705	C706	A2
C707	C708	C709	C710	C711	VC1	A3
$V\dot{C}1$	EV					A4

Variable	Description
VS	Supply voltage (volts)
C700	Skid detection threshold current (amps)
C701	(EG-VC1) coeff equ V6 (MHOS)
C702	Const equ V6 (AMPS)
C705	Reciprocal of capacitance C1 (volt/ amp sec)
C706	(EG-VC1) coeff equ R1 (MHOS)
C707	Const equ R1 (AMPS)

Variable	Description
C708	(EG-VC1) coeff equ V2 (MHOS)
C709	(EG-VC1) coeff equ V4-1 (MHOS)
C710	Const equ V4-1 (AMPS)
C711	ABQ1 coeff equ V4-1 (DIMLS)
VC1	Voltage across capacitor C1 at time=0 (VOLTS)
$V\dot{C}1$	Capacitor C1 voltage change rate (volts/sec)
EV	Anti-skid valve voltage (VOLTS)

OUTPUT DATA

If microfilm output data is expected, indicate "16mm print" on job sheet and write "33-4020 PR" under Setups. Only the data outputted from the modules will be microfilmed. This data is printed every "P" seconds (see Card 1) of the total run "R" (see Card 1). The internal data print is an optional print, after the outputted data print, which consists of data inside a particular module, not outputted to other modules.

RESTRICTIONS AND ERRORS

A. Restrictions

No single time step should be greater than the run time of the problem. Each time step should be greater than zero. The internal print frequencies may be zero, but the print frequency for external data should never be zero.

B. Errors

If any of the following errors occur, a message giving the error number will be printed out.

Error	Explanation
100	Microfilm option not 1, 2, or 3
101	Run time is zero
102	External print frequency is zero
103 or 120	Brake time step is zero
104 or 131	Hydraulic time step is zero
105 or 125	Airplane time step is zero
106 or 130	Wheel and tire time step is zero
107 or 127	Wheel speed sensor time step is zero

Error	Explanation
108, 133 or 126	Control system time step is zero
109 or 128	Control valve time step is zero
110 or 160	Pitch control time step is zero
111	Airplane runway option not 1 or 2
112	Wheel speed sensor option not 1 or 2
113	Number of points for nose gear airload curve less than one or greater than 20
114	Number of points for nose gear damping curve less than one or greater than 20
115	Number of points for main gear airload curve is less than 1 or greater than 20
116	Number of points for main gear damping curve (ZSM 0) less than 1 or greater than 20
117	Hydraulic option is not 1, 2, or 3

The Simplified Antiskid Analysis Procedure Digital Computer Program Listing, CDC 6600 Procedure A6A, follows.

```
      PROGRAM  A6A (INPUT,OUTPUT,TAPE5=INPUT,TAPE6=OUTPUT,TAPE22<
C
C
C
C          ANTISKID BRAKE SYSTEM  --  SIMPLIFIED MODEL
C
      COMMON /KEY/ TSTEP, TEND, TRITE, MICRC, IOPT(2), T, TINTP
     1        /SIMS/ ALPHA, ALPHB, ABP, ABPS, XGDD, VFD, ACVL,
     2 CBPL, CBPU, CG, CSCVR, DG, ET, FNM, GCV, PBO, PCP, PFB,
     3 PR, RBT, RR, RTD, SCL, SCVO, SCVA, SCVR, TCP, UB1, UB2,
     4 UT1, UT2, VF, VRO, WG, WT, WIT, XCV, XSCM, XSCR, XB, XG, XGD,
     5 XF, XFD    /AFTT/  XCVD, WTD, XBC
     5        /ICHECK/ IT
     6         /WSD/EG
     7        /CSO/ EV                   /FRST/ FLG1,FLG3
     8 /A6AC1/ VMIN, ACVRD, ACVSD, NR, PCVB
     9 /CSI/ VC1, VC2, VC3, VC4, VC1D, VC2D, VC3D, VC4D
     A /CSU/ VC1D1, VC2D1, VC3D1, VC4D1
      DATA WF /26.29/
      F1(XD,XD1,X1,H)       = (H/2.)  * (XD+XD1) + X1
      FN(XD,XD1,XD2,X1,H) = (H/12.) * (5.*XD + 8.*XD1 - XD2) + X1
C
C     SIMPLIFIED BRAKE CONTROL
    5 CALL INPUT
      KNT = 0
      FLG1 = 0.
      TIOUT = TINTP
      T = 0.
      TOUT = TRITE
      VC1D1 = VC1D
      VC2D1 = VC2D
      VC3D1 = VC3D
      VC4D1 = VC4D
   10 FLG3 = 0.
      FLG2 = 1.0
   20 XGDD1 = XGDD
      XGD2  = XGD1
      XGD1  = XGD
      XG1   = XG
```

```
      XBD2  = XBD1                                          A6AA040
      XBD1  = XBD                                           A6AA041
      XB1   = XB                                            A6AA042
      XCVD2 = XCVD1                                         A6AA043
      XCVD1 = XCVD                                          A6AA044
      XCV1  = XCV                                           A6AA045
      WTD2  = WTD1                                          A6AA046
      WTD1  = WTD                                           A6AA047
      WT1   = WT                                            A6AA048
      VFD2 = VFD1                                           A6AA049
      VFD1 = VFD                                            A6AA050
      VF1  = VF                                             A6AA051
      XFD2 = XFD1                                           A6AA052
      XFD1 = XFD                                            A6AA053
      XF1  = XF                                             A6AA054
C                                                           A6AA055
C     EQUATION 3                                            A6AA056
      IF (T - TCP) 30,30,40                                 A6AA057
   30 PMV = T * (PCP - PR)/TCP + PR                         A6AA058
      GO TO 50                                              A6AA059
   40 PMV = PCP                                             A6AA060
C                                                           A6AA061
C     EQUATION  4                                           A6AA062
   50 IF (XCV - SCL - SCVO) 60, 70, 70                      A6AA063
   60 ACVS = AMAX1 (ACVL,(XCV-SCL)*ACVSO/SCVO)              A6AA064
      GO TO 80                                              A6AA065
   70 ACVS = ACVSO                                          A6AA066
C                                                           A6AA067
C     EQUATION  5                                           A6AA068
   80 IF (-XCV-SCL-SCVO) 90, 100, 100                       A6AA069
   90 ACVR = AMAX1 (ACVL,(-SCL-XCV)*ACVRO/SCVO)             A6AA070
      GO TO 110                                             A6AA071
  100 ACVR = ACVRO                                          A6AA072
  110 CONTINUE                                              A6AA073
C                                                           A6AA074
C                                                           A6AA075
C     EQUATION 10                                           A6AA076
      IF (XB) 150, 150, 160                                 A6AA077
  150 PB # CBPL * XB & PBO                                  A6AA078
```

```
      GO TO 170                                                         A6AA079
  160 PB # CBPU * XB & PBO                                              A6AA080
C     EQUATION 6 AND 7                                                  A6AA081
  170 QCVS = ACVS * SIGN(1.,PMV-PB) * SQRT (ABS(PMV - PB))              A6AA082
      QCVR = ACVR * SIGN(1.,PB-PR)  * SQRT (ABS(PB-PR))                 A6AA083
C                                                                       A6AA084
C     EQUATION 8                                                        A6AA085
      QB = QCVS - QCVR                                                  A6AA086
C                                                                       A6AA087
C     EQUATION 9                                                        A6AA088
      XBD = QB/ABPS                                                     A6AA089
C                                                                       A6AA090
C     EQUATION 11                                                       A6AA091
      XSC # CSCVR * EV                                                  A6AA092
C                                                                       A6AA093
C     EQUATION 12                                                       A6AA094
      IF (XSC.LE.XSCM) GO TO 200                                        A6AA095
      IF (XSC.LT.XSCR) GO TO 210                                        A6AA096
      RSC = 0.                                                          A6AA097
      GO TO 220                                                         A6AA098
  200 RSC = 1.                                                          A6AA099
      GO TO 220                                                         A6AA100
  210 RSC = (XSCR - XSC)/(XSCR - XSCM)                                  A6AA101
C                                                                       A6AA102
C     EQUATION 13                                                       A6AA103
  220 PSC = RSC * (PMV - PR) + PR + PCVE                                A6AA104
C                                                                       A6AA105
C     EQUATION 14                                                       A6AA106
      VCV = GCV * (PSC - PB)                                            A6AA107
C                                                                       A6AA108
C     EQUATION 15                                                       A6AA109
      IF (XCV.GE.SCVA) GO TC 240                                        A6AA110
      IF (XCV.GT.SCVR) GO TO 230                                        A6AA111
      XCVD = AMAX1 (0,VCV)                                              A6AA112
      GO TO 250                                                         A6AA113
  230 XCVD = VCV                                                        A6AA114
      GO TO 250                                                         A6AA115
  240 XCVD = AMIN1 (0,VCV)                                              A6AA116
C                                                                       A6AA117
```

```
C     EQUATION 16                                                       A6AA118
  250 TEMP = PFB * SIGN(1.,XBD)                                         A6AA119
      PE = AMAX1 (O,PB-PBO-TEMP)                                        A6AA120
C                                                                       A6AA121
C     EQUATION 17                                                       A6AA122
      VB = RBT * WT                                                     A6AA123
C                                                                       A6AA124
C     EQUATION 18                                                       A6AA125
      IF (VB)  300, 310, 320                                            A6AA126
  300 UB = -UB1 - UB2 * EXP(ALPHB * VB)                                 A6AA127
      GO TO 330                                                         A6AA128
  310 UB = 0.                                                           A6AA129
      GO TO 330                                                         A6AA130
  320 UB = UB1 + UB2 * EXP (-ALPHE * VB)                                A6AA131
C                                                                       A6AA132
C     EQUATION 19                                                       A6AA133
  330 TBT = ABP * RBT * 2.0 * NR * PE * UB                              A6AA134
C                                                                       A6AA135
C     EQUATION 20                                                       A6AA136
      FG = -CG*XG - DG*XGD                                              A6AA137
C                                                                       A6AA138
C     EQUATION 23                                                       A6AA139
      VR = VF + XGD - RR*WT                                             A6AA140
C                                                                       A6AA141
C     EQUATION 25                                                       A6AA142
      IF (VR.GT.VRO)  GO TO 400                                         A6AA143
      IF (VR.GT.-VRO) GO TO 410                                         A6AA144
      UT = -UT1 -(UT2 - ET * VF) * EXP (ALPHA*(VR+VRO))                 A6AA145
      GO TO 420                                                         A6AA146
  400 UT = UT1 + (UT2 - ET *VF) * EXP(-ALPHA*(VR-VRO))                  A6AA147
      GO TO 420                                                         A6AA148
  410 UT = (VR/VRO) * (UT1+UT2-ET*VF)                                   A6AA14
C                                                                       A6AA
C     EQUATION  24                                                      A6AA151
  420 FBT = FNM * UT                                                    A6AA152
C                                                                       A6AA153
C     EQUATION 26                                                       A6AA154
      VFD = -FBT / WF                                                   A6AA155
C                                                                       A6AA156
```

```
C     EQUATION 27                                                    A6AA157
      XFO  = VF / 12.0                                               A6AA158
C                                                                    A6AA159
C     EQUATION 21                                                    A6AA16D
      XGDO = (FG - FBT)/WG                                           A6AA161
C                                                                    A6AA162
C     EQUATION 22                                                    A6AA163
      WTD = (FBT * RTO - TBT)/WIT                                    A6AA164
      IF%FLG1.NE.0.< GOTO 433                                        A6AA165
      IF%FLG2.NE.0.< GOTO 434                                        A6AA166
      XGDO1 # XGDD                                                   A6AA167
  433 IF (FLG2.EQ.0.) GO TO 500                                      A6AA168
  434 IF (TINTP.EQ.D.) GO TU 50D                                     A6AA169
      IF (T - TIOUT)  5D0, 450, 450                                  A6AA170
  450 TIOUT = TIOUT + TINTP                                          A6AA171
      FLG3 = 1.                                                      A6AA172
      WRITE (22,2DDD) T, ACVR, ACVS, EV, FG, FBT, PB, PE, PMV,       A6AA173
     1PSC, QB, QCVR, QCVS, RSC, TBT, UB, UT, VB, VCV, WT, WTO,       A6AA174
     2XCV, XCVD, XSC, XB, XBC, XG, XGC, XCCC, VR                     A6AA175
 200D FORMAT (* *,*SIMPLIFIED BRAKE CCNTRCL INTERNAL CATA*/          A6AA176
     1 *      T=*,F15.8,*   ACVR=*,E11.4,*   ACVS=*,E11.4,           A6AA177
     2 *     EV=*,E11.4,*     FG=*,E11.4,*    FBT=*,E11.4/           A6AA178
     3 *     PB=*,E11.4,*     PE=*,E11.4,*    PMV=*,E11.4,           A6AA179
     4 *    PSC=*,E11.4,*     QB=*,E11.4,*   CCVR=*,E11.4/           A6AA18D
     5 *   QCVS=*,E11.4,*    RSC=*,E11.4,*    TBT=*,E11.4,           A6AA181
     6 *     UB=*,E11.4,*     UT=*,E11.4,*     VB=*,E11.4/           A6AA182
     7 *    VCV=*,E11.4,*     WT=*,E11.4,*    WTD=*,E11.4,           A6AA183
     8 *    XCV=*,E11.4,*   XCVO=*,E11.4,*    XSC=*,E11.4/           A6AA184
     9 *     XB=*,E11.4,*    XBD=*,E11.4,*     XG=*,E11.4,           A6AA185
     A *    XGO=*,E11.4,*   XGOD=*,E11.4,*     VR=*,E11.4/)          A6AA186
  5D0 XGD = F1(XGCD,XCOD1,XGD1,TSTEP)                                A6AA187
      IF (FLG1.NE.D.) GO TO 510                                      A6AA188
      XG  = F1(XGD,XGD1,XG1,TSTEP)                                   A6AA189
      XB  = F1(XBC,XBD1,XB1,TSTEP)                                   A6AA190
      XCV = F1(XCVO,XCVD1,XCV1,TSTEP)                                A6AA191
      WT  = F1(WTC,WTD1,WT1,TSTEP)                                   A6AA192
      VF = F1(VFD,VFD1,VF1,TSTEP)                                    A6AA193
      XF = F1(XFO,XFD1,XF1,TSTEP)                                    A6AA194
      GO TO 520                                                      A6AA195
```

```
510 XG   = FN(XGD,XG01,XG02,XG1,TSTEP)                                  A6AA196
    XB   = FN(XBD,XB01,XB02,XB1,TSTEP)                                  A6AA197
    XCV  = FN(XCVD,XCVD1,XCVD2,XCV1,TSTEP)                              A6AA198
    WT   = FN(WTO,WTD1,WT02,WT1,TSTEP)                                  A6AA199
    VF = FN(VFD,VFD1,VFD2,VF1,TSTEP)                                    A6AA200
    XF = FN(XFO,XFO!,XFD2,XF1,TSTEP)                                    A6AA201
520 IF (FLG2.NE.0.) GO TO 530                                           A6AA202
    FLG2 = 1.                                                           A6AA203
    GO TO 20                                                            A6AA204
530 CALL WHSPSN                                                         A6AA205
    IF%IOPT%2<.EQ.2< GO TO 540                                          A6AA206
    CALL CONSYS                                                         A6AA207
    GO TO 545                                                           A6AA208
540 CALL CONCIR                                                         A6AA209
545 FLG1 = 1.                                                           A6AA210
    T = T + TSTEP                                                       A6AA211
    IF (VF .LE. VMIN) GO TC 600                                         A6AA212
    IF (T - TEND) 550, 605, 605                                         A6AA213
550 IF (T - TOUT)  10, 600, 600                                         A6AA214
600 TOUT = TOUT + TRITE                                                 A6AA215
605 WRITE (6,6010) T, TBT, XB, PB, PMV, XCV, EG, EV, WT, XF,XG,VF       A6AA216
6010 FORMAT (*0*,T50,*TIME =*,F16.8/* *,T14,*SIMPLIFIED BRAKE*/* *,     A6AA217
   1T14,*CONTROL SYSTEM*,T30,*   TBT=*,E11.4,*   XB=*,E11.4,*    PB=*,  A6AA218
   2E11.4/* *,T30,*   PMV=*,E11.4,*   XCV=*,E11.4,*  EG=*,E11.4/        A6AA219
   3 * *,T3C,*    EV=*,E11.4,*   WT=*,E11.4,*   XF=*,E11.4/             A6AA220
   4 * *,T30,*    XG=*,E11.4,*   VF=*,E11.4/)                           A6AA221
    IF (VF .LE. VMIN) GO TO 5                                           A6AA222
    IF (T - TENO) 610, 5, 5                                             A6AA223
610 KNT = KNT +1                                                        A6AA224
    IF (MOD(KNT,8))  10, 62C, 1C                                        A6AA225
620 CALL EJECT                                                          A6AA226
    GO TO 1C                                                            A6AA227
    END                                                                 A6AA228
```

```
                SUBROUTINE   WHSPSN
C
C                  THE WHEEL SPEED SENSOR SYSTEM
C
      COMMON /KEY/ TSTEP,TEND,TRITE,MICRO,IOPT(2),T,TINTP
     1          /FRST/ FLG1,FLG3     /CSO/ EV
     2          /WSC/  CCGV,  CWG,  CWS,  DWS,  GWS, GWCC,  WWS, ESN
     3          /WSI/   XWS, XWSD
     4          /WSO/ EG
     5          /SIMS/ SIMP(44)
      EQUIVALENCE  (WT,SIMP(35))
C
      IF(IOPT(1).EQ.2)  GO TO 60
      FLG4 = 0.
C
   10 XWSD01 = XWSDD
      XWSD2  = XWSD1
      XWSD1  = XWSD
      XWS1   = XWS
C
C     EQUATION  (1)
      EWS = GWS * WT
C
C     EQUATION  (2)
      FWS = CWG * EWS
C
C     EQUATION  (3)
      XWSDD = FWS/WWS - (CWS/WWS) * XWS - (DWS/WWS) * XWSD
C
C     EQUATION  (4)
      EG = CCGV * XWS + ESN
C
C     CHECK FOR INTERNAL PRINT
      IF (FLG4.EQ.0.) GO TO 30
      IF (FLG3.EQ.0.) GO TO 30
   20 WRITE(22,6000) T, ESN, EG, EWS, FWS, XWS, XWSD, XWSDD
 6000 FORMAT(*0WHEEL SPEED SENSOR   OPT=1*/
     1    *  T=*,E15.8,*    ESN=*,E11.4,*     EG=*,E11.4,
     2*    EWS=*,E11.4,*    FWS=*,E11.4,*    XWS=*,E11.4/
```

```
     3*    XWSD=*,E11.4,*  XWSDD=*,E11.4)                                  A6AI040
C                                                                          A6AI041
C      PERFORM INTEGRATION                                                 A6AI042
   30 XSWD =  (TSTEP/2.) * (XWSDD + XWSDD1) + XWSD1                        A6AI043
      IF (FLG1.NE.0.) GO TO 40                                             A6AI044
      XWS =  (TSTEP/2.) * (XWSD + XWSDI) + XWS1                            A6AI045
      GO TO 50                                                             A6AI046
   40 XWS =  (TSTEP/12.) * (5.*XWSD + 8.*XWSD1 - XWSD2) + XWS1             A6AI047
   50 IF (FLG4.NE.0.) GO TO 55                                             A6AI048
      FLG4 = 1.                                                            A6AI049
      GO TO 10                                                             A6AI050
   55 RETURN                                                               A6AI051
C                                                                          A6AI052
C      EQUATION  (5)    OPTION 2                                           A6AI053
   60 EG = GWOC * WT + ESN                                                 A6AI054
      IF ( TINTP.EQ.0.) GO TO 80                                           A6AI055
      IF ( FLG3.EQ.0.)  GC TO 80                                           A6AI056
      WRITE (22,6010)  T, EG, WT, ESN                                      A6AI057
 6010 FORMAT(*0 WHEEL SPEED SENSOR*/*  T=*,F15.8,                          A6AI058
     1*    EG=*,E11.4,*    WT=*,E11.4,*   ESN=*,E11.4)                     A6AI059
   80 RETURN                                                               A6AI060
C                                                                          A6AI061
      END                                                                  A6AI062
C                                                                          A6AL001
C                                                                          A6AL002
```

```
                 S U B R O U T I N E    C O N S Y S                       A6AL003
C                                                                         A6AL004
C                THE  MOOULATEO  ANTISKIO  CCNTRCL  CIRCUIT               A6AL005
C                                                                         A6AL006
      COMMON /KEY/ TSTEP, TENO, TRITE, MICRG, IOPT(2), T, TINTP           A6AL007
     1       /SIMS/ SIMP(44)                                              A6AL008
     2       /FRST/ FLG1,FLG3                                             A6AL009
     3       /CSI/  VC1,  VC2,  VC3,  VC4, VC10, VC2D, VC3D, VC40         A6AL010
     4       /CSO/  EV                                                    A6AL011
     5       /WSO/  EG                                                    A6AL012
      COMMON /CSC/ CM, C404, C405, C406, C407, C446, C447, C448,          A6AL013
     1           C449, C450, C451, C452, C456, C457, C458, C459,          A6AL014
     2           C460, C461, C462, C526, C527, C528, C529, C530,          A6AL015
     3           C531, C532, C533, C534, C535, C565, C566, C567,          A6AL016
     4           C568, C569, C570, C571, C575, C576, C577, C578,          A6AL017
     5           C579, C580, C581, C604, C605, C606, C607, C608,          A6AL018
     6           C609, C610, C611, C612, C613, C614, C615, C616,          A6AL019
     7           C617, C618, C619, C620, C621, C622, C623, C800,          A6AL020
     8           C801, C802, C803, C804, C805, C806, C807, C808,          A6AL021
     9           C809, C810, C811, C812, N                                A6AL022
     A /CSU/ VC101, VC201, VC301, VC4D1                                   A6AL023
      EQUIVALENCE (VF,SIMP(32))                                           A6AL024
C                                                                         A6AL025
      F1(XO,XO1,X1,H) = H*.5*(XO + XD1) + X1                              A6AL026
      FN(XO,XD1,XO2,X1,H) =(H/12.)*(5.*XD + 8.*XO1 - XD2) + X1            A6AL027
C                                                                         A6AL028
      TO = TSTEP                                                          A6AL029
      FLG5 = 1.0                                                          A6AL030
   10 VC102 = VC1D1                                                       A6AL031
      VC101 = VC10                                                        A6AL032
      VC11  = VC1                                                         A6AL033
      VC2D2 = VC201                                                       A6AL034
      VC201 = VC20                                                        A6AL035
      VC21  = VC2                                                         A6AL036
      VC302 = VC301                                                       A6AL037
      VC301 = VC30                                                        A6AL038
      VC31  = VC3                                                         A6AL039
      VC402 = VC401                                                       A6AL040
      VC401 = VC4D                                                        A6AL041
```

```
      VC41  = VC4                                                      A6AL042
C                                                                      A6AL043
C     EQUATION  (5)                                                    A6AL044
      EGMVC1 = EG - VC1                                                A6AL045
C                                                                      A6AL046
C     EQUATION  (R10)                                                  A6AL047
      VALUE = C621 / C620                                              A6AL048
      AD8 = 0.                                                         A6AL049
      IF (EGMVC1 .GT. VALUE) AD8 = EGMVC1 * C620 - C621                A6AL050
C                                                                      A6AL051
C     EQUATION  (Q-1C)                                                 A6AL052
      IF    (EGMVC1) 20, 25, 25                                        A6AL053
   20 ACQ1 = C604 - C605 * VC2                                         A6AL054
      IF (VC2 - C604/C605)  30, 25, 25                                 A6AL055
   25 ACQ1 = 0.                                                        A6AL056
C                                                                      A6AL057
C     EQUATION  (6)                                                    A6AL058
   30 ALWS = 0.                                                        A6AL059
      IF (VF .GT. C615 .AND. EG .LT. C616) GC TC 600                   A6AL060
C                                                                      A6AL061
C     EQUATION  (VQ4)                                                  A6AL062
      VALU = VC3 - VC2                                                 A6AL063
      ABQ4 = 0.                                                        A6AL064
      IF (VALU .GT. C623/C622) ABQ4 = VALU * C622 - C623               A6AL065
C                                                                      A6AL066
C     CIRCUIT CONDITICN TEST EQUATIONS    TABLE VI-2  A,B,C            A6AL067
      K = 1                                                            A6AL068
      VC34 = VC3 + VC4                                                 A6AL069
      VC24 = VC2 + VC4                                                 A6AL070
   40 GO TO (50,60,70,80,90,100,110,120,130,14C,15C,160), N            A6AL071
  600 ALWS = C617                                                      A6AL072
      WRITE (6,6040) ALWS, VF,C615,EG,C616                             A6AL073
 6040 FORMAT(*0MODULATED CONTROL CIRCUIT  ALWS TEST CCNDITION FAILED.* A6AL074
     1/* ALWS = *,E11.4,* VF = *,E11.4, * C615 = *,E11.4,              A6AL075
     2 * EG= *,E11.4,* C616 = *,E11.4)                                 A6AL076
      CALL EXIT                                                        A6AL077
   45 K = C                                                            A6AL078
      VC34 = VC3 + VC4                                                 A6AL079
      VC24 = VC2 + VC4                                                 A6AL080
```

```
C
C        CIRCUIT  CONDITION    1
   50 AEQ2 = - EGMVC1*C456 - VC34*C457 + C458
      IF (AEQ2 - C6C7) 51, 51, 53
   51 IF (AEQ2 .LT. 0.0) AEQ2 = 0.0
      V8 = VC2*CM + AEQ2*C801 - C800
      IF (V8) 52, 52, 53
   52 AC4  = AEQ2 * C806 - VC34 * C804 - C8C7
      IF (AC4)  53, 53, 54
   53 IF (K) 180, 60, 45
   54 N = 1
      GO TO 180
C
C        CIRCUIT  CONDITICN   2
   60 AEQ2 = VC2*C461 - EGMVC1*C459 - VC34*C46C + C462
      IF (AEQ2 - C607) 61, 61, 63
   61 IF (AEQ2 .LT. 0.0) AEQ2 = 0.0
      VB = VC2*CM + AEQ2*C801 - C800
      IF (VB) 63, 63, 62
   62 AC4 = AEQ2 * C8C6 - VC34 * C804 - C807
      IF (AC4) 63, 63, 64
   63 IF (K) 180, 70, 45
   64 N = 2
      GO TO 180
C
C        CIRCUIT  CONDITION    3
   70 AEQ2 = - EGMVC1*C446 - VC34*C447 + C448
      IF (AEQ2 - C607) 73, 73, 71
   71 IF (AEQ2 .GT. C802) AEQ2 = C802
      VB = VC2*CM + AEQ2*C801 - C80C
      IF (VB) 72, 72, 73
   72 AC4 = AEQ2 * C803 - VC34 * C804 - C805
      IF (AC4) 73, 73, 74
   73 IF (K) 180, 80, 45
   74 N = 3
      GO TO 180
C
C        CIRCUIT  CONDITION    4
```

```
   80 AEQ2 = VC2*C450 - EGMVC1*C449 - VC34*C451 + C452            A6AL119
      IF (AEQ2 - C607) 83, 83, 81                                A6AL120
   81 IF (AEQ2 .GT. C802) AEQ2 = C8C2                            A6AL121
      V8 = VC2*CM + AEQ2*C801 - C800                             A6AL122
      IF (V8) 83, 83, 82                                         A6AL123
   82 AC4 = AEQ2 * C803 - VC34 * C804 - C8C5                     A6AL124
      IF (AC4) 83, 83, 84                                        A6AL125
   83 IF (K) 180, 90, 45                                         A6AL126
   84 N = 4                                                      A6AL127
      GO TO 180                                                  A6AL128
C                                                                A6AL129
C     CIRCUIT  CONOITION   5                                     A6AL130
   90 AEQ2 = - EGMVC1*C531 + C532                                A6AL131
      IF (AEQ2 - C607) 91, 91, 94                                A6AL132
   91 IF (AEQ2 .LT. 0.0) AEQ2 = 0.0                              A6AL133
      V8 = VC2*CM + AEQ2*C8C1 - C8CC                             A6AL134
      IF (V8) 92,  92,  94                                       A6AL135
   92 AC4 = 0.0                                                  A6AL136
      TEMP1 = AEQ2 * C806 - VC34 * C8C4 - C8C7                   A6AL137
      IF (TEMP1) 93, 93, 94                                      A6AL138
   93 TEMP2 = AEQ2 * C811 - VC24 * C809 - C812                   A6AL139
      IF (TEMP2) 94, 95, 95                                      A6AL140
   94 IF (K) 180, 100, 45                                        A6AL141
   95 N = 5                                                      A6AL142
      GO TO 180                                                  A6AL143
C                                                                A6AL144
C     CIRCUIT  CONDITION   6                                     A6AL145
  100 AEQ2 = VC2*C533 - EGMVC1*C534 - C535                       A6AL146
      IF (AEQ2 - C607) 101, 101, 104                             A6AL147
  101 IF (AEQ2 .LT. 0.0) AEQ2 = 0.0                              A6AL148
      VB = VC2*CM + AEQ2*C801 - C800                             A6AL149
      IF (VB) 104, 104, 102                                      A6AL150
  102 AC4 = 0.0                                                  A6AL151
      TEMP1 = AEQ2 * C806 - VC34 * C804 - C807                   A6AL152
      IF (TEMP1) 103, 103, 104                                   A6AL153
  103 TEMP2 = AEQ2 * C811 - VC24 * C809 - C812                   A6AL154
      IF (TEMP2) 104, 105, 105                                   A6AL155
  104 IF (K) 180, 110, 45                                        A6AL156
  105 N = 6                                                      A6AL157
      GO TO 180                                                  A6AL158
```

```
C                                                                       A6AL159
C     CIRCUIT  CONDITION   7                                            A6AL160
  110 AEQ2 = - EGMVC1*C526 + C527                                       A6AL161
      IF (AEQ2 - C607) 114, 114, 111                                    A6AL162
  111 IF (AEQ2 .GT. C802) AEQ2 = C802                                   A6AL163
      V8 = VC2*CM + AEQ2*C801 - C800                                    A6AL164
      IF (V8) 112, 112, 114                                             A6AL165
  112 AC4 = 0.0                                                         A6AL166
      TEMP1 = AEQ2 * C803 - VC34 * C804 - C805                          A6AL167
      IF (TEMP1) 113, 113, 114                                          A6AL168
  113 TEMP2 = AEQ2 * C808 - VC24 * C809 - C810                          A6AL169
      IF (TEMP2) 114, 115, 115                                          A6AL170
  114 IF (K) 180, 120, 45                                               A6AL171
  115 N = 7                                                             A6AL172
      GO TO 180                                                         A6AL173
C                                                                       A6AL174
C     CIRCUIT  CONDITION   8                                            A6AL175
  120 AEQ2 = VC2*C528 - EGMVC1*C529 - C530                              A6AL176
      IF (AEQ2 - C607) 124, 124, 121                                    A6AL177
  121 IF (AEQ2 .GT. C802) AEQ2 = C802                                   A6AL178
      V8 = VC2*CM + AEQ2*C801 - C800                                    A6AL179
      IF (V8) 124, 124, 122                                             A6AL180
  122 AC4 = 0.0                                                         A6AL181
      TEMP1 = AEQ2 * C803 - VC34 * C804 - C805                          A6AL182
      IF (TEMP1) 123, 123, 124                                          A6AL183
  123 TEMP2 = AEQ2 * C808 - VC24 * C809 - C810                          A6AL184
      IF (TEMP2) 124, 125, 125                                          A6AL185
  124 IF (K) 180, 130, 45                                               A6AL186
  125 N = 8                                                             A6AL187
      GO TO 180                                                         A6AL188
C                                                                       A6AL189
C     CIRCUIT  CONDITION   9                                            A6AL190
  130 AEQ2 = - EGMVC1*C565 - VC24*C566 + C567                           A6AL191
      IF (AEQ2 - C607) 131, 131, 133                                    A6AL192
  131 IF (AEQ2 .LT. 0.0) AEQ2 = 0.0                                     A6AL193
      V8 = VC2*CM + AEQ2*C801 - C800                                    A6AL194
      IF (V8) 132, 132, 133                                             A6AL195
  132 AC4 = AEQ2 * C811 - VC24  * C809 - C812                           A6AL196
      IF (AC4) 134, 133, 133                                            A6AL197
```

```
  133 IF (K) 180, 140, 45
  134 N = 9
      GO TO 180
C
C     CIRCUIT  CONDITION  10
  140 AEQ2 = VC2*C568 - EGMVC1*C569 - VC24*C570 - C571
      IF (AEQ2 - C607) 141, 141, 143
  141 IF (AEQ2 .LT. 0.0) AEQ2 = 0.0
      V8 = VC2*CM + AEQ2*C801 - C800
      IF (V8) 143, 143, 142
  142 AC4 = AEQ2 * C811 - VC24  * C809 - C812
      IF (AC4) 144, 143, 143
  143 IF (K) 180, 150, 45
  144 N = 10
      GO TO 180
C
C     CIRCUIT  CONDITION  11
  150 AEQ2 = - EGMVC1*C575 - VC24*C576 + C577
      IF (AEQ2 - C607) 153, 153, 151
  151 IF (AEQ2 .GT. C802) AEQ2 = C802
      V8 = VC2*CM + AEQ2*C801 - C800
      IF (V8) 152, 152, 153
  152 AC4 = AEQ2 * C808 - VC24  * C809 - C810
      IF (AC4) 154, 153, 153
  153 IF (K) 180, 160, 45
  154 N = 11
      GO TO 180
C
C     CIRCUIT  CONDITION  12
  160 AEQ2 = VC2*C578 - EGMVC1*C579 - VC24*C580 - C581
      IF (AEQ2 - C607) 163, 163, 161
  161 IF (AEQ2 .GT. C802) AEQ2 = C802
      V8 = VC2*CM + AEQ2*C801 - C800
      IF (V8) 163, 163, 162
  162 AC4 = AEQ2 * C808 - VC24  * C809 - C810
      IF (AC4) 164, 163, 163
  163 IF (K) 180, 170, 45
  164 N = 12
      GO TO 180
```

```
  170 K = -1
      GO TO 40
  180 CONTINUE
C
C     EQUATION  (LW-1)
      AVA1 = AEQ2 + ALWS
C
C     EQUATION  (N5)   TABLE VI-3
      GO TO (190,190,200,200,210,210,22C,220,230,230,240,240), N
  190 AD5 = AVA1*C606 - AC4
      GO TO 250
  200 AD5 = AVA1*C606*C404 - C405 - AC4
      GO TO 250
  210 AD5 = AVA1 * C6C6
      GO TO 250
  220 AD5 = AVA1*C606*C404 - C405
      GO TO 250
  230 AD5 = AVA1*C606 - AC4
      GO TO 250
  240 A05 = AVA1*C606*C404 - C405 - AC4
  250 IF (A05 .LT.0.) AD5 = C.
C
C     EQUATION  (N4)
      EV = A05 * C406 + C407
C
C     EQUATION  (N10)
      AR3 = AEQ2*C612 + (EV - EGMVC1)*C613
C
C     EQUATION  (N11)
      AC1 = AC8 - AR3 - ACQ1
C
C     EQUATION  (A1)
      VC10 = AC1 * C608
C
C     EQUATION (N14)
C
      IF (AC4) 260, 270, 270
  260 AC2 = ABQ4 * C614 + AC4 - VC2 *C618
      GO TO 280
```

```
  270 AC2 = ABQ4 * C614 - VC2 * C618
C
C     EQUATION  (A2)
  280 VC2D = AC2 * C609
C
C     EQUATION  (N3)
      IF (AC4) 29D, 290, 30D
  290 AC3 = - C619*VC3 - ABQ4
      GO TO 310
  3D0 AC3 = AC4 - VC3*C619 - ABQ4
C
C     EQUATION  (A3)
  31D VC3D = AC3 * C61D
C
C     EQUATION  (A4)
      VC40 = AC4 * C611
C
C     CHECK PRINT INTERVAL
      IF (FLG5.EQ.0.) GO TO 33D
      IF (FLG3.EQ.0.) GO TO 330
  320 WRITE(22,6D10) T, ABQ4, AC1, AC2, AC3, AC4, ACQ1, AD5, AD8,
     1  AEQ2, AEQ4, ALWS, AR3, VB, VC1, VC10, VC2, VC2O, VC3,
     2  VC3D, VC4, VC40, EV, N
 6D1D FORMAT (*0 CONTROLLER INTERNAL DATA*/
     1      *  T=*,E15.8,*   ABQ4=*,E11.4,*    AC1=*,E11.4,
     2*      AC2=*,E11.4,*    AC3=*,E11.4,*    AC4=*,E11.4/
     3*    ACQ1=*,E11.4,*    AO5=*,E11.4,*    AO8=*,E11.4,
     4*    AEQ2=*,E11.4,*   AEQ4=*,E11.4,*   ALWS=*,E11.4/
     5*     AR3=*,E11.4,*     VB=*,E11.4,*    VC1=*,E11.4,
     6*    VC1D=*,E11.4,*    VC2=*,E11.4,*   VC2O=*,E11.4/
     7*     VC3=*,E11.4,*   VC3D=*,E11.4,*    VC4=*,E11.4,
     8*    VC4D=*,E11.4,*     EV=*,E11.4,*      N=*,I3)
C
C     PERFORM  INTEGRATION
  330 IF (FLG1.NE.0.) GO TO 340
      VC1 = F1(VC10,VC101,VC11,TD)
      VC2 = F1(VC2D,VC201,VC21,TO)
      VC3 = F1(VC30,VC3D1,VC31,TD)
      VC4 = F1(VC4D,VC4D1,VC41,TD)
```

```
      GO TO 350                                                         A6AL315
  340 VC1 = FN(VC1D,VC1D1,VC1D2,VC11,TC)                                A6AL316
      VC2 = FN(VC2D,VC2D1,VC2D2,VC21,TD)                                A6AL317
      VC3 = FN(VC3D,VC3D1,VC3D2,VC31,TD)                                A6AL318
      VC4 = FN(VC4D,VC4D1,VC4D2,VC41,TD)                                A6AL319
C                                                                       A6AL320
  350 WRITE (6,1005) N, VC1, VC2, VC3, VC4                              A6AL321
 1005 FORMAT (*0*,T14,*SUBROUTINE CONSYS*,T31,*  N=*,I2,*   VC1=*,E11.4,A6AL322
     1 *   VC2=*,E11.4/ * *,T30, *           VC3=*,E11.4,*   VC4=*,E11.4 A6AL323
     2 /)                                                               A6AL324
      IF (FLG5.NE.0.) GO TO 360                                         A6AL325
      FLG5 = 1.                                                         A6AL326
      GO TO 10                                                          A6AL327
  360 RETURN                                                            A6AL328
      END                                                               A6AL329
```

```
C
C
                   S U B R O U T I N E      I N P U T
C
C         THIS ROUTINE REAOS THE PRCBLEM CATA AND PRINTS A LISTING.
C
      COMMON /KEY/ TSTEP,TENO,TRITE,MICRO,ICPTI2),T,TINTP
     1         /SIMS/ SIMPI44)
      COMMON /WSC/ CCGV, CWG, CWS, OWS, GWS, GWCC, WWS, ESN
     1         /WSI/ XWS, XWSO       /WSO/ EG
     C         /CSC/ CS(76), N      /CSI/ C(8)
     0         /CSO/  EV
     E /AFTT/XCVO,WTO,XBO
     F /A6AC1/ VMIN, ACVRO, ACVSO, NR, PCVB
      COMMON /ICHECK/ IT   /CCC/ CC(11)   /CCI/  VC1, VC10
      COMMON /DAT/ JOB, OAY, IPAGE, PAGE(2)
      OIMENSICN IOI3)
      OATA IDASH/1H-/
C
      IT= 0
      CALL DATE IDAY)
      IPAGE = 100000
      REAO I5,4000) IO, JOB, MICRO
      JOB = (JOB.ANO.77777777777700777777B).OR. 46000000B
 4000 FORMAT (3A10,6X,A9,I2)
      IF IECF(5)) 210, 1
    1 CONTINUE
      REAO I5,5000) TSTEP, TINTP, TENO, TRITE
 5000 FORMAT (4F10.0)
      REAO (5,5005) ACVRO, ACVSO, PCVB, VMIN, NR
 5005 FORMAT (4F10.0, I5)
C     SIMPLIFIEO BRAKE CCNTRCL
      REAO (5,5010) SIMP
 5010 FORMATI6F10.0)
      REAO%5,5010< XCVD,WTO,XBD
      REAO (5,5020) ICPTI1)
 5C20 FORMAT (I2)
      IF IIOPT(1).EQ.2) GO TO 17
      REAO I5,5010) CCGV, CWG, CWS, OWS, GWS, WWS, ESN,XWS, XSWO, EG
```

```
      GO TO 18                                                          A6AM040
   17 READ (5,5010) GWOC, ESN, EG                                       A6AM041
   18 CONTINUE                                                          A6AM042
C     CONTROLLER                                                        A6AM043
      READ (5,5020) ICPT(2)                                             A6AM044
      IF (IOPT(2).EQ.2) GO TO 20                                        A6AM045
      READ (5,5010) CS, C, EV                                           A6AM046
      GO TO 24                                                          A6AM047
   20 READ (5,5010) CC, VC1, VC10, EV                                   A6AM048
   24 CALL EJECT                                                        A6AM049
   25 WRITE (6,6000) IO, TSTEP, TENO, TRITE, MICRC, TINTP               A6AM050
 6000 FORMAT  (//1HO,T55,19HI N P U T   O A T A//1HO,T10,               A6AM051
     1 *TIME BETWEEN*,T30,*SYSTEM*,T60,*SYSTEM PRINT*,T88,              A6AM052
     2 3A10/ * *,T10,*STEPS=*,E11.4,T30,*RUN TIME = *,                  A6AM053
     3 E11.4,T60,*INTERVAL = *,E11.4,T88,*MICROFILM OPT=   *,I2//       A6AM054
     4 * *,T10,*INTERNAL PRINT INTERVAL =*,E11.4//)                     A6AM055
      WRITE (6,5007) ACVRO, ACVSO, PCVB, VMIN, NR                       A6AM056
 5CC7 FORMAT (1HO, * ACVRC = *,E11.4, 5X, * ACVSO = *,E11.4, 5X, * PCVB A6AM057
     1= *,E11.4, 5X, * VMIN = *,E11.4, 5X, * NR = *,I3//)               A6AM058
      WRITE (6,6020) SIMP                                               A6AM059
 6020 FORMAT (1H ,T44,*S I M P L I F I E D   B R A K E   C O N T R O L*/A6AM060
     1 *O*,T10,*  ALPHA=*,E11.4,*  ALPHB=*,E11.4,*    ABP=*,E11.4,      A6AM061
     2         *    ABPS=*,E11.4,*    ACR=*,E11.4,*   ACVO=*,E11.4/     A6AM062
     3 * *,T1C,*  ACVL=*,E11.4,*   CBPL=*,E11.4,*   CBPU=*,E11.4,       A6AM063
     4         *      CG=*,E11.4,*  CSCVR=*,E11.4,*     OG=*,E11.4/     A6AM064
     5 * *,T10,*      ET=*,E11.4,*    FNP=*,E11.4,*    GCV=*,E11.4,     A6AM065
     6         *     PBO=*,E11.4,*    PCP=*,E11.4,*    PFB=*,E11.4/     A6AM066
     7 * *,T10,*      PR=*,E11.4,*    RBT=*,E11.4,*     RR=*,E11.4,     A6AM067
     8         *     RTO=*,E11.4,*    SCL=*,E11.4,*   SCVC=*,E11.4/     A6AM068
     9 * *,T10,*    SCVA=*,E11.4,*   SCVR=*,E11.4,*    TCP=*,E11.4,     A6AM069
     A         *     UB1=*,E11.4,*    UB2=*,E11.4,*    UT1=*,E11.4/     A6AM070
     B * *,T10,*     UT2=*,E11.4,*     VF=*,E11.4,*    VRO=*,E11.4,     A6AM071
     C         *      WG=*,E11.4,*    WTO=*,E11.4,*    WIT=*,E11.4/     A6AM072
     D * *,T1C,*   XCVO=*,E11.4,*   XSCP=*,E11.4,*   XSCR=*,E11.4,      A6AM073
     E         *     XBO=*,E11.4,*    XGO=*,E11.4,*   XOGO=*,E11.4/     A6AM074
     F * *,T10,*     XFO=*,E11.4,*   XFDO=*,E11.4/)                     A6AM075
C     WHEEL SPEED SENSOR                                                A6AM076
      IF (IOPT(1).EQ.2) GO TO 83                                        A6AM077
      WRITE (6,6050) ICPT(1), CCGV, CWG, CWS, OWS, GWS, WWS,ESN,        A6AM078
```

```
     1 XWS, XWSD, EG                                                    A6AM079
 6050 FORMAT(1H ,T10,6HOPTICN,I3,T41,35HW H E E L   S P E E D   S E N S A6AM080
     10 R/                                                              A6AM081
     2 1HO,T10,8H   CCGV=,E11.4,8H    CWG=,E11.4,8H    CWS=,E11.4,      A6AM082
     3         8H    DWS=,E11.4,8H    GWS=,E11.4,8H    WWS=,E11.4/      A6AM083
     4 1HO,T1C,8H    ESN=,E11.4,8H    XWS=,E11.4,8H   XWSC=,E11.4,      A6AM084
     5         8H     EG=,E11.4///)                                     A6AM085
      GO TO 84                                                          A6AM086
   83 WRITE (6,6051) IOPT(1), GWOC, ESN, EG                             A6AM087
 6051 FORMAT(1H ,T10,6HOPTION,I3,T41,35HW H E E L   S P E E D   S E N S A6AM088
     10 R/                                                              A6AM089
     2 1HO,T10,8H   GWOC=,E11.4,8H    ESN=,E11.4,8H      EG=,E11.4//)   A6AM090
C                                                                       A6AM091
C      CONTROL  SYSTEM                                                  A6AM092
   84 IF (IOPT(2).EQ.2) GO TO 90                                        A6AM093
      WRITE (6,6060) (CS(L),L=1,29)                                     A6AM094
 6060 FORMAT(*0*,T46,*CONTROLLER*/                                      A6AM095
     1 *0*,T10,*     CM=*,E11.4,                                        A6AM096
     2         *   C404=*,E11.4,*   C405=*,E11.4,*   C406=*,E11.4/      A6AM097
     3 * *,T10,*   C407=*,E11.4,*   C446=*,E11.4,*   C447=*,E11.4,      A6AM098
     4         *   C448=*,E11.4,*   C449=*,E11.4,*   C450=*,E11.4/      A6AM099
     5 * *,T10,*   C451=*,E11.4,*   C452=*,E11.4,*   C456=*,E11.4,      A6AM100
     6         *   C457=*,E11.4,*   C458=*,E11.4,*   C459=*,E11.4/      A6AM101
     7 * *,T1C,*   C460=*,E11.4,*   C461=*,E11.4,*   C462=*,E11.4,      A6AM102
     8         *   C526=*,E11.4,*   C527=*,E11.4,*   C528=*,E11.4/      A6AM103
     9 * *,T1C,*   C529=*,E11.4,*   C530=*,E11.4,*   C531=*,E11.4,      A6AM104
     A         *   C532=*,E11.4,*   C533=*,E11.4,*   C534=*,E11.4/      A6AM105
     B * *,T10,*   C535=*,E11.4)                                        A6AM106
      WRITE (6,6065) (CS(L),L=30,43)                                    A6AM107
 6065 FORMAT(                                                           A6AM108
     1 * *,T10,*   C565=*,E11.4,*   C566=*,E11.4,*   C567=*,E11.4,      A6AM109
     2         *   C568=*,E11.4,*   C569=*,E11.4,*   C570=*,E11.4/      A6AM110
     3 * *,T1C,*   C571=*,E11.4,*   C575=*,E11.4,*   C576=*,E11.4,      A6AM111
     4         *   C577=*,E11.4,*   C578=*,E11.4,*   C579=*,E11.4/      A6AM112
     5 * * T10,*   C580=*,E11.4,*   C581=*,E11.4)                       A6AM113
      WRITE (6,6069) (CS(L),L=44,76), C, EV                             A6AM114
 6069 FORMAT(                                                           A6AM115
     1 * *,T1C,*   C604=*,E11.4,*   C605=*,E11.4,*   C606=*,E11.4,      A6AM116
     2         *   C607=*,E11.4,*   C608=*,E11.4,*   C609=*,E11.4/      A6AM117
```

```
    3 * *,T10,*   C610=*,E11.4,*   C611=*,E11.4,*   C612=*,E11.4,      A6AM118
    4          *  C613=*,E11.4,*   C614=*,E11.4,*   C615=*,E11.4/      A6AM119
    5 * *,T10,*   C616=*,E11.4,*   C617=*,E11.4,*   C618=*,E11.4,      A6AM120
    6          *  C619=*,E11.4,*   C620=*,E11.4,*   C621=*,E11.4/      A6AM121
    7 * *,T10,*   C622=*,E11.4,*   C623=*,E11.4,*   C800=*,E11.4,      A6AM122
    8          *  C801=*,E11.4,*   C8C2=*,E11.4,*   C8C3=*,E11.4/      A6AM123
    9 * *,T10,*   C804=*,E11.4,*   C805=*,E11.4,*   C8C6=*,E11.4,      A6AM124
    A          *  C8C7=*,E11.4,*   C8C8=*,F11.4,*   C809=*,E11.4/      A6AM125
    B * *,T10,*   C810=*,E11.4,*   C8II=*,EI1.4,*   C812=*,E11.4,      A6AM126
    C          *    VC1=*,E11.4,*    VC2=*,E11.4,*    VC3=*,E11.4/     A6AM127
    D * *,T10,*     VC4=*,E11.4,*  VC1D=*,E11.4,*  VC2D=*,E11.4,       A6AM128
    E          *  VC3D=*,E11.4,*   VC4D=*,E11.4,*     EV=*,E11.4//)    A6AM129
      GO TO 95                                                         A6AM130
   90 WRITE (6,6080) CC, VC1, VC1D, EV                                 A6AM131
 6C8C FORMAT (* *,T46,*CCNTRCLLER*/                                    A6AM132
    1 *0*,T10,*      VS=*,E11.4,                                       A6AM133
    2          *  C700=*,E11.4,*   C701=*,E11.4,*   C7C2=*,EII.4/      A6AM134
    3 * *,T1C,*   C7C5=*,E11.4,*   C706=*,E11.4,*   C707=*,E11.4,      A6AM135
    4          *  C7C8=*,E11.4,*   C7C9=*,E11.4,*   C7I0=*,E11.4/      A6AM136
    5 * *,T10,*   C711=*,E11.4,*    VC1=*,E11.4,*  VC1D=*,E11.4,       A6AM137
    6          *     EV=*,E11.4)                                       A6AM138
   95 CALL EJECT                                                       A6AM139
C                                                                      A6AM140
C     ERROR CHECKS                                                     A6AM141
  100 IF (MICRC .GT. 0 .AND. MICRO .LT. 4) GO TO 110                   A6AM142
      IT= 100                                                          A6AM143
      WRITE (6,6100)  IT                                               A6AM144
 6100 FORMAT(*0       ERROR *, I3, * CCCURREC. *      )                A6AM145
  110 IF (TEND .GT. 0.) GO TO 120                                      A6AM146
      IT= 101                                                          A6AM147
      WRITE (6,6100)  IT                                               A6AM148
  120 IF (TRITE .GT. 0.) GO TO 13C                                     A6AM149
      IT= 102                                                          A6AM150
      WRITE (6,61C0) IT                                                A6AM151
  130 IF(TSTEP.GT.0.) GO TO 140                                        A6AM152
      IT = 103                                                         A6AM153
      WRITE (6,6100) IT                                                A6AM154
  140 IF (IOPT(1).EQ.1.OR.IOPT(1).EQ.2)  GO TO 15C                     A6AM155
      IT = 104                                                         A6AM156
```

```
      WRITE (6,6100) IT                                                 A6AM157
  150 IF (IOPT(2).EQ.1.OR.IOPT(2).EQ.2)  GO TC 200                     A6AM158
      IT # 105                                                          A6AM159
      WRITE (6,6100) IT                                                 A6AM160
C                                                                       A6AM161
  200 N = 1                                                             A6AM162
      RETURN                                                            A6AM163
  210 CALL EJECT                                                        A6AM164
      WRITE(6,6600)                                                     A6AM165
 6600 FORMAT(22HOTHIS JOB IS CCMPLETE. )                                A6AM166
      CALL EXIT                                                         A6AM167
      RETURN                                                            A6AM168
      END                                                               A6AM169
```

```
C
C
                    S U B R O U T I N E     C O N C I R
C
C                    ON-OFF ANTISKID CONTROL CIRCUIT (2)
C
      COMMON /KEY/ TSTEP, TEND, TRITE, MICRO, IOPT(2), T, TINTP
     1       /CSO/ EV
     2       /CCC/ VS,   C700, C701, C702, C705, C706, C707, C708,
     3             C709, C710, C711
     4       /CCI/ VC1, VC1D
     5       /FRST/ FLG1,FLG3
     6       /WSO/ EG
C
      FLG6 = 0.
   10 VC1D2 = VC1D1
      VC1D1 = VC1D
      VC11  = VC1
C
C     EQUATION  (3)
      EGMVC1 = EG - VC1
C
C     EQUATION  (R1)
      AD1 = 0.
      IF (EGMVC1 .GT. C707/C706) AD1 = EGMVC1*C706 - C707
C
C     EQUATION  (V2)
      AR4 = EGMVC1 * C708
C
C     EQUATION  (V6)
      ABQ1 = 0.
      IF (-EGMVC1.GT. C702/C701) ABQ1 = -EGMVC1 * C701 - C702
C
C     EQUATION  (V4-1)
      AR1 = 0.
      IF (ABQ1 .LT. C700) AR1 = -EGMVC1*C709 - ABQ1*C711 - C710
C
C     EQUATION (EV)
      EV = 0.
```

```
      IF (ABQ1 .GE. C700) EV = VS
C
C     EQUATION  (N1)
      AD2 = ABQ1 + AR1
      IF (AD2 .LT. 0.) AD2 = 0.
      AC1 = AD1 + AR4 - AD2
C
C     EQUATION  (A1)
      VC1D = AC1 * C705
C
C     CHECK FOR PRINTCUT
      IF(FLG6.EQ.0.) GO TO 30
      IF(FLG3.EQ.0.) GO TO 30
   20 WRITE(22,6010) T, VC1, VC1D, ABQ1, AC1, AD1, AR1, AR4, EV ,EG
 6010 FORMAT (*0 CONTROLLER INTERNAL DATA*/
     1*  T=*,E15.8,*    VC1=*,E11.4,*   VC1C=*,E11.4,
     2*   ABQ1=*,E11.4,*    AC1=*,E11.4,*    AD1=*,E11.4/
     3*    AR1=*,E11.4,*    AR4=*,E11.4,*     EV=*,E11.4,
     4 8H     EG=,E11.4)
C
   30 IF(FLG1.NE.C.) GO TO 40
      VC1 = TSTEP*.5*(VC1D+VC1D1) + VC11
      GO TO 50
   40 VC1 = (TSTEP/12.) * (5.*VC1D + 8.*VC1D1 - VC1C2) + VC11
C
   5C IF (FLG6.NE.0.)  GC TO 70
      FLG6 = 1.
      GO TO  10
   70 RETURN
      END
```

```
C
                    S U B R O U T I N E   E J E C T
C
      COMMON /DAT/ JCB, DAY, IPAGE, PAGE(2)
C
      IPAGE = IPAGE + 1
      ENCODE(14,50,PAGE)IPAGE
   50 FORMAT(I14)
      WRITE(6,60) JOB, DAY,  PAGE(2)
   60 FORMAT(78H1GENERAL DYNAMICS        CCNVAIR AERCSPACE CIVISION
     1  FORT WORTH OPERATICN /37H 6600 PROCECURE A1C          PROBLEM ,
     2 A9,11X,A10,2X,5HPAGE ,A4/)
      RETURN
      END
```

CC = 00871